

On the value of systematics for the study of evolution: insights from the reptiles and amphibians of Madagascar



Dissertation zur Erlangung des Doktorgrades der Naturwissenschaften der
Fakultät für Biologie der Ludwig-Maximilians-Universität München
*Dissertation to Obtain a Doctoral Degree in Natural Sciences from the
Faculty of Biology of the Ludwig-Maximilian University of Munich*

vorgelegt von
presented by

Mark D. Scherz

März 2019

Cover art: *Plethodontohyla guentheri* Glaw & Vences 2007 and
Gephyromantis (Duboisimantis) saturnini Scherz, Rakotoarison, Ratsoavina, Hawlitschek, Vences & Glaw, 2018, two frogs from northern Madagascar. Illustration by Gabriel Ugueto.

Erstgutachter: Prof. Dr. Gerhard Haszprunar
Zweitgutachter: Prof. Dr. Roland Melzer

Tag der Einreichung: 21 März 2019
Tag der mündlichen Prüfung: 11 Juli 2019

A hundred million years ago
Gondwanaland was split
and Indiagascar's continent
rifted off of it.
India and Madagascar
soon were parted ways.
So Madagascar, in the sea,
now isolated lays.

It shifted south, it shifted north;
ran hot and cool and wet;
and from the KPg event
its biota reset.
Then sailing from across the sea
there came, by drip and drab,
new fauna and new flora, there
to Evolution's Lab.

The mountains in particular,
with mists, and rains, and fogs,
produced a thousand different kinds
of reptiles and of frogs.
This isolated 'continent'
where selection went mad
became a unique paradise
for research to be had.

Over six hundred frogs but just
three hundred fifty named—
filling this Linnean gap
is where this thesis aimed.
We need to name them all if we
are ever to connect them;
to understand their ancestry,
and somehow to protect them.

And so it is this thesis starts,
systematics at the fore:
how it works and what it does
and why we need it more.
For names are anchors of all life;
the way we group and bin things,
and how we reconstruct the tree
'from such simple beginnings'.

Eidesstattliche Erklärung

Ich versichere hiermit an Eides statt, dass die vorgelegte Dissertation von mir selbständig und ohne unerlaubte Hilfe angefertigt wurde.

München, den

7. August 2019

Mark D. Scherz

Erklärung

Hiermit erkläre ich, dass die Dissertation nicht ganz oder in wesentlichen Teilen einer anderen Prüfungskommission vorgelegt worden ist und dass ich mich nicht anderweitig einer Doktorprüfung ohne Erfolg unterzogen habe.

München, den

7. August 2019

Mark D. Scherz

Contents

Acknowledgements	vii
Taxonomic Disclaimer	ix
Abbreviations	ix
Declaration of contributions as a co-author	x
Summary	1
Zusammenfassung	2
Introduction	4
<i>Categorising a continuum: Species concepts and the philosophy of taxonomy</i>	5
<i>Taxonomy in the 21st century</i>	7
<i>Evolution on islands</i>	9
<i>Madagascar: a systematist's paradise, and an ideal island study system for continental evolution</i>	10
<i>Herpetofaunal diversity of Madagascar</i>	12
<i>Thesis outline</i>	14
Results	17
<i>Section 1: Conserving complexes requires taxonomic clarity</i>	17
Chapter 1. MANUSCRIPT (in review): Species complexes and the importance of Data Deficient classification in Red List assessments: the case of <i>Hylobatrachus</i> frogs	17
<i>Section 2: Biogeography through the lens of systematics</i>	46
Chapter 2. PAPER: A new frog species of the subgenus <i>Asperomantis</i> (Anura, Mantellidae, <i>Gephyromantis</i>) from the Bealanana District of northern Madagascar	46
Chapter 3. PAPER: A distinctive new frog species (Anura, Mantellidae) supports the biogeographic linkage of the montane rainforest massifs of northern Madagascar	63
Chapter 4. PAPER: Yet another small brown frog from high altitude on the Marojejy Massif, northeastern Madagascar (Anura: Mantellidae)	79
Chapter 5. PAPER: Two new Madagascan frog species of the <i>Gephyromantis</i> (<i>Duboimantis</i>) <i>tandroka</i> complex from northern Madagascar	91
<i>Section 3: Ecomorphological evolution through the lens of systematics</i>	121
Chapter 6. PAPER: Two new species of terrestrial microhylid frogs (Microhylidae: Coprophylinae: <i>Rhombophryne</i>) from northeastern Madagascar	121
Chapter 7. PAPER: A review of the taxonomy and osteology of the <i>Rhombophryne serratopalpebrosa</i> species group (Anura: Microhylidae) from Madagascar, with comments on the value of volume rendering of micro-CT data to taxonomists	138
Chapter 8. PAPER: Reconciling molecular phylogeny, morphological divergence and classification of Madagascan narrow-mouthed frogs (Amphibia: Microhylidae)	179
Chapter 9. MANUSCRIPT (accepted): Morphological and ecological convergence at the lower size limit for vertebrates highlighted by five new miniaturised microhylid frog spe-	

cies from three different Madagascan genera	190
Chapter 10. MANUSCRIPT (in prep.): Ecomorphological evolution of Madagascar's narrow-mouthed frogs (Anura, Microhylidae)	237
<i>Section 4: Consolidating taxonomic datasets for macroevolutionary studies</i>	265
Chapter 11. MANUSCRIPT (in prep.): Genital and external ornaments are evolutionarily uncoupled in chameleons.	265
Discussion	281
<i>Conservation implications</i>	281
<i>Biogeography of herpetofauna in northern Madagascar</i>	283
<i>Ecomorphological evolution in cophylines</i>	287
<i>Macroevolution and taxonomy</i>	289
<i>Madagascar as an island model system for continental evolution</i>	290
Conclusions	293
References	294
Curriculum Vitae	311

Acknowledgements

My gratitude to the numerous people who have been instrumental in the preparation of this thesis can hardly be expressed. It has been a huge privilege to work on a subject that I love with such wonderful colleagues, and with the encouragement and support of my friends and family.

First of all, I would like to give my warmest thanks to Dr Frank Glaw and Prof. Miguel Vences, who have played such an important role in my development as a researcher over not only the period of this doctoral thesis, but years before that—even before we met. Frank’s knowledge of the herpetofauna of Madagascar is second to none and is always a source of awe. His attention to detail and fastidiousness are always inspiring and make me strive to achieve the same levels of care and accuracy in my work. Miguel’s astounding efficiency and focus have changed the way that I work, driving me to think about my projects in a bigger context, and challenging me to focus on hypotheses and questions. Miguel and Frank have shaped the way that I think, and have been a constant source of encouragement and thoughtful feedback. I could not have hoped for a more welcoming work environment.

I thank my friend and colleague Dr Andolalao Rakotoarison for her continued passion for the frogs of Madagascar, for her dependability, and for her help in various aspects of my work in Madagascar over the years since we met. I am glad that the frogs of Madagascar have a Malagasy voice of such strength and determination speaking for them.

I thank also my other colleagues, David Prötz, Dr Oliver Hawlitschek, Frederic Schedel, and Michael Franzen, who have been great companions in the museum over the past years; who have offered me stimulating conversations and heartfelt commiserations when needed, shared highly productive collaborations, and celebrated successes with me. Also, to the various master’s and bachelor’s students who I have worked with over the last few years, who have reminded me of the importance of passing on knowledge, and the potential of malleable minds committed to intellectual pursuits.

To my colleagues in the Zoological Institute in Braunschweig I am also grateful for their help and good humour during my occasional short visits. Especially to the tireless laboratory technicians, Gabriele Keunecke and Meike Kondermann, who sequenced or organised the sequencing of countless specimens for me.

I thank also the rest of my colleagues working in Madagascar for their friendship, support, and collaboration. There are many of them, so I cannot list them all here, but I would like to particularly thank Dr Angelica Crottini, Dr Jörn Köhler, Carl Hutter, and Dr Fanomezana M Ratsoavina, with whom I have had extremely rewarding collaborations. These dedicated researchers, foreign and Malagasy, are working to push our knowledge of the herpetofauna of Madagascar forward every day, and have been most inspiring and enthusiastic collaborators.

I thank the dozens of friends and colleagues on Twitter whom I have never met in person, but who have nevertheless been important influences over the course of my PhD. I have been able to turn to them for help in R, for advice on life decisions, for celebration of successes big and small, and for sympathy when things have not gone exactly to plan. It is always a huge comfort to know that there are so many inspiring and amazing scientists out there, sharing their work, inspiring new generations, and showing what it means to work on what you love.

My greatest thanks must go to my parents. It was an unbelievable privilege to be encouraged in my youth to pursue my passion for animals, and, as I grew older, to fulfil my dream of researching the amphibians and reptiles of Madagascar; to never hear a word of discouragement regarding my decision to work in an obscure field of research, often under precarious circumstances far from home. To have had such unwavering support is something I now know to be rare, and I appreciate it more than I can say.

Finally, I would like to thank my beloved partner, Ella Z. Lattenkamp, without whom I cannot

imagine having completed this thesis. Her encouragement and understanding have been unwavering. Her clear-headedness and organisation helped calm the chaos of my own ‘organisation’ system (or lack thereof) and gave me the structure and clarity I needed when I was overwhelmed. She has been a constant source of support and comfort, with pragmatic solutions and thoughtful critique. She has challenged my worldview and thoughts, and pushed me to be a better person. She has been patience herself in every aspect of our life together, especially in dealing with my absent-mindedness and forgetfulness, particularly in the months during which I was writing the body of this thesis. I could not hope for a more compassionate, stronger partner. For this and more, she has my enduring gratitude.



Rhombocephryne vaventy

Taxonomic Disclaimer

This thesis contains names of species established in papers that are still in press or under review. For the sake of practicality, the names included in these papers are used throughout the thesis. However, I hereby disclaim all of the unpublished names in this thesis for nomenclatural purposes, and state that they are not to be considered available in the sense of the International Code of Zoological Nomenclature (ICZN), in accordance with Article 8.3 of that Code.

Abbreviations

- 3D — three-dimensional
b.p. — before present
BCS — Biological Species Concept
BioGeoBEARS — Biogeography with Bayesian (and Likelihood) Evolutionary Analysis in R Scripts
cf. — *confer* (Latin, meaning ‘compare with’)
DD — Data Deficient
diceCT — diffusible iodine contrast-enhanced computed tomography
DNA — deoxyribonucleic acid
ECS — Evolutionary Species Concept
ESS — effective sample size
ICZN — International Code of Zoological Nomenclature
IUCN — International Union for the Conservation of Nature
KPg — Cretaceous-Palaeogene
m a.s.l. — metres above sea level
Ma — mega-annum
Micro-CT — micro-computed tomography
ML — maximum likelihood
MSC — Multispecies Coalescent
NMDS — non-metric multidimensional scaling
nt — nucleotides
OTU — operational taxonomic unit
p-distance — pairwise distance
RNA — ribonucleic acid
SC — sequence capture
SE — standard error
SOD — sexual ornamentation dimorphism
SSD — sexual size dimorphism
s. l. — *sensu lato* (Latin, meaning ‘in the broad sense’)
sp. — species
sp. aff. — *species affinis* (Latin, meaning ‘species with affinities to’)
s. s. — *sensu stricto* (Latin, meaning ‘in the strict sense’)
UCS — Unified Species Concept
UCE — ultra-conserved element

Declaration of contributions as a co-author

I declare that I have contributed to the chapters contained in this cumulative dissertation as follows:

I independently carried out the research under the guidance of my supervisors Professor Miguel Vences and Dr Frank Glaw, including the conceptual design, planning, data collection and processing, data analysis, manuscript preparation, submission, and revision, and all other associated work, with input from my colleagues. Notable exceptions are listed below, indicated by the initials of the following co-authors: Franco Andreone, Lawrence Ball, Molly C. Bletz, James Borrell, Wolfgang Böhme, Teddy Bruy, Angelica Crottini, Naidi M. Dixit, Carmen Drehlich, Joan Garcia-Porta, Frank Glaw, Julian Glos, Oliver Hawlitschek, Carl R. Hutter, Iker Irisarri, Jörn Köhler, Sven Künzel, Steve Megson, Axel Meyer, Serge H. Ndriantsoa, Denise H. Nomenjanahary, Duncan Parker, Hervé Philippe, David Prötz, Jeanneney Rabearivony, Andolalao Rakotoarison, Marius Rakotondratsima, Loïs Rancilhac, Fanomezana M. Ratsoavina, Elidiot Razafimandimby, Jary H. Razafindraibe, Jana C. Riemann, Mark-Oliver Rödel, Sam Hyde Roberts, Thomas Starnes, Dominik Stützer, Krystal Tolley, Miguel Vences.

Chapter 1. Scherz, M.D., Glaw, F., Hutter, C.R., Bletz, M.C., Rakotoarison, A., Köhler, J. & Vences, M. (in review) Species complexes and the importance of Data Deficient classification in Red List assessments: the case of *Hylobatrachus* frogs. Unpublished manuscript.

- Fieldwork was conducted by all coauthors.
- Molecular genetic laboratory work was done in the lab of MV by laboratory technicians (M. Kondermann or G. Keunecke), and phylogenetic reconstruction conducted by MV.
- Recordings were collected by CRH and FG and analysed by JK.
- Specimens were measured by MV.

Chapter 2. Scherz, M.D., Vences, M., Borrell, J., Ball, L., Nomenjanahary, D.H., Parker, D., Rakotondratsima, M., Razafimandimby, E., Starnes, T., Rabearivony, J. & Glaw, F. (2017) A new frog species of the subgenus *Asperomantis* (Anura, Mantellidae, *Gephyromantis*) from the Bealanana District of northern Madagascar. *Zoosystematics and Evolution*, 93(2):451–466. DOI: 10.3897/zse.93.14906

- Molecular genetic laboratory work was done in the lab of MV by laboratory technicians (M. Kondermann or G. Keunecke).
- Fieldwork was conducted by all authors except FG.

Chapter 3. Scherz, M.D., Hawlitschek, O., Razafindraibe, J.H., Megson, S., Ratsoavina, F.M., Rakotoarison, A., Bletz, M.C., Glaw, F. & Vences, M. (2018) A distinctive new frog species (Anura, Mantellidae) supports the biogeographic linkage of the montane rainforest massifs of northern Madagascar. *Zoosystematics and Evolution*, 94(2):247–261. DOI: 10.3897/zse.94.21037

- Molecular genetic laboratory work was done in the lab of MV by laboratory technicians (M. Kondermann or G. Keunecke), and phylogenetic reconstruction conducted by MV.
- Fieldwork was conducted by all coauthors.

Chapter 4. Scherz, M.D., Razafindraibe, J.H., Rakotoarison, A., Dixit, N.M., Bletz, M.C., Glaw, F. & Vences, M. (2017) Yet another small brown frog from high altitude on the Marojejy Massif, northeastern Madagascar (Anura: Mantellidae). *Zootaxa*, 4347(3):572–582. DOI: 10.11646/zootaxa.4347.3.9

Declaration of contributions as a co-author

- Molecular genetic laboratory work was done by NMD and MV, and phylogenetic reconstruction conducted by MV.
- Fieldwork was conducted together with JHR, AR, MCB, and MV, and additional samples were included that were sampled by FG, OH, FMR, and AR.

Chapter 5. Scherz, M.D., Rakotoarison, A., Ratsoavina, F.M., Hawlitschek, O., Vences, M. & Glaw, F. (2018) Two new Madagascan frog species of the *Gephyromantis (Duboimantis) tandroka* complex from northern Madagascar. *Alytes*, 36:130–158.

- Molecular genetic laboratory work was done in the lab of MV by laboratory technicians (M. Kondermann or G. Keunecke), and phylogenetic reconstruction conducted by MV.
- Fieldwork was conducted by all coauthors.
- Bioacoustic analysis was conducted by MV.

Chapter 6. Scherz, M.D., Glaw, F., Vences, M., Andreone, F. & Crottini, A. (2016) Two new species of terrestrial microhylid frogs (Microhylidae: Cophylinae: *Rhombophryne*) from northeastern Madagascar. *Salamandra*, 52(2):91–106.

- Fieldwork was conducted by FG, MV, AF, and AC.
- Molecular genetic laboratory work was done in the lab of MV by laboratory technicians (M. Kondermann or G. Keunecke), and phylogenetic reconstruction conducted by MV.

Chapter 7. Scherz, M.D., Hawlitschek, O., Andreone, F., Rakotoarison, A., Vences, M. & Glaw, F. (2017) A review of the taxonomy and osteology of the *Rhombophryne serratopalpebrosa* species group (Anura: Microhylidae) from Madagascar, with comments on the value of volume rendering of micro-CT data to taxonomists. *Zootaxa*, 4273(3):301–340. DOI: 10.11646/zootaxa.4273.3.1

- Fieldwork was conducted by OH, AF, AR, MV, FG, and FMR.
- Molecular genetic laboratory work was done in the lab of MV by laboratory technicians (M. Kondermann or G. Keunecke), and phylogenetic reconstruction conducted by MV.

Chapter 8. Scherz, M.D., Vences, M., Rakotoarison, A., Andreone, F., Köhler, J., Glaw, F. & Crottini, A. (2016) Reconciling molecular phylogeny, morphological divergence and classification of Madagascan narrow-mouthed frogs (Amphibia: Microhylidae). *Molecular Phylogenetics and Evolution*, 100(2016):372–381. DOI: 10.1016/j.ympev.2016.04.019

- Samples used were collected by various researchers over the last 30 years.
- Molecular genetic laboratory work was done in the labs of MV and AC, in part by laboratory technicians, and in part by AC.
- Phylogenetic reconstruction was done by AC and MV.

Chapter 9. Scherz, M.D., Hutter, C.R., Rakotoarison, A., Riemann, J.C., Rödel, M.-O., Ndriantsoa, S.H., Glos, J., Hyde Roberts, S., Crottini, A., Vences, M. & Glaw, F. (accepted) Morphological and ecological convergence at the lower size limit for vertebrates highlighted by five new miniaturised microhylid frog species from three different Madagascan genera. *PLoS One*.

- Fieldwork was conducted over several expeditions between 2000 and 2017 by AR, JCR, MOR, SHN, JG, SHR, AC, MV, and FG, and colleagues.
- Molecular genetic laboratory work was done by AC.
- Bioacoustic analysis was conducted by MV and me.

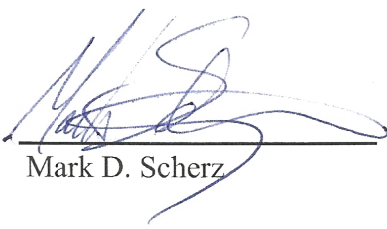
Chapter 10. Scherz, M.D., Hutter, C.R., Rödel, M.-O., Rancilhac, L., Künzel, S., Rakotoarison, A., Drehlich, C., Philippe, H., Glaw, F., Vences, M. Ecomorphological evolution of Madagascar's narrow-mouthed frogs (Anura, Microhylidae). Unpublished manuscript

- Transcriptome libraries were prepared by SK and were sequenced at the Max Planck Institute for Evolutionary Biology in Plön.
- Molecular genetic laboratory work for single markers was done by CD with the aid of laboratory technicians (M. Kondermann or G. Keunecke) and MV.
- Target capture sequencing and phylogenomic reconstruction was conducted by CRH. Phylogenetic methods were also written largely by CRH.
- Biogeographic analysis in BioGeoBEARS was coded by me and run by CRH.

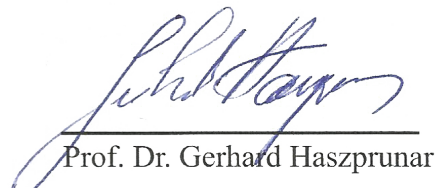
Chapter 11. Scherz, M.D., Rancilhac, L., Garcia-Porta, J., Bruy, T., Irisarri, I., Künzel, S., Stützer, D., Glaw, F., Prötz, D., Tolley, K.A., Meyer, A., Böhme, W., Philippe, H. & Vences, M. Genital and external ornaments are evolutionarily uncoupled in chameleons. Unpublished manuscript.

- Transcriptome libraries were prepared by SK and were sequenced at the Max Planck Institute for Evolutionary Biology in Plön.
- Transcriptome filtering was done by HP and LR.
- Phylogenetic transcriptomics was conducted by LR and MV, with input from KT, II, HP, and me.
- Supplementary methods pertaining to genomics were written by LR and II.
- Molecular genetic laboratory work for single markers was done by DS with the aid of laboratory technicians (M. Kondermann or G. Keunecke) and MV.
- Morphological database was assembled by TB, AM, MV, DP, and me.
- Statistical analysis was conducted by me, with input from JGP, MV, TB, and ES.

Furthermore, all published articles were peer reviewed, and revised following suggestions of the reviewers, with the input of their respective co-authors. Photographs and call recordings were taken by the co-authors or me, unless otherwise stated. Figures were prepared by me, MV, or JK. Figures in the introduction and discussion of this thesis, as well as frog and chameleon photographs included were made by me.



Mark D. Scherz



Prof. Dr. Gerhard Haszprunar

Summary

Background

Systematics, divided into the two subfields of taxonomy and phylogeny, is a field concerned with deducing evolutionary relationships among branches of the tree of life. Species form the substrate of systematics that is drawn upon by almost all other biological fields, from conservation policy to community ecology to evolutionary biology. We have so far named nearly 2 million eukaryotes. Yet, there may be as many as 100 million species on Earth, and our current rate of description is just 20,000 new species and subspecies per year. Thus, a vast amount of taxonomic work remains to be done. Systematic research helps us to complete this inventory, while at the same time shedding light on numerous other aspects of biology.

In this thesis, I focus on the systematics of reptiles and amphibians in Madagascar, an island model for continent-scale evolutionary dynamics. I revise the taxonomy of several different groups, and in doing so, reveal facets of their evolution, ecology, and conservation. I also demonstrate that narrow-scope taxonomic works can be harvested as data sources to address broad-scope research questions, for example in the realm of macroevolution.

Results

The studies presented here are divided into four sections encompassing eleven chapters:

In section 1, I present a paper (chapter 1) in which my colleagues and I describe two new species of frogs of the genus *Mantidactylus* and discuss their conservation; I demonstrate the important link between taxonomy and conservation, and the way in which conservation policy is currently not taking full advantage of taxonomic knowledge or highlighting gaps in that knowledge.

In section 2, I present four papers (chapters 2–5), in which my colleagues and I describe five new species of frogs of the genus *Gephyromantis* and discuss in particular their biogeographic relationships; I show that examining the patterns in the different subgenera concerned points toward general patterns, giving us insights on the biogeographic history of northern of Madagascar. In the discussion I provide comparative examples from other taxa distributed in the same area and show that patterns hold across amphibians and reptiles, but apparently not small mammals.

In section 3, I present five chapters (chapters 6–10), three of which are taxonomic and two of which are more phylogenetic in focus, together resulting in nine new species and two new genera of microhylid frogs of the subfamily Cophylinae; I illustrate how taxonomy can take advantage of new technological advantages to resolve taxonomically challenging cases, and provide insights into the ecomorphological evolution of these frogs.

In section 4, I present a paper (chapter 11) in which my colleagues and I use a dataset generated from taxonomic literature in a comparative phylogenetic framework to analyse the evolution of sexual ornamentation across chameleons. I show that the difference in sexual selection acting on genital and external morphological ornamentation results in their evolutionary uncoupling.

Conclusions

In this thesis, I describe 16 new species and two new genera of frogs from Madagascar and provide new data on their phylogeny and evolution. I also demonstrate that the existing taxonomic literature on chameleons can become a source of data for studies to addressing questions about their evolution in more detail. Taxonomic progress on the herpetofauna of Madagascar is proceeding apace, and as we are approaching a completion of the island's biodiversity inventory, we are gaining valuable insights into the relationships among its fauna, their ecology, evolution, and origins, while also learning about which species need to be protected and how best to do so. Completion of this picture will have broad implications, as the evolutionary Petri dish that is Madagascar can be scaled up to understand patterns governing the generation and perpetuation of biodiversity at a continental scale.

Zusammenfassung

Hintergrund

Die Systematik, unterteilt in die beiden Teilbereiche Taxonomie und Phylogenie, befasst sich mit der Ableitung evolutionärer Verwandschaftsbeziehungen. Arten bilden die Basis der Systematik, auf der fast alle anderen biologischen Bereiche aufbauen – von der Naturschutzpolitik über die Ökologie bis hin zur Evolutionsbiologie. Bisher wurden fast 2 Millionen Eukaryoten benannt. Schätzungen zur Gesamtzahl sprechen von bis zu 100 Millionen Arten auf der Erde; unsere derzeitige Beschreibungsrate hingegen beträgt nur etwa 20.000 neue Arten und Unterarten pro Jahr. Es bleibt also noch viel zu tun im taxonomischen Bereich. Systematik hilft uns dabei, die Inventarisierung der Biodiversität voranzutreiben und gleichzeitig zahlreiche andere Aspekte der Biologie zu beleuchten.

In dieser Arbeit konzentriere ich mich auf die Systematik der Reptilien und Amphibien von Madagaskar, einem Inselmodell für die evolutionäre Dynamik auf kontinentaler Ebene. Ich überarbeite die Taxonomie verschiedener Gruppen und lege dabei Facetten ihrer Entwicklung, ihrer Ökologie und ihrer Erhaltung dar. Ich zeige auch, dass eng begrenzte taxonomische Arbeiten als Datenquellen für breiter angelegte Forschungsfragen genutzt werden können, beispielsweise im Bereich der Makroevolution.

Ergebnisse

Die hier vorgestellten Studien sind in vier Abschnitte unterteilt, die insgesamt elf Kapitel umfassen:

In Abschnitt 1 stelle ich eine Arbeit (Kapitel 1) vor, in der zwei neue Froscharten der Gattung *Mantidactylus* beschrieben werden und deren Erhaltung besprochen wird. Es wird gezeigt, dass die Verbindung zwischen Taxonomie und Naturschutz äußerst wichtig ist, und dass die Naturschutzpolitik derzeit das taxonomische Wissen nicht vollständig ausschöpft.

In Abschnitt 2 stelle ich vier Artikel (Kapitel 2–5) vor, in denen fünf neue Froscharten der Gattung *Gephyromantis* beschrieben werden und insbesondere ihre biogeographischen Beziehungen diskutiert wird. Es wird deutlich, dass die Untersuchung der Muster in den verschiedenen betroffenen Untergattungen auf allgemeine Muster hinweist und Einblicke in die biogeographische Geschichte des Nordens von Madagaskar ermöglicht. In der Diskussion zeigen Vergleichsbeispiele aus anderen Tiergruppen, die in demselben Gebiet verteilt sind, dass diese Muster bei Amphibien und Reptilien deutlicher sind als bei Säugetieren.

In Abschnitt 3 stelle ich fünf Kapitel vor (Kapitel 6–10), von denen drei taxonomisch und zwei phylogenetisch sind und zusammen neun neue Arten und zwei neue Gattungen von Engmaulfröschen der Unterfamilie Cophylinae ergeben. Es wird erläutert, wie die Taxonomie neue technologische Vorteile nutzen kann, um taxonomisch herausfordernde Fälle zu lösen, und Einblicke in der Evolutionsgeschichte dieser Frösche zu gewinnen.

In Abschnitt 4 stelle ich eine Arbeit vor (Kapitel 11), in der einen aus taxonomischer Literatur erstellten Datensatz in einem vergleichenden phylogenetischen Rahmen verwendet wird, um die Entwicklung der sexuellen Ornamentierung zwischen Chamäleonarten zu analysieren und zu zeigen, dass die genitalen und äußeren morphologischen Ornamente wegen verschiedener Auswirkungen der sexuellen Selektion entkoppelt evolvieren.

Schlussfolgerungen

In dieser Arbeit werden 16 neue Arten und zwei neue Froschgattungen aus Madagaskar beschrieben, zusammen mit neuen Daten zu ihrer Phylogenie und Evolution. Es wird auch gezeigt, dass die bereits existierende taxonomische Literatur über Chamäleons zu einer Datenquelle für Studien werden kann, die Fragen zu ihrer Evolution genauer behandeln. Der taxonomische Fortschritt der Beschreibung der Herpetofauna auf Madagaskar schreitet zügig voran. Wenn wir uns dem Ab-

Zusammenfassung

schluss des Biodiversitätsinventars der Insel nähern, bekommen wir auch wertvolle Einblicke in die Beziehungen zwischen seiner Fauna, ihrer Ökologie, ihrer Evolution und ihrer Herkunft und erfahren auch, welche Arten geschützt werden müssen und, möglicherweise, wie dies am besten zu tun ist. Die Entschlüsselung dieses Puzzles wird weitreichende Auswirkungen haben, nicht nur in Bezug auf Madagaskar selber, sondern auch für die Art- und Gemeinschaftsbildung auf Kontinenten.

Taxon Box

This thesis focuses broadly on two groups of frogs from Madagascar, and specifically on one group of lizards. For ease of understanding, the following summarises briefly the groups that are discussed.

Amphibians:

Microhylidae — A family of pantropical neobatrachian ranoid frogs, containing 11 recognised subfamilies (AmphibiaWeb 2019). Three are endemic and exclusive to Madagascar:

Cophylinae — Highly diverse subfamily, containing 103 described species. Sister to **Scaphiophryininae**.

Scaphiophryininae — Moderately diverse subfamily, containing 13 described species. Sister to **Cophylinae**.

Dyscophinae — A subfamily containing just 3 species. This subfamily is currently thought be sister to the Asian **Microhylinae** (Tu et al. 2018).

Mantellidae — A family of afrobatrachian neobatrachian ranoid frogs endemic to Madagascar and the Comoro archipelago. Sister to the family **Rhacophoridae** from Australasia.

Reptiles:

Chamaeleonidae — The chameleon family, divided into two subfamilies:

Chamaeleoninae — Small to large, mostly arboreal chameleons. Ten genera from Madagascar, Africa, Europe, and Asia.

Brookesiinae — Small, generally terrestrial chameleons. Two genera endemic to Madagascar.

Introduction

'The beginning of wisdom is to call things by their proper name.'

— Chinese Proverb

'It is through careful, thorough, competent descriptive taxonomy that the most fascinating details of evolutionary history are revealed'

— Quentin D. Wheeler, 2013, *New Phytologist* 201:370–371

In Douglas Adams' 'The Restaurant at the End of the Universe', the second book in the Hitchhiker's Guide series, there is a machine known as the Total Perspective Vortex (Adams 1980). The intent of this torture device is to show the user the 'infinity of creation', driving them mad by virtue of the enormity of the universe and their insignificance therein. Such a device, used merely for the scope of Life on Earth, would be quite effective enough: it would reveal the millions upon millions of species; an overwhelming chaos of multitudes, and humans just a blip in their midst. Place a systematic biologist into such a machine, however, and that effect would be short-lived. For systematics is the science of naming, categorising, sorting, and classifying life on earth. It is the joining of the two disciplines of taxonomy, the science of naming life, and phylogenetics, the science of deducing the evolutionary relationships between branches of life. Inside the Total Perspective Vortex of Life on Earth, a systematist would classify the multitudes, rank and collate them, seek to understand their evolutionary connections, and thereby unravel the apparent chaos that is life.

Outside the Vortex, this work is well underway, but the scope of the problem is immense. Just how immense is unclear; estimates of living eukaryotic diversity range from 2 to 100 million species (reviewed by Chapman 2009 and Scheffers et al. 2012), without beginning to consider the domains of Archaea and Bacteria. Part of the reason for the uncertainty in this estimate is that only ca. 1.8 million Eukaryote species have been described (<http://www.catalogueoflife.org/>). This 'taxonomic gap' or 'Linnean shortfall' (Hortal et al. 2015), presents a major scientific challenge that has not yet been overcome; at present rates of description (around 20,000 species and subspecies per year; <http://www.organismnames.com/>), an end to the Linnean shortfall cannot be imagined within the next century (Scheffers et al. 2012). This is a critical deficiency, because taxa—that is to say, the names that anchor our understanding of life on earth—have a central role in all organismal biology. Despite disputes about definitions of species and the problems of species delimitation over time and space (discussed below), they remain fundamental biological units by which ecosystems at a single point in time and space are structured, and thus have broad biological relevance, and are not simply academic, artificial units for 'stamp collectors'. They are the foundation of comparative biology and much of our understanding of evolution and ecology. Species are also central to our approach to conservation; while unnamed, a species cannot effectively be protected or managed (Dubois 2003; de Carvalho et al. 2007; Vogel Ely et al. 2017)—a function of particular importance in the current global biodiversity crisis (Dubois 2003; de Carvalho et al. 2007; Barlow et al. 2018).

There is thus a great need for taxonomic research in its own right, but taxonomic work can also be much more than simply descriptive text, and these contributions are arguably of nearly equal importance. In this thesis, I describe numerous new species and two new genera of frogs from Madagascar, shedding light on their evolution and biogeography, and providing a foundation for their conservation. In a final chapter, I also demonstrate the way that data from taxonomic descriptions can be harvested in order to perform macroevolutionary analysis. I argue that these contribu-

tions are made more important by their taxonomic foundation, and that taxonomy and evolutionary biology are tied together, to their mutual benefit.

Categorising a continuum: Species concepts and the philosophy of taxonomy

Having a robust definition of what constitutes a species is of great importance and a central philosophical concern of taxonomists. The biological species concept (BSC, Mayr 1942), which posits that ‘species are groups of interbreeding natural populations that are reproductively isolated from other such groups’, was long held as a gold standard for species definition. Yet it has numerous pitfalls, not least of which are the uncertainty of its application to asexually reproducing organisms, the time-consuming nature of proving its applicability in any given system, and the increasing evidence that species need not be wholly reproductively isolated in order to be evolutionarily distinct (de Queiroz 2005a). Reticulate speciation and hybrid species are also increasingly well known, even among vertebrates (Schliewen and Klee 2004; Burbrink and Gehara 2018). The clean-cut biological species concept is simply not universally applicable.

Dozens of other species concepts have been put forward since the 1940s (reviewed by Mayden 1997; de Queiroz 2005b, 2007; and Hausdorf 2011), but none are universally applicable or accepted, and opinions can vary greatly as to which is the most appropriate to apply to any given group. Part of the trouble is that a species that satisfies one concept might not satisfy another. As a result, one scientist might consider a group of individuals to comprise just one species, while another, preferring an alternative species concept, might regard the same group as multiple species, without either being technically incorrect. For taxonomy to have a stable footing, consensus is desirable, yet while so much subjectivity remains, the problem of stably defining a species becomes intractable.

Consideration of the process of speciation itself is important if we are to arrive at a stable and broadly applicable species concept (Hausdorf 2011). At what point does a diverging group of individuals become two species? Moreover, what is the role of time? Does an ancestral species immediately go extinct when it becomes divided into two descendant species? Speciation is, in most cases, a gradual and continuous process (de Queiroz 1998; Coyne and Orr 2004; Roux et al. 2016). Any number of factors may simultaneously be at play in driving the process, and in some cases, it may never fully complete, or may indeed reverse and revert back to a single panmictic species (reviewed by Seehausen et al. 2008). It is also frequently not a simple binary case, but can include anagenesis (speciation without bifurcation), multifurcation, and fusion (de Queiroz 2005b; Kuchta and Wake 2016). The result is that there is a grey zone between where a lineage is one and where it becomes two species, and species limits can only be applied at a given point in time (Mayden 1997; de Queiroz 1998, 2005b, 2007; Roux et al. 2016).

How are taxonomists to reconcile this continuity and variability in the speciation process? One option would be to consider it futile and give up on the pursuit of naming species. After all, our categorical naming system is hardly appropriate for a reality that is continuous over space, genomes, and time. However, to appropriate a quote from statistician George E. P. Box, ‘all models are wrong, but some are useful’ (Box 1976). As I have already suggested above, and as will be reinforced throughout this thesis, I contend that the utility of taxonomic names is sufficiently great that, even if they are gross simplifications, and thus technically ‘wrong’, they are nonetheless highly useful.

To maximise the utility of taxonomic names in light of our growing understanding of the speciation process, we must adapt our concepts. Mayden (1997) and de Queiroz (1998) took the first steps toward reconciliation of the conceptual paradigm shift in adapting species concepts. Both argued that, while separate concepts use different definitions, they do not differ in resting upon the conceptualization of a species as some kind of cohesive unit evolutionarily separated

from other such units. Mayden (1997) noted that most concepts conflated the question of species definition with species diagnosis, the notable exception being the Evolutionary Species Concept (ESC) coined by Simpson (1961), which states that a species is ‘a lineage (an ancestral-descendant sequence of populations) evolving separately from others and with its own unitary evolutionary role and tendencies’. The other concepts, Mayden held, fail to incorporate the individual-based nature of species, are insufficiently general, are overtly operational in nature, and are not broadly applicable. The ESC, he argued, is universally applicable, and should therefore form the primary species concept. However, he also noted that the ESC requires operational bridges in order to be implemented, so-called ‘secondary concepts’ coined by Mayr (1957). These take the form of the other species concepts, which he suggested could be organised into numerous different hierarchies based on a variety of criteria.

Apparently without having read Mayden’s work, de Queiroz (1998) came to the same realisation. He proposed an alternative solution to it, however. He saw all the various concepts as revolving around a unifying idea of what a species should constitute. This central concept he dubbed the General Lineage Concept (GLC), which holds that ‘species are segments of population level evolutionary lineages’. de Queiroz argued that the universal agreement among existing concepts meant that these were all conditional derivatives of the universal GLC. Some earlier concepts, such as the ESC, had been attempts to define this same concept, while others, such as the BSC, had conflated what a species is with how it can be recognised. The aspects of these concepts pertaining to ways in which species could be delimitated or identified would then constitute ‘species criteria’; conditions that, if satisfied, would be sufficient to qualify a lineage as a species. Fundamentally, this is not very different from Mayden’s (and Mayr’s) notion of primary and secondary species concepts, but conceptually it is somewhat more advanced for two reasons. Firstly, de Queiroz (1998) emphasised that the usually gradual process of speciation results in criteria being satisfied in a time-dependent manner; as speciation proceeds, so too does the number of criteria satisfied that make the two lineages distinct species, so the overall picture of separation becomes more clear. Secondly, he recognised that the order in which criteria are recruited is arbitrary, as is which criteria are involved and which are never satisfied.

The GLC was the foundation that de Queiroz later built on in his establishment of the Unified Species Concept (USC, de Queiroz 2005b, 2007). The difference between these two concepts is subtle, but important. Both rely upon the central concept that a species is a ‘separately evolving metapopulation lineage’, but the GLC can be seen as a generalization of, and not an alternative to, most previous species concepts, and relies upon secondary properties for them to be defined as a species (de Queiroz 2005b). The USC, by contrast, takes the central concept of separately evolving metapopulation lineages as the only required condition for a species. It is thus not a generalisation of other concepts, but an alternative to them (de Queiroz 2005b). The species hypothesis is thus founded on this central premise, and various species criteria are recruited to lend support to it. The more species criteria are satisfied, the stronger the evidence for evolutionary separation. Which criteria are satisfied is then informative about the nature of separation, be it reproductive isolation, ecological distinctness, or otherwise.

Like all species concepts, the USC is not without flaws. It was particularly criticised by Hausdorf (2011) as being vaguely defined, and of shifting the problem of ‘what is a species?’ to ‘what is a lineage or a segment of a lineage?’. An important concern with the USC is that it can be used to justify evolutionary independence down to the individual (or pair) level; Kuchta and Wake (2016) gave the example of a gravid lizard rafting onto an island and becoming isolated, and thereby instantaneously setting out on a new evolutionary trajectory. Although the degree of ephemerality of lineages can be taken into account to minimise the inflation of species recognised under the USC, this is nonetheless a challenge that does not appear to have an objective solution. Additionally, ring species under the USC also present a challenge, because the gene flow between neighbouring

Introduction

populations can be high, but the ends of the ring can still be reproductively isolated, rendering the independence of lineages tenuous (Kuchta and Wake 2016).

On the other hand, there are numerous advantages of the USC. To enumerate just a handful: (1) It already agrees with most if not all previously used species concepts. (2) It reconciles the differences in evolutionary trajectory that sometimes occur by chance, resulting in non-comparability among species defined using former restrictive concepts. (3) Because its stipulations are few, it can be applied across the tree of life, making it nearly universally applicable, and much less restrictive than previous definitions. (4) It is highly feasible for rapid application based on whichever data types are available, giving it a distinct advantage over an approach where a single concept is chosen for a whole group, and all members of that group must be tested on the same criterion, which may not be universally relevant. (5) Finally, because it has, as its central tenet, a concept that is common to almost all existing species concepts, it shifts the focus from conceptual debate on the topic of ‘what is a species?’ to the methodological and empirical debate over how reliable any given method is for identifying the independence of lineages (Kuchta and Wake 2016). Together, these aspects make the USC a very appealing concept for taxonomists, and it has been widely adopted. It is therefore the species concept I have adopted implicitly and explicitly throughout this thesis.

Taxonomy in the 21st century

Despite the central role of taxonomy in anchoring much of the rest of biology, there has been much recent discussion of the ‘crisis’ facing the field of taxonomy (Dubois 2003; Agnarsson and Kuntner 2007; Kotov and Gololobova 2016; but see also Joppa et al. 2011), and the so-called ‘taxonomic impediment’, i.e. the inability of the taxonomist to meet the demand for taxonomic information. In recent years, the fields of evolutionary biology and cladistics have flourished. Some have alleged meanwhile that taxonomy has stagnated (e.g. Paknia et al. 2015), but this is highly debatable (see Joppa et al. 2011); in reality, more taxonomists are working today than ever (Costello et al. 2013). It is true, however, that the inability of impact factors, the metrics by which science ‘importance’ is often assessed, to capture the importance and quality of taxonomic research causes an underestimation of the significance and widespread value of taxonomy, as has been highlighted by numerous authors (e.g. Dubois 2003; Agnarsson and Kuntner 2007; Kotov and Gololobova 2016; Vogel Ely et al. 2017). Nonetheless, taxonomists are managing to remain innovative, and are constantly increasing the quality and quantity of descriptive works.

Over the last 30 years, genetic methods have emerged as a means to rapidly recognise units of biological diversity. DNA barcoding in particular has been widely adopted and is orders of magnitude faster than any hitherto available methods (Hebert et al. 2003; Blaxter et al. 2005; Smith et al. 2005; Vences et al. 2005a; Vences et al. 2005b; Fouquet et al. 2007; Ratnasingham and Hebert 2007). This method allows us to flag genetic lineages (generally mitochondrial in animals and plastid in plants) with particularly strong divergence as potentially meaningful biological units, with utility both in rapid estimation of total diversity and in identification of potentially undescribed species-level lineages (e.g. Smith et al. 2005; Fouquet et al. 2007; Vieites et al. 2009; Nagy et al. 2012).

Taking this a step further, multispecies coalescent (MSC) models have been developed, which seek to reconcile evolutionary lineages over different gene histories and delimit species level-units from the coalescence of these histories (Yang and Rannala 2010). These methods have great potential to help us understand genetic diversity and population structure and delimit meaningful units from complicated or only subtly differing clusters. However, they have also been criticised recently because they are prone to delineation of geographically, but not biologically meaningful units (e.g. Skukumaran and Knowles 2017; literature on this topic was nicely summarised by Hillis

2019); uncritical taxonomic action based on MSC outputs can result in over-splitting, or division of continuums into arbitrary and meaningless slices (Skukumaran and Knowles 2017; Hillis 2019).

The emergence of affordable genetic methods has coincided with and strongly stimulated the popularisation of an ‘integrative’ approach to taxonomy (Dayrat 2005; Will et al. 2005; Padial and de la Riva 2010; Padial et al. 2010; reviewed by Schlick-Steiner et al. 2010). Integrative taxonomy takes advantage of a breadth of methods for generating different datasets and uses multiple lines of evidence to distinguish species-level lineages; the more lines of evidence that support a distinction between any two species, the more confident one can be that they constitute evolutionarily independent units warranting species-level recognition. As such, integrative taxonomy is ideally suited to work together with the USC discussed above.

An integrative approach can also be used in explicit species delimitation algorithms in the MSC framework; by considering additional lines of evidence, MSC may better reflect biologically meaningful units. Recently, Solís-Lemus et al. (2015) proposed to integrate quantitative trait data into a Bayesian MSC framework to test for discordance and concordance between morphometric and genetic signals to overcome the problem of over-splitting. Their software, iBPP (integrated Bayesian phylogenetics and phylogeography, Solís-Lemus et al. 2015), has been implemented successfully in a number of studies (e.g. Pavón-Vázquez et al. 2018; Ramos et al. 2019), but has not yet been widely adopted, for reasons that are unclear. This avenue is a potentially valuable one, however, as it has the potential to assist greatly in the rapid recognition and simultaneous diagnosis of species-level units. Integration of more lines of evidence, particularly categorical trait data, may further enhance this approach.

Whether at the simple DNA barcode level or the more complex MSC methods, it is clear that genetic methods have a major role to play in the recognition and characterisation of undescribed diversity (e.g. Smith et al. 2005; Fouquet et al. 2007; Vieites et al. 2009; Nagy et al. 2012). Some proposals have taken this still further, suggesting that characteristic mutations could potentially be integrated in species diagnoses to expand the diagnostic features used in unravelling particularly stubborn species complexes, permitting an increased rate of taxonomic resolution in difficult-to-resolve taxa, while also making diagnoses ‘sharper’ (Tautz et al. 2003; Renner 2016).

Affordable, mass-sequencing methods have also led to the emergence of ‘rapid’, ‘turbo’, or ‘fast-track’ taxonomy, which involves rapid mass-descriptions of taxa (e.g. Riedel et al. 2014). Riedel et al. (2013) proposed taxonomic descriptions be stripped back to the bare minimum in order to decrease the effort required to produce them en masse, focussing, for example, on only describing diagnostic characters, and removing comparative diagnoses altogether. While this proposal may better reflect the quintessential minimums of species description (Renner 2016), I contend that it is extreme, because it reduces the amount of useful information in the papers so dramatically, especially when considering the usefulness of taxonomic literature outside the field of taxonomy itself. Intermediate approaches, using an integrative approach applied in a streamlined manner to describe swathes of new species, while also including adequate descriptive information to be useful for future taxonomic work and other yet unforeseen uses outside the realm of taxonomy, provide a method for achieving considerably elevated rates of description over historical rates, without compromising quality and usability (Rakotoarison et al. 2017).

In the integrative era of taxonomy, the emergence of new technologies for extracting hitherto inaccessible information from specimens is continuing to provide substrate for taxonomic progress that was previously impeded by ambiguity. Foremost among these emerging technologies are those that increase the volume, rate, and/or quality of DNA sequence data, and particularly exciting are the emerging technologies that promise to provide sequence data from museum material hitherto thought too damaged or too old for DNA extraction, which promise to dramatically speed up the unambiguous assignment of taxonomic names to extant populations by genetic verification of the type material (Burrell et al. 2015; McCormack et al. 2016; Ruane and Austin 2017; Allentoft

et al. 2018).

Methods for digitising morphology are also progressing rapidly. Photogrammetry (a method to capture the 3D shape of objects using cameras) using compact systems has been popularised especially in entomology, providing access to high-resolution 3D morphological data that can be digitally examined by anyone with a computer and an internet connection. This has the double benefit of democratising the material (available to anyone worldwide, not only local scientists or people able to travel) while at the same time preventing further damage to material caused by reducing the amount that it must be handled (Wheeler et al. 2012; Nguyen et al. 2014; Adams et al. 2015). Internal anatomy has also become accessible without necessitating dissection, meaning that it can now be examined from valuable type material. The most popular method for digital acquisition of internal anatomy imagery is currently micro-computed tomography (micro-CT) (reviewed by Faulwetter et al. 2013 and Broeckhoven and du Plessis 2018). Micro-CT scans of vertebrates provide access to their skeletons, which are often a rich source of taxonomically valuable information (e.g. **chapters 6–9** of this thesis). By making use of staining methods, micro-CT contrast can be enhanced in soft tissues, providing additional access to organ systems for taxonomic purposes (Gignac et al. 2016; Broeckhoven and du Plessis 2018).

By taking advantage of these myriad emerging technologies, taxonomy is remaining a modern science. With the strengthening and deepening of this solid foundation, discoveries and innovations in other systematic disciplines including evolutionary biology, are facilitated.

Evolution on islands

Since Darwin's sojourn in the Galapagos, where he remarked particularly on the patterns of beak shape differences in finches of the genus *Geospiza* among the islands (Darwin 1845), islands have been of central interest for evolutionary biology and biogeography. The vast size and extremely long history of biological assemblages on continents complicate analyses of the evolutionary histories of their inhabitants (Warren et al. 2015). Islands, on the other hand, act as evolutionary laboratories. They are often populated by largely endemic flora and fauna, making them ideal locations for research on processes involved in the generation and radiation of biological diversity (MacArthur and Wilson 1963; reviewed by Whittaker and Fernández-Palacios 2007; Losos and Ricklefs 2009; and Warren et al. 2015). Island species radiations, such as Darwin's finches (*Geospiza*) in the Galapagos (reviewed by Grant and Grant 2003) and anoles (family Dactyloidae) in the Greater Antilles (reviewed by Losos 2011), provide elegant demonstrations of evolutionary principles, while island communities give insight into fundamental ecological principles. Studies with either goal favour in particular the use of archipelagos, which provide replicate islands for comparison (Warren et al. 2015; Ali and Meiri in press; reviewed by Shaw and Gillespie 2016).

However, scalability of island patterns and phenomena to continental landmasses is questionable. Species assemblages on islands are often skewed in comparison to continents as a result of colonisation history; Darwin himself remarked 'Oceanic islands are sometimes deficient in certain classes, and their places are apparently occupied by the other inhabitants' (Darwin 1859). Biodiversity on islands correlates with island size and distance from a mainland (MacArthur and Wilson 1963; Ali and Meiri in press), but the influence of age of the island is also not to be forgotten; older islands should have greater degrees of endemism (Heaney 2007; Gillespie and Baldwin 2010), but volcanic islands are typically short-lived. Continental biotic communities are strongly affected by palaeoclimatic variation (Hewitt 2000). Some continental species have very large range sizes, which can be fragmented through climatic shifts to produce allopatric species in ways to which small islands cannot compare (e.g. Maestri et al. 2017). Island radiations may be more limited in available niche space than continental radiations (Derryberry et al. 2011). Finally, a recent study on anoles suggested that gaps in community composition (specifically the lack of predators) may

allow island radiations to diversify in ecomorph in ways not possible on continents (Poe and Anderson 2019).

An ideal compromise would consist of a study system that is (1) an island or island-like landmass of (2) large size that is (3) isolated by hundreds of kilometres from other major landmasses, with (4) heterogeneous climate zones and (5) hyper-diverse in flora and fauna, but (6) populated largely with endemic radiations. Only few such landmasses exist: Papua (New Guinea), Kalimantan (Borneo), and Madagascar. Of these, Madagascar is the smallest, but is also the oldest, most isolated, and the most climatically heterogeneous, and, most importantly, has the highest level of endemism, especially at higher taxonomic levels (Goodman and Benstead 2005). As a result, it has been hailed as an ideal location to study speciation and diversification (Vences et al. 2009).

Madagascar: a systematist's paradise, and an ideal island study system for continental evolution

Madagascar is the oldest and fourth largest island on Earth. Spanning ca. 1600 km at its longest point (NNE–SSW), and ca. 580 km at its widest point, it has an area of 586,884 km², making it slightly larger than mainland France. It sits isolated ca. 500 km off the east coast of Africa. Geologically, it is a continental landmass, with potential ties to the Somali micro-plate (Kusky et al. 2010). Indeed, there is some debate as to whether or not it should be regarded as an island at all (de Wit 2003). It was formerly located within the supercontinent Gondwana, wedged between the Indian and East African plates. Indiagascar, the landmass composed of India and Madagascar, separated from what is now Africa some 165 Ma before present (b.p.) (de Wit 2003; Wells 2003; Yoder and Nowak 2006), before India and Madagascar separated 84–93 Ma b.p. (reviewed by Chatterjee et al. 2013). It may have maintained land bridge connections with India and Antarctica, and through Antarctica, South America and possibly Australasia (Briggs 2003; Chatterjee et al. 2013), becoming fully isolated and stabilising in its current position relative to Africa around 84 Ma (de Wit 2003; Yoder and Nowak 2006), while India rapidly moved northwards to collide with the Central Asian Plate and form the Himalayas (Chatterjee et al. 2013; Jagoutz et al. 2015).

Much as it would any tectonic landmass that is never submerged, palaeoclimate played an important role in the formation of Madagascar's modern ecosystems, but the location of Madagascar made these patterns particularly pronounced in comparison to analogously large and ancient landmasses like Greenland (de Wit 2003). The literature on this topic was reviewed by Wells (2003), from whom I summarise briefly here: following its isolation, Madagascar moved northwards through an aridifying high-pressure belt from the Cretaceous to the Eocene, leading to eradication of most if not all xeric-adapted flora and fauna. This dry zone was pushed to the south of the island as it drifted north, and so too was its adapted biota. The island became moister from the north as it moved northwards into the trade winds, starting in the Eocene, and warmth was added through ocean currents from the Late Eocene or Oligocene (see Ali and Huber 2010), leading to the formation of northern and eastern humid forests. Moisture in northwestern Madagascar has increased in the last few millennia, as Madagascar has moved into the path of monsoon winds.

Today, Madagascar is divided into five relatively distinct bioclimatic zones: a subarid zone in the southwest, a dry zone along the west coast and most of the north, a subhumid zone across the central highlands, and a humid zone along the east coast, with montane zones scattered across its mountain peaks (Schatz 2000; forest cover is shown in Fig. 1). The zonation results largely from the relief of the island. From the east coast, a lowland area rises rapidly into a mountain chain running nearly the length of the island, west of which is a highland plateau that slowly declines toward the west coast. The result of this geography combined with prevailing winds from the east and north is that rain is dispensed predominantly on the eastern escarpment and decreases westward, forming an east–west gradient in precipitation (Jury 2003). The distance between the north-

Introduction

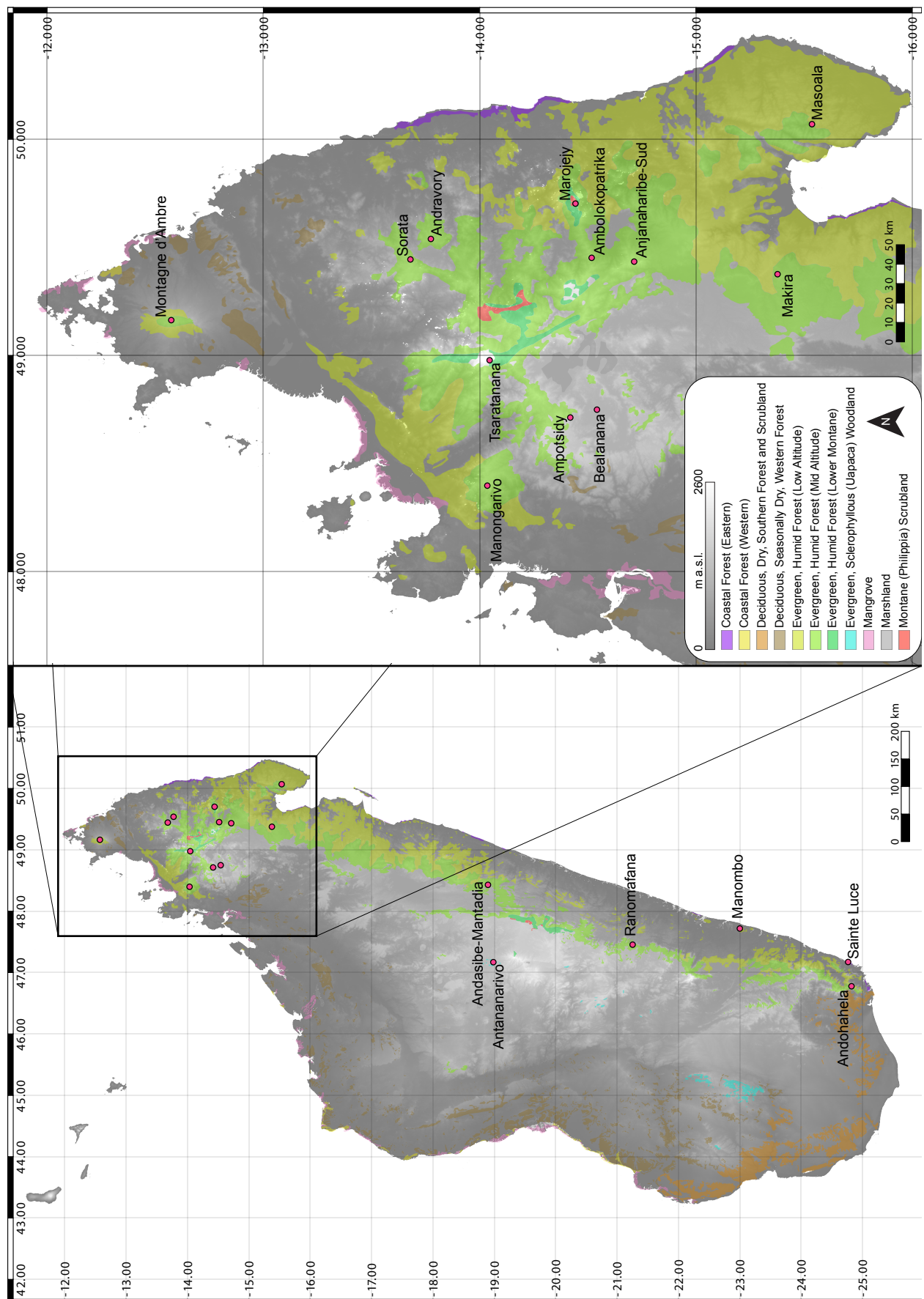


Figure 1. Map of Madagascar highlighting important location names mentioned in this thesis.

Basemap is the SRTM 1 Arc-Minute dataset, overlain with vegetation distribution data from Du Puy and Moat (2003).

ern- and southern-most points is such that a further gradient of moisture is formed in a north-south direction, so that the driest area of the island is the southwest, and the wettest in the northeast. The simplicity of these gradients makes the island particularly well-suited for studies of evolution and biogeography (Vences et al. 2009; Brown et al. 2014, 2016).

Considering its ancient isolation, we might expect that Madagascar would today harbour a unique fauna, largely of Gondwanan origin. This, however, is not the case. Madagascar has a rich vertebrate fossil history before the Tertiary, including a wide array of dinosaurs, reptiles, and frogs (reviewed by Flynn and Wyss 2003 and Krause 2003, but for more recent discoveries see also Krause et al. 2003; Evans et al. 2008; Laduke et al. 2010). This fossil data suggests that the island indeed retained a diverse Gondwanan fauna even after its isolation. Post-KPg extinction, pre-Pleistocene fossils are practically absent from Madagascar (Flynn and Wyss 2003; Samonds et al. 2012, 2013), and as a result, we must look to the extant fauna for information about the biogeographic history of the island after the KPg extinction event. Yoder and Nowak (2006), Poux et al. (2005), Ali and Huber (2010), and especially Crottini et al. (2012a) showed that almost no vertebrate species on Madagascar are remnants from its Gondwanan past, but instead the majority of species represent post-KPg colonisations. Recent work (Yuan et al. 2018) suggests that major biotic interchanges between Madagascar, Africa, and Asia through India were made possible for an intermediate period via land bridges, or at least island chains (Briggs 2003; Warren et al. 2010; Chatterjee et al. 2013), which appears to have been pivotal to Madagascar's recolonization in the Cenozoic after its biotic 'slate' was wiped clean by the KPg extinction event, combined with its aridification during its traversal of the high-pressure belt around the same period.

Despite lacking the predicted Gondwanan fauna, Madagascar today has unparalleled levels of endemism of flora and fauna (reviewed by Goodman and Benstead 2005); for example, 84% of its 11,641 known naturalised vascular plants (Lowry II et al. 2019; Madagascar Catalogue 2019) are endemic. Endemism and species richness are especially high among its vertebrates; it is home to seven endemic families of terrestrial mammals (Goodman et al. 2019), and 99.5% of the 355 frog species (AmphibiaWeb 2019) and 98% of the 426 terrestrial reptile species are endemic (Uetz and Hošek 2016). The concentration of extremely great diversity makes it one of the world's hottest biodiversity hotspots (Myers et al. 2000; Ganzhorn et al. 2009), a priority for conservation (Raxworthy 1988; Andreone 2008; Horning 2008; Kremen et al. 2008; Ganzhorn et al. 2009; Martin et al. 2009; Jenkins et al. 2014), and an ideal location for research on diversification mechanisms (Vences et al. 2009). As a result of the climatic and topological heterogeneity of the island, diversity and endemism levels vary strongly by group across the island (Wilmé et al. 2006), and many groups have high rates of species turnover over small geographic scales (Wilmé et al. 2006; Brown et al. 2014, 2016).

Altogether, the age, size, isolation, cardinal simplicity of climatic heterogeneity, and extreme diversity and microendemism of largely Cenozoic-colonizing plants and animals make Madagascar an ideal island parallel for continental-scale evolution and biogeography (de Wit 2003; Raxworthy et al. 2008; Vences et al. 2009).

Herpetofaunal diversity of Madagascar

Ideal study organisms for the study of continent-like biogeography and evolution should be diverse endemic radiations of ecologically sensitive species of low vagility. The combination of ecological sensitivity and low vagility is key, because it tends to generate a great deal of microendemism. As a result of their poikilothermic ectothermic physiology (behaviourally regulated, extrinsically determined body temperature), amphibians and reptiles are strongly dependent on abiotic environmental parameters. Amphibians are still more strongly susceptible to biotic and abiotic factors as a result of their permeable eggs and skin. Consequently, reptiles and amphibians, together 'herpe-

Introduction

to fauna', are often used as indicators of environmental quality (e.g. Scott et al. 2006; Gardner et al. 2007; Ramanamanjato 2008; Sung et al. 2012). But this dependency of herpetofauna on their environments, as well as their generally low vagility (Pabijan et al. 2012), also makes them ideally suited for biogeographic study (Brown et al. 2014, 2016). This has been exploited across the world (e.g. Blackburn 2008; Wiens et al. 2011; Hawlitschek et al. 2016; Poe et al. 2017; Zimkus et al. 2017; Meiri 2018; Esquerré et al. 2019).

Madagascar's reptiles and amphibians are spectacularly diverse. Currently, 355 amphibian species and 426 non-marine non-avian reptiles are described from the island (Uetz and Hošek 2016; AmphibiaWeb 2019). Of the amphibians, represented only by frogs, just one of the native species, *Ptychadena mascareniensis*, is not exclusive to the island (but even it is composed of endemic, possibly species-level lineages; Zimkus et al. 2017). Of reptiles, 98% are endemic, and a few species are shared with the Comoro archipelago (Glaw and Vences 2007; Hawlitschek et al. 2018). What is more, only a few of the island's amphibians or reptiles are widespread; the herpetofauna is typified by extremely high levels of microendemism (Wollenberg et al. 2011; Pabijan et al. 2012; Brown et al. 2014), especially in the north (Raxworthy and Nussbaum 1996; Andreone 2004; Wollenberg et al. 2008; Andreone et al. 2009).

The majority of named species of non-avian reptiles and amphibians in Madagascar have been DNA barcoded (Vieites et al. 2009; Nagy et al. 2012; Perl et al. 2014), preparing them for systematic and evolutionary work. These DNA barcoding efforts revealed a major Linnean shortfall in Madagascan herpetofauna, especially in the frogs; Vieites et al. (2009) showed that only half of the diversity of frogs in Madagascar had been described—at the time, fewer than 250 species had been described, but estimates for the full diversity revealed by deep genetic lineages was placed at 373–465 species, which was later increased to 533 (Perl et al. 2014). Since that time, still more species have been discovered which were not included in these estimates (e.g. Andreone et al. 2010; Scherz et al. 2015a; Rakotoarison et al. 2017; Bletz et al. 2018; Glaw et al. 2018; **chapters 3–6 and 8–10** of this thesis). As a result, although the rate of species description for amphibians has skyrocketed in the last fifteen years, it is somewhat tempered by continued fieldwork resulting in further discoveries.

Among reptiles, a smaller shortfall was discovered by Nagy et al. (2012), with 50 candidate species revealed, but their barcoding survey was less complete, containing only 64% of known diversity, and still more undescribed species are likely to be revealed with expanded barcode surveys. Among non-avian reptiles too, continued species discovery and the resolution of species complexes, especially in the chameleons (e.g. the *Calumma nasutum* species group, which has risen from seven to nineteen species since 2012; Gehring et al. 2012; Prötz et al. 2015, 2017, 2018b, 2018c, submitted), has continued to push up the diversity estimates of the island. As a result, although around 40 species have been described since 2012, considerable undescribed reptilian diversity remains. Despite the Linnean shortfall in Madagascan herpetofauna, the fact that so much of the diversity of reptiles and amphibians has been genetically characterised lends further weight to its value as a study system for evolutionary biology and biogeography.

Green and Sussman (1990) predicted that forest on Madagascar would be wiped out except on the steepest slopes by the year 2025. While this no longer looks likely, the country still has an exceedingly high rate of deforestation (Consiglio et al. 2006; Harper et al. 2007; Clayton 2011). At present, roughly 46% of Madagascar's frogs are considered threatened (status of Vulnerable, Endangered, or Critically Endangered; IUCN 2019) and 5% Data Deficient (the rest are in unthreatened categories, Least Concern, or Near Threatened). Roughly 35% of the island's reptiles are threatened and 11% are Data Deficient (IUCN 2019). The dominant threat to these species is habitat loss. That habitat loss is probably also causing us to lose much of the diversity that is not yet known to science, as indicated by recent discoveries of new species in small and isolated forest fragments (e.g. Gehring et al. 2010; Prötz et al. 2018c). Work on these animals is therefore cur-

rently proceeding with a sense of urgency.

At present, the Linnean shortfall in Madagascar's reptiles and amphibians is rapidly closing, but barcoding studies have shown that there is a long way to go, made still more challenging by the high rate of additional species discovery. There also remains a great deal to be understood about the systematics of Madagascar's herpetofauna, their origins and evolution. Studying the taxonomy and systematics of these animals is critical if they are to be protected. As I show in this thesis, by studying these aspects, we can gain a greater understanding of the biogeography of their environment and the principles governing their evolution. From these insights, we can gain a greater understanding of the processes behind them.

Thesis outline

The results of my thesis research are organised into four sections, each representing a different application for which systematic research can not only enhance our knowledge of biological diversity, but also shed light on broader questions in evolutionary biology. The **first section**, comprising **chapter 1**, highlights the importance of taxonomic accuracy in conservation assessments, especially pertaining to species complexes. The **second section**, comprising **chapters 2–5**, focusses on insights into biogeography afforded via taxonomic treatment. The **third section**, comprising **chapters 6–10**, focusses on the understanding of morphological evolution through taxonomic resolution. The **fourth section**, comprising **chapter 11**, showcases the potential for taxonomic papers to provide baseline data for macroevolutionary studies.

Section 1: Conserving complexes requires taxonomic clarity

In this section, I present a paper that discusses the importance of taxonomic accuracy and clarity when assessing species that are from known complexes (i.e. species complexes that are genetically characterised and known to consist of multiple similar or cryptic species), via the case study of mantelline mantellid frogs of the *Mantidactylus* subgenus *Hylobatrachus*. *Hylobatrachus* are torrent frogs found in and near streams along Madagascar's eastern mountain chain. Until now, only two species of this subgenus have been known, and I was involved in their IUCN Red List assessment in 2016. One of the species was known to constitute a species complex, but we followed IUCN recommendations in treating the species complex as a single good species. In **chapter 1**, my colleagues and I argue that this practice is detrimental to the conservation of such species complexes, and that change is needed to the way the IUCN handles species complexes. We demonstrate this by describing two new species, one of which had been included in the broad circumscription of a complex. In the **Discussion**, I highlight the disparity between conservation's foundation on good taxonomy and current policies that seem to sweep taxonomic uncertainty under the rug. I discuss the dual fates of Data Deficient species in policy making, and their value in representing the state of knowledge without extrapolating from inadequate or flawed data. Finally, I argue that species complexes are a taxonomically and globally widespread phenomenon, and the impacts of current policies are therefore globally relevant and worthy of reconsideration.

Section 2: Biogeography through the lens of systematics

In this section, I present a case study for biogeographical patterns that have emerged as a result of my systematic work on the mantellid frog genus *Gephyromantis*. The frogs of the genus *Gephyromantis* are widespread across Madagascar's humid forests but have their centre of endemism and diversity in the north of the island (Brown et al. 2016). The genus consists of 47 species, which are organised into six subgenera, some with starkly differing morphology and ecology and with deep genetic divergences (Glaw and Vences 2006). The genus was highlighted by Vieites et al. (2009) as

Introduction

containing a large number of candidate species. Biogeographic patterns in the genus have not been closely examined in the past. In this section, I show that the inter-relationships of *Gephyromantis* species, inferred using molecular phylogenies, are highly informative about the biogeography of northern Madagascar, and elevation is a particularly limiting factor. Central points established are (1) the role of the Tsaratanana massif in isolating mid-elevation populations to its northeast (Sorata) and southwest (Bealanana District) from one another (**chapters 2 and 5**), (2) the flow of species/genetics between Marojejy and Sorata along the intervening mountain chain at mid-elevations (**chapters 3–5**), with stronger connection at intermediate elevations and especially loss of connection between high-elevation endemics (**chapters 3–5**), and (3) presence of connection between Marojejy and the southwestern slopes of the northern mountain range (**chapters 2 and 5**). In the **Discussion**, I examine the biogeography of the genus *Gephyromantis* in greater detail and relate the observed patterns in northern Madagascar to other taxa, showing parallels between different groups of frogs and also with chameleons, but rather different patterns in small mammals according to Maminirina et al. (2008). I discuss the curious pattern of greatest community similarity 200 metres above the point of minimum connection and argue that this suggests a dynamic palaeoclimatic influence on herpetofaunal biogeography in this area. I argue that the emerging patterns, combined with the ecological differences among subgenera, will make these frogs well suited to modelling approaches in order to understand the influence of ecology on biogeography.

Section 3: Ecomorphological evolution through the lens of systematics

In this section, I present a case study for ecomorphological evolution that has emerged as a result of my systematic and taxonomic work on narrow-mouthed frogs of the subfamily Cophylinae from Madagascar. The Cophylinae are endemic to Madagascar and highly diverse (Wollenberg et al. 2008; Vieites et al. 2009; **chapters 8 and 10**). As a subfamily, they are widespread across eastern and northern Madagascar, with only a few species occurring also in the drier west (Glaw et al. 2007), but their centre of endemism and diversity is in the north of Madagascar (Brown et al. 2016). Previous work has established that these frogs have a dynamic history of morphological evolution, evidenced by non-monophyly of long-established taxa that was revealed when genetics became available (Andreone et al. 2005; Wollenberg et al. 2008). They were also found to have a particularly large Linnean shortfall (Vieites et al. 2009). In this section, I show that (1) osteological characters are often needed for taxonomic resolution of species in this subfamily (**chapters 6 and 7**), and (2) ecological convergence within this group seems to occur in such a way that while the resulting phenotype may be highly similar externally, osteologically it generally shows hallmarks of its genetic history (**chapters 8 and 9**)—that is to say, ecomorphological convergence is a compromise of determinism and contingency. As a result, characters of particular taxonomic value at supraspecific levels are to be found in the skeletons of these frogs (**chapters 8 and 9**). These are particularly valuable, as burrowing, climbing, and miniaturisation have evolved repeatedly within these frogs, as highlighted by the phylogeny-focussed **chapters 8 and 10**. In the **Discussion**, I emphasise the expanding picture of morphological evolution that has emerged as a result of the rapid taxonomic work made on this subfamily over the last six years, and the particular importance of osteological and genetic datasets in this transformation. A great deal more about these frogs remains to be explored, but much of it will be facilitated by taxonomic resolution of the group, which is now in sight.

Section 4: Consolidating taxonomic datasets for macroevolutionary studies

In this section, I present an example of the way that taxonomic datasets can be used as data sources for larger evolutionary analyses, from the lizard family Chamaeleonidae. Chameleons are among the most morphologically specialised of all lizards, adapted for crypsis and precision long-distance

prey capture. But chameleons are also among the most ornamented of all animals, and, as a family, have the greatest variety of physical ornaments of any vertebrates, extinct or extant (D. Hone, pers. comm.), including horns, spines, skin flaps, crests, sails, and ridges. With over 200 species, the group is an excellent system not only for the study of ecomorphological evolution, but also for the study of the evolution of sexual ornamentation. Around half of the family Chamaeleonidae is found on Madagascar, while the other half is found across Africa, extending even into southern Europe and Asia (Tilbury 2018). Chameleon taxonomy is rapidly progressing, especially in Madagascar (Glaw et al. 2009, 2012; Gehring et al. 2010, 2011; Crottini et al. 2012b; Prötzl et al. 2015, 2017, 2018a, 2018b, 2018c, submitted; Scherz et al. 2019) and sub-Saharan Africa (e.g. Tilbury and Tolley 2009; Stipala et al. 2012; Branch et al. 2014; Tilbury and Tolley 2015; Hughes et al. 2017). In **chapter 11**, I use data on external and genital morphology mined largely from taxonomic literature and field guides in a phylogenetic comparative framework using a new, phylotranscriptomics-anchored species-level phylogeny to test hypotheses surrounding the evolution of external and genital ornamentation. I show that genital and external ornamentation are largely uncoupled evolutionarily, and while both are influenced by body size and ecology, the patterns in genitals are more consistent with intrasexual selection and mating system as drivers, while those in external ornaments are more compatible with mate choice and extrinsic factors. This shows that ornamentation of genitals and head morphology are affected by different forms of sexual selection. In the **Discussion**, I highlight the wealth of data made available by taxonomists every year, and the ability to tap into this resource as a foundation from which to build datasets to test macroevolutionary hypotheses. This process relies on detailed and accurate taxonomic accounts for these purposes.



Mantidactylus (Hylobatrachus) petakorona sp. nov.
described in Chapter 1

Results

Section 1: Conserving complexes requires taxonomic clarity

In this section, I present a single chapter in which we highlight the critical importance of taxonomy for accurate conservation assessment and make recommendations for how the IUCN might change their policy to better handle taxonomic conundrums.

Chapter 1. MANUSCRIPT (in review): Species complexes and the importance of Data Deficient classification in Red List assessments: the case of *Hylobatrachus* frogs

The IUCN Red List recommends that whole species complexes with one named and several unnamed lineages should be assessed as though they belong to a single species. The result is that the assessment of the named lineage includes the distribution of the whole complex, representative of no single member at all. As assessments of such poorly known species are often based on the criterion that pertains to range size and known locations (Criterion B; IUCN 2012), these complexes are consequently given optimistic non-threatened statuses. In this chapter, I present a manuscript in which we argue that this practice is not only unhelpful, but that it is actively detrimental; erroneously overestimated conservation statuses do not reflect the fact that any single member of the species complex could be insidiously nearing extinction. We argue that this is because taxonomy is not being appropriately valued by the IUCN. The real status of whole species complexes should be Data Deficient, and the importance of taxonomic reassessment of the complex should be brought to the fore: resolving their taxonomy is the only way that directed action can be taken to protect the species. We demonstrate this principle by partly resolving the taxonomy of frogs of the mantellid genus *Mantidactylus* from the subgenus *Hylobatrachus*. We confine the definition of one species, previously assessed by the IUCN while including other members of the complex, to a specific genetic lineage, and describe two new species.

Scherz, M.D., Glaw, F., Hutter, C.R., Bletz, M.C., Rakotoarison, A., Köhler, J. & Vences, M. (in review) Species complexes and the importance of Data Deficient classification in Red List assessments: the case of *Hylobatrachus* frogs. Unpublished manuscript.

Currently in review in PLoS ONE.

Species complexes and the importance of Data Deficient classification in Red List assessments: the case of *Hylobatrachus* frogs

Mark D. Scherz^{1,2*}, Frank Glaw¹, Carl R. Hutter³, Molly C. Bletz⁴, Andolalao Rakotoarison⁵, Jörn Köhler⁶, Miguel Vences²

Short title: Species complexes and the Red List

¹Zoologische Staatssammlung München (ZSM-SNSB), Münchhausenstraße 21, 81247 München, Germany

²Braunschweig University of Technology, Zoological Institute, Mendelssohnstraße 4, 38106 Braunschweig, Germany

³Biodiversity Institute and Department of Ecology and Evolutionary Biology, University of Kansas, Lawrence, KS 66045-7561, USA

⁴Department of Biology, University of Massachusetts Boston, Boston, MA, USA

⁵Zoologie et Biodiversité Animale, Université d'Antananarivo, BP 906, Antananarivo, 101 Madagascar

⁶Hessisches Landesmuseum Darmstadt, Friedensplatz 1, 64283 Darmstadt, Germany

*corresponding author, e-mail: mark.scherz@gmail.com

Abstract

Taxonomy is the cornerstone of conservation assessments. Currently, the IUCN Red List treats species complexes either under a single overarching species or omits them altogether. Unless the assessment is as Data Deficient (DD), the former results in an unhelpfully broad and often over-estimated assessment that does not apply to any one species, while the latter may result in the omission of species that should be assessed. We here provide a partial taxonomic revision of *Mantidactylus* subgenus *Hylobatrachus*, a case study for the discussion of the application of conservation assessments to species complexes. These rheophilous frogs from eastern Madagascar consist of two named species, *M. lugubris* and *M. cowanii*, but several undescribed candidate species are recognised, and the application of the currently available names is not unambiguous. Our genetic survey of these frogs confirms that these lineages are mitochondrially well segregated, but share haplotypes in the nuclear RAG1 gene, further complicating their taxonomic resolution. As a first step towards a taxonomic revision, we describe two of the lineages for which sufficient data are available: one from southeastern Madagascar, *Mantidactylus (Hylobatrachus) atsimo* sp. nov., and the other from the Marojejy Massif in northeastern Madagascar, *Mantidactylus (Hylobatrachus) petakorona* sp. nov. Description of the remaining candidate species within this subgenus, and understanding their systematics and evolution, will require additional field samples and probably also phylogenomic or population genomic approaches. Our data helps to restrict the name *M. lugubris* and gives a clear picture of the distribution of the species to which it is currently applied, and we propose to re-assess its Red List status under a more restrictive definition that omits other candidate species. We make recommendations for reducing the ambiguity and over-estimation involved in assessing species complexes. We emphasise that DD is a valuable category that should be actively used when data deficiency is taxonomic in nature, especially in the case of species complexes, and that more emphasis should be placed on the importance of taxonomy in understanding the conservation status of species.

Keywords:

Amphibia, Data Deficient, International Union for the Conservation of Nature, *Mantidactylus atsimo* sp. nov., *Mantidactylus petakorona* sp. nov., *Hylobatrachus*, molecular genetics, morphology, species complex

Introduction*Species complexes and the IUCN Red List*

Species complexes are entities of multiple separate species-level lineages that cannot be separated based on current knowledge. Often their resolution (i.e. describing their constituent species) is hampered because they consist of cryptic lineages, that is, species-level units that are difficult if not impossible to distinguish with traditional methods, for example based on external morphology. Such cryptic diversity is often discovered when DNA barcoding [1] reveals that a ‘species’ consists of multiple, deeply separated lineages. Further difficulties in resolving species complexes can arise from uncertainty in the application of available names, when these cannot be easily assigned to any one lineage, and the type material is too old or damaged to PCR-amplify DNA from it (although new opportunities are opening up with massively parallel target capture sequencing methods, e.g. [2]), in poor condition, and/or without helpful type locality.

Although species complexes are difficult to quantify, there is no disputing that they are pervasive across all domains of life. This presents a major challenge to species-driven conservation. At its core, the International Union for the Conservation of Nature (IUCN) Red List of Threatened Species (hereafter IUCN Red List) is anchored on taxon names, and it can therefore only be as re-

liable as its underlying taxonomy. The IUCN's policy is that species with complicated or uncertain taxonomy should either be regarded a priori as 'good species' and assessed following the standard procedure and criteria, or simply not be listed [3]. A consequence of this is that species complexes under single names are assessed with the distribution range of all of their lineages. This gives them a large range, often resulting in a status of Least Concern, although the status of each of the constituent species-level lineages may be threatened [4]. This is problematic as it overestimates the distribution and underestimates the threat status of the one species to which the assessment ostensibly applies, as well as all of the unnamed members of the complex included in its assessment. It also means that every taxonomic revision that resolves part of a species complex requires the threat status of the whole complex to be reassessed. In the case where the complex has been characterised genetically (e.g. through DNA barcoding), candidate species (*sensu* [5, 6]) established, and the definition of available names restricted as far as possible, this could be avoided if the threat assessment were restricted to omit undescribed members of the species complex.

Here we present a case study for the discussion of the application of Red List assessments to known and characterised species complexes: the *Mantidactylus* subgenus *Hylobatrachus*, a clade of taxonomically challenging rheophilous mantellid frogs from Madagascar.

Hylobatrachus: an enigmatic and complex clade of frogs

The genus *Mantidactylus* of the largely Madagascar-endemic neobatrachian family Mantellidae contains 31 described species. It is divided into six subgenera, *Mantidactylus* (2 species), *Brygoomantis* (11), *Maitsoamantis* (1), *Hylobatrachus* (2), *Ochthomantis* (5), and *Chonomantis* (9), which are ecologically and morphologically distinct [7]. Most are found in close association with lotic water, with some (e.g. *Brygoomantis*) preferring slow and shallow streams and sometimes also nearby lentic water bodies, and others, particularly *Hylobatrachus*, preferring fast-flowing waters with rapids. Each subgenus of *Mantidactylus* hosts numerous candidate species, and at present at least 56 candidate species are recognised across all subgenera [8-10]. Most of these candidates are involved in species complexes, which impedes progress towards taxonomic resolution.

The subgenus *Hylobatrachus* contains riparian frogs, closely associated with fast-flowing streams where they are mostly found on and among rocks [7, 11], and are defined by their highly derived larval morphology [12]. This clade was defined as the *Mantidactylus lugubris* group by Blommers-Schlösser [13], and assumed to contain a single taxon, *Mantidactylus lugubris* (Duméril, 1853) by Blommers-Schlösser and Blanc [14]. The only further nomen associated to this group is *Mantidactylus cowanii* (Boulenger, 1882), which was considered a junior synonym of *M. lugubris* by Guibé [15] and Blommers-Schlösser and Blanc [16] but resurrected as distinct species by Glaw and Vences [7]. The two currently accepted species in the subgenus *Hylobatrachus* are *Mantidactylus cowanii* and *M. lugubris*. While the former has a fairly precise type locality (Ankafana in the East Betsileo region), the latter was described with the imprecise locality information 'Madagascar'.

Previous studies (e.g. [8-10]) have provided evidence for the presence of unrecognized lineages in the *Hylobatrachus* clade, with six candidate species defined so far. Taxonomic progress has been hampered by the morphological similarity among species, apparent variation among specimens genetically assigned to the same lineage, and lack of bioacoustic data for most lineages. So, while a taxonomic revision of the subgenus is long overdue, it remains challenging.

In our recent re-assessment of all of Madagascar's frogs, we assessed *M. cowanii* (<http://dx.doi.org/10.2305/IUCN.UK.2017-2.RLTS.T135907A84184849.en>) and *M. lugubris* (<http://dx.doi.org/10.2305/IUCN.UK.2016-3.RLTS.T57496A84173405.en>), as Near Threatened and Least Concern, respectively. The status of *M. cowanii* was based only on specimens confidently assigned to that species, while that of *M. lugubris* was based on a broad circumscription that intentionally

Results

included part of the known undescribed diversity of the complex under the umbrella-name ‘*lugubris*’. While this followed the IUCN policy, it created a spuriously optimistic assessment that refers to an entity that is known to not constitute a single species and therefore management unit [4]. It is therefore of questionable value.

Here, we provide new data on members of the subgenus *Hylobatrachus* and their relationships, based on newly collected material and newly generated sequence data, and provide formal descriptions of two of the candidate species. We then discuss the connotations of our revision for the IUCN Red List status of the species of this subgenus, and make recommendations for best practices for dealing with species complexes in IUCN Red List assessments.

Materials and Methods

Ethics statement: Approval for this study by an Institutional Animal Care and Use Committee (IACUC) was not required by Malagasy law, but all work complied with the guidelines for field research compiled by the American Society of Ichthyologists and Herpetologists (ASIH), the Herpetologists’ League (HL), and the Society for the Study of Amphibians and Reptiles (SSAR). All field research, collecting of specimens, including in situ euthanasia of specimens, were approved by the Madagascan Ministère de l’Environnement des Eaux et des Forêts (Direction des Eaux et Forêts, DEF) under the permit numbers 215/16/MEEF/SG/DGF/DSAP/SCB.Re, 238-MINENV.EF/SG/DGEF/DPB/SCBLF/RECH, 285/MEADR/DEF/SEFLFB/FF/Aut, 238-MINENVEF/SG/DGEF/DPB/SCBLF, 218-MEEF/DEF/SPN/FFE/AUT, and 282/16/MEEF/SG/DGF/DSAP/SCB.Re, and exported under the permits 107N-EA04/MG17, 094C-EA03/MG04, and 105N-EA04/MG17. Specimens were anaesthetised and subsequently euthanized following approved methods (MS222 solution; approved by the American Veterinary Medical Association) that do not require approval by an ethics committee, after consultation of the animal welfare officer of TU Braunschweig.

For molecular analysis, tissue samples were taken from thigh muscle and preserved in pure ethanol. Studied specimens are deposited at the Zoologische Staatssammlung München (ZSM), the Zoologisches Forschungsmuseum Alexander Koenig (ZFMK), the Université d’Antananarivo, Département de Biologie Animale (UADBA), and the Muséum National d’Histoire Naturelle in Paris (MNHN). Field numbers FGMV, FGZC, MV and ZCMV refer to the zoological collections of F. Glaw and M. Vences; CRH refers to Carl R. Hutter field numbers.

The following morphometric measurements were taken by MV with a digital calliper to the nearest 0.1 mm: snout–vent length (SVL); maximum head width (HW); head length from tip of snout to posterior edge of snout opening (HL); horizontal tympanum diameter (TD); horizontal eye diameter (ED); distance between anterior edge of eye and nostril (END); distance between nostril and tip of snout (NSD); distance between both nostrils (NND); forelimb length, from limb insertion to tip of longest finger (FORL); hand length, to the tip of the longest finger (HAL); hindlimb length, from the cloaca to the tip of the longest toe (HIL); foot length (FOL); foot length including tarsus (FOTL); foot length (FL), and tibia length (TIBL). Hand length/body length ratio and foot length/body ratio were also calculated. Webbing formulae are given according to Blommers-Schlösser [13].

Call recordings were made in the field using various different tape and digital recorders with external microphones. Recordings were digitized at 22.05 kHz and 32-bit resolution, and computer-analysed using the software Adobe Audition 1.5. Frequency information was obtained through Fast Fourier Transformation (FFT; width 1024 points). Spectrograms were obtained at Hanning window function with 256 bands resolution. Temporal measurements are exclusively given as range (small sample size). Terminology of call descriptions follows Köhler et al. [17].

Genomic DNA was extracted from muscle tissue samples preserved in 100% ethanol using a

standard salt extraction protocol [18]. We sequenced a segment of the 16S rRNA gene using primers 16SA-L and 16SB-H [19] using protocols as in Vences et al. [20]. Furthermore, a fragment of the nuclear recombination-activating gene 1 (RAG1) was amplified with primers Rag1-Manti-F1 (CGTGACAGAGTSAAAGGAGT) and Rag1-Manti-R1 (TCAATGATCTCTGGAACGTG) from Vences et al. [21], using the following PCR protocol: 120 seconds at 94°C, followed by 35 cycles of (20 s at 94°C, 50 s at 53°C, 180 s at 72°C), and 600 s at 72°C.

PCR products were cleaned with enzymatic purification: 0.15 units of Shrimp Alkaline Phosphatase (SAP) and 1 unit of Exonuclease I (New England Biolabs) incubated for 15 min at 37°C followed by 15 min at 80°C. Purified PCR products were sequenced on an automated DNA sequencer (Applied Biosystems ABI 3130XL). Sequencing reactions (10 µl) contained 0.2 or 0.3 µl of PCR product, 0.5 µl of BigDye 3.1 (Applied Biosystems) and 0.3 µmol of primer. Sequences were checked and edited, and heterozygous positions in both nuclear genes inferred, in the software CodonCode Aligner 3.7.1 (CodonCode Corporation). All newly determined sequences will be submitted to GenBank upon manuscript acceptance.

Sequences of the 16S rRNA gene were aligned with those from previous studies in MEGA 7 [22] using the MUSCLE algorithm. We determined the best-fitting substitution model (SYM+G) by the Bayesian Information Criterion in jModelTest 2.1. [23]. We computed a phylogenetic tree in MEGA 7 under the Maximum Likelihood (ML) optimality criterion under the GTR+G model (as it is the most similar to the SYM model, which cannot be implemented in MEGA). Node support was assessed with 2000 full heuristic bootstrap replicates.

Haplotypes of nuclear gene sequences were inferred using the PHASE algorithm implemented in DnaSP [24] and a Maximum Likelihood tree of phased sequences was calculated in MEGA 7 [22]. Haplotype networks were then reconstructed in HapViewer (Haplovieviewer), written by G. B. Ewing (<http://www.cibiv.at/~greg/haplovieviewer>), which infers haplotype networks applying the methodological approach of Salzburger et al. [25].

The electronic version of this article in Portable Document Format (PDF) will represent a published work according to the International Commission on Zoological Nomenclature (ICZN), and hence the new names contained in the electronic version are effectively published under that Code from the electronic edition. This published work and the nomenclatural acts it contains will be registered in ZooBank, the online registration system for the ICZN. The published version of this work will be archived and made available from the following digital repositories: LOCKSS and PubMed Central.

Results

*Species diversity in the subgenus *Hylobatrachus* assessed by molecular markers*

Our alignment for the 16S rRNA mitochondrial gene consisted of 507 bp for 112 individuals of the subgenus *Hylobatrachus*. The obtained ML tree (Fig 1) confirmed the eight previously defined species and candidate species in the subgenus as deep mitochondrial lineages, several of which had additional geographic structure (Figs 1–2). Note that the purpose of this single-marker tree was not to resolve the deep relationships of *Hylobatrachus* but to assign specimens to distinct lineages.

Three candidate species from northern Madagascar (*Mantidactylus* sp. Ca50, Ca53 and Ca54) were represented by single samples only and will not be further discussed in this study. The two nominal species, *Mantidactylus cowanii* and *M. lugubris*, comprised samples from multiple locations: for *M. cowanii*, specimens from Ambohitantely were placed in a separate subclade, sister to the subclade with samples from Mantadia, Vohidrazana, and Vohimana; for *M. lugubris*, specimens from northeastern coastal localities (Befanjana forest: Ambodirafia and Ambatoroma) formed one clade, a sample from another northeastern locality (Sahavontsira) formed a second clade, and specimens from the northern central east (Mantadia, Vohidrazana and Vohimana) formed a third clade.

Results

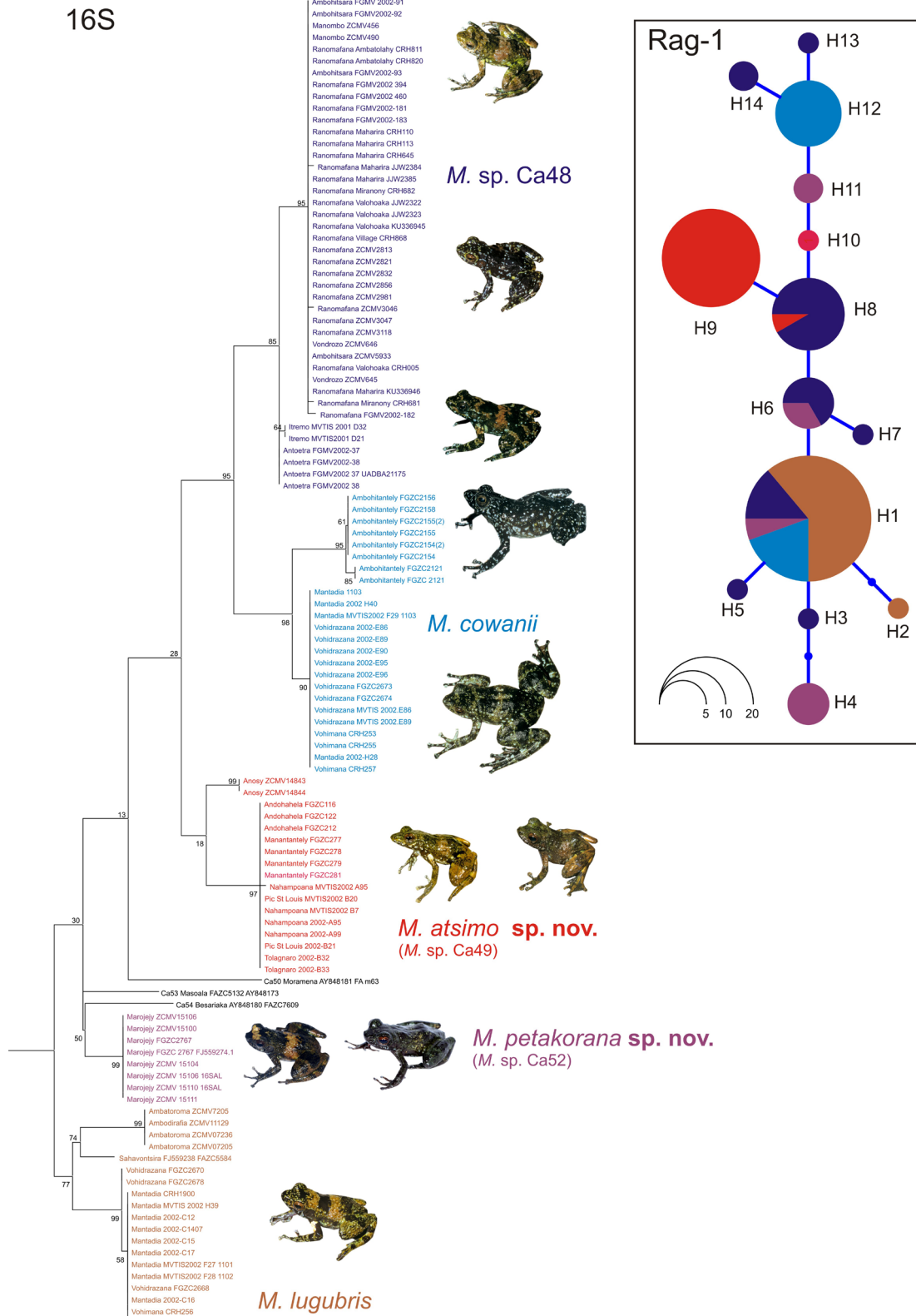


Fig 1. Maximum likelihood tree of 112 individuals belonging to the subgenus *Hylobatrachus*, based on DNA sequences (507 bp) of the mitochondrial 16S gene.

The inset pictures show representative individuals of the respective species. Values at nodes are support values in percent of a bootstrap analysis (2000 replicates). The tree was rooted with *Mantidactylus femoralis* (subgenus *Ochthomantis*) as the outgroup (removed from the graphic for better visualization of ingroup relationships). The inset haplotype network is based on haplotypes inferred from 572 bp of the nuclear RAG1 gene for 54 individuals (haplotypes numbered H1–H14). Colours correspond to those used in the tree.

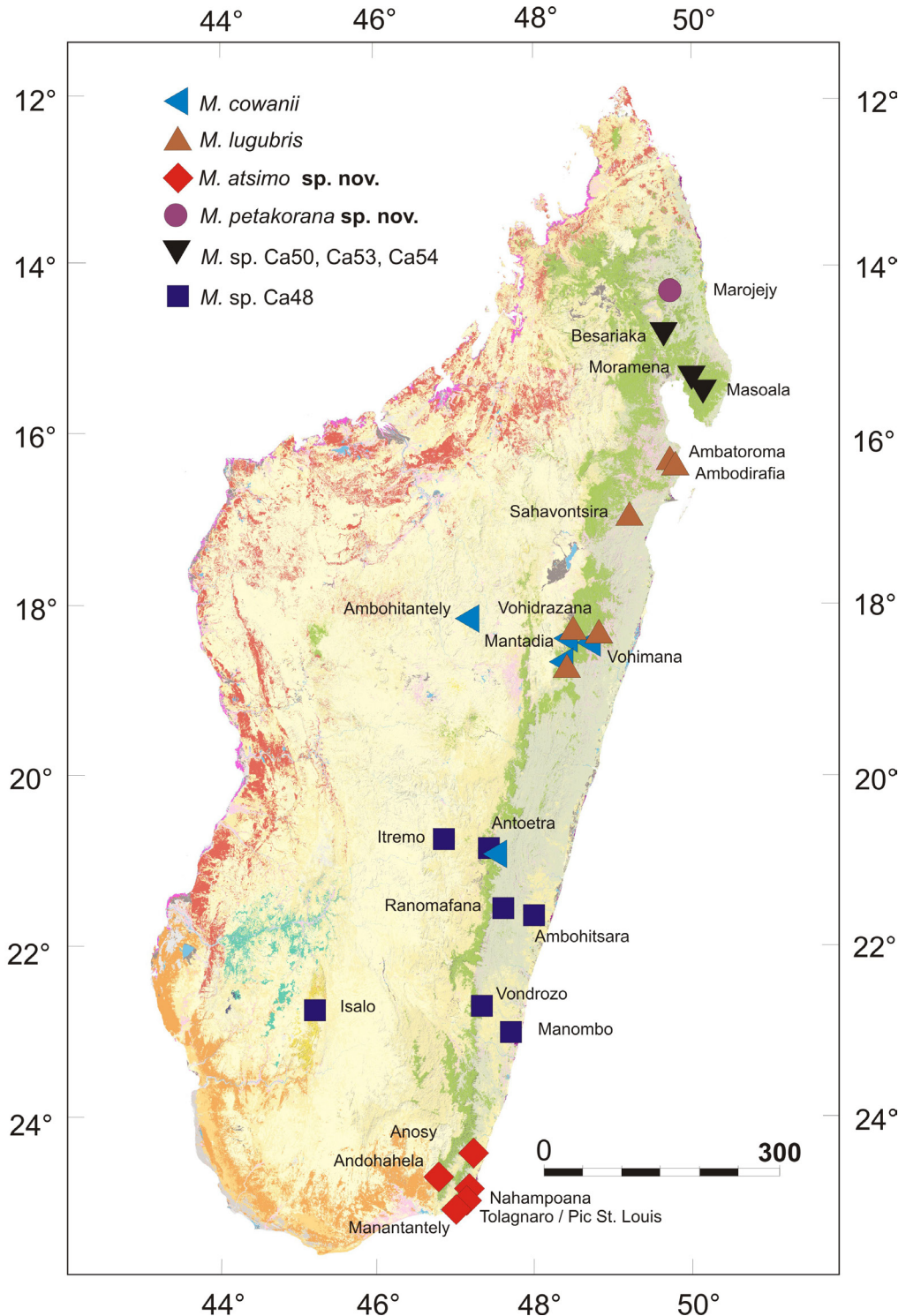


Fig 2. Map of Madagascar showing the known distribution of *Mantidactylus* species and candidate species in the subgenus *Hylobatrachus*.

Only records confirmed by molecular data in Fig 1 are shown, except the *M. cowanii* record in Antoetra (see text) and the *M. sp. Ca48* record from Isalo (molecular data in [26]).

Note that at the latter three localities, our data suggest syntopic co-occurrence of *M. cowanii* and *M. lugubris*, and this was also corroborated for these sites by morphological comparison of the voucher specimens (Table 1) which showed the differences in colour pattern and partly in body size characteristic for this species, with *M. cowanii* being usually characterised by being larger and having a darker dorsal colour with irregular light spotting (see Figs 3–5 and Table 1; Vohimana specimens not measured but confirmed by CRH).

Three additional lineages in our phylogenetic tree were represented by multiple individuals: (1) one lineage from the Marojejy Massif in the northeast, corresponding to *M.* sp. Ca52; Vieites et al. 2009); one lineage from several localities in the southeast (Andohahela, Manantantely, Nahampoana, Tolagnaro/Pic St Louis, and probably Anosy Mountains) corresponding to *M.* sp. Ca49; (3) and one lineage from various sites in southern central Madagascar, corresponding to *M.* sp. Ca48. All of these lineages, as well as *M. lugubris* and *M. cowanii*, were supported by bootstrap support values >70%, except for *M.* sp. Ca49 where most individuals had near-identical sequences placed in a highly supported clade (bootstrap proportion 97%), but the placement of the two specimens from the Anosy mountains was unsupported (18%) and remains tentative.

Genetic divergences among the main lineages in *Hylobatrachus* were high. 16S uncorrected pairwise divergences as reported in Table 2 were 3.6–7.6%. The highest divergence (7.6%) corresponded to the sympatric species pair, *M. cowanii* and *M. lugubris*.

The alignment of the nuclear gene fragment, RAG1, consisted of 572 nucleotide positions for 54 individuals of *Hylobatrachus*. The haplotype network reconstructed from these sequences contained 14 haplotypes (H1–H14 in Fig 1) which, however, did not reveal a pattern of differentiation consistent with the mitochondrial tree. Every lineage showed haplotype sharing with at least one other lineage, and one haplotype (H1) was found in four of the lineages. However, some haplotypes were more common in some species; for instance, most individuals of *M.* sp. Ca49 had one exclusive RAG1 haplotype not shared with any other of the lineages (H9), and a large proportion of *M. cowanii* sequences corresponded to one haplotype exclusive for this species (H12).

The extensive haplotype sharing in RAG1 might indicate incomplete lineage sorting or limited gene flow among species and candidate species of *Hylobatrachus*. This necessarily hampers species delimitation which, based on the available data, cannot rely on the genealogical concordance

Table 1 Morphometric data of examined specimens of *Hylobatrachus* (all in mm)
For abbreviations of measurements, see Methods. Additional abbreviations: M, male; F, female, HT, holotype, ST, syntype. The column 16S indicates individuals for which a fragment of the 16S rRNA gene has been sequenced and included in the phylogenetic tree (Fig 1).

Voucher number	Field number (tissue number)	Sex	16S	Location	SVL	HW	HL	TD	ED	NSD	NND	FORL	HAL	HIL	FOTL	FOL	TBL
<i>M. lugubris</i>																	
MNHN 1994.1750 (ST)	–	F		Madagascar	38.0	11.6	13.7	2.9	4.8	3.1	1.8	3.4	21.7	10.7	59.7	26.4	18.3
MNHN 1994.1751 (ST)	–	M		Madagascar	31.5	10.3	11.9	3.6	4.3	3.0	1.3	3.3	19.0	9.4	49.4	22.5	15.6
MNHN 1994.1752 (ST)	–	M		Madagascar	32.0	10.3	11.5	3.7	4.1	3.0	1.7	2.8	19.0	9.4	51.6	23.8	16.3
MNHN 4583 (ST)	–	M		Madagascar	32.0	11.2	11.5	3.9	4.3	3.0	1.6	3.8	21.1	9.8	54.3	25.6	17.6
ZSM 166/2002	MV 2001.1101	F	+	Mantadia	35.7	10.9	12.7	3.2	4.5	3.5	2.0	3.7	22.4	11.2	59.9	28.3	19.7
ZSM 167/2002	MV 2001.1102	M	+	Mantadia	33.6	11.3	13.0	4.1	4.5	3.3	1.8	3.1	21.4	10.6	54.8	26.4	18.1
ZSM 750/2009	ZCMV 7206	M	+	Ambatorama	33.6	11.0	12.7	3.8	4.8	3.5	1.8	3.6	19.4	9.6	48.2	23.2	16.4
ZSM 749/2009	ZCMV 7205	M		Ambatorama	31.3	10.3	11.8	3.7	4.6	2.9	1.9	3.6	19.3	9.5	50.4	23.1	16.1
ZSM 751/2009	ZCMV 7236	M	+	Ambatorama	31.9	11.2	12.0	3.4	4.8	2.8	2.4	3.8	19.5	9.1	50.0	21.5	13.8
ZSM 747/2009	ZCMV 11124	F	+	Ambodirafia	35.8	13.3	13.7	3.5	5.3	3.0	2.1	3.5	22.2	10.8	58.3	26.8	18.8
ZSM 748/2009	ZCMV 11129	F	+	Ambodirafia	36.8	12.0	13.0	3.0	5.4	3.4	1.7	3.9	22.6	10.8	56.1	25.7	18.1

Table 1 cont.

ZSM 65/2002	MV 2001.1364 (2002-H39)	Mantadia	36.0	13.0	14.7	3.8	4.7	3.5	2.2	3.9	NM	10.7	NM	18.3	18.9
ZSM 299/2005	FGZC 2668	Vohidrazana	36.2	12.7	14.2	3.6	5.4	3.8	2.2	3.7	24.1	11.2	56.3	28.5	19.3
ZSM 300/2005	FGZC 2670	Vohidrazana	36.8	12.1	14.0	3.9	5.5	3.3	2.2	4.1	21.3	11.0	56.1	27.4	17.4
M. cowanii															17.6
ZSM 63/2002	MV 2001.1353 (2002-H28)	Mantadia	43.5	14.1	15.6	2.9	5.3	3.9	2.7	4.1	28.5	12.9	67.1	28.6	17.8
ZSM 64/2002	MV 2001.1365 (2002-H40)	Mantadia	32.9	11.2	12.8	3.7	4.1	3.1	1.9	2.7	21.0	8.8	54.3	24.1	12.7
ZSM 306/2005	FGZC 2121	Ambohitantely	41.3	13.6	14.8	3.3	5.2	3.8	2.1	3.9	23.2	11.8	62.4	28.8	19.5
ZSM 301/2005	FGZC 2673	Vohidrazana	35.7	12.2	13.5	3.3	4.9	3.6	2.3	4.3	23.1	9.8	60.8	27.7	18.1
ZSM 302/2005	FGZC 2674	Vohidrazana	34.2	11.9	12.2	3.9	4.2	2.9	2.2	3.6	21.1	9.2	55.3	26.2	17.1
ZSM 171/2002	MV 2001.1103 (2002-F29)	Mantadia	40.4	13.7	14.3	3.2	5.1	3.5	2.5	4.0	25.3	12.5	68.4	31.5	21.6
ZSM 297/2005	FGZC 2155	Ambohitantely	38.7	12.8	13.1	2.9	4.2	3.2	2.1	3.4	22.9	11.8	62.5	29.1	20.2
ZSM 298/2005	FGZC 2158	Ambohitantely	39.9	13.1	13.5	2.8	4.3	3.3	2.6	4.0	22.1	11.1	64.9	29.5	20.7
ZSM 296/2005	FGZC 2154	Ambohitantely	31.9	11.1	11.5	2.9	4.3	3.2	2.0	3.8	19.8	9.3	54.0	23.8	16.4
M. petakorona sp. nov.															16.1
ZSM 305/2005	FGZC 2767	Marojejy	29.0	10.1	10.8	2.6	3.5	2.8	1.5	3.1	19.3	8.9	53.9	25.3	14.9
ZSM 501/2016	ZCMV 15100	Marojejy	31.3	10.0	11.6	3.7	4.9	3.0	1.8	3.1	19.6	8.8	52.8	24.2	14.7
ZSM 502/2016	ZCMV 15104	Marojejy	34.0	10.1	11.7	2.9	4.9	2.8	1.7	3.1	20.4	8.2	58.2	26.0	16.1
ZSM 503/2016	ZCMV 15106	Marojejy	28.9	9.2	10.6	3.4	4.4	2.7	1.5	2.5	18.3	8.4	46.9	22.5	16.9
ZSM 504/2016 (HT)	ZCMV 15110	Marojejy	34.0	11.4	12.0	2.8	6.3	2.6	2.1	3.3	20.7	9.7	57.7	26.2	15.3
ZSM 505/2016	ZCMV 15111	Marojejy	27.0	9.2	10.1	2.0	4.8	1.9	1.5	2.2	17.7	8.6	50.4	23.0	18.3
M. atsimo sp. nov.															16.1
ZSM 149/2004	FGZC 277	Manantantely	34.8	11.7	12.3	2.7	4.6	3.8	1.8	3.1	22.0	10.7	56.7	26.0	17.5
ZSM 150/2004	FGZC 281	Manantantely	33.7	11.9	12.5	2.4	4.6	3.8	2.1	3.5	20.1	10.0	50.6	24.0	15.9
ZSM 72/2004	FGZC 122	Andohahela	34.6	11.9	12.3	2.6	4.3	3.7	1.6	2.9	21.0	10.1	56.2	25.0	16.9
ZSM 69/2004 (HT)	FGZC 116	Andohahela	34.5	11.8	12.8	2.2	5.4	3.5	2.0	3.7	20.7	10.3	53.3	24.2	16.7

criterion [27]. Yet, the sympatric occurrence of *M. lugubris* and *M. cowanii*, where individuals can clearly be recognised by morphology (body size and colour pattern) clearly supports the existence of more than one species in the subgenus. While the available evidence for multiple species is weaker in *Hylobatrachus* than in other groups of recently revised Malagasy anurans (e.g. [28,

Results

Table 1 cont.

ZSM 174/2002	MV 2001.1483 (2002-B20=B21)	F +	Pic St Louis	33.8	11.9	12.2	2.7	4.8	3.4	1.6	3.1	19.7	9.6	53.6	23.4	15.7	16.1
ZSM 253/2002	2002-A95/A99/B7	F +	Nahampoana	31.2	10.5	11.4	2.2	4.3	3.4	1.6	3.0	18.6	8.9	52.2	23.3	15.5	16.6
ZSM 172/2002	MV 2001.1476 (2002-A95/A99/B7)	F +	Nahampoana	34.1	11.7	12.6	2.2	4.9	3.2	1.7	2.8	21.0	9.6	56.1	24.7	16.6	16.6
ZSM 367/2016	ZCMV14843	M +	Anosy Massif	25.2	9.9	11.4	3.0	5.2	3.0	1.8	3.0	17.4	8.7	46.3	21.2	11.0	15.0
ZSM 368/2016	ZCMV14844	M +	Anosy Massif	28.0	10.2	12.0	3.3	5.0	3.0	2.0	2.8	17.0	8.3	47.7	21.8	14.3	14.9
<i>M. sp. Ca48</i>																	
ZSM 493/2006	ZCMV2821	M	Ranomafana	31.5	10.4	12.5	3.6	4.5	2.9	1.9	2.5	19.0	9.0	49.0	22.9	14.7	16.5
ZSM 494/2006	ZCMV2832	F	Ranomafana	37.8	13.1	14.8	2.7	5.6	3.2	2.5	2.5	24.9	10.7	62.7	28.5	18.9	18.6
ZSM 495/2006	ZCMV2856	F	Ranomafana	36.1	13.6	14.5	3.2	5.7	3.5	2.2	2.9	23.8	11.0	62.0	27.9	17.5	19.0
ZSM 496/2006	ZCMV2981	M	Ranomafana	26.9	10.2	11.8	3.1	4.5	2.1	1.5	3.3	19.4	8.9	52.2	23.1	13.6	15.7
ZSM 497/2006	ZCMV3046	M	Ranomafana	26.0	9.4	11.6	2.8	4.7	2.4	2.0	2.6	16.2	7.4	45.1	20.9	14.5	14.4
ZSM 498/2006	ZCMV3047	F	Ranomafana	38.1	15.2	14.8	2.9	4.7	3.6	2.2	2.9	22.4	11.0	58.2	27.2	18.4	17.8
ZSM 499/2006	ZCMV3118	M	Ranomafana	29.7	11.1	12.1	3.2	4.7	3.2	1.6	3.2	20.8	9.5	52.4	25.3	15.7	17.6
ZSM 717/2003	FGMV 2002.0379	?	Ranomafana	30.0	10.6	12.3	3.6	5.2	3.0	1.6	3.6	18.2	9.5	49.0	22.7	15.3	15.1
ZSM 718/2003	FGMV 2002.0385	F	Ranomafana	36.5	12.2	12.7	4.1	5.0	2.9	2.3	4.6	21.0	10.3	58.7	27.2	15.1	17.7
ZSM 719/2003	FGMV 2002.0386	M	Ranomafana	29.2	10.3	12.3	3.2	4.6	2.9	2.0	3.2	18.7	9.3	52.3	24.1	14.3	15.2
ZSM 720/2003	FGMV 2002.0391	F +	Ambohitara	38.0	12.5	14.5	3.1	5.8	3.0	1.8	3.1	23.2	10.9	65.7	28.9	17.9	19.5
ZSM 721/2003	FGMV 2002.0392	M +	Ambohitara	28.6	10.9	12.7	3.5	5.0	2.9	2.0	3.2	19.4	8.8	50.6	23.1	15.0	16.1
ZSM 722/2003	FGMV 2002.0394	M	Ranomafana	30.1	10.9	12.0	2.4	4.8	3.2	2.1	4.5	20.6	9.4	57.2	26.1	16.7	17.7
ZSM 898/2006	ZCMV2813	F	Ranomafana	39.0	12.2	13.9	3.1	5.0	3.5	2.9	2.6	23.7	11.3	61.0	28.2	19.3	18.8
ZSM 2412/2007	ZCMV5933	M?	Ambohitara	26.7	9.7	11.2	3.7	3.6	3.2	1.3	2.8	18.6	8.5	47.5	21.0	10.9	14.6
ZSM 730/2003	FGMV 2002.0454	M	Ranomafana	26.8	10.3	11.8	2.8	5.0	2.9	1.8	3.2	19.3	7.9	48.7	23.2	13.2	19.5
ZSM 734/2003	FGMV 2002.0460	M	Ranomafana	27.7	9.8	11.8	3.4	3.9	2.8	1.9	4.4	18.9	8.0	51.2	23.1	14.2	15.2
ZSM 646/2003	FGMV 2002.181	F +?	Ranomafana	37.2	12.0	13.4	2.7	5.2	3.4	2.3	3.7	22.4	11.4	59.1	27.8	19.1	18.3
ZSM 744/2001	MV 2001.467 (2001-D21?)	M +?	Itremo	26.8	8.9	9.5	2.2	3.9	2.1	1.6	2.4	16.6	8.1	44.9	20.8	13.5	13.7
ZSM 745/2001	MV 2001.468 (2001-D21?)	M +?	Itremo	27.4	8.9	10.1	3.1	3.9	2.5	1.6	3.2	16.9	8.0	44.3	20.1	13.8	13.4

29]) we are still convinced that in light of the available evidence, a taxonomic hypothesis dividing the subgenus into various species reflects biological reality better than a one-species or two-species hypothesis—especially in light of the high divergences in mitochondrial DNA identified within *Hylobatrachus*. As a first step, we here decided to formally recognise the geographically most

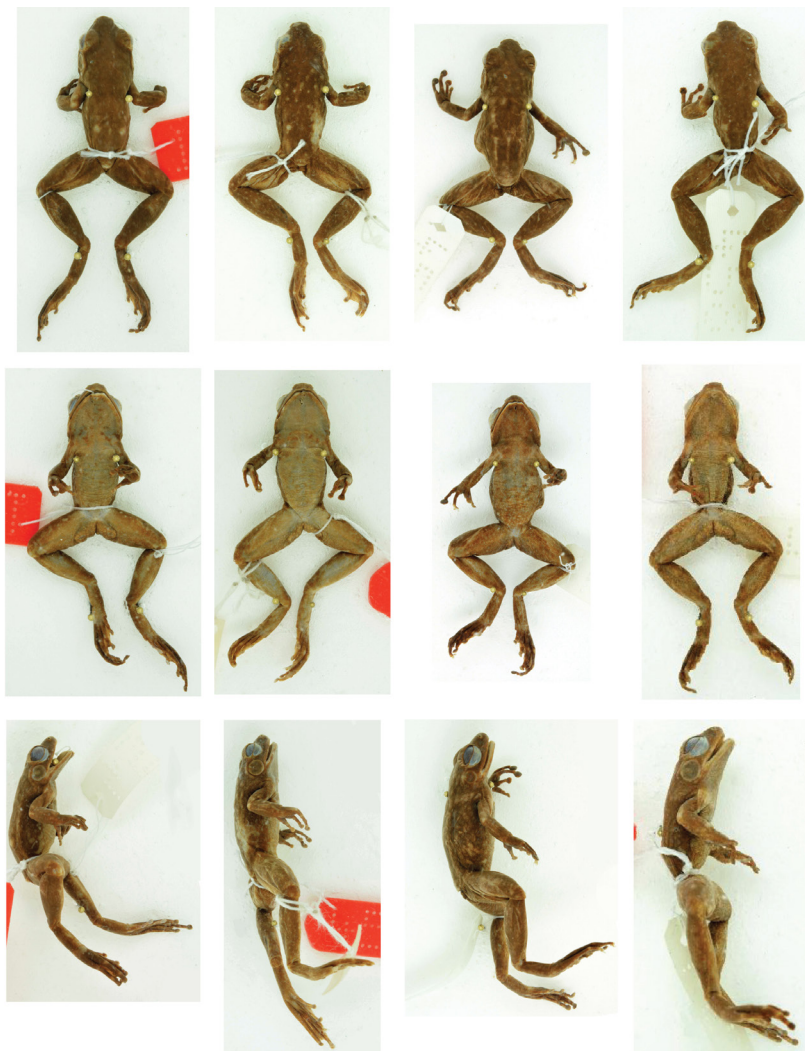


Fig 3. Preserved syntype specimens of *Mantidactylus lugubris* from MNHN database.

MNHN 1994.1752, 4583, MNHN 1994.1750, MNHN 1994.1751 are presented (left to right) in dorsal (top), ventral (middle) and lateral (bottom) view.

separated lineages, *M. sp. Ca49* and *52*, as distinct species, given that these also show some consistent morphological differentiation from the other lineages, as presented in more detail in the diagnoses below.

Identity of described taxa in the subgenus Hylobatrachus

The first step to achieve an improved taxonomic resolution in *Hylobatrachus* consists of assigning each of the available names, *cowanii* and *lugubris*, to one of the genetic lineages. Preserved syntypes of *M. lugubris* are shown in Fig 3 and two living individuals assigned to this species in Fig 4. Living individuals assigned to *M. cowanii* are shown in Fig 5. Living and fixed specimens of *M. sp. Ca52* are shown in Figs 6–7, and living specimens of *M. sp. Ca49* are shown in Fig 8, and of *M. sp. Ca48* in Fig 9.

We here follow the definition of *M. lugubris* and *M. cowanii* given by Glaw and Vences [11], but we are aware that it might partly be in need of revision. These authors, building on Glaw and Vences [7], defined *M. lugubris* (a species without clearly defined type locality) as the main lineage of olive-green coloured stream frogs occurring in the Mantadia/Andasibe region in the Northern Central East of Madagascar, considering that numerous species described by early researchers had been collected in this general region (SVL of syntypes 32–38 mm, see measurements in Table 1). Furthermore, Glaw and Vences [7], Glaw and Vences [11] defined *Mantidactylus cowanii* (type localities: Ankafana and East Betsileo) as corresponding to a large-sized species that occurs syntopically with *M. lugubris* at Mantadia, Vohidrazana and Vohimana, characterised by rather

Results

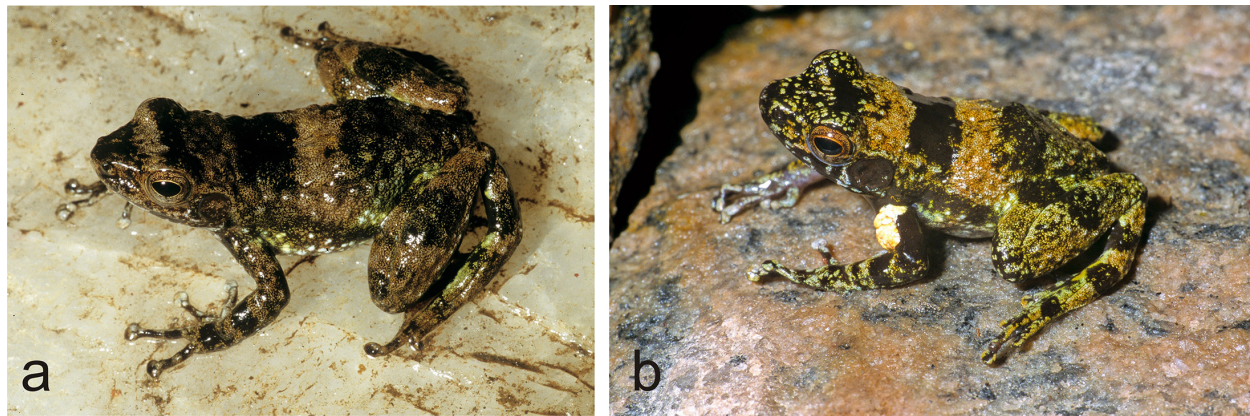
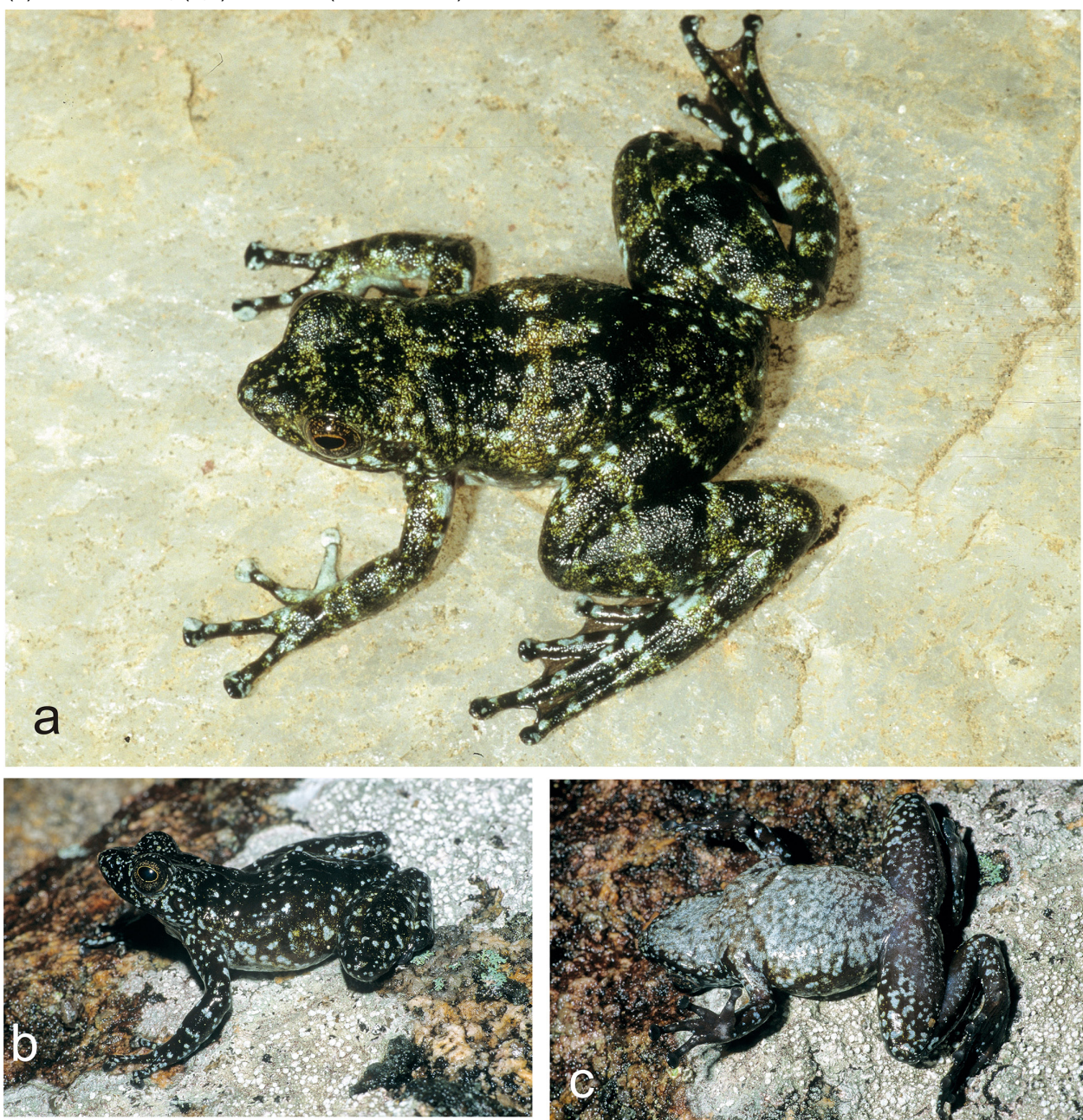


Fig 4. Specimens assigned to *Mantidactylus lugubris* in life.

(a) Vohidrazana, (b) Mantadia.

Fig 5. Specimens assigned to *Mantidactylus cowanii* in life.

(a) Vohidrazana, (b,c) Antoetra (Soamazaka).



uniform blackish colour with irregular light spotting, in agreement with the *M. cowanii* type specimen, described by Boulenger [30] as being dorsally brown, ‘sometimes minutely punctuated with whitish’, with whitish flanks and lateral hindlimbs, measuring 42 mm in SVL.

This definition is not as clear-cut as first hoped. Our samples closest to the type locality of *M. cowanii* originate from Antoetra, and correspond to *M. sp. Ca48*, a candidate species that has previously been referred to as *Mantidactylus* sp. aff. *cowanii* ‘small’. This candidate species is widespread, occurring in Manombo, Antoetra, Itremo, Ranomafana, and Ambohitara (Fig 2). However, large-sized specimens matching the description of *M. cowanii* have also been found at Antoetra (Fig 5), but no tissue samples of these individuals are available for molecular analysis. Therefore, we hypothesise that both *M. sp. Ca48* and the larger-sized *M. cowanii* occur at Antoetra, which would support our definition of the latter taxon.

Despite all of the uncertainty surrounding the identity of *M. lugubris*, *M. cowanii*, and *M. sp. Ca48*, it seems clear to us that neither of the two available names, *M. lugubris* or *M. cowanii*, refers to either the genetically divergent Marojejy lineage, or *M. sp. Ca49* from the far south of Madagascar. This is based on the following rationale: (1) *M. cowanii* was described from Eastern Betsileo, i.e., from the Southern Central East of Madagascar, and no specimens belonging to either of these genetic lineages are known from this part of Madagascar. Furthermore, the size given in the original description (42 mm) clearly exceeds that of specimens from either Marojejy or the extreme southeast of Madagascar (Table 1). (2) *M. lugubris* was described without precise locality information, but of the early-described anurans from Madagascar, none is an endemic from northeastern or extreme southeastern Madagascar. Furthermore, the syntypes of *M. lugubris* differ morphologically from at least the Marojejy specimens (especially by a longer snout; Table 1).

Consequently, it seems sufficiently clear that none of the two available names refers to the candidate species from the northeast or southeast of Madagascar (*M. sp. Ca49* and *M. sp. Ca52*). These two candidate species also show some morphological differentiation from other *Hylobatrachus*: the northeastern *M. sp. Ca52* often has a conspicuously short snout and large eyes, and most individuals of *M. sp. Ca49* have a uniformly coloured, silvery white ventral side as well as rather large terminal discs on fingers and toes. This combined with their 16S divergence of >3%, above the threshold typically defining evolutionarily distinct species of neobatrachian frogs [8, 31], led us to propose their formal taxonomic descriptions in the following.

Table 2. Mean uncorrected pairwise distances among species and candidate species of *Hylobatrachus* in a fragment of 507 bp of the mitochondrial 16S rRNA gene.

	<i>M. lugubris</i>	<i>M. cowanii</i>	<i>M. atsimo</i> (Ca49)	<i>M. petakorona</i> (Ca52)	<i>M. sp. Ca48</i>	<i>M. sp. Ca50</i>	<i>M. sp. Ca53</i>
<i>M. cowanii</i>	7.6						
<i>M. atsimo</i> (Ca49)	4.7	6.1					
<i>M. petakorona</i> (Ca52)	3.9	7.1	5.5				
<i>M. sp. Ca48</i>	7.5	4.5	5.2	6.8			
<i>M. sp. Ca50</i>	6.7	8.5	5.9	5.8	6.8		
<i>M. sp. Ca53</i>	4.5	6.7	5.4	3.6	6.7	5.8	
<i>M. sp. Ca54</i>	5.0	7.1	6.0	3.4	6.3	6.0	4.2

Taxonomy

Mantidactylus petakorona sp. nov.

Remarks. This species was previously considered as *Mantidactylus* sp. aff. *lugubris* “Marojejy”

Results

by Glaw and Vences (2007: 250–251) and as *Mantidactylus* sp. Ca52 by Vieites et al. (2009, suppl.), Wollenberg et al. (2011, suppl.) and Perl et al. (2014, suppl.).

Holotype. ZSM 504/2016 (field number ZCMV 15110), adult female (Fig 6–7), collected at Camp 0 in Marojejy National Park (ca. 14.4463°S, 49.7852°E, ~310 m a.s.l.), Sava Region, former Antsiranana Province, northeastern Madagascar, on 15 November 2016, by M. Bletz, M. D. Scherz, J. H. Razafindraibe, A. Rakotoarison, M. Vences, and A. Razafimanantsoa.

Paratypes. ZSM 501–503/2016 (field numbers ZCMV 15100, 15104, 15106), ZSM 505/2016 (ZCMV 15111), and UADBA-A uncatalogued (ZCMV 15105, 15121), six specimens with the same collection data as holotype. ZSM 305/2005 (FGZC 2767) collected at Camp Mantella in Marojejy National Park (14.4377°S, 49.7756°E, 481 m a.s.l.) on 14 February 2005 by F. Glaw, M. Vences, and R.D. Randrianiaina; ZFMK 57420, adult (possibly female), collected around a temporary low altitude camp (ca. 300–400 m a.s.l.) in Marojejy National Park on 27 March 1994 by F. Glaw, N. Rabibisoa and O. Ramilison; ZFMK 59909, adult female, collected at a temporary low altitude camp (ca. 300–400 m a.s.l.) in Marojejy National Park on 22–23 February 1995 by F. Glaw and O. Ramilison.

Etymology. The specific epithet is a Malagasy word meaning ‘flat face’ or ‘flat nose’, in reference to the distinctly shorter snout of this species. It is treated as an invariable noun in apposition to the genus name.

Diagnosis. *Mantidactylus petakorona* sp. nov. differs from all other species of *Mantidactylus*, subgenus *Hylobatrachus*, by a divergence of 5.9–8.7% uncorrected pairwise distance in a fragment of the 16S gene (uncorrected pairwise distances of *M. petakorona* to *M. cowanii* (8.7%), to *M. lugubris* (5.6%), to *M. sp. Ca49*, described below (6.5%)). The new species is characterised by the possession of the following suite of characters: (1) SVL 27–34 mm, (2) absence of white dorsal and lateral spotting, (3) squared snout in dorsal view, (4) large eyes (ED/HL = 0.32–0.52), (5) almost complete webbing of the fourth toe, and (6) a dark venter.

Among members of the subgenus *Hylobatrachus*, *M. (H.) petakorona* can be distinguished from *M. cowanii* as defined by Glaw and Vences [7], Glaw and Vences [11] by its distinctly smaller adult SVL (27–34 mm vs. 34–39 mm), shorter relative head length in males (HW/HL 0.86–0.87 vs. 0.90–0.98), generally smaller relative tympanum diameter in females (TD/ED 0.42–0.59 vs. 0.55–0.69, probably due to larger eye size), relatively longer hindlimbs in females (HIL/SVL 1.7–1.87 vs. 1.51–1.63), and lack of rather consistent white dorsal and lateral spotting (vs. presence); from *M. lugubris* by a distinctly more squared snout in dorsal view (vs. pointed) and by larger eyes evidenced by smaller TD/ED ratio and larger ED/HL ratio (see Table 1), and relatively longer hindlimbs in females (HIL/SVL 1.70–1.87 vs. 1.52–1.68). For diagnosis against *M. sp. Ca49*, see the description of that species, below.

Description of the holotype. Adult female in good state of preservation; SVL 34.0 mm; body relatively slender; head slightly longer than wide, of same width as body; snout rounded, slightly squared in dorsal view, slightly pointed in lateral view; nostrils directed laterally, slightly protuberant, nearer to tip of snout than to eye; canthus rostralis rather indistinct, straight; loreal region slightly concave; tympanum distinct, circular, its horizontal diameter 44% of eye diameter; supratympanic fold slightly distinct; tongue attached anteriorly, distinctly bilobate posteriorly, lobes rounded (right lobe slightly shorter than left lobe); maxillary teeth present; vomerine odontophores

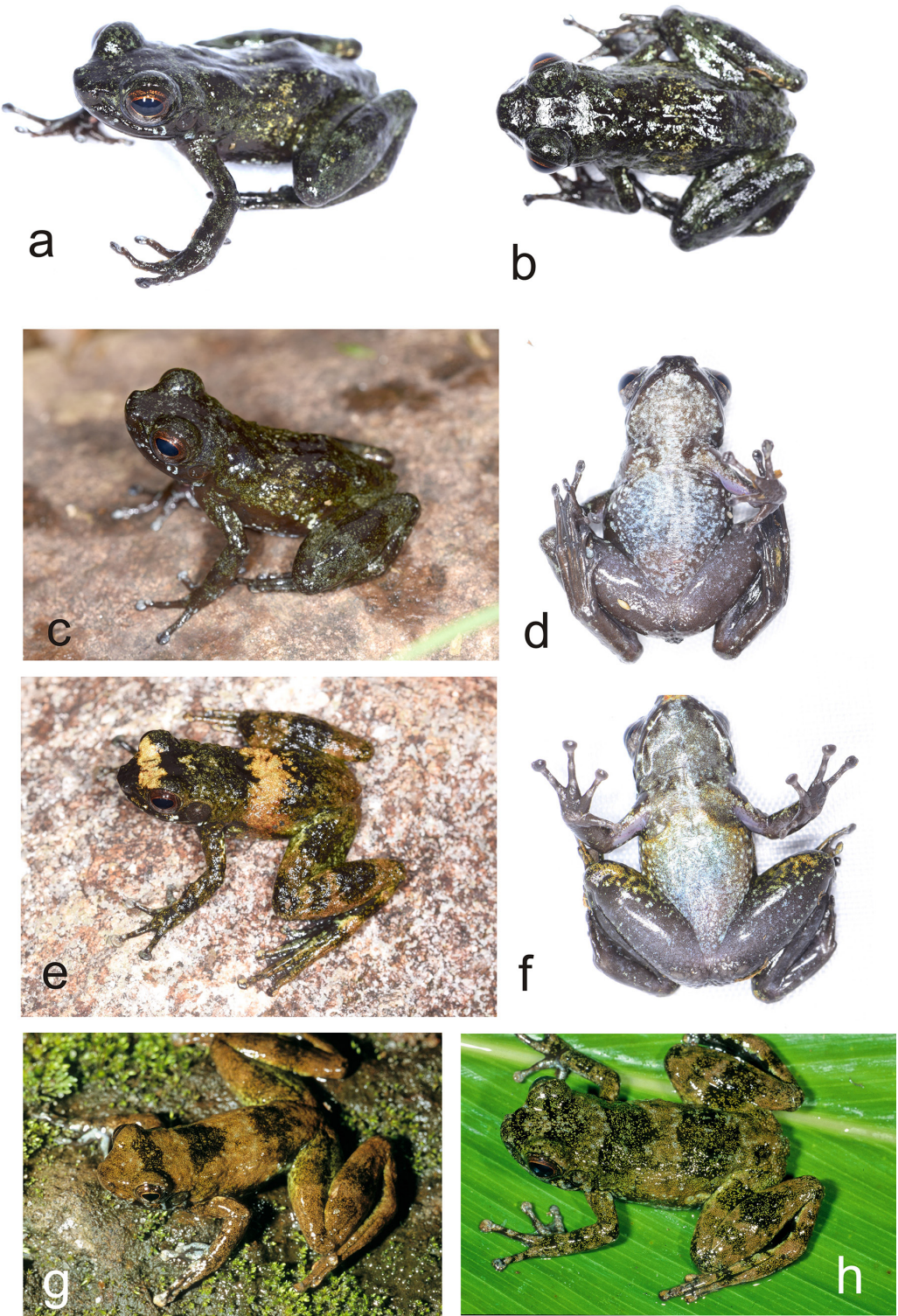


Fig 6. Specimens of *Mantidactylus petakorona* sp. nov. from Marojejy (low elevation localities around Camp 'Mantella') in life.

(a-d) holotype ZSM 504/2016, (e-f) paratype ZCMV 15121, (g) paratype ZSM 305/2005, (h) probably paratype ZFMK 59909, photographed in 1995.

distinct, one rounded patch on each side of buccal roof, positioned posteromedial to choana; choanae small, rounded. Arms slender, subarticular tubercles distinct, single; inner metacarpal tubercle and outer metacarpal tubercle not clearly recognizable; fingers without webbing; comparative finger length 1<2<4<3, second finger distinctly shorter than fourth finger; finger disks slightly

Results

Mantidactylus petakorona sp. nov.



Mantidactylus atsimo sp. nov.



Fig 7. Preserved holotypes of *Mantidactylus petakorona* sp. nov. from Marojejy (ZSM 504/2016), and of *Mantidactylus atsimo* sp. nov. from Andohahela (ZSM 69/2004).

enlarged. Hindlimbs slender; tibiotarsal articulation reaches slightly beyond the anterior corner of the eye when the hindlimb is adpressed forward along the body; lateral metatarsalia separated by webbing; comparative toe length $1<2<3<5<4$; fifth toe only slightly longer than third toe; inner metatarsal tubercle slightly distinct, outer metatarsal tubercle not recognizable; webbing between toes strongly expressed, formula 1 (0), 2i (0.25), 2e (0), 3i (0.5), 3e (0), 4i (0), 4e (0), 5 (0). Dorsal skin smooth; dorsum with slightly distinct dorsolateral folds; ventral skin smooth, including in the cloacal region, where there are no distinct tubercles. For extensive measurements see Table 1.

In preservative (Fig 7), dorsal colour dusky brown from top of head and dorsal abdomen; flanks transitioning from dorsal to ventral from light to dark dirty brown with whitish speckles situated near the hindlimbs; ventral background drab cinnamon with whitish speckles, darker, less speckled colour extending from the attachment of the arm, chin less speckled than the abdomen; dorsal forelimbs a dusky brown, ventral forelimbs centrally translucent surrounded by drab cinnamon, dorsal

hindlimbs dusky brown, transition zone from dorsal to ventral surface is speckled with pale buff, ventral hindlimbs drab with pale buff speckles, hindlimbs have distinctly less speckled than ventral abdomen; toe tips dusky brown.

In life (Fig 6a–d), the dorsal background was a blackish granite in colour, with light greenish grey speckling on head and dorsum, discontinuous lateral band pattern on mid dorsum with light greenish grey and light lime green colouring; ventral background a pale grey-brown brown with extensive white to pale blue mottling; dorsal forelimbs dusky brown-black with light greenish-grey speckling, ventral forelimbs centrally translucent surrounded by brownish olive, dorsal hindlimbs dusky brown-black with distinct light greenish grey bands, ventral hindlimbs brownish olive with random white to white-blue flecks. Iris copper coloured. Toe tips lighter in colour.

Variation. Morphologically studied paratypes include two males (ZCMV 15106, ZCMV 15100) and two individuals with unknown sex (ZCMV 15111, ZCMV 15104, ZCMV 15121). Males appear to be smaller in size (29–31 mm) than the holotype female (34 mm). Femoral glands appear indistinct in male specimens. See Table 1 for detailed morphological measurements. Colour patterns vary between individuals with (1) the extent of lateral banding on the dorsum varying from no apparent bands to multiple distinct bands, (2) lateral bands varying in colour from light greenish to buff yellow, and in the extent of whitish speckling on the ventral abdomen and chin.

Distribution and Natural History. Typically found on rocks in small- to medium-sized rainforest streams with moderate flow velocity and on rocks along the stream banks. The call of the species is not known, nor are any data available on its reproductive habits. It is currently only known from Marojejy National Park at low elevation (Fig 2).

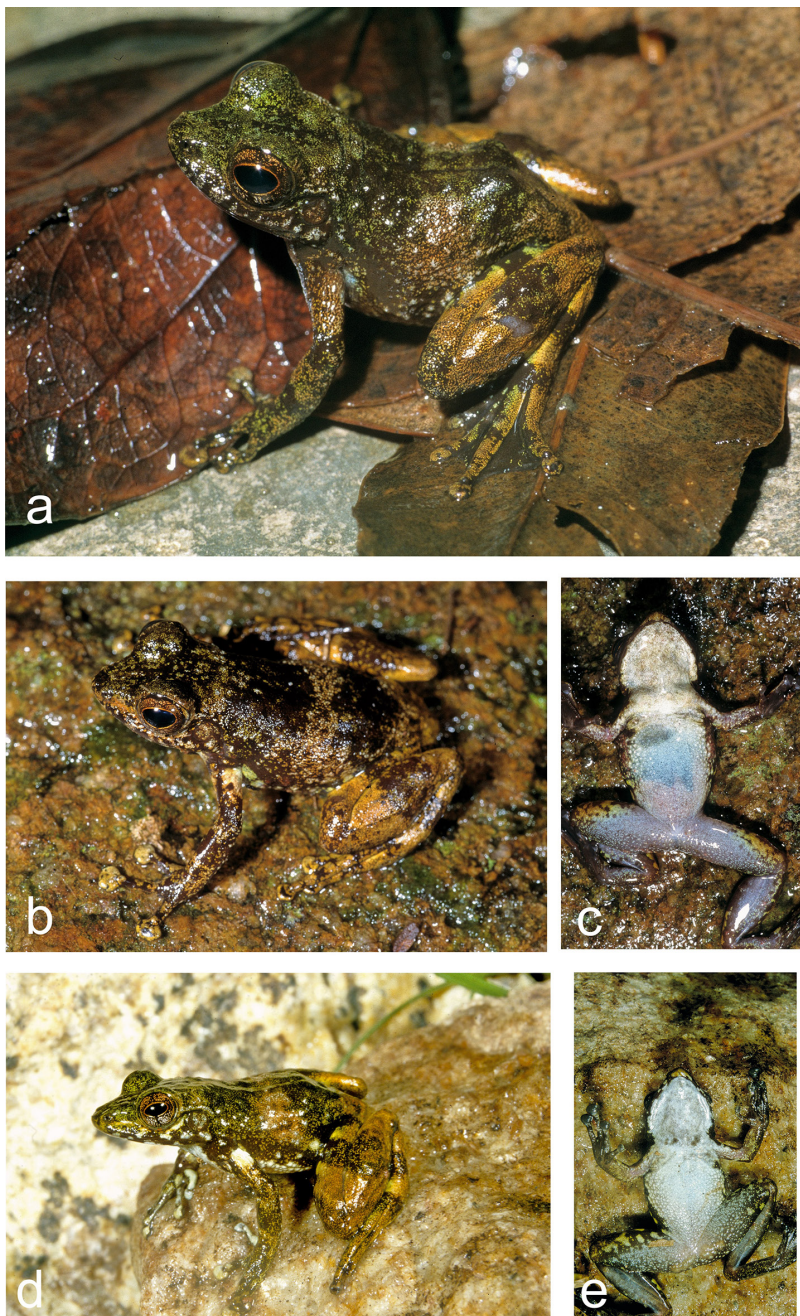


Fig 8. Specimens of *Mantidactylus atsimo* sp. nov. from south-eastern Madagascar in life.

(a) a specimen from Nahampoana photographed 2001, (b–c) holotype ZSM 69/2004 from Andohahela Camp 1, photographed 2004, (d–e) specimen from near Tolagnaro (Pic St Louis) photographed 1991.



Fig 9. Specimens of *Mantidactylus* sp. Ca48 in life.

(a–b) specimen from Ranomafana, photographed 2003; (c–d) specimen from Ranomafana, photographed 2003; (e–f) specimen from Antoetra, photographed 2003; (g–h) specimen from Antoetra, photographed 2003; (i) specimen from Itremo, photographed 2001; (j) specimen from Ranomafana, photographed 2003; (k) tadpole from Antoetra, photographed 2003.

Pic St. Louis (25.0106°S , 46.9731°E , 365 m a.s.l.), Anosy Region, southeastern Madagascar, in December 2001 by M. Vences. ZFMK 52686–9, a subadult, two females, and a juvenile, respectively, all collected near the peak of Pic St. Louis and the forest near Nahampoana in southeastern Madagascar on 22–27 February 1991 by F. Glaw and M. Vences. ZFMK 53673–9, seven female specimens, all collected near the peak of Pic St. Louis and the forest near Nahampoana in southeastern Madagascar between 22 December 1991 and 12 March 1992 by F. Glaw and J. Müller.

Referred material. ZSM 367–368/2016 (ZCMV 14843–14844), two adult males, collected in Sampanandrano (24.1399°S , 47.0742°E , 539 m a.s.l.), Anosy Region, southern Madagascar, on 16 December 2016 by A. Rakotoarison, E. Rajeriarison, and J.W. Ranaivosolo.

Etymology. The specific epithet is a Malagasy word meaning ‘south’. It is treated as an invariable noun in apposition to the genus name.

Diagnosis. *Mantidactylus atsimo* sp. nov. differs from all other species of *Mantidactylus*, subgenus *Hylobatrachus*, by a divergence of 4.7–6.1% uncorrected pairwise distance in a fragment of the 16S gene (uncorrected pairwise distances of *M. atsimo* to *M. cowani* (6.1%), to *M. lugubris* (4.7%), to *M. petakorona* (5.5%). The new species is characterised by the possession of the following characters: (1) SVL 25–35 mm, (2) banded dorsal colouration, (3) relatively long snout, pointed in lateral view, (4) moderately sized eyes ($\text{ED}/\text{HL} = 0.35–0.46$), (5) fully webbed feet, and

(6) whitish venter without dark brown markings. Females also have comparatively shallow snouts.

Among members of the subgenus *Hylobatrachus*, *M. (H.) atsimo* can be distinguished from *M. cowanii* as defined by Glaw and Vences [7,11] by its generally smaller adult SVL (25–35 mm versus 34–39 mm) and lack of rather consistent white dorsal and lateral spotting (vs. presence); from *M. lugubris* by lighter belly colouration, larger brown flecks on males, smaller relative tympanum size in males (TD/ED 0.58–0.66 vs. 0.71–0.91) and females (TD/ED 0.41–0.60 vs. 0.60–0.71), females with a rounded, slightly protruding snout (vs. acute snout); and from *M. petakorona* by slightly longer relative snout length in males (END/SVL 0.11–0.12 vs. 0.09–0.10) and typically whitish ventral colouration (vs. dark coloured), discs of third finger broader (pad of third toe ca. twice as broad as finger vs. ca. 1.5 times as broad), snout pointed in ventral view (vs. truncate) in females.

Description of the holotype. Adult female in good state of preservation; SVL 34.5 mm; body relatively slender; head slightly longer than wide (HW/HL 0.92), slightly wider than the body; snout rounded in dorsal view, slightly pointed in lateral view; nostrils directed laterally, protuberant, nearer to tip of snout than to eye; canthus rostralis distinct, slightly curved; loreal region concave; tympanum distinct, circular, its horizontal diameter 41% of eye diameter; supratympanic fold slightly distinct; tongue taken as tissue sample; maxillary teeth present; vomerine odontophores distinct, one rounded patch on each side of buccal roof, positioned posteromedial to choana; choanae small, rounded. Arms slender, subarticular tubercles indistinct, single; inner metacarpal tubercle and outer metacarpal tubercle not clearly recognizable; fingers without webbing; comparative finger length 1<2<4<3, second finger distinctly shorter than fourth finger; finger disks distinctly enlarged. Hindlimbs slender with a robust thigh; tibiotarsal articulation reaches the eye when the hindlimb is adpressed forward along the body; lateral metatarsalia separated by webbing; comparative toe length 1<2<3<5<4; fifth toe slightly longer than third toe; inner metatarsal tubercle slightly distinct, outer metatarsal tubercle not recognizable; toes completely webbed, formula 1 (0), 2i (0), 2e (0), 3i (0), 3e (0), 4i (0), 4e (0), 5 (0). Dorsal skin smooth; dorsum without dorsolateral folds; ventral skin smooth on the chin but granular over the abdomen and in the cloacal region; no distinct tubercles in the cloacal region. For measurements see Table 1.

In preservative (Fig 7), dorsal colour chocolate brown, lighter over the head and one band on the mid-body; flanks transitioning from dorsal to ventral from chocolate brown to burnt umber, with a moderately distinct colour border at the junction of the ventral colouration, which is a pale cream over the anterior body and more yellowish posteriorly and on the ventral legs, where it mixes with brown. The forelimbs are dorsally as the trunk in colour, and ventrally cream except on the hands, which are brown. The toe pads are a brown-grey, both on hands and feet. The hindlimbs are banded dark brown, milky brown, and red-brown. When the leg is bent (at rest), these crossbands line up to form consistent bands over thigh, shank, and foot. The hidden surfaces of the legs are chocolate brown as the dorsum, and the anterior thigh also has large blotches of burnt umber bordered in pale cream. The webbing is drab brown in colour.

Colouration in life (Fig 8b–c) was much more vibrant and contrasting in colour than in preservative, but the pattern was the same. The dorsal trunk was dark burnt umber with chocolate-brown band at mid-body and speckled chocolate on the head. A honey-brown stripe was present in the loreal region. The forelimb was as the dorsum in colouration, with a cream spot near the axilla, and a yellow-green marking on the flank beside the axilla. The dorsal hindlimbs were honey-brown cross-banded with burnt umber. The venter was taupe over the posterior abdomen and hindlimbs, bluish over the anterior abdomen, and dirty white on the chin and pectoral region. The iris was bronze.

Results

Variation. Individuals morphologically studied in detail include six female paratypes and two males tentatively attributed to *M. atsimo* (Table 1). Males appear to be slightly smaller than females (25 and 28 mm vs. 31–35 mm). Femoral glands are moderately distinct in males (Fig 8e). Colour patterns are relatively similar among all ZSM paratypes, including the presence of crossbands on the body and hindlimbs, and the presence of distinct light spots in the axilla. Ventral colouration is more variable, with most specimens having white chins except ZSM 174/2002, 149/2004 and 150/2004. ZSM 149/2004 has an unusual pathology of the right thigh, with a large subcutaneous growth. Specimens from the Anosy mountains that are tentatively assigned to this species differ in possessing dark spots on their venters, white toe tips, and distinct femoral glands in males (ZSM 367/2016 and 368/2016).

Natural History. Typically found on rocks in small to medium sized rainforest streams with moderate flow velocity and on rocks along the stream banks, also in heavily degraded forest near the peak of Pic St. Louis. During the day, females were sitting on rocks close to the water level. When disturbed, the frogs jump across the surface of the water at great velocity, coming to rest only at the next available rock (again at the water level). This way, they were able to cross a stream of several metres widths within a few seconds. They avoid diving in the water, probably due to high predation pressure (e.g. by large aquatic crustaceans). Almost all collected specimens were females, suggesting different habits of males and females. The calls and the clutches of the species

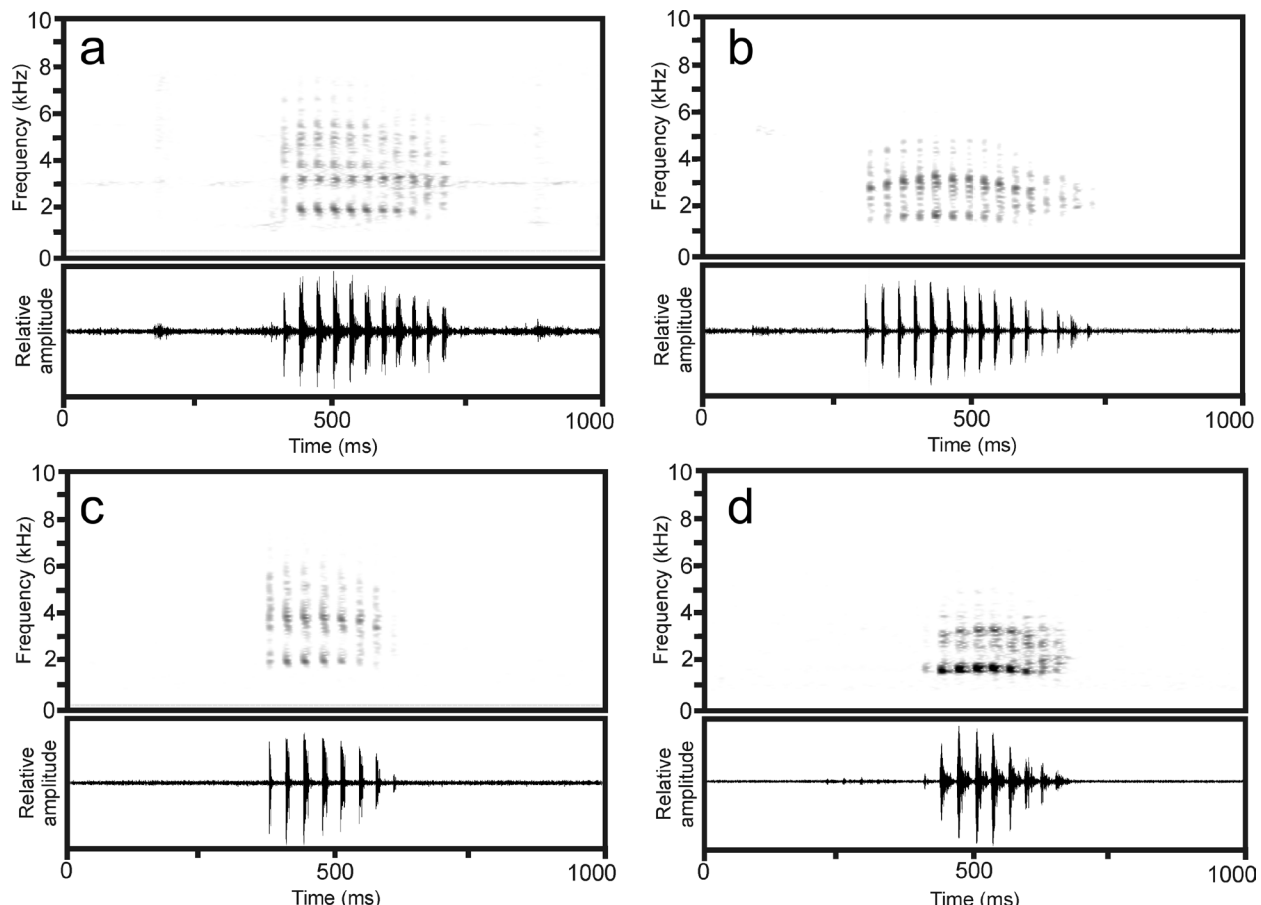


Fig 10. Spectrograms and oscillograms of calls of members of *Mantidactylus* (*Hylobatrachus*).

(a) A call of *Mantidactylus* sp. (*lugubris* or *cowanii*), recorded on 14 January 1995 near Andasibe at 22.1°C air temperature; (b) a call of *Mantidactylus lugubris*, recorded on 15 January 2016 in Vohidrazana at 17.3°C air temperature; (c) a call tentatively assigned to *Mantidactylus* sp. Ca48, recorded on 10 February 1997 in Ifanadiana at 21°C air temperature; (d) a call tentatively assigned to *Mantidactylus* sp. Ca48, recorded on 29 October 1995 in Ranomafana village at 27.2°C air temperature, bandpass filtered (800–9000 Hz).

are unknown. The blackish and elongated tadpoles were roughly described by Glaw and Vences (1994, page 167 and Figs 192, 193, Tad 28) based on individuals from near the peak of Pic St. Louis and Nahampoana. They are exotrophic and live on the ground of the streams. The highly specialised mouthparts without horny beak and labial teeth appear to be a filter apparatus. Metamorphosis was observed in December/January and juveniles measured 10–11 mm SVL.

Distribution. Currently known from Andohahela, Manantantely, Nahampoana, and Pic St Louis, all in southeastern Madagascar. Specimens from Sampanandrano in the Anosy mountains referred to this species require taxonomic clarification, but these expand the distribution of this species considerably northwards.

Vocalizations in Hylobatrachus

Despite being relatively common along rocky streams in Madagascar's rainforests, *Hylobatrachus* are bioacoustically remarkably inconspicuous. Only on few occasions have advertisement calls been recorded. These calls are described in the following, to provide a baseline for future bioacoustic comparisons in this group of frogs.

Mantidactylus sp. (probably *lugubris*, but might refer to *cowanii* which also occurs in nearby areas). – Two calls recorded from a male (not collected), sitting on a tree trunk ca. 2 m above the water level of a quietly running stream, on 14 January 1995 near Andasibe (at the border of Analamazaotra reserve) by F. Glaw, at 22.1°C air temperature (one call provided by Vences et al. [32]: CD2, Track 88, Cut 4) each consist of a single short, strongly and regularly pulsed note (Fig 10a) with the following parameters: note duration (= call duration) 314–320 ms; 11 pulses/note; pulse duration varies from 14–18 ms; inter-pulse intervals 12–18 ms; pulse repetition rate is 34–35 pulses/s; dominant frequency 1520–2020 Hz; prevalent bandwidth 1500–7200 Hz. Moderate amplitude modulation is recognizable among pulses, with the initial pulse emitted with much lower energy, followed by 3–4 pulses with high amplitude that decreases slightly in subsequent pulses towards the end of the note. Call repetition rate of reasonably motivated calls unknown.

Mantidactylus lugubris. – Two calls recorded at night on 15 January 2016 at Vohidrazana by C. Hutter, at 17.3°C air temperature, from a male confirmed by its typical colour pattern to be *M. lugubris* (voucher specimen CRH1293) each consist of a single short, strongly and regularly pulsed note (Fig 10b) and have the following parameters: note duration (= call duration) 428–430 ms; 15 pulses/note; pulse duration varies from 9–14 ms, with initial pulses of a note being the shortest; inter-pulse intervals 18–24 ms; pulse repetition rate ca. 32–35 pulses/s; dominant frequency 1540–1690 Hz; prevalent bandwidth 1400–6500 Hz. Amplitude modulation is recognizable among pulses, with highest energy present in fourth pulse of the note. Frequency modulation is apparent within notes, with dominant frequency slightly increasing from the beginning to the middle of the note, and continuing with dropping dominant frequency towards the end of the note, reaching a slightly lower level than that of the beginning. Call repetition rate of reasonably motivated calls is unknown.

Mantidactylus sp. cf. Ca48. – Calls are tentatively assigned to this candidate species based on the recording localities as in this region of Madagascar (Ranomafana region) only this lineage of *Hylobatrachus* has so far been identified (no calling voucher specimens available).

Seven calls recorded on 10 February 1997 in Ifanadiana by F. Andreone (partly provided in Vences et al. 2006: CD2, Track 88, Cuts 1–3) at 21°C air temperature each consist of a single short,

Results

strongly and regularly pulsed note (Fig 10c) and have the following parameters: note duration (= call duration) 217–248 ms (240 ± 11 ms, $n = 7$), 7–8 pulses/note ($n=7$); pulse duration varies from 4–15 ms (10 ± 3 ms, $n = 55$), with the initial pulse of a note being the shortest; inter-pulse intervals 19–28 ms (24 ± 2 ms, $n = 48$); pulse repetition rate 32.3–33.8/s (32.7 ± 0.5 /s, $n = 7$); dominant frequency 1860–2050 Hz; prevalent bandwidth 1600–7000 Hz. Slight amplitude modulation is recognizable among pulses, with highest energy present in third and fourth pulses of the note.

Three calls recorded on 29 October 1995 at Ranomafana village by J. Köhler at 27.2°C air temperature (23°C water temperature) each consist of a single short, strongly and regularly pulsed note (Fig 10d) and have the following parameters: note duration (= call duration) 235–284 ms; 8–9 pulses/note; pulse duration varies from 10–14 ms, with initial pulses of a note being the shortest; inter-pulse intervals 19–22 ms; pulse repetition rate app. 29–32 pulses/s; dominant frequency 1540–1690 Hz; prevalent bandwidth 1350–6500 Hz. Amplitude modulation is recognizable among pulses, with highest energy present in third and fourth pulses of the note. Compared to the call from Ifanadiana, pulses appear to be less well spaced, but this is probably due to echo effects in the stony river bed of the Ranomafana river where the recording was obtained. Call repetition rate of reasonably motivated calls is unknown.

Discussion

*First steps toward resolving the taxonomy of *Hylobatrachus*, and its integrative future*

The frogs of the subgenus *Hylobatrachus* are among the most enigmatic members of the genus *Mantidactylus*. Their reproductive habits are poorly known, as are their highly specialised tadpoles [12], vocalization and diet. Only one species was recognised as valid until Glaw and Vences [7] resurrected *M. cowanii* from synonymy with *M. lugubris*. Genetic evidence revealed that this was still a considerable underrepresentation of the species diversity of this subgenus, and that several new candidate species exist within it [8]. Small sample sizes and the aforementioned poor knowledge concerning these frogs hampered that revision, and only now has it been possible to assemble the modest sample size we report from just the two candidate species addressed here.

In this revision, we have described the two new species, *M. petakorona* and *M. atsimo*. Both have been recognised as potentially distinct since at least 2007 [11]. *Mantidactylus petakorona*, characterised by a distinct short snout and large eyes, is restricted to Marojejy, and is the northern-most representative of the subgenus, while *M. atsimo*, characterised by a typically white belly and dorsal crossbands, as well as complete webbing of its feet, is the southern-most representative. We have here refrained from revisiting the taxonomy of *M. cowanii* and *M. lugubris*, for which large sample sizes are available, as those taxa are currently considered relatively stable. However, we note that the description of the lineage called *M. sp. Ca48* will require the careful reassessment of the assignment of these names, given its wide distribution and similarity to those species. The identity of the candidate species *M. sp. Ca50*, *M. sp. Ca53*, and *M. sp. Ca54* will also require future efforts, as those lineages are currently known from only few samples.

Recordings of calls of these frogs are rare and hard to get. The sparse bioacoustic data available do not contribute much to the understanding of species limits in *Hylobatrachus*, as they provide an ambiguous and inconclusive picture. Comparison of calls referred reliably or tentatively assigned to *M. lugubris* with those corresponding to *M. sp. Ca48* reveals slight differences in numerical parameters (e.g., note duration, number of pulses per note). The greatest difference is that *M. lugubris* calls have a larger number of pulses than *M. sp. Ca48* (11–15 vs. 7–9 pulses), but the general call structure of all the calls recorded is very similar and usually would not qualify as species-specific differences, particularly not among allopatric populations (see Köhler et al. 2017). However, this picture may change once more call recordings become available, and deserves future attention.

While we have succeeded in identifying morphological characters differentiating these species, we have also shown that haplotype sharing in at least some nuclear genes is rather high within this subgenus. It is in this light that we emphasise that future testing may falsify some of our results. For example, the identity of the specimens here tentatively referred to *M. atsimo* from Sampanandranano in the Anosy Mountains will require future study to clarify, as these specimens, though genetically closely related to *M. atsimo* from Andohahela and other areas further south, differ in having dark spots on their venters, rather than the white that is typical of *M. atsimo* and one of the most valuable taxonomic characters of that species. Nevertheless, we consider the proposed new species here likely to be robust, given their high mitochondrial divergence and concordance with morphological differences.

Biogeographically, the genus *Hylobatrachus* presents an interesting pattern that is worthy of cursory remark: The known diversity of this subgenus is distributed from the far southeast of Madagascar to Marojejy in the north, and exceptionally in two locations in the highlands of central Madagascar, Itremo and Ambohitantely. It is curious that no representatives have yet been found in any part of the northwestern end of the eastern escarpment, that is, the chain of mountains that runs from Anjanaharibe-Sud northwest to Tsaratanana, then southwest to Manongarivo, and northeast to Sorata. All other subgenera of *Mantidactylus*, except the monotypic *Maitsoamantis*, are represented in this region by at least one species, yet for some reason *Hylobatrachus* is apparently not. Rather than speculating on why this might be, we here simply highlight this as a point of interest and recommend that it be investigated in detail in the future. As fieldwork in this area has been less intense than in eastern Madagascar, there is a chance that *Hylobatrachus* have simply been overlooked. However, it is also evident that *Hylobatrachus* is absent in the well-studied northernmost Malagasy rainforest of Montagne d'Ambre.

The need for changes to the way the IUCN Red List treats species complexes

We recently re-assessed *Mantidactylus cowanii* and *M. lugubris* as Near Threatened and Least Concern, respectively, but while we considered only specimens confidently assigned to the former species (and validated by the genetic results presented here), the assessment of *M. lugubris* was based on a broad circumscription that includes several undescribed candidate species. On the one hand, this strategy had the benefit of including undescribed lineages that would otherwise go unassessed until described, but on the other hand it resulted in an assessment that is inaccurate for the species for which it is intended. This raises the issue of best practices for IUCN assessments for known species complexes.

According to the IUCN Standards and Petitions Subcommittee [3], species with complicated or uncertain taxonomy should either be regarded a priori as ‘good species’, or should be omitted from the Red List. However, where a taxon is known to consist of multiple species-level lineages, i.e. in a species complex, the guidelines are somewhat ambiguous. The relevant recommendation reads: ‘Where a species name is widely accepted as containing multiple taxa that may deserve species-level recognition (a “species complex”) AND there is insufficient information (direct or indirect) to apply the Red List Categories and Criteria, the “species complex” should be listed as Data Deficient’ [3]. Treated as an a priori ‘good species’, there is often enough data to assess a species complex under Criterion B, pertaining to geographic range and trends of decreasing habitat, range, or population. However, as we have outlined, and as discussed by McLeod [4], this is not valuable. But if being a species complex constitutes sufficient uncertainty that it can be considered ‘insufficient information’, then most complexes should be Data Deficient (DD). Following this logic strictly, a very large proportion of Madagascar’s frogs (not to mention innumerable other taxa, both in Madagascar and worldwide) would still be considered Data Deficient (DD).

We suggest two ways of handling species complexes that may help to reduce ambiguity and

Results

over-estimation, while at the same time minimising the need for DD status for species that do not warrant that categorisation. (1) Where species complexes consist of a moderately clear nominal species and a number of undescribed candidate species that have at least partly been characterised (e.g. clearly distinct genetic units from the nominal species), we suggest that the assessment of the species should, as far as possible, be restricted to the nominal form and candidate species should remain omitted from the Red List altogether. (2) Where the identity of nominal species within the species complex is unclear, the complex should be assessed as DD.

Taxonomy is the foundation of the IUCN Red List, and indeed much species-directed conservation planning. Without a solid foundation for the units to which assessments are applied (species), they cannot be used in conservation practice [33, 34]. Providing non-DD assessments for species complexes can amount to pseudo-precision, for example by overestimating species distribution and population statuses (as for *Mantidactylus lugubris*, but also e.g. *Dendropsophis minutus* [35] and *Scinax ruber* [36]), while omitting taxa from the Red List can lead to their being forgotten for future assessments. Thus, the statement that ‘taxonomic uncertainty alone is not a reason for listing as Data Deficient’ [37], while true according to the current recommendations, belies the importance of taxonomy in anchoring conservation assessments. Despite IUCN guidelines discouraging the ‘liberal use’ of DD [38], it is a valuable category, especially when the justification is taxonomic in nature. It highlights the importance of taxonomy in facilitating and promoting conservation. DD species are also valuable in the establishment of priority areas for research, including taxonomic work [39]. Numerous studies have attempted to use modelling or other approaches to extract conservation priorities from DD species (e.g. [39-42]), but an emphasis on the importance of clarifying taxonomic conundrums has been lacking.

*Revising and refining the IUCN Red List assessments of *Hylobatrachus* species, and the future for yet undescribed candidate species*

Following the description of the two new species provided here, we can also suggest modifications of the IUCN Red List assessment of all three species. *Mantidactylus lugubris*, as currently understood, is distributed from Ambatorama and Ambodirafia in the north Central East, to Vohimana, Vohidrazana, and Mantadia in the Central East; all other regions currently included in the IUCN status of that species refer to other species. As such, it has an EOO of ca. 7000 km², although it probably occurs more widely in, for example, the poorly surveyed Zahamena National Park. As is currently included in its assessment, the species ‘requires clear streams and so cannot survive in fully transformed agricultural landscapes,’ and its habitat is experiencing on-going habitat decline. It therefore qualifies for a status of Vulnerable under IUCN Red List criterion B1ab(iii).

Mantidactylus petakorona is found in Marojejy National Park and is currently not known from any other locations. It occurs in streams at low-elevation. We here follow the assessments for other species from this area, e.g. *Rhombophryne savaka*, in considering the species Endangered under criterion B1ab(iii), due to an estimated Extent of Occurrence (EOO) of < 1000 km², records from a single threat-defined location, and on-going decline in the extent and quality of appropriate habitat.

Mantidactylus atsimo is found in five threat-defined locations in southeastern Madagascar, including Anosy, Andohahela, Manantantely, Pic St. Louis, and Nahampoana. These span an estimated EOO of ca. 4500 km². Throughout this area, there is, however, dramatic habitat decline, with extensive deforestation. The species is thus a borderline case between Endangered and Vulnerable under B1ab(iii). A small extension of its known range northwards would render its EOO over 5000 km². We therefore conservatively propose a status of Vulnerable B1ab(iii) for *M. atsimo*.

The remainder of the recognised candidate species within the subgenus *Hylobatrachus* cannot be assessed while they remain undescribed. This too emphasises the importance of taxonomy, as well as the importance of continued field collections. Species that are undescribed cannot be

adequately protected. Recognition of candidate species does not constitute description, and while candidate species can be included on faunistic lists to lend weight to the importance of protecting certain areas (e.g. [26, 43, 44], they remain unavailable for species-level management. The extensive availability of characterised candidate species of reptiles and amphibians is exceptional in Madagascar [8, 10, 45], giving conservation on the island an edge, but the importance of taxonomic assessment of these species remains unabated. Elsewhere, DNA barcoding can also be used as a first line for species discovery, but except at landscape conservation levels, taxonomic description of the discovered species will be needed to ensure their protection.

Acknowledgments

We are grateful to numerous colleagues, students and field assistants who have accompanied us in the field during the numerous expeditions needed to obtain the material analyzed here, in particular F. Andreone, P. Bora, A. Conover, S. Lambert, J. Müller, J. Steinbrecher, M. Puente, N. Rabibisoa, O. Ramilison, J.E. Randrianirina, R.D. Randrianiaina, F. Ratsoavina, A. Razafimanantsoa, M. Thomas, D. Vallan, and D.R. Vieites. This work was carried out in collaboration with the Mention Zoologie et Biodiversité Animale, Université d’Anananarivo. We are grateful to the Malagasy authorities for research, collection and export permits.

References

1. Hebert PDN, Cywinska A, Ball SL, DeWaard JR. Biological identifications through DNA barcodes. *Proceedings of the Royal Society of London B*. 2003;270(1512):313–21. doi: 10.1098/rspb.2002.2218.
2. Ruane S, Austin CC. Phylogenomics using formalin-fixed and 100+ year-old intractable natural history specimens. *Molecular Ecology Resources*. 2017;17(5):1003–8. doi: 10.1111/1755-0998.12655.
3. IUCN Standards and Petitions Subcommittee. Guidelines for using the IUCN Red List categories and criteria. Version 13. Gland, CH: IUCN; 2017.
4. McLeod DS. Of Least Concern? Systematics of a cryptic species complex: *Limnonectes kuhlii* (Amphibia: Anura: Dic平glossidae). *Molecular Phylogenetics and Evolution*. 2010;56:991–1000. doi: 10.1016/j.ympev.2010.04.004.
5. Vences M, Thomas M, Bonett RM, Vieites DR. Deciphering amphibian diversity through DNA barcoding: chances and challenges. *Philosophical Transactions of the Royal Society B*. 2005;360:1859–68. doi: 10.1098/rstb.2005.1717.
6. Vences M, Thomas M, van der Meijden A, Chiari Y, Vieites DR. Comparative performance of the 16S rRNA gene in DNA barcoding of amphibians. *Frontiers in Zoology*. 2005;2:5. doi: 10.1186/1742-9994-2-5.
7. Glaw F, Vences M. Phylogeny and genus-level classification of mantellid frogs (Amphibia, Anura). *Organisms Diversity & Evolution*. 2006;6(3):236–53. doi: 10.1016/j.ode.2005.12.001.
8. Vieites DR, Wollenberg KC, Andreone F, Köhler J, Glaw F, Vences M. Vast underestimation of Madagascar’s biodiversity evidenced by an integrative amphibian inventory. *Proceedings of the National Academy of Sciences of the USA*. 2009;106(20):8267–72. Epub 2009/05/07. doi: 10.1073/pnas.0810821106. PubMed PMID: 19416818; PubMed Central PMCID: PMC2688882.
9. Wollenberg KC, Vieites DR, Glaw F, Vences M. Speciation in little: the role of range and body size in the diversification of Malagasy mantellid frogs. *BMC Evolutionary Biology*. 2011;11:217. Epub 2011/07/23. doi: 10.1186/1471-2148-11-217. PubMed PMID: 21777445;

Results

- PubMed Central PMCID: PMC3199771.
10. Perl RGB, Nagy ZT, Sonet G, Glaw F, Wollenberg KC, Vences M. DNA barcoding Madagascar's amphibian fauna. *Amphibia-Reptilia*. 2014;35:197–206. doi: 10.1163/15685381-00002942.
 11. Glaw F, Vences M. A field guide to the amphibians and reptiles of Madagascar. 3rd Edition ed. Cologne, Germany: Vences & Glaw Verlags GbR; 2007. 496 p.
 12. Altig R, McDiarmid RW. Descriptions and biological notes on three unusual mantellid tadpoles (Amphibia: Anura: Mantellidae) from southeastern Madagascar. *Proceedings of the Biological Society of Washington*. 2006;119(3):418–25.
 13. Blommers-Schöller RMA. Biosystematics of the Malagasy frogs. I. Mantellinae (Ranidae). *Beaufortia*. 1979;352:1–77.
 14. Blommers-Schöller RMA, Blanc CP. Amphibiens (duxième partie). *Faune de Madagascar*. 1993;75(2):385–530.
 15. Guibé J. Les batraciens de Madagascar. *Bonner zoologische Monographien*. 1978;11:1–140.
 16. Blommers-Schöller RMA, Blanc CP. Amphibiens (première partie). *Faune de Madagascar*. 1991;75(1):1–397.
 17. Köhler J, Jansen M, Rodríguez A, Kok PJR, Toledo LF, Emmrich M, et al. The use of bioacoustics in anuran taxonomy: theory, terminology, methods and recommendations for best practice. *Zootaxa*. 2017;4251(1):1–124. doi: 10.11646/zootaxa.4251.1.1.
 18. Bruford MW, Hanotte O, Brookfield JFY, Burke T. Single-locus and multilocus DNA fingerprint. In: Hoelzel AR, editor. *Molecular Genetic Analysis of Populations: A Practical Approach*. Oxford: IRL Press; 1992. p. 225–70.
 19. Palumbi SR, Martin A, Romano S, McMillan WO, Stice L, Grabowski G. The simple fool's guide to PCR, Version 2.0. University of Hawaii: Privately published; 1991.
 20. Vences M, Kosuch J, Glaw F, Böhme W, Veith M. Molecular phylogeny of hyperoliid treefrogs: biogeographic origin of Malagasy and Seychellean taxa and re-analysis of familial paraphyly. *Journal of Zoological Systematics and Evolutionary Research*. 2003;41:205–15. doi: 10.1046/j.1439-0469.2003.00205.x.
 21. Vences M, Hildenbrand A, Warmuth KM, Andreone F, Glaw F. A new riparian *Mantidactylus (Brygoomantis)* frog from the Tsaratanana and Manongarivo Massifs in northern Madagascar. *Zootaxa*. 2018;4486(4):575–88. doi: 10.11646/zootaxa.4486.4.10.
 22. Kumar S, Stecher G, Tamura K. MEGA7: Molecular Evolutionary Genetics Analysis version 7.0 for bigger datasets. *Molecular Biology and Evolution*. 2016;33(7):1870–4. doi: 10.1093/molbev/msw054.
 23. Darriba D, Taboada GL, Doallo R, Posada D. jModelTest 2: more models, new heuristics and parallel computing. *Nature Methods*. 2012;9:772.
 24. Librado P, Rozas J. DnaSP v5: A software for comprehensive analysis of DNA polymorphism data. *Bioinformatics*. 2009;25:1451–2. doi: 10.1093/bioinformatics/btp187.
 25. Salzburger W, Ewing GB, Von Haeseler A. The performance of phylogenetic algorithms in estimating haplotype genealogies with migration. *Molecular Ecology*. 2011;20:1952–63. doi: 10.1111/j.1365-294X.2011.05066.x.
 26. Cocca W, Rosa GM, Andreone F, Aprea G, Bergò PE, Mattioli F, et al. The herpetofauna (Amphibia, Crocodylia, Squamata, Testudines) of the Isalo Massif, Southwest Madagascar: combining morphological, molecular and museum data. *Salamandra*. 2018;54:178–200.
 27. Avise JC, Ball RM. Principles of genealogical concordance in species concepts and biological taxonomy. In: Futuyma D, Antonovics J, editors. *Oxford surveys in evolutionary biology*. Ox-

- ford, UK: Oxford University Press; 1990. p. 45–67.
- 28. Rakotoarison A, Scherz MD, Glaw F, Köhler J, Andreone F, Franzen M, et al. Describing the smaller majority: Integrative fast-track taxonomy reveals twenty-six new species of tiny microhylid frogs (genus *Stumpffia*) from Madagascar. *Vertebrate Zoology*. 2017;67(3):271–398.
 - 29. Vences M, Köhler J, Pabijan M, Bletz M, Gehring P-S, Hawlitschek O, et al. Taxonomy and geographic distribution of Malagasy frogs of the *Gephyromantis asper* clade, with description of a new subgenus and revalidation of *Gephyromantis ceratophrys*. *Salamandra*. 2017;53(1):77–98.
 - 30. Boulenger GA. Catalogue of the Batrachia Salientia s. Ecaudata in the Collection of the British Museum. 2nd Edition ed. London, UK: Taylor and Francis; 1882.
 - 31. Fouquet A, Gilles A, Vences M, Marty C, Blanc M, Gemmell NJ. Underestimation of species richness in neotropical frogs revealed by mtDNA analyses. *PLoS One*. 2007;2(10):e1109. doi: 10.1371/journal.pone.0001109.
 - 32. Vences M, Glaw F, Marquez R, editors. The Calls of the Frogs of Madagascar. 3 Audio CD's and booklet. Madrid, Spain: Fonoteca Zoológica; 2006.
 - 33. Vogel Ely C, de Loreto Bordignon SA, Trevisan R, Boldrini II. Implications of poor taxonomy in conservation. *Journal for Nature Conservation*. 2017;36:10–3. doi: 10.1016/j.jnc.2017.01.003.
 - 34. Dubois A. The relationships between taxonomy and conservation biology in the century of extinctions. *Comptes Rendus Biologies*. 2003;326:9–21. doi: 10.1016/S1631-0691(03)00022-2.
 - 35. Gehara M, Crawford AJ, Orrico VGD, Rodríguez A, Lötters S, Fouquet A, et al. High levels of diversity uncovered in a widespread nominal taxon: continental phylogeography of the Neotropical tree frog *Dendropsophus minutus*. *PLoS One*. 2014;9(9):e103958. doi: 10.1371/journal.pone.0103958.
 - 36. Fouquet A, Vences M, Salducci M-D, Meyer A, Marty C, Blanc M, et al. Revealing cryptic diversity using molecular phylogenetics and phylogeography in frogs of the *Scinax ruber* and *Rhinella margaritifera* species groups. *Molecular Phylogenetics and Evolution*. 2007;43(2):567–82. doi: 10.1016/j.ympev.2006.12.006.
 - 37. Butchart SHM, Bird JP. Data Deficient birds on the IUCN Red List: What don't we know and why does it matter? *Biological Conservation*. 2010;143(1):239–47. doi: 10.1016/j.biocon.2009.10.008.
 - 38. IUCN. IUCN Red List Categories and Criteria: Version 3.1. 2nd Edition ed. Gland, Switzerland and Cambridge, UK: IUCN; 2012.
 - 39. Nori J, Villalobos F, Loyola R. Global priority areas for amphibian research. *Journal of Biogeography*. in press. doi: 10.1111/jbi.13435.
 - 40. Howard SD, Bickford DP. Amphibians over the edge: silent extinction risk of Data Deficient species. *Diversity and Distributions*. 2014;20(7):837–46. doi: 10.1111/ddi.12218.
 - 41. Nori J, Loyola R. On the Worrying Fate of Data Deficient Amphibians. *PLoS One*. 2015;10(5):e0125055. doi: 10.1371/journal.pone.0125055.
 - 42. Jetz W, Freckleton RP. Towards a general framework for predicting threat status of data-deficient species from phylogenetic, spatial and environmental information. *Philosophical Transactions of the Royal Society B: Biological Sciences*. 2015;370(1662). doi: 10.1098/rstb.2014.0016.
 - 43. Penny SG, Crottini A, Andreone F, Bellati A, Rakotozafy LMS, Holderied MW, et al. Combining old and new evidence to increase the known biodiversity value of the Sahamalaza Peninsula, Northwest Madagascar. *Contributions to Zoology*. 2017;86(4):273–96.

Results

44. Rosa GM, Andreone F, Crottini A, Hauswaldt JS, Noël J, Rabibisoa NH, et al. The amphibians of the relict Betampona low-elevation rainforest, eastern Madagascar: an application of the integrative taxonomy approach to biodiversity assessments. *Biodiversity and Conservation*. 2012;21(6):1531–59. doi: 10.1007/s10531-012-0262-x.
45. Nagy ZT, Sonet G, Glaw F, Vences M. First large-scale DNA barcoding assessment of reptiles in the biodiversity hotspot of Madagascar, based on newly designed COI primers. *PLoS ONE*. 2012;7(3):e34506. Epub 2012/04/06. doi: 10.1371/journal.pone.0034506. PubMed PMID: 22479636; PubMed Central PMCID: PMC3316696.

Section 2: Biogeography through the lens of systematics

In this section, I present a series of papers pertaining to the genus *Gephyromantis* in northern Madagascar. These include descriptions of five new species of frogs, each giving insight into the biogeography of the group. Together, these taxonomic papers shed light on the biogeography of these frogs in northern Madagascar, and open interesting avenues for future research into the properties governing species distribution in the forests of northern Madagascar.

Chapter 2. PAPER: A new frog species of the subgenus *Asperomantis* (Anura, Mantellidae, *Gephyromantis*) from the Bealanana District of northern Madagascar

In this chapter, I present the description of a new species of *Gephyromantis* from the subgenus *Asperomantis*. This subgenus was recently described (Vences et al. 2017), with a candidate species identified from north Madagascar that was not taxonomically assessed because of inadequate material. In December 2015–January 2016, I collected additional material of this species, and in this chapter, my colleagues and I describe it in this chapter as *Gephyromantis (Asperomantis) angano*. It is found in two localities within the Bealanana District in the Diana Region of northern Madagascar. A population of frogs from the southwest of the Bealanana District is genetically only weakly differentiated from *G. (A.) angano* but is bioacoustically strongly different and is also slightly larger in size. We consider it to be a new candidate species in need of assessment—possibly these lineages constitute a case of incipient speciation that is in the process of being reinforced by intense deforestation in the region preventing connectivity among populations. We also find strong genetic differentiation between *G. (A.) ambohitra* populations from Montagne d'Ambre and Manongarivo, suggesting the need for work to assess the taxonomic status of these populations. Curiously, *G. (A.) tahotra*, which was found in sympatry with *G. (A.) angano* in the Bealanana District, lacks genetic differentiation from the population in Marojejy at the same elevation (Glaw et al. 2011), suggesting that these areas may have recent or on-going gene flow at elevations of ca. 1350 m a.s.l. No explanation is currently obvious for why *G. (A.) angano* does not appear to have a similar range, given that the two species have very similar ecologies.

Scherz, M.D., Vences, M., Borrell, J., Ball, L., Nomenjanahary, D.H., Parker, D., Rakotondratrima, M., Razafimandimby, E., Starnes, T., Rabearivony, J. & Glaw, F. (2017) A new frog species of the subgenus *Asperomantis* (Anura, Mantellidae, *Gephyromantis*) from the Bealanana District of northern Madagascar. *Zoosystematics and Evolution*, 93(2):451–466. DOI: 10.3897/zse.93.14906

Digital Supplementary Materials on appended CD:

Supplementary Material 1 — Recording 1

Supplementary Material 2 — Recording 2

Supplementary Material 3 — Recording 3

Supplementary Material 4 — Recording 4

Supplementary Material 5 — Figure S1

Supplementary Material 6 — Table S1

A new frog species of the subgenus *Asperomantis* (Anura, Mantellidae, *Gephyromantis*) from the Bealanana District of northern Madagascar

Mark D. Scherz^{1,2}, Miguel Vences², James Borrell³, Lawrence Ball⁴,
Denise Herizo Nomenjanahary⁵, Duncan Parker⁶, Marius Rakotondratsima⁷,
Elidiot Razafimandimby⁵, Thomas Starnes⁸, Jeanneney Rabearivony⁵, Frank Glaw¹

1 Zoologische Staatssammlung München (ZSM-SNSB), Münchhausenstr. 21, 81247 München, Germany

2 Zoologisches Institut, Technische Universität Braunschweig, Mendelssohnstr. 4, 38106 Braunschweig, Germany

3 School of Biological and Chemical Sciences, Queen Mary University of London, Mile End Road, London, E1 4NS, UK

4 The Durrell Institute of Conservation and Ecology, School of Anthropology and Conservation, Marlowe Building, The University of Kent, Canterbury, Kent, CT27NR, UK

5 Faculté des Sciences, Université d'Antsiranana, Antsiranana 201, Madagascar

6 Falcon Productions, 1 St Andrews Road, Bristol, BS6 5EH, UK

7 The Peregrine Fund's Project in Madagascar, B. P. 4113, Antananarivo 101, Madagascar

8 Amphibian and Reptile Conservation Trust, 655A Christchurch Road, Bournemouth BH1 4AP, UK

<http://zoobank.org/7EE704F2-05B4-48D1-AE41-929676D91E08>

Corresponding author: Mark D. Scherz (mark.scherz@gmail.com)

Abstract

Received 7 July 2017

Accepted 24 August 2017

Published 15 November 2017

Academic editor:

Johannes Penner

Key Words

Amphibia
Bioacoustics
Incipient speciation
Candidate species
Mantellinae

A recent study on a group of rough-skinned *Gephyromantis* frogs from Madagascar (Anura: Mantellidae: Mantellinae) established a new subgenus, *Asperomantis*, with five described species and one undescribed candidate species. Based on newly collected material from the Bealanana District, we address the taxonomy of this candidate species, and reveal that it consists of two populations with low genetic and morphological divergence but considerable bioacoustic differences that are obvious to the human ear. As a result, we describe some of the specimens formerly assigned to *Gephyromantis* sp. Ca28 as *G. angano* sp. n. and assign the remaining specimens from a locality between Bealanana and Antsohihy to a new Unconfirmed Candidate Species, *G. sp. Ca29*. *Gephyromantis angano* sp. n. is a small species that strongly resembles *G. asper* and *G. ceratophrys*, but it differs from these and all other *Gephyromantis* species by a unique, clinking advertisement call. The new species may be highly threatened by habitat fragmentation, but at present we recommend it be treated as Data Deficient until more data are available to assess its distribution. We discuss the curious relationship between *G. angano* sp. n. and *G. sp. Ca29*, which we suspect may represent a case of incipient speciation. We also identify two additional new Unconfirmed Candidate Species of *Gephyromantis* based on sequence data from other specimens collected during our surveys in the Bealanana District.

Introduction

Madagascar's 317 nominal frog species belong to six families: Mantellidae Laurent, 1946 (213 species), Microhylidae Günther, 1858 (91 species), Hyperoliidae Laurent, 1943 (11 species), Ptychadenidae Dubois, 1987 (1 species), Dicroidiidae Anderson, 1871 (1 species, introduced), and Bufonidae Gray, 1825 (1

species, introduced) (AmphibiaWeb 2017). Mantellidae is the island's most diverse radiation, and among the amphibians, the only family-level unit wholly endemic to Madagascar and the nearby Comoros (two undescribed species are found on nearby Mayotte; Vences et al. 2003). It is divided into three subfamilies, of which the Mantellinae Laurent, 1946 is the most diverse, comprising 129 species in seven genera. The most diverse of

these genera is *Gephyromantis* Methuen, 1920, with 42 nominal species.

Gephyromantis is currently divided into six subgenera: *Asperomantis* Vences, Köhler, Pabijan, Bletz, Gehring, Hawlitschek, Rakotoarison, Ratsoavina, Andreone, Crottini & Glaw, 2017, *Duboimantis* Glaw & Vences, 2006, *Gephyromantis* Methuen, 1920, *Laurentomantis* Dubois, 1980, *Phylacomantis* Glaw & Vences, 1994, and *Vatomantis* Glaw & Vences, 2006 (Kaffenberger et al. 2012, Vences et al. 2017). In their recent study, Vences et al. (2017) erected the subgenus *Asperomantis* for the *Gephyromantis asper* clade, which contains five nominal species: *G. ambohitra* (Vences & Glaw, 2001), *G. asper* (Boulenger, 1882), *G. ceratophrys* (Ahl, 1929), *G. tahoatra* Glaw, Köhler & Vences, 2011, and *G. spinifer* (Blommers-Schöller & Blanc, 1991). A sixth species that was identified by Perl et al. (2014), *G. sp. Ca28*, clearly belongs to this subgenus as well based on its morphology and genetic affinities (Vences et al. 2017). It was originally detected based on DNA sequences of a specimen from 'Antsahan'i Ledy', and later two additional specimens from a site between Bealanana and Antsohihy were added to it (Vences et al. 2017), but no adult male specimen or bioacoustic data have been available until now.

Here, we address the taxonomy of *G. sp. Ca28* using an integrative taxonomic approach based on bioacoustics, morphology, morphometrics, and genetics, from new material collected between December 2015 and January 2016. We also provide additional sequence data and new localities for a selection of *Gephyromantis* species encountered during the collection of the new species.

Materials and methods

Fieldwork was conducted at two sites: Ampotsidy mountains, near Beandradezona (14.410–14.432°S, 48.710–48.727°E) in the Bealanana District of the Sofia Region between the 17th of December 2015 and 9th of January 2016; and in several small forest fragments near the southern border of the Bealanana District (14.701–14.758°S, 48.493–48.587°E) between the 13th and 17th of January 2016. These two locations are separated by ca. 40 km.

Specimens were captured by hand, euthanized using MS222, fixed in ~90% ethanol, and kept thereafter in 75% ethanol. Prior to fixation, a piece of muscle from the thigh was taken as a tissue sample for subsequent DNA analysis, deposited in 99% ethanol. Field numbers refer to Mark D. Scherz (MSZC), Miguel Vences (ZCMV), and David R. Vieites (DRV). Institutional abbreviations are: ZSM (Zoologische Staatssammlung München), and UADBA-A (Université d'Antananarivo Département de Biologie Animale, Amphibiens).

Call recordings were made with a Sennheiser KE66+K6 super-cardioid microphone on a Marantz PMD 661 MKII field recorder, at 44.1 kHz sampling. Bioacoustic analysis was performed in COOL EDIT PRO. Frequency information was obtained through Fast Fourier Transformations

(FFT; width 1024 points). Spectrograms were obtained with a Hanning window of 512-bands resolution. Temporal measurements are given as mean ± standard deviation with range in parentheses. Terminology in call descriptions follows the call-centred terminology of Köhler et al. (2017). Recordings are deposited in the Animal Sound Archive of the Museum für Naturkunde, Berlin and are provided as Supplementary materials 1–4.

We analysed a segment of the mitochondrial DNA (mtDNA) 16S rRNA gene (*16S*). We used a salt-extraction protocol to extract DNA from tissue samples as described by Kaffenberger et al. (2012). We PCR-amplified the *16S* segment used as standard for barcoding Madagascan amphibians (Vences et al. 2005, Vieites et al. 2009) with the primer pairs AC16SAR-L/AC16SBR-H (Crottini et al. 2014) and 16SFrogL1/16SFrogH1 (Vences et al. 2010). Purification of PCR product was done using Exonuclease I and Shrimp Alkaline Phosphatase digestion. Amplicons were sequenced using the BigDye v. 3.1 cycle sequencing chemistry on a 3130xl genetic analyser (Applied Biosystems). Assembly and quality-checking was performed in CODONCODE ALIGNER v. 3.0.3 (CodonCode Corporation). Newly generated sequences were deposited in GenBank under accession numbers MF768444–MF768467.

Comparative sequences were retrieved from Vieites et al. (2009) and Vences et al. (2017), for almost all known *Gephyromantis* species including candidate species, for a total of 123 terminals. We aligned sequences using the ClustalW algorithm in MEGA7 (Kumar et al. 2016), with *Boophis madagascariensis* (Mantellidae: Boophinae) and *Guibemantis liber* (Mantellidae: Mantellinae) as hierarchical outgroups. Gaps were treated as missing data. Due to the short length of the alignment, hypervariable regions were not removed. Uncorrected pairwise distances (p-distances) between and within species in the *16S* dataset were calculated using MEGA7.

Phylogenies were calculated using Bayesian Inference (BI) in MRBAYES v. 3.2.6 (Ronquist et al. 2012) under the JC69 model in order to reduce the risk of over-parameterisation with our small dataset. The Markov chain Monte Carlo sampling included two runs of four chains each (three heated, one cold) sampled every 10³ generations for a total of 10⁶ generations. The first 25% of samples were discarded as burn-in. Parameter convergence was assessed in TRACER v 1.5 (Rambaut and Drummond 2007). For comparative purposes, we ran a maximum likelihood (ML) tree in RAXML (Stamatakis 2014) with 500 bootstrap replicates under the GTR+G model.

Morphometrics of the new material were obtained for comparison primarily with values reported by Vences et al. (2017). Measurements were taken by MV to the nearest 0.1 mm with a precision calliper, for the following characters (reiterated verbatim from Vences et al. 2017): snout–vent length (SVL), maximum head width (HW), head length from posterior maxillary commissure to snout tip (HL), horizontal eye diameter (ED), horizontal tympanum diameter (TD), distance from eye to nostril

(END), distance from nostril to snout tip (NSD), distance between nostrils (NND), foot length (FOL), foot length including tarsus (FOTL), hindlimb length from cloaca to tip of longest toe (HIL), forelimb length from axilla to tip of longest finger (FORL), length and width of femoral gland (FGL, FGW), and number of femoral gland granules (FGG) given as left/right. Webbing formulae follow Blommers-Schöller (1979); femoral gland terminology follows Glaw et al. (2000).

The electronic version of this article in Portable Document Format (PDF) will represent a published work according to the International Commission on Zoological Nomenclature (ICZN), and hence the new names contained in the electronic version are effectively published under that Code from the electronic edition alone. This published work and the nomenclatural act it contains have been registered in ZooBank, the online registration system for the ICZN. The ZooBank LSIDs (Life Science Identifiers) can be resolved and the associated information viewed through any standard web browser by appending the LSID to the prefix <http://zoobank.org/>. The LSID for this publication is urn:lsid:zoobank.org:pub:7EE704F2-05B4-48D1-AE41-929676D91E08. The online version of this work will be archived and made available from the following digital repositories: CLOCKSS and Zenodo.

Results

During fieldwork in Ampotsidy we encountered several *Gephyromantis* species. Most notable among these was an abundant species of the subgenus *Asperomantis*, with a characteristic, high pitched, clinking call. Later, during fieldwork ca. 40 km SSW, near the road between Bealanana and Antsohihy in a forest patch locally called Andranonafindra, we encountered another relatively abundant *Asperomantis* with a lower, rasping call, similar to that called '*Gephyromantis* sp. aff. *ambohitra*' in Vences et al. (2006). Genetically the former population is assignable to the first specimen of *G. sp.* Ca28 from Antsahan'i Ledy, whereas the latter is assignable to the specimens from between Antsohihy and Bealanana (very near Andranonafindra) added to this candidate species by Vences et al. (2017) (genetics are discussed and displayed in more detail below). We investigated whether these specimens represented one or two species using an integrative approach based on bioacoustics, morphology, and molecular phylogenetics.

Bioacoustics

Advertisement calls of the *Asperomantis* species from Ampotsidy and from Andranonafindra exhibited strong and clear differences in call parameters. To illustrate these differences, we here describe these calls:

Ampotsidy: Based on call voucher ZSM 68/2016 (MSZC 0172): Calls recorded at 22h40 on the 8th of January, 2016, 50 cm above the ground on a fern above a muddy spring in primary rainforest, calling as part of a

small chorus, at 14.41949°S, 48.71938°E, 1340 m a.s.l., at an estimated air temperature between 15 and 20°C (Fig. 1, Suppl. material 1). Call series are composed of 9–25 (mean 16.7 ± 6.5 , n = 6) rapidly emitted, short (call duration 41–98 ms, mean = 59.4 ± 10.4 ms, n = 27), unpulsed, tonal, single-note calls (call series duration 2798–5917 ms, n = 6), with silent inter-call intervals of 148–239 ms (mean 193 ± 22 ms, n = 25). The inter-series intervals are highly variable (26.0–64.2 s, 41.5 ± 20 s, n = 3). Before some call series, one or two pairs of calls are released, here termed 'warm-up calls', which we here do not consider as part of a call series, as some other series do not include these. The silent interval between warm-up calls and main call series is 1233–1335 ms (n = 2). The call series is amplitude modulated, with the initial few calls being of considerably lower amplitude than the subsequent calls, followed by calls at constant amplitude until the end of the series. Dominant frequency of calls is 3803 ± 59 Hz (3703–3875 Hz, n = 6), with a 90% bandwidth from ca. 3700 to ca. 4050 Hz. Other calls recorded were not vouchered, but shared these parameters (Suppl. material 2). Calls highly similar to the human ear in frequency and structure were heard on a daily basis from numerous individuals across several sites up to three kilometres from the coordinates of this specimen during the three week observation period, sometimes in extremely motivated, dense choruses. We infer these calls to be typical advertisement calls as they occurred both in isolation and in dense choruses, and no other calls were heard from these frogs.

Andranonafindra: Based on call voucher ZSM 58/2016 (MSZC 0196): Calls recorded at 18h40 on the 14th of January, 2016 on a broad fleshy leaf 4 m from a slow stream in degraded primary rainforest, calling as part of a large chorus, at 14.73600°S, 48.54831°E, 1180 m a.s.l., at an estimated air temperature of 17–23°C (Fig. 2, Suppl. material 3). Call series are ill-defined, composed of an indefinite number of rapidly emitted, short (call duration 51–96 ms, 59.8 ± 13 ms, n = 10), single-note calls, each of which is highly pulsed containing 16–21 pulses (mean 18.2 ± 1.4 , n = 10), the maxima of which are separated by 2–3 ms (mean 2.8 ± 0.4 ms, n = 10). Calls are generally separated by inter-call intervals of 210–268 ms duration (mean 226.3 ± 16.3 , n = 10, silence of these intervals is inferred as background calls and noise in the recording make it difficult to be certain of silence). Each call is amplitude modulated, with greatest energy at the beginning, decreasing toward the end of the call, but the call series shows no pattern of modulation (Fig. 2). Dominant frequency of calls is 3703 ± 0 Hz (n = 10), with a 90% bandwidth from ca. 1560 to ca. 3800 Hz. Calls of a second vouchered specimen, ZSM 59/2016 (MSZC 0203), from the same locality, had the same structure as ZSM 58/2016, but were shorter (16–68 ms, 44.0 ± 15.4 ms, n = 10), had slightly fewer pulses (3–19, mean 11.5 ± 4.9 , n = 10), and had shorter inter-call intervals (169.0 ± 53 ms, 97–243 ms, n = 10), but roughly the same dominant frequency (3716 ± 86 Hz, 3617–3875 ms, n = 10) (Suppl. material 4).

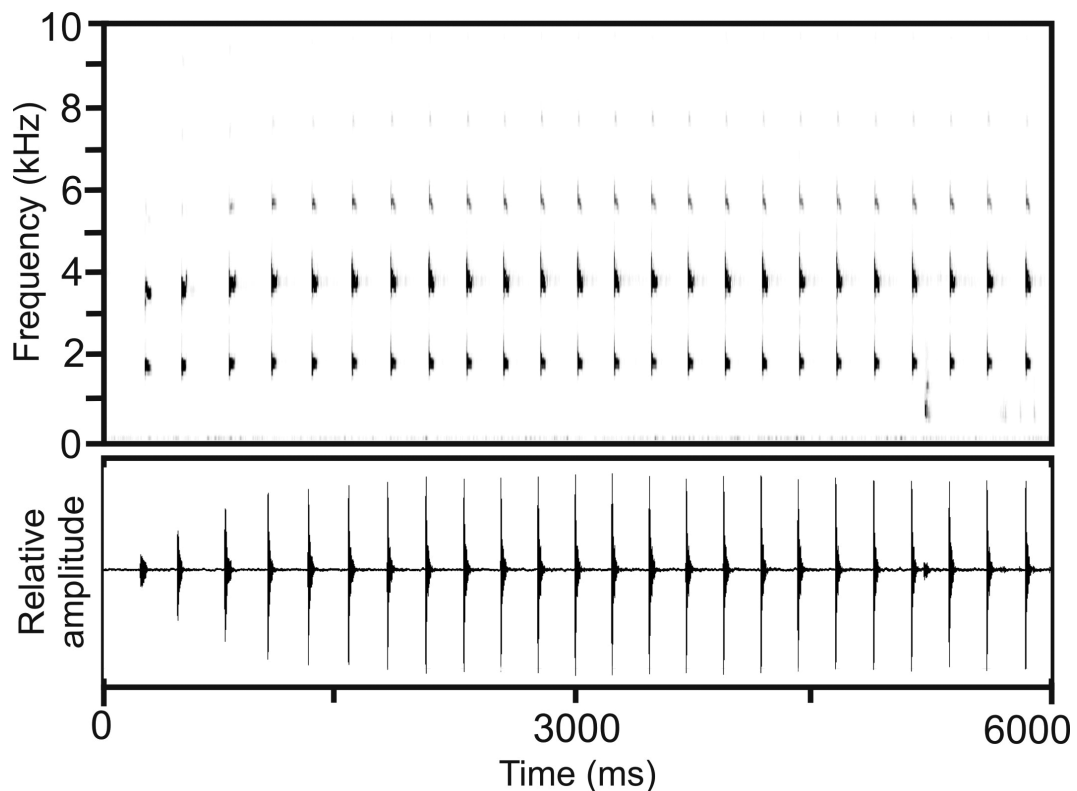


Figure 1. Spectrogram (above) and oscillogram (below) of a call series of the holotype of *Gephyromantis angano* sp. n., ZSM 68/2016 (MSZC 0172) from Ampotsidy. For the conditions of the call, see the text. The call is provided in Suppl. material 1.

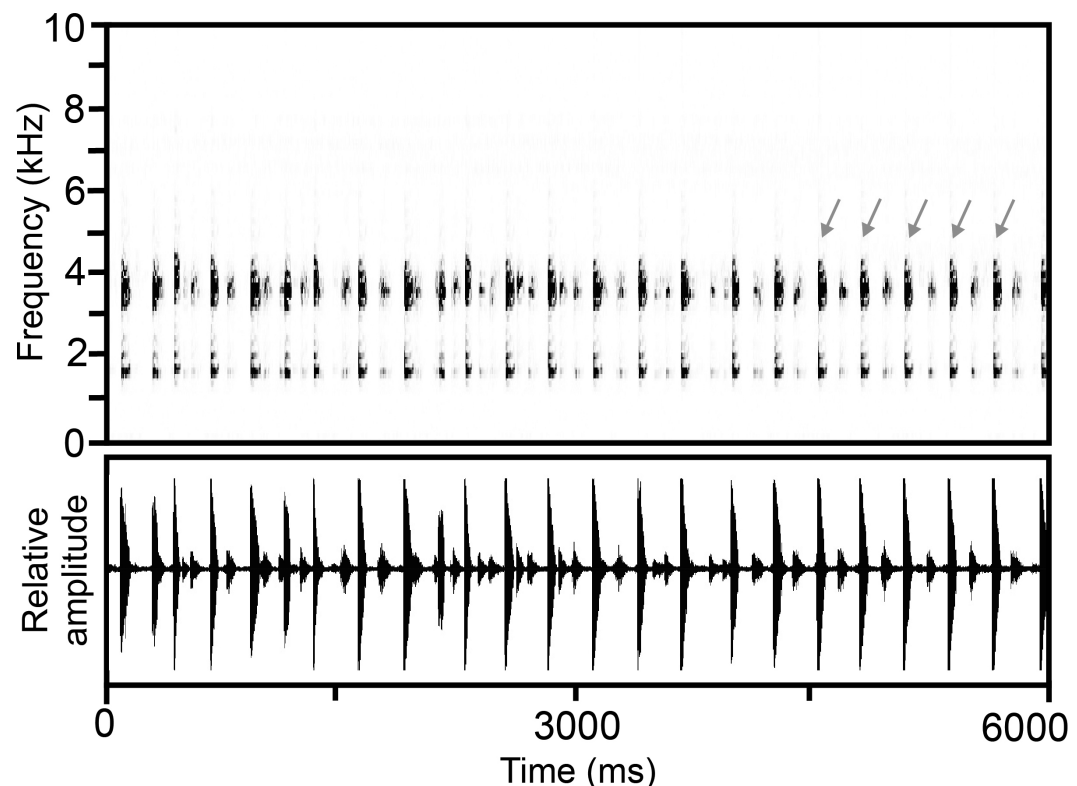


Figure 2. Spectrogram (above) and oscillogram (below) of a part of a long call series of *Gephyromantis* sp. Ca29 (ZSM 58/2016 = MSZC 0196) from Andranonafindra. For the conditions of the call, see the text. Note that in between the calls of the main recorded male (closest to the microphone), other males can be heard. In the second half of the spectrogram, five calls of the male closest to the microphone are marked with small arrows. The call is provided in Suppl. material 3.

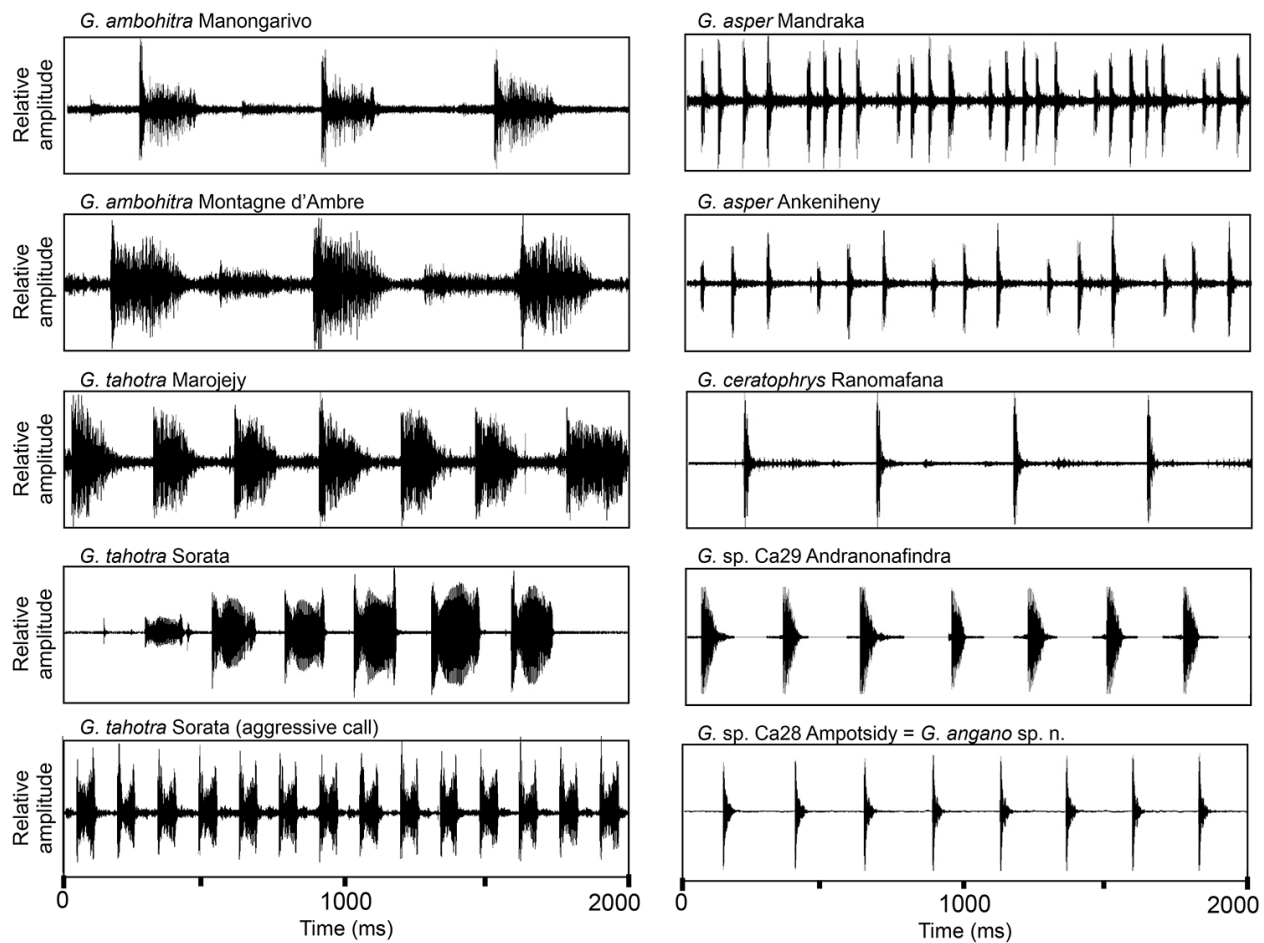


Figure 3. Bioacoustic differences among *Gephyromantis* (*Asperomantis*) species, as evident from oscillograms of their calls, adapted from Vences et al. (2017) in comparison with *Gephyromantis angano* sp. n. and *Gephyromantis* sp. Ca29.

Calls highly similar to the human ear in frequency and structure were heard on two non-consecutive nights in the vicinity of the recorded specimens during the brief survey period in this area of forest, but were not heard in other nearby patches of forest in between these nights. However, no suitable habitats (slow-flowing, shallow water) were found in the other surveyed forest patches, so their absence was anticipated. We suppose these calls also to be advertisement calls as the circumstances under which they were recorded were similar to those under which specimens from Ampotsidy were observed, but the observation period was admittedly much shorter and the sample size is small.

The advertisement calls of both of these populations are distinct from all other *Asperomantis* species (see Fig. 3, and compare data provided in Vences et al. 2017). By their short call duration, they are slightly similar to calls of *G. asper* and *G. ceratophrys*, but differ by longer note duration (mean 59.4 ± 10.4 ms vs. mean range 10.3–28.6 ms in *G. asper* and *G. ceratophrys*), by being evenly spaced (rather than arranged in fast call groups as in *G. asper*), and apparently by being more rapidly repeated than in *G. ceratophrys* (Fig. 3).

The vocalizations from Ampotsidy and Andranonafindra are also different from one another, especially in that specimens from Ampotsidy emit a tonal, unpulsed call in a clearly defined call series, whereas specimens from Andranonafindra emit a rough, strongly pulsed call without clear call series formulation. The sound impression of calls from both populations is very different to the human ear, mostly as a result of the tonal calls of specimens from Ampotsidy as opposed to the pulsed calls of specimens from Andranonafindra, although their temporal parameters are remarkably similar (call duration 59.4 ± 10.4 ms vs. 59.8 ± 13 ms; inter-call interval duration 193 ± 22 ms vs. 226.3 ± 16.3 ms). Thus the measured differences are smaller than those between other species in the subgenus *Asperomantis* (Fig. 3), but the calls are as distinguishable from one another. It is possible that the different calls represent two separate call types of the same species, as is known from *G. tahotra* (Glaw et al. 2011; Fig. 3; discussed below). However, in either location only one of the respective call types was heard, unlike in *G. tahotra*, where both call types can be heard simultaneously or independently in a single population and switching among calls appears to occur sporadically (e.g. within a single evening).

Morphology and colouration

Morphological measurements are given in Table 1. The newly collected adults are smaller than most other *Asperomantis* material, resembling in size primarily *G. asper* and *G. cera-**tophrys*. Male specimens from Ampotsidy and Andranonafindra are highly similar, and the only notable difference is body size (SVL 29.1–29.6 mm [n = 2] in Ampotsidy vs. 30.6–32.7 mm [n = 2] in Andranonafindra). There is a slight difference in the shape of the femoral glands, with those of specimens from Ampotsidy being slightly longer relative to their width than those of specimens from Andranonafindra. The number of femoral gland granules between the two species overlaps, being exceptionally variable in specimens from Ampotsidy with 26–69 granules per gland, whereas specimens from Andranonafindra have 42–49 (note that not all values are reported in Table 1 as some specimens from which granule number could be counted from photos were not available for measurements). Females were not available from Andranonafindra. All other measurements do not differ. The colouration of specimens is also similar (see photos in life below), and it must be noted that colouration is highly variable in all *Asperomantis* species (Vences et al. 2017). In summary, the morphological differences between these populations are on par with both inter- and intraspecific variation of other *Asperomantis* species (Vences et al. 2017).

Molecular phylogenetics

We produced new *16S* DNA sequences for 20 specimens. Our *16S* alignment of these and 103 other terminals contained 619 characters and a total of 283 variable sites, of which 241 were parsimony informative (excluding outgroups). BI and ML phylogenies of the *16S* alignment agreed in topology of the *Asperomantis* subgenus (Fig. 4), with small differences in other subgenera throughout the genus *Gephyromantis* (Suppl. material 5); the overall tree topology agrees well

with more comprehensive multi-gene studies (Kaffenberger et al. 2012). Support for the BI tree was generally high, whereas support for the ML phylogeny was rather low (Fig. 4, Suppl. material 5). Uncorrected pairwise distances (p-distances) are given for *Asperomantis* in Table 2 and for all other *Gephyromantis* species in Suppl. material 6. Specimens from Ampotsidy and Andranonafindra belong to four or five species: *G. sp. Ca28* (one or two species; discussed in the next paragraph), *G. tahotra*, *G. horridus* (3% divergent from other *G. horridus* and recovered with negligible support as closer related to *G. ranjomavo* in our tree, so requiring closer investigation), and two divergent lineages well over 3% genetically divergent from all other *Gephyromantis* species, identified here as Unconfirmed Candidate Species sensu Vieites et al. (2009) for the first time, *G. sp. Ca30* (a *Duboinantis* with affinities to *G. tandroka*, separated by 6.4% uncorrected p-distance) and *G. sp. Ca31* (a *Phylacomantis* with affinities to *G. azzurrae*, separated by 5.5% uncorrected p-distance; Suppl. material 6).

Populations of *Gephyromantis* sp. Ca28 from Ampotsidy and Andranonafindra are genetically assortative; specimens from Ampotsidy cluster with a specimen from Antsahan'i Ledy, while specimens from Andranonafindra cluster with specimens from between Antsohihy and Bealanana (Fig. 4; the names *G. angano* sp. n. and *G. sp. Ca29* for these two populations are used pre-emptively here and in Table 1 and Fig. 3). These clades have an uncorrected p-distance between them of 1.0–3.0% (Table 1). This distance is below the typical threshold of genetic distance used to identify candidate species based on *16S* DNA barcode sequence data (Vieites et al. 2009), and agrees with intraspecific distances among other species of *Asperomantis* (see Table 2). Note that the intraspecific variation in *G. ambohitra* is exceptionally high as a result of the distance between its two clades (Fig. 4) of 5.6–7.1%; distances within these clades are 0.4–2.1% (data not shown). On the

Table 1. Morphological measurements of *Gephyromantis angano* sp. n. (formerly *G. sp. Ca28*) from Ampotsidy and Antsahan'i Ledy, and *G. sp. Ca29* from Andranonafindra, plus two newly collected specimens of *G. tahotra* from Ampotsidy. All measurements are given in mm. Measurement abbreviations are given in the Materials and methods. The bolded specimen is the holotype of the new species described below.

Species	Field number	Sex	SVL	HW	HL	TD	ED	END	NSD	NND	FORL	HAL	HIL	FOTL	FOL	TIBL	FGG	FGL	FGW
<i>G. angano</i> (Ampotsidy)	MSZC 0172	M	29.6	10.4	11.0	2.7	3.8	3.0	1.8	2.8	19.1	9.3	53.7	23.3	15.8	17.2	36/44	6.6	3.0
<i>G. angano</i> (Ampotsidy)	MSZC 0021	M	29.1	9.9	11.0	2.5	3.7	3.2	1.7	2.4	18.3	8.8	50.2	22.3	15.2	16.0	30/26	6.2	2.4
<i>G. angano</i> (Ampotsidy)	MSZC 0112	F	30.5	9.8	11.4	2.3	3.8	3.3	1.9	2.4	20.0	9.6	54.3	23.7	15.9	17.8	n/a	absent	absent
<i>G. angano</i> (Antsahan'i Ledy)	ZSM 1731/2010	F	26.2	8.8	10.4	2.2	3.4	2.8	1.4	2.2	18.1	8.4	50.1	21.6	15.6	15.5	n/a	absent	absent
<i>G. sp. Ca29</i> (Andranonafindra)	MSZC 0203	M	30.6	10.5	13.1	2.4	4.0	3.5	1.7	2.6	18.7	9.0	54.3	23.8	16.0	17.4	48/47	6.2	3.1
<i>G. sp. Ca29</i> (Andranonafindra)	MSZC 0196	M	32.7	10.7	12.0	3.0	4.0	3.3	2.0	2.7	20.3	9.9	54.9	24.6	16.8	17.5	42/49	6.1	2.9
<i>G. tahotra</i> (Ampotsidy)	MSZC 0142	M	32.0	11.9	12.2	2.5	4.3	3.2	2.0	2.8	19.8	10.5	59.4	26.1	18.0	19.0	7/3	indistinct	indistinct
<i>G. tahotra</i> (Ampotsidy)	MSZC 0148	M	33.4	11.7	12.9	3.1	4.3	3.4	2.4	3.0	20.1	10.8	60.0	26.2	18.1	19.3	22/22	indistinct	indistinct

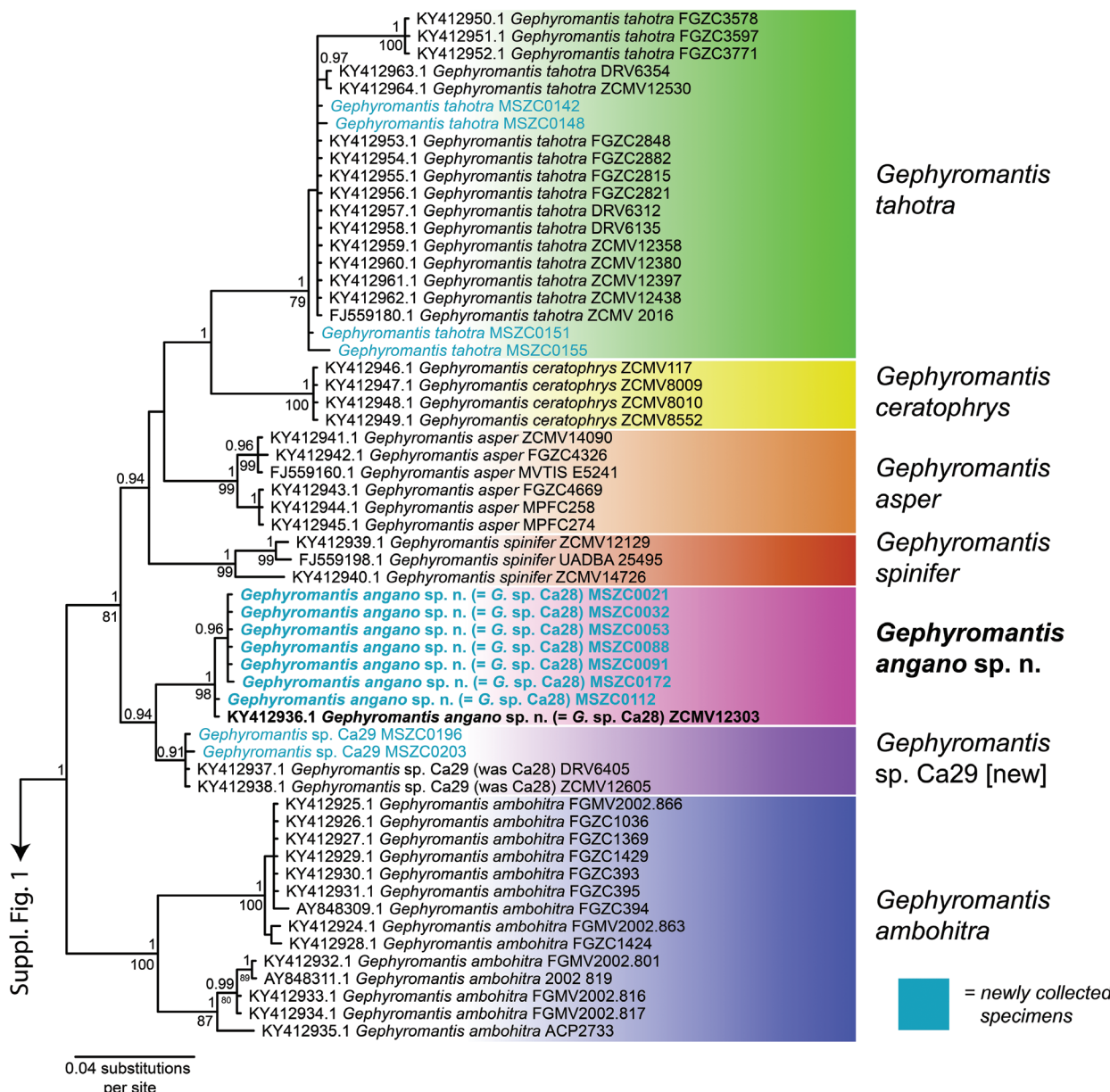


Figure 4. Phylogenetic relationships of the subgenus *Asperomantis*, reconstructed by Bayesian Inference analysis of a fragment of the mitochondrial 16S rRNA gene. Numbers above nodes denote Bayesian Posterior Probability (PP) from Bayesian Inference analysis; numbers below nodes indicate bootstrap support (%) from Maximum Likelihood analysis. PP lower than 0.9 and bootstrap support lower than 70% are not shown. Other *Gephyromantis* and outgroups are shown in Suppl. material 5. Numbers before taxon names are GenBank numbers; numbers after taxon names are field numbers.

other hand, the Ampotsidy and Andranonafindra sequences differ from all described *Asperomantis* species by high distances of 3.3–9.3% and are phylogenetically distinct from other *Asperomantis*. It is thus clear that the current taxonomy requires revision and the bioacoustic and genetic distinctness of these frogs needs to be carefully evaluated.

Taxonomic conclusions

Genetically, specimens from Ampotsidy+Antsahan'i Ledy and Andranonafindra+Bealanana-Antsohihy are separated by 1–3% in the segment of the 16S rRNA gene typically used for candidate species designation

in Madagascan amphibians (Vieites et al. 2009). This is relatively low, and the typical threshold for establishment of candidate species (3% uncorrected p-distance) is barely achieved. However, bioacoustics tells a different story: the differences in the sound of the call (tonal and unpulsed vs. noisy and pulsed; fairly short, isolated series vs. long, ill-defined series) are remarkable. Morphological data among these populations are equivocal; although males from Ampotsidy are smaller than those from Andranonafindra and the dimensions of their femoral glands differ somewhat, all other characters show no distinction among the populations, albeit with low sample

Table 2. Uncorrected pairwise distances among members of the subfamily *Asperomantis* in the *16S* marker; the diagonal values refer to intra-specific distinction. For uncorrected p-distances for the whole genus *Gephyromantis*, see Supplementary material 6.

	1	2	3	4	5	6	7
1. <i>Gephyromantis</i> sp. Ca29	0.0%						
2. <i>Gephyromantis</i> angano sp. n.	1.0–3.0%	0.0–0.2%					
3. <i>Gephyromantis</i> tahotra	6.5–8.9%	7.3–9.3%	0.0–3.3%				
4. <i>Gephyromantis</i> ceratophrys	6.1–6.5%	6.0–6.7%	6.9–8.2%	0.0%			
5. <i>Gephyromantis</i> asper	3.3–4.5%	3.9–5.9%	6.1–8.6%	7.1–7.8%	0.0–1.4%		
6. <i>Gephyromantis</i> spinifer	4.9–6.7%	5.3–7.5%	7.9–9.4%	7.6–7.8%	5.2–7.3%	0.6–3.1%	
7. <i>Gephyromantis</i> ambohitra	6.7–8.5%	7.4–9.3%	11.5–14.8%	11.0–11.3%	9.6–11.7%	9.7–11.8%	0.0–7.1%

sizes. This is typical of some *Asperomantis* species however, and a similar lack of morphological difference is to be found between *G. asper* and *G. ceratophrys* (Vences et al. 2017).

In summary, evidence from mitochondrial DNA, biacoustics, and morphology currently suggests a weak degree of differentiation between these two populations, with the greatest differences being in sound and structure of the advertisement calls. It may thus be possible that both of these forms represent separate species. We therefore assign the populations from Andranonafindra and Bealanana-Antsohihy a new candidate species number, *Gephyromantis* sp. Ca29, and consider it an Unconfirmed Candidate Species sensu Vieites et al. (2009). It is apparent however that specimens from Antsahan'i Ledy and Ampotsidy, representing *G. sp. Ca28* in the original sense (Perl et al. 2014), are distinct from all currently described *Gephyromantis* species. We therefore describe this form as a new species in the following. Whether *G. sp. Ca29* indeed represents an independent evolutionary lineage also meriting formal description, or if it is better seen as deep conspecific lineage of the new species described here, can only be decided with further genetic and field data.

Gephyromantis (Asperomantis) angano sp. n.

<http://zoobank.org/B1DA196D-21E4-4A45-9D4A-B6E8DBF912F6>

Figures 1, 3–7, Suppl. material 1, 2, 5

Gephyromantis sp. Ca28 — Perl et al. (2014)

Holotype. ZSM 68/2016 (MSZC 0172), an adult male, collected at 22h40 on 8th January 2016 in Ampotsidy (14.41949°S, 48.71938°E, 1340 m a.s.l.), roughly 15 km north of Bealanana in the Bealanana District, Sofia Region, northern Madagascar, by Mark D. Scherz, James Borrell, Lawrence Ball, Thomas Starnes, Elidiot Razafimandimby, Denise Herizo Nomenjanahary, and Jeanneney Rabearivony.

Paratypes. ZSM 67/2016 (MSZC 0112) adult female, collected at night on 30th December 2015 in Ampotsidy (14.41734°S, 48.71858°E, 1363 m a.s.l.); ZSM 69/2016 (MSZC 0021) adult male, collected at 22h00 on 19th December 2015 in Ampotsidy (14.41956°S, 48.71946°E, 1357 m a.s.l.); UADBA-A uncatalogued (MSZC 0032)

adult male, collected in the late morning on the 21st December 2015 in Ampotsidy (14.41435°S, 48.71155°E, 1431 m a.s.l.); UADBA-A uncatalogued (MSZC 0053) subadult, collected at 20h43 on 22nd December 2015 in Ampotsidy (14.41382°S, 48.71178°E, 1443 m a.s.l.); UADBA-A uncatalogued (MSZC 0091), an adult female collected at night on 30th December 2015 in Ampotsidy (14.41208°S, 48.71609°E, 1513 m a.s.l.); all collected by Mark D. Scherz, James Borrell, Lawrence Ball, Thomas Starnes, Elidiot Razafimandimby, Denise Herizo Nomenjanahary, and Jeanneney Rabearivony. ZSM 1731/2010 (ZCMV 12303), adult female, collected on 9th June 2010 on the Tsaratanana massif, in the forest near camp 0 (Antsahan'i Ledy; 14.2332°S, 48.9800°E, 1207 m a.s.l.) by Miguel Vences, David R. Vieites, Roger-Daniel Randrianiaina, Fanomezana Ratsoavina, Soloheray Rasamison, Andolalao Rakotoarison, Emile Rajeriarison, and Theo Rajoafiarison.

Diagnosis. A *Gephyromantis* species assigned to the subgenus *Asperomantis* based on the presence of small dermal spines on the elbow and heel, presence of inner and outer dorsal ridges as defined by Vences and Glaw (2001), Type 2 femoral glands sensu Glaw et al. (2000)Glaw et al. (2000), moderately enlarged finger and toe tips, absence of webbing between fingers, moderate webbing between toes, presence of paired blackish sub-gular vocal sacs in males, and a distinct whitish spot in the middle of the tympanic field (Vences et al. 2017). DNA sequence data from a fragment of the *16S* gene supports this assignment. *Gephyromantis angano* sp. n. is characterized by the following suite of morphological characters: (1) adult SVL 29.1–30.5 mm, (2) TD/ED 0.61–0.71, (3) small supraocular spines, (4) large femoral glands consisting of numerous small granules, (5) moderately raised dorsal ridges, (6) granular dorsal skin, (7) relatively short hindlimbs (HIL/SVL 1.73–1.81 in males), and (7) its unique call (see above).

Within the subgenus *Asperomantis*, *Gephyromantis angano* sp. n. can be distinguished from *G. ambohitra*, *G. spinifer*, and *G. tahotra* by its smaller size (male SVL < 30 mm, vs. >31 mm, female SVL up to 30.5 mm vs. >32 mm); from *G. spinifer* by its less granular dorsal skin and smaller supraocular spines; from *G. asper* and *G. ceratophrys* by its generally shorter hindlimbs in males (HIL/SVL 1.73–1.81 vs. 1.77–2.11); and from *G. ceratophrys* by more granules per femoral gland (26–69 vs. 14–20).

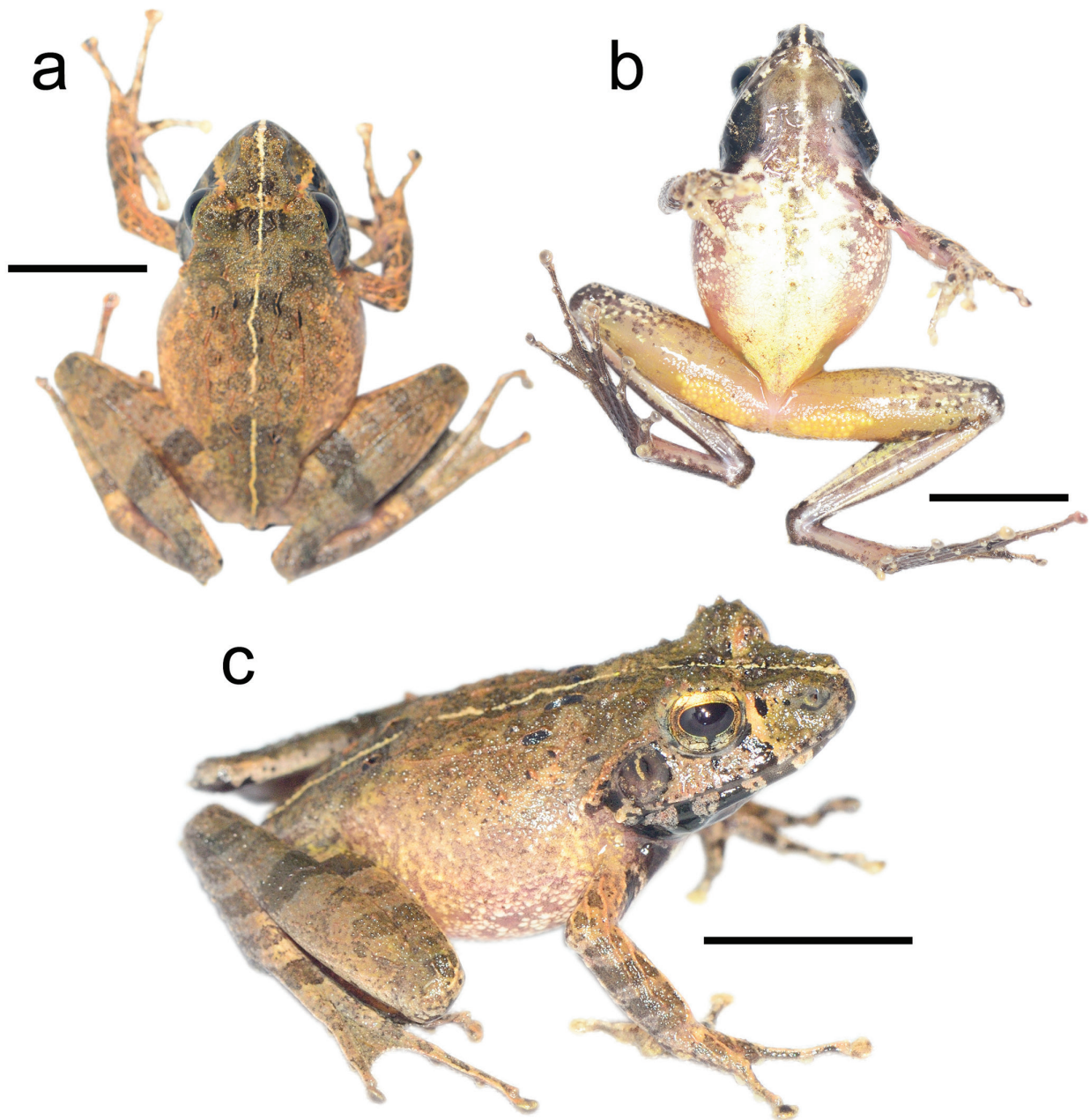


Figure 5. The holotype of *Gephyromantis angano* sp. n., ZSM 68/2016 (MSZC 0172) in life in (a) dorsal, (b) ventral, and (c) lateral view. Scale bars indicate 10 mm.

Bioacoustically, it is distinguished from all of these species by its call duration (41–98 ms vs. 5–44 ms in *G. asper* and *G. ceratophrys*, and 98–274 ms in *G. ambohitra* and *G. tahotra*), unpulsed calls (vs. pulsed in *G. ambohitra* and *G. tahotra*), calls repeated faster than in *G. ceratophrys*, and dominant frequency (3703–3875 Hz vs. 1435–3366 Hz in *G. ambohitra*, and *G. tahotra*).

Description of the holotype. A specimen in a good state of preservation, the left thigh cut for DNA tissue sample and to expose the inner face of the femoral gland. Snout-vent length 29.6 mm. For other measurements see Table 1. Body rather rounded; head longer than wide, as wide as the body; snout acuminate in dorsal view, truncate in lateral

view; nostrils directed laterally, slightly protuberant, much nearer to tip of snout than to eye; canthus rostralis distinct, concave; loreal region concave and moderately oblique; tympanum distinct, round, its diameter 71% of eye diameter; supratympanic fold distinct, curving ventrally; tongue ovoid, distinctly bifid posteriorly; vomerine teeth distinct, in two small aggregations, positioned posteromedially to choanae; choanae rounded. Dark dermal fold (the inflatable parts of the vocal sacs) running along each lower jaw from commissure of mouth to middle of lower jaw. Arms slender, subarticular tubercles single; outer metacarpal tubercle very poorly developed and inner metacarpal tubercle relatively well developed; fingers without webbing; relative length of fingers 1 < 2 < 4 < 3, second finger dis-

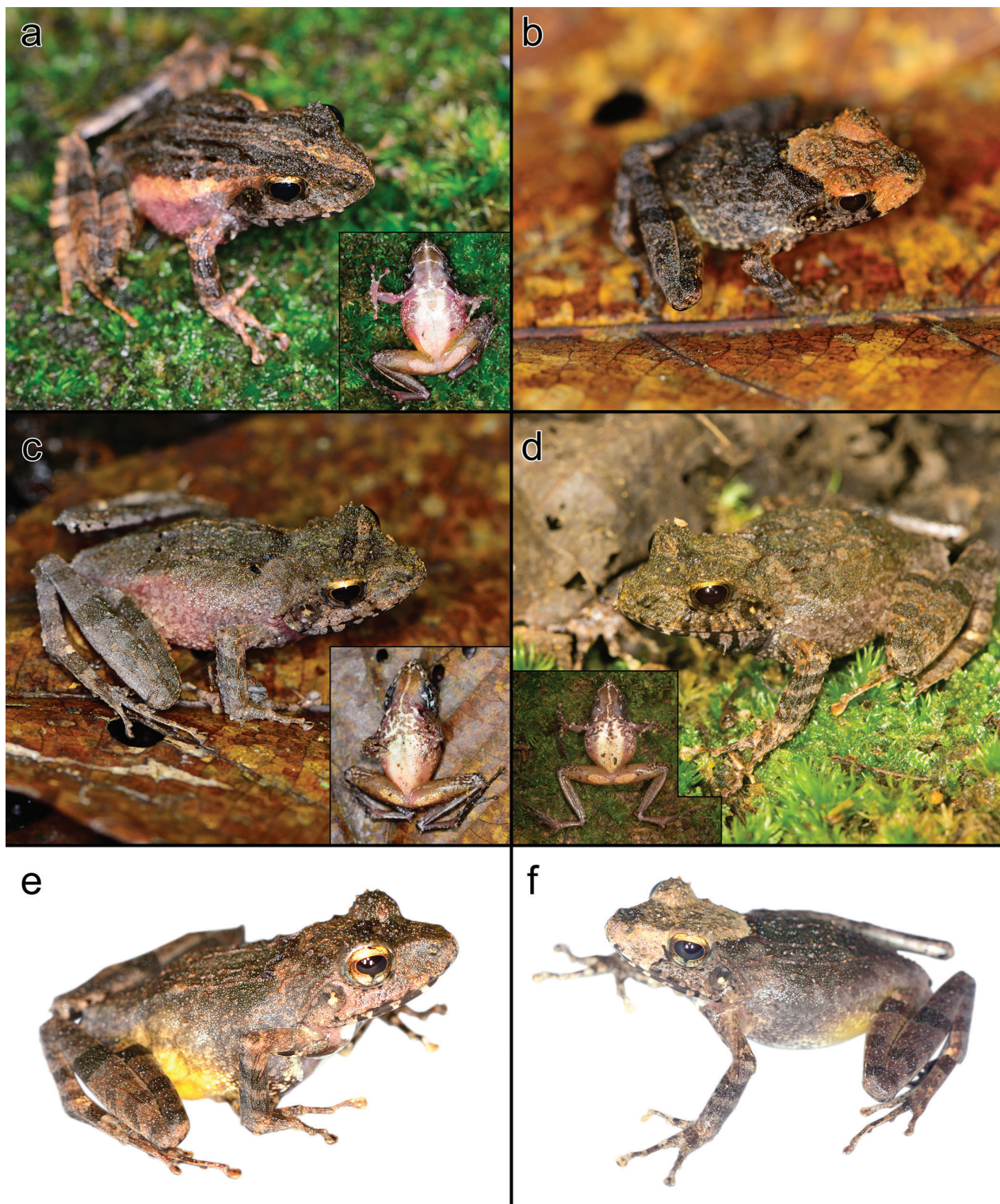


Figure 6. Variation in *Gephyromantis angano* sp. n. (a) UADBA-A uncatalogued (MSZC 0032), adult male (FGG = 69/56), (b) UADBA-A uncatalogued (MSZC 0053), juvenile, (c) ZSM 67/2016 (MSZC 0021), adult male (FGG = 30/26), (d) UADBA-A uncatalogued (MSZC 0091), adult male (FGG = 57/55), (e) Université d'Antsiranana uncatalogued (MSZC 0088), adult female (not in the type series), (f) ZSM 69/2016 (MSZC 0112), adult female. Insets show specimens in ventral view. Not to scale.

tinctly shorter than fourth; finger discs distinctly enlarged, nuptial pads absent. Hindlimbs slender; tibiotarsal articulation reaching beyond snout tip when hindlimb is adpressed along body; lateral metatarsals separated by webbing; in-

ner metatarsal tubercle distinct, outer metatarsal tubercle very faint but present; webbing formula of foot according to Blommers-Schlösser (1979) 1(1), 2i(1.5), 2e(1), 3i(2), 3e(1), 4i(2.5), 4e(2), 5(0.5); relative toe length $1 < 2 < 5$

$< 3 < 4$; toe discs distinctly enlarged. Skin dorsally granular; ridges bordering mid-dorsal band elevated, starting approximately 1 mm behind eyes (starting off bifurcated and converging toward the mid-line) and gradually becoming less distinct posteriorly; additional, interrupted and less distinct ridges are present posterior to the suprascapular region; two dark inter-ocular ridges are present either side of a fine cream-coloured vertebral band; supraocular tubercles are weakly enlarged, and do not form strong spines above the eyes; a modest dermal tarsal spine is present. Ventral skin smooth on throat and limbs, granular in posterior portion of abdomen. Femoral glands well delimited externally, consisting of 36 small granules on the left side and 44 small granules on the right side.

Dorsal colouration after one and a half years in preservative sepia, becoming increasingly grey posteriorly, mottled with almost black and brownish markings; dorsal folds are blackened over the suprascapular region but are otherwise brown; the tympanum is darker brown than the surrounding area; the lateral head has a cream stripe before the eye, immediately followed by a black stripe roughly 1 mm wide, and then mottled dark and light until the tympanum; bottom lip has alternating brown and cream annulations; dorsal forelimbs mottled blackish and Mikado brown reticulated with cream; dorsal hind-limbs brown with burnt umber crossbands on the thigh (three), shank (four), and foot (four); the cloacal region has a trapezoid of burnt umber around it; flank colouration fades from the sepia dorsal colouration through grey to the cream of the venter; ventrally the chin is medium fawn with a cream mid-ventral stripe and blackish vocal sacs, becoming blotched fawn among cream posteriorly to fully cream on the abdomen; the ventral legs are cream with brown and black areas toward the knees and on the anteroventral edge of the shank, including the femoral glands, which are distinct only in their texture and shape, and not in colour; the ventral foot is dark brown.

Colouration in life was as in preservative but more vibrant; see Figure 5.

Variation. For a summary of measurement variation, see Table 1. All morphologically examined paratypes strongly resemble the holotype in morphology. Ridges between the eyes vary somewhat in shape, and in some specimens are black but in others do not have a distinct colouration from the surrounding head surface. The dorsal ridges vary from strongly to weakly pronounced, but are always present. There is no sexual dimorphism in inner metacarpal tubercle size. Snout shape in lateral view varies from rounded to square. The supraciliary spines of all specimens are fairly low and indistinct. The femoral glands are remarkably variable, ranging from 26 granules in the right gland of ZSM 69/2016 to 69 granules in the left gland of MSZC 0032 (Fig. 6). Variation in colouration is as variable as is typical for members of this subgenus. A thin vertebral line can be present. The arms are always reticulated with whitish to light brown colouration. The head of ZSM 69/2016 (Fig. 6f) has a diamond-shaped lighter colouration

covering its dorsal surface. The ventral colouration of this specimen is remarkably similar to that of all males, except that the blackish vocal sacs are absent. A juvenile, MSZC 0032, also had this diamond-shaped brown marking on its head (Fig. 6b).

Etymology. *Angano* is a Malagasy word meaning ‘fable’. The new material for this species was collected on Expedition Angano, a research expedition to the Bealanana District of northern Madagascar to assess the impacts of forest fragmentation on the reptiles and amphibians. The epithet is used as an invariable noun in apposition to the genus name.

Call. See the description provided above.

Natural history and distribution. One specimen of this species has been collected in Antsahan’i Ledy, and numerous specimens of this species were encountered during fieldwork on the Ampotsidy mountains (Fig. 7). Calling males were generally found in association with slow flowing water, in the case of the holotype at the source of a spring, in close syntopy with *Boophis madagascariensis* and a *Mantidactylus* (*Brygoomantis*) species. Males called up to 1 m above the ground from fern fronds and other low foliage. Females were found both near to and away from water, during the day and at night, but were less commonly encountered. No eggs were observed, but highly ovigerous females were found in January (e.g. Fig. 6e). The call of the species is loud and carries over long distances, so that it can be heard alongside the calls of *Boophis madagascariensis* from well outside of some small forest fragments in the vicinity of Ampotsidy. In a small forest fragment where vouchers of *Gephyromantis* (*Asperomantis*) *tahotra* were collected (14.41689°S, 048.71435°E, 1368 m a.s.l.), *G. angano* sp. n. could also be heard; this appears to be the first ever record of any two *Asperomantis* species occurring in close syntopy (Vences et al. 2017).

Discussion

Gephyromantis is one of the most diverse genera of frogs in Madagascar. Since the first major barcoding study of all of Madagascar’s amphibians in 2009 (Vieites et al. 2009), five species of *Gephyromantis* have been described (Crottini et al. 2011, Glaw et al. 2011, Glaw and Vences 2011, Vieites et al. 2012, Wollenberg et al. 2012), two have been resurrected (Wollenberg et al. 2012, Vences et al. 2017), and numerous undescribed species remain, including two that are in description (Scherz et al. in press; submitted). During our fieldwork in the Bealanana District of northern Madagascar, we encountered a total of six *Gephyromantis* species verified by DNA barcoding (Suppl. material 5), including three in the subgenus *Asperomantis* (*G. angano* sp. n., *G. sp. Ca29* [new; Fig. 8] and *G. tahotra*, Fig. 4), one in the subgenus *Laurentomantis* (identified as *G. horridus*, but separated from other *G. horridus* by 3% 16S divergence and requiring closer investigation), one in the

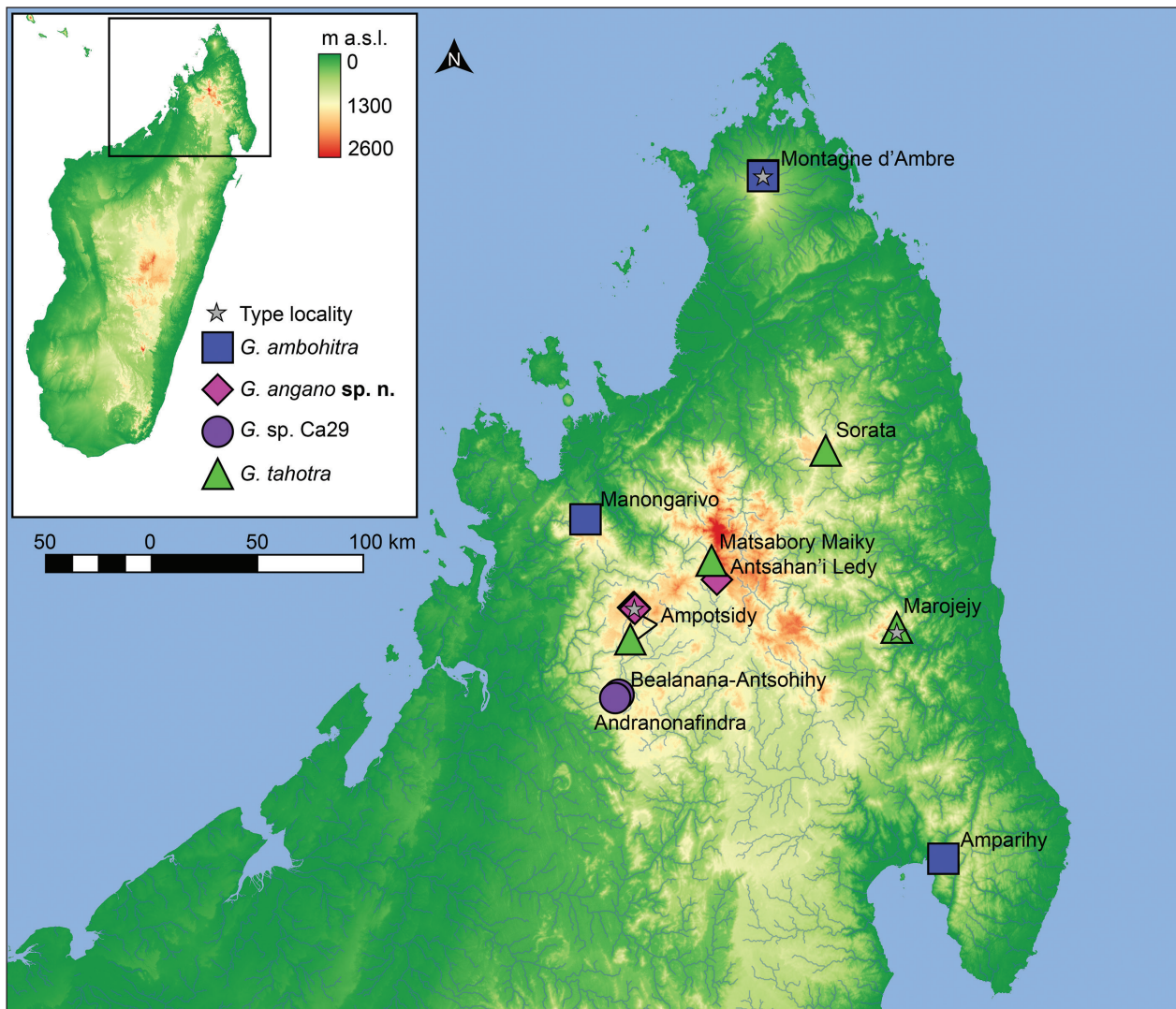


Figure 7. Map of northern Madagascar indicating the known distribution of *Asperomantis* species. Colours correspond to species in Fig. 4. Three arc second SRTM basemap from Jarvis et al. (2008).

subgenus *Duboimantis* (a new candidate species close to *G. tandroka*, here dubbed *G. sp. Ca30*), and one in the subgenus *Phylacomantis* (a new candidate species close to *G. azzurrae*, here dubbed *G. sp. Ca31*) (see Suppl. material 5). Of these, only two (*G. tahotra* and *G. horridus*) are already described, and Ampotsidy represents a new locality for both of them. The new Unconfirmed Candidate Species of *Duboimantis* and *Phylacomantis* are numbered and rationalised following Vieites et al. (2009). In summary, although recent advances have brought major improvements to the supraspecific taxonomy of *Gephyromantis* (Kaffenberger et al. 2012, Vences et al. 2017), work on the species-level taxonomy of the genus is far from finished.

Several hypotheses may be put forward to explain the differences between *G. angano* sp. n. and its bioacoustically divergent but genetically and morphologically similar sister lineage *G. sp. Ca29* (shown in Fig. 8): (1) these represent two call types for the same species, as is known from the closely related *G. tahotra*, and also *Boophis tampoka*, a tree frog from Madagascar that also has two

call types that are not genetically assortative and change by locality or temporally (Vences et al. 2011) (considered unlikely, as the calls were heard within five days of one another at the two sites, and neither call was ever heard at both sites despite numerous calling individuals being observed, and over three weeks of observations from one of the sites), (2) the calls form two ends of a continuum of variation over the distribution of a single species (seemingly unlikely, given they are correlated with genetic differences and are rather important, affecting several call variables), (3) the calls represent local dialects caused by a slight structural modification of the vocal apparatus, (4) the two populations are undergoing incipient speciation or (5) they are two distinct, recently diverged species. In frogs, advertisement calls play a strong role in sexual selection and mate recognition (Hoskin et al. 2005, Köhler et al. 2017), and call differences may function as drivers and/or reinforcers of divergence (Hoskin et al. 2005). In either case, they can evolve exceptionally quickly, in a way that can greatly exceed signals of typical drift-based

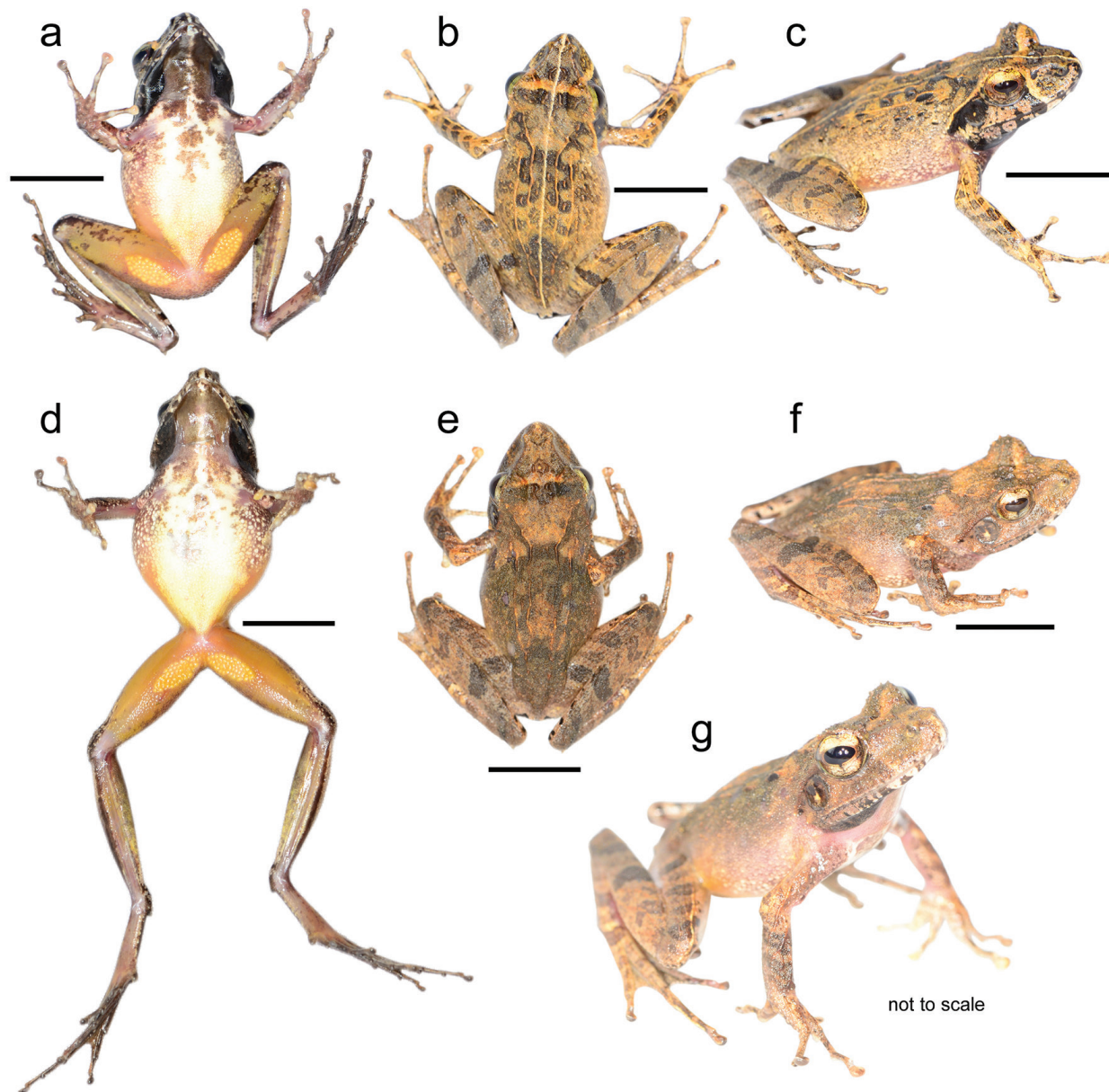


Figure 8. *Gephyromantis* sp. Ca29 from Andranonafindra in life. Photos show (a–c) ZSM 59/2016 (MSZC 0203), adult male (FGG = 48/47), and (e–g) ZSM 58/2016 (MSZC 0196), adult male (FGG = 42/49). Scale bars indicate 10 mm.

divergence, which can lead to cases where signals from mitochondrial genes simply have not yet caught up, but are likely to do so. With greater sampling and sequencing of nuclear genes, we may be able to reveal which of these hypotheses is most credible, but at present data are insufficient to draw convincing conclusions on this matter. Denser sampling across a greater area of the Bealanana basin to identify possible contact or hybrid zones will also be critical in understanding the divergence pattern and phylogeography of these frogs, but such work will undoubtedly be challenging, given the extreme fragmentation of forests in this area, and how difficult it is for research teams to access its more remote reaches.

The new species *Gephyromantis angano* sp. n. is restricted to primary and secondary mid-altitude rainforest

(Fig. 7). These forests are disappearing rapidly in the Bealanana District, becoming increasingly fragmented, with fragments decreasing in size. Based on bioacoustic surveys while crossing between large forest fragments, it seems that *G. angano* sp. n. is able to survive in even tiny forest remnants, but a degree of connectivity is doubtless required in order to facilitate gene flow. At present the two known localities make up an area of just 90 km², most of which is devoid of forest. As such, the species could warrant treatment as Critically Endangered. However, due to its relative abundance, and because we suspect that it is more widespread, we recommend that it instead be assessed as Data Deficient for the IUCN Red List until better sampling in the Bealanana District can be carried out.

Acknowledgements

Field research for Expedition Angano (specimens collected in 2015 and 2016) was made possible by grants from the Royal Geographical Society, the Zoological Society of London, Cadogan Tate, The Scientific Exploration Society, and crowdfunding via Indiegogo. Research in 2015–2016 was conducted under the permit N° 224/15/MEEMF/SG/DGF/DAPT/SCBT. Specimens were exported under N° 030N-EA01/MG16. We thank our guides and cooks in the field, Brian Fisher and his team for logistical support in Madagascar, as well as our driver Davy Heritiana, and MICET for handling logistics. We thank Jörn Köhler for providing a helpful and constructive review of this paper. The publication of this article in *Zoosystematics and Evolution* was made possible by the Museum für Naturkunde Berlin.

References

- AmphibiaWeb (2017) AmphibiaWeb: Information on amphibian biology and conservation. AmphibiaWeb, Berkley, California. [Accessed 6. July 2017]
- Blommers-Schöller RMA (1979) Biosystematics of the Malagasy frogs. I. *Mantellinae* (Ranidae). *Beaufortia* 352: 1–77.
- Crottini A, Glaw F, Casiraghi M, Jenkins RBK, Mercurio V, Randrianantoandro C, Randrianirina JE, Andreone F (2011) A new *Gephyromantis* (*Phylacomantis*) frog species from the pinnacle karst of Bemaraha, western Madagascar. *Zookeys* 81: 51–71. <https://doi.org/10.3897/zookeys.81.1111>
- Crottini A, Harris DJ, Miralles A, Glaw F, Jenkins RKB, Randrianantoandro JC, Bauer AM, Vences M (2014) Morphology and molecules reveal two new species of the poorly studied gecko genus *Paragehyra* (Squamata: Gekkonidae) from Madagascar. *Organisms Diversity & Evolution* 15(1): 175–198. <https://doi.org/10.1007/s13127-014-0191-5>
- Glaw F, Köhler J, Vences M (2011) New species of *Gephyromantis* from Marojejy National Park, northeast Madagascar. *Journal of Herpetology* 45(2): 155–160. <https://doi.org/10.1670/10-058.1>
- Glaw F, Vences M (2011) Description of a new frog species of *Gephyromantis* (subgenus *Laurentomantis*) with tibial glands from Madagascar. *Spixiana* 34(1): 121–127.
- Glaw F, Vences M, Gossmann V (2000) A new species of *Mantidactylus* (subgenus *Guibemantis*) from Madagascar, with a comparative survey of internal femoral gland structure in the genus (Amphibia: Ranidae: Mantellinae). *Journal of Natural History* 34: 1135–1154. <https://doi.org/10.1080/00222930050020140>
- Hoskin CJ, Higgle M, McDonald KR, Moritz C (2005) Reinforcement drives rapid allopatric speciation. *Nature* 437: 1353–1356. <https://doi.org/10.1038/nature04004>
- Jarvis A, Reuter HI, Nelson A, Guevara E (2008) Hole-filled seamless SRTM data V4, International Centre for Tropical Agriculture (CIAT). <http://srtm.csi.cgiar.org>.
- Kaffenberger N, Wollenberg KC, Köhler J, Glaw F, Vieites DR, Vences M (2012) Molecular phylogeny and biogeography of Malagasy frogs of the genus *Gephyromantis*. *Molecular Phylogenetics and Evolution* 62(1): 555–560. <https://doi.org/10.1016/j.ympev.2011.09.023>
- Köhler J, Jansen M, Rodríguez A, Kok PJR, Toledo LF, Emmrich M, Glaw F, Haddad CFB, Rödel M-O, Vences M (2017) The use of bioacoustics in anuran taxonomy: theory, terminology, methods and recommendations for best practice. *Zootaxa* 4251(1): 1–124. <https://doi.org/10.11646/zootaxa.4251.1.1>
- Kumar S, Stecher G, Tamura K (2016) MEGA7: Molecular Evolutionary Genetics Analysis version 7.0 for bigger datasets. *Molecular Biology and Evolution* 33(7): 1870–1874. <https://doi.org/10.1093/molbev/msw054>
- Perl RGB, Nagy ZT, Sonet G, Glaw F, Wollenberg KC, Vences M (2014) DNA barcoding Madagascar's amphibian fauna. *Amphibia-Reptilia* 35: 197–206. <https://doi.org/10.1163/15685381-00002942>
- Rambaut A, Drummond AJ (2007) Tracer v1.5. <http://beast.bio.ed.ac.uk/Tracer>.
- Ronquist F, Teslenko M, van der Mark P, Ayres DL, Darling A, Höhna S, Larget B, Liu L, Suchard MA, Huelsenbeck JP (2012) MRBAYES 3.2: Efficient Bayesian phylogenetic inference and model selection across a large model space. *Systematic Biology* 61(3): 539–542. <https://doi.org/10.1093/sysbio/sys029>
- Scherz MD, Hawlitschek O, Razafindraibe JH, Megson S, Ratsoavina FM, Rakotoarison A, Bletz MC, Glaw F, Vences M (submitted) A distinctive new frog species supports the biogeographic linkage of two montane rainforest massifs in northern Madagascar. *Zoosystematics and Evolution*.
- Scherz MD, Razafindraibe JH, Rakotoarison A, Bletz MC, Glaw F, Vences M (in press) Yet another small brown frog from high altitude on the Marojejy Massif, northeastern Madagascar. *Zootaxa*
- Stamatakis A (2014) RAXML Version 8: A tool for phylogenetic analysis and post-analysis of large phylogenies. *Bioinformatics* 30(9): 1312–1313. <https://doi.org/10.1093/bioinformatics/btu033>
- Vences M, Glaw F (2001) Systematic review and molecular phylogenetic relationships of the direct developing Malagasy anurans of the *Mantidactylus asper* group (Amphibia, Mantellidae). *Alytes* 19(2-4): 107–139.
- Vences M, Glaw F, Marquez R (2006) The Calls of the Frogs of Madagascar. 3 Audio CD's and booklet. Fonoteca Zoológica, Madrid, Spain, 44 pp.
- Vences M, Köhler J, Pabijan M, Bletz M, Gehring P-S, Hawlitschek O, Rakotoarison A, Ratsoavina FM, Andreone F, Crottini A, Glaw F (2017) Taxonomy and geographic distribution of Malagasy frogs of the *Gephyromantis asper* clade, with description of a new subgenus and revalidation of *Gephyromantis ceratophrys*. *Salamandra* 53(1): 77–98.
- Vences M, Köhler J, Pabijan M, Glaw F (2010) Two syntopic and microendemic new frogs of the genus *Blommersia* from the east coast of Madagascar. *African Journal of Herpetology* 59(2): 133–156. <https://doi.org/10.1080/21564574.2010.512961>
- Vences M, Köhler J, Vieites DR, Glaw F (2011) Molecular and bioacoustic differentiation of deep conspecific lineages of the Malagasy treefrogs *Boophis tampoka* and *B. luteus*. *Herpetology Notes* 4: 239–246.
- Vences M, Thomas M, Bonett RM, Vieites DR (2005) Deciphering amphibian diversity through DNA barcoding: chances and challenges. *Philosophical Transactions of the Royal Society B* 360: 1859–1868. <https://doi.org/10.1098/rstb.2005.1717>
- Vences M, Vieites DR, Glaw F, Brinkmann H, Kosuch J, Veith M, Meyer A (2003) Multiple overseas dispersal in amphibians. *Proceedings*

- of the Royal Society of London B 270(1532): 2435–2442. <https://doi.org/10.1098/rspb.2003.2516>
- Vieites DR, Wollenberg KC, Andreone F, Köhler J, Glaw F, Vences M (2009) Vast underestimation of Madagascar's biodiversity evidenced by an integrative amphibian inventory. Proceedings of the National Academy of Sciences of the USA 106(20): 8267–8272. <https://doi.org/10.1073/pnas.0810821106>
- Vieites DR, Wollenberg KC, Vences M (2012) Not all little brown frogs are the same; a new species of secretive and cryptic *Gephyromantis* (Anura: Mantellidae) from Madagascar. Zootaxa 3344: 34–46.
- Wollenberg KC, Glaw F, Vences M (2012) Revision of the little brown frogs in the *Gephyromantis decaryi* complex with description of a new species. Zootaxa 3421: 32–60.

Supplementary material 1

Recording 1

Authors: Mark D. Scherz, Miguel Vences, James Borrell, Lawrence Ball, Denise Herizo Nomenjanahary, Duncan Parker, Marius Rakotondratsima, Elidiot Razafimandimby, Thomas Starnes, Jeanneney Rabearivony, Frank Glaw

Data type: FLAC File (.flac)

Explanation note: Call recording of *Gephyromantis angano* sp. n. ZSM 68/2016. Call recorded at 22h40 on the 8th of January, 2016, 50 cm above the ground on a fern above a muddy spring in primary rainforest, calling as part of a small chorus, at 14.41949°S, 48.71938°E, 1340 m a.s.l., at an estimated air temperature between 15 and 20°C. Animal Sound Archive: http://wwwtierstimmenarchiv.de/webinterface/contents/showdetails.php?edit=-1&unique_id=TSA:Gephyromantis_angano_Scherz_1_1_0

Copyright notice: This dataset is made available under the Open Database License (<http://opendatacommons.org/licenses/odbl/1.0/>). The Open Database License (ODbL) is a license agreement intended to allow users to freely share, modify, and use this Dataset while maintaining this same freedom for others, provided that the original source and author(s) are credited.

Link: <https://doi.org/10.3897/zse.93.14906.suppl1>

Supplementary material 2

Recording 2

Authors: Mark D. Scherz, Miguel Vences, James Borrell, Lawrence Ball, Denise Herizo Nomenjanahary, Duncan Parker, Marius Rakotondratsima, Elidiot Razafimandimby, Thomas Starnes, Jeanneney Rabearivony, Frank Glaw

Data type: WAV File (.wav)

Explanation note: Call recordings of *Gephyromantis angano* sp. n. uncollected specimens. Call recorded at ca. 03h30 on the 8th of January, 2016 near a muddy spring in primary rainforest, at 14.41949°S, 48.71938°E,

1340 m a.s.l. Animal Sound Archive: http://wwwtierstimmenarchiv.de/webinterface/contents/showdetails.php?edit=-1&unique_id=TSA:Gephyromantis_angano_Scherz_1_2_0

Copyright notice: This dataset is made available under the Open Database License (<http://opendatacommons.org/licenses/odbl/1.0/>). The Open Database License (ODbL) is a license agreement intended to allow users to freely share, modify, and use this Dataset while maintaining this same freedom for others, provided that the original source and author(s) are credited.

Link: <https://doi.org/10.3897/zse.93.14906.suppl2>

Supplementary material 3

Recording 3

Authors: Mark D. Scherz, Miguel Vences, James Borrell, Lawrence Ball, Denise Herizo Nomenjanahary, Duncan Parker, Marius Rakotondratsima, Elidiot Razafimandimby, Thomas Starnes, Jeanneney Rabearivony, Frank Glaw

Data type: WAV File (.wav)

Explanation note: Call recording of *Gephyromantis* sp. Ca29 ZSM 58/2016. Call recorded at 18h40 on the 14th of January, 2016 on a broad fleshy leaf 4 m from a slow stream in degraded primary rainforest, calling as part of a large chorus, at 14.73600°S, 48.54831°E, 1180 m a.s.l., at an estimated air temperature of 17–23°C. Animal Sound Archive: http://wwwtierstimmenarchiv.de/webinterface/contents/showdetails.php?edit=-1&unique_id=TSA:Gephyromantis_sp_Ca_29_Scherz_1_3_0

Copyright notice: This dataset is made available under the Open Database License (<http://opendatacommons.org/licenses/odbl/1.0/>). The Open Database License (ODbL) is a license agreement intended to allow users to freely share, modify, and use this Dataset while maintaining this same freedom for others, provided that the original source and author(s) are credited.

Link: <https://doi.org/10.3897/zse.93.14906.suppl3>

Supplementary material 4

Recording 4

Authors: Mark D. Scherz, Miguel Vences, James Borrell, Lawrence Ball, Denise Herizo Nomenjanahary, Duncan Parker, Marius Rakotondratsima, Elidiot Razafimandimby, Thomas Starnes, Jeanneney Rabearivony, Frank Glaw

Data type: WAV File (.wav)

Explanation note: Call recording of *Gephyromantis* sp. Ca29 ZSM 59/2016. Call recorded at 18h25 on the 14th of January, 2016 on a leaf 50 cm above ground several metres from a slow stream in degraded primary rainforest, calling as part of a large chorus, at 14.73600°S,

48.54831°E, 1180 m a.s.l., at an estimated air temperature of 17–23°C. Animal Sound Archive: http://www.tierstimmenarchiv.de/webinterface/contents/showdetails.php?edit=-1&unique_id=TSA:Gephyromantis_sp_Ca_29_Scherz_1_4_0

Copyright notice: This dataset is made available under the Open Database License (<http://opendatacommons.org/licenses/odbl/1.0/>). The Open Database License (ODbL) is a license agreement intended to allow users to freely share, modify, and use this Dataset while maintaining this same freedom for others, provided that the original source and author(s) are credited.

Link: <https://doi.org/10.3897/zse.93.14906.suppl4>

Supplementary material 5

Figure S1

Authors: Mark D. Scherz, Miguel Vences, James Borrell, Lawrence Ball, Denise Herizo Nomenjanahary, Duncan Parker, Marius Rakotondratsima, Elidiot Razafimandimby, Thomas Starnes, Jeanneney Rabearivony, Frank Glaw

Data type: Encapsulated PostScript (.eps)

Explanation note: Phylogeny of *Gephyromantis* based on the BI consensus tree reconstructed by Bayesian Inference analysis of a fragment of the mitochondrial 16S rRNA gene. Numbers above nodes denote Bayesian Posterior Probability (PP); numbers below nodes indicate bootstrap support (%). PP lower than 0.9 and bootstrap support lower than 70% are not shown.

Numbers before taxon names are GenBank numbers; numbers after taxon names are field numbers.

Copyright notice: This dataset is made available under the Open Database License (<http://opendatacommons.org/licenses/odbl/1.0/>). The Open Database License (ODbL) is a license agreement intended to allow users to freely share, modify, and use this Dataset while maintaining this same freedom for others, provided that the original source and author(s) are credited.

Link: <https://doi.org/10.3897/zse.93.14906.suppl5>

Supplementary material 6

Table S1

Authors: Mark D. Scherz, Miguel Vences, James Borrell, Lawrence Ball, Denise Herizo Nomenjanahary, Duncan Parker, Marius Rakotondratsima, Elidiot Razafimandimby, Thomas Starnes, Jeanneney Rabearivony, Frank Glaw

Data type: Microsoft Excel 97-2003 Worksheet (.xls)

Explanation note: Average uncorrected pairwise-distances in a fragment of the 16S rRNA gene among *Gephyromantis* species.

Copyright notice: This dataset is made available under the Open Database License (<http://opendatacommons.org/licenses/odbl/1.0/>). The Open Database License (ODbL) is a license agreement intended to allow users to freely share, modify, and use this Dataset while maintaining this same freedom for others, provided that the original source and author(s) are credited.

Link: <https://doi.org/10.3897/zse.93.14906.suppl6>

Chapter 3. PAPER: A distinctive new frog species (Anura, Mantellidae) supports the biogeographic linkage of the montane rainforest massifs of northern Madagascar

In this chapter, I present the description of a new species of *Gephyromantis* from the subgenus *Vatomantis* that was first discovered on an expedition to Sorata in 2012, and then also found by my colleagues and me in Marojejy, and by another set of colleagues in Andravory in 2016. This species, *Gephyromantis (Vatomantis) lomorina*, occurs between 1150 and 1400 m a.s.l. across all three areas. There is a small mitochondrial differentiation between populations from Marojejy and Sorata, but the difference amounts only to intraspecific variation. We suggest that the presence of the species, which only occurs above 1150 m a.s.l., across all three mountain massifs, implies historical or on-going biogeographic connection between these areas around these elevations. This chapter thus establishes that the Marojejy massif is not only connected to the Bealanana District as demonstrated in **chapter 2**, but also to the Sorata massif and nearby Andravory.

Scherz, M.D., Hawlitschek, O., Razafindraibe, J.H., Megson, S., Ratsoavina, F.M., Rakotoarison, A., Bletz, M.C., Glaw, F. & Vences, M. (2018) A distinctive new frog species (Anura, Mantellidae) supports the biogeographic linkage of the montane rainforest massifs of northern Madagascar. *Zoosystematics and Evolution*, 94(2):247–261. DOI: 10.3897/zse.94.21037

Post-publication comments and errata:

Page 258. It is stated that connection between Marojejy, Sorata, and Manongarivo reaches ‘up to 1400 m’. This connection in fact limited to ca. 1120 m a.s.l. This point is emphasised in the **Discussion**, as it has paleoclimatic and biogeographic implications.

Digital Supplementary Materials on appended CD:

Supplementary Material 1 — Recording 1

Supplementary Material 2 — Recording 2

A distinctive new frog species (Anura, Mantellidae) supports the biogeographic linkage of two montane rainforest massifs in northern Madagascar

Mark D. Scherz^{1,2}, Oliver Hawlitschek², Jary H. Razafindraibe³,
Steven Megson⁴, Fanomezana Mihaja Ratsoavina³, Andolalao Rakotoarison^{2,3},
Molly C. Bletz^{2,5}, Frank Glaw¹, Miguel Vences²

1 *Zoologische Staatssammlung München (ZSM-SNSB), Münchhausenstr. 21, 81247 Munich, Germany*

2 *Zoologisches Institut, Technische Universität Braunschweig, Mendelsohnstr. 4, 38106 Braunschweig, Germany*

3 *Mention Zoologie et Biodiversité Animale, Université d'Antananarivo, BP 906, Antananarivo 101, Madagascar*

4 *School of Science and the Environment, Manchester Metropolitan University, Manchester, M1 5GD, UK*

5 *Department of Biology, University of Massachusetts Boston, 100 Morrissey Boulevard, Boston, MA 02125, USA*

<http://zoobank.org/8A83DE58-A2EE-494F-A03C-820DC836CDDF>

Corresponding author: Mark D. Scherz (mark.scherz@gmail.com)

Abstract

Received 16 September 2017

Accepted 26 February 2018

Published 15 March 2018

Academic editor:
Johannes Penner

Key Words

Bioacoustics
Biogeography
Marojejy
Montane Endemism
Sorata
Taxonomy

We describe a new species of the genus *Gephyromantis*, subgenus *Vatomantis* (Mantellidae, Mantellinae), from moderately high elevation (1164–1394 m a.s.l.) on the Marojejy, Sorata, and Andravory Massifs in northern Madagascar. The new species, *Gephyromantis (Vatomantis) lomorina* sp. n. is highly distinct from all other species, and was immediately recognisable as an undescribed taxon upon its discovery. It is characterised by a granular, mottled black and green skin, reddish eyes, paired subgular vocal sacs of partly white colour, bulbous femoral glands present only in males and consisting of three large granules, white ventral spotting, and a unique, amplitude-modulated advertisement call consisting of a series of 24–29 rapid, quiet notes at a dominant frequency of 5124–5512 Hz. Genetically the species is also strongly distinct from its congeners, with uncorrected pairwise distances $\geq 10\%$ in a fragment of the mitochondrial 16S rRNA gene to all other nominal *Gephyromantis* species. A molecular phylogeny based on 16S sequences places it in a clade with species of the subgenera *Laurentomantis* and *Vatomantis*, and we assign it to the latter subgenus based on its morphological resemblance to members of *Vatomantis*. We discuss the biogeography of reptiles and amphibians across the massifs of northern Madagascar, the evidence for a strong link between Marojejy and Sorata, and the role of elevation in determining community sharing across this landscape.

Introduction

In recent decades, the number of frog species that have been discovered in Madagascar, while steadily increasing (Köhler et al. 2005), often included species that were not immediately recognizable as new to science, though with occasional exceptions, e.g. *Boophis lichenoides* (Vallan et al. 1998), *Scaphiophryne boribory* (Vences et al. 2003), and *Tsingymantis antitra* (Glaw et al. 2006). The majority of newly discovered taxa are assignable to existing complexes and must be investigated closely before it can

be confirmed whether or not they constitute new species (e.g. Vieites et al. 2012). Differing from this general pattern, on a 2012 expedition to the Sorata massif in northern Madagascar, we discovered a small green frog of the genus *Gephyromantis* that was immediately recognisable as a new species. It was not given a candidate species number at the time, and no sequences of this species were included in the barcoding assessment of Perl et al. (2014). In a 2016 survey in Andravory, near Sorata, and a 2016 survey of Marojejy National Park in northeastern Madagascar, we encountered the same species.

At present, 44 species of *Gephyromantis* are recognized and assigned to six subgenera (*Asperomantis*, *Duboinmantis*, *Gephyromantis*, *Laurentomantis*, *Phylacomantis*, and *Vatomantis*) based on molecular and morphological criteria (Glaw and Vences 2006, Vences et al. 2017). This classification is largely in agreement with the molecular multi-gene phylogeny of Kaffenberger et al. (2012). However, this phylogenetic study revealed that the subgenera *Laurentomantis* and *Vatomantis* are closely related, and that *Gephyromantis klemmeri* Guibé, 1974, morphologically similar to other species of the subgenus *Gephyromantis*, is sister to the *Laurentomantis* clade, suggesting the need for an improved classification. We here provide a description of the new species, which has potential implications for the supraspecific taxonomy of *Gephyromantis*, and the biogeographical linkage of the rainforest massifs of northern Madagascar.

Materials and methods

Specimen collection and morphological measurement

Specimens were collected at night using head torches along montane streams, euthanized using MS222 anaesthesia and subsequent overdose, fixed in 96 % ethanol, and deposited in 75 % ethanol for long-term storage. Tissue samples were stored in 96 % ethanol. Field numbers refer to the zoological collections of Miguel Vences (ZCMV), Frank Glaw (FGZC), and Steven Megson (SM). Specimens were deposited in the amphibian collections of the Mention Zoologie et Biodiversité Animale, Université d'Antananarivo (UADBA-A) and the Zoologische Staatssammlung München (ZSM).

Morphological measurements were taken to the nearest 0.1 mm using a digital calliper. Measurement schemes followed generally previous work on the genus (e.g. Vences et al. 2017) with modifications to decrease the risk of damaging the fragile limbs of the specimens when ascertaining limb lengths: snout–vent length (SVL), maximum head width (HW), head length from posterior edge of tympanum to snout tip (HL), horizontal eye diameter (ED), horizontal tympanum diameter (TD), distance from eye to nostril (END), distance from nostril to snout tip (NSD), distance between nostrils (NND), upper arm length from the articulation of the arm with the trunk to the elbow (UAL), lower arm length from the elbow to the base of the hand (LAL), hand length from the base of the hand to the tip of the longest finger (HAL), fore-limb length (FORL*, given by the sum of UAL, LAL, and HAL), forearm length (FARL, given by the sum of LAL and HAL), thigh length from cloaca to knee (THIL), tibia length from knee to heel (TIBL), tarsus length from heel to base of foot (TARL), foot length from base of foot to tip of longest toe (FOL), hindlimb length (HIL*, given by the sum of THIL, TIBL, TARL and FOL), and length and width of femoral gland (FGL, FGW). Asterisks in this list indicate measurements that have the same abbreviation as the analogous single-measurement of previous studies

(e.g. Vences et al. 2017) but are cumulative here and therefore not necessarily equivalent; comparison of such values must be done cautiously.

Sequencing and analysis of DNA sequences

DNA was extracted from tissue samples using a Qiagen DNeasy blood & tissue kit (Qiagen, Hilden, Germany), or standard salt extraction protocols. For two samples from Sorata and one sample from Marojejy (ZCMV 15269), we amplified a fragment of the mitochondrial 16S rRNA gene (hereafter 16S) in 25 µl polymerase chain reactions with the primers 16Sra-L and 16Sb-H (Palumbi et al. 1991), 1 µl of template DNA, and the following steps: initial denaturation for 3 min at 94 °C, followed by denaturation with 35 cycles of 30 sec each at 94 °C, 30 sec of annealing at 55 °C and 60 sec of elongation at 72 °C, and a final elongation step of 10 min at 72 °C. Sequencing was conducted using the BigDye Terminator v1.1 Cycle Sequencing Kit on ABI 3730 and ABI 3130xl capillary sequencers. Newly determined sequences were deposited in GenBank (accession numbers MG926811–MG926823). For an additional nine specimens from Marojejy, we sequenced a shorter, highly variable stretch of 250 bp of the same 16S region by an Illumina amplicon approach (Vences et al. 2016) to confirm their identification (data not shown).

For an exploratory analysis, we aligned the new sequences with 16S sequences used by Kaffenberger et al. (2012) for all nominal species of *Gephyromantis*. Because the obtained tree (not shown) confirmed the new species to be related to the *Laurentomantis/Vatomantis* clade as also strongly suggested by morphology, we focused our analysis on this subgroup, i.e., all nominal species of the subgenera *Laurentomantis* and *Vatomantis*, and *G. klemmeri* which is known to be related to these subgenera (Kaffenberger et al. 2012), as well as *G. granulatus* (subgenus *Duboinmantis*) as outgroup.

We aligned sequences in MEGA 7 (Kumar et al. 2016), yielding an alignment of 532 positions of the sequenced stretch of the 16S rRNA gene. As only a few indels were found in this alignment, we did not exclude any positions for further analysis. We used the Bayesian Information Criterion in jModelTest 2.1.4 (Darriba et al. 2012) to determine a SYM+G substitution model as best-fitting our data. We implemented this model in MrBayes 3.2 (Ronquist et al. 2012) and computed a Bayesian inference phylogenetic analysis, with two independent runs of 20 million generations, each comprising four Markov Chains (three heated and one cold), sampling every 1000 generations. Chain mixing and stationarity were assessed by examining the standard deviation of split frequencies and by plotting the -lnL per generation using Tracer 1.5 software (Rambaut and Drummond 2007). Results were combined to obtain a 50 %-majority rule consensus tree and the respective posterior probabilities of nodes, after discarding 25 % of the generations as burn-in (all compatible nodes with probabilities <0.5 kept). In addition, we computed a Maximum Likelihood (ML) tree in MEGA 7, with a GTR+G model (as the SYM model is not available

in this program), SPR level 5 branch swapping, and 500 nonparametric bootstrap replicates. Genetic distances (uncorrected pairwise p-distances) were also calculated in MEGA 7.

Bioacoustic analyses

Recordings from Marojejy were made on a Marantz PMD661 MKII with a Sennheiser ME66/K6 supercardioid microphone, at a bandwidth of 44.1 kHz. Recordings from Sorata were made on an Edirol R-09 with its internal microphone. Call analysis was conducted in Cooedit 2.0 (Syntrillium Corp.). To obtain frequency information, the recording was transformed with Fast Fourier Transformation (FFT; width 1024 points). Spectrograms were created with a Hanning window of 512 or 256 bands. Measurements are given as mean \pm one standard deviation, with range in parentheses. Terminology follows the recently-published recommendations of Köhler et al. (2017) with a note-centred approach. This definition is different from that of Vences et al. (2002) for *Laurentomantis* and Sabino-Pinto et al. (2014) for *Vatomantis*; the ‘pulses’ of those studies are here treated as notes, because each of these units in the new species described herein are distinctly pulsed, and therefore are treated as individual notes following Köhler et al. (2017). Recordings are deposited in the Animal Sound Archive of the Museum für Naturkunde, Berlin (DOI: 10.7479/nmx8-aq7v), and are available as Suppl. materials 1–2.

Taxonomic work

The electronic version of this article in Portable Document Format (PDF) will represent a published work according to the International Commission on Zoological Nomenclature (ICZN), and hence the new names contained in the electronic version are effectively published under that Code from the electronic edition alone. This published work and the nomenclatural act it contains have been registered in ZooBank, the online registration system for the ICZN. The ZooBank LSIDs (Life Science Identifiers) can be resolved and the associated information viewed through any standard web browser by appending the LSID to the prefix <http://zoobank.org/>. The LSID for this publication is urn:lsid:zoobank.org:pub:8A83DE58-A2EE-494F-A03C-820DC836CDDE. The online version of this work will be archived and made available from the following digital repositories: CLOCKSS and Zenodo.

Results

Based on 16S sequences, the newly collected specimens represent an undescribed and hitherto unknown species of *Gephyromantis* that is highly distinct from all others ($\geq 10\%$ p-distance). Exploratory phylogenetic analyses including all species of *Gephyromantis* clearly suggested their relationships with the subgenera *Laurentomantis* and *Vatomantis*, which also is strongly supported by morphological affinities, in particular by the greenish dorsal

colour, granular skin, riparian habits, and paired subgular vocal sacs of partly white colour in males (see Diagnosis below for more details). A phylogenetic analysis of 16S sequences (total alignment length 532 bp) for all described species of *Laurentomantis* and *Vatomantis* as well as *G. klemmeri*, which was related to these subgenera in the multi-gene analysis of Kaffenberger et al. (2012), places the newly collected specimens sister to a clade with all described species of *Vatomantis*. *Gephyromantis klemmeri* is placed sister to *Laurentomantis*, although these basal nodes did not receive relevant support from ML bootstrap values or Bayesian posterior probabilities (Fig. 1). Genetic distances of the new specimens to all other species were high: 10.9–15.4 % to the three described species of *Vatomantis*, 10.0–13.2 % to species of *Laurentomantis*, and 12.2–12.5 % to *G. klemmeri*. The newly collected specimens from Sorata and Marojejy differed by 2.9 %, while no sequence differences were detected within each of these two localities, except for two mutations observed in one Marojejy specimen (ZCMV 15219).

Phenotypically the new specimens bear resemblance to both *Laurentomantis* and *Vatomantis*. Their advertisement call is more similar to *Laurentomantis*, but their morphological resemblance to *Vatomantis* is greater (see the diagnosis below). We here tentatively assign them to *Vatomantis* due to their morphological affinities and preliminary phylogenetic relationships. Given their very high genetic divergence to all other *Gephyromantis*, isolated phylogenetic position (not placed as close sister group to any other species), and morphological and bioacoustic differences, there is no doubt that these specimens belong to a new species, which we describe below.

Gephyromantis (Vatomantis) lomorina sp. n.

<http://zoobank.org/5D2109C8-AD0A-434D-816F-51722FE7DCD7>

Figs 1–4, Table 1, Suppl. materials 1–2

Holotype. ZSM 419/2016 (ZCMV 15221), adult male, collected at 21h20 on 18 November 2016 near Camp Simpona (ca. 14.4366°S, ca. 49.7434°E, ca. 1325 m a.s.l.) in Marojejy National Park, Sava Region, northeastern Madagascar, by M. D. Scherz, J. H. Razafindraibe, M. C. Bletz, A. Rakotoarison, A. Razafimanantsoa, and M. Vences (Fig. 2).

Paratypes. ZSM 418/2016 (ZCMV 15220), female, and ZSM 420–421/2016 (ZCMV 15222 and 15271), two males, collected between 17 and 19 November 2016 from the same locality and by the same collectors as the holotype; UADBA-A 60294–60299 (ZCMV 15219, 15223, 15247, 15270, 15272, and 15273), one male, three females, a subadult and an unsexed adult, collected between 17 and 19 November 2016 from the same locality and by the same collectors as the holotype; ZSM 1549/2012 (FGZC 3714), adult male, collected on 30 November 2012 in a creek near the campsite on the Sorata massif (13.6829°S, 49.4403°E, 1325 m a.s.l.), Sava Region, northeastern Madagascar,

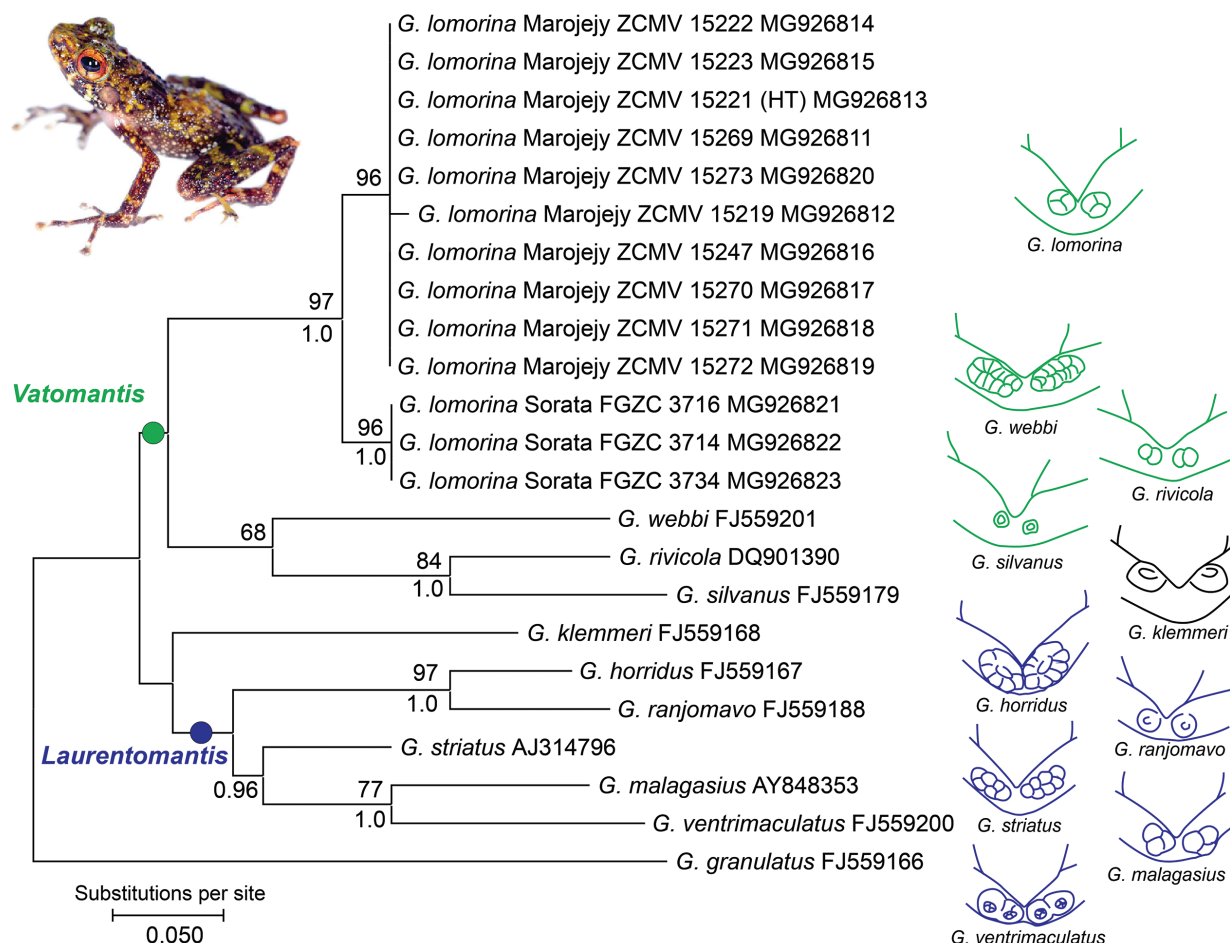


Figure 1. Preliminary phylogenetic tree of *Gephyromantis (Vatomantis) lomorina* sp. n., based on Maximum Likelihood analysis of a 532 bp fragment of the mitochondrial 16S rRNA gene. Numbers at nodes indicate bootstrap values in percent (500 replicates, above) and posterior probabilities from a Bayesian Inference analysis (20 million generations, below), shown only if >50 % (bootstrap) or >90 % (posterior probabilities). Each specimen/species is followed by the corresponding GenBank accession number used in the alignment. Schematic drawings of femoral glands of all species in the subgenera *Laurentomantis* and *Vatomantis* as well as of *G. klemmeri* are shown to the right of the phylogeny, and coloured according to the subgenus to which they are assigned.

by O. Hawlitschek, F. Glaw, A. Rakotoarison, F. M. Ratsoavina, T. Rajoafiarison, and A. Razafimanantsoa; ZSM 1545–1547/2012 (FGZC 3716, 3734, and 3664), adult males, and ZSM 1548/2012 (FGZC 3721), adult female, collected between 28 and 30 November 2012 from a creek below a bamboo forest on the Sorata massif (13.6772°S, 49.4413°E, 1394 m above sea level), Sava Region, northeastern Madagascar, by O. Hawlitschek, F. Glaw, A. Rakotoarison, F. M. Ratsoavina, T. Rajoafiarison, and A. Razafimanantsoa; ZSM 318/2016 (SM AEA 063), adult female, and UADBA-A uncatalogued (SM AEA 062), unsexed adult, collected between 18h45 and 18h50 on 30 May 2016 in Andravory (13.7385–13.7388°S, 49.5310°E, 1164–1179 m a.s.l.), Sava Region, Antsiranana Province, northeastern Madagascar, by S. Megson, R. Walker, W.-Y. Crawley, and T. H. Rafeliarisoa (Figs 3–4).

Diagnosis. A species assigned to the genus *Gephyromantis* on the basis of its granular skin, moderately en-

larged finger tips, small femoral glands consisting of a small number of large granules and present in males only (thus of type 2 as defined by Glaw et al. 2000), and bifid tongue. Within the genus *Gephyromantis*, assigned to the subgenus *Vatomantis* on the basis of its small size, connected lateral metatarsalia, absence of an outer metatarsal tubercle, paired subgular vocal sacs of partly whitish colour, greenish skin colouration, and riparian ecology. *Gephyromantis lomorina* sp. n. is characterized by the possession of the following suite of morphological characters: (1) granular skin, (2) reddish eyes, (3) mottled green and black skin, (4) males with paired subgular vocal sacs of partly white colour, (5) males with bulbous type 2 femoral glands consisting of a small number (2–3) of large granules, (6) white spots on the venter, (7) SVL 20.2–25.5 mm, and (8) fourth finger much longer than second. Furthermore, the species is characterised by distinctive, 1681–1827 ms advertisement calls of relatively low intensity, consisting of 24–30 individual pulsed notes,

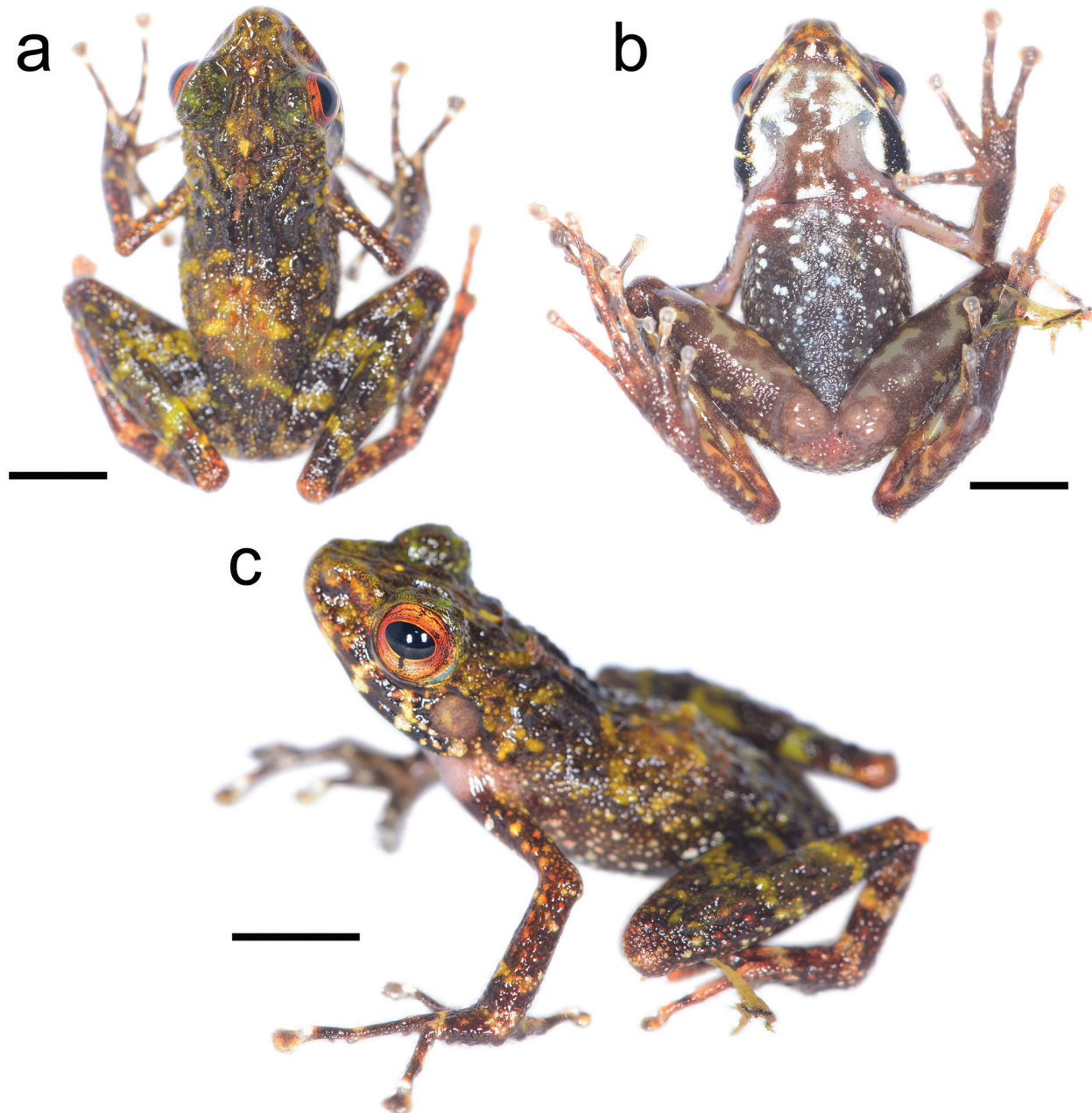


Figure 2. The holotype of *Gephyromantis lomorina* sp. n., ZSM 419/2016 (ZCMV 15221) in life. (a) Dorsal; (b) ventral; and (c) dorsolateral view. Scale bars indicate 5 mm.

with 2–4 pulses per note, an inter-note interval of 41–75 ms, and a dominant frequency of 5124–5555 Hz. DNA sequence data from the 16S gene fragment supports the high divergence of this taxon to all other *Gephyromantis*, and is in agreement with its subgeneric assignment, albeit without statistical support (Fig. 1).

Within the genus *Gephyromantis*, *G. lomorina* sp. n. can be distinguished from all subgenera except *Laurentomantis* and *Vatomantis* on the basis of the combination of femoral glands composed of few large granules (vs. composed of many, small granules; note that *G. klemmeri* is here treated separately from all other subgenera, below, due to its unclear assignment), SVL < 26 mm (vs. > 27 mm

in all other subgenera except *Gephyromantis*), absence of a white stripe along the upper lip (vs. general presence in subgenus *Gephyromantis*), and absence of distinctly enlarged supraocular spines (vs. presence in *Asperomantis* and some *Duboimantis*). It may be distinguished from all members of the subgenus *Laurentomantis* (*G. ventrimaculatus* (Angel), *G. malagasius* (Methuen & Hewitt), *G. striatus* (Vences, Glaw, Andreone, Jesu & Schimmenti), *G. horridus* (Boettger), and *G. ranjomavo* Glaw & Vences) by paired subgular vocal sacs (vs. single), absence of outer metatarsal tubercles (vs. presence), and at least partly greenish dorsal skin (vs. mostly yellowish to brown to reddish), and from several of these by the

Table 1. Morphological data on specimens of *Gephyromantis lomorina* sp. n. Abbreviations: m = male, f = female, sa = subadult; for measurement abbreviations, see the Materials and methods. The holotype is bolded. Additive measurements (FARL, FORL, and HIL) are not explicitly shown but can be deduced from these data.

Catalogue (field number)	Sex	SVL	HW	HL	TD	ED	END	NSD	NND	UAL	LAL	HAL	THIL	TIBL	TARL	FOL	FGL	FGW
ZSM 419/2016 (ZCMV 15221)	m	23.3	7.2	8.5	2.1	4.0	2.2	1.4	2.2	6.0	7.3	8.2	13.4	13.9	7.4	12.1	2.8	2.0
ZSM 421/2016 (ZCMV 15271)	m	22.2	6.6	8.2	1.9	3.4	2.1	1.5	2.2	4.8	6.0	8.0	12.2	12.8	7.0	10.6	2.2	1.8
ZSM 420/2016 (ZCMV 15222)	m	23.0	7.3	9.1	1.9	3.0	1.9	1.5	2.1	5.1	6.8	8.2	11.5	13.3	7.0	11.8	2.2	1.5
ZSM 418/2016 (ZCMV 15220)	f	25.5	7.7	9.1	2.0	4.1	2.4	1.4	2.1	5.2	7.7	8.4	13.6	14.8	6.7	12.6	n/a	n/a
UADBA-A 60294 (ZCMV 15270)	m	22.1	6.5	8.0	2.7	3.4	1.5	1.4	1.9	4.9	6.1	7.2	10.8	12.3	6.4	11.0	2.6	1.6
UADBA-A 60298 (ZCMV 15273)	f	24.6	7.6	9.0	2.0	3.8	2.2	1.4	2.1	6.4	6.4	8.3	12.1	13.5	7.3	12.4	n/a	n/a
UADBA-A 60296 (ZCMV 15223)	sa	20.2	5.7	7.8	1.6	3.1	1.9	1.6	1.9	4.8	5.9	7.6	11.1	12.0	6.6	9.5	n/a	n/a
UADBA-A 60297 (ZCMV 15272)	f	24.6	8.0	8.7	2.1	3.5	2.4	1.3	2.2	5.7	6.1	8.6	12.4	14.7	7.3	12.0	n/a	n/a
UADBA-A 60295 (ZCMV 15219)	f	23.2	6.8	8.5	2.0	3.6	2.0	1.4	2.0	5.6	6.9	8.1	12.6	14.9	7.6	11.6	n/a	n/a
UADBA-A 60299 (ZCMV 15247)	f	22.0	7.0	8.1	2.1	3.5	2.3	1.5	2.0	5.0	6.0	7.5	10.4	12.4	7.0	11.6	n/a	n/a
ZSM 1549/2012 (FGZC 3714)	m	23.3	8.0	8.3	2.3	3.3	2.6	1.5	1.9	5.8	6.7	8.8	11.1	13.2	6.7	12.6	3.0	2.1
ZSM 1545/2012 (FGZC 3716)	m	22.8	7.1	8.0	2.2	3.0	2.8	1.5	2.1	6.0	6.9	8.1	11.9	13.1	6.7	13.2	2.9	2.1
ZSM 1546/2012 (FGZC 3734)	m	24.6	8.0	9.7	2.2	3.3	2.8	1.6	2.3	7.0	7.5	9.3	13.1	14.5	6.6	13.4	3.4	2.5
ZSM 1547/2012 (FGZC 3664)	m	23.9	8.1	9.1	2.2	3.4	2.6	1.6	2.2	6.4	7.0	9.5	12.1	14.2	6.5	13.6	2.5	2.1
ZSM 1548/2012 (FGZC 3721)	f	24.1	7.7	9.2	2.2	2.8	2.8	1.4	2.2	5.5	6.6	9.3	12.5	14.0	6.5	13.8	n/a	n/a
ZSM 318/2016 (SM AEA 063)	f	25.2	7.9	9.4	2.1	2.6	3.0	2.0	2.4	7.1	6.4	8.9	13.6	14.2	7.2	13.6	n/a	n/a

absence of tibial glands in males (vs. typical presence). Within the subgenus *Vatomantis*, *G. lomorina* sp. n. may be distinguished from all species by its more granular dorsal skin (vs. granular but not rough) and venter spotted with white (vs. generally without whitish spotting except on the chin and over the sternum); from *G. rivicola* (Vences, Glaw & Andreone) and *G. webbi* (Grandison) by its reddish iris colouration (vs. copper and greenish, respectively); from *G. silvanus* (Vences, Glaw & Andreone) by its smaller size (SVL 20.5–25.5 mm vs. 31 mm) and partly whitish vocal sacs (vs. yellowish); from *G. webbi* by femoral glands composed of few large granules (vs. composed of many, small granules) and large inner metatarsal tubercle (vs. small). *Gephyromantis lomorina* sp. n. may be distinguished from *G. klemmeri* by its roughly granular dorsal skin (vs. smooth to shagreened), greenish skin colour (vs. brownish), reddish iris (vs. gold), and strongly protruding inner metatarsal tubercle (vs. small and not protruding).

The call of *G. lomorina* sp. n. may be distinguished from all *Vatomantis* and *Laurentomantis* species in having notes that are clearly pulsed (vs. unpulsed

notes in all species except *G. ventrimaculatus*); *Gephyromantis ventrimaculatus* has a higher number of pulses per note than *G. lomorina* sp. n. (ca. 6 pulses per note vs. 2–4 in *G. lomorina* sp. n.). The call of *G. lomorina* sp. n. is somewhat similar to that of *G. klemmeri*, especially in having pulsed notes, but the call duration is much longer (1681–1827 ms vs. 626–982 ms), the call has a more distinct amplitude decay (vs. complex amplitude modulation, see Vences et al. 1997), the notes of the call are more homogeneous (vs. distinct components of the call), and it lacks frequency modulation (vs. frequency modulated toward the end of the call).

Description of the holotype. A specimen in a good state of preservation, a piece of tissue taken from the left thigh. SVL 23.3 mm; for other body measurements see Table 1. Body slender. Widest part of head marginally wider than widest part of body. Snout rounded in dorsal and lateral view, protruding slightly over upper jaw in lateral view. Nostrils not distinctly protruding, with lateral openings. Canthus rostralis distinct, concave. Loreal re-

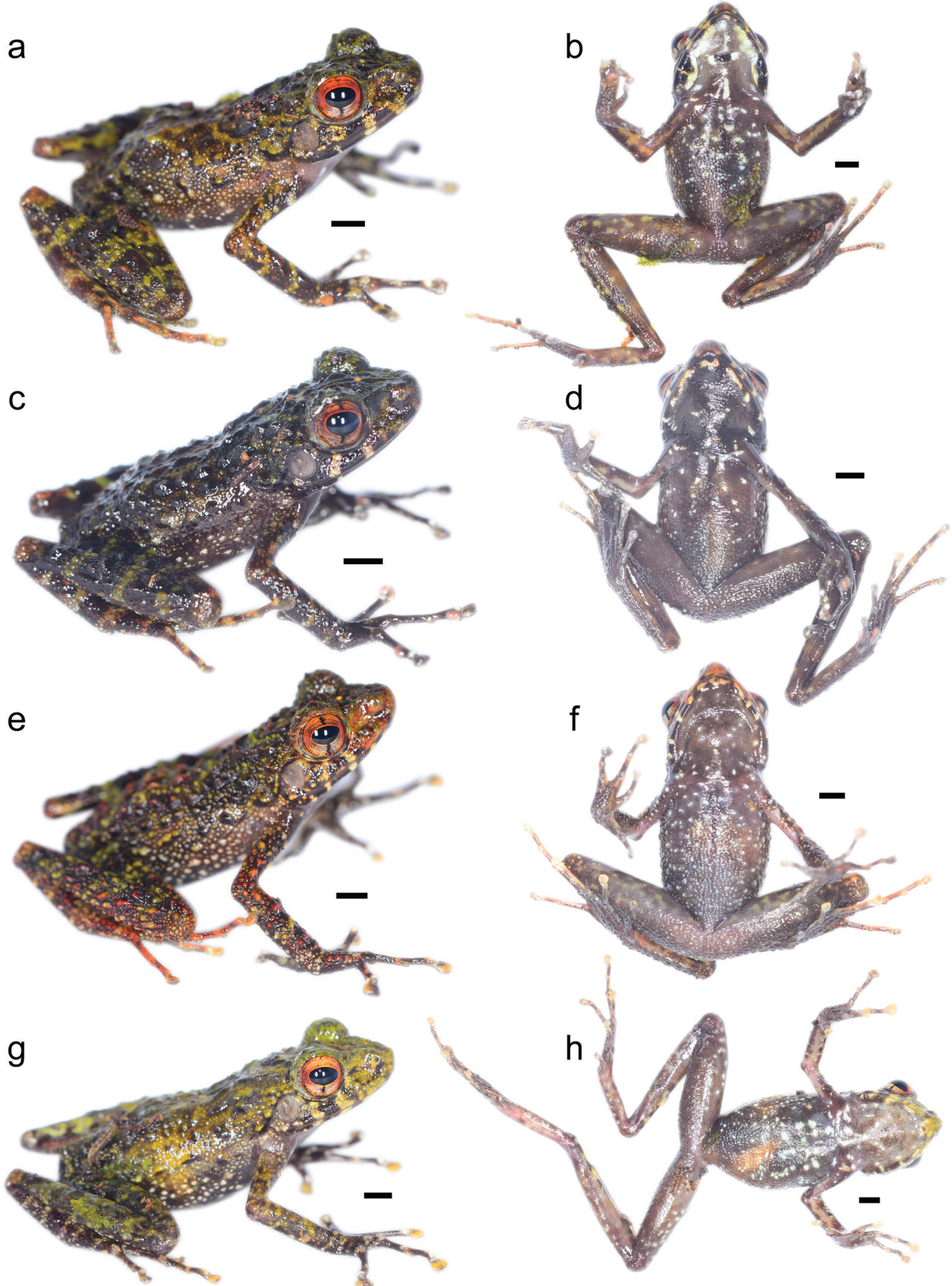


Figure 3. Morphological and chromatic variation among paratypes of *Gephyromantis (Vatomantis) lomorina* sp. n. from Marojejy in life. (a–b) ZSM 420/2016; (c–d) UADBA-A 60296; (e–f) UADBA-A 60295; and (g–h) ZSM 418/2016. Scale bars indicate 2 mm.

gion concave, vertical. Tympanum distinct, fairly small, 53% of eye diameter. Supraocular spines absent. Weakly distinct supratympanic fold running from the eye over the tympanum to above the insertion of the arm. Fore-

limbs and hindlimbs slender. Inner and outer metacarpal tubercle present, both indistinct. Finger discs enlarged, round. Subarticular tubercles distinct, dark in colour. No webbing between fingers. Comparative finger lengths



Figure 4. Photographs of *Gephyromantis (Vatomantis) lomorina* sp. n. and its habitat in Sorata. (a,d) ZSM 1545/2012; (b,e) ZSM 1547/2012; and (c,f) ZSM 1549/2012, not to scale; (g) habitat where several specimens were found in Sorata, showing (h,i) the appearance of the species in situ whilst calling at night.

$1 < 2 < 4 < 3$, fourth finger much longer than second finger. Toe discs slightly enlarged, smaller than finger discs. Traces of webbing between toes. Comparative toe length

$1 < 2 < 3 = 5 < 4$. Inner metatarsal tubercle rather large (length about 1.3 mm), protruding strongly distally to resemble a toe. Outer metatarsal tubercle absent. Lateral

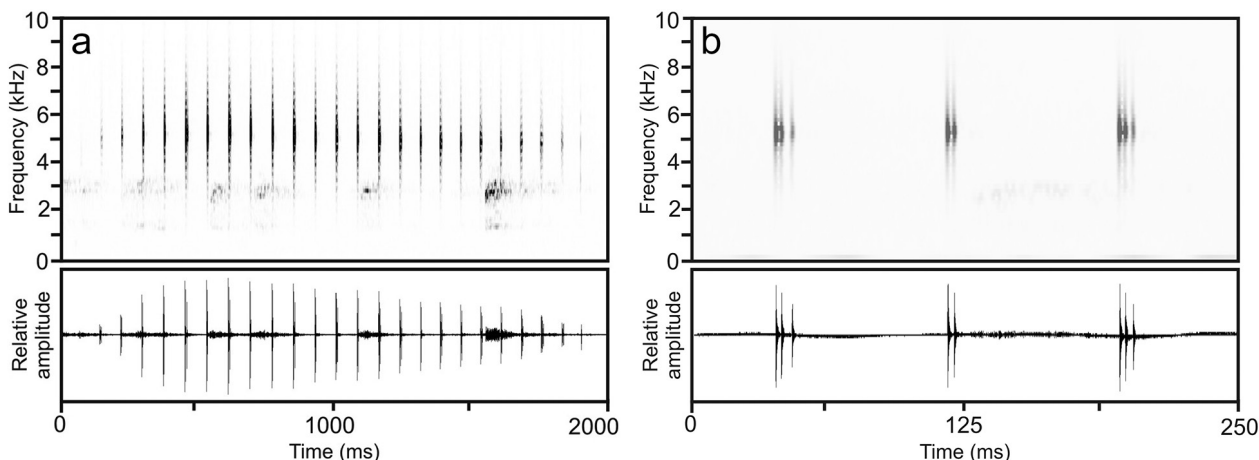


Figure 5. Spectrogram (above) and waveform (below) of a call of the holotype of *Gephyromantis (Vatomantis) lomorina* sp. n., ZSM 419/2016, from Marojejy. (a) A full call (spectrogram shown using FFT of 512 points to visualise call structure); and (b) a 250 ms section from the middle of a call, showing the degree of pulsation of each note (spectrogram shown using FFT of 128 points to visualise note structure).

metatarsalia connected. Dorsal skin granular, with numerous small tubercles arranged in mostly parallel lines running posteriorly over the dorsum, with convergent lines of tubercles on the posterior head, and weak rows of tubercles on the hindlimbs and forelimbs. Femoral glands round, consisting of three large granules with an indentation in their middle (similar to type 2 sensu Glaw et al. 2000). Vomerine teeth absent. Maxillary teeth present. Choanae small and lateral. Subgular vocal sacs whitish in distensible portion, blackish on the jaw, fairly small. Tongue bifid, free posteriorly.

Colouration in life (Fig. 2) dorsally mottled with greens, browns, blacks, and yellows. Particularly green over the eyes. Raised ridges on the back were mostly yellowish, but some also with an orange hint. Flanks and lateral head as dorsum. Legs dark brown with yellow-green cross-bands, three on the thigh, three on the shank, and two on the tarsus. The tarsus and dorsal foot were a more ruddy brown than the rest of the body, mottled with a tan orange on the toes and on the heel. A few tubercles on the legs were red. A whitish annulus was present before the terminal disc of each toe and finger. The forelimbs were as the shanks and foot, ruddy brown mottled with yellow-green and dark brown, with a few red tubercles. Whitish spots were present in the inguinal region and the ventral portion of the flank, and also two cream stripes were present below the eye that continued on the bottom lip. The tympanum was distinctly brownish. The venter was umber in base colour with more reddish portions of translucent skin on the ventral side of the arms. The chin had white portions along the lip and especially on the vocal sacs, but the jaw itself was blackish. The venter had distinct white spots. The ventral hindlimbs were umber with irregular pale olive and yellow patches on the ventral thigh and shank. The ventral tarsus, foot, and hand were umber. The femoral glands were fleshy in colour, and the area ventral to the cloaca was pinkish. The iris was copper above and below, and rusty anteriorly and

posteriorly, with blackish reticulations and a blackish line above and below the centre of the pupil.

After six months in preservative, the colouration of the holotype has faded to become more uniformly brownish, and areas that were greenish in life have become cream. White areas of the venter are still immaculately white.

Variation. All paratypes resemble the holotype in gross morphology; see Table 1 for morphological variation. Tympanum diameter ranges from 47–79 % of eye, without strong sexual dimorphism in tympanum size. Females are marginally but not significantly larger than males (t -test, $t = -1.9215$, $df = 13$, $p = 0.07687$). Several paratypes have smaller femoral glands than the holotype. Femoral glands are composed of 2 or 3 large granules (mean 2.875 ± 0.35 , $n = 8$; all but one of eight examined specimens with 3 granules). Females have minuscule raised bumps in the femoral area. There is considerable variation in colouration of the specimens, with some individuals being much darker, and others being more green (Figs 3–4). The chin of females is more solidly dark than that of males, and they lack most white spots. A pair of cream stripes below the eye that continue on the lower lip is present in all specimens. Two specimens (UADBA-A 60299, and ZSM 1545/2012, Fig. 4) have a bright vertebral stripe.

Bioacoustics. Call recordings were made in Marojejy from the holotype ZSM 419/2016 at its collection locality at a distance of 0.5 m during light rain (Suppl. material 1, DOI: 10.7479/nmx8-aq7v). The call is interpreted as an advertisement call as it resembles the advertisement calls of the subgenus *Laurentomantis*, and was emitted without close proximity to other individuals, and while the frog was otherwise inactive (Köhler et al. 2017). Air temperature was not recorded. A strict FFT bandwidth filter was applied to the dataset to remove all sound below 400 Hz in order to remove wind artefacts. Two calls were recorded from the holotype, but numerous calls

were heard whilst searching for this species along the river where it was found. Calls consisted of a rapid series of 24–29 extremely short notes (note duration 6.3 ± 1.9 ms, range 2–10 ms, $n = 53$; Fig. 5a), each of which had 2.6 ± 0.6 pulses (2–4 pulses, $n = 50$), the peak amplitudes of which were separated by 2.7 ± 0.6 ms (1–4 ms, $n = 53$; Fig. 5b). Notes were separated by silent inter-note intervals of 64.6 ± 5.5 ms (47–75 ms, $n = 51$). The call was amplitude modulated, increasing in amplitude quickly and slowly decaying toward the end of the call. Call duration was 1769–1827 ms ($n = 2$), with one inter-call interval recorded of 2399 ms. Generally, however, the calls appeared to be emitted rather irregularly. Dominant frequency was 5124–5512 Hz, and the 90 % bandwidth was from 2723–2759 to 6391–6462 Hz.

Similar calls were recorded in Sorata from ZSM 1549/2012 at its collection locality (Suppl. material 2, DOI: 10.7479/nmx8-aq7v). Air temperature was not recorded. The calls strongly resembled those recorded from the holotype. Three calls were recorded, but one was cut off and another had loud calls of *Gephyromantis (Dubomantis)* sp. in the background, so only one was analysed. The call consisted of a rapid series of 31 extremely short notes (note duration 6.9 ± 0.8 ms, range 6–10 ms, $n = 27$ analysed), each of which had 2.0 ± 0.2 pulses (2–3 pulses, $n = 27$), the peak amplitudes of which were separated by 3.0 ± 0.4 ms (2–4 ms, $n = 27$). Notes were separated by silent inter-note intervals of 46.3 ± 3.8 ms (41–55 ms, $n = 27$). The call was amplitude modulated in the same way as that of ZSM 419/2016. Call duration was 1681 ms, and one inter-call interval was ca. 1900 ms. In general however calling was irregular. The dominant frequency was 5555 Hz, and the 90 % bandwidth was from 4979 to 6003 Hz. The call with a loud *Gephyromantis (Dubomantis)* sp. in the background was considerably shorter, and consisted of just 11 notes over a duration of 515 ms, but we suppose this call may have been disturbed as it lacked amplitude reduction toward its end.

Distribution. The new species is known from three localities in northeastern Madagascar: (1) Marojejy National Park (type locality), (2) Sorata massif, and (3) Andravory massif (Fig. 6). All specimens were collected between 1164 and 1394 m a.s.l.

Natural history. Specimens were collected near mountain streams in pristine montane riparian rainforest (Fig. 4g). In Marojejy National Park they were encountered during and after light rain, sitting in inconspicuous locations, especially on the fronds of tree ferns, but also on other low vegetation, between a few centimetres and up to 2 m above the ground. Specimens in Sorata were found in similar positions during dry weather, in the days just before the beginning of the rainy season. Males called irregularly and softly (see the call description above). Population density in Marojejy was remarkably high, with around three or four individuals being found along a 10 m stretch of stream. The observed density in Sorata was lower, possibly due

to the absence of rain during the observation period. The species occurred in close sympatry with a number of other mantellids, but only few of these (especially *Mantidactylus* aff. *femoralis*) were found in the same microhabitat. Several specimens from Marojejy had pinkish mites (probably of the genus *Endotrombicula*; see Wohltmann et al. 2007) embedded within translucent whitish pustules on the skin of their fingers, toes, and bodies. Nothing is known about the reproduction of this species, but the calling sites suggest an association with lotic water.

Available names. There are no other, earlier names currently available (e.g., junior synonyms) that are assignable to the subgenera *Vatomantis* or *Laurentomantis* and that could apply to the new species.

Etymology. The specific epithet is the Malagasy word *lomorina*, meaning ‘covered in moss’, in reference to the green, mossy appearance of the species in life. It is used as an invariable noun in apposition to the genus name.

Conservation. The species occurs in two regions with very different conservation situations: the highly protected forests of Marojejy National Park, and the unprotected, isolated, and highly threatened forests of Sorata and Andravory. Maminirina et al. (2008) report a study site in the rainforest of Sorata at 970 m a.s.l., but in our surveys in 2012, we detected larger patches of forest only at elevations of ca. 1270 m and above. The new species was collected at lower elevation in Andravory (1164–1179 m a.s.l.), where forest persists. Higher elevation levels of Sorata are covered by high-elevation forests different to those where *G. lomorina* sp. n. was found, and these therefore may not support this species. In this area, the species is therefore directly threatened by the loss of the only forests in which it has been detected.

By contrast in Marojejy, forest extends down to roughly 200 m a.s.l., is highly protected, and the high elevation forest where this species occurs does not seem to be facing any immediate threats. Although the tourist load to Marojejy is relatively high, and the area upslope from the collection locality of the holotype and several paratypes is somewhat polluted with refuse from the nearby tourist camp, the species was abundant around this stream during our survey there in 2016, and presumably inhabits other streams around the same elevation across the massif.

Accommodating this spread of risk is a challenge for the IUCN Red List status. However, *G. (V.) lomorina* sp. n. is not the first species to have almost exactly this distribution. *Rhombophryne vaventy* Scherz, Ruthensteiner, Vences & Glaw was recently recovered from Sorata (Peloso et al. 2016, Scherz et al. 2016, Lambert et al. 2017) after initially having been described from the same type locality as *G. lomorina* sp. n. (Scherz et al. 2014). In the case of this species, Scherz et al. (2017a) argued for a classification of Endangered under IUCN criterion B1ab(iii), i.e. an extent of occurrence under 5000 km^2 (B1), known from fewer than five

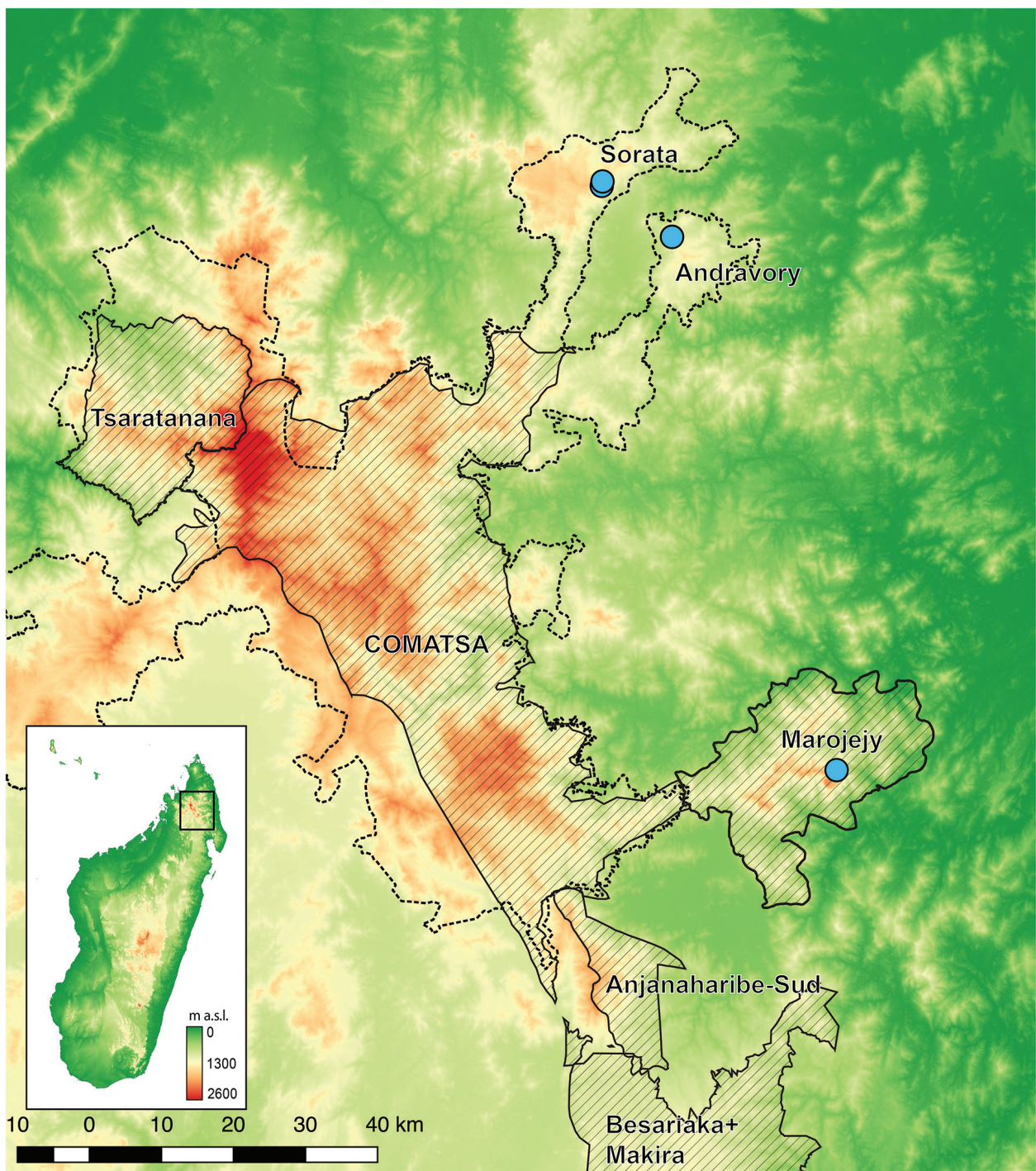


Figure 6. Distribution of *Gephyromantis (Vatomantis) lomorina* sp. n. in northern Madagascar. Areas with diagonal lines are official protected areas. The dotted outline indicates the proposed area with the scope of the WWF protection plan for this part of Madagascar (Biodev Madagascar Consulting 2014, WWF Madagascar 2015). Three arc second SRTM data from Jarvis et al. (2008).

threat-defined locations (a), and an observed, estimated, inferred, or projected decline (b) in the area, extent, and/or quality of habitat (iii). Given the similar situation in *G. lomorina* sp. n., i.e., very similar, limited distribution and ongoing reduction and threat to a substantial part of its habitat (i.e., the forests of Sorata and Andravory), we propose that the same threat status and justification be given for this species.

Discussion

Gephyromantis (Vatomantis) lomorina sp. n. is a distinctive species, mostly due to its granular, greenish skin, which is rougher than in all other members of the subgenus *Vatomantis*, but not as rugose as in many species of the subgenus *Laurentomantis*. Indeed, it is in several aspects intermediate between these subgenera, having a

call that sounds similar to both (Vences et al. 2006). Its phylogenetic position is at present basically unresolved between these two subgenera. However, its morphology is clearly more similar to *Vatomantis* than to *Laurentomantis*, as it lacks an outer metatarsal tubercle (present in *Laurentomantis*), has a distinct brown tympanum (less distinct in *Laurentomantis*), lacks a broadened head (usually distinctly broadened in *Laurentomantis*) and has paired subgular vocal sacs (single in *Laurentomantis*) (Glaw and Vences 2006).

Gephyromantis (Vatomantis) rivicola, *G. (V.) silvanus*, *G. (V.) lomorina* sp. n., and most *Laurentomantis* species share a unique femoral gland morphology with glands being composed of a small number of large, round granules (each granule representing a single gland within the femoral macrogland; Vences et al. 2007; Fig. 1). Glaw et al. (2000) interpreted these unusual glands as possible intermediate steps between Type 2 glands (sharply delimited groups of numerous granules of up to 0.9 mm diameter) toward Type 3 and 4 glands (a rounded structure composed of few, large granules and an external central depression). The position of *G. (V.) lomorina* sp. n. appears to make this situation more complicated; formerly, it seemed that granule size had increased and number decreased in *G. (V.) rivicola* and *G. (V.) silvanus* while *G. (V.) webbi* had retained Type 2 glands typical of most other *Gephyromantis* species (Glaw et al. 2000, Vences et al. 2007). However, given the split of *G. (V.) lomorina* from a more basal node in that clade (Fig. 1), and given the ubiquity of these unusual glands in the sister subgenus *Laurentomantis* (Glaw et al. 2000, Kaffenberger et al. 2012), it seems that Type 2 femoral glands may have independently originated one or more times in this clade. A better resolved phylogeny of the clade will be necessary to better understand the evolution of their femoral gland morphology.

The apparently highly divergent *G. (V.) lomorina* sp. n. sheds some light on questions regarding the relationships of *G. klemmeri*. Formerly, *G. klemmeri* was considered a member of the subgenus *Gephyromantis*, but Kaffenberger et al. (2012) showed that it has affinities between *Laurentomantis* and *Vatomantis*. They forestalled action on transferring it to one of these subgenera until more data become available, as single genes disagreed as to its position. *Gephyromantis klemmeri* shares femoral gland morphology with both *Laurentomantis* and *Vatomantis*, having large glands with a small number of large granules. This lends credence both to its phylogenetic position being close to these subgenera, and also to the hypothesis that smaller numbers of larger granules in the femoral glands may be ancestral in this clade.

Kaffenberger et al. (2012) suggested three possible alternatives to dealing with the phylogenetic affinities of *G. klemmeri*: (a) including *G. klemmeri* in *Laurentomantis* (its position sister to *Laurentomantis* was supported with 94 % bootstrap support from maximum likelihood and >0.99 posterior probability, but was not supported in maximum parsimony analysis), (b) erecting a new monotypic subgenus, or (c) redefining a more inclusive sub-

nus *Laurentomantis* that besides *G. klemmeri* would also include *Vatomantis* as a junior synonym (the clade containing *Laurentomantis*, *Vatomantis*, and *G. klemmeri* was supported with 100 % bootstrap support from maximum likelihood, >0.99 posterior probability, and 86 % bootstrap support from maximum parsimony). Determining the best course of taxonomic action will in part depend on the resolution of the phylogenetic relationships of *G. klemmeri* and of *G. (V.) lomorina* sp. n., in the framework of a more comprehensive revision of *Laurentomantis* and *Vatomantis*, as these subgenera still contain further candidate species requiring in-depth analysis (Vieites et al. 2009).

Gephyromantis (Vatomantis) lomorina sp. n. also sheds light on the biogeography of northern Madagascar, providing yet more evidence for a strong link between Sorata and Marojejy. The environmental conditions of these two regions are similar (Brown et al. 2016), and various species originally described from one of the two areas have subsequently been discovered in the other, e.g. *Rhombophryne vaventy* (Peloso et al. 2016, Scherz et al. 2016, 2017a, Lambert et al. 2017), *Gephyromantis (Asperomanitis) tahotra* (Glaw et al. 2011, Vences et al. 2017), and *G. (D.) schilfi* (Glaw and Vences 2000, Scherz et al. 2017b). These similarities are generally limited to species found above 1200 m, probably because forest below 1200 m in Sorata has been mostly eradicated.

We predict that similarities between faunal compositions of the mountainous massifs of northern Madagascar are limited by elevational connectivity. For instance, there is continued connectivity between regions of elevation up to 1400 m from Sorata to Marojejy and indeed roughly to the Manongarivo massif as well. There is no connectivity above this elevation however; areas of over 1400 m across the different massifs are separated by lower elevations, leading to island-like isolation of peak areas. Therefore, we predict that species occurring above 1400 m will show a greater degree of microendemism, and those below this elevation will have a greater probability of occurring more widely; the higher a species' centre of elevational distribution is located, the greater its chance of being microendemic. No absolute threshold of turnover is expected, because major climate fluctuations in the past will likely have blurred elevational boundaries over time.

So far, evidence appears to support this hypothesis; as already stated, several species from around 1300 m are shared between Marojejy and Sorata (and Andravory, though at present only limited and generally unpublished data are available from this forest), and some species known from higher elevations are so far thought to be microendemic to either region, e.g. *Rhombophryne longicrus* (Scherz et al. 2015), *Gephyromantis (Duboimanitis) tohatra* (Scherz et al. 2017b), *Calumma jeiy*, and *C. peyrierasi*. Assuming this hypothesis is correct, it raises questions about species that are microendemic at lower elevations, but opportunities to study and understand these taxa are increasingly limited by the fact that forest at lower elevations is disappearing outside of protected

areas. Conservation efforts must be redoubled to ensure that these study systems may remain long enough to be investigated and understood.

Acknowledgements

As always, we are grateful to the Malagasy authorities of the Ministry of Environments and Forests for providing us with permits. Field research was conducted under permit N° 215/16/MEEF/SG/DGF/DSAP/SCB.Re (dated 5 September 2016) and N° 265/12/MEF/SG/DGF/DCB.SAP/SCB (dated 18 October 2012). Specimens were exported under permits N° 010N-EA01/MG17 (dated 4 January 2017) and N° 163N-EA12/MG12 (dated 17 December 2012). This work was carried out in collaboration with the Mention Zoologie et Biodiversité Animale, Université d'Antananarivo, to whom we are also grateful for the loan of the paratype series. We are also grateful to R. Walker, W.-Y. Crawley, T. H. Rafeliarisoa, and the Andraovory team for their help in Andraovory, and A. Razafimanantsoa and T. Rajoafiarison for their help in Marojejy and Sorata. AR and MCB were supported by fellowships of the Deutscher Akademischer Austauschdienst. MV and MDS were supported by grants of the Deutsche Forschungsgemeinschaft (VE247/13-1 and 15-1). The fieldwork of OH, FG, AR, and FR was supported by the Mohamed bin Zayed Species Conservation Fund (project 11253064). The publication of this article in Zoosystematics and Evolution was made possible by the Museum für Naturkunde Berlin.

References

- Biodev Madagascar Consulting (2014) Document de référence sur la NAP complexe Ambohimirahavavy Marivorahona en vue de l'évaluation environnementale par le CTE. Unpublished report. Accessed 14 June 2017. Available from: <https://goo.gl/4KgD9W> [Archived by WebCite® at <http://www.webcitation.org/6saYQDhEv>]
- Brown JL, Sillero N, Glaw F, Bora P, Vieites DR, Vences M (2016) Spatial biodiversity patterns of Madagascar's amphibians and reptiles. *PLoS One* 11(1): e0144076. <https://doi.org/10.1371/journal.pone.0144076>
- Darriba D, Taboada GL, Doallo R, Posada D (2012) jModelTest 2: more models, new heuristics and parallel computing. *Nature Methods* 9: 772. <https://doi.org/10.1038/nmeth.2109>
- Glaw F, Hoegg S, Vences M (2006) Discovery of a new basal relict lineage of Madagascan frogs and its implications for mantellid evolution. *Zootaxa* 1334: 27–43.
- Glaw F, Köhler J, Vences M (2011) New species of *Gephyromantis* from Marojejy National Park, northeast Madagascar. *Journal of Herpetology* 45(2): 155–160. <https://doi.org/10.1670/10-058.1>
- Glaw F, Vences M (2000) A new species of *Mantidactylus* from northeastern Madagascar (Amphibia, Anura, Ranidae) with resurrection of *Mantidactylus blanci* (Guibé, 1974). *Spixiana* 23(1): 71–83.
- Glaw F, Vences M (2001) Two new sibling species of *Mantidactylus cornutus* from Madagascar. *Spixiana* 24(2): 177–190.
- Glaw F, Vences M (2006) Phylogeny and genus-level classification of mantellid frogs (Amphibia, Anura). *Organisms Diversity & Evolution* 6(3): 236–253. <https://doi.org/10.1016/j.ode.2005.12.001>
- Glaw F, Vences M, Gossmann V (2000) A new species of *Mantidactylus* (subgenus *Guibemantis*) from Madagascar, with a comparative survey of internal femoral gland structure in the genus (Amphibia: Ranidae: Mantellinae). *Journal of Natural History* 34: 1135–1154. <https://doi.org/10.1080/00222930050020140>
- Jarvis A, Reuter HI, Nelson A, Guevara E (2008) Hole-filled seamless SRTM data V4, International Centre for Tropical Agriculture (CIAT). Available from: <http://srtm.csi.cgiar.org>.
- Kaffenberger N, Wollenberg KC, Köhler J, Glaw F, Vieites DR, Vences M (2012) Molecular phylogeny and biogeography of Malagasy frogs of the genus *Gephyromantis*. *Molecular Phylogenetics and Evolution* 62(1): 555–560. <https://doi.org/10.1016/j.ympev.2011.09.023>
- Köhler J, Jansen M, Rodríguez A, Kok PJR, Toledo LF, Emmrich M, Glaw F, Haddad CFB, Rödel M-O, Vences M (2017) The use of bioacoustics in anuran taxonomy: theory, terminology, methods and recommendations for best practice. *Zootaxa* 4251(1): 1–124. <https://doi.org/10.11646/zotaxa.4251.1.1>
- Köhler J, Vieites DR, Bonett RM, García FH, Glaw F, Steinke D, Vences M (2005) New amphibians and global conservation: a boost in species discoveries in a highly endangered vertebrate group. *BioScience* 55(8): 693–696. [https://doi.org/10.1641/0006-3568\(2005\)055\[0693:NAAGCA\]2.0.CO;2](https://doi.org/10.1641/0006-3568(2005)055[0693:NAAGCA]2.0.CO;2)
- Kumar S, Stecher G, Tamura K (2016) MEGA7: Molecular Evolutionary Genetics Analysis version 7.0 for bigger datasets. *Molecular Biology and Evolution* 33(7): 1870–1874. <https://doi.org/10.1093/molbev/msw054>
- Lambert SM, Hutter CR, Scherz MD (2017) Diamond in the rough: a new species of fossorial diamond frog (*Rhombophryne*) from Ranomafana National Park, southeastern Madagascar. *Zoosystematics and Evolution* 93(1): 143–155. <https://doi.org/10.3897/zse.93.10188>
- Maminirina CP, Goodman SM, Raxworthy CJ (2008) Les micro-mammifères (Mammalia, Rodentia, Afrosoricida et Soricomorpha) du massif du Tsaratanana et biogéographie des forêts de montagne de Madagascar. *Zoosystema* 30: 695–721.
- Palumbi SR, Martin A, Romano S, McMillan WO, Stice L, Grabowski G (1991) The simple fool's guide to PCR, Version 2.0. Privately published, University of Hawaii.
- Peloso PLV, Frost DR, Richards SJ, Rodrigues MT, Donnellan S, Matsui M, Raxworthy CJ, Biju SD, Lemmon EM, Lemmon AR, Wheeler WC (2016) The impact of anchored phylogenomics and taxon sampling on phylogenetic inference in narrow-mouthed frogs (Anura, Microhylidae). *Cladistics* 32(2): 113–140. <https://doi.org/10.1111/cla.12118>
- Perl RGB, Nagy ZT, Sonet G, Glaw F, Wollenberg KC, Vences M (2014) DNA barcoding Madagascar's amphibian fauna. *Amphibia-Reptilia* 35: 197–206. <https://doi.org/10.1163/15685381-00002942>
- Rambaut A, Drummond AJ (2007) Tracer v1.5. Available from: <http://beast.bio.ed.ac.uk/Tracer>.
- Ronquist F, Teslenko M, van der Mark P, Ayres DL, Darling A, Höhna S, Larget B, Liu L, Suchard MA, Huelsenbeck JP (2012) MRBAYES 3.2: Efficient Bayesian phylogenetic inference and model selection across a large model space. *Systematic Biology* 61(3): 539–542. <https://doi.org/10.1093/sysbio/sys029>
- Sabino-Pinto J, Mayer CJ, Meilink WRM, Grasso D, Raajmakers CCB, Russo VG, Segal M, Stegen G, Clegg J, Srikanthan AN, Glaw F, Vences M (2014) Descriptions of the advertisement calls of three sympatric frog species in the subgenus *Vatomantis* (genus *Gephyromantis*) from Madagascar. *Herpetology Notes* 7: 67–73.

- Scherz MD, Hawlitschek O, Andreone F, Rakotoarison A, Vences M, Glaw F (2017a) A review of the taxonomy and osteology of the *Rhombophryne serratopalpebrosa* species group (Anura: Microhylidae) from Madagascar, with comments on the value of volume rendering of micro-CT data to taxonomists. *Zootaxa* 4273(3): 301–340. <https://doi.org/10.11646/zootaxa.4273.3.1>
- Scherz MD, Rakotoarison A, Hawlitschek O, Vences M, Glaw F (2015) Leaping towards a saltatorial lifestyle? An unusually long-legged new species of *Rhombophryne* (Anura, Microhylidae) from the So-rata massif in northern Madagascar. *Zoosystematics and Evolution* 91(2): 105–114. <https://doi.org/10.3897/zse.91.4979>
- Scherz MD, Razafindraibe JH, Rakotoarison A, Bletz MC, Glaw F, Vences M (2017b) Yet another small brown frog from high altitude on the Marojejy Massif, northeastern Madagascar. *Zootaxa* 4347(3): 572–582. <https://doi.org/10.11646/zootaxa.4347.3.9>
- Scherz MD, Ruthensteiner B, Vences M, Glaw F (2014) A new microhylid frog, genus *Rhombophryne*, from northeastern Madagascar, and a re-description of *R. serratopalpebrosa* using micro-computed tomography. *Zootaxa* 3860(6): 547–560. <https://doi.org/10.11646/zootaxa.3860.6.3>
- Scherz MD, Vences M, Rakotoarison A, Andreone F, Köhler J, Glaw F, Crottini A (2016) Reconciling molecular phylogeny, morphological divergence and classification of Madagascan narrow-mouthed frogs (Amphibia: Microhylidae). *Molecular Phylogenetics and Evolution* 100: 372–381. <https://doi.org/10.1016/j.ympev.2016.04.019>
- Vallan D, Glaw F, Andreone F, Cadle JE (1998) A new treefrog species of the genus *Boophis* (Anura: Ranidae: Rhacophorinae) with dermal fringes from Madagascar. *Amphibia-Reptilia* 19(4): 357–368. <https://doi.org/10.1163/156853898X00025>
- Vences M, Glaw F, Andreone F (1997) Description of two new frogs of the genus *Mantidactylus* from Madagascar, with notes on *Mantidactylus klemmeri* (Guibe, 1974) and *Mantidactylus webbi* (Grandison, 1953) (Amphibia, Ranidae, Mantellinae). *Alytes* 14(4): 130–146.
- Vences M, Glaw F, Andreone F, Jesu R, Schimmenti G (2002) Systematic revision of the enigmatic Malagasy broad-headed frogs (*Lau-rentomantis* Dubois, 1980), and their phylogenetic position within the endemic mantellid radiation of Madagascar. *Contributions to Zoology* 70(4): 191–212.
- Vences M, Glaw F, Marquez R (2006) The Calls of the Frogs of Madagascar. 3 Audio CD's and booklet. Fonoteca Zoológica, Madrid, Spain, 44 pp.
- Vences M, Köhler J, Pabijan M, Bletz M, Gehring P-S, Hawlitschek O, Rakotoarison A, Ratsoavina FM, Andreone F, Crottini A, Glaw F (2017) Taxonomy and geographic distribution of Malagasy frogs of the *Gephyromantis asper* clade, with description of a new subgenus and revalidation of *Gephyromantis ceratophrys*. *Salamandra* 53(1): 77–98.
- Vences M, Lyra ML, Perl BRG, Bletz MC, Stankovic D, Geffers R, Haddad CFB, Steinfartz S, Martins Lopes C, Jarek M, Bhuju S (2016) Freshwater vertebrate metabarcoding on Illumina platforms using double-indexed primers of the mitochondrial 16S rRNA gene. *Conservation Genetics Resources* 8(1): 1–5. <https://doi.org/10.1007/s12686-016-0550-y>
- Vences M, Raxworthy CJ, Nussbaum RA, Glaw F (2003) A revision of the *Scaphiophryne marmorata* complex of marbled toads from Madagascar, including the description of a new species. *Herpetological Journal* 13: 69–79.
- Vences M, Wahl-Boos G, Hoegg S, Glaw F, Oliveira ES, Meyer A, Perry S (2007) Molecular systematics of mantelline frogs from Madagascar and the evolution of their femoral glands. *Biological Journal of the Linnean Society* 92(2007): 529–539.
- Vieites DR, Wollenberg KC, Andreone F, Köhler J, Glaw F, Vences M (2009) Vast underestimation of Madagascar's biodiversity evidenced by an integrative amphibian inventory. *Proceedings of the National Academy of Sciences of the USA* 106(20): 8267–8272. <https://doi.org/10.1073/pnas.0810821106>
- Vieites DR, Wollenberg KC, Vences M (2012) Not all little brown frogs are the same: a new species of secretive and cryptic *Gephyromantis* (Anura: Mantellidae) from Madagascar. *Zootaxa* 3344: 34–46.
- Wohltmann A, du Preez L, Rödel M-O, Köhler J, Vences M (2007) Endoparasitic mites of the genus *Endotrombicula* Ewing, 1931 (Acari: Prostigmata: Parasitengona: Trombiculidae) from African and Madagascan anurans, with description of a new species. 54: 225–235. <https://doi.org/10.14411/fp.2007.031>
- WWF Madagascar (2015) Plan d'Aménagement et de gestion intégré du complexe d'aires protégées Ambohimirahavavy Marivorahona, Report Draft. Accessed 14 June 2017. Available from goo.gl/GGXP2D

Supplementary material 1

Advertisement call of *Gephyromantis lomorina* sp. n.

Authors: Mark D. Scherz, Oliver Hawlitschek, Jary H. Razafindraibe, Steven Megson, Fanomezana Mihaja Ratsoavina, Andolalao Rakotoarison, Molly C. Bletz, Frank Glaw, Miguel Vences

Data type: WAV File (.wav)

Explanation note: Call recording of *Gephyromantis (Vatomantis) lomorina* sp. n. ZSM 419/2016 (ZCMV 15221). Calls recorded at 21h20 on 18 November 2016 near Camp Simpona (ca. 14.4366°S, ca. 49.7434°E, ca. 1325 m a.s.l.) in Marojejy National Park, Sava Region, Antsiranana Province, northeastern Madagascar, by M. D. Scherz. Frog was ca. 1 m above the ground on a fern near a small river, calling occasionally during light rain. Air temperature was not taken. Recording distance was 0.5 m. Animal Sound Archive: <https://doi.org/10.7479/nmx8-aq7v>.

Copyright notice: This dataset is made available under the Open Database License (<http://opendatacommons.org/licenses/odbl/1.0/>). The Open Database License (ODbL) is a license agreement intended to allow users to freely share, modify, and use this Dataset while maintaining this same freedom for others, provided that the original source and author(s) are credited.

Link: <https://doi.org/10.3897/zse.94.21037.suppl1>

Supplementary material 2

Advertisement call of *Gephyromantis lomorina* sp. n.

Authors: Mark D. Scherz, Oliver Hawlitschek, Jary H. Razafindraibe, Steven Megson, Fanomezana Mihaja Ratsoavina, Andolalao Rakotoarison, Molly C. Bletz, Frank Glaw, Miguel Vences

Data type: WAV File (.wav)

Explanation note: Call recording of *Gephyromantis (Vatomantis) lomorina* sp. n. ZSM 1549/2012 (FGZC 3714). Calls recorded at night on 30 November 2012 on the Sorata massif (creek near campsite, 13.6829°S, 49.4403°E, 1325 m a.s.l.), Sava Region, Antsiranana Province, northeastern Madagascar, by O. Hawlitschek. Ecological data not available. Air temperature and recording distance were not noted. Animal Sound Archive: <https://doi.org/10.7479/nmx8-aq7v>.

Copyright notice: This dataset is made available under the Open Database License (<http://opendatacommons.org/licenses/odbl/1.0/>). The Open Database License (ODbL) is a license agreement intended to allow users to freely share, modify, and use this Dataset while maintaining this same freedom for others, provided that the original source and author(s) are credited.

Link: <https://doi.org/10.3897/zse.94.21037.suppl2>

Chapter 4. PAPER: Yet another small brown frog from high altitude on the Marojejy Massif, northeastern Madagascar (Anura: Mantellidae)

In this chapter, I present the description of a new species of *Gephyromantis* from the subgenus *Duboimantis* that my colleagues and I discovered on an expedition to the Marojejy massif in 2016. The new species, *Gephyromantis (Duboimantis) tohatra*, is a high-elevation endemic, occurring at elevations over 1700 m a.s.l. It is sister to another species from lower on Marojejy, *G. (D.) schilfi* (1250–1800 m a.s.l.), which we show also occurs on the Sorata massif. This corroborates the connection between these massifs around the same elevation reported in **chapter 3**. The contrast of the higher elevation endemic (*G. (D.) tohatra*) with the species that ranges into lower elevations and has a broader distribution (*G. (D.) schilfi*), suggests elevation-limited distribution potential of species. Yet, we show also that there is strong genetic differentiation between *G. (D.) tandroka* from Marojejy and a sister lineage from Sorata around this same elevation, suggesting a more complex pattern (illuminated in **chapter 5**).

Scherz, M.D., Razafindraibe, J.H., Rakotoarison, A., Dixit, N.M., Bletz, M.C., Glaw, F. & Vences, M. (2017) Yet another small brown frog from high altitude on the Marojejy Massif, north-eastern Madagascar (Anura: Mantellidae). *Zootaxa*, 4347(3):572–582. DOI: 10.11646/zootaxa.4347.3.9



Gephyromantis (Duboimantis) tohatra in life

<https://doi.org/10.11164/zootaxa.4347.3.9>
<http://zoobank.org/urn:lsid:zoobank.org:pub:BF851FBA-98F3-4DB8-A69F-73D930773AFE>

Yet another small brown frog from high altitude on the Marojejy Massif, northeastern Madagascar (Anura: Mantellidae)

MARK D. SCHERZ^{1,2}, JARY H. RAZAFINDRAIBE³, ANDOLALAO RAKOTOARISON^{2,3}, NADI M. DIXIT⁴, MOLLY C. BLETZ², FRANK GLAW¹ & MIGUEL VENCES^{2,5}

¹Zoologische Staatssammlung München (ZSM-SNSB), Münchhausenstr. 21, 81247 München, Germany

²Zoologisches Institut, Technische Universität Braunschweig, Mendelssohnstr. 4, 38106 Braunschweig, Germany

³Faculté des Sciences, Zoologie et Biodiversité Animale, Université d'Antananarivo, BP 906, Antananarivo 101, Madagascar

⁴Indian Institute of Science Education and Research, near Jersey Farm, Maruthamala PO, Vithura- 695551, Thiruvananthapuram, Kerala, India

⁵Corresponding author. E-mail: m.vinces@tu-braunschweig.de

Abstract

Madagascar hosts a high diversity of small brown frogs. In this paper, we add another one by describing *Gephyromantis (Duboimantis) tohatra* sp. nov. The new species is a small brown mantellid frog discovered on a recent expedition to Marojejy National Park in northeastern Madagascar. It is characterised, among other things, by its small size (snout-vent length ~33 mm), an orange to yellowish belly, two dorsolateral ridges, and a distinctive call composed of 7–10 pulsed notes. The new species occurs sympatrically with other members of the subgenus *Duboimantis* at high altitude (~1700 m above sea level), including its sister species *G. schilfii* from which it radically differs by advertisement call and by a substantial genetic divergence of 4.3% uncorrected pairwise distance in the mitochondrial 16S rRNA gene. It thus joins the diverse assemblage of *Gephyromantis* species known from high altitudes on the mountain massifs of northern Madagascar.

Key words: Amphibia, Anura, Mantellidae, *Gephyromantis*, *Gephyromantis tohatra* sp. nov., *Gephyromantis schilfii*, *Gephyromantis tandroka*

Introduction

Marojejy National Park is a reserve protecting rainforest and high-altitude vegetation of the Marojejy Massif in northeastern Madagascar. The amphibian diversity of this national park currently consists of roughly 56 described frog species (Raselimanana *et al.* 2000), but at least 25 additional candidate species are currently known from this area (Vieites *et al.* 2009). Recent descriptions have included several microhylids (Glaw & Vences 2007; Glaw *et al.* 2012; Scherz *et al.* 2014, 2016), and mantellids (Glaw & Vences 2000, 2001, 2011; Glaw *et al.* 2011), with especially large numbers of species described in the genus *Gephyromantis* (*G. tahotra*, *G. tandroka*, *G. ranjomavo*, *G. rivicola*, *G. striatus*, *G. schilfii*); currently 12 *Gephyromantis* species are known from the Marojejy massif, most of which are restricted to narrow altitudinal ranges. A remarkable diversity is found between 1000 and 2000 m a.s.l., with five species currently described: *G. klemmeri*, *G. ranjomavo*, *G. schilfii*, *G. tahotra*, and *G. tandroka*. A sixth species is in description elsewhere by M.D. Scherz and collaborators.

Gephyromantis currently contains 42 species (Frost 2017), which are divided into six subgenera: *Asperomantis*, *Duboimantis*, *Gephyromantis*, *Laurentomantis*, *Phylacomantis*, and *Vatomantis* (Glaw & Vences 2006; Vences *et al.* 2017). The species found between 1000 and 2000 m a.s.l. on the Marojejy Massif belong to the subgenera *Asperomantis*, *Duboimantis*, *Gephyromantis*, *Laurentomantis*, and *Vatomantis* (a member of the latter being in description). That so many species of relatively closely related frogs can be found in close sympatry speaks to the significant niche differentiation among these subgenera. Each is represented by a single species, with the exception of *Duboimantis*, which at present has two named species in this high altitudinal zone in Marojejy (*G. tandroka* and *G. schilfii*).

Vences *et al.* (2017) transferred a series of species to the new subgenus *Asperomantis*, leaving the subgenus

Results

Duboimantis with 10 medium- to large-sized species of scansorial frogs largely confined to rainforest, and with a centre of diversity in northern Madagascar (Kaffenberger *et al.* 2012). Six species assigned to the latter subgenus are currently known from Marojejy: *G. granulatus*, *G. sp. Ca17*, *G. cf. moseri*, *G. redimitus*, *G. schilfi*, and *G. tandroka*. In this paper, we describe a third species of *Duboimantis* from high altitude on Marojejy, which represents the seventh species of *Duboimantis* from Marojejy National Park. Species status of this new taxon is justified by its radically different advertisement calls and genetic divergence compared to its sympatric sister species, *G. schilfi*. We also briefly discuss the possible reasons behind the relatively high diversity of *Duboimantis* compared to other subgenera of *Gephyromantis* that occur at high altitudes in northern Madagascar.

Materials and methods

Specimens were located at night by following their distinctive advertisement calls. After being photographed, they were euthanized with MS222, fixed in 95% ethanol, and thereafter deposited in 75% ethanol for long-term storage. Field numbers refer to the zoological collections of Miguel Vences (ZCMV) and Frank Glaw (FGZC). Specimens were deposited in the Zoologische Staatssammlung München (ZSM) and the Université d'Antananarivo, Zoologie et Biodiversité Animale (UADBA).

Morphological measurements were taken using a digital calliper to 0.1 mm by AR. The measurement scheme followed previous work on this genus, e.g. Vences *et al.* (2017), modified to deal with the relatively strong fixation of the measured specimens; measurements that required straightening of limbs were replaced with piece-by-piece measurements: snout–vent length (SVL), maximum head width (HW), head length from posterior maxillary commissure to snout tip (HL), horizontal eye diameter (ED), horizontal tympanum diameter (TD), distance from eye to nostril (END), distance from nostril to snout tip (NSD), distance between nostrils (NND), foot length (FOL), tarsus length (TARL), tibia length (TIBL), thigh length from cloaca to knee (THIL), upper arm length from the insertion of the arm to the elbow (UAL), lower arm length from the elbow to the base of the hand (LAL), hand length from the base of the hand to the length of the longest finger (HAL), and length and width of femoral gland (FGL, FGW). Webbing formulae follow Blommers-Schlösser (1979); femoral gland terminology follows Glaw *et al.* (2000), and dorsolateral ridges are named following Vences & Glaw (2001).

DNA sequences were obtained using previously established protocols described elsewhere (e.g. Vences *et al.* 2003, 2017). In brief, DNA was extracted using a standard salt extraction protocol from samples of muscle tissue preserved in 99% ethanol in the field. Polymerase Chain Reaction carried out with universal primers to amplify fragments of the mitochondrial genes for 16S rRNA (16S) and 12S rRNA (12S), and these amplicons were directly sequenced on an automated capillary DNA sequencer (ABI 3130xl). All new DNA sequences were submitted to GenBank (accession numbers MF683128–MF683165). We used MEGA7 (Kumar *et al.* 2016) to align sequences to reference sequences of other *Gephyromantis* from previous studies. We then used the Bayesian Information Criterion in jModeltest (Darriba *et al.* 2012) to determine the best-suited substitution model for the sequences (a HKY+G model), and implemented it in Maximum Likelihood (ML) and Bayesian Inference (BI) reconstructions of phylogeny. ML was run in MEGA7 and node support assessed with 2000 non-parametric ML bootstraps. BI was run in MrBayes 3.2 (Ronquist *et al.* 2012), running two parallel runs for 20 million generations, sampling every 1000th tree, and discarding 25% of the sampled trees as burn-in. Chain mixing and stationarity were assessed by examining the standard deviation of split frequencies and by plotting the -lnL per generation using Tracer 1.5 software (Rambaut & Drummond 2007). In addition, we conducted non-parametric bootstrapping under Maximum Parsimony (MP) in MEGA7. To quantify genetic divergences we calculated uncorrected pairwise distances among the sequences (p-distances). The fragment typically used for DNA barcoding of Madagascar's amphibians (a 3'-terminal stretch of 16S; e.g., Vieites *et al.* 2009) could not be reliably sequenced for *G. schilfi* due to a long C-repeat within this sequence. Therefore, divergences reported herein refer to the 5'-terminal stretch of the 16S gene which, in general, yields sequence divergence values comparable to those of the 3'-terminal portion of the gene.

Calls of two specimens were recorded with different recording equipment (Tascam DR05 and DR07, digital recorders with built-in microphones). We analysed calls in the software Cooledit 2.0 (Syntrillium Corp.). Frequency information was obtained through Fast Fourier Transformation (FFT; width 1024 points). The spectrogram was obtained using the Hanning window function with 256 bands resolution. Terminology of call descriptions follows Köhler *et al.* (2017); in order to facilitate comparisons with previous call descriptions of *Gephyromantis*, we followed a note-centred terminology of call subunits as defined in Köhler *et al.* (2017).

Results

Exploratory comparisons with DNA sequences of all species of *Gephyromantis* (not shown) suggested close relationships of the newly collected, bioacoustically divergent specimens from Marojejy with species of the subgenus *Duboimantis*, and more specifically with a subclade that, according to Kaffenberger *et al.* (2011), contains *G. salegy*, *G. schilfi*, and *G. tandroka*. We therefore analysed in more depth the DNA sequences of the new material along with all samples of these species available to us. All methods of phylogenetic inference used (BI, ML, MP) recovered the same topology (Fig. 1) and identified five main lineages: (1) *G. salegy*, which was placed sister to a clade of the other four lineages; (2) *G. tandroka*; (3) its deeply divergent sister lineage; (4) *G. schilfi*; and (5) a lineage containing the two bioacoustically divergent specimens from Marojejy, placed as sister group to *G. schilfi*. The placement of this new lineage sister to *G. schilfi* received maximum support from BI posterior probabilities (PP=1.0) but was only very weakly supported by ML and MP bootstrap proportions (36% and 45%, respectively). Their distinct position in the mitochondrial phylogeny, high genetic divergence to all *Gephyromantis* (see diagnosis below), and strong bioacoustic differences to all *Gephyromantis* except the larger-sized *G. salegy* indicate that the newly collected individuals from Marojejy represent a new species described in the following.

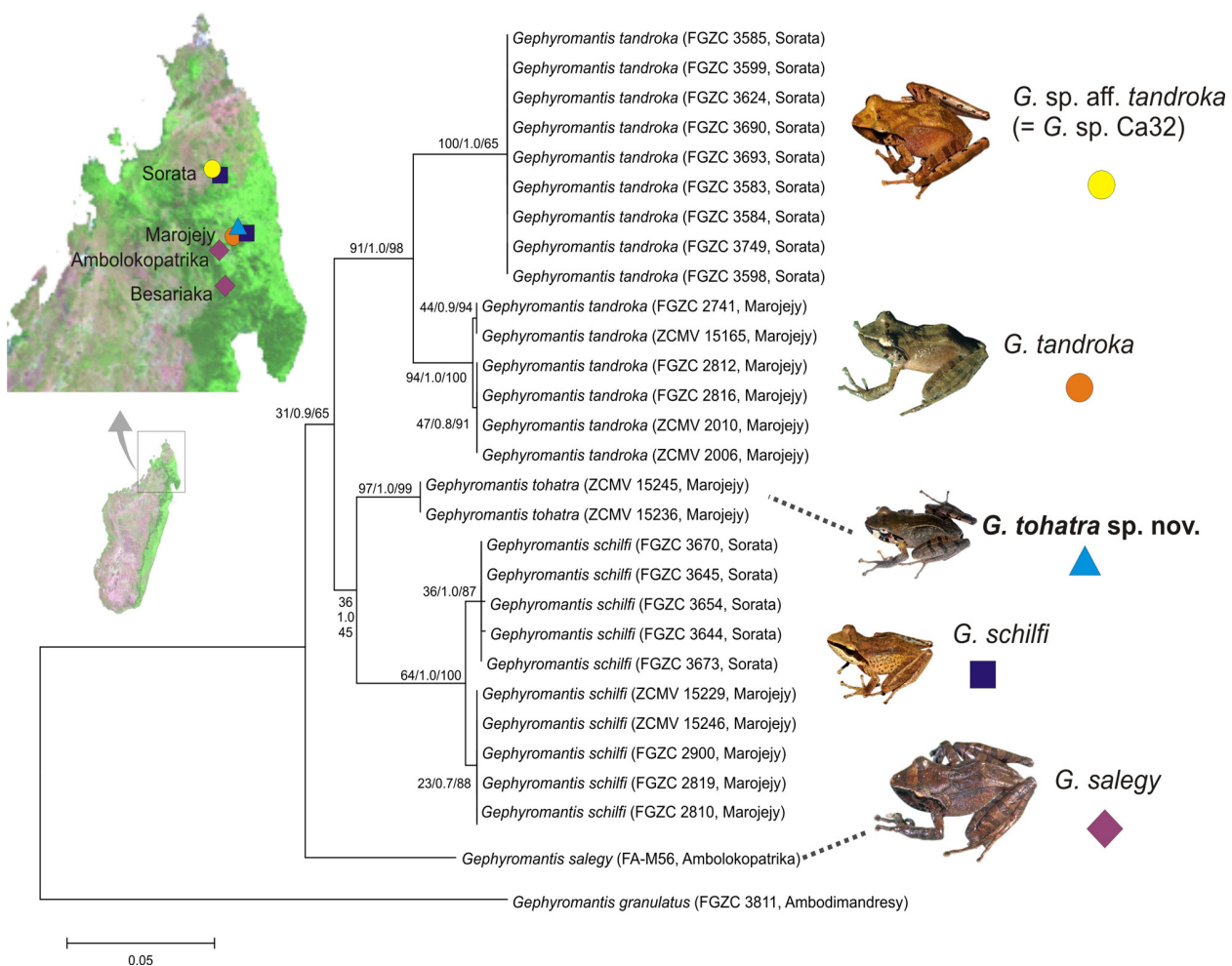


FIGURE 1. Maximum Likelihood tree based on 1106 bp of the mitochondrial 12S and 16S rRNA genes, showing relationships of *G. tohatra* sp. nov. to three other related *Gephyromantis* species and one candidate species from northern Madagascar. Support at nodes are ML likelihood bootstrap values, BI posterior probabilities, and MP bootstrap values. *Gephyromantis granulatus* was used as the outgroup. Inset map shows the four localities from which these species are known (with jitter to reveal overlapping species). Inset photos show representative individuals of the four target species, size of the pictures roughly proportional to body size differences among the species.

Results

Gephyromantis tohatra sp. nov.

(Figs. 2–3)

Holotype. ZSM 422/2016 (ZCMV 15245), adult male, collected at a site along the main trail leading from Camp Simpona to the summit of the Marojejy Massif, Sava Region, northeastern Madagascar, at geographical coordinates 14.44400°S, 49.73791°E and an elevation of 1758 m above sea level (Fig. 2, 3a–b) by M. D. Scherz, M. Vences, J. H. Razafindraibe, and M. Bletz, in the evening of the 19th of November 2016.

Paratype. UADBA uncatalogued (ZCMV 15236), adult male, with the same collection data as the holotype.

Diagnosis. The new species is assigned to the genus *Gephyromantis* and subgenus *Duboimantis* on the basis of its mostly connected lateral metatarsalia, moderately enlarged finger tips, type 2 femoral glands (Glaw *et al.* 2000), inner and outer dorsolateral ridges sensu Vences & Glaw (2001), presence of webbing between the toes, absence of a distinct white spot in the centre of the tympanum, and presence of small supraocular spines. It is characterised by the following unique suite of characters: (1) SVL at least up to 33 mm, (2) orange to yellowish ventral colouration in males, (3) type 2 femoral glands with 10–21 small granules, (4) strongly distinct inner and outer dorsolateral ridges sensu Vences & Glaw (2001), (5) a pale loreal region and broad pale marking covering most of the anterior edge of the tympanum, (6) second finger much shorter than fourth, (7) third toe much shorter than fifth, and (8) 7–10 distinct pulsed notes per call.

Gephyromantis tohatra sp. nov. differs from the majority of *Duboimantis* species by smaller body size: adult male SVL 33 vs. >35 mm in *G. granulatus*, *G. cornutus*, *G. redimitus*, *G. tschenki*, *G. salegy*, *G. tandroka*, *G. luteus*, *G. sculpturatus*, *G. plicifer*, and *G. zavona*. It can also be distinguished from all other species of *Duboimantis* by its orange to yellowish venter (typically whitish in all other species). Additionally, the presence of distinct inner and outer dorsolateral ridges distinguishes the new species in particular from *G. granulatus*, *G. redimitus*, and *G. zavona* in which these folds (in particular the inner dorsolateral ridges) are absent or very weakly expressed. *Gephyromantis luteus*, *G. plicifer*, and *G. sculpturatus* have dark concave markings in the suprascapular region (absent in the new species) and much more extensive webbing on the feet. *Gephyromantis cornutus*, *G. tschenki*, and *G. tandroka* have strongly expressed interocular tubercles (absent in the new species).

Three species of *Duboimantis* overlap with the new species in body size. *Gephyromantis leucomaculatus* is typically larger (adult male SVL 32–41 mm) and differs by absence of inner dorsolateral ridges and straight outer dorsolateral ridges (vs. anteriorly curved). *Gephyromantis moseri* (adult male SVL 27–40 mm) has a granular dorsum without or with interrupted dorsolateral ridges (vs. smooth or reticulated dorsum and continuous dorsolateral ridges in the new species) and interocular tubercles (vs. absence). *Gephyromantis schilfi* (adult male SVL 27–30 mm) occurs in close syntopy with the new species but differs from it by the absence of distinct inner and outer dorsolateral ridges (vs. presence in the new species).

Bioacoustically, the new species differs from all species in *Duboimantis* by advertisement call structure. Most species in this subgenus emit regularly repeated calls, each of which consists of a single, typically pulsed or pulsatile note (*G. granulatus*, *G. cornutus*, *G. leucomaculatus*, *G. moseri*, *G. redimitus*, *G. schilfi*, *G. tschenki*, *G. tandroka*, *G. plicifer*, *G. zavona*). In many of these species, notes can also be more irregularly arranged in short series, but calls do not consist of a regular number of 7–10 short and rapidly repeated notes as in *G. tohatra* sp. nov. This characteristic is particularly helpful in its distinction from the sympatrically occurring and morphologically similar *G. schilfi*, which emits a single, densely pulsed note. *Gephyromantis sculpturatus* and *G. luteus* emit a fast series of squeaking, unpulsed notes that are very distinct from the call of *G. tohatra*. The only other *Duboimantis* with a surprisingly similar call structure to the new species is *G. salegy*, which however differs by a substantially larger body size of 45–48 mm in adult males and by a larger number of granules in femoral glands (36–38 vs. 10–21).

G. tohatra sp. nov. differs from its probable sister species *G. schilfi* (Fig. 1) by a substantial genetic differentiation of 4.3% uncorrected pairwise distance (p-distance) in the *16S* gene, and from all other species of *Duboimantis* by a *16S* p-distance >6%. The bioacoustically similar *G. salegy* differs by 6.8% *16S* p-distance and is not the sister taxon of the new species.

Holotype description. A specimen in a good state of preservation, the right thigh muscle taken for DNA tissue samples. SVL 32.7 mm. For other measurements see below. Body gracile; head longer than wide, wider than body; snout pointed in dorsal and lateral view; nostrils directed laterally, protruding slightly, much nearer to tip of snout than to eye; canthus rostralis distinct, straight; loreal region concave and weakly oblique; tympanum indistinct,

oval, its horizontal diameter 42% of eye diameter; supratympanic fold distinct, straight, following the line of the eyelid to above the insertion of the arm; tongue fairly narrow, posteriorly bifid; vomerine teeth clearly distinct, arranged in two small aggregations on either side of the midline of the palate at the level of the anterior edge of the eye, posteromedial to choanae; choanae small and rounded and laterally displaced. Dark, translucent dermal fold below each jaw starting at the level of the mid-eye. Arms slender, subarticular tubercles single, highly distinct; outer metacarpal tubercle small and indistinct and inner metacarpal tubercle relatively well developed; fingers without webbing; relative length of fingers $1 < 2 < 4 < 3$, second finger much shorter than fourth; finger discs distinctly enlarged, round, nuptial pads absent. Hindlimbs slender; lateral metatarsals slightly separated distally with webbing; inner metatarsal tubercle distinct, anteriorly oriented, outer metatarsal tubercle absent; webbing formula of foot according to the scheme of Blommers-Schlösser (1979) 1(1), 2i(1.75), 2e(1), 3i(2.25), 3e(1.5), 4i(2.5), 4e(2.5), 5(1.25); relative toe length $1 < 2 < 3 < 5 < 4$, third toe much shorter than fifth; toe discs distinctly enlarged. Skin dorsally smooth, with reticulated fine ridges, and two sets of distinct dorsolateral ridges on the dorsum, one pair from the posterior eye running medially to over the suprascapular region, the other pair running dorsolaterally from the suprascapular region to the hip; no ridges or bumps are present on the dorsal head; diminutive supraocular spines present; a diminutive dermal flap is present on the heel; ventral skin smooth on chin and limbs, but highly granular on the abdomen. Femoral glands type 2 sensu Glaw *et al.* (2000), consisting of roughly 16 granules on the right thigh and 21 on the left thigh.



FIGURE 2. Preserved holotype of *G. tohatra* sp. nov. (ZSM 422/2016, field number ZCMV 15245, SVL 32.7 mm), in dorsal and ventral view. Scale bar corresponds to 5 mm.

Measurements, all in mm: SVL, 32.7; HW, 9.5; HL, 12.0; TD, 1.9; ED, 4.5; END, 3.3; NSD, 2.7; NND, 3.8; UAL, 6.7; LAL, 8.0; HAL, 11.0; THIL, 17.7; TIBL, 19.4; TARL, 9.5; FOL, 18.2.

In life (Fig. 3a,b), the dorsum was a medium brown with the external dorsolateral ridges distinctly tan, the internal ridges less distinct but also light in colour. The dorsal surface of head was not distinct from the dorsum, with a slightly darker brown band between the eyes. The flank fades to a more grey-brown ventrally. The dorsal surfaces of hindlimbs were as the flank in colour, with three dark brown crossbands on the thigh, three on the shank, and no crossbands on the foot. The dorsal surface of forelimb was similar to the lower leg in colour. No light annulus was present before the tip of each toe or finger. The lateral head was distinctly differentiated from the dorsal head, being almost black along the canthus rostralis, from the nostril to the tip of the snout, over the dorsal portion of the tympanic region beneath the supratympanic fold, and beneath the eye. An immaculate white spot was present anterior to the eye, with a more faded spot posterior to the eye over part of the tympanum. The iris was whitish above, and dark brown below the pupil. The lower lip was yellowish. Ventrally, the hands, forearms, tarsus and feet were all burnt umber in colour, with pale yellowish subarticular tubercles on the fingers, the subarticular tubercles of the toes being more orange in colour. The ventral chin and throat were burnt umber, especially on the jaw, making a distinct line anterior to the pectoral girdle, posterior to which the abdomen was orange with a few

Results

dark brown flecks anteriorly. The ventral thighs were also orange. The femoral glands were a creamy orange. The ventral humerus was semi-translucent.

After six months in preservative, the coloration has faded. Dorsally, areas that were brown have become grey to silver, with light grey dorsolateral ridges. The head colouration is mostly retained. The ventral colouration has lost its orange hue, and is now a yellow-cream. All elements of the colour pattern are however retained.

G. tohatra sp. nov.



G. schilfii



FIGURE 3. Adult male specimens of *Gephyromantis tohatra* sp. nov. and syntopic *G. schilfii* from Marojejy National Park in life, in dorsolateral and ventral views. (a,b) Holotype of *G. tohatra* (ZSM 422/2016, field number ZCMV 15245, SVL 32.7 mm); (c,d) paratype of *G. tohatra* (UADBA uncatologued, field number ZCMV 15236, SVL unknown). (e,f) call voucher of *G. schilfii* (ZSM 415/2016, field number ZCMV 15246, SVL 29.8 mm).

Variation. The paratype was not available for measurements but was of similar size as assessed in the field. Its colour in life (Fig. 3c,d) was generally similar to the holotype, but it lacked the bright whitish marking anterior to

the eye, had only one dark brown marking below the eye (two in the holotype), had slightly broader crossbands on the legs, and its outer dorsolateral ridges were less distinctly coloured than those of the holotype. Ventrally it was also similar to the holotype but its abdomen was more yellowish, with yellow-cream patches posterior to the pectoral girdle.

Etymology. The specific name is a noun in apposition, derived from the Malagasy word ‘tohatra,’ meaning ‘stairs,’ in reference to the difficulty of hiking up Marojejy on very steep trails with stair-like stretches between Camp Marojejia and Camp Simpona, and especially from Camp Simpona to the summit, necessary to discover this species.

Natural history. Calling males were heard at night at a site between Camp 3 (= Camp Simpona) and the summit of the Marojejy Massif, within montane rainforest of rather low canopy height and in an area of very steep slopes. Most specimens were calling in a dry headwater area of a small stream, in between very dense bushy undergrowth, at perch heights of 0.5–1 m above the ground from leaves and branches. In some areas the call could be heard from far outside the forest.

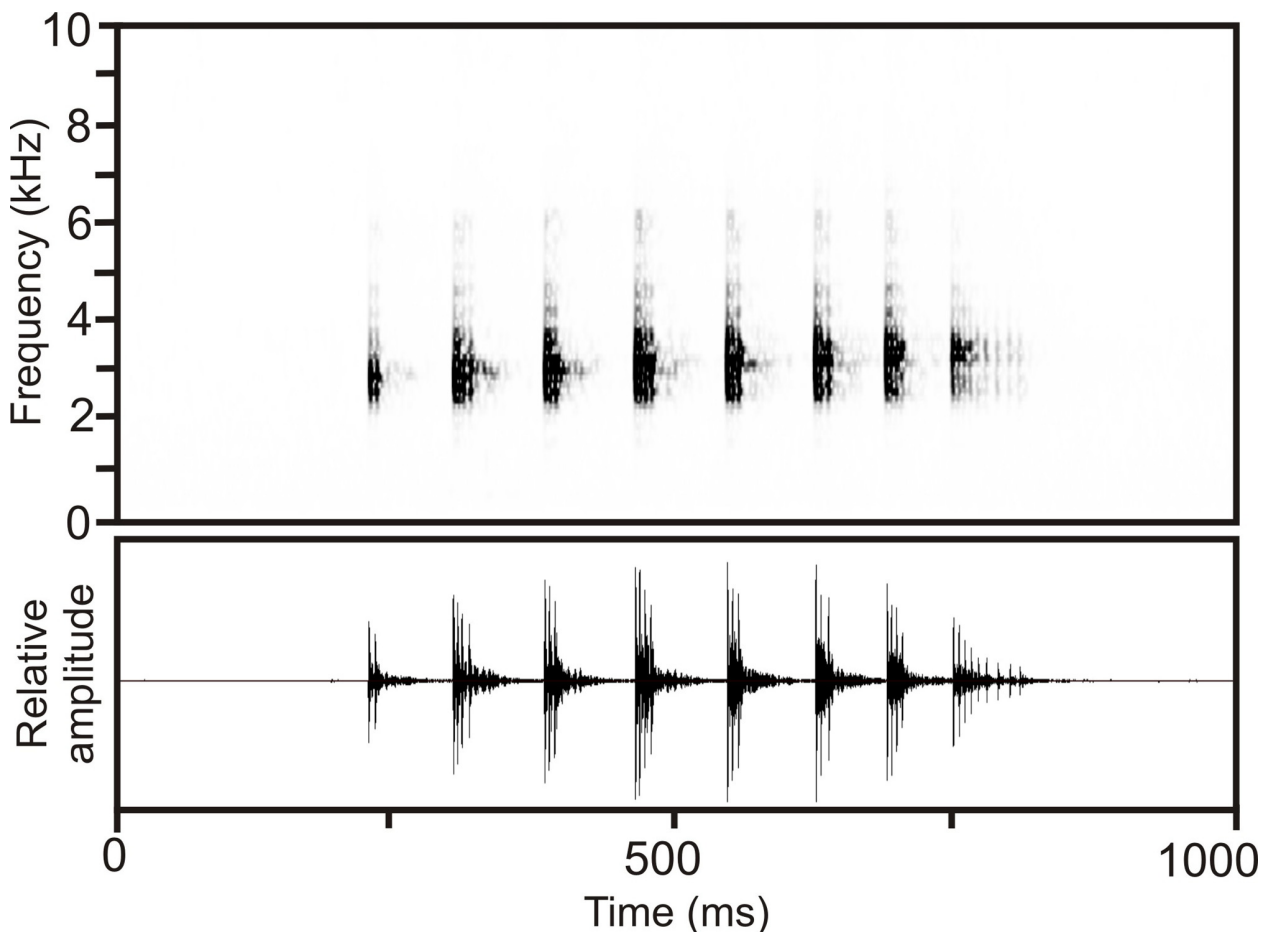


FIGURE 4. Audiospectrogram (above) and oscillogram (below) of a call of the holotype of *Gephyromantis tohatra* sp. nov. (ZSM 422/2016), recorded on 19 November 2016 on the Marojejy Massif in the North East of Madagascar. This call is here interpreted as consisting of eight notes, each with a distinct pulsed structure, and the last note containing more pulses than the preceding notes. Calls were filtered with a high pass filter to remove frequencies below 400 Hz in order to reduce wind artefacts.

Advertisement calls. Call recordings were made in an area where several (>5) males were calling relatively close to one another, and were obtained from the holotype and the paratype. The calls are considered advertisement calls because they were loud, stereotyped calls emitted by males without any sign of conflict with conspecifics. Calls consist of 7–10 pulsed notes (Fig. 4). Calls are separated by long and rather irregular intervals. In the holotype, call duration was 547–640 ms (594 ± 38 ms; $n = 9$), inter-call interval 1258–2306 ms (1622 ± 398 ms; $n = 8$), dominant frequency 3014–3273 Hz, and approximate prevalent band width 2000–5000 Hz. Each note had

Results

three to four recognizable pulses, with the last note of the call having more pulses (about 8). Characteristics of notes were measured in two calls. Pulses were not separated by distinct silent intervals. Intensity of each note was highest in the first pulse of each note. Note and interval duration are only tentatively presented, as there remains a weak background sound energy during these periods. Call 1: Note duration 34–78 ms (53 ± 14 ms, $n = 7$), inter-note interval duration 19–40 ms (30 ± 8 ms, $n = 6$), pulses per note 3–8 (4 ± 2 , $n = 7$). Call 2: Note duration 45–77 ms (57 ± 11 ms, $n = 7$), inter-note interval duration 7–36 ms (26 ± 12 ms, $n = 6$), pulses per note 3–9 (4 ± 2 , $n = 8$). Calls of the paratype were similar in most parameters but differed in that the pulses in notes were neither distinct nor clearly distinguishable; clear silent intervals between notes were not present, possibly due to background noise, and a weak frequency modulation was apparent in each note. Call duration was 502–798 ms (698 ± 117 ms, $n = 5$), inter-call interval duration 1458–1461 ($n = 2$), notes per call 7–10 (9 ± 1 ms, $n = 5$), dominant frequency of first three notes in a call 2454–2713 Hz (2637 ± 124 Hz, $n = 4$), dominant frequency of last 2–3 notes in a call 3014–3229 Hz (3122 ± 124 Hz, $n = 4$), time between start of one note and subsequent note 73–86 ms (82 ± 4 , $n = 17$ notes from 2 calls).

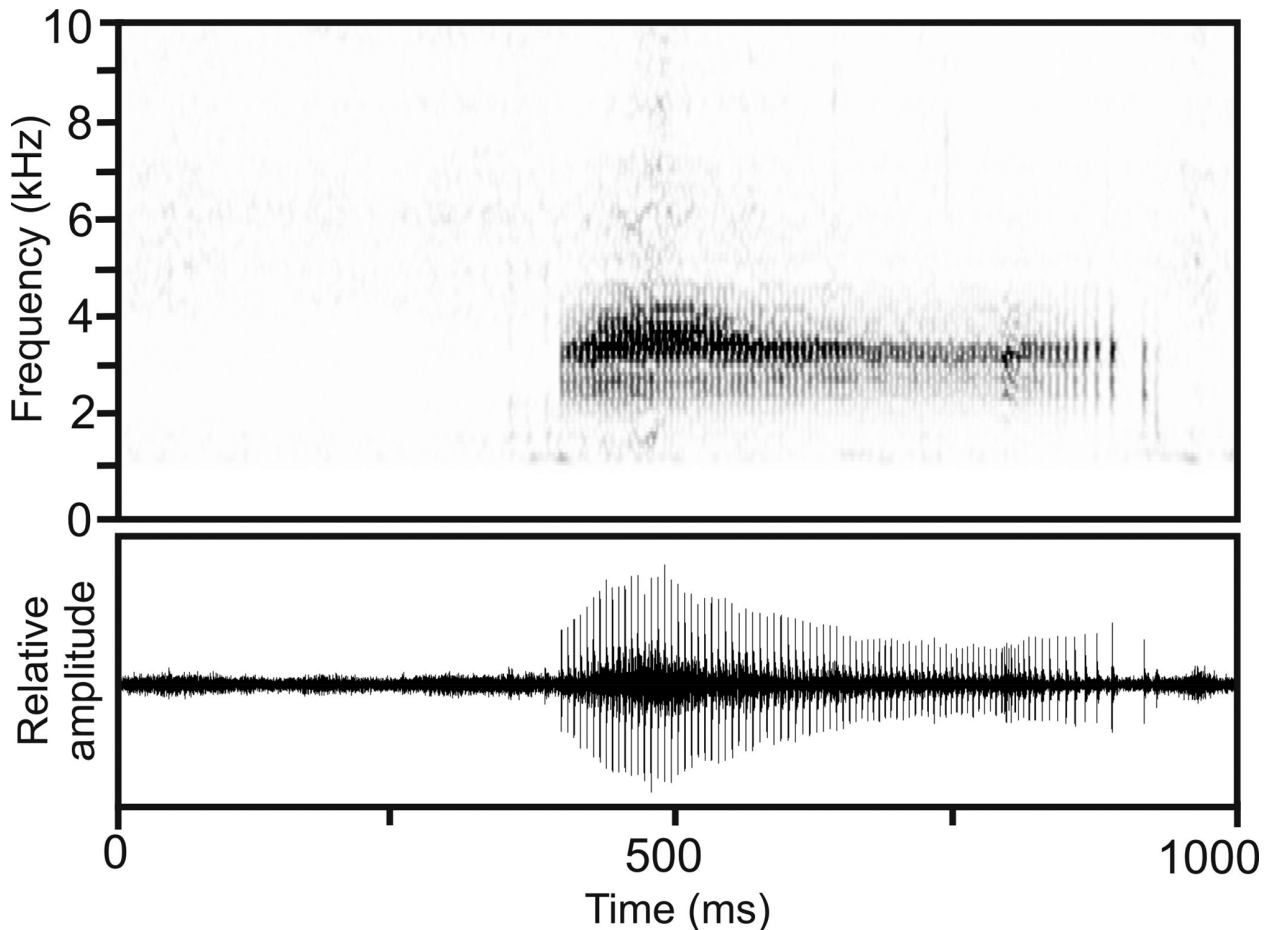


FIGURE 5. Audiospectrogram (above) and oscillogram (below) of a call of a specimen of *G. schilfi* (ZSM 415/2016 = ZCMV 15246), recorded on 19 November 2016 in proximity of the *G. tohatra* type locality on the Marojejy Massif. Calls were filtered with a high pass filter to remove frequencies below 1000 Hz in order to reduce wind artefacts.

Comparative data for syntopic *G. schilfi*. A few individuals of *G. schilfi* were heard emitting advertisement calls very close to the site in which *G. tohatra* sp. nov. individuals were heard and collected, on the same day and ca. 15 minutes after collecting *G. tohatra* sp. nov. One adult calling male was recorded and collected (voucher ZSM 415/2016, field number ZCMV 15246) from dense vegetation at a perch height of ca. 1 m above the ground, in a rainforest area on a steep mountain slope. Measurements: SVL, 29.8; HW, 9.5; HL, 11.6; TD, 1.9; ED, 4.6; END, 2.9; NSD, 2.5; NND, 2.6; UAL, 4.8; LAL, 7.5; HAL, 9.3; THIL, 15.6; TIBL, 18.3; TARL, 9.2; FOL, 16.5. As previously described (Glaw & Vences 2000), the call is a single pulsed note emitted after long and rather irregular silent intervals (Fig. 5). Call duration is 483–538 ms (518 ± 25 ms; $n = 4$), inter-call interval duration is

2917–5121 ms (3672 ± 1255 ms, $n = 3$), one note consists of ca. 73–89 pulses (80 ± 7 ; $n = 5$). Pulses were not clearly separated by silent intervals and in some cases not unambiguously distinguishable from each other. The intervals between pulse intensity maxima were somewhat irregular, becoming longer towards the end of the call, with a duration of about 5 ms at the beginning of the call and 7–12 ms at the end of the call. Dominant frequency was 3402–3445 Hz and approximate prevalent bandwidth was between 2000–4000 Hz.

Range extension for *G. schilfi* and *G. tandroka*. The goal of this study is not a comprehensive reassessment of the phylogeny within the subgenus *Duboimantis* and molecular analyses were thus limited to a subset of taxa. In exploratory analyses, the new species clustered with *G. salegy*, *G. schilfi*, and *G. tandroka*, three species that formed a highly supported subclade of *Duboimantis* in the analyses of Wollenberg *et al.* (2011) and Kaffenberger *et al.* (2012). For our analysis we thus expanded the sampling for these three species with additional individuals. We found molecular evidence for new populations of *G. schilfi* and *G. tandroka*, both of which were so far known only from Marojejy. Both these species were now also found on the Sorata Massif north of Marojejy, and had different degrees of genetic differentiation. While the populations of *G. schilfi* (Sorata vs. Marojejy) differed by only 0.6–0.8% uncorrected *16S* p-distance, those of *G. tandroka* had a higher divergence of 5.4% which suggests their taxonomic status requires revision and we therefore here flag the Sorata population as new Unconfirmed Candidate Species, *Gephyromantis* sp. Ca32, rationalised following Vieites *et al.* (2009). Another candidate species of *Duboimantis* (*G.* sp. Ca30 from the Bealanana district of northern Madagascar) that was also recently identified (Scherz *et al.* in press) was not included in our analysis here, but we have confirmed that it is not conspecific with *G.* sp. Ca32 (data not shown).

Discussion

This study adds one additional *Gephyromantis* of the subgenus *Duboimantis* to the ever-growing inventory of inconspicuous and morphologically similar brown-coloured frogs inhabiting Madagascar's rainforests. It is worth emphasizing that this species had not been included in previous DNA barcoding assessments of Madagascar's undescribed amphibian diversity (Vieites *et al.* 2009; Perl *et al.* 2014) but was a genuine new discovery during fieldwork in 2016. The congruence between molecular, bioacoustic and morphological characters unambiguously supports it as a new species, but its relationships require further investigation.

The available data suggest that *G. tohatra* is the sister species of the sympatric *G. schilfi*. Yet, its advertisement calls are remarkably similar to those of *G. salegy* from Ambolokopatrika described by Andreone *et al.* (2003), as shown by a comparison of the main temporal characteristics (values for *G. tohatra* in parentheses): Call duration 695–698 ms (502–798 ms), notes per call 8–11 (7–10), note duration 34–53 ms (34–78 ms), duration of inter-note intervals 42–50 ms (7–40 ms). A notable difference in dominant frequency is present, as calls of *G. salegy* have a dominant frequency of around 2600 Hz, whereas the calls of *G. tohatra* have a higher dominant frequency around 3000 Hz as expected by its smaller body size. Also, notes of *G. salegy* calls are not as clearly pulsed as those of *G. tohatra* and as a further weak difference, inter-note intervals were more distinct and more clearly silent in *G. salegy*. While the differentiation between *G. tohatra* and *G. salegy* is obvious by the drastic size differences (adult male SVL 33 mm in *G. tohatra* versus 46–48 mm in *G. salegy*) and the genetic divergence, their extreme bioacoustic similarity flags the calls of *G. salegy* as in need of confirmation. In fact, these calls were described without assigning them to a specific *G. salegy* specimen (Andreone *et al.* 2003). As *G. tohatra* at first glance looks like a small *G. salegy*, it is conceivable (although highly unlikely) that this species occurs syntopically with *G. salegy* in Ambolokopatrika, the type locality of the latter species, and that the two species were confused when call recordings were made.

Gephyromantis tohatra is currently known from only two male specimens, and nothing is known of its reproduction. Since the encountered individuals were calling along a dried headwater of a small rainforest stream, it is probable that their habits are similar to other species in the subgenus *Duboimantis* and they reproduce by endotrophic (non-feeding) tadpoles that complete their metamorphosis in slow-moving headwater stretches of such streams.

Biogeographically, most *Duboimantis* are known from northern Madagascar, and this remains true after the erection of the subgenus *Asperomantis* for several species previously included in *Duboimantis* (Vences *et al.* 2017). Of the described species in the subgenus, currently six species are restricted to a small portion of Madagascar north

Results

of ca. 15.5°S (*G. granulatus*, *G. salegy*, *G. schilfi*, *G. tandroka*, *G. tohatra*, *G. zavona*), while only four species (*G. cornutus*, *G. tschenki*, *G. plicifer* and *G. sculpturatus*) are restricted to south of this line, and another four species *G. leucomaculatus*, *G. luteus*, *G. moseri*, and *G. redimitus* occur both north and south of 15.5°S. The majority of species also remain north of 15.5°S when all known candidate species of this subgenus are also taken into account (*G. spp.* Ca16 [Masoala], Ca17 [Marojejy], Ca20 [Sahavontsira, south of 15.5°S], Ca21 [Antoetra, south of 15.5°S], Ca22 [Mahasoa, south of 15.5°S], Ca30 [Bealanana district], and the newly identified Ca32 [Sorata]), although three of these are known only from south of this line. This confirms this area as a centre of endemism and diversity for *Duboimantis*, as is also the case for numerous other groups of amphibians and reptiles (Brown *et al.* 2016).

The diversity of *Gephyromantis*, and in particular *Duboimantis*, at high altitudes on the Marojejy massif is remarkable. At present seven species including the newly described *G. tohatra* are known from above 1000 m a.s.l. in this area, three of which belong to *Duboimantis*: *G. tandroka*, *G. schilfi*, and *G. tohatra*. These species, which probably have endotrophic tadpoles (Randrianiaina *et al.* 2011), may be especially well suited to reproduction in forested upper reaches of mountains where flowing water is scarce and temporary. Given the apparent sister-group relationship between *G. schilfi* and *G. tohatra*, and their sympatric occurrence (individuals of both species captured within 50 metres of one another), it seems possible that these taxa may have diverged in sympatry. The question of how their ecology and mating habits differ, however, will require further study.

Acknowledgements

We are grateful to A. Razafimanantsoa and E. Mahazandry for their assistance in the field, to M. Kondermann and G. Keunecke for help with laboratory work, and to J. Köhler for his constructive review of the manuscript. This work was carried out in the framework of collaboration accords of the Technische Universität Braunschweig and the Zoologische Staatssammlung München with the Université d'Antananarivo, Faculté des Sciences (Zoologie et Biodiversité Animale). We are grateful to the Malagasy authorities for issuing permits for research, collection and export of specimens, and both to the staff of Madagascar National Parks in the central office and at Marojejy for their support. AR and MCB were supported by fellowships of the Deutscher Akademischer Austauschdienst. MV and MDS were supported by grants of the Deutsche Forschungsgemeinschaft (VE247/13-1 and 15-1).

References

- Andreone, F., Aprea, G., Vences, M. & Odierna, G. (2003) A new frog of the genus *Mantidactylus* from the rainforests of north-eastern Madagascar, and its karyological affinities. *Amphibia-Reptilia*, 24, 285–303.
<https://doi.org/10.1163/156853803322440763>
- Blommers-Schlösser, R.M.A. (1979) Biosystematics of the Malagasy frogs. I. Mantellinae (Ranidae). *Beaufortia*, 352, 1–77.
- Brown, J.L., Sillero, N., Glaw, F., Parfait, B., Vieites, D.R. & Vences, M. (2016) Spatial biodiversity patterns of Madagascar's amphibians and reptiles. *PLoS ONE*, 11, e0144076.
<https://doi.org/10.1371/journal.pone.0144076>
- Darriba, D., Taboada, G.L., Doallo, R. & Posada, D. (2012) jModelTest 2: more models, new heuristics and parallel computing. *Nature Methods*, 9, 772.
<https://doi.org/10.1038/nmeth.2109>
- Frost, D.R. (2017) Amphibian Species of the World: an Online Reference. Version 6.0 American Museum of Natural History, New York, USA. Electronic Database. Available from: <http://research.amnh.org/herpetology/amphibia/index.html> (accessed 21 May 2017)
- Glaw, F., Köhler, J. & Vences, M. (2011) New species of *Gephyromantis* from Marojejy National Park, northeast Madagascar. *Journal of Herpetology*, 45, 155–160.
<https://doi.org/10.1670/10-058.1>
- Glaw, F., Köhler, J. & Vences, M. (2012) A tiny new species of *Platypelis* from the Marojejy National Park in northeastern Madagascar (Amphibia: Microhylidae). *European Journal of Taxonomy*, 9, 1–9.
<https://doi.org/10.5852/ejt.2012.9>
- Glaw, F. & Vences, M. (2000) A new species of *Mantidactylus* from northeastern Madagascar (Amphibia, Anura, Ranidae) with resurrection of *Mantidactylus blanci* (Guibé, 1974). *Spixiana*, 23, 71–83.
- Glaw, F. & Vences, M. (2001) Two new sibling species of *Mantidactylus cornutus* from Madagascar. *Spixiana*, 24, 177–190.
- Glaw, F. & Vences, M. (2006) Phylogeny and genus-level classification of mantellid frogs (Amphibia, Anura). *Organisms*

- Diversity & Evolution*, 6, 236–253.
<https://doi.org/10.1016/j.ode.2005.12.001>
- Glaw, F. & Vences, M. (2007) *Plethodontohyla guentheri*, a new montane microhylid frog species from northeastern Madagascar. *Mitteilungen aus dem Museum für Naturkunde in Berlin – Zoologische Reihe*, 83, 33–39.
<https://doi.org/10.1002/mmnez.200600023>
- Glaw, F. & Vences, M. (2011) Description of a new frog species of *Gephyromantis* (subgenus *Laurentomantis*) with tibial glands from Madagascar. *Spixiana*, 34, 121–127.
- Glaw, F., Vences, M. & Gossmann, V. (2000) A new species of *Mantidactylus* (subgenus *Guibemantis*) from Madagascar, with a comparative survey of internal femoral gland structure in the genus (Amphibia: Ranidae: Mantellinae). *Journal of Natural History*, 34, 1135–1154.
<https://doi.org/10.1080/00222930050020140>
- Kaffenberger, N., Wollenberg, K.C., Köhler, J., Glaw, F., Vieites, D.R. & Vences, M. (2012) Molecular phylogeny and biogeography of Malagasy frogs of the genus *Gephyromantis*. *Molecular Phylogenetics and Evolution*, 62, 555–560.
<https://doi.org/10.1016/j.ympev.2011.09.023>
- Köhler, J., Jansen, M., Rodríguez, A., Kok, P.J.R., Toledo, L.F., Emmrich, M., Glaw, F., Haddad, C.F.B., Rödel, M.-O. & Vences, M. (2017) The use of bioacoustics in anuran taxonomy: theory, terminology, methods and recommendations for best practice. *Zootaxa*, 4251 (1), 1–124.
<https://doi.org/10.11646/zootaxa.4251.1.1>
- Kumar, S., Stecher, G. & Tamura, K. (2016) MEGA7: Molecular Evolutionary Genetics Analysis version 7.0 for bigger datasets. *Molecular Biology and Evolution*, 33, 1870–1874.
<https://doi.org/10.1093/molbev/msw054>
- Perl, R.G.B., Nagy, Z.T., Sonet, G., Glaw, F., Wollenberg, K.C. & Vences, M. (2014) DNA barcoding Madagascar's amphibian fauna. *Amphibia-Reptilia*, 35, 197–206.
<https://doi.org/10.1163/15685381-00002942>
- Rambaut, A. & Drummond, A.J. (2007) Tracer v1.5. Available from: <http://beast.bio.ed.ac.uk/Tracer> (accessed 29 August 2017)
- Randrianiaina, R.D., Wollenberg, K.C., Rasoloniatovo Hiobiarilanto, T., Strauß, A., Glos, J. & Vences, M. (2011) Nidicolous tadpoles rather than direct development in Malagasy frogs of the genus *Gephyromantis*. *Journal of Natural History*, 45, 2871–2900.
<https://doi.org/10.1080/00222933.2011.596952>
- Raselimanana, A.P., Raxworthy, C.J. & Nussbaum, R.A. (2000) Herpetofaunal species diversity and elevational distribution within the Parc National de Marojejy, Mad[a]agascar. *Fieldiana Zoology*, New Series, 97, 157–174.
- Ronquist, F., Teslenko, M., van der Mark, P., Ayres, D.L., Darling, A., Höhna, S., Larget, B., Liu, L., Suchard, M.A. & Huelsenbeck, J.P. (2012) MRBAYES 3.2: Efficient Bayesian phylogenetic inference and model selection across a large model space. *Systematic Biology*, 61, 539–542.
<https://doi.org/10.1093/sysbio/sys029>
- Scherz, M.D., Glaw, F., Vences, M., Andreone, F. & Crottini, A. (2016) Two new species of terrestrial microhylid frogs (Microhylidae: Cophylinae: *Rhombophryne*) from northeastern Madagascar. *Salamandra*, 52, 91–106.
- Scherz, M.D., Ruthensteiner, B., Vences, M. & Glaw, F. (2014) A new microhylid frog, genus *Rhombophryne*, from northeastern Madagascar, and a re-description of *R. serratopalpebrosa* using micro-computed tomography. *Zootaxa*, 3860 (6), 547–560.
<https://doi.org/10.11646/zootaxa.3860.6.3>
- Scherz, M.D., Vences, M., Borrell, J., Ball, L., Nomenjanahary, D.H., Parker, D., Rakotondratsima, M., Razafimandimby, E., Starnes, T., Rabearivony, J. & Glaw, F. (in press) A new frog species of the subgenus *Asperomantis* (Anura: Mantellidae: *Gephyromantis*) from the Bealanana District of northern Madagascar. *Zoosystematics and Evolution*.
- Vences, M. & Glaw, F. (2001) Systematic review and molecular phylogenetic relationships of the direct developing Malagasy anurans of the *Mantidactylus asper* group (Amphibia, Mantellidae). *Alytes*, 19, 107–139.
- Vences, M., Köhler, J., Pabijan, M., Bletz, M., Gehring, P.-S., Hawlitschek, O., Rakotoarison, A., Ratsoavina, F.M., Andreone, F., Crottini, A. & Glaw, F. (2017) Taxonomy and geographic distribution of Malagasy frogs of the *Gephyromantis asper* clade, with description of a new subgenus and revalidation of *Gephyromantis ceratophrys*. *Salamandra*, 53, 77–98.
- Vences, M., Kosuch, J., Glaw, F., Böhme, W. & Veith, M. (2003) Molecular phylogeny of hyperoliid treefrogs: biogeographic origin of Malagasy and Seychellean taxa and re-analysis of familial paraphyly. *Journal of Zoological Systematics and Evolutionary Research*, 41, 205–215.
<https://doi.org/10.1046/j.1439-0469.2003.00205.x>
- Vieites, D.R., Wollenberg, K.C., Andreone, F., Köhler, J., Glaw, F. & Vences, M. (2009) Vast underestimation of Madagascar's biodiversity evidenced by an integrative amphibian inventory. *Proceedings of the National Academy of Sciences of the USA*, 106, 8267–8272.
<https://doi.org/10.1073/pnas.0810821106>
- Wollenberg, K.C., Vieites, D.R., Glaw, F. & Vences, M. (2011) Speciation in little: the role of range and body size in the diversification of Malagasy mantellid frogs. *BMC Evolutionary Biology*, 11, 217.
<https://doi.org/10.1186/1471-2148-11-217>

Results

Chapter 5. PAPER: Two new Madagascan frog species of the *Gephyromantis (Duboimantis) tandroka* complex from northern Madagascar

In this chapter we describe the genetically isolated lineage sister to *G. (Duboimantis) tandroka*, identified in **chapter 4**, as *G. (D.) grosjeani*, and a further species that I discovered in the Bealanana District in 2015–2016, as *G. (D.) saturnini* (first identified and given a candidate number in **chapter 2**), which falls sister to *G. (D.) schilfi*, which occurs in both Marojejy and Sorata (shown in **chapter 4**). The level of divergence among taxa occurring in Marojejy and Sorata thus varies from conspecific levels to species-level differences, suggesting that connection between these areas may have been of considerable duration, or that their ability to maintain gene flow over large distances and complex topologies differs. This paper thus illuminates the pattern of connectedness among the massifs of Marojejy, Sorata+Andravory, and the Bealanana District.

Scherz, M.D., Rakotoarison, A., Ratsoavina, F.M., Hawlitschek, O., Vences, M. & Glaw, F. (2018)
Two new Madagascan frog species of the *Gephyromantis (Duboimantis) tandroka* complex
from northern Madagascar. *Alytes*, 36:130–158.

Alytes, 2018, **36** (1–4): 130–158.



Two new Madagascan frog species of the *Gephyromantis (Duboimantis) tandroka* complex from northern Madagascar

Mark D. SCHERZ^{1,2*}, Andolalao RAKOTOARISON³, Fanomezana Mihaja RATSOAVINA³, Oliver HAWLITSCHER¹, Miguel VENCES^{2*} & Frank GLAW¹

¹Zoologische Staatssammlung München (ZSM-SNSB), Münchhausenstr. 21, 81247 München, Germany.

²Zoologisches Institut, Technische Universität Braunschweig, Mendelssohnstr. 4, 38106 Braunschweig, Germany.

³Mention Zoologie et Biodiversité Animale, Université d'Antananarivo, BP 906, Antananarivo 101, Madagascar.

* Corresponding authors. <mark.scherz@gmail.com>, <m.vences@tu-bs.de>.

We describe two new frog species of the Madagascar-endemic genus *Gephyromantis*, belonging to the *G. tandroka* complex in the subgenus *Duboimantis*. *Gephyromantis (Duboimantis) saturnini* sp. nov. is known from specimens collected at Ampotsidy, in the District de Bealanana of the Région Sofia of northern Madagascar. It is a large and genetically distinct species with small interocular tubercles and indistinct femoral glands that emits calls in series composed of couplets and triplets. Morphologically and bioacoustically, it is most similar to *G. tandroka*, but genetically it was recovered as sister to *G. schilfi*, from which it is separated by an uncorrected p-distance of 5.1 % in the mitochondrial 16S rRNA gene. *Gephyromantis (Duboimantis) grosjeani* sp. nov. was collected on the Sorata massif, in the District de Vohemar of the Région Sava of northern Madagascar. It is a medium-sized species with large and distinct femoral glands, which are a distinctive characteristic from other members of this complex. Genetically, it is distinguished from all other *Gephyromantis* species by uncorrected p-distances of at least 5.1 % in the 16S rRNA gene.

urn:lsid:zoobank.org:pub:2A5B3873-3512-4088-B992-B1D69CA9EB8B

INTRODUCTION

The Madagascar-endemic mantellid frog genus *Gephyromantis* is currently divided into six subgenera: *Asperomantis* Vences, Köhler, Pabijan, Bletz, Gehring, Hawlitschek, Rakotoarison, Ratsoavina, Andreone, Crottini & Glaw, 2017, *Duboimantis* Glaw & Vences, 2006, *Gephyromantis* Methuen, 1920, *Laurentomantis* Dubois, 1980, *Phylacomantis* Glaw & Vences, 1994, and *Vatomantis* Glaw & Vences, 2006. The most diverse of these subgenera is *Duboimantis*, with 14 described species (Scherz *et al.* 2017b). *Duboimantis* has its centre of diversity in northeastern Madagascar (Kaffenberger *et al.* 2012), and in some areas, as many as seven species can occur in sympatry – and up to three species in close syntopy (e.g. Marojejy: Raselimanana *et al.* 2000; Glaw & Vences 2007; Scherz *et al.* 2017a). *Duboimantis* frogs typically inhabit primary rainforest, with only few representatives (e.g., *G. granulatus*) sometimes occurring in degraded areas and secondary forest. Adult males range in size from snout-vent lengths of 27 mm to 53 mm (Glaw & Vences 2007). They are scansorial, often found during the day in the leaf litter on the forest floor, and at night perching in the vegetation whence the males emit their advertisement calls (Glaw & Vences 2000, 2001, 2007; Vences & Glaw 2001). As far as known, these frogs have endotrophic (non-feeding) tadpoles that probably hatch in terrestrial nests and at least sometimes are washed into streams where they complete metamorphosis (Randrianaaina *et al.* 2011). Species of *Duboimantis* tend to be difficult to distinguish morphologically, and although they are rather vocal and their loud calls are easily heard, in some of the species groups even bioacoustic differences require specific experience to tell apart.

During fieldwork on the Sorata massif in the District de Vohemar of the Région Sava of northern Madagascar in 2012, we encountered numerous specimens of a large *Duboimantis* species, which resembles *G. (D.) tandroka* (Glaw & Vences 2001). Analysis of a fragment of the 16S rRNA mitochondrial barcode gene region showed that these specimens are genetically separated from that species, and the clade they formed was designated as a new candidate species, *G. (D.)* sp. Ca32 (Scherz *et al.* 2017a). On a separate expedition to Ampotsidy, an area of mountains north of Beandrarezona in the District de Bealanana of the Région Sofia of northern Madagascar in 2015–2016, we collected three specimens of another large *Duboimantis* species which represent another undescribed candidate species dubbed *G. (D.)* sp. Ca30, which also has affinities to *G. (D.) tandroka* (Scherz *et al.* 2017b). Herein, we address the taxonomy of these two candidate species.

METHODS

Specimens were located in the field by following their calls or opportunistically found on nocturnal transects. When possible, specimens were photographed in situ and recorded calling prior to capture. Specimens were anaesthetized with aqueous MS 222 solution and subsequently killed with an MS 222 overdose, fixed with 90 % ethanol, and then transferred to 70 % ethanol for long-term storage. Tissue samples taken prior to fixation were deposited in 99 % ethanol for molecular study. Field numbers MSZC, FGZC and ZCMV refer to the zoological collections of Mark D. Scherz, Frank Glaw and Miguel Vences, respectively. Specimens were deposited in the Zoologische

Staatssammlung München (ZSM) and the amphibian collections of the Université d'Antananarivo, Mention Zoologie et Biodiversité Animale (UADBA-A). Additional institutional abbreviations used are MNHN (Muséum National d'Histoire Naturelle, Paris), MRSN (Museo Regionale di Scienze Naturali di Torino) and ZFMK (Zoologisches Forschungsmuseum Alexander Koenig, Bonn).

Research was conducted under permit No. 224/15/MEEMF/SG/DGF/DAPT/SCBT, 215/16/MEEF/SG/DGF/DSAP/SCB.Re and 265/12/MEF/SG/DGF/DCB.SAP/SCB provided by the Direction Générale des Forêts at the Ministère de l'Environement, de l'Ecologie et des Forêts (MEEF) of Madagascar. Specimens were exported under permit No. 030N-EA01/MG16, 010N-EA01/MG17 and 163N-EA12/MG12.

Measurements were taken by MV to the nearest 0.1 mm using the standard scheme employed in other recent *Gephyromantis* species descriptions (Scherz *et al.* 2017a, b; Vences *et al.* 2017), provided here again for better comparability: snout-vent length (SVL), maximum head width (HW), head length from posterior maxillary commissure to snout tip (HL), horizontal eye diameter (ED), horizontal tympanum diameter (TD), distance from eye to nostril (END), distance from nostril to snout tip (NSD), distance between nostrils (NND), foot length (FOL), foot length including tarsus (FOTL), hindlimb length from cloaca to tip of longest toe (HIL), forelimb length from axilla to tip of longest finger (FORL), hand length from the base of the hand to the length of the longest finger (HAL) and femoral gland granule number (FGG). Webbing formulae follow Blommers-Schlösser (1979); femoral gland terminology follows Glaw *et al.* (2000); skin ridge and tubercle terminology follows Vences & Glaw (2001).

Previous analyses (Scherz *et al.* 2017a, b) had attributed the two target candidate species to the *G. salegy* subclade recovered in the multigene analysis of Kaffenberger *et al.* (2012). We therefore added sequences of the mitochondrial 16S rRNA gene (16S) from Scherz *et al.* (2017b) for *Gephyromantis* sp. Ca30 to the alignment of Scherz *et al.* (2017a) which included all described species of this subclade, and complemented this dataset with newly obtained sequences of a second 16S rRNA fragment, and of a fragment of the 12S rRNA gene (12S) for this candidate species. We extracted DNA using a standard salt extraction protocol from samples of muscle tissue preserved in 99 % ethanol in the field, used polymerase chain reaction to amplify and sequence the target fragments, and sequenced these directly on an automated capillary DNA sequencer. Primers and amplification protocols used were as follows (Vences *et al.* 2003): 12S, primer 12SAL (AAACTGGGATTAGATACCCCACTAT), and 12SBH (GAGGGTGACGGCGGTGTGT), 35 cycles of 94°C (45 s), 50°C (60 s), 74°C (120 s). 16S, primer 16SL3 (AGCAAAGAHYWWACCTCGTACCTTTGCAT and 16SAH (ATGTTTTGATAAACAGGCG), 94°C (90 s) followed by 33 cycles of 94°C (45 s), 55°C (45 s), 72°C (90 s). All new DNA sequences were submitted to GenBank (accession numbers MH307657–MH307659 and MH307662–MH307664).

For phylogenetic analysis based on model selection under the Bayesian Information Criterion in jModeltest 2 (Darriba *et al.* 2012), we implemented a HKY+G substitution model in Maximum Likelihood (ML) and Bayesian Inference (BI) analyses. ML was run in MEGA7 (Kumar *et al.* 2016) and node support assessed with 2000 non-parametric ML bootstraps. BI was run in MrBayes 3.2 (Ronquist *et al.* 2012), with two parallel runs for 50 million generations, sampling every 1000th tree, and discarding 25 % of the sampled trees as burn-in. Chain mixing and stationarity were assessed by

examining the standard deviation of split frequencies and by plotting the -lnL per generation using Tracer 1.5 software (Rambaut & Drummond 2007). Genetic divergences are quantified as uncorrected pairwise distances (p-distances).

Call recordings from Ampotsidy (District de Bealanana, Région Sofia, Madagascar) and Marojejy (District d'Andapa, Région Sava, Madagascar) were made on a Marantz PMD661 MKII with a Sennheiser ME66/K6 supercardioid microphone, at 44.1 kHz. Recordings from Sorata (District de Vohemar, Région Sava, Madagascar) were made on an Edirol R-09 with its internal microphone. Bioacoustic analysis was performed in Cooledit Pro 2.0 (Syntrillium Corp.). Air temperatures were measured to the nearest 0.1°C after recording using an infrared thermometer pointed in the general direction of the calling specimen when possible. Terminology of call descriptions follows Köhler *et al.* (2017).

RESULTS

Phylogenetic analysis of three segments of the mitochondrial 16S and 12S genes (fig. 1) produced a tree with relatively high Bayesian posterior probability values (PP) at most nodes, but moderate to low Maximum Likelihood bootstrap support (BS). *Gephyromantis* sp. Ca30 was recovered as sister to *G. (D.) schilfi* (Glaw & Vences 2000) with fairly high support (PP 1.0, BS 84 %) from which it is separated by an uncorrected p-distance of 5.1 % in the region of the 16S gene fragment typically used for the molecular taxonomic identification (barcoding) of Madagascan frogs (e.g. Vieites *et al.* 2009). *Gephyromantis (Duboimantis)* sp. Ca32 was recovered as sister to *G. tandroka* with high support (PP 1.0, BS 92 %), from which it is also separated by an uncorrected p-distance of 5.1 %. The recently described *G. (D.) tohatra* Scherz, Razafindraibe, Rakotoarison, Dixit, Bletz, Glaw & Vences, 2017 was recovered without support as sister to the clade containing *G. (D.)* sp. Ca30 and *G. (D.) schilfi*. Two clades were formed within *G. (D.) schilfi* corresponding to the two localities (Marojejy and Sorata) whence this species is known, but the genetic differences between these two clades were much lower (0.6–0.8 %; see Scherz *et al.* 2017a).

We compared the morphology of *G. (D.)* sp. Ca30 and *G. (D.)* sp. Ca32 to other members of the subgenus *Duboimantis*, and to *G. (D.) tandroka* and *G. (D.) schilfi* in particular as these were found to be their respective sister species. We found *G. (D.)* sp. Ca30 (SVL 39–43 mm in adult males) to be larger than *G. (D.) tandroka* (36–40 mm in adult males). Otherwise these two species are highly similar—far more so than *G. (D.)* sp. Ca30 to its sister species (as suggested by mitochondrial DNA) *G. (D.) schilfi*, which is much smaller (27–30 mm in adult males). Males of *Gephyromantis (D.)* sp. Ca32 are morphologically quite distinctive as they are characterised by large, distinct femoral glands, which are indistinct in most other members of the *G. (D.) tandroka* complex. We investigated the bioacoustics of the two candidate species in comparison to other members of the *G. tandroka* complex in the subgenus *Duboimantis* (fig. 2–3). To facilitate this comparison, we provide a new description of calls of *G. (D.) tandroka* recorded in 2005 (Vences *et al.* 2006) and 2016 (deposited in the Tierstimmenarchiv, DOI: 10.7479/vd5c-3waj).

Calls of one male *G. (D.) tandroka* (ZSM 417/2016; fig. 2–3) were recorded on 17 November 2016 at 19 h 15 at an estimated air temperature of 17°C, at the type

locality, Camp 3 in Marojejy, ca. 1300 m a.s.l. A call consists of a single pulsatile note, with a call (or note) duration of 77–94 ms (88 ± 5 ms; $N = 10$), repeated for long periods with regular inter-call intervals of 1542–2034 ms (1721 ± 128 ms; $N = 10$). Each call (or note) consists of approximately 21–24 indistinct pulses (22.5 ± 1.4 ; $N = 10$), without silent interval between them. Pulse intensity decreases towards the end of the call. The dominant frequency is between 2885–3100 Hz (3048 ± 81 Hz; $N = 10$). The approximate prevalent bandwidth is between 1100–5900 Hz, with relevant energy bands also between 6000–9000 Hz.

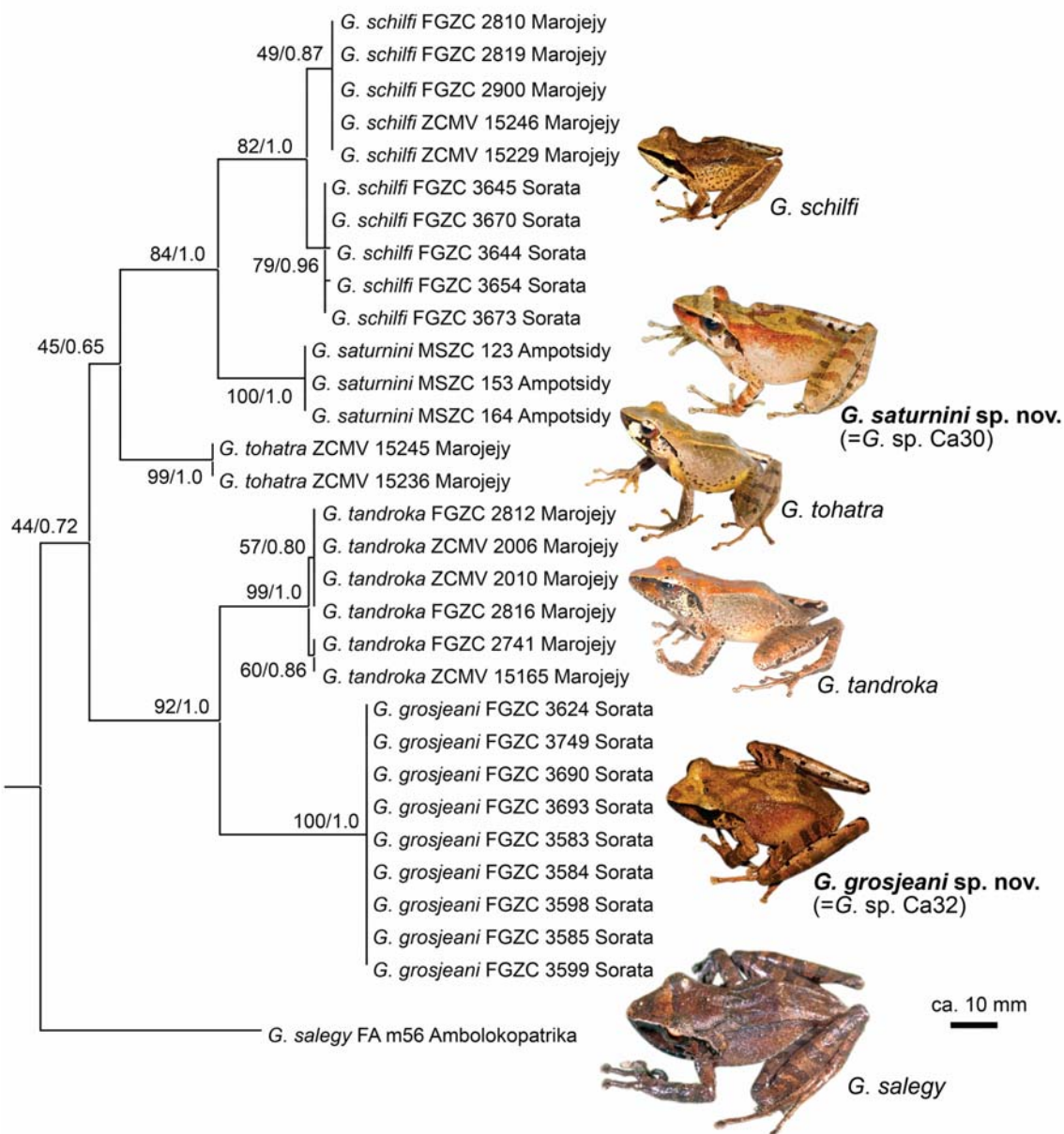


Figure 1. Maximum Likelihood tree based on 1106 bp of the mitochondrial 12S and 16S rRNA gene fragments, showing phylogenetic relationships of the two new species to their closest relatives among *Gephyromantis*. Support values at nodes are ML likelihood bootstrap values and BI posterior probabilities. *Gephyromantis granulatus* was used as outgroup (removed for better graphical representation). Inset photos show representative individuals of the target species, size of the pictures roughly to scale.

Additional calls were recorded on 16 February 2005 at the same site, at an air temperature of ca. 21°C (fig. 2–3). This recording, available in Vences *et al.* (2006), is of poorer quality and was done with a tape recorder. Calls are in general similar to those recorded in 2016, but the calls of various males in a chorus all have longer call durations, caused by a noisy ‘tail’ at the end which might be artefactual. The calls are pulsatile, but single pulses cannot be reliably recognized. Temporal and spectral measurements of one male ($N = 10$ calls) are as follows: call duration 113–152 ms (123 \pm 14 ms), inter-call interval duration 1877–2447 ms (2226 \pm 207 ms), dominant frequency 2842–3186 Hz (3082 \pm 116 Hz), approximate prevalent bandwidth 1200–5500 Hz. In very large and persistent choruses, heard over numerous nights in 2005 and 2016, we do not recall hearing multi-note calls from *G. tandroka*.

Calls recorded from two individuals of *G. (D.)* sp. Ca30 (ZSM 61/2016 and 62/2016; fig. 2–3) were highly similar to one another, and, although similar note-for-note to the calls of *G. (D.) tandroka*, differ strongly in call structure, being typically composed of pairs or triplets of notes except the first few calls, compared to the single-note calls of that species. In this respect they resemble more closely the calls of *G. zavona* and *G. leucomaculatus* (Vences *et al.* 2006). They bear little similarity to the calls of *G. (D.) schilfi*, which are long, highly pulsed single-note calls (Glaw & Vences 2000; Vences *et al.* 2006). Calls from a single individual of *G. (D.)* sp. Ca32 were more similar to *G. (D.) tandroka* in call structure, being also composed of single calls (fig. 2–3), but differed in other call parameters, especially in call and inter-call interval duration; for details see below.

In light of their strong genetic differentiation together with morphological and bioacoustic differences from all described species of the *G. tandroka* complex in the subgenus *Duboimantis*, we describe *G. (D.)* sp. Ca30 and *G. (D.)* sp. Ca32 as new species:

Gephyromantis (Duboimantis) saturnini sp. nov.

(fig. 1–7, Table 1)

LSID: urn:lsid:zoobank.org:act:8CD78532-677C-4352-AEE8-C291B0715A11

Gephyromantis (Duboimantis) sp. Ca30 – (Scherz *et al.* 2017a, b)

Specimens allocated to new species

Holotype

ZSM 61/2016 (MSZC 0123), an adult male collected in the eastern parcel of the Ampotsidy mountains (14.4133°S, 48.7175°E, 1450 m a.s.l.), District de Bealanana, Région Sofia, northern Madagascar, at 18 h 30 on 31 December 2015 by M. D. Scherz, J. Borrell, L. Ball, T. Starnes, E. Razafimandimby, D. H. Nomenjanahary and J. Rabearivony.

Paratypes

UADBA-A 61674 (ex-ZSM 66/2016, MSZC 0164), an adult male collected between 20 h 30 and 21 h 55 on 7 January 2016 in the western parcel of the Ampotsidy mountains (14.4123°S, 48.7118°E, 1481 m a.s.l.), and ZSM 62/2016 (MSZC 0153), an adult male collected at 23 h 50 on 6 January 2016 in the eastern parcel of the Ampotsidy mountains (14.4134°S, 48.7173°E, 1476 m a.s.l.), District de Bealanana, Région Sofia, northern Madagascar, by M. D. Scherz, J. Borrell, L. Ball, T. Starnes, E. Razafimandimby, D. H. Nomenjanahary and J. Rabearivony.

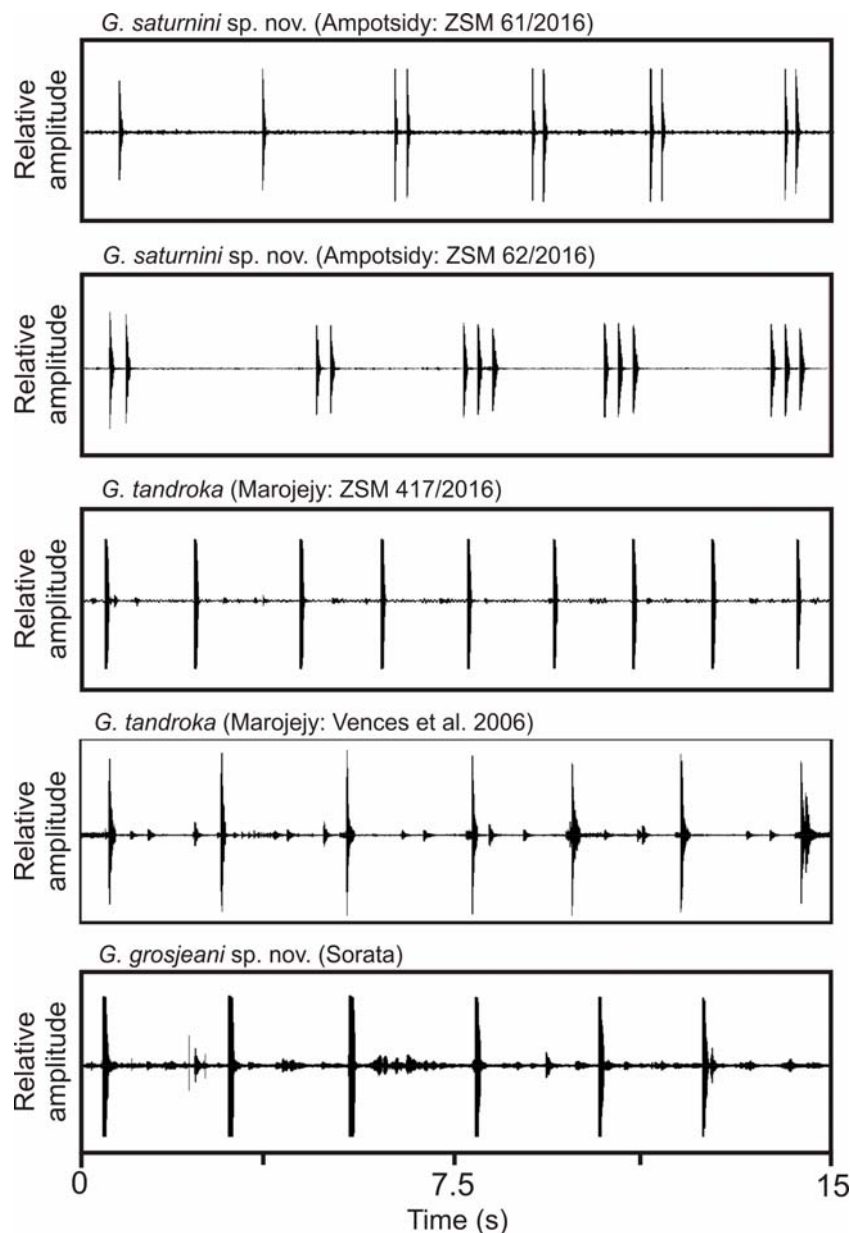


Figure 2. Comparative oscillograms of parts of call series of some representative of the *G. tandroka* complex in the subgenus *Duboimantis*. The figure shows the typical pattern of multi-note calls in *Gephyromantis (Duboimantis) saturnini* sp. nov. vs. *G. (D.) tandroka* and *G. (D.) grosjeani* sp. nov. The recording of *G. tandroka* from 2005 (taken from Vences *et al.* 2006) is of a chorus of multiple specimens; for visualization, the amplitude of calls of other specimens was strongly reduced to highlight the calls of the specimens closest to the microphone.

Diagnosis

A *Gephyromantis* species assigned to the subgenus *Duboimantis* on the basis of its fairly smooth skin, interocular tubercles, large body size and presence of inner and outer dorsolateral folds. *Gephyromantis saturnini* is characterised by the following unique suite of characters: (1) large body size (SVL 39.4–42.8 mm in adult males), (2) paired subgular vocal sacs, (3) HIL/SVL 1.79–1.87, (4) TD/ED 0.48–0.56, (5) presence of inner and outer dorsolateral folds, (6) reticulated low ridges on the dorsum, (7) distinct interocular tubercles, (8) indistinct femoral glands consisting of 9–16 faint granules. It is furthermore characterised by advertisement calls consisting of 1–3 pulsatile notes, emitted in series of 7–8 calls.

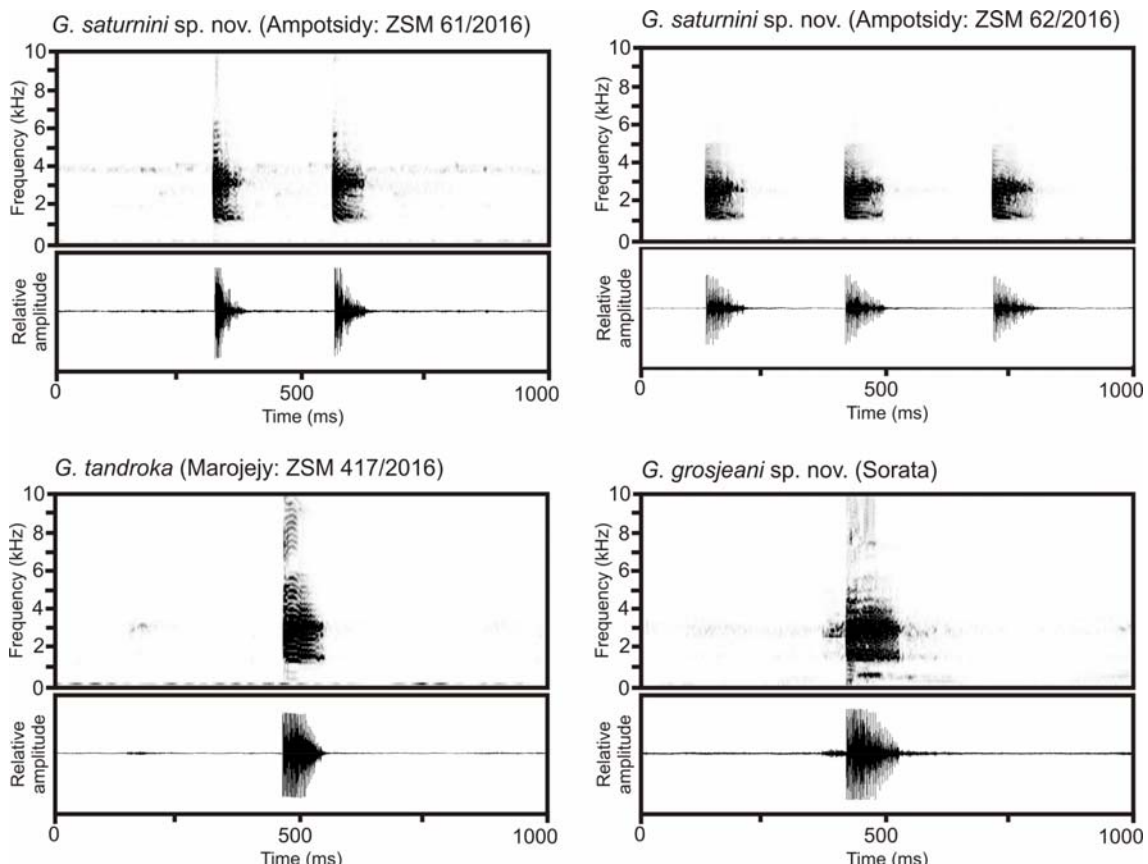


Figure 3. Comparative spectrograms and oscillograms of calls of some representatives of the *G. tandroka* complex in the subgenus *Duboimantis*.

Comparisons

Within the genus *Gephyromantis*, *G. saturnini* may be distinguished from all members of the subgenus *Gephyromantis* on the basis of much larger body size (SVL 39.4–42.8 mm vs. 20–33 mm); from all members of the subgenus *Asperomantis* on the basis of generally larger body size (SVL 39.4–42.8 mm vs. 26.6–40.7 mm); from all members of the subgenus *Phylacomantis* on the basis of the presence of distinct dorsolateral ridges (vs. absent or discontinuous), indistinct femoral glands (vs. distinct), more slender body shape and absence of outer metatarsal tubercle (vs. presence); from all members of the subgenus *Laurentomantis* on the basis of much larger body size (SVL 39.4–42.8 mm vs. 20–34 mm), smooth skin (vs. highly granular to rugose); and from all members of the subgenus *Vatomantis* on the basis of much larger body size (SVL 39.4–42.8 mm vs. 23–31 mm), lack of greenish skin colouration (vs. presence) and less slender limbs. Within the subgenus *Duboimantis*, it may be distinguished from *G. (D.) cornutus* (Glaw & Vences, 1992) and *G. (D.) redimitus* (Boulenger, 1889) by the possession of paired subgular vocal sacs (vs. single); from *G. (D.) luteus* (Methuen & Hewitt, 1913), *G. (D.) sculpturatus* (Ahl, 1929) and *G. (D.) plicifer* (Boulenger, 1882) by less webbed toes, lack of concave black suprascapular markings (vs. usually present) and presence of only diminutive heel spines (vs. distinct heel spines); from *G. (D.) moseri* (Glaw & Vences, 2002) by the much less rugose dorsum and smaller supraocular tubercles; from *G. (D.) salegy* (Andreone, Aprea, Vences & Odierna, 2003) and *G. (D.) redimitus* by considerably smaller body size (SVL 39.4–42.8 mm vs. 46–53 mm); from *G. (D.) schilfii*, *G. (D.) tschenki* (Glaw & Vences, 2001) and *G. (D.) tohatra* by much larger body size (SVL 39.4–42.8 mm vs. 27–36 mm); from *G. (D.) zavona* (Vences, Andreone, Glaw & Randrianirina, 2003), *G. (D.) leucomaculatus* (Guibé, 1975) and *G. (D.) granulatus* (Boettger, 1881) by the presence of distinct interocular tubercles (vs. absence). From the most similar species, *G. (D.) tandroka*, *G. (D.) saturnini* may be distinguished by generally larger adult male size (SVL 39.4–42.8 mm vs. 35.6–40.1 mm; see Table 1).

Bioacoustically, *G. (D.) saturnini* most strongly resembles *G. (D.) tandroka* to the human ear, but differs consistently in call series structure (1–3 notes per call vs. always single-note calls). Its call series structure resembles more strongly *G. (D.) leucomaculatus* and *G. (D.) zavona* in this respect, but it differs from *G. (D.) zavona* in having a maximum of three notes per call (vs. up to five) and a lower dominant frequency (2497–2670 Hz vs. 3171–3785 Hz); and from *G. (D.) leucomaculatus* in having a longer inter-note interval within two-note calls (150–237 ms vs. 83–116 ms) and a lower dominant frequency (2497–2670 Hz vs. 2917–3168 Hz). To compare the calls by ear to other members of the subgenus *Duboimantis*, the reader is referred to our deposited calls and those available from Vences *et al.* (2006), which are also available online at www.fonozoo.com.

Genetically, the species is distinguished from all other species of *Gephyromantis* by uncorrected p-distances of at least 5.1 % in the analysed 16S rRNA gene fragment.

Results

Table 1. Morphometric measurements of examined specimens of *Duboimantis*. For abbreviations, see Methods section. HT marks the holotype, PT the paratypes of the respective species. Measurements for *G. (D.) solegy* are from Andreone *et al.* (2003), *G. (D.) tohatra* are from Scherz *et al.* (2017a) and *G. (D.) schilli* are from Glaw & Vences (2000) and Scherz *et al.* (2017a).

Voucher	Type status	SVL	HW	HL	TD	ED	END	NSD	NND	FORL	HAL	HIL	FOTL	FOL
<i>Gephyromantis landolaka</i> (Marojejy) - males														
MNHN 1973.922	PT	38.9	13.1	14.5	2.2	4.8	3.4	2.2	3.7	26.6	13.0	74.4	32.8	21.8
MNHN 1973.924	HT	38.7	13.2	14.6	2.4	4.8	3.5	1.9	3.9	26.0	12.7	70.2	32.9	21.9
MNHN 1973.927	PT	38.8	14.0	15.6	2.4	5.1	3.8	2.3	3.5	26.3	12.7	73.3	32.8	21.9
MNHN 1973.929	PT	38.8	13.1	15.0	2.4	5.2	3.8	2.4	4.1	23.3	12.5	73.5	31.7	22.1
ZSM.321/2005 (FGZC 2812)		35.6	12.9	14.2	2.7	5.0	3.6	2.0	3.8	24.3	12.3	65.5	29.8	20.3
ZSM.322/2005 (FGZC 2816)		37.0	13.1	15.2	2.7	5.0	4.0	2.1	3.8	23.9	11.1	66.7	28.9	18.7
ZSM.417/2016 (ZCMV 15165)		40.1	14.8	16.0	2.6	6.1	4.1	2.1	4.4	26.7	13.4	74.3	32.4	22.4
<i>Gephyromantis grosjeani</i> (Sorata) - males														
ZSM.1553/2012 (FGZC 3749)	PT	36.1	12.3	14.1	2.8	5.3	3.8	1.8	4.0	23.9	12.0	70.9	31.3	21.2
ZSM.1554/2012 (FGZC 3584)	HT	38.4	13.0	14.2	2.6	4.5	3.6	2.1	3.4	24.8	12.1	70.9	32.2	22.1
<i>Gephyromantis saturnini</i> (Bealanana) - males														
ZSM.61/2016 (MSZC 123)	HT	39.4	13.4	14.7	2.8	5.0	4.1	2.5	4.7	24.0	12.5	73.7	32.5	21.9
ZSM.62/2016 (MSZC 153)	PT	41.7	13.7	15.3	2.4	5.0	4.2	2.3	4.2	24.1	12.0	74.5	33.9	22.9
UADBA-A61674 (ex-ZSM.66/2016, MSZC 164)	PT	42.8	14.5	15.8	2.8	5.5	4.3	2.4	4.3	26.2	13.2	77.6	35.1	24.0
<i>Gephyromantis tohatra</i> (Marojejy) - male														
ZSM.422/2016 (ZCMV 15245)	HT	32.7	9.5	12.0	1.9	4.5	3.3	2.7	3.8		11.0			18.2
<i>Gephyromantis solegy</i> (Ambolokopatra) - males														
MRSN.A2038	HT	47.8	16.2	18.0	3.0	5.9	4.7	2.8	4.5	29.4	14.4	86.5	38.7	25.9
MRSN.A2043	PT	45.8	15.5	16.5	2.5	5.2	5.0	2.2	4.4	29.8	13.6	84.4	37.9	25.3
ZSM.48/2011 (ex-MRSN.A2044)	PT	47.0	15.5	17.2	3.0	5.3	5.1	2.5	4.2	29.9	14.1	88.3	38.2	26.7
<i>Gephyromantis schilli</i> (Marojejy) - male														
ZFMK.59885	HT	29.0	9.5	11.6	1.9	4.6	3.8	2.5	2.6			9.3		16.5
ZSM.415/2016 (ZCMV 15246)		29.8												

Voucher	Type status	SVL	HW	HL	TD	ED	END	NSD	NND	FORL	HAL	HIL	FOTL	FOL
<i>Gephyromantis tandroka</i> (Marojejy) - females														
MNHN 1973.912	PT	43.2	14.9	16.4	2.9	5.1	4.1	2.5	4.6	29.2	13.9	81.8	36.2	24.2
MNHN 1973.926	PT	44.7	15.3	16.7	2.8	5.4	4.4	2.5	4.2	28.8	14.5	84.1	37.6	24.5
MNHN 1973.928	PT	39.8	13.3	14.8	2.2	5.1	3.8	2.3	3.8	25.8	12.6	78.4	34.3	22.4
ZFMK 59894	PT	39.6	15.0	16.5	2.3	5.4	4.3	2.7	4.7	27.0	13.6	80.1	36.0	23.1
ZSM 937/2000	PT	41.5	15.3	16.6	2.3	5.6	4.3	2.6	4.3	28.3	14.0	85.0	38.1	24.3
ZSM 320/2005 (FGZC 2741)	PT	39.8	13.6	15.8	3.2	5.4	4.2	2.2	3.9	27.3	12.4	78.7	34.2	22.1
<i>Gephyromantis grosjeani</i> (Sorata) - females														
ZSM 1552/2012 (FGZC 3693)	PT	41.0	13.8	15.3	2.9	5.4	3.8	2.5	4.7	25.5	13.3	83.2	36.9	25.0
ZSM 1555/2012 (FGZC 3585)	PT	40.8	13.5	15.5	2.7	4.6	3.7	2.4	4.0	25.7	12.2	77.5	33.2	22.4
<i>Gephyromantis solegy</i> (Ambolokopatra) - females														
MRSN A2039	PT	49.3	16.3	17.8	2.8	6.1	5.1	2.7	4.2	29.8	14.8	90.8	39.5	26.0
MRSN A2040	PT	44.6	15.0	16.8	2.6	6.0	4.5	2.6	4.4	28.4	13.2	86.4	39.0	24.7
MRSN A2041	PT	47.0	15.5	16.9	2.5	5.4	4.8	2.3	4.6	30.3	14.9	89.5	39.8	26.9
MRSN A2046	PT	50.1	16.8	19.0	2.6	5.6	5.0	2.7	4.5	33.0	15.3	97.1	43.0	28.5
MRSN A2045	PT	43.3	14.7	17.2	2.8	-	5.3	-	3.7	28.6	13.5	87.4	39.1	25.2
<i>Gephyromantis tandroka</i> (Marojejy) - subadult														
MNHN 1973.93	PT	33.9	11.6	13.0	2.4	4.3	3.4	1.9	3.6	23.8	11.1	72.3	32.3	20.0

Description of holotype ZSM 61/2016, adult male

Specimen in a good state of preservation, a tissue sample taken from the left thigh. SVL 39.4 mm. For other measurements see Table 1. Body somewhat gracile; head longer than wide, not as wide as body (body is somewhat inflated in preservative); snout pointed in dorsal and lateral view; nostrils directed laterally, protruding slightly, much nearer to tip of snout than to eye; canthus rostralis distinct, straight; loreal region concave and weakly oblique; tympanum distinct, oval, its horizontal diameter 56 % of eye diameter; supratympanic fold distinct, weakly curved, from the posterior corner of the eye to above the insertion of the arm; tongue fairly broad, posteriorly bifid; vomerine teeth clearly distinct, arranged in two small aggregations on either side of the midline of the palate at the level of the anterior edge of the eye, posteromedial to choanae; choanae small and rounded and laterally displaced. Dark, translucent dermal fold below each jaw starting at the level of the anterior edge of the eye. Arms slender, subarticular tubercles single, highly distinct; outer metacarpal tubercle small and oval and inner metacarpal tubercle small; fingers without webbing; relative length of fingers $1 < 2 < 4 < 3$, second finger distinctly shorter than fourth; finger discs distinctly enlarged, round, nuptial pads absent. Hindlimbs slender; lateral metatarsalia slightly separated distally with webbing; subarticular tubercles highly distinct; inner metatarsal tubercle distinct, anteriorly oriented, outer metatarsal tubercle absent; webbing formula of foot according to the scheme of Blommers-Schlösser (1979) 1(1), 2i(1.5), 2e(1), 3i(2), 3e(1.25), 4i(2.5), 4e(2.25), 5(1); relative toe length $1 < 2 < 3 < 5 < 4$, third toe much shorter than fifth; toe discs distinctly enlarged. Skin dorsally granular, with two pairs of distinct dorsolateral ridges, corresponding to the inner and outer ridges of Vences & Glaw (2001), one pair running from the posterior of the eye to the suprascapular region, and the other pair along the dorsolateral ridge of the body; between these ridges over the dorsum posterior to the head is a reticulated pattern of fine ridges; a small pair of interocular spines is present, and each eye is adorned with two small supraocular spines; a diminutive dermal flap is present on the heel; ventral skin smooth on chin and forelimbs, but highly granular on the abdomen and ventral thighs. Femoral glands indistinguishable in the fixed specimen, but visible from images of the specimen in life (fig. 4): type 2 sensu Glaw *et al.* (2000), 4.6 mm long, 2.2 mm wide (measured in internal view), consisting of 16 granules on the right thigh and 15 on the left thigh.

In life (fig. 4) the dorsum was a light mocha, with rust markings on the upper flanks, in a W-shaped marking on the mid-dorsum, on the lateral head and posterior surface of the eyes, and in an oblong patch over the hips. The light colouration of the dorsal surface of the head continued as a medial rostral stripe visible in ventral and anterior view. The inner and outer dorsolateral folds were not remarkably coloured. A mottled dark line was present between the eyes, with black around the interocular tubercles. The larger of the two supraocular spines was also surrounded in black. A thin black stripe was present from the nostril to the eye along the canthus rostralis, and the lower edge of the supratympanic fold and the tympanum itself were dark brown. A further dark brown marking was present on the upper lip below the eye. The limbs exhibited extensive crossbanding: the forelimb had one faint crossband on the upper arm, and three crossbands on the lower arm, each of the rust colour of the dorsum, with black on the inner surface; the fingers lacked crossbands but had black flecks, without any distinctive colouration of the distal discs. The hindlimbs had five crossbands of

dark brown tinged with rust and black on the thigh, six on the shank, three on the tibiotarsus, and two on the foot. The chin was mottled translucent and light yellow ventrally, only slightly darker on the vocal sacs, becoming translucent over the pectoral region, and then cream over the abdomen, in turn fading to egg-yolk yellow near the hip and over the surface of the thighs. The thighs were distally flecked with brown, the lower legs mottled yellow, beige and brown. The foot was mocha brown ventrally with tinges of rust on the subarticular tubercles. The hand was also brown ventrally, but its tubercles were cream in colour.

After roughly two years in preservative, the colour pattern is unchanged, but the colour itself has faded (fig. 5). Dorsally, areas that were light mocha have become grey to silver, with light grey dorsolateral ridges, while areas that were rust in life are now mauve. Both the chin and the pectoral region have lost their translucence and the colouration on the chin has become darker, and the W-shaped marking on the mid-dorsum has faded but is still visible. All traces of yellow in the ventral colouration has been replaced by a dirty cream.

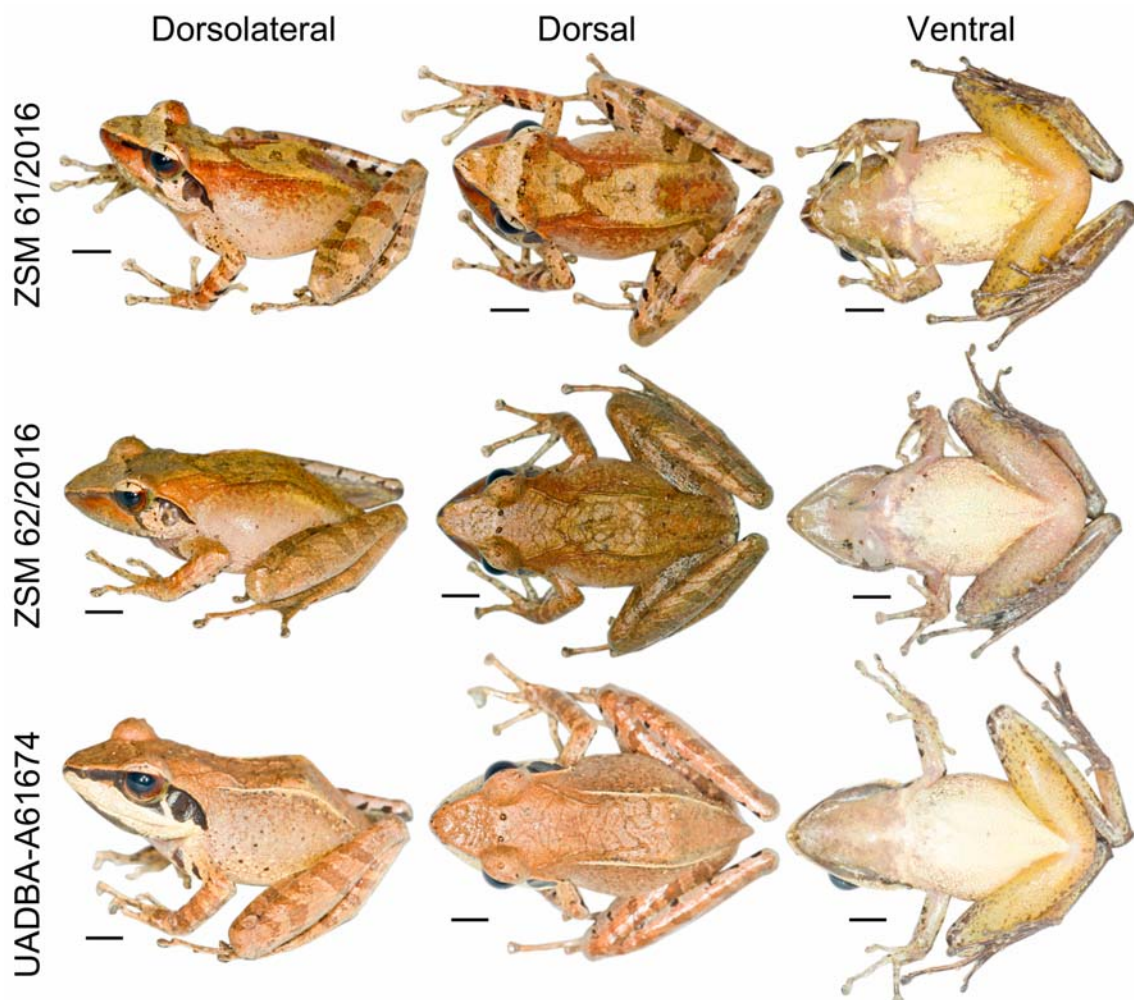


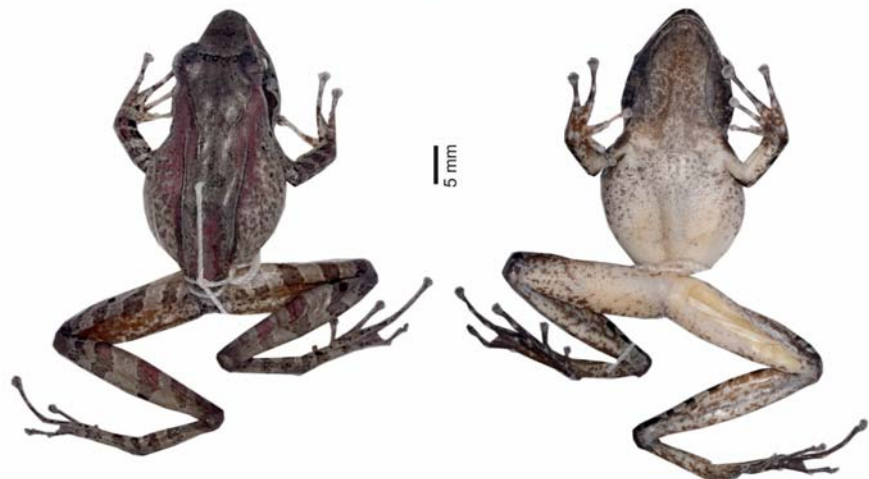
Figure 4. Type series of *Gephyromantis saturnini* sp. nov. in dorsolateral, dorsal and ventral view. Scale bars indicate 5 mm. Femoral gland granules (FGG): ZSM 61/2016, 15 left/16 right, ZSM 62/2016, 10/9, UADBA-A 61674, 13/10.

Morphological and chromatic variation

In morphology, the paratypes strongly resemble the holotype; for variation in measurements, see Table 1. Webbing formula varies in 3e (1 in the paratypes vs. 1.25 in the holotype) and 5i (0.75–1 in the paratypes). The femoral glands are equally poorly distinguishable in all specimens, but can be identified with strong magnification (fig 6); the number of granules varies from 9–16, but they are always indistinct.

Although they are consistently brown in overall colour, the colour patterns of the type specimens are highly varied (fig. 4), and only a few characteristics are consistent: the dark canthal stripe is consistently present in the type series, though much thicker in UADBA-A 61674 than the other paratypes. Crossbands are always present on the limbs, but the number is variable. The ventral abdomen is consistently cream in colour, and the mottling of the thighs distally is also fairly consistent among the specimens. The rostral stripe is present in all of the type series.

Gephyromantis (Duboimantis) saturnini sp. nov.
ZSM 61/2016



Gephyromantis (Duboimantis) grosjeani sp. nov.
ZSM 1554/2012

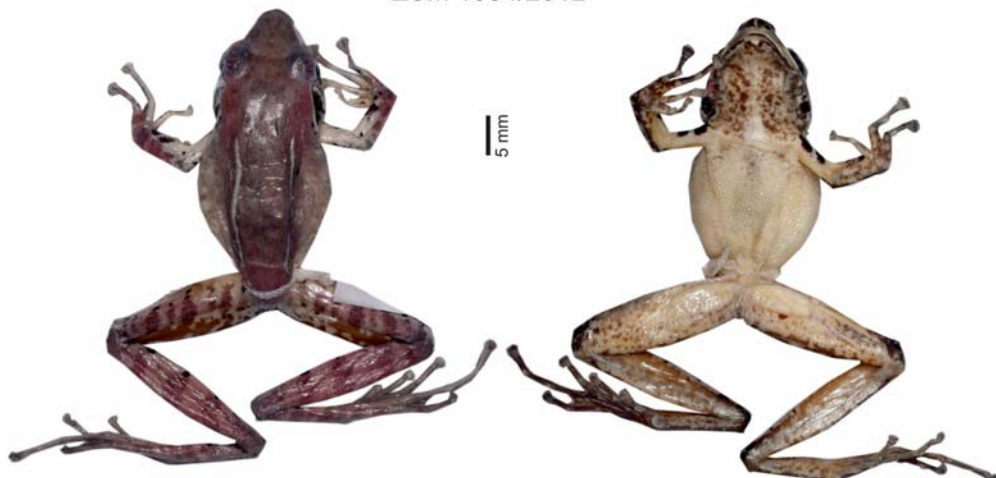


Figure 5. Holotypes of *Gephyromantis (Duboimantis) saturnini* sp. nov. (ZSM 61/2016) and *G. (D.) grosjeani* sp. nov. (ZSM 1554/2012) in dorsal (left) and ventral (right) view.

Bioacoustics

The calls of two recorded individuals consisted of pulsatile notes, which were arranged in note groups of 1–3 notes, and these note groups emitted in a finite series of 7–8 note groups. We here define each note group as a call. In this definition, calls are thus arranged in call series consisting of 7–8 calls, and each call consists of 1–3 notes. In the holotype ZSM 61/2016 (recorded on 31 December 2015 at 18 h 30, air temperature unknown), two call series contained calls with 1–2 notes, and lasted 22.7 s (7 calls) and 27.3 s (8 calls). Note duration was 56–78 ms (63 ± 6 ms; $N = 10$), and each note consisted of 12–18 very poorly distinguishable pulses (16 ± 2 ; $N = 10$), without silent intervals between them. Inter-call interval duration was 2054–8436 ms (3912 ± 2246 ms; $N = 10$) and decreased toward the end of the call series, i.e., calls were repeated faster and contained more notes towards the end of a call series. Within two-note calls, the interval duration between notes was 150–181 ms (165 ± 12 ms; $N = 8$). Dominant frequency was between 3057–3227 Hz (3100 ± 57 Hz; $N = 10$), approximate prevalent bandwidth is between 1000–4500 Hz.

The calls of paratype ZSM 62/2016 (recorded on 6 January 2016 at 23 h 45 at an air temperature of 15.9°C) were very similar; one call series of 7 calls was available for analysis. Of these, the first two calls had 1 note, the third and fourth call had two notes and the last three calls had three notes each. As in the holotype, inter-call interval duration decreased toward the end of the call series. Temporal and spectral measurements were as follows: Note duration 87–100 ms (91 ± 5 ms; $N = 12$), inter-call interval duration 2158–5944 ms (3500 ± 1385 ms; $N = 6$), inter-note interval within one call 199–237 ms (209 ± 13 ms; $N = 8$), dominant frequency 2497–2670 Hz (2583 ± 45 Hz; $N = 10$), approximate prevalent bandwidth 1000–5000 Hz.

Natural history and conservation status

Very little is known of the ecology of this species. Male specimens were collected at night, sitting on leaves in primary rainforest at 1.1–3 m above the ground. ZSM 61/2016 was collected 20 m from a small stream on a steep slope. The confirmed elevational range of the collected specimens is 1450–1481 m a.s.l. and we did not encounter them below 1400 m a.s.l. Our survey work above 1500 m a.s.l. was insufficient to be conclusive as to the upper ranges of the distribution of this species, but the Ampotsidy mountains have a maximum elevation of ca. 1860 m a.s.l.

At present this species is known from just three collected specimens, though several others were heard in the vicinity of the collected individuals at low density (MDS pers. obs.). It is known from one area of fragmented forests, which are in an active state of decline due to ongoing slash-and-burn agriculture, cattle grazing and logging. However, like other species collected in Ampotsidy (e.g. *Gephyromantis [Asperomantis] angano*, Scherz *et al.* 2017b; *Calumma gehringi*, Prötzl *et al.* 2017; *Uroplatus fotsivava*, Ratsosavina *et al.* 2017), we suspect that the species will occur more broadly within the poorly surveyed District de Bealanana. As such, any evaluation of its conservation status based on current knowledge is liable to dramatically overestimate its threat status: at present it qualifies as Critically Endangered under IUCN (2012) criterion B1ab(iii) due to its range of below 100 km² (B1) from one threat-defined location (a) undergoing active decline in extent and quality of its habitat

(b[iii]). To avoid being inflationary, we recommend that the species be considered Data Deficient until further survey work has been conducted in the District de Bealanana.

Etymology

We dedicate this species of *Duboimantis* to Saturnin Pojarski, a pseudonym of Alain Dubois during his time as a late-night radio presenter on Radio Carbone 14, a ‘pirate’ station that was part of the free radio movement in France in the 1980s. Saturnin also makes an appearance in a children’s book (Dubois & Ohler 2010) as a grandfather transmitting the enthusiasm for and knowledge of amphibian biology to his grandson, Augustin.



Figure 6. Femoral glands of male specimens of *Gephyromantis tandroka* ZSM 321/2005 (FGZC 2812), femoral gland granules (FGG) 24 left/21 right (above), *G. saturnini* sp. nov. Holotype ZSM 61/2016 (MSZC 123), FGG 16/15 (middle) and *G. grosjeani* sp. nov. (unidentified UADBA specimen), FGG, 41/34 (below). Note the much more distinct glands in the latter species.

Gephyromantis (Duboimantis) grosjeani sp. nov.

(fig. 1–3, 5–9, Table 1)

LSID: urn:lsid:zoobank.org:act:2D5B8810-A9CD-4363-A960-3F8AA6C61D41

Gephyromantis (Duboimantis) sp. Ca32 – (Scherz *et al.* 2017a)*Specimens allocated to new species**Holotype*

ZSM 1554/2012 (FGZC 3584), an adult male collected at high elevation on the Sorata massif (13.67–13.69°S, 49.43–49.44°E, ca. 1400–1500 m a.s.l.), District de Vohemar, Région Sava, northern Madagascar, at night on 26 November 2012 by F. Glaw, O. Hawlitschek, T. Rajoafiarison, A. Rakotoarison, F. M. Ratsoavina and A. Razafimanantsoa.

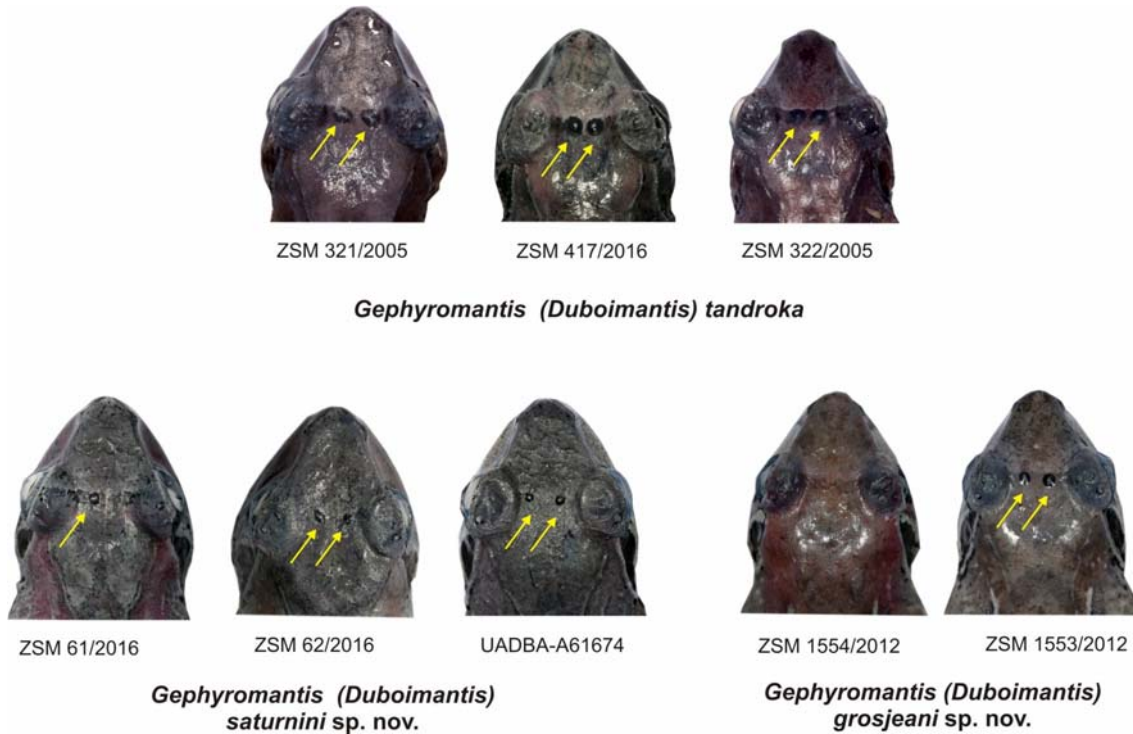


Figure 7. Heads of *Gephyromantis (Duboimantis) saturnini* sp. nov. and *G. (D.) grosjeani* sp. nov. in dorsal view compared to *G. (D.) tandroka*. Arrows indicate the interocular tubercles, which appear less expressed especially in *G. (D.) saturnini* sp. nov. than in *G. (D.) tandroka*.

Paratypes

ZSM 1555/2012 (FGZC 3585) and UADBA uncatalogued (FGZC 3583), two adult females and UADBA uncatalogued (FGZC 3599), an adult male with the same collection data as the holotype. ZSM 1553/2012 (FGZC 3749), a male, ZSM 1552/2012 (FGZC 3693), a female and UADBA uncatalogued (FGZC 3690), an unsexed individual, collected in bamboo forest above the campsite in Sorata (ca. 13.6752°S, ca. 49.4410°E, ca. 1485 m a.s.l.), District de Vohemar, Région Sava, northern Madagascar, at night between 28–30 November 2012 by F. Glaw, O. Hawlitschek, T. Rajoafiarison, A. Rakotoarison, F. M. Ratsoavina and A. Razafimanantsoa. UADBA uncatalogued (FGZC 3598), an adult male collected above the campsite in Sorata (13.6829°S, 49.4419°E, 1312 m a.s.l.), District de Vohemar, Région Sava, northern Madagascar, at night on 26 November 2012 by F. Glaw, O. Hawlitschek, T. Rajoafiarison, A. Rakotoarison, F. M. Ratsoavina and A. Razafimanantsoa.

Diagnosis

A *Gephyromantis* species assigned to the subgenus *Duboimantis* on the basis of its fairly smooth skin, interocular tubercles generally present, moderately large body size and presence of inner and outer dorsolateral folds. *Gephyromantis grosjeani* is characterised by the following unique suite of characters: (1) large body size (36.1–38.4 mm in adult males, 40.8–41.0 mm in adult females), (2) paired subgular vocal sacs, (3) HIL/SVL 1.84–2.03, (4) TD/ED 0.53–0.59, (5) presence of inner and outer dorsolateral folds, with the inner folds being generally weak, (6) reticulated low ridges on the dorsum, (7) large, distinct femoral glands in males consisting of 25–41 granules. It is furthermore characterised by advertisement calls consisting of pulsatile single-note calls arranged in undefined series.

Comparisons

Within the genus *Gephyromantis*, *G. grosjeani* may be distinguished from all members of the subgenus *Gephyromantis* on the basis of larger body size (SVL 36.1–41.0 mm vs. 20–33 mm); from all members of the subgenus *Asperomantis* by less rough dorsal skin, less distinct inner dorsolateral ridges, less pronounced supraocular spines and absence of a pale spot in the middle of the tympanum; from all members of the subgenus *Phylacomantis* on the basis of the presence of distinct dorsolateral ridges (vs. absent or discontinuous), more slender body shape and absence of outer metatarsal tubercle (vs. presence); from all members of the subgenus *Laurentomantis* on the basis of larger body size (SVL 36.1–41.0 mm vs. 20–34 mm), smooth skin (vs. highly granular to rugose); and from all members of the subgenus *Vatomantis* on the basis of much larger body size (SVL 36.1–41.0 mm vs. 23–31 mm), lack of greenish skin colouration (vs. presence) and less slender limbs. Within the subgenus *Duboimantis*, it may be distinguished from all species except *G. (D.) salegy*, *G. (D.) redimitus*, *G. (D.) plicifer* and *G. (D.) moseri* by larger and/or more distinct femoral glands in males. Additionally, it may be distinguished from *G. (D.) cornutus* and *G. (D.) redimitus* by the possession of paired subgular vocal sacs (vs. single); from *G. (D.) luteus*, *G. (D.) sculpturatus* and *G. (D.) plicifer* by less webbed toes, lack of concave black suprascapular markings (vs. usually present) and presence of only diminutive heel

spines (vs. distinct heel spines); from *G. (D.) moseri* by the much less rugose dorsum and smaller supraocular tubercles; from *G. (D.) salegy* and *G. (D.) redimitus* by much smaller body size (SVL 36.1–41.0 mm vs. 46–53 mm); from *G. (D.) saturnini* by smaller adult male body size (36.1–38.4 mm vs. 39.4–42.8 mm) and less distinct inner dorsolateral folds; from *G. (D.) schilfii*, *G. (D.) tschenki* and *G. (D.) tohatra* by larger body size (SVL 36.1–41.0 mm vs. 27–36 mm); from *G. (D.) zavona*, *G. (D.) leucomaculatus* and *G. (D.) granulatus* by the general presence of interocular tubercles (vs. absence). From the highly similar *G. (D.) tandroka*, it may be distinguished most reliably by the distinct femoral glands in males (fig. 6) and provisionally (due to low sample sizes) males may differ by slightly longer relative foot length (FOL/SVL 0.58–0.59 vs. 0.51–0.57) and females may differ by slightly longer relative forelimb length (FORL/SVL 0.62–0.63 vs. 0.64–0.69). The interocular spines of this species appear to be smaller and less distinct than those of *G. tandroka*, even when they are present (fig. 7).

Genetically, the species is distinguished from all other species of *Gephyromantis* by uncorrected p-distances of at least 5.1 % in the analysed 16S rRNA gene fragment.

The calls of *G. (D.) grosjeani* strongly resemble those of *G. (D.) tandroka*, but differ slightly in call duration (119–128 ms vs. 77–94 ms) and inter-call interval duration (1977–2720 ms vs. 1524–2034 ms), but the assessment of the diagnostic value of these differences requires additional data.

Description of holotype ZSM 1554/2012, adult male

Specimen in a good state of preservation, a tissue sample taken from the left thigh. SVL 38.4 mm. For other measurements see Table 1. Body somewhat gracile; head longer than wide, not as wide as body (body is somewhat inflated in preservative); snout pointed in dorsal view, rounded in lateral view; nostrils directed laterally, protruding slightly, much nearer to tip of snout than to eye; canthus rostralis distinct, straight; loreal region concave and weakly oblique; tympanum indistinct, oval, its horizontal diameter 58 % of eye diameter; supratympanic fold distinct, curved, from the posterior corner of the eye to above the insertion of the arm; tongue fairly narrow, posteriorly bifid; vomerine teeth clearly distinct, arranged in two small aggregations on either side of the midline of the palate at the level of the anterior edge of the eye, posteromedial to choanae; choanae small and rounded and laterally displaced. Pigmented translucent dermal fold below each jaw starting at the level of the anterior edge of the eye. Arms quite stocky, subarticular tubercles single, highly distinct; outer metacarpal tubercle small and oval and inner metacarpal tubercle relatively well developed; fingers without webbing; relative length of fingers $1 < 2 < 4 < 3$, second finger distinctly shorter than fourth; finger discs distinctly enlarged, round, nuptial pads absent. Hindlimbs slender; lateral metatarsalia separated distally with webbing; subarticular tubercles highly distinct; inner metatarsal tubercle distinct, anteriorly oriented, outer metatarsal tubercle absent; webbing formula of foot according to the scheme of Blommers-Schlosser (1979) 1(1), 2i(1.5), 2e(1), 3i(2), 3e(1.5), 4i(2.75), 4e(2.5), 5(1); relative toe length $1 < 2 < 3 = 5 < 4$, third toe equal in length to fifth; toe discs distinctly enlarged. Skin dorsally smooth, with one pair of distinct dorsolateral ridges running from the suprascapular region to the hip, and weak suggestion of a pair of inner dorsolateral ridges as termed by Vences & Glaw (2001) only over the suprascapular region; interocular spines absent; two diminutive supraocular spines

present; a diminutive dermal flap is present on the heel; skin smooth on chin, forelimbs and hindlimbs ventrally, but highly granular on the abdomen and lower flanks. Femoral glands distinct, large, type 2 sensu Glaw *et al.* (2000), 8.1 mm long, 3.6 mm wide (measured in external view), consisting of 37 granules on the right thigh and 31 on the left thigh (counted in internal view).

The colouration in life is unknown. After six years in preservative (fig. 5), the dorsum is grey-beige fading through salmon laterally onto grey flanks; the outer dorsolateral folds are cream. The lateral head is distinctly different in colour from the dorsum, with burnt umber patches over the tympanum, under the eye, along the canthus rostralis and around the nostril, separated by cream patches. The forelimb is cream in base-colour with thin blackish markings along the posterior edge of the upper forelimb, with salmon-grey crossbands with blackish internal markings from the hand to the elbow. The dorsal surface of the hand is externally the same salmon-grey colour, and internally cream. The dorsal hindlimb is light salmon in base colour with numerous mauve crossbands dorsally that darken to nearly black on the leading and trailing edges; there are roughly seven crossbands on the thigh, four or five on the shank and five becoming more indistinct on the foot; the toes lack crossbands. The hidden surfaces of the posterior thigh are a coffee brown towards the knee, becoming dappled with cream toward the cloaca, with a poorly-defined dark brown trapezoid below the cloaca. The ventral base colour is cream, immaculate over the abdomen and ventral surfaces of the forelimbs, but dappled with dark brown on the chin. The ventral surfaces of the hands and feet are a muddy grey. The thighs are cream with irregular small light brown spots all over except on the femoral glands ventrally, which are cream.

Morphological and chromatic variation

In morphology, the paratypes strongly resemble the holotype; for variation in measurements, see Table 1. Females are apparently larger than males (40.8–41.0 mm vs. 36.1–38.4 mm in males), but no other sexual dimorphisms are visible except the absence of the distinct femoral glands in females. Males have clearly bilobed subgular vocal sacs (fig. 8) The distinctiveness of the inner dorsolateral folds is variable, being distinct in ZSM 1552/2012, but weak or almost absent in the other specimens examined. Interocular tubercle presence is variable: present in ZSM 1552/2012 and 1553/2012, but absent in the holotype and ZSM 1555/2012 (fig. 7). The strength of the supraocular tubercles is slightly less variable, being small in all specimens, but exceptionally so in ZSM 1555/2012. Femoral glands vary in the number of granules (25–41) and the shape of the gland (fig. 6 & 9); the glands of ZSM 1553/2012 measure 5.4 mm long by 2.7 mm wide.

The dorsal colouration of this species is highly variable (fig. 9), while the ventral colouration is largely consistent, even between males and females except that the females lack the different colouration of the vocal sacs present in males. Dorsal base-colour ranges from the beige to salmon of the holotype to dark brown in preservative. The outer dorsolateral folds can be distinctly cream as in the holotype, or indistinct in colour as in ZSM 1552/2012. ZSM 1555/2012 differs dramatically in body colouration in having a strong colour border on the whole body between the dark brown dorsum and the light cream flanks. Laterally, the head can be solid black above with a white lip (e.g. ZSM 1553/2012) or wholly cream with only dark brown on the tympanum (ZSM

1555/2012). The number of crossbands on the limbs is wholly variable. When present, interocular tubercles are surrounded with blackish circles.

Bioacoustics

The advertisement call, recorded on 29 November 2012 at 20 h 30 at an elevation of ca. 1400 m a.s.l. in moderately disturbed primary montane forest (air temperature not recorded), consists of a single pulsatile note, with a call (= note) duration of 119–128 ms (121 ± 4 ms; $N = 10$ calls of one male), repeated for long periods with regular inter-call intervals of a duration of 1977–2720 ms (2363 ± 226 ms; $N = 10$). Each call (or note) consists of approximately 23–25 indistinct pulses (23.9 ± 0.7 ; $N = 10$), without clear silent interval between them. Pulse intensity decreases towards the end of the call, and pulses appear longer and more densely packed in the beginning of the call, becoming more distinct and more widely spaced toward the end. Dominant frequency is between 2713–3186 Hz (2936 ± 120 Hz; $N = 10$). Approximate prevalent bandwidth is between 1200–5800 Hz.



Figure 8. A calling male specimen of *Gephyromantis (Duboisianus) grosjeani* sp. nov. (specimen unidentified). Note the clearly bilobed subgular vocal sacs.



Figure 9. Photos in life of four specimens of *Gephyromantis (Duboimantis) grosjeani* sp. nov. from Sorata. (a-f) unidentified males (UADBA-A specimens) with femoral gland granule (FGG) numbers of (b) 41 left/34 right, (d) 31/34 and (f) 25/27; (g-h) female ZSM 1552/2012 (FGZC 3693).

Natural history and conservation status

Numerous male individuals were heard calling at night at the end of November, sitting on branches and leaves, especially of ferns, in disturbed primary rainforest and bamboo forest, ca. 1–3 m above the ground at an elevation of ca. 1300–1500 m a.s.l., but we suspect that the species will be distributed more widely in the poorly surveyed Sorata and Andavory regions and perhaps other high-altitude rainforests in northern Madagascar. Similarly to *G. saturnini* sp. nov. described above, an evaluation of the conservation status of *G. grosjeani* sp. nov. based on current knowledge is liable to dramatically overestimate its threat status: at present it qualifies as Critically Endangered under IUCN (2012) criterion B1ab(iii) due to its range of below 100 km² (B1) from essentially one threat-defined location (a) undergoing relative dramatic decline in extent and quality of its habitats (b[iii]). To avoid being inflationary, we recommend that the species be considered Data Deficient until further survey work has been conducted in surrounding rainforest areas.

Etymology

We dedicate this species to Stéphane Grosjean, who completed his PhD studies under the mentorship of Alain Dubois, in recognition of his valuable contributions to the knowledge of Madagascan frog larvae (e.g. Grosjean *et al.* 2007, 2011a, b).

DISCUSSION

The mitochondrial data on *Gephyromantis (Duboisianus) saturnini* suggests close affinities to *G. (D.) schilfi*, both in terms of uncorrected p-distance (5.1 %) and phylogenetic relationships (fig. 1). These two species however bear little resemblance to one another; *G. (D.) saturnini* is much more similar in appearance to *G. (D.) tandroka* (compare fig. 4 with fig. 10) and *G. (D.) grosjeani*, in terms of size, overall morphology and bioacoustics. Although it is at present poorly resolved, the position of *G. (D.) tohatra* outside of this clade is surprising, because that species is morphologically more similar to *G. (D.) schilfi* than is *G. (D.) saturnini*. These relationships suggest discordance between overall phenotype and mitochondrial sequence data, and therefore require further testing with sequences of nuclear genes. The observed discordance could be the result of one or more recent or ancient hybridisation events, which could be revealed by mitochondrial-nuclear gene tree discordance.

If our phylogeny is correct in representing relationships, the biogeography of this complex of frogs is interesting (fig. 11). The type localities of the two new species are separated by a mere ca. 112 km in a straight line, and the elevations of 1312–1500 m a.s.l. for *G. (D.) grosjeani* and 1450–1481 m a.s.l. for *G. (D.) saturnini* overlap, yet these two species are each more closely related to taxa in Marojejy (*G. [D.] grosjeani* to *G. [D.] tandroka*) and Marojejy plus Sorata (*G. (D.) saturnini* to *G. [D.] schilfi*), respectively. Marojejy is almost equally distant from both localities (90–120 km; see fig. 11). This suggests greater connectivity between Marojejy and Sorata, and Marojejy and the Bealanana area, than between Sorata and the Bealanana area. In other amphibian taxa we have found a similar level of isolation between species from Sorata and the Bealanana side of the Tsaratanana massif (Scherz *et al.* 2015; 2017c), and at

present very few species are known to occur both in the Bealanana area and Sorata. Those that do occur at these two sites can also be found in Marojejy (e.g. *G. [Asperomantis] tahotra* Glaw, Köhler & Vences, 2011). Indeed, Sorata shares several species with Marojejy (Cramer *et al.* 2008; Scherz *et al.* 2017c, 2018; Prötzl *et al.* 2018). The emerging pattern suggests that the Tsaratanana massif, probably due to its great elevation, is acting as a barrier to gene flow between areas to its North-East and South-West, at least to species that occur at sufficiently low elevations to not have ring-shaped ranges including both sides of the massif. Gene flow along either side of the massif is less inhibited, resulting in the connectivity we see between Sorata and Marojejy and, to a lesser degree, the Bealanana area and Marojejy.

With the description of these two new species, we bring the subgenus *Duboimantis* to 16 described species. The centre of diversity of this subgenus is unquestionably northeastern Madagascar (Kaffenberger *et al.* 2012), although some members are more widespread throughout the east of the island (Glaw & Vences 2007). The new species described here conform to this pattern. Although all members of the *G. (D.) tandroka* complex are relatively high-elevation species, they are not as ecologically conserved as this might suggest. Forests above 1300 m a.s.l. in Marojejy (type localities of *G. [D.] schilfi*, *G. [D.] tohatra* and *G. [D.] tandroka*) are montane high-elevation forest with a low canopy and dense epiphyte coverage. The type locality of *G. (D.) grosjeani* is similar in these regards, but it occurs also in bamboo forest, which was not seen at this elevation in Marojejy. The forests of Ampotsidy from 1400–1600 m a.s.l. (type locality of *G. [D.] saturnini*) are rather humid forests, with little understory, a high canopy and relatively few epiphytes. This habitat is somewhat different from those of the other members of this complex, and its ecology may differ accordingly. More data are needed on its reproductive habits before we can draw conclusions to this effect however.

Finally, we are pleased to note that the type localities of both of the new species, as well as most members of the *G. (D.) tandroka* complex, are within the network of protected areas that have recently been expanding in northern Madagascar (Gardner *et al.* 2018, fig. 11). Although these protected areas are in relatively early states of establishment and as such the habitat within them is still liable to decline through anthropogenic activity, the future outlook is a positive one.



Figure 10. Photos in life of four specimens of *Gephyromantis (Duboimantis) tandroka* from Marojejy. (a,b) an uncollected male specimen photographed in 2016, femoral gland granules 10 left/8 right, (c,d) ZSM 321/2005 (FGZC 2812), FGG 23/21, (e,f) ZSM 937/2000, (g–i) ZSM 417/2016 (ZCMV 15165), FGG 18/12.

Results

SCHERZ *et al.*

155

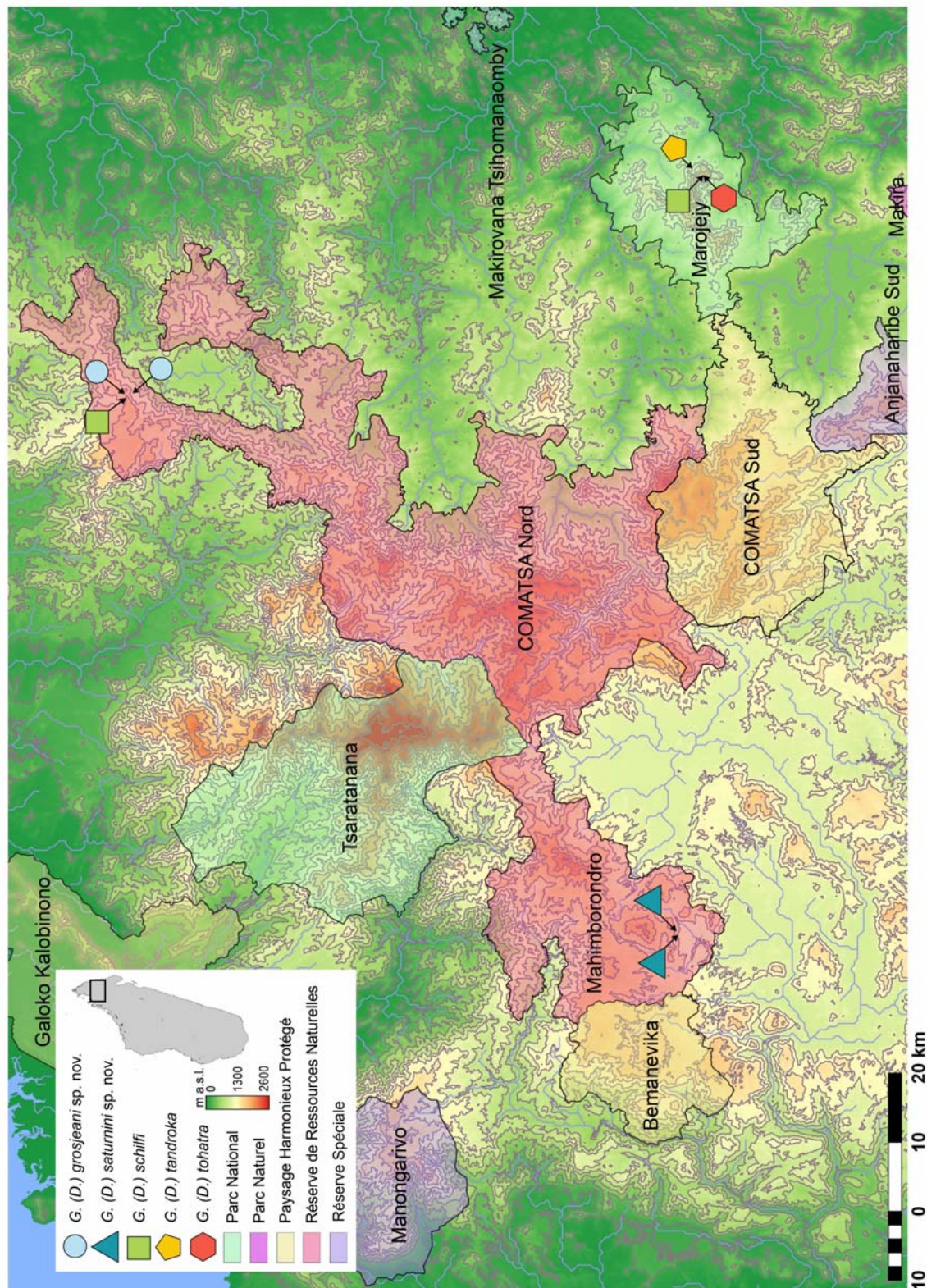


Figure 11. Map of current distribution records of the *Gephyromantis (Duboimantis) tandroka* species complex, with reference to the network of protected areas in northern Madagascar. Isolines indicate 200 m.

ACKNOWLEDGEMENTS

We thank J. Borrell, L. Ball, T. Starnes, D. Parker, D. H. Nomenjanahary, T. Rajoafiarison, A. Razafimanantsoa and E. Razafimandimby, and our cooks and guides for their assistance in the field. We thank MICET for facilitation of our fieldwork, the Madagascar Ministry for Environment, Water and Forests for issuing research, collection and export permits, and B. Fisher and the team of the Madagascar Biodiversity Center for their support. Fieldwork in 2012 was supported financially by the Mohamed bin Zayed Species Conservation Fund, and in 2016 was supported financially by the Royal Geographical Society, the Zoological Society of London, Cadogan Tate, The Scientific Exploration Society, crowdfunding via Indiegogo, the Freunde der Zoologischen Staatssammlung München and the Deutsche Forschungsgemeinschaft.

LITERATURE CITED

- Ahl, E. (1929) Beschreibung neuer Frösche aus Madagascar. *Mitteilungen aus dem zoologischen Museum in Berlin*, **14**: 469–484.
- Andreone, F., Aprea, G., Vences, M. & Odierna, G. (2003) A new frog of the genus *Mantidactylus* from the rainforests of north-eastern Madagascar, and its karyological affinities. *Amphibia-Reptilia*, **24**: 285–303.
- Blommers-Schöller, R. M. A. (1979) Biosystematics of the Malagasy frogs. I. Mantellinae (Ranidae). *Beaufortia*, **352**: 1–77.
- Boettger, O. (1881) Diagnoses reptilium et batrachiorum novorum ab ill. Antonio Stumpff in insula Nossi-Bé Madagascariensi lectorum. *Zoologischer Anzeiger*, **4**: 358–362.
- Boulenger, G. A. (1882) *Catalogue of the Batrachia Salientia s. Ecaudata in the Collection of the British Museum*. Second Edition. London (Taylor and Francis): i–xvi, 1–503, 30 pl.
- Boulenger, G. A. (1889) Descriptions of new reptiles and batrachians from Madagascar. *Annals and Magazine of natural History, Ser. 6*, **4**: 244–248.
- Cramer, A. F., Rabibisoa, N. H. C. & Raxworthy, C. J. (2008) Descriptions of two new *Spinomantis* frogs from Madagascar (Amphibia: Mantellidae), and new morphological data for *S. brunae* and *S. massorum*. *American Museum Novitates*, **3618**: 1–22. <10.1206/594.1>.
- Darriba, D., Taboada, G. L., Doallo, R. & Posada, D. (2012) jModelTest 2: more models, new heuristics and parallel computing. *Nature Methods*, **9**: 772.
- Dubois, A. (1980) Un nom de remplacement pour un genre de ranidés de Madagascar (Amphibiens, Anoures). *Bulletin du Muséum national d'Histoire naturelle, Paris, Section A, Zoologie, Biologie et Ecologie animales*, **2**: 349–351.
- Dubois, A. & Ohler, A. (2010) *La vie des grenouilles*. Paris (Editions Le Pommier): 1–61.
- Gardner, C. J., Nicoll, M. E., Birkinshaw, C., Harris, A., Lewis, R. E., Rakotomalala, D. & Ratsifandrihamanana, A. N. (2018) The rapid expansion of Madagascar's protected area system. *Biological Conservation*, **220**: 29–36. <10.1016/j.biocon.2018.02.011>.
- Glaw, F., Köhler, J. & Vences, M. (2011) New species of *Gephyromantis* from Marojejy National Park, northeast Madagascar. *Journal of Herpetology*, **45**: 155–160. <10.1670/10-058.1>.
- Glaw, F. & Vences, M. (1992) *A fieldguide to the amphibians and reptiles of Madagascar*. First Edition, Cologne (Vences & Glaw Verlags GbR): 1–335.
- Glaw, F. & Vences, M. (1994) *A fieldguide to the amphibians and reptiles of Madagascar*. Second Edition, Cologne (Vences & Glaw Verlags GbR): 1–478.
- Glaw, F. & Vences, M. (2000) A new species of *Mantidactylus* from northeastern Madagascar (Amphibia, Anura, Ranidae) with resurrection of *Mantidactylus blanchi* (Guibé, 1974). *Spixiana*, **23**: 71–83.
- Glaw, F. & Vences, M. (2001) Two new sibling species of *Mantidactylus cornutus* from Madagascar. *Spixiana*, **24**: 177–190.
- Glaw, F. & Vences, M. (2002) A new species of *Mantidactylus* (Anura: Mantellidae) from Andasibe in eastern Madagascar. *Journal of Herpetology*, **36**: 372–378.

- Glaw, F. & Vences, M. (2006) Phylogeny and genus-level classification of mantellid frogs (Amphibia, Anura). *Organisms Diversity & Evolution*, **6**: 236–253. <10.1016/j.ode.2005.12.001>.
- Glaw, F. & Vences, M. (2007) *A field guide to the amphibians and reptiles of Madagascar*. Third Edition, Cologne (Vences & Glaw Verlags GbR): 1–496.
- Glaw, F., Vences, M. & Gossmann, V. (2000) A new species of *Mantidactylus* (subgenus *Guibemantis*) from Madagascar, with a comparative survey of internal femoral gland structure in the genus (Amphibia: Ranidae: Mantellinae). *Journal of Natural History*, **34**: 1135–1154.
- Grosjean, S., Glos, J., Teschke, M., Glaw, F. & Vences, M. (2007) Comparative larval morphology of Madagascan toadlets of the genus *Scaphiophryne*: phylogenetic and taxonomic inferences. *Zoological Journal of the Linnean Society*, **151**: 555–576.
- Grosjean, S., Randriaina, R.-D., Strauß, A. & Vences, M. (2011a) Sand-eating tadpoles in Madagascar: morphology and ecology of the unique larvae of the treefrog *Boophis picturatus*. *Salamandra*, **47**: 63–76.
- Grosjean, S., Strauß, A., Glos, J., Randriaina, R.-D., Ohler, A. & Vences, M. (2011b) Morphological and ecological uniformity in the funnel-mouthed tadpoles of Malagasy litter frogs, subgenus *Chonomantis*. *Zoological Journal of the Linnean Society*, **162**: 149–183.
- Guibé, J. (1975) Batraciens nouveaux de Madagascar. *Bulletin du Muséum national d'Histoire naturelle*, **3**: 1081–1089.
- Anonymous (IUCN) (2012) *IUCN Red List Categories and Criteria: Version 3.1*. IUCN, 2nd Edition, Gland & Cambridge (IUCN)
- Kaffenberger, N., Wollenberg, K. C., Köhler, J., Glaw, F., Vieites, D. R. & Vences, M. (2012) Molecular phylogeny and biogeography of Malagasy frogs of the genus *Gephyromantis*. *Molecular Phylogenetics and Evolution*, **62**: 555–560. <10.1016/j.ympev.2011.09.023>.
- Köhler, J., Jansen, M., Rodríguez, A., Kok, P. J. R., Toledo, L. F., Emmrich, M., Glaw, F., Haddad, C. F. B., Rödel, M.-O. & Vences, M. (2017) The use of bioacoustics in anuran taxonomy: theory, terminology, methods and recommendations for best practice. *Zootaxa*, **4251**: 1–124. <10.11646/zotaxa.4251.1.1>.
- Kumar, S., Stecher, G. & Tamura, K. (2016) MEGA7: Molecular Evolutionary Genetics Analysis version 7.0 for bigger datasets. *Molecular Biology and Evolution*, **33**: 1870–1874. <10.1093/molbev/msw054>.
- Methuen, P. A. (1920) Descriptions of a new snake from the Transvaal, together with a new diagnosis and key to the genus *Xenocalamus*, and of some Batrachia from Madagascar. *Proceedings of the zoological Society of London*, **1919**: 349–355.
- Methuen, P. A. & Hewitt, J. (1913) On a collection of Batrachia from Madagascar made during the year 1911. *Annals of the Transvaal Museum*, **4**: 49–64.
- Prötz, D., Vences, M., Hawlitschek, O., Scherz, M. D., Ratsoavina, F. M. & Glaw, F. (2018) Endangered beauties: three new species of chameleons in the *Calumma boettgeri* complex (Squamata: Chamaeleonidae). *Zoological Journal of the Linnean Society*, advanced access: zlx112.
- Prötz, D., Vences, M., Scherz, M. D., Vieites, D. R. & Glaw, F. (2017) Splitting and lumping: An integrative taxonomic assessment of Malagasy chameleons in the *Calumma guibei* complex results in the new species *C. gehringi* sp. nov. *Vertebrate Zoology*, **67**: 231–249.
- Rambaut, A. & Drummond, A. J. (2007) Tracer v1.5. Available from: <http://beast.bio.ed.ac.uk/Tracer>.
- Randriaina, R. D., Wollenberg, K. C., Rasolontjatovo Hiobiarilanto, T., Strauß, A., Glos, J. & Vences, M. (2011) Nidicolous tadpoles rather than direct development in Malagasy frogs of the genus *Gephyromantis*. *Journal of natural History*, **45**: 2871–2900. <10.1080/00222933.2011.596952>.
- Raselimanana, A. P., Raxworthy, C. J. & Nussbaum, R. A. (2000) Herpetofaunal species diversity and elevational distribution within the Parc National de Marojejy, Mad[a]gascar. *Fieldiana: Zoology*, (New Series), **97**: 157–174.
- Ratsoavina, F. M., Gehring, P.-S., Scherz, M. D., Vieites, D. R., Glaw, F. & Vences, M. (2017) Two new species of leaf-tailed geckos (*Uroplatus*) from the Tsaratanana mountain massif in northern Madagascar. *Zootaxa*, **4347**: 446–464. <10.11646/zootaxa.4347.3.2>.
- Ronquist, F., Teslenko, M., van der Mark, P., Ayres, D. L., Darling, A., Höhna, S., Larget, B., Liu, L., Suchard, M. A. & Huelsenbeck, J. P. (2012) MRBAYES 3.2: Efficient Bayesian phylogenetic inference and model selection across a large model space. *Systematic Biology*, **61**: 539–542. <10.1093/sysbio/sys029>.
- Scherz, M. D., Hawlitschek, O., Andreone, F., Rakotoarison, A., Vences, M. & Glaw, F. (2017c) A review of the taxonomy and osteology of the *Rhombophryne serratopalpebrosa* species group (Anura:

- Microhylidae) from Madagascar, with comments on the value of volume rendering of micro-CT data to taxonomists. *Zootaxa*, **4273**: 301–340. <10.11646/zootaxa.4273.3.1>.
- Scherz, M. D., Hawlitschek, O., Razafindraibe, J. H., Megson, S., Ratsoavina, F. M., Rakotoarison, A., Bletz, M. C., Glaw, F. & Vences, M. (2018) A distinctive new frog species supports the biogeographic linkage of the montane rainforest massifs of northern Madagascar. *Zoosystematics and Evolution*, **94**: 247–261. <10.3897/zse.94.21037>
- Scherz, M. D., Razafindraibe, J. H., Rakotoarison, A., Bletz, M. C., Glaw, F. & Vences, M. (2017a) Yet another small brown frog from high altitude on the Marojejy Massif, northeastern Madagascar. *Zootaxa*, **4347**: 572–582. <10.11646/zootaxa.4347.3.9>.
- Scherz, M. D., Ruthensteiner, B., Vieites, D. R., Vences, M. & Glaw, F. (2015) Two new microhylid frogs of the genus *Rhombophryne* with supraciliary spines from the Tsaratanana Massif in northern Madagascar. *Herpetologica*, **71**: 310–321. <10.1655/HERPETOLOGICA-D-14-00048>.
- Scherz, M. D., Vences, M., Borrell, J., Ball, L., Nomenjanahary, D. H., Parker, D., Rakotondratsima, M., Razafimandimby, E., Starnes, T., Rabearivony, J. & Glaw, F. (2017b) A new frog species of the subgenus *Asperomantis* (Anura: Mantellidae: *Gephyromantis*) from the Bealanana District of northern Madagascar. *Zoosystematics and Evolution*, **93**: 451–466. <10.3897/zse.93.14906>.
- Vences, M., Andreone, F., Glaw, F. & Randrianirina, J. E. (2003) Molecular and bioacoustic divergence in *Mantidactylus granulatus* and *M. zavona* n.sp. (Anura: Mantellidae): bearings for the biogeography of northern Madagascar. *African Zoology*, **38**: 67–78.
- Vences, M. & Glaw, F. (2001) Systematic review and molecular phylogenetic relationships of the direct developing Malagasy anurans of the *Mantidactylus asper* group (Amphibia, Mantellidae). *Alytes*, **19**: 107–139.
- Vences, M., Glaw, F. & Marquez, R. (2006) *The calls of the frogs of Madagascar. 3 Audio CD's and booklet*. Foneteca Zoológica, Foneteca Zoológica, Madrid, Spain.
- Vences, M., Köhler, J., Pabijan, M., Bletz, M., Gehring, P.-S., Hawlitschek, O., Rakotoarison, A., Ratsoavina, F. M., Andreone, F., Crottini, A. & Glaw, F. (2017) Taxonomy and geographic distribution of Malagasy frogs of the *Gephyromantis asper* clade, with description of a new subgenus and revalidation of *Gephyromantis ceratophrys*. *Salamandra*, **53**: 77–98.
- Vences, M., Kosuch, J., Glaw, F., Böhme, W. & Veith, M. (2003) Molecular phylogeny of hyperoliid treefrogs: biogeographic origin of Malagasy and Seychellean taxa and re-analysis of familial paraphyly. *Journal of zoological Systematics and evolutionary Research*, **41**: 205–215.
- Vieites, D. R., Wollenberg, K. C., Andreone, F., Köhler, J., Glaw, F. & Vences, M. (2009) Vast underestimation of Madagascar's biodiversity evidenced by an integrative amphibian inventory. *Proceedings of the National Academy of Sciences of the USA*, **106**: 8267–8272. <10.1073/pnas.0810821106>.

Submitted: 28 February 2018.

Accepted: 29 April 2018.

Published: 4 June 2018.

Corresponding editor: Annemarie Ohler.

Section 3: Ecomorphological evolution through the lens of systematics

In this section, I present a series of papers pertaining to the Madagascar-endemic subfamily Cophylineae. These include the descriptions of nine new species and two new genera of frogs, as well as two studies with a greater focus on the phylogeny and evolutionary history of the group. Particular emphasis is placed on the evidence for body size and ecological transitions that is becoming obvious from the increasing clarity given to these groups by systematic treatments.

Chapter 6. PAPER: Two new species of terrestrial microhylid frogs (Microhylidae: Cophylineae: *Rhombophryne*) from northeastern Madagascar

In this chapter I present the description of two new species of *Rhombophryne*, moderately small, partially fossorial narrow-mouthed frogs from northeastern Madagascar. *Rhombophryne savaka* is a fairly small species related to *R. mangabensis*, while *R. botabota* is a medium-sized species related to *R. laevipes*. The fully developed clavicles of *R. savaka*, compared to the absence of clavicles in *R. mangabensis*, suggests a more dynamic history of clavicle loss in *Rhombophryne* than hitherto thought. This paper sheds light on the usefulness of osteological data in the field of systematics, using micro-CT scan data to examine skeletal morphology in a non-destructive manner.

Scherz, M.D., Glaw, F., Vences, M., Andreone, F. & Crottini, A. (2016) Two new species of terrestrial microhylid frogs (Microhylidae: Cophylineae: *Rhombophryne*) from northeastern Madagascar. *Salamandra*, 52(2):91–106.

Digital Supplementary Materials on appended CD:

Supplementary Material — PDF-embedded 3D models of skeletal anatomy of *R. botabota* and *R. savaka*



Rhombophryne savaka in life

Two new species of terrestrial microhylid frogs (Microhylidae: Cophylinae: *Rhombophryne*) from northeastern Madagascar

MARK D. SCHERZ¹, FRANK GLAW¹, MIGUEL VENES², FRANCO ANDREONE³ & ANGELICA CROTTINI⁴

¹⁾ Zoologische Staatssammlung München (ZSM-SNSB), Münchhausenstr. 21, 81247 München, Germany

²⁾ Zoologisches Institut, Technische Universität Braunschweig, Mendelssohnstr. 4, 38106 Braunschweig, Germany

³⁾ Museo Regionale di Scienze Naturali, Via G. Giolitti, 36, 10123 Torino, Italy

⁴⁾ CIBIO, Research Centre in Biodiversity and Genetic Resources, InBIO, Universidade do Porto, Campus Agrário de Vairão, Rua Padre Armando Quintas, Nº 7, 4485-661 Vairão, Portugal

Corresponding author: MARK D. SCHERZ, e-mail: mark.scherz@gmail.com

Manuscript received: 6 December 2015

Accepted: 22 February 2016 by JÖRN KÖHLER

Abstract. We describe two new microhylid frog species of the genus *Rhombophryne* from the humid forests of northeastern Madagascar: *Rhombophryne botabota* sp. n. and *R. savaka* sp. n. The former is a medium-sized species, characterised by darkened lateral sides of the head (present in only one other congener, *R. laevipes*) and a unique combination of morphological, osteological, and molecular characters. The latter is a rather small species, characterised by medially undivided vomerine teeth with two large lateral diastemata, and presence of inguinal spots. *Rhombophryne savaka* sp. n. is the first species of the genus known from Makira Natural Park, and is reported also from Marojejy National Park and Ambolokopatrika (Betaolana Forest). Although its distribution range is relatively large compared to those of congeners, its known extent of occurrence is less than 2,000 km². As deforestation and habitat degradation persist as threats despite formal legal protection, we suggest an IUCN Red List status of Vulnerable for this species. *Rhombophryne savaka* sp. n. is possibly endemic to the Marojejy National Park, like several other *Rhombophryne* species, but is unusual in being found at a relatively low altitude. As such, it is likely to be at high risk of habitat loss and decreasing range, and we propose a status of Endangered for it. We discuss the affinities of these new species and the variability of calls in this genus.

Key words. Amphibia, Anura, bioacoustics, Makira Natural Park, Marojejy National Park, Ambolokopatrika, *Rhombophryne mangabensis*, *R. alluaudi*, new species, COMATSA.

Introduction

Madagascar's diamond frogs, genus *Rhombophryne* BOETTGER, 1880 (Microhylidae: Cophylinae), consist of 14 currently valid nominal species (AmphibiaWeb 2016, SCHERZ et al. 2015a). They were recently recognized as having a high proportion of undescribed diversity, with more candidate species than named species (WOLLENBERG et al. 2008, VIEITES et al. 2009, PERL et al. 2014). We have worked on reducing this taxonomic gap, both to improve our understanding of this genus and to improve the conservation prospects of its species. Seven new species of *Rhombophryne* have been described since the year 2000, but several new ones are still awaiting formal description.

We here describe two new species from northeastern Madagascar. The phylogenetic position of one of these has already been resolved in a previous study based on

a multigene dataset of DNA sequences (SCHERZ et al. in press); we here provide an assessment of the genetic variation of these two new species based on the mitochondrial 16S rRNA gene fragment, which is traditionally used for the taxonomic identity assessment of Malagasy amphibians. X-ray Micro-Computed Tomography (micro-CT) was used to aid in identifying differences between the new species and their congeners.

Materials and methods

Individuals were collected by targeting calling specimens and by pitfall trapping. They were euthanised by immersion in 0.5% MS 222, fixed in 90% ethanol or 10% buffered formalin, and subsequently transferred to 70% ethanol for permanent storage. ZCMV and MVTIS refer to the zoo-

Results

MARK D. SCHERZ et al.

logical collection of MIGUEL VENCES and FGZC to that of FRANK GLAW, while FAZC and FN refer to the zoological collection of FRANCO ANDREONE. Specimens were deposited in the herpetological collections of the Université d'Antananarivo Département de Biologie Animale (UAD-BA), the Zoologische Staatssammlung München (ZSM), and the Museo Regionale di Scienze Naturali, Torino (MRSN).

This published work and the nomenclatural acts it contains have been registered in ZooBank, the online registration system for the ICBN. The LSID (Life Science Identifier) for this publication is: urn:lsid:zoobank.org:pub:21CB910D-7B42-4BE1-8B8A-461578F4818B. The electronic edition of this work will be archived at and available from the following digital repositories: www.salamandra-journal.com and www.zenodo.org.

Sound recordings were made on a Tascam DR07 digital field recorder with its built-in microphone, sampled at 44.1 kHz, and saved at 24-bit uncompressed resolution. Audio files were processed and analysed in Audacity® 2.1.0 (Audacity Team 2014), including noise reduction and manual silencing of noisy segments. Frequency information was obtained through Fast Fourier Transformation (FFT; width 512 points). We define 'core call duration' as the duration of the main peak in amplitude of a call to the exclusion of a trailing tail. Figures were produced in R (R Core Team 2014) using the spectro() function in the Seewave package (SUEUR et al. 2008). We follow GLAW & VENCES (1994) and RAKOTOARISON et al. (2015) in considering a 'call' of these frogs to consist of a single note, and will use the terms 'inter-call interval' and 'call duration' accordingly. All times were rounded to the nearest ms, and frequencies to the nearest Hz.

Morphometric data was measured using a digital caliper accurate to 0.01 mm, rounded to the nearest 0.1 mm. Morphometric ratios were calculated prior to rounding. We measured the following characters: SVL (snout-vent length), HW (maximum head width), HL (head length, from the maxillary commissure to the snout tip along the jaw), ED (horizontal eye diameter), END (eye-nostril distance), NSD (nostril-snout tip distance), NND (internarial distance), TDH (horizontal tympanum diameter), TDV (vertical tympanum diameter), HAL (hand length, from the metacarpal–radioulnar articulation to the tip of the longest finger), LAL (lower arm length, from the metacarpal–radioulnar articulation to the radioulnar–humeral articulation), UAL (upper arm length, from the radioulnar–humeral articulation to the trunk, measured along the posterior aspect of the arm), FORL (forelimb length as the sum of HAL + LAL + UAL), FOL (foot length, from the tarsal–metatarsal articulation to the tip of the longest toe), TARL (tarsal length, from the tarsal–metatarsal articulation to the tarsal–tibiofibular articulation), FOTL (foot length including tarsus as the sum of FOL + TARL), TIBL (tibiofibula length), TIBW (tibiofibula width), THIL (thigh length, from the vent to the femoral–tibiofibular articulation), THIW (thigh width at thickest point, measured in supine position), HIL (hind

limb length as the sum of FOL + TARL + TIBL + THIL), IMCL (maximum length of inner metacarpal tubercle), IMTL (maximum length of the inner metatarsal tubercle). See SCHERZ et al. (2015b) for a figure showing this measurement scheme.

Micro-CT scanning was conducted using a phoenix nanotom m (GE Measurement & Control, Wunstorf, Germany). Specimens were mounted on a polystyrene base-plate using wooden struts, and placed inside a polyethylene vessel. Scans were conducted at a voltage of 140 kV and current of 80 mA, for 2,440 projections over 20 minutes. Volumes initially rendered in phoenix|x reconstruction software (GE Measurement & Control) were examined in VG Studio Max 2.2 (Volume Graphics GMBH, Heidelberg, Germany). Surface models were produced in Amira 6.0. Our osteological terminology follows TRUEB (1968, 1973). Supplementary PDF-embedded 3D models were constructed using the Adobe® 3D Toolkit and Adobe® Acrobat X Pro. Micro-CT does not render cartilage, and cartilage structures are therefore omitted from our osteological descriptions.

Four samples of *R. botabota* sp. n., one sample of *R. aluaudi* (MOCQUARD, 1901), two samples of *R. savaka* sp. n., one sample of *Rhombophryne* sp. from Sorata, four samples of *R. mangabensis* GLAW, KÖHLER & VENCES, 2010, and one of *R. guentherpetersi* (GUIBÉ, 1974) were newly analysed genetically for this study. Toe clippings or thigh muscle were collected as tissue samples. Total genomic DNA was extracted from the tissue samples by applying proteinase K digestion (10 mg/ml concentration) followed by a standard salt extraction protocol (BRUFORD et al. 1992). We sequenced a fragment of ca 550 bp of the 3' terminus of the mitochondrial rrnL (large ribosomal RNA, or 16S rRNA gene). For primers used and cycling protocols applied, see CROTTINI et al. (2011). Standard polymerase chain reactions were performed in a final volume of 11 µl and using 0.3 µl each of 10 pmol primer, 0.25 µl of total dNTP 10 mM (Promega, Fitchburg, WI, USA), 0.08 µl of 5 U/ml GoTaq, and 2.5 µl 5X Green GoTaq Reaction Buffer (Promega). Successfully amplified PCR products, treated with ExoSAP-IT (Affymetrix, Santa Clara, CA, USA) to inactivate remaining primers and dNTPs, were directly used for the cycle sequencing reaction, using dye-labelled terminators (Applied Biosystems, Foster City, CA, USA) with the amplification primers. Labelled fragments were analysed on an ABI 3130 automated DNA sequencer (Applied Biosystems). Sequences were compared with GenBank sequences and chromatographs were visually checked and edited, when necessary, using CodonCode Aligner 3.7.1 (CodonCode Corporation, Centerville, MA, USA). This alignment required the inclusion of gaps to account for indels in only a few cases. For GenBank accession numbers of the sequences used, see Table 1.

Molecular analyses included one sequence of each described *Rhombophryne* species, plus all sequences available to us of *R. botabota* sp. n., *R. savaka* sp. n., and their closest relatives, *R. aluaudi* and *R. mangabensis* (see Table 1). We also included one sequence each of two unde-

Two new *Rhombophryne* from northeastern Madagascar

Table 1. List of samples included in the present study for molecular analyses (ID), species identification, localities, GenBank accession numbers.

ID	Species	Locality	16S
MRSN A2620	<i>R. alluaudi</i>	Tsararano	AY594105
ZSM 3/2002	<i>R. alluaudi</i>	Andasibe	DQ019606
ZCMV 2209	<i>R. alluaudi</i>	Andasibe	KU724170
ZCMV 968	<i>R. alluaudi</i>	Torotorofotsy	EU341105
FGZC 3631	<i>R. sp.</i>	Sorata	KU724171
FGZC 3651	<i>R. longicrus</i>	Sorata	KR025897
DRV 5836	<i>R. botabota</i>	Makira	KU724172
ZCMV 11473	<i>R. botabota</i>	Makira	KU724173
ZCMV 11474	<i>R. botabota</i>	Makira	KU724174
FGZC 2896	<i>R. botabota</i>	Marojejy	FJ559297
MRSN A2640	<i>R. botabota</i>	Ambolokopatrika	AY594104
MRSN A2956	<i>R. botabota</i>	Ambolokopatrika	KU724175
ZCMV 2065	<i>R. savaka</i>	Marojejy	KU724176
ZCMV 2079	<i>R. savaka</i>	Marojejy	KU724177
ZSM 694/2001	<i>R. coronata</i>	Mandraka	EU341103
FAZC 13887	<i>R. coudreaulti</i>	Betampona	FJ559299
DRV 6220	<i>R. guentheri</i> <i>petersi</i>	Tsaratanana	KU724178
FGZC 423	<i>R. laevipes</i>	Montagne d'Ambre	EU341104
ZCMV 886	<i>R. mangabensis</i>	Nosy Mangabe	EU341109
FGZC 1888	<i>R. matavy</i>	Forêt d'Ambre	J559298
FGZC 2899	<i>R. minuta</i>	Marojejy	EU341106
ZCMV 12384	<i>R. ornata</i>	Tsaratanana	KP895584
FAZC 7292	<i>R. sp.</i>	Ambolokopatrika	EU341111
ZCMV 12359	<i>R. tany</i>	Tsaratanana	KP895585
ZSM 475/2000	<i>R. testudo</i>	Nosy Be	AY594125
FGZC 2842	<i>R. vaventy</i>	Marojejy	EU341107
MVTIS 2001/	<i>S. psologlossa</i>	Benavony	EU341066
G54			
ZCMV 2118	<i>R. mangabensis</i>	Nosy Mangabe	KU724179
ZCMV 2119	<i>R. mangabensis</i>	Nosy Mangabe	KU724180
ZCMV 886	<i>R. mangabensis</i>	Nosy Mangabe	KU724181
ZCMV 891	<i>R. mangabensis</i>	Nosy Mangabe	KU724182

scribed species from Ambolokopatrika and Sorata, respectively, in order to confirm whether these new species are different from the ones we describe here. A homologous 16S rRNA gene sequence of *Stumpffia psologlossa* BOETTGER, 1881 from Benavony was added to the 16S gene fragment alignment for outgroup rooting in the phylogenetic analyses. The purpose of the presented phylogenetic analyses is to show the closest relationships of the two new species to *R. mangabensis* and *R. alluaudi*, rather than provide a strongly supported phylogenetic hypothesis of the relationships between all *Rhombophryne* species.

Uncorrected pairwise distances (p-distance transformed into percentage) between individuals of the same species and between analysed *Rhombophryne* species and

S. psologlossa were computed using MEGA 6.06 (TAMURA et al. 2013) (see Table 2).

Bayesian inference searches of the mitochondrial 16S rRNA gene fragment (Fig. 1) were conducted in MrBayes 3.2.1 (RONQUIST et al. 2012). The simple JC model of substitution was used because this non-overparametrised model produced a more realistic topology for this short gene segment. We performed two runs of 10 million generations (started on random trees) and four incrementally heated Markov chains (using default heating values), sampling the Markov chains at intervals of 1000 generations. Stabilization and convergence of likelihood values were checked by visualizing the log likelihoods associated with the posterior distribution of trees in the software Tracer (RAMBAUT & DRUMMOND 2007), and occurred after about 3.5–4 million generations. The first four million generations were therefore discarded, and six million trees were retained post burn-in and summarized to generate a majority-rule consensus tree.

Results

Two candidate species of *Rhombophryne* have been recognized from Marojejy, Ambolokopatrika, and Makira based on DNA sequence data (VIEITES et al. 2009, PERL et al. 2014): *R. sp. Ca2* and *R. sp. Ca4*. These taxa are superficially similar in external appearance, and thus far they have had an unstable phylogenetic position, mostly due to the lack of a robust phylogeny of the genus. However, based on our newly obtained DNA sequence data, we were able to correct previous sequences and provide a new hypothesis on the position of these candidate taxa (see Fig. 1). The two Bayesian analyses resulted in identical trees. *Rhombophryne* sp. Ca2, hereinafter referred to as *R. botabota* sp. n., was recovered as a member of the *R. alluaudi* complex (posterior probability 0.99), and *R. sp. Ca4*, hereinafter called *R. savaka* sp. n., was recovered as the sister species of *R. mangabensis* (posterior probability 1.00). Our data also reveal genetic differentiation between the populations of *R. botabota* from Makira and Marojejy + Ambolokopatrika (see Fig. 1), with an intraspecific mean uncorrected p-distance of 1.2% (Table 2). At interspecific level, the lowest mean uncorrected p-distances were observed between *R. botabota* sp. n. and *R. alluaudi* (3.6%) and between *R. savaka* sp. n. and *R. mangabensis* (8.4%); the highest mean uncorrected p-distances were observed between *R. botabota* sp. n. and *R. savaka* sp. n. versus *R. matavy* D'CRUZE, KÖHLER, VENCES & GLAW, 2010 (10.7%, 13.9%, respectively) (for intraspecific comparisons and comparisons with other *Rhombophryne* species, see Table 2).

In conclusion, the two new species, *R. botabota* sp. n. and *R. savaka* sp. n., are genetically distinct from all congeners (mitochondrial genetic differentiation \geq 3.6%; see Fig. 1 and Table 2). This genetic distinction is corroborated by osteological and morphological differences, and we here provide their formal taxonomic description.

Results

MARK D. SCHERZ et al.

Table 2. Within- (bold) and among-species genetic divergence values of the analysed 16S rRNA mitochondrial gene fragment, based on uncorrected pairwise-distance for the analysed species of the genus *Rhombophryne* and *Stumpffia psologlossa*.

	<i>S. psologlossa</i>									
<i>R. vaventy</i>	1.2%									
<i>R. testudo</i>	9.2%									
<i>R. tany</i>	8.2%									
<i>R. sp. Ambolokopatrika</i>	10.0%									
<i>R. ornata</i>	3.6%									
<i>R. minuta</i>	9.2%									
<i>R. matavy</i>	10.0%									
<i>R. mangabensis</i>	12.9%									
<i>R. laevipes</i>	9.6%									
<i>R. guentherpetersi</i>	13.5%									
<i>R. coudreaui</i>	9.0%									
<i>R. savaka</i> sp. n.	11.6%									
<i>R. botabota</i> sp. n.	10.3%									
<i>R. coronata</i>	9.0%									
<i>R. longicrus</i>	11.5%									
<i>R. alluaudi</i>	8.6%									
<i>R. sp. Sorata</i>	9.0%									
<i>R. sp. Ambolokopatrika</i>	9.0%									
<i>R. tany</i>	1.2%									
<i>R. testudo</i>	—									
<i>R. vaventy</i>	—									
<i>R. ornata</i>	—									
<i>R. minuta</i>	—									
<i>R. matavy</i>	—									
<i>R. mangabensis</i>	—									
<i>R. laevipes</i>	—									
<i>R. guentherpetersi</i>	—									
<i>R. coudreaui</i>	—									
<i>R. coronata</i>	—									
<i>R. savaka</i> sp. n.	—									
<i>R. botabota</i> sp. n.	—									
<i>R. longicrus</i>	—									
<i>R. sp. Sorata</i>	—									
<i>R. alluaudi</i>	—									
<i>R. sp. Ambolokopatrika</i>	—									
<i>R. tany</i>	—									
<i>R. testudo</i>	—									
<i>R. vaventy</i>	—									
<i>S. psologlossa</i>	—									

Two new *Rhombophryne* from northeastern Madagascar***Rhombophryne botabota* sp. n.**
(Figs 1–5)

ZooBank LSID: urn:lsid:zoobank.org:act:B95E889C-C2E2-4362-B20C-37E8C7999A81
Suggested common name: Chubby diamond frog

Holotype: ZSM 358/2005 (FGZC 2896), an adult male collected in Marojejy National Park ('Camp Simpona'), 14.4364° S, 49.7433° E, 1,326 m above sea level (a.s.l.), Sava Region, northeastern Madagascar, on 18 February 2005 by F. GLAW, M. VENCES, and R. D. RANDRIANIAINA.

Paratypes: ZSM 538/2009 (ZCMV 11473), ZSM 539/2009 (ZCMV 11474), two presumably immature males collected at Angozongahy, on the western side of the Makira plateau (Camp 1), 15.4370° S, 49.1186° E, 1,009 m a.s.l., Analanjirofo Region, northeastern Madagascar, on 21 June 2009 by M. VENCES, D. R. VIEITES, F. RATSOAVINA, R. RANDRIANIAINA, E. RAJERIARISON, T. RAJOFIARISON, and J. PATTON; MRSN A2956 (FN 7164), A2640 (FN 7238), A2954 (FN 7281), A2955 (FN 7300), two males and two females collected at a site known as 'Andranomadio' on the Ambo-

lokopatrika/Betaolana ridge which connects the massifs of Marojejy and Anjanaharibe-Sud (ANDREONE et al. 2000, RAKOTOMALALA & RASELIMANANA 2003), 14.5304° S, 49.4383° E, 860 m a.s.l., Sava Region, northeastern Madagascar, on 9–15 December 1997 by F. ANDREONE, G. APREA, and J. E. RANDRIANIRINA.

Remark: This species was included in the phylogenies produced by VIEITES et al. (2009) and PERL et al. (2014) as *R. sp. 2* (EU341102) and *R. sp. Ca2* (KF611585), respectively. The GenBank accession number erroneously given in the Supplementary Information of VIEITES et al. (2009) for *R. sp. 4* (FJ559297) also referred to *R. botabota* (FGZC 2896) and the sequence of *R. sp. Ca4* in SCHERZ et al. (2015b) therefore represents *R. botabota* as well.

Diagnosis: A Malagasy microhylid frog assigned to the genus *Rhombophryne* on the basis of its possessing clavicles coupled with knobbed rather than Y-shaped terminal phalanges (SCHERZ et al. in press) and phylogenetic position based on our analysis of the 16S rRNA gene. *Rhombophryne botabota* sp. n. is characterised by the following combination of features: medium size (SVL 24.2–

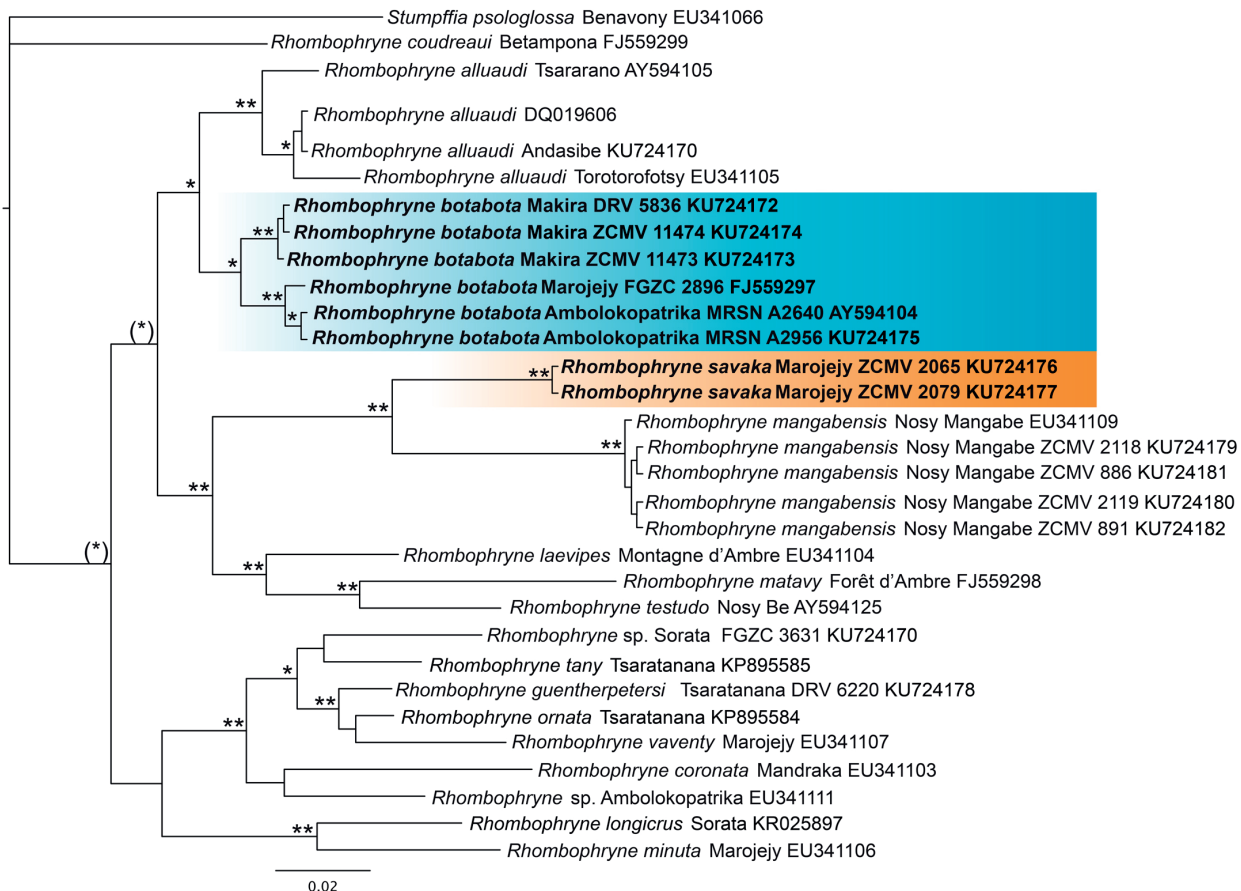


Figure 1. Bayesian inference tree of *Rhombophryne* species based on 545 bp of the mitochondrial 16S rRNA gene fragment. Asterisks denote Bayesian posterior probabilities values: (*): 97–98%; *: 99%; **: 100%. The two new species described herein are highlighted.

Results

MARK D. SCHERZ et al.

32.2 mm); TDH 51.0–70.5% of ED; FORL 43.5–55.2% of SVL; TIBL 38.4–45.7% of SVL; TIBW 26.5–36.0% of TIBL; HIL 141–164% of SVL; HW 144.2–169.5% of HL; tibiotarsal articulation reaching the tympanum or the eye; distinct colour border between lateral head and dorsum in most specimens; possession of curved clavicles, and maxillary and vomerine teeth; vomerine teeth sigmoidal, medially separated by a small cleft; an uncorrected p-distance of at least 3.6% in the analysed 16S rRNA gene fragment, and a unique call (see below).

Within the genus *Rhombophryne*, *R. botabota* sp. n. may be distinguished from the *R. serratopalpebrosa* group (*R. serratopalpebrosa*, *R. vaventy*, *R. coronata*, *R. ornata*, *R. tany*, and *R. guentherpetersi*) by the absence of superciliary spines (but see below for additional comments on its differentiation from *R. guentherpetersi* in which the superciliary spines are small). It is distinguished from all other described *Rhombophryne* species except *R. laevipes* by typically having a distinct colour border between its dorsum and lateral head. Additionally, *R. botabota* sp. n. may be distinguished from *R. minuta* and *R. mangabensis* by its larger SVL (24.2–32.2 mm vs 15.4–23.2 mm); from *R. laevipes* and *R. alluaudi* by its smaller SVL (24.2–32.2 mm vs 36.4–56.3) and the absence of inguinal ocelli (vs presence); from *R. minuta* and *R. longicrus* by its shorter forelimbs (FORL 43.5–55.2% vs 70.4–74.7% of SVL), robust legs (vs slim), larger tympanum (TDH 51.0–70.5% vs 39.5–48.3% of ED), and wider head (HW 144.2–169.5% vs 122.5–142.8% of HL); from *R. minuta*, *R. longicrus*, and *R. laevipes* by its shorter TIBL (TIBL 38.4–45.7% vs 48.3–52.3% of SVL) and shorter HIL (HIL 141–164% vs 175–184% of SVL); from *R. mangabensis*, *R. testudo*, *R. matavy*, and *R. coudreau* by its smooth skin (vs tubercular), possession of ossified clavicles (vs not ossified, reduced, or absent), and narrower vertebral transverse processes; from *R. mangabensis* by its higher call repetition rate (inter-call interval 2,359 vs 6,420 ms), lower dominant call frequency (1,272 Hz vs 2,800–7,800 Hz), and a call without frequency modulation (vs with); and from *R. testudo*, *R. matavy*, and *R. coudreau* by its longer TIBL (TIBL 38.4–45.7% vs 30.3–37.2% of SVL), and tibiotarsal articulation reaching the tympanum or eye (vs not exceeding the axilla). Some specimens of *R. botabota* sp. n. superficially resemble *R. guentherpetersi*, the superciliary spines of which are sometimes difficult to observe, but can easily be distinguished from this species by the absence of tibial glands. For a distinction from *R. savaka* sp. n., see the description of that species, below.

Rhombophryne botabota sp. n. is most similar to *R. alluaudi* (which is also its sister species). It may be distinguished from that species (as it is currently understood; see Discussion) by the absence of light dorsolateral markings (vs presence), absence of inguinal ocelli (vs presence), smaller SVL (24.2–32.2 mm vs 36.4–42.6 mm), higher dominant call frequency ($1,272 \pm 13$ Hz vs 798 ± 23 Hz), and higher fundamental call frequency (621 ± 11 Hz vs 379 ± 34 Hz). One micro-CT scanned specimen of *R. alluaudi* (ZSM 3/2002) differed from *R. botabota* sp. n. in having a less ossified skeleton, fusion of presacral VIII and sacrum

(vs not fused), and the dorsal crest of urostyle running almost its full length (vs ~75% of its length). More micro-CT scans of *R. alluaudi* are needed to identify non-variable skeletal characters useful for distinguishing it from *R. botabota* sp. n.

Rhombophryne botabota sp. n. differs from all species of *Plethodontohyla* BOULENGER, 1882 except *P. mihanika*, *P. inguinalis*, and *P. fonetana* by possessing a clavicle; from *P. mihanika* and *P. inguinalis* by the absence of expanded digital discs and a dorsolateral colour border, and from these two species and *P. fonetana* by possessing knob-like terminal phalanges (vs Y-shaped). In its external morphology, this species could be confused with *P. brevipes*, but its supratympanic fold is dark (vs whitish), and it lacks inguinal spots (vs usually present). As far as is known, the two species do not overlap in distribution, so confusion in the field should not occur.

Description of holotype: The specimen is in a good state of preservation. A tissue sample was taken from the right thigh for molecular analyses. An incision running from side to side across the posterior abdomen was made to check sex and access gut contents, leaving the testes clearly visible.

Body robust. Head wider than long. Pupils small, round. Snout rounded in dorsal and lateral views. Canthus rostralis distinct, concave. Loreal region concave. Nostril closer to eye than to tip of snout, slightly protuberant. Tympanum indistinct, rounded, TDH 51.0% of ED. Supratympanic fold distinct, weakly raised, curving slightly from posterior corner of eye over tympanum toward axilla. Superciliary spines absent. Tongue very broad, attached anteriorly, unlobed. Maxillary and vomerine teeth present, vomerine teeth distinct, forming two curved rows posteromedial to choanae, separated by a small medial gap. Choanae oblong.

Forelimbs relatively thick. Fingers without webbing, relative lengths $1 < 2 < 4 < 3$, fourth finger slightly longer than second; finger tips not enlarged; subarticular tubercles faint, single; nuptial pads absent; inner metacarpal tubercle present, outer metatarsal tubercle absent. Hind limb thick; tibiotarsal articulation reaching tympanum; tibia length 38.4% of SVL. Inner metatarsal tubercle present, slightly enlarged; outer metatarsal tubercle absent. Toes not webbed; relative lengths $1 < 2 < 5 < 3 < 4$, fifth toe distinctly shorter than third; without subarticular tubercles; toe tips not enlarged.

Osteology of holotype: The skeleton of the holotype is fairly typical of *Rhombophryne* (see SCHERZ et al. 2015a, b for detailed accounts of other species in this genus). It is well ossified, without any broken bones. Unusually, the inter-vertebral spaces are highly X-ray absorbent, giving the impression of an almost ankylosed spine.

Anterior braincase laterally and anteriorly closed by sphenethmoid (or an intersphenethmoid calcium deposit). Vomerine teeth consisting of a sigmoidal row on either side of the parasphenoid, separated at the midline by a small gap. Maxillary teeth small, poorly defined.

Sternum not ossified. Clavicle well developed, curved. Humerus with crista ventralis roughly 50% of its length;

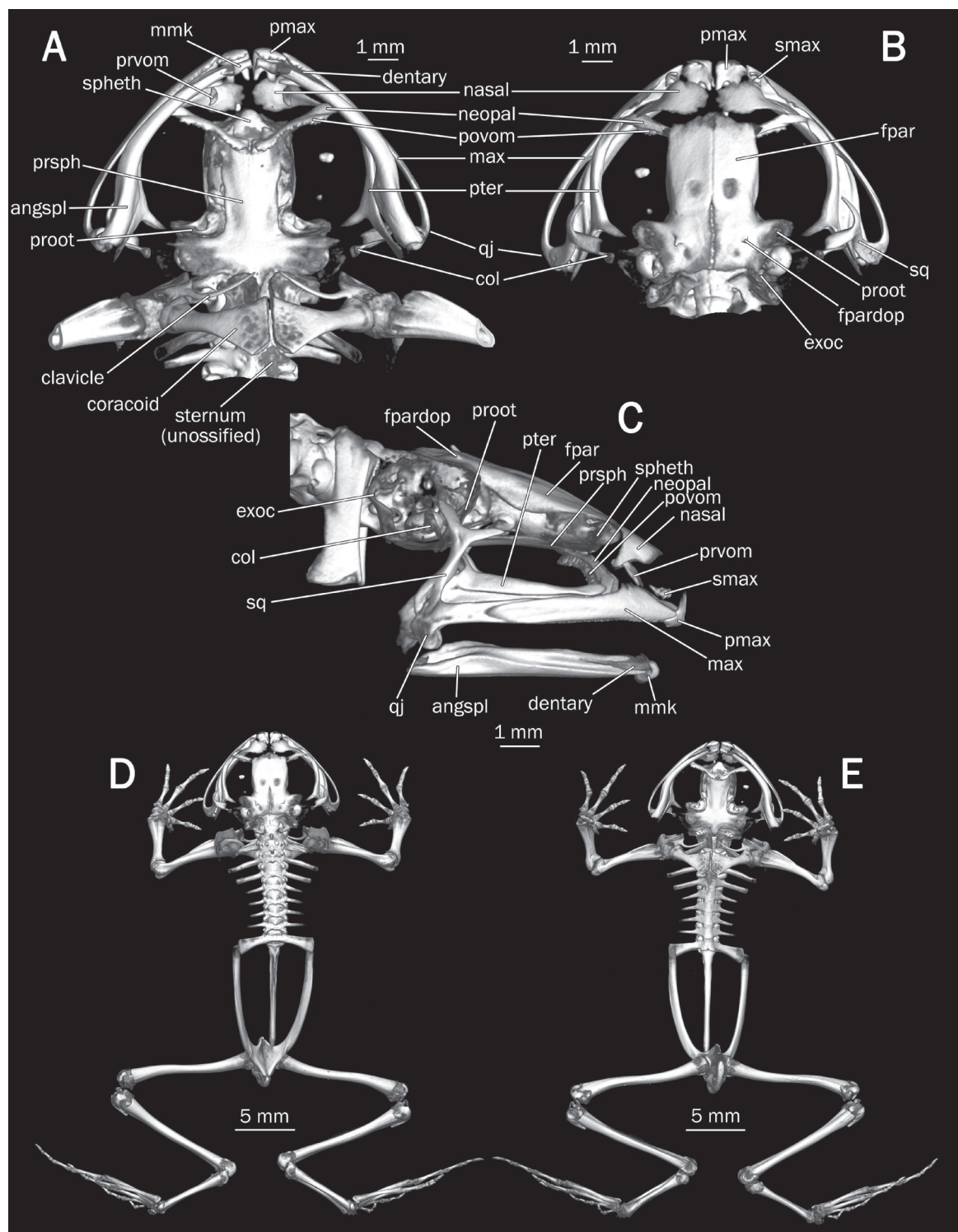
Two new *Rhombophryne* from northeastern Madagascar

Figure 2. Osteology of *Rhombophryne botabota* sp. n. (holotype, ZSM 358/2005), showing the skull in A) ventral, B) dorsal, and C) lateral views, and the full skeleton in D) dorsal and E) ventral views. Abbreviations as follows: angspl – angulosplenial; col – columella; dentary – dentary bone; exoc – exoccipital; fpar – frontoparietal; fpardop – dorsal process of frontoparietal; max – maxilla; mmk – mentomeckelian bone; nasal – nasal bone; neopal – neopalatine; povom – postchoanal vomer; pmax – premaxilla; proot – prootic; prsph – parasphenoid; prvom – prechoanal vomer; pter – pterygoid; qj – quadratojugal; smax – septomaxilla; spheth – sphenethmoid; sq – squamosal. A PDF-embedded 3D model is provided in the supplementary material online.

Results

MARK D. SCHERZ et al.

crista lateralis weak. Terminal phalanges of fingers and toes with small distal knobs. Phalangeal formula of fingers 2-2-3; of toes 2-2-3-4-3. Femur without cristae. Prepollex ossified, relatively small. Prehallux not ossified.

Neural spines decreasing in size posteriorly. Dorsal crest of urostyle running roughly 75% along its shaft. Iliosacral articulation type IIA sensu EMERSON (1979). Iliac shafts bearing weak dorsal tubercles, with dorsal crests running roughly 90% of their length. Pubis ossified.

Colour pattern of holotype: After ten years in preservative, specimen dorsally light brown (Fig. 3). Symmetric markings present behind scapular region. Thin cream stripes run obliquely over each scapula. Dorsum faintly striped with darker and lighter brown, in lines, running roughly from inguinal region obliquely toward midline. Inguinal spots absent. Lateral side of head dark brown, strongly distinct from dorsal coloration, limited by canthus rostralis, eyelid, and supratympanic fold. On flanks, the dorsal brown merges with the translucent cream ventral coloration. Ventral belly immaculate cream. Chin cream, heavily flecked with brown. Cloacal region dark brown. Legs dorsally light brown with two dark cross-bands on the thigh (oblique), three on the shank, two on the tarsus. Thighs ventrally cream, flecked with brown anteriorly and posteriorly, anterodorsally brown with cream flecks, posteriorly proximally cream, distally becoming dark brown and ocellated with cream. Shank ventrally distally and externally cream, flecked lightly with brown, but brown ocellated

with cream toward the inside of the knee. Tarsus ventrally cream with brown flecks. External foot as the tarsus, with one dark brown area. Sole of foot brown with small cream flecks. Toes speckled cream and light brown. Toe tips dark brown. Arms ventrally cream with brown flecks, dorsally light brown with a dark brown cross band on the lower arm. Interior hand finely speckled with cream and brown. Fingers light brown with small dark brown and cream regions. Colour in life as in preservative (see Figs 4a, b).

Variation: In general, all paratypes agree strongly with the holotype in morphology, but not in coloration. For full details of variation in measurements, see Table 3. SVL ranges from 24.2 to 32.2 mm, FORL from 43.5 to 55.2% of SVL, TIBL from 38.4 to 45.7% of SVL, TIBW from 26.5 to 36.0% of TIBL, HIL from 141 to 164% of SVL, TDH from 65.0 to 80.8% of ED, and HW from 144.2 to 169.5% of HL. Finger ratios vary slightly, but in general the second and fourth finger are subequal in length. The two specimens from Makira (ZSM 538/2009 and 539/2009) are considerably smaller than the other specimens. The paratypes vary quite strongly in coloration. In all specimens, light, oblique, thin lines are present across the scapular region. The dark spots posterior to these are present in specimens MRSN A2955 and A2956, but absent from all others. In all specimens, the side of the head is darker than the dorsum. The posterior dorsal/inguinal stripes are present in MRSN A2954-2956, but absent from all other paratypes. The ocelli on

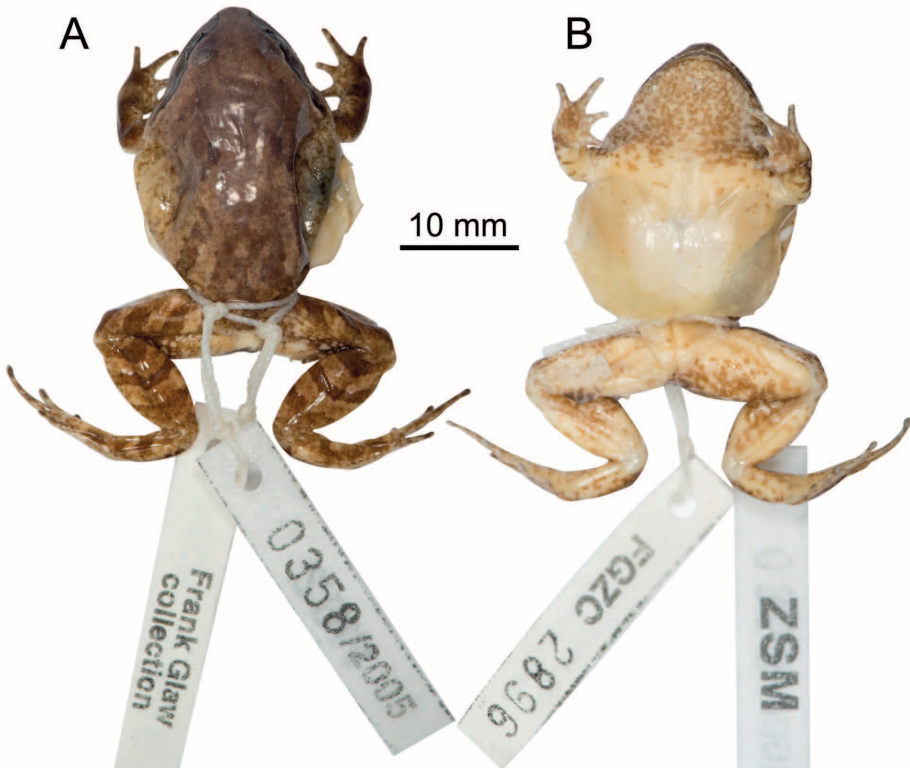


Figure 3. The holotype of *Rhombophryne botabota* sp. n. (ZSM 358/2005) in preservative, in A) dorsal and B) ventral views.

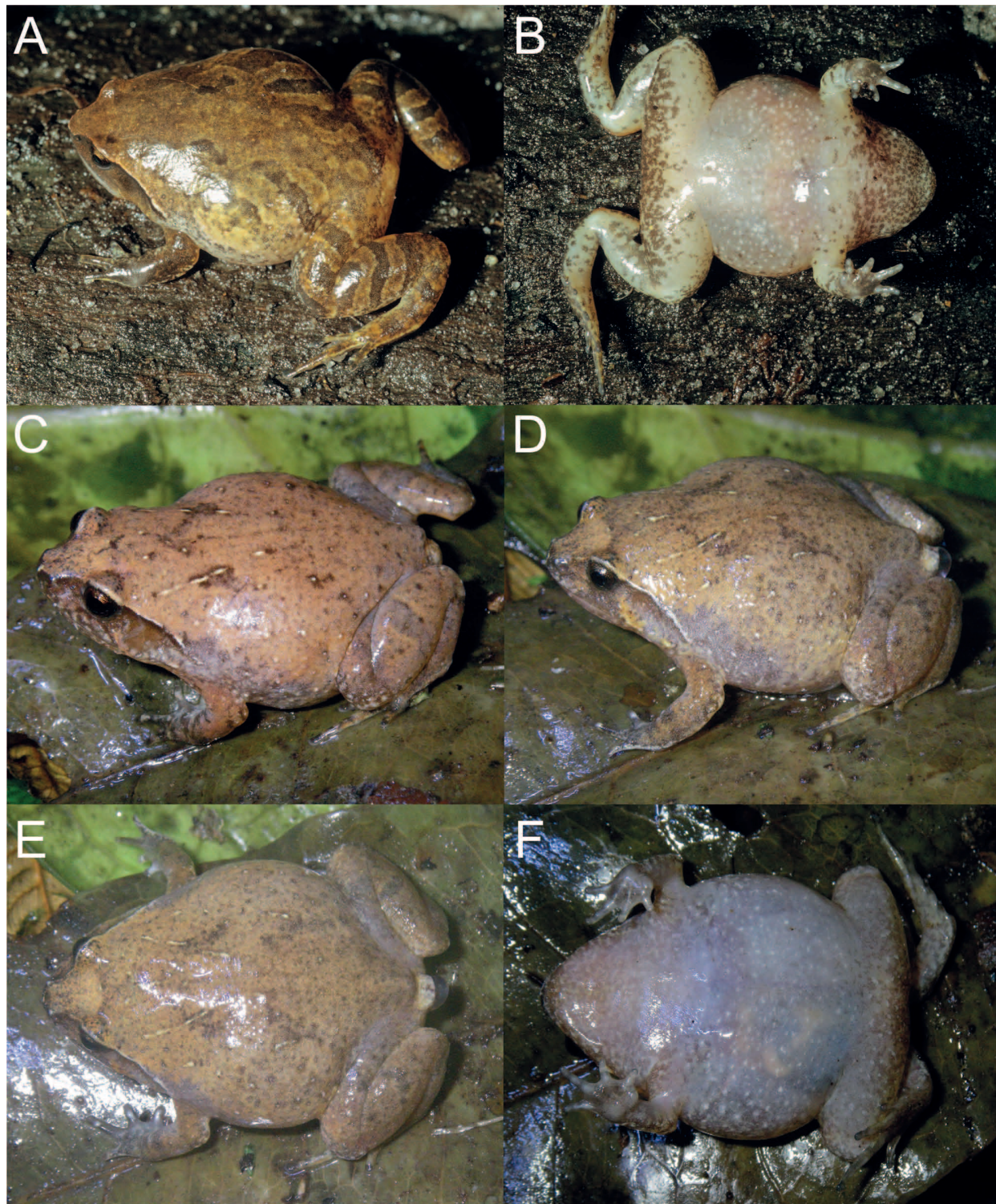
Two new *Rhombophryne* from northeastern Madagascar

Figure 4. *Rhombophryne botabota* sp. n. in life. A–B) ZSM 358/2005 (holotype) from Marojejy National Park in dorsolateral and ventral views; C) ZSM 539/2009 from Angozongahy (Makira) in dorsolateral view; D–F) ZSM 538/2009 from Angozongahy (Makira) in dorsolateral, dorsal, and ventral views.

Results

MARK D. SCHERZ et al.

Table 3. Morphological measurements of *Rhombophryne botabota* sp. n. and *R. savaka* sp. n. Measurements were rounded to the nearest 0.1 mm. Abbreviations are defined in the chapter Materials and methods except HT (holotype), PT (paratype), M (male), and F (female).

Collection No.	ZSM 358/2005	MRSN A2640	MRSN A2954	MRSN A2955	MRSN A2956	ZSM 538/2009	ZSM 539/2009	ZSM 468/2005
Field No.	FGZC 2896	FN 7238	FN 7281	FN 7300	FN 7164	ZCMV 11473	ZCMV 11474	ZCMV 2065
Species	<i>R. botabota</i>	<i>R. savaka</i>						
Locality	Marojejy	Amboloko-patrika	Amboloko-patrika	Amboloko-patrika	Amboloko-patrika	Makira	Makira	Marojejy
Status	HT	PT	PT	PT	PT	PT	PT	HT
Sex	M	M	F	M	F	M	M	M
SVL	30.2	30.4	32.2	30.8	28.6	25.4	24.2	20.4
HW	11.5	12.3	13.3	12.7	11.8	10.9	9.6	9.2
HL	6.8	7.7	7.9	7.8	7.5	6.8	6.6	5.1
ED	2.6	2.5	2.6	2.7	2.6	2.4	2.4	2.0
END	1.6	1.9	2.3	2.1	1.7	1.9	1.6	1.2
NSD	1.6	1.4	1.6	1.5	1.5	1.1	1.1	1.1
NND	2.9	2.9	3.0	2.8	2.7	2.4	2.2	2.5
TDH	1.3	1.5	1.8	1.6	1.7	1.4	1.4	1.2
TDV	1.7	1.8	1.9	1.7	1.6	1.7	1.5	1.4
HAL	6.5	7.0	6.8	7.1	6.0	5.9	5.1	3.7
UAL	2.4	3.9	3.5	2.7	3.4	1.6	3.2	1.7
LAL	4.3	5.9	5.0	5.0	3.6	4.8	4.4	3.5
FORL	13.1	16.8	15.3	14.8	13.1	12.3	12.7	8.8
THIL	11.4	13.1	13.4	13.6	13.4	11.2	10.7	8.1
THIW	5.7	5.4	6.1	5.5	5.1	4.6	4.8	5.3
TIBL	11.6	13.5	13.9	12.8	13.1	10.2	10.2	7.6
TIBW	4.2	4.2	3.7	4.2	4.0	3.2	3.3	3.6
TARL	7.1	6.5	7.4	6.7	7.0	6.3	6.4	4.4
FOL	12.5	14.4	15.0	13.4	13.4	11.0	10.9	7.8
FOTL	19.5	20.9	22.4	20.0	20.5	17.3	17.3	12.2
HIL	42.5	47.5	49.7	46.4	46.9	38.7	38.2	27.9
IMCL	1.4	1.4	1.5	1.2	1.3	1.1	1.0	0.8
IMTL	1.5	1.5	1.4	1.5	1.1	1.0	1.1	0.9

the posterior thigh are present in MRSN A2954 and ZSM 538/2009 and 539/2009, weakly expressed in MRSN A2955 and A2956, and absent in MRSN A2955 and A2640. Thigh cross-bands are present only in MRSN A2955 and the holotype. Shank cross-bands are present in most specimens, but vary in number (one in MRSN A2955, three in MRSN A2954), and intensity (almost invisible in ZSM 538/2009, clearly visible in MRSN A2954). Ventral coloration is more or less consistent across all specimens.

In the paratype ZSM 538/2009, the spine is malformed: first and second presacrals fused but atypically so, sacral articulation with urostyle differentiated to form a regular vertebral articulation instead of the typical bicondylar articulation found in this genus (SCHERZ et al. 2015a,b). Urostyle possessing a lateral parapophysis anteriorly on its right side.

Advertisement call: A single individual was recorded by MV during the day on 24 June 2009 in Makira (Ango-zongahy site), calling from the leaf litter in dense primary rainforest at an estimated ambient temperature of 22–24°C.

The individual in question was not seen during the recording, but we are confident that the call belongs to this species because of its resemblance to the call of *R. alluaudi* and because this was the only *Rhombophryne* found near the location of the call. In fact, more calling individuals were heard and the two paratypes were collected, all from the same small area of an estimated 50 m². The advertisement call of this species consists of a series of harmonious honking notes repeated at regular intervals (Fig. 5). The following analysis is based on a recording of just four calls and is therefore tentative. Call duration was 505 ± 76 ms (range: 405–582 ms, n = 4), but this includes a long tapering tail; the core-call duration was 151 ± 18 ms (134–175 ms, n = 4). Inter-call intervals were 2359 ± 44 ms (range: 2313–2363 ms, n = 3). Fundamental frequency was 621 ± 11 Hz (610–634, n = 4). Dominant frequency peaked at 1272 ± 13 Hz (1259–1289, n = 4), i.e., the first harmonic. A harmonic band appeared at $1,893 \pm 24$ Hz (1,869–1,923) in all calls; one call had further harmonics at 2,537 and 3,185 Hz. No frequency modulation or pulsing was recognizable.

Two new *Rhombophryne* from northeastern Madagascar

Ecology: The stomach of one of the paratypes (ZSM 538/2009) contained a small snail (tentatively identified as a member of Subulinidae, possibly the non-native *Subulina octona*) measuring 8.6 mm (measured in VG Studio Max 2.2). This is the first record of *Rhombophryne* predating on gastropods. The paratypes currently housed in MRSN were collected using pitfall traps, as described by ANDREONE et al. (2000). This provides further support for a fossorial lifestyle and rather secretive behaviour of this species.

IUCN Red List status: This species has been found at three localities: Marojejy, Ambolokopatrika, and Makira. These areas span a distance of 128.5 km. A simple minimum convex polygon (triangle) of the three collection sites covers an area of 1,457 km². Current records include two large protected areas: Makira Natural Park, consisting of 3,850 km² of protected forest surrounded by community-managed protected zones; and Marojejy National Park, consisting of 597.5 km² of protected forest. Ambolokopatrika is at present unprotected, but forms part of a proposed protected area encompassing the forest corridor connecting Marojejy with Tsaratanana (COMATSA; see RABE-RIVONY et al. 2015). Based on these records, the altitudinal range of this species extends from 860 to 1,326 m a.s.l.

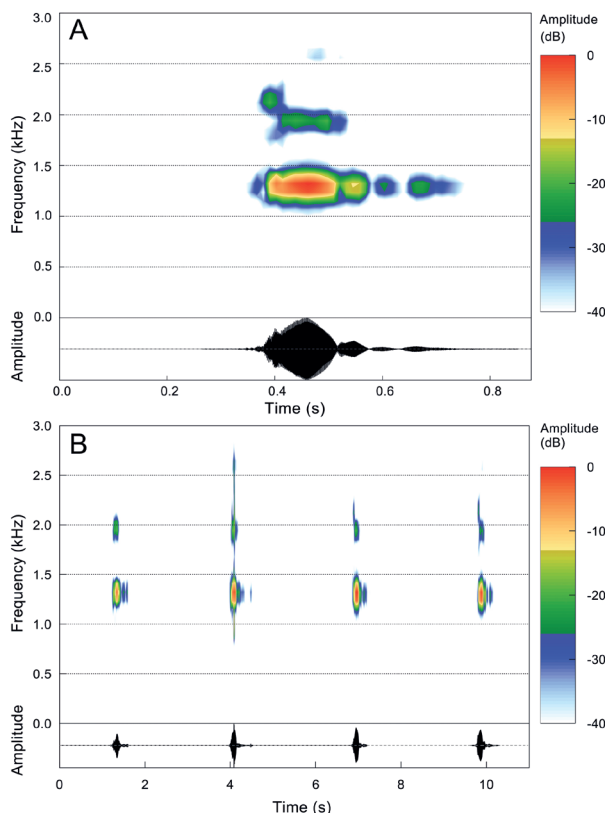


Figure 5. Oscillograms and spectrograms of *Rhombophryne botabota* sp. n., showing A) the structure of a single call and B) the structure of a call series. The second call is probably over-modulated.

Within the protected areas, anthropogenic activities continue to compromise the quality and coverage of forest (PATEL & WELCH 2013). This is even more true for the expanses of forest between them, including the Anjanaharibe-Sud Special Reserve and COMATSA. Mining and harvesting of hardwood trees (RANDRIAMALALA & LIU 2010, PATEL & WELCH 2013) are the two most important factors diminishing the quality of these forests.

Current knowledge provides an extent of occurrence (EOO) of 1,457 km², but this is probably an underestimate. Two of the three known localities are relatively well protected, but threats, including declining forest expanse and quality, persist. We propose a status of Vulnerable for this species, under IUCN Red List Criteria B1ab(iii) (IUCN 2012).

Etymology: The specific epithet *botabota* (pronounced 'buddha-buddha') is a Malagasy word meaning 'chubby' in allusion to the plump appearance of this frog. It is to be considered a noun in the nominative singular in apposition to the generic name.

***Rhombophryne savaka* sp. n.**
(Figs 1, 6, 7)

ZooBank LSID: urn:lsid:zoobank.org:act:D75DoA22-35EE-41C4-A385-1D02F896E6DB

Suggested common name: Savaka diamond frog

Holotype: ZSM 468/2005 (ZCMV 2065), a male collected in Marojejy National Park ('Camp Marojejia'), 14.435° S, 49.7605° E, 746 m a.s.l., Sava Region, northeastern Madagascar, on 18 February 2005 by F. GLAW, M. VENCES, and R. D. RANDRIANIAINA.

Paratype: UADBA-A uncatalogued (ZCMV 2079), a specimen of unknown age and sex with the same collection data as the holotype. This specimen could not be examined for this study, but its 16S sequence was 100% identical with the holotype, and we are therefore sure of its assignment to this taxon.

Remark: This species was included as *R. sp. Ca4* in the phylogenies produced by VIEITES et al. (2009) and PERL et al. (2014). However, the sequence accession number FJ559297 given in the Supplementary Information of VIEITES et al. (2009) for this species had incorrect voucher information and in reality referred to a sequence of *R. botabota* (specimen FGZC 2896).

Diagnosis: A Malagasy microhylid frog assigned to the genus *Rhombophryne* on the basis of possessing clavicles coupled with knobbed, rather than Y-shaped terminal phalanges (SCHERZ et al. in press) and phylogenetic position based on our analysis of the 16S rRNA gene. *Rhombophryne savaka* sp. n. is characterized by the following combination of features: small size (SVL 20.4 mm), TDH

Results

MARK D. SCHERZ et al.

60.0% of ED; FORL 43.3% of SVL; TIBL 37.4% of SVL; TIBW 47% of TIBL; HIL 137% of SVL; HW 179.5% of HL; tibiotarsal articulation reaching the tympanum; possession of inguinal spots; possession of thin, curved clavicles, and maxillary and vomerine teeth; vomerine teeth with large lateral diastemata, medially fused; well-ossified braincase; well-developed prehallux; and an uncorrected p-distance of at least 8.4% in the analysed 16S rRNA gene fragment.

Within the genus *Rhombophryne*, *R. savaka* sp. n. is unique in having inguinal spots and medially fused vomers, and has the largest lateral vomerine diastemata yet observed. This species may be distinguished from the *R. serratopalpebrosa* group (*R. serratopalpebrosa*, *R. vaventy*, *R. coronata*, *R. ornata*, *R. tany*, and *R. guentherpetersi*) by the absence of superciliary spines; from *R. longicrus*, *R. laevipes*, *R. alluaudi*, *R. testudo*, *R. matavy*, *R. coudreaui*, and *R. botabota* possibly by its smaller size (SVL 20.4 vs 23.8–56.3 mm); from *R. longicrus*, *R. minuta*, and *R. botabota* by its broader head (HW 179.5% vs 122.5–169.4% of HL); from *R. testudo* by its narrower head (HW 179.5% vs 200.4–259.9% of HL); from *R. minuta* and *R. longicrus* by its larger tympanum (TDH 60.0% vs 39.5–48.3% of ED) and shorter forelimbs (FORL 43.3% vs 70.4–74.7% of SVL); from *R. minuta*, *R. longicrus*, and *R. laevipes* by its shorter tibia length (TIBL 37.4% vs 47.2–52.3% of SVL); from *R. minuta*, *R. longicrus*, *R. laevipes*, and possibly *R. alluaudi* by its shorter hind limbs (HIL 137% vs 146–184% of SVL); and from *R. testudo*, *R. matavy*, *R. mangabensis*, and *R. coudreaui* by its possessing clavicles (vs absence) and smooth skin (vs tubercular). As for *R. botabota*, this species can be easily distinguished from *R. guentherpetersi* by the absence of tibial glands.

Rhombophryne savaka sp. n. is most similar to *R. mangabensis* (which is also its sister species) and some individuals of *R. botabota* sp. n., described above. It may be distinguished from either species by the presence of inguinal spots (vs absence), possibly slightly shorter hind limbs (HIL 137% vs 141–164% of SVL), and possessing medial fused vomerine teeth with a large mid-row diastema on either side (vs medially separated with either no or just a small diastema), and from *R. mangabensis* by the presence of clavicles (vs absence), shorter forelimbs (FORL 37.4% vs 43.9–45.9% of SVL), and smooth skin (vs tubercular).

Rhombophryne savaka sp. n. differs from all *Plethodontohyla* species except *P. mihanika*, *P. inguinalis*, and *P. fonetana* by possessing a clavicle; from *P. mihanika* and *P. inguinalis* by the absence of expanded digital discs, and from these two species and *P. fonetana* by possessing knob-like terminal phalanges (vs Y-shaped). Externally, it resembles *P. bipunctata* and *P. brevipes*, but can be distinguished from these species by its shorter relative forelimb length (FORL 43.3% vs 48.1–54.3% of SVL), and broader shanks (TIBW 47.2% vs 29.4–40.8% of TIBL). It is not known to co-occur with either of these two taxa.

Description of holotype: Specimen in an excellent state of preservation. A small tissue sample for sequencing was taken from the right thigh. A small incision for sexing was

made on the left flank, revealing that the testes are large and distinct.

Body robust. Head wider than long. Pupils small, round. Snout rounded in dorsal and lateral views. Canthus rostralis distinct, concave. Loreal region concave. Nostril closer to eye than to tip of snout, directed laterally, slightly protuberant. Tympanum indistinct, rounded, TDH 60.0% of ED. Supratympanic fold distinct, not raised, indicated by a dark marking, running from the posterior corner of the eye and over the tympanum, curving toward but not extending to the axilla. Superciliary spines absent. Maxillary teeth present. Vomerine teeth distinct, forming a broad, U-shaped central patch and two additional patches laterally that are clearly separated by a small diastema. Choanae oblong.

Forelimbs stubby. Fingers without webbing, relative lengths 1 < 2 = 4 < 3; finger tips not expanded; fingers not reduced; nuptial pads absent; inner metacarpal tubercle distinct, outer metacarpal indistinct; subarticular tubercles faint. Hind limbs short and strongly built; tibiotarsal articulation reaching the tympanum; tibia length 37.4% of SVL. Inner metatarsal tubercle present, outer metatarsal tubercle present, light in colour but not raised. Toes not webbed; relative lengths 1 < 2 < 5 < 3 < 4, fifth toe distinctly shorter than third. Toe tips not expanded.

Osteology of holotype: The osteology of the holotype is typical of *Rhombophryne*. It is well ossified, without any broken bones.

Anterior braincase laterally closed by sphenethmoid, anteriorly with a small fenestra. Vomerine teeth medially fused in a central patch, laterally bearing large (0.5 mm) diastemata in the middle of each lateral extension, so that three patches of vomerine teeth are present (one central and two lateral ones). Maxillary teeth small. Otic capsule dorsally partly ossified.

Sternum not ossified. Clavicle thin, not well ossified, curved. Humerus with crista ventralis roughly 60% of its length; crista lateralis weak. Terminal phalanges of fingers and toes with small distal knobs. Phalangeal formula of fingers 2-2-3-3; of toes 2-2-3-4-3. Femur without cristae. Prepollex ossified and relatively small. Prehallux well developed.

Neural spines decreasing in size posteriorly. Dorsal crest of urostyle running roughly 60% along its shaft. Iliosacral articulation type IIA sensu EMERSON (1979). Iliac shafts with almost no dorsal tubercles or oblique grooves; dorsal crests running roughly 90% of their length. Pubis well ossified.

Colour of holotype: After ten years in preservative, light brown dorsally, cream ventrally (Fig. 7). A lighter scapular region bordered anteriorly and posteriorly by darker areas. Dark supratympanic fold running from posterior corner of eye and curving over the tympanum but not reaching the axilla. Large, comma-shaped, dark inguinal spots. Dorsal coloration dissolving increasingly into speckles before fading to cream ventrally. Ventrally immaculate cream posterior to the chin. Chin cream with brown speckling. Cloacal region dark brown. Legs light brown dorsally, cream ventrally. Two dark cross bands on the thigh, one on the shank, one on the tarsus. Posterior side of thighs translu-

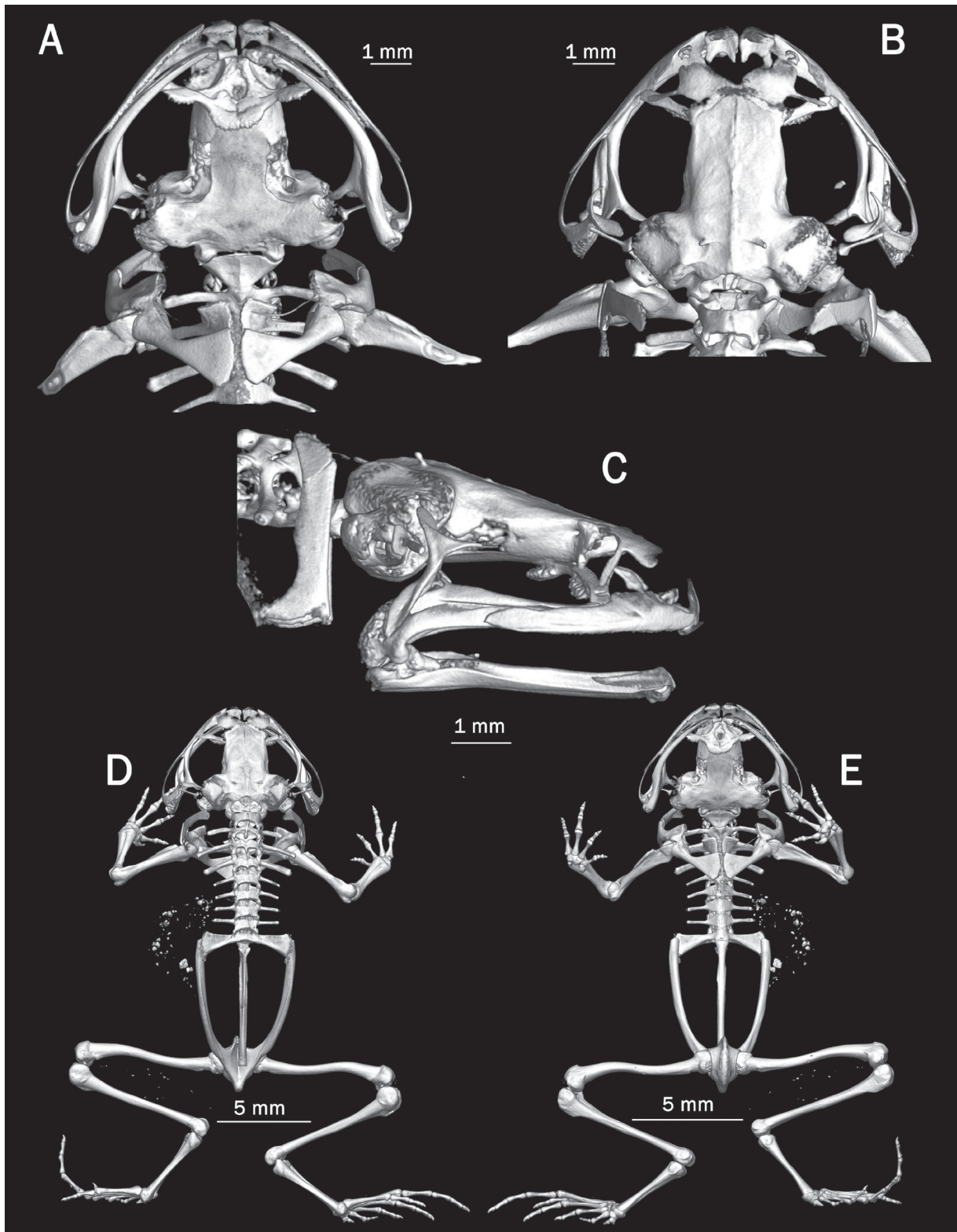
Two new *Rhombophryne* from northeastern Madagascar

Figure 6. Osteology of *Rhombophryne savaka* sp. n. (holotype, ZSM 468/2005) from Marojejy National Park, showing the skull in A) ventral, B) dorsal, and C) lateral views, and the full skeleton in D) dorsal and E) ventral views. See Fig. 2 for bone names. A PDF-embedded 3D model is provided in the supplementary material online.

Results

MARK D. SCHERZ et al.

cent cream. Tarsus with a dark brown posterior face. Sole of foot light brown. Toes light brown with cream stripes anterior to the tips. Arms dorsally light brown with a single cross band on the lower arm, ventrally cream. Fingers lightly striped with cream.

Ecology: The sole two known specimens were captured in pitfall traps in primary rainforest suggesting terrestrial or fossorial habits. No further field observations are available. The gut of the holotype specimen contained the head of a large ant of the genus *Mystrium* (YOSHIMURA & FISHER 2014).

IUCN Red List status: This species is known only from two individuals captured at 746 m a.s.l. in the Marojejy National Park. The location of capture is roughly 600 m from degraded forest to the east, and 4.9 km in a straight line from the edge of the protected area and the forest. Most *Rhombophryne* species are microendemic to narrow altitudinal ranges and areas (WOLLENBERG et al. 2008). As this species occurs in a forest around 746 m a.s.l., it might be less strictly restricted to the Marojejy Massif than higher altitude species (e.g., *R. vaventy* and *R. serratopalpebrosa*), and could possibly be found in other parts of the northern rainforest chain, too. However, as the majority of species of *Rhombophryne* are known from fewer than five localities, we think it unlikely that it occurs in an area much larger than the size of the Marojejy National Park, which is 5975 km². Therefore, due to a projected small extent of occurrence (< 5,000 km²), its being known from just one threatened location and the higher rate of forest alteration at lower altitudes in this area (PATEL & WELCH 2013, RABEARIVONY et al. 2015), this species qualifies as Endangered B1ab(iii) under the IUCN Red List criteria (IUCN 2012).

Etymology: The specific epithet *savaka* is a Malagasy word meaning 'diastema' in reference to the diastemata in the vomerine teeth of this species. It is to be considered a noun in the nominative singular in apposition to the genus name.

Discussion

VIEITES et al. (2009) identified ten candidate species in the genus *Rhombophryne* that were possibly in need of description. This number was increased to twelve by PERL et al. (2014) after the discovery of two new candidate species of this genus from Tsaratanana. Here, we have described candidates *R. sp. Ca2* and *R. sp. Ca4* as *R. botabota* and *R. savaka*, respectively. *Ca5* was described by GLAW et al. (2010) as *R. mangabensis*, *Ca6* by SCHERZ et al. (2014) as *R. vaventy*, *Ca8* by D'CRUZE et al. (2010) as *R. matavy*, and *Ca11* and *Ca12* were described by SCHERZ et al. (2015a) as *R. ornata* and *R. tany*, respectively. We have recently demonstrated that *R. sp. Ca7* probably represents a member of a new genus of miniaturized frogs (SCHERZ et al. in press). Thus, only candidates 1, 3, 9, and 10 still remain to be described. These potential species – and others discovered since the major barcode studies on Madagascar's amphibians (VIEITES et al. 2009, PERL et al. 2014) – will be the subject of a revision of the genus *Rhombophryne* (CROTTINI et al. in prep.). We also anticipate that the status and definition of *R. alluaudi* will likely need to be adjusted in the course of forthcoming revisions. Nevertheless, we here chose to keep the definition of *R. alluaudi* in line with current taxonomy as it was established by BLOMMERS-SCHLÖSSER (1975), who first defined stout microhylids from the Northern Central East of Madagascar (i.e., the region around Andasibe) as being referable to this species.

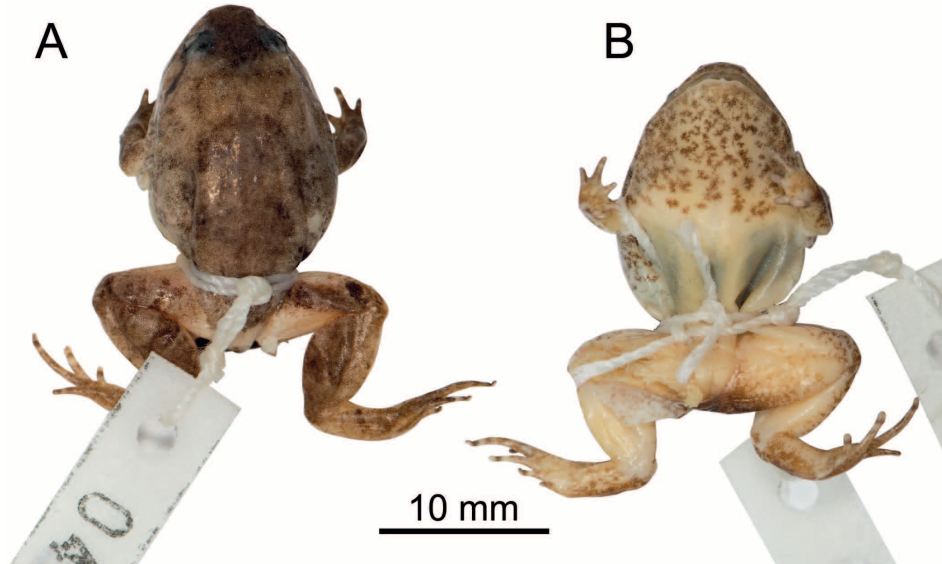


Figure 7. The holotype of *Rhombophryne savaka* sp. n. (ZSM 468/2005) in preservative, in A) dorsal and B) ventral views.

Two new *Rhombophryne* from northeastern Madagascar

The skeletons of microhylids are notoriously variable (NOBLE & PARKER 1926, PARKER 1934, DUELLMAN & TRUEB 1986). *Rhombophryne* has proven to be no exception to this pattern (SCHERZ et al. 2014, 2015a, b, in press). The new species *R. savaka* is sister to *R. mangabensis*, but unlike that species, it possesses fully developed, albeit poorly ossified, clavicles. Three other species, *R. testudo*, *R. matavy*, and *R. coudreaui* also lack clavicles, while all other known members of this genus possess them. Although our 16S rRNA gene fragment phylogeny could not resolve the position of *R. coudreaui*, the monophyly of these three clavicle-lacking species is suggested by their morphology and ecology (GLAW & VENCES 2007, M. D. SCHERZ unpubl. data). *Rhombophryne mangabensis* is related to this group, but clearly more closely to *R. savaka*. Because *R. savaka* possesses clavicles, we may infer that *R. mangabensis* has lost its clavicles independently. It might be tempting to conclude that the most fossorial species of *Rhombophryne* tend to have lost their clavicles, but clavicles are otherwise absent in arboreal taxa of other genera within the Cophylinae (BLOMMERS-SCHLÖSSER & BLANC 1991, RAKOTOARISON et al. 2015, SCHERZ et al. in press), and there is little or no correlation between ecology and pectoral girdle morphology in frogs in general (EMERSON 1984).

The new species *R. botabota* has most often been recovered as being closely related to the *R. alluaudi* complex (VIEITES et al. 2009, PERL et al. 2014), although in SCHERZ et al. (in press) it is recovered as the sister of *R. mangabensis* and another undescribed miniaturized *Rhombophryne* from Andapa, without support. *Rhombophryne botabota* resembles *R. alluaudi* and *R. laevipes* in external morphology, but it is smaller and lacks inguinal ocelli. Like other members of this species complex, *R. botabota* occurs at moderate altitudes. It is remarkable that this species apparently also occupies a moderately large distributional range compared to other members of the genus *Rhombophryne*, although this range is still much smaller than that of *R. laevipes*.

In addition to its morphology, the call of *R. botabota* also closely resembles *R. alluaudi* (VENCES et al. 2006) in that it has long inter-call intervals, a low frequency, an unmodulated note structure, and is emitted during daylight hours from concealed positions in the leaf litter. In these aspects it is also quite similar to those of *R. matavy* and *R. testudo* (VENCES et al. 2006, D'CRUZE et al. 2010), and rather dissimilar to those of *R. mangabensis* and *R. minuta* (VENCES et al. 2006, GLAW et al. 2010). Together, osteology and bioacoustics seem to have a strong potential for taxonomic differentiation within this genus.

Acknowledgements

This research was conducted under multiple permits issued to the authors by the Département d'Eaux et des Forêts over the last two decades of research. R. D. RANDRIANAINA, D. R. VIEITES, F. RATSOAVINA, R. RANDRIANAINA, E. RAJERIARISON, T. RAJOAFIARISON, J. PATTON, G. APREA, and J. E. RANDRIANIRINA helped with fieldwork. Thanks go to J. LUEDTKE and J. ABLE for their as-

sistance with suggestions for Red List assessments. Thanks are due to C. HUTTER and E. Z. LATDENKAMP for their help with bioacoustic analyses, and to A. RAKOTOARISON for helping with Malagasy grammar. Special thanks go to B. SCOTT and M. SCHILTHUIZEN for their help with molluscan identification, and B. Fisher for help with ant identification. The work of MDS was supported by a Wilhelm-Peters Fund grant by the Deutsche Gesellschaft für Herpetologie und Terrarienkunde (DGHT). The work of AC is supported by an Investigador FCT (IF) grant from the Portuguese "Fundação para a Ciencia e a Tecnologia" (IF/00209/2014), funded by Programa Operacional Potencial Humano (POPH) – Quadro de Referencia Estratégico Nacional (QREN) from the European Social Fund.

References

- AmphibiaWeb (2016): Berkeley, California: AmphibiaWeb: Information on amphibian biology and conservation. – Available at <http://amphibiaweb.org/>, accessed 21 February 2016.
- ANDREONE, F., J. E. RANDRIANIRINA, P. D. JENKINS & G. APREA (2000): Species diversity of Amphibia, Reptilia and Lipotyphla (Mammalia) at Ambolokopatrika, a rainforest between the Anjanaharibe-Sud and Marojejy massifs, NE Madagascar. – Biodiversity and Conservation, **9**: 1587–1622.
- Audacity Team (2014): Audacity(R): Free Audio Editor and Recorder. v2.1.0. – Available at <http://audacity.sourceforge.net/>.
- BLOMMERS-SCHLÖSSER, R. M. A. (1975): Observations on the larval development of some Malagasy frogs, with notes on their ecology and biology (Anura: Dyscophinae, Scaphiophryninae, and Cophylinae). – Beaufortia, **24**: 7–26.
- BLOMMERS-SCHLÖSSER, R. M. A. & C. P. BLANC (1991): Amphibiens (première partie). – Faune de Madagascar, **75**: 1–397.
- BRUFORD, M. W., O. HANOTTE, J. F. Y. BROOKFIELD & T. BURKE (1992): Single-locus and multilocus DNA fingerprint. – pp. 225–270 in: HOELZEL, A. R. (ed.) Molecular Genetic Analysis of Populations: A Practical Approach. – IRL Press, Oxford.
- CROTTINI, A., F. GLAW, M. CASIRAGHI, R. K. JENKINS, V. MERCURIO, C. RANDRIANANTANDRO, J. E. RANDRIANIRINA & F. ANDREONE (2011): A new *Gephyromantis* (*Phylacomantis*) frog species from the pinnacle karst of Bemaraha, western Madagascar. – Zookeys, **81**: 51–71. <http://dx.doi.org/10.3897/zookeys.81.1111>.
- D'CRUZE, N., J. KÖHLER, M. VENCES & F. GLAW (2010): A new fat fossorial frog (Microhylidae: Cophylinae: *Rhombophryne*) from the rainforest of the Forêt d'Ambre Special Reserve, northern Madagascar. – Herpetologica, **66**: 182–191, <http://dx.doi.org/10.1655/09-008r1.1>.
- DUELLMAN, W. E. & L. TRUEB (1986): Biology of Amphibians. – John Hopkins University Press, Baltimore.
- EMERSON, S. B. (1979): The ilio-sacral articulation in frogs: form and function. – Biological Journal of the Linnaean Society, **11**: 153–168.
- EMERSON, S. B. (1984): Morphological variation in frog pectoral girdles: Testing alternatives to a traditional adaptive explanation. – Evolution, **38**: 376–388.
- GLAW, F. & M. VENCES (1994): A Fieldguide to the Amphibians and Reptiles of Madagascar. – Vences & Glaw Verlags GbR, Cologne, Germany, 480 pp.
- GLAW, F. & M. VENCES (2007): A Field Guide to the Amphibians and Reptiles of Madagascar. – Vences & Glaw Verlags GbR, Köln, Germany, 496 pp.

Results

MARK D. SCHERZ et al.

- GLAW, F., J. KÖHLER & M. VENCES (2010): A new fossorial frog, genus *Rhombophryne*, from Nosy Mangabe Special Reserve, Madagascar. – *Zoosystematics and Evolution*, **86**: 235–243, <http://dx.doi.org/10.1002/zoos.201000006>.
- IUCN (2012): IUCN Red List Categories and Criteria: Version 3.1. – IUCN, Gland, Switzerland and Cambridge, UK.
- NOBLE, G. K. & H. W. PARKER (1926): A synopsis of the brevicipitid toads of Madagascar. – *American Museum Novitates*, **232**: 1–21.
- PARKER, H. W. (1934): Monograph of the frogs of the family Microhylidae. – Trustees of the British Museum, London, UK.
- PATEL, E. R. & C. WELCH (2013): Marojejy National Park and Anjanaharibe-Sud Special Reserve. – pp. 54–55 in: DAVIES, N. et al. (eds): Lemurs of Madagascar: A Strategy for their Conservation 2013–2016. – IUCN/SSC Primate Specialist Group, Conservation International, Bristol Conservation and Science Foundation.
- PERL, R. G. B., Z. T. NAGY, G. SONET, F. GLAW, K. C. WOLLENBERG & M. VENCES (2014): DNA barcoding Madagascar's amphibian fauna. – *Amphibia-Reptilia*, **35**: 197–206.
- R Core Team (2014): R: A language and environment for statistical computing. – R Foundation for Statistical Computing, Vienna, Austria. – Available at <http://www.R-project.org/>.
- RABEARIVONY, J., M. RASAMOELINA, J. RAVELOSON, H. RAKOTOMANANA, A. P. RASELIMANANA, N. R. RAMINOSOA & J. R. ZAONARIVELO (2015): Roles of a forest corridor between Marojejy, Anjanaharibe-Sud and Tsaratanana protected areas, northern Madagascar, in maintaining endemic and threatened Malagasy taxa. – *Madagascar Conservation & Development*, **10**: 85–92, <http://dx.doi.org/10.4314/mcd.v10i2.7>.
- RAKOTOARISON, A., A. CROTTINI, J. MÜLLER, M.-O. RÖDEL, F. GLAW & M. VENCES (2015): Revision and phylogeny of narrow-mouthed treefrogs (*Cophyla*) from northern Madagascar: integration of molecular, osteological, and bioacoustic data reveals three new species. – *Zootaxa*, **3937**: 61–89, <http://dx.doi.org/10.11646/zootaxa.3937.1.3>.
- RAKOTOMALALA, D. & A. P. RASELIMANANA (2003): Les amphibiens et reptiles des massifs de Marojejy, d'Anjanaharibe-Sud et du couloir forestier de Betaolana. – pp. 146–202 in: GOODMAN, S. M. & L. WILMÉ (eds): Nouveaux résultats d'inventaires biologiques faisant référence à l'altitude dans la région des massifs montagneux de Marojejy et d'Anjanaharibe-Sud. Antananarivo.
- RAMBAUT, A. & A. J. DRUMMOND (2007): Tracer. v1.5. – Available at <http://beast.bio.ed.ac.uk/Tracer>.
- RANDRIAMALALA, H. & Z. LIU (2010): Rosewood of Madagascar: between democracy and conservation. – *Madagascar Conservation & Development*, **5**: 11–22, <http://dx.doi.org/10.4314/mcd.v5i1.57336>.
- RONQUIST, F., M. TESLENKO, P. VAN DER MARK, D. L. AYRES, A. DARLING, S. HÖHNA, B. LARGET, L. LIU, M. A. SUCHARD & J. P. HUELSENBECK (2012): MRBAYES 3.2: Efficient Bayesian phylogenetic inference and model selection across a large model space. – *Systematic Biology*, **61**: 539–542, <http://dx.doi.org/10.1093/sysbio/sys029>.
- SCHERZ, M. D., B. RUTHENSTEINER, M. VENCES & F. GLAW (2014): A new microhylid frog, genus *Rhombophryne*, from northeastern Madagascar, and a re-description of *R. serratopalpebrosa* using micro-computed tomography. – *Zootaxa*, **3860**: 547–560, <http://dx.doi.org/10.11646/zootaxa.3860.6.3>.
- SCHERZ, M. D., B. RUTHENSTEINER, D. R. VIEITES, M. VENCES & F. GLAW (2015a): Two new microhylid frogs of the genus *Rhombophryne* with superciliary spines from the Tsaratanana Massif in northern Madagascar. – *Herpetologica*, **71**: 310–321, <http://dx.doi.org/10.1655/HERPETOLOGICA-D-14-00048>.
- SCHERZ, M. D., A. RAKOTOARISON, O. HAWLITSCHKE, M. VENCES & F. GLAW (2015b): Leaping towards a saltatorial lifestyle? An unusually long-legged new species of *Rhombophryne* (Anura, Microhylidae) from the Sorata massif in northern Madagascar. – *Zoosystematics and Evolution*, **91**: 105–114, <http://dx.doi.org/10.3897/zse.91.4979>.
- SCHERZ, M. D., M. VENCES, A. RAKOTOARISON, F. ANDREONE, J. KÖHLER, F. GLAW & A. CROTTINI (in press): Reconciling molecular phylogeny, morphological divergence and classification of Madagascan narrow-mouthed frogs (Amphibia: Microhylidae). – *Molecular Phylogenetics and Evolution*, <http://dx.doi.org/10.1016/j.ympev.2016.04.019>.
- SUEUR, J., T. AUBIN & C. SIMONIS (2008): Seewave: a free modular tool for sound analysis and synthesis. – *Bioacoustics*, **18**: 213–226.
- TAMURA, K., G. STECHER, D. PETERSON, A. FILIPSKI & S. KUMAR (2013): MEGA6: Molecular Evolutionary Genetics Analysis Version 6.0. – *Molecular Biology and Evolution*, **30**: 2725–2729.
- TRUEB, L. (1968): Cranial osteology of the hylid frog, *Smilisca baudini*. – University of Kansas Publications, Museum of Natural History, **18**: 11–35.
- TRUEB, L. (1973): Bones, frogs, and evolution. – pp. 65–132 in: VIAL, J. L. (ed.) Evolutionary biology of the anurans: Contemporary research on major problems. – University of Missouri Press, USA.
- VENCES, M., F. GLAW & R. MARQUEZ (2006): The Calls of the Frogs of Madagascar. 3 Audio CD's and booklet. – Madrid, Spain, Foneteca Zoológica, 44 pp.
- VIEITES, D. R., K. C. WOLLENBERG, F. ANDREONE, J. KÖHLER, F. GLAW & M. VENCES (2009): Vast underestimation of Madagascar's biodiversity evidenced by an integrative amphibian inventory. – *Proceedings of the National Academy of Sciences of the USA*, **106**: 8267–8272, <http://dx.doi.org/10.1073/pnas.0810821106>.
- WOLLENBERG, K. C., D. R. VIEITES, A. VAN DER MEIJDEN, F. GLAW, D. C. CANNATELLA & M. VENCES (2008): Patterns of endemism and species richness in Malagasy cophyline frogs support a key role of mountainous areas for speciation. – *Evolution*, **62**: 1890–1907, <http://dx.doi.org/10.1111/j.1558-5646.2008.00420.x>.
- YOSHIMURA, M. & B. L. FISHER (2014): A revision of the ant genus *Mystrum* in the Malagasy region with description of six new species and remarks on *Amblyopone* and *Stigmatomma* (Hymenoptera, Formicidae, Amblyoponinae). – *Zookeys*, **394**: 1–99, <http://dx.doi.org/10.3897/zookeys.394.6446>.

Supplementary material

Additional information is available in the online version of this article at <http://www.salamandra-journal.com>

PDF-embedded 3D models of the skeletons of the holotypes of *Rhombophryne botabota* sp. n. and *Rhombophryne savaka* sp. n.

Chapter 7. PAPER: A review of the taxonomy and osteology of the *Rhombophryne serratopalpebrosa* species group (Anura: Microhylidae) from Madagascar, with comments on the value of volume rendering of micro-CT data to taxonomists

In this chapter I present a taxonomic revision of the *Rhombophryne serratopalpebrosa* species group, describing two new species, re-describing *R. guentherpetersi*, and providing an osteological revision of the whole group. The species group is typified by small dermal spines above the eyes, called ‘superciliary spines’, present in all of its members (hitherto overlooked in *R. guentherpetersi*). The revision of this complex was hindered by uncertainty surrounding the identity *R. serratopalpebrosa*. That species remains unavailable for genetic investigation, and the type specimen (the only known specimen) is in poor condition. As in other species of *Rhombophryne* (chapter 6), osteological investigation enabled us to disentangle this complex. Work on it began in 2014 (Scherz et al. 2014, 2015b), and culminated in this paper. By means of a comparative overview of the skeletal anatomy of all eight species in this species group, my colleagues and I show that the osteology of the group is quite conserved, but at least two species, *Rhombophryne coronata* and *R. guentherpetersi*, each have a number of apomorphies that differentiate them from the other species. This paper also provides updates and corrections on previously published osteological information from members of this group, and highlights in particular that some of the previous conclusions (e.g. ossification of the pubis bone) were based on misrepresentation of the anatomy as a result of the technique used to render micro-CT scans. We therefore used this paper as an opportunity to make recommendations about best practice for micro-CT scan rendering.

Scherz, M.D., Hawlitschek, O., Andreone, F., Rakotoarison, A., Vences, M. & Glaw, F. (2017) A review of the taxonomy and osteology of the *Rhombophryne serratopalpebrosa* species group (Anura: Microhylidae) from Madagascar, with comments on the value of volume rendering of micro-CT data to taxonomists. *Zootaxa*, 4273(3):301–340. DOI: 10.11646/zootaxa.4273.3.1

Digital Supplementary Materials on appended CD:

Supplementary Figures 1–12 — PDF-embedded 3D models of skeletal anatomy of species concerned in this paper

<https://doi.org/10.11646/zootaxa.4273.3.1>

<http://zoobank.org/urn:lsid:zoobank.org:pub:4D576A21-DA71-41C2-9408-96BB24B9CFD>

A review of the taxonomy and osteology of the *Rhombophryne serratopalpebrosa* species group (Anura: Microhylidae) from Madagascar, with comments on the value of volume rendering of micro-CT data to taxonomists

MARK D. SCHERZ^{1,6}, OLIVER HAWLITSCHEK^{1,2}, FRANCO ANDREONE³,
ANDOLALAO RAKOTOARISON^{4,5}, MIGUEL VENCES⁴ & FRANK GLAW¹

¹Zoologische Staatssammlung München (ZSM-SNSB), Münchhausenstr. 21, 81247 Munich, Germany.

E-mail: mark.scherz@gmail.com, Frank.Glaw@zsm.mwn.de

²Institut de Biología Evolutiva (CSIC-Universitat Pompeu Fabra), Passeig Marítim de la Barceloneta 37, 08003 Barcelona, Spain,
Email: oliver.hawlitschek@gmx.de

³Museo Regionale di Scienze Naturali, Via G. Giolitti, 36, 10123 Torino, Italy. E-mail: Franco.Andreone@regione.piemonte.it

⁴Division of Evolutionary Biology, Zoological Institute, Technical University of Braunschweig, Mendelsohnstr. 4, 38106 Braunschweig, Germany. E-mail: andomailaka@gmail.com, m.vences@tu-braunschweig.de

⁵Mention Zoologie et Biodiversité Animale, Faculté des Sciences, Université d'Antananarivo, Antananarivo 101

⁶Corresponding author. E-mail: mark.scherz@gmail.com

Abstract

Over the last three years, three new species of saw-browed diamond frogs (*Rhombophryne serratopalpebrosa* species group)—a clade of cophyline microhylid frogs native to northern and eastern Madagascar—have been described. We here review the taxonomy of these frogs based on a new multi-gene phylogeny of the group, which confirms its monophyly but is insufficiently resolved to clarify most intra-group relationships. We confirm *Rhombophryne guentherpetersi* (Guibé, 1974) to be a member of this group, and we re-describe it based on its type series and newly collected material; the species is characterised by small supraciliary spines (overlooked in its original description), as well as large tibial glands and an unusually laterally compressed pectoral girdle. We go on to describe two new species of this group from northern Madagascar: both *R. diadema* sp. nov. from the Sorata Massif and *R. regalis* sp. nov. from several sites in the northeast of the island possess three supraciliary spines, but they are characterised by several subtle morphological and osteological differences. The new species are separated from all known congeners by an uncorrected pairwise distance of at least 5.1% in a ca. 550 bp fragment of the 16S rRNA gene. In order to highlight the significance of the skeleton in the taxonomy of this group, we provide a detailed description of its generalized osteology based on volume-rendered micro-CT scans of all described members, revisiting already-described skeletons of some species, and describing the skeletons of *R. guentherpetersi*, *R. coronata*, and the new taxa for the first time. Use of volume rendering, instead of surface rendering of micro-CT data, resulted in some discrepancies due to the properties of each method. We discuss these inconsistencies and their bearing on the relative value of surface and volume rendering in the taxonomist's toolkit. We argue that, while surface models are more practical for the reader, volumes are generally a more objective representation of the data. Thus, taxonomic description work should be based on volume rendering when possible, with surface models presented as an aid to the reader.

Key words: *Rhombophryne diadema* sp. nov., *Rhombophryne regalis* sp. nov., micro-Computed Tomography, Cophylineae, integrative taxonomy

Introduction

Cophylineae Cope, 1889 is the most diverse of Madagascar's three endemic microhylid subfamilies, with 73 described species (AmphibiaWeb 2017; Lambert *et al.* 2017). Mitochondrial DNA barcoding studies have suggested that the number of described species of this subfamily covers barely half of its total diversity (Vieites *et al.* 2009; Perl *et al.* 2014). More than 70 candidate species were revealed by Andreone *et al.* (2005), Wollenberg *et al.* (2008), Vieites *et al.* (2009), and Perl *et al.* (2014), and although several of these candidates have already been

described in the meantime (e.g. D'Cruze *et al.* 2010; Glaw *et al.* 2010; Köhler *et al.* 2010; Vences *et al.* 2010), the taxonomic gap in this subfamily remains large.

Recently, we have been applying an integrative systematic approach (Dayrat 2005; Padial *et al.* 2008, 2010; Padial & de la Riva 2010) to the resolution of a species complex in the cophyline genus *Rhombophryne* Boettger, 1880 (diamond frogs). The *Rhombophryne serratopalpebrosa* species group (saw-browed diamond frogs), as defined by Scherz *et al.* (2015a), contained numerous morphologically cryptic species, as revealed by DNA barcoding (Vieites *et al.* 2009; Perl *et al.* 2014). Progress resolving this complex had been constrained by the lack of diagnostic external morphological characters and the poor condition of the holotype of *R. serratopalpebrosa* (Guibé, 1975). Only *R. coronata* (Vences & Glaw, 2003) could be described due to its clearly different morphology from *R. serratopalpebrosa* (Vences & Glaw 2003).

X-ray micro-Computed Tomography (micro-CT) scanning allowed us to investigate the osteology of the holotype of *R. serratopalpebrosa* in spite of its poor condition, thereby making available a taxonomically valuable set of characters (Scherz *et al.* 2014). Pairing digital osteological data with mainstream modern data types—DNA sequence data (which remains unavailable from *R. serratopalpebrosa*, but is available from all other members of the group), external morphology, morphometrics, and colouration—has so far resulted in a total of three new species being described from this complex (*R. vaventy* Scherz, Ruthensteiner, Vences & Glaw, 2014, *R. ornata* Scherz, Ruthensteiner, Vieites, Vences & Glaw, 2015, *R. tany* Scherz, Ruthensteiner, Vieites, Vences & Glaw, 2015; see Fig. 1), and phylogenetic analysis of genetic data has suggested that a further species, *R. guentherpetersi* (Guibé, 1974), is also a member of this group (Scherz *et al.* 2016a,b).

This paper concludes our integrative review of the *R. serratopalpebrosa* species group. Here we provide a new multi-gene phylogeny of the group, describe two new species, and re-describe the enigmatic *R. guentherpetersi*. As it has been central to the taxonomy of this group, we provide a detailed osteological description of all of the included species, focussing on differences among species. We take this opportunity to deal with an important issue in the presentation, interpretation, and analysis of micro-CT data, namely visualization methods.

Micro-CT data can be visualised in two quintessentially different ways: isosurfaces (also called ‘isocontouring’ or ‘surface rendering’), which are polygonal single-density meshes used to bound the areas of interest (in our case, typically bone); or volumes (or ‘volume rendering’), which are grey-value varied density clouds of the whole dataset (or a segmented subset of it), where the opacity (and colour) of each three-dimensional pixel (termed ‘voxel’) is set according to its grey value. Until now, most of our work on this genus has been based on surface rendering (Scherz *et al.* 2014, 2015a,b), due to its ease of use—in particular the ability to produce PDF-embedded 3D models that can be examined on demand at a personal computer (Ruthensteiner & Heß 2008). To compare the performance of this method with volume rendering, we analysed volume-rendered data from all members of the *R. serratopalpebrosa* group. We found several significant discrepancies between the two methods, and discuss their implications for taxonomists.

Materials and methods

Specimens were captured by hand or in pitfall traps, euthanized by anaesthetic overdose following approved ethics standards, and fixed in either 96% ethanol or 10% buffered formalin, before transfer to 75% ethanol for storage in research institutions. CRH, DRV, FGZC, ZCMV, and FN refer to the field numbers of Carl R. Hutter, David R. Vieites, Frank Glaw, Miguel Vences, and Franco Andreone, respectively. Institutional abbreviations are: ZSM, Zoologische Staatssammlung München, Munich, Germany; MNHN, Muséum National d'Histoire Naturelle, Paris, France; MRSN, Museo Regionale di Scienze Naturali, Torino, Italy; UADBA, Université d'Antananarivo, Département de Biologie Animale, Antananarivo, Madagascar; AMNH, American Museum of Natural History; KU, Kansas University. All geographic coordinates are given in WGS84.

Micro-computed tomography. X-ray micro-Computed Tomography (micro-CT) scans were produced using a phoenix|x nanotom m cone beam scanner (GE Measurement & Control, Wunstorf, Germany), employing a tungsten target and a 0.1 mm copper filter. Specimens were scanned at a voltage of 140 kV and a current of 80 µA for 2440 projections over 20 or 30 minutes (timing of 500 ms or 750 ms, respectively; one scan of *R. vaventy* was produced with a diamond target and 0.1 mm copper filter, at 60 kV and 120 µA for 2440 projections over 30 minutes). These were reconstructed into 3D volumes in datos|x reconstruction software (GE Measurement &

Results

Control, Wunstorf, Germany), and then converted to 8-bit and exported using VG Studio Max 2.2 (Volume Graphics GMBH, Heidelberg, Germany).

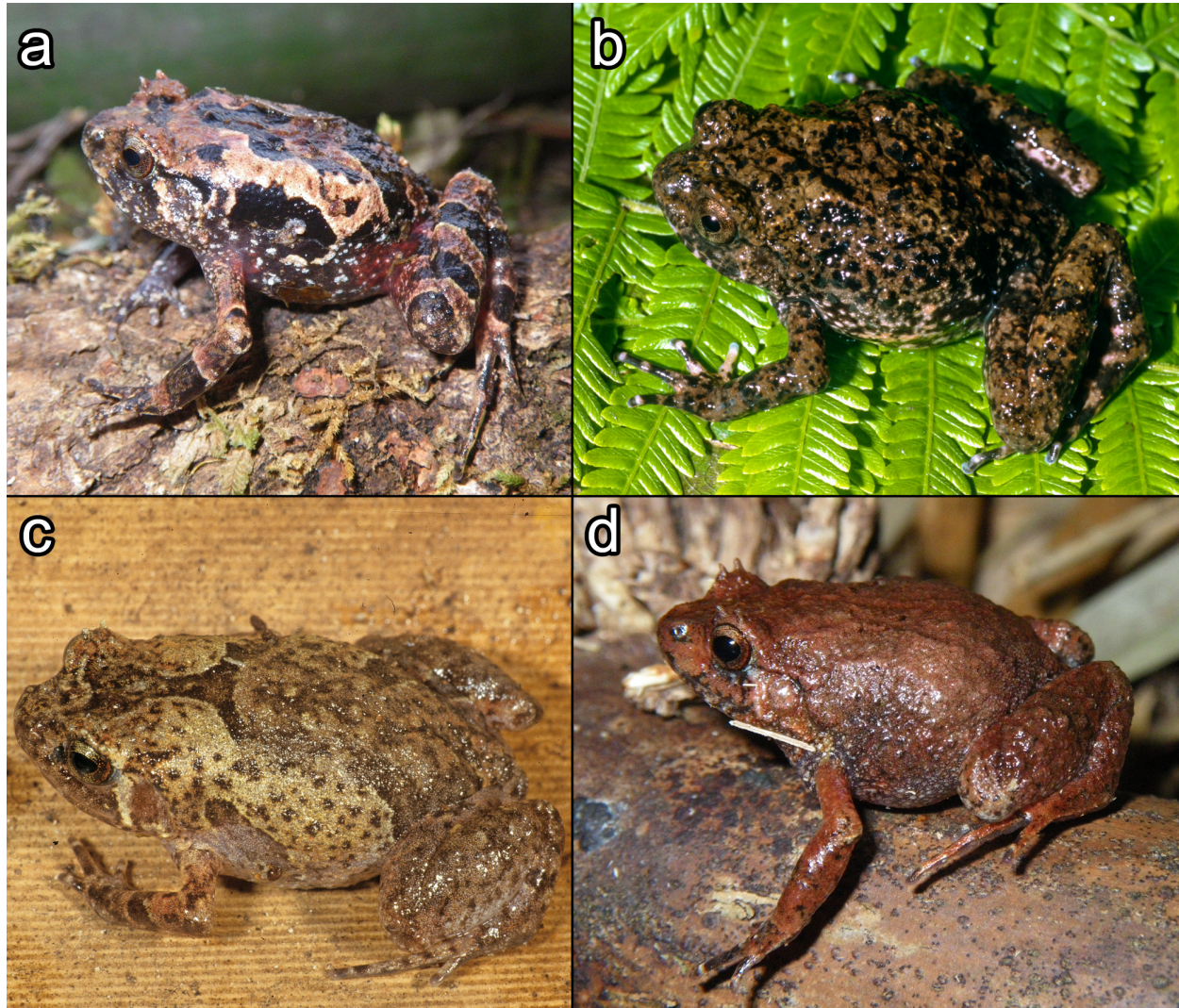


FIGURE 1. Four of the named species from the *Rhombophryne serratopalpebrosa* group. (a) *R. ornata*, (b) *R. vaventy*, (c) *R. coronata*, and (d) *R. tany*. No photos in life of *R. serratopalpebrosa* are available. *Rhombophryne guentherpetersi* is shown in Fig. 6.

Osteological descriptions are based on volumes rendered in VG Studio Max using the phong renderer with a custom preset (available from the corresponding author upon request), adjusted for each scan to reveal the skeleton but not the rest of the matrix. Models were registered using Simple Registration to facilitate their examination. Osteological terminology follows Trueb (1968, 1973), with that of the carpals and tarsals following Fabrezi & Alberch (1996). Measurements were taken from these models using the Calliper Tool to 0.01 mm. Fig. 2 shows the skeletal measurement scheme. Figures were prepared from screenshots taken in orthographic view. Scans with edge and beam-hardening artefacts were refined using local thresholds, clipping planes, and/or segmentation.

Rotational videos of the skeletons were produced using the Animation tools: specimens were visualised in right orthographic view and the animation was produced using the option ‘circle vertical, as seen’. The animation was set to run for 10 s at 12 frames per second and a resolution of 120 dpi. Videos were exported using the Microsoft Video 1 codec, and subsequently compressed with the H.264 codec and the .M4V container in VLC Media Player (VideoLAN Organization, Paris, France). These videos and DICOM image stacks of the scans are deposited at http://morphosource.org/Detail/ProjectDetail>Show/project_id/254. Readers are advised that micro-CT does not render most cartilage. As too few specimens are available for clearing and staining, we have opted to omit cartilage descriptions from our skeletal descriptions below.

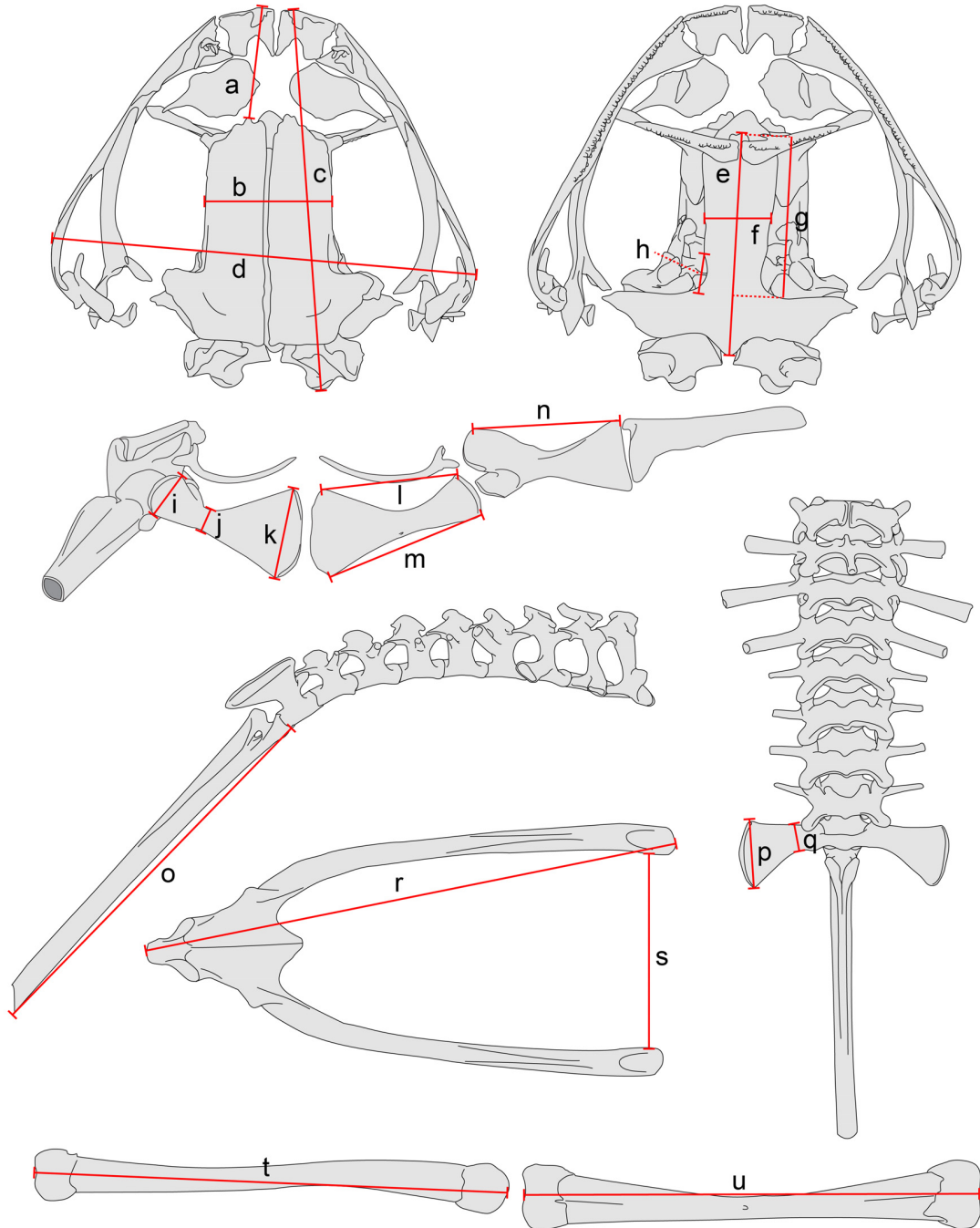


FIGURE 2. Definition of skeletal measurements taken for this study: (a) snout length, from the anterior frontoparietal to the anterior premaxilla; (b) brain case width, at mid-orbit; (c) skull length, from occipital condyle of exoccipital to the anterior premaxilla; (d) maximum skull width, typically at the middle of the quadratojugal (not landmark-based); (e) parasphenoid length; (f) parasphenoid width, at mid-orbit; (g) length of parasphenoid cultriform process; (h) distance from parasphenoid alae to waist of cultriform process (the waist being a distinct discontinuity in the angle of expansion of the cultriform process); (i) coracoid width at glenoid socket; (j) coracoid width at thinnest point; (k) coracoid width at sternal end; (l) length of anterior edge of coracoid; (m) length of posterior edge of coracoid; (n) length of anterior face of scapula, (o) length of urostyle; (p) distal width of sacral diapophysis; (q) base width of sacral diapophysis; (r) length of acetabulum; (s) distance between anterior tips of iliac shafts; (t) length of femur from condyle to condyle; (u) length of tibiofibula from condyle to condyle. Not to scale.

Results

Surface models of scans were made in Amira 5.4.5 or 6.0 (FEI Visualisation Sciences Group, Burlington, MA, USA), and refined using local manual thresholding and segmentation. These were embedded into portable document files (PDFs) using Adobe® 3D Toolkit and Adobe® Acrobat Pro XI, essentially following Ruthensteiner & Heß (2008). These PDFs are provided as supplementary 3D models (Figs S1–S12).

External morphological measurements. Morphometric data were produced using a digital calliper to 0.01 mm, rounded to the nearest 0.1 mm (note: ratios were calculated using non-rounded values and subsequently rounded). We measured the following characters: SVL (snout–vent length), HW (maximum head width), HL (head length, from the maxillary commissure to the snout tip. Note: this is measured along the jaw, and not parallel to the longitudinal axis of the animal), ED (horizontal eye diameter), END (eye–nostril distance, from the anterior eye to the posterior of the naris), NSD (nostril–snout tip distance, from the centre of the naris), NND (internarial distance, from the centre of each naris), TDH (horizontal tympanum diameter), TDV (vertical tympanum diameter), HAL (hand length, from the carpal–radioulnar articulation to the tip of the longest finger), LAL (lower arm length, from the carpal–radioulnar articulation to the radioulna–humeral articulation), UAL (upper arm length, from the radioulna–humeral articulation to the trunk, measured along the posterior aspect of the arm), FORL (forelimb length, given by the sum of HAL, LAL, and UAL), FOL (foot length, from the tarsal–metatarsal articulation to the tip of the longest toe), TARL (tarsal length, from the tarsal–metatarsal articulation to the tarsal–tibiofibular articulation), FOTL (foot length including tarsus, given by the sum of FOL and TARL), TIBL (tibiofibula length, from the femoral–tibiofibular articulation to the tarsal–tibiofibular articulation), TIBW (maximum tibiofibula [=shank] width), THIL (thigh length, from the vent to the femoral–tibiofibular articulation), THIW (thigh width at thickest point, measured in supine position), HIL (hindlimb length, given by the sum FOL, TARL, TIBL, and THIL), IMCL (maximum length of inner metacarpal tubercle), IMTL (maximum length of the inner metatarsal tubercle). For a figure of the application of this scheme, readers are referred to Scherz *et al.* (2015b); for the sake of consistency, we here retain the abbreviations we have used previously instead of those proposed by Watters *et al.* (2016). A table including all morphological measurements is provided as Appendix 1.

DNA sequencing. We extracted total genomic data from tissue samples stored in 99% ethanol using proteinase K (final concentration 1 mg/mL). DNA was isolated using a standard salt extraction protocol (Bruford *et al.* 1992). We used previously published sequences of the mitochondrial genes for cytochrome c oxidase subunit 1 (*cox1*) and 16S rRNA (16S, two separate non-overlapping segments) as summarized by Scherz *et al.* (2016b), and we complemented these by additional sequencing of previously unrepresented taxa. Furthermore, for several representatives of the *R. serratopalpebrosa* group we sequenced a segment of the nuclear gene for sacsin (*sacs*). DNA segments were amplified for the 5'-terminus of 16S using primers 16S-L3 and 16S-AH (Vences *et al.* 2003); for the 3'-terminus of 16S using primers 16Sar-L and 16Sbr-H (Palumbi *et al.* 1991); for *cox1* using primers dgLCO1490 and dgHCO2198 (Meyer *et al.* 2005), and for *sacs* using a nested PCR approach with the primer pairs SACS2/SACSR2 and SACS2/SACSNR2 of Shen *et al.* (2012). PCR conditions followed Vences *et al.* (2003) for 16S, Perl *et al.* (2014) for *cox1*, and Shen *et al.* (2012) for *sacs*.

Sequences were resolved using an ABI 3130xl automated DNA sequencer (Applied Biosystems) and deposited in GenBank (accession numbers KY748094–KY748115). Sequences were error-checked in CodonCode Aligner v. 5.1.4 (CodonCode Corp.) and aligned using the MUSCLE algorithm (Edgar 2004) in MEGA 7 (Kumar *et al.* 2016). Sequences of *cox1* and *sacs* were translated into amino acids for confirmation. All hypervariable regions of the 16S gene were conservatively excluded from analysis; exploratory analyses however showed that retention of these stretches resulted in an identical topology and similar support. Our matrix included all available samples of the *R. serratopalpebrosa* group from the analysis of Scherz *et al.* (2016b), complemented by sequences of various additional individuals of this group. Because *Stumpffia* is the sister taxon of *Rhombophryne* (Scherz *et al.* 2016b), we used *Stumpffia psologlossa* (the type species of *Stumpffia*) as the outgroup, and also added sequences from Scherz *et al.* (2016b) of all *Rhombophryne* not belonging to the *R. serratopalpebrosa* group to the analysis, to serve as hierarchical outgroups.

We used PartitionFinder v. 1.1.1 (Lanfear *et al.* 2012) to determine partitions and substitution models for our data set and ran a partitioned Bayesian Inference (BI) analysis in MrBayes 3.2 (Ronquist *et al.* 2012). Two independent runs of 20 million generations, each comprising four Markov chains (three heated and one cold), were sampled every 10,000 generations. Mixing and stationarity were assessed by examining the standard deviation of split frequencies and plotting the -lnL per generation using Tracer v1.5 software (Rambaut & Drummond 2007). The runs were combined to obtain a 50%-majority-rule consensus tree, with 25% of generations discarded as burn-in (all compatible nodes with probabilities > 0.5 kept).

Results

The concatenated alignment of four segments of three genes (*16S*, *cox1*, *sacs*) used for analysis consisted of 2491 nucleotide characters. Of these, 581 were variable and 406 of these were parsimony informative. Most new sequences used for this study were added for species of the *R. serratopalpebrosa* species group only. As expected, the relationships among other *Rhombophryne* were insufficiently resolved and are, therefore, neither shown nor further discussed here; see Scherz *et al.* (2016b) for a complete tree including these species. The *R. serratopalpebrosa* group was found to form a highly supported monophyletic group within the genus *Rhombophryne* (Fig. 3). The tree also confirms *R. longicrus* Scherz, Rakotoarison, Hawlitschek, Vences & Glaw, 2015 and *R. minuta* (Guibé, 1975) as forming a clade that is sister to the *R. serratopalpebrosa* species group (as previously suspected; see Scherz *et al.* 2015b, 2016b). The *R. serratopalpebrosa* group contains all *Rhombophryne* species with distinct supraocular spines, as well as *R. guentherpetersi*, a species in which these spines are quite small and not obvious at first glance, thereby confirming the phylogenetic placement of this species by Scherz *et al.* (2016a,b).

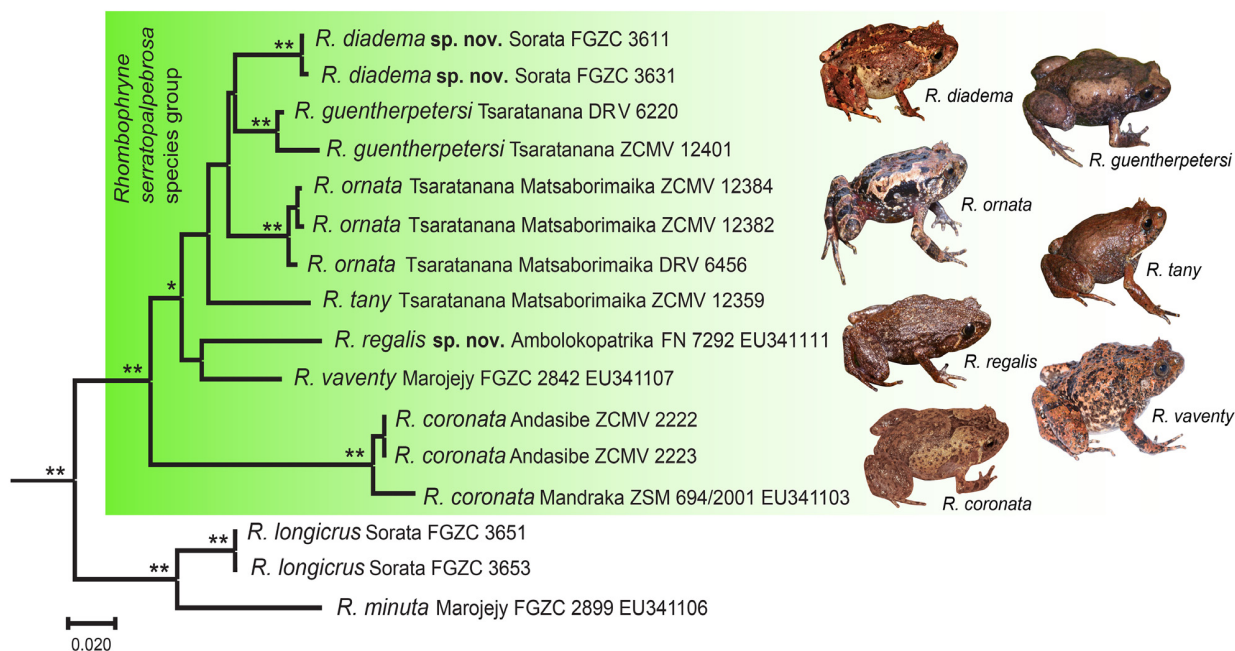


FIGURE 3. Majority-rule consensus tree of the *Rhombophryne serratopalpebrosa* species group and its sister clade, obtained by partitioned BI analysis, based on 2491 nucleotide characters of two mitochondrial and one nuclear gene (*16S*, *cox1*, *sacs*). Asterisks indicate Bayesian posterior probability values (*0.95–0.98, **0.99–1.0; not shown if <0.95). *Stumpffia psologlossa* and other species of *Rhombophryne* were used as hierarchical outgroups and are here excluded from the figure as they are not the subject of this study. Members of the *R. serratopalpebrosa* species group are depicted in life, not to scale.

Genetic data are not available from *R. serratopalpebrosa* itself. However, monophyly of all species of *Rhombophryne* with supraocular spines has been recovered strongly and consistently here and in previous studies (e.g. Scherz *et al.* 2016b), which provides strong support for our assignment of *R. serratopalpebrosa* to this group. Furthermore, other morphological similarities between it and the other members of the group, such as the presence of an S-shaped fold posterior to the nostril (otherwise found only in a new species described below), and relatively long limbs and feet without a strongly rounded body shape (typical of most members of the *R. serratopalpebrosa* species group but also its sister clade *R. minuta*+*R. longicrus*), support this assignment. A more extensive analysis of the morphological (including osteological) and morphometric similarities of various different species clusters in the genus *Rhombophryne* will be included in a forthcoming study.

Within the *R. serratopalpebrosa* species group, *R. coronata* is confirmed as the sister taxon to all other species, but all other interspecific relationships are poorly resolved. For instance, despite a high genetic similarity of *R. guentherpetersi* with *R. ornata* in one *16S* segment (see below), these two species were not resolved as sister

Results

species. Exploratory single-gene analyses suggest a possible mitochondrial-nuclear gene tree discordance causing the poor resolution within the group: the mitochondrial genes suggest a close relationship between *R. guentherpetersi*, *R. ornata*, and *R. tany*, whereas the single nuclear gene *sacs* places *R. guentherpetersi* basal to a clade containing *R. ornata*, *R. tany*, and a new species from Sorata described below (not available for the remaining species).

All species of the *R. serratopalpebrosa* group for which multiple individuals were available were resolved, respectively, as monophyletic groups (Fig. 3) and these were distinguished from each other by substantial genetic distances. In the 3'-terminal segment of *16S* used by Vieites *et al.* (2009) to define candidate species of Malagasy frogs, all species differed by >4% uncorrected pairwise distance (Table 1), except for *R. guentherpetersi* and *R. ornata*, which had only 2.4–3.4% distance. However, this probably just reflects a coincidental and rare similarity between two distinct species, given that in the second *16S* segment their pairwise distances amounted to 5.0–7.2%. Pairwise distances in *cox1*, among the species for which this gene was sequenced, ranged from 5.8–11.6% (Table 1). None of the species sequenced for *sacs* (*R. coronata*, *R. guentherpetersi*, *R. ornata*, *R. tany*, *R. vaventy*, and the new species from Sorata described below) shared haplotypes of this nuclear gene.

Two lineages were found to be genetically distinct from all nominal species. We describe these as new species due to the congruence of their large genetic distances with morphological differences. Furthermore, we provide a re-description of the poorly known *R. guentherpetersi*, which both the mitochondrial and the nuclear data support as reliably embedded within the *R. serratopalpebrosa* group.

TABLE 1. Uncorrected p-distances (in percent) in the ca. 550 bp 3'-terminal segment of the *16S* gene (lower diagonal) and in a ca. 600 bp segment of the *cox1* gene (upper diagonal). Grey cells are within-group distances in *16S*. Note that not all available sequences were included in the comparisons because some sequences of much shorter length were excluded. NA, not applicable (due to missing sequences for distance calculation).

	<i>R. c.</i>	<i>R. d.</i>	<i>R. g.</i>	<i>R. o.</i>	<i>R. r.</i>	<i>R. t.</i>	<i>R. v.</i>
<i>Rhombophryne coronata</i> (N=1)	NA	NA	10.3%	11.6%	NA	11.4%	11.4%
<i>Rhombophryne diadema</i> sp. nov. (N=2)	9.1%	0.0%	NA	NA	NA	NA	NA
<i>Rhombophryne guentherpetersi</i> (N=2)	8.1–8.5%	5.1–5.3%	0.8%	5.8%	NA	7.7%	6.7%
<i>Rhombophryne ornata</i> (N=2)	9.2–9.4%	5.5–5.6%	2.4–3.4%	0.2%	NA	8.4%	7.4%
<i>Rhombophryne regalis</i> sp. nov. (N=1)	8.1%	5.9%	6.1–6.6%	6.1–6.3%	NA	NA	NA
<i>Rhombophryne tany</i> (N=1)	8.6%	5.4–5.5%	4.4–4.5%	3.8–4.1%	6.7%	NA	7.4%
<i>Rhombophryne vaventy</i> (N=1)	9.4%	6.9%	5.2–6.0%	4.9–5.1%	6.7%	7.3%	NA

Taxonomic accounts

Rhombophryne guentherpetersi (Guibé, 1974)

Common name: Tsaratanana saw-browed diamond frog (modified from Frank & Ramus 1995) (Figs 4–7, S1–S2)

Mantipus guentherpetersi Guibé, 1974: 1181–1182

Plethodontohyla guentherpetersi—Blommers-Schöller & Blanc, 1991: 56–57. First depicted in life under this name in Stuart *et al.* (2008).

Rhombophryne guentherpetersi—Glaw & Vences, 2007: 118. The photo provided on page 119 of this book is misattributed and depicts an undescribed species (Scherz *et al.* unpubl. data).

Holotype. MNHN 1953.165, an adult female specimen captured by an unknown collector on an unknown date on the Tsaratanana Massif at 2600 m a.s.l. (Figs 4, 5, S2)

Paratypes. MNHN 1953.165A and MNHN 1953.165B, a juvenile and adult female with the same collection data as the holotype. MNHN 1973.592 and MNHN 1973.593, a subadult female and juvenile collected by Charles P. Blanc in 1966 on Mission ORSTOM from the same location as the holotype.

Referred specimens. ZSM 606/2014 (DRV 6220), a female, ZSM 607/2014 (DRV 6223), a male, and ZSM 608/2014 (DRV 6231), a female (Fig. S1), three adult specimens collected by D. Vieites, M. Vences, R.D.

Randrianiaina, F.M. Ratsoavina, S. Rasamison, A. Rakotoarison, E. Rajeriarison, F. Randrianasolo, F. Randrianasolo and T. Rajoafiarison, ZSM 606/2014 and 607/2014 on the 16th of June 2010 at Andranomadio (camp 4), Tsaratanana, 14.0801°S, 48.9854°E, 2503 m a.s.l.; ZSM 608/2014 on the 18th of June 2010 at a site on the Tsaratanana mountain 14.0665°S, 48.9832°E, 2732 m a.s.l. A further three specimens from Andranomadio (with same collecting data as ZSM specimens from this site) were deposited in the UADBA collection: UADBA-A 60775 (DRV 6210) and UADBA-A 60776 (ZCMV 12401), adults; UADBA-A 60782 (ZCMV 12435), subadult.

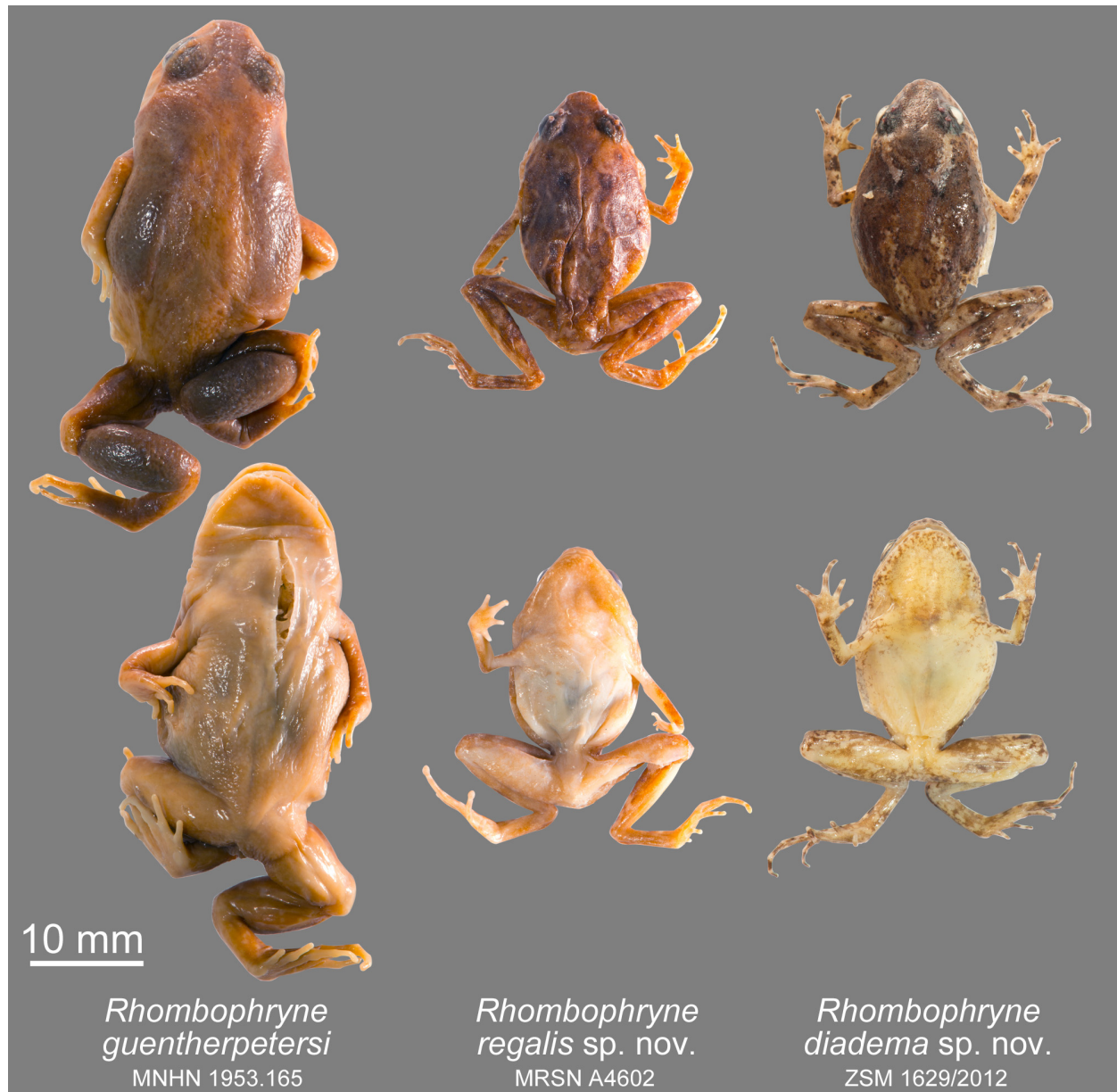


FIGURE 4. Photographs of the holotypes of the species treated in this manuscript, in dorsal (top row) and ventral (bottom row) views.

Diagnosis and comparisons. *Rhombophryne guentherpetersi* is a member of the genus *Rhombophryne* on the basis of molecular phylogenetic affinities (Fig. 3) and the possession of a clavicle combined with the absence of T- or Y-shaped terminal phalanges (vs. either absence of a clavicle or possession of a clavicle combined with T- or Y-shaped terminal phalanges in the morphologically similar *Plethodontohyla* Boulenger, 1882). Within the genus *Rhombophryne*, it is assigned to the *R. serratopalpebrosa* species group on the basis of possessing supraciliary spines and of molecular phylogenetic affinities (Fig. 3, Table 1).

Rhombophryne guentherpetersi is distinguished from all other described congeners by the following unique

Results

suite of characters: adult SVL 27.3–35.7 mm; TDH/ED = 0.45–0.66; a weak supratympanic fold running from the rear corner of the eye to curve slightly over and behind the tympanum toward the axilla; two or three small supraciliary spines; distinct, raised dorsolateral glands, and bulbous tibial glands. The pectoral girdle is distinctly narrower than that seen in its congeners (see Fig. 7; 8.2–9.4% of SVL). Furthermore, *R. guentherpetersi* is separated from all other *Rhombophryne* species except *R. ornata* and *R. serratopalpebrosa* by uncorrected pairwise distances of at least 4.4% in a segment of the 16S rRNA mitochondrial gene (see Table 1; no molecular data available for *R. serratopalpebrosa*)—for distinction from *R. ornata*, see below.

Rhombophryne guentherpetersi is distinguished from all *Rhombophryne* species except the *R. serratopalpebrosa* group by the possession of supraciliary spines, and from all members of this group, and indeed all cophyline microhylids, by the possession of bulbous tibial glands. Genetically, *R. guentherpetersi* is very closely related to *R. ornata*—they are separated by just 2.4–3.4% in one fragment of the 16S gene (see Table 1), which is lower than our standard threshold for candidate species recognition (Vieites *et al.* 2009). However, the two species are highly morphologically distinct, differing not just in the presence or absence of tibial glands, but also in the shorter relative hindlimb length of *R. guentherpetersi* (HIL/SVL 1.33–1.45 vs. 1.46–1.64), tibiotarsal articulation reaching the axilla or tympanum (vs. between the tympanum and the eye), absence (vs. presence) of red colouration in the inguinal region, partially ossified limb epiphyses and carpals (vs. unossified), and much narrower pectoral girdle (length of coracoid <10% of SVL vs. >12%; see Fig. 7). A differential diagnosis from all other cophyline microhylids is unnecessary because the tibial glands allow easy unambiguous distinction. These are noticeable, if not well developed, even in subadults.

Re-description of the holotype. (Figs 4, 5) An adult female specimen in moderately good state of preservation. Ventral incision and left lateral incision present.



FIGURE 5. Comparative morphology of the heads, feet, and hands of members of the *Rhombophryne serratopalpebrosa* species group. All specimens are the holotypes of their respective species, except *R. coronata*, which is paratype ZSM 694/2001. Asterisks indicate mirrored images. Not to scale.

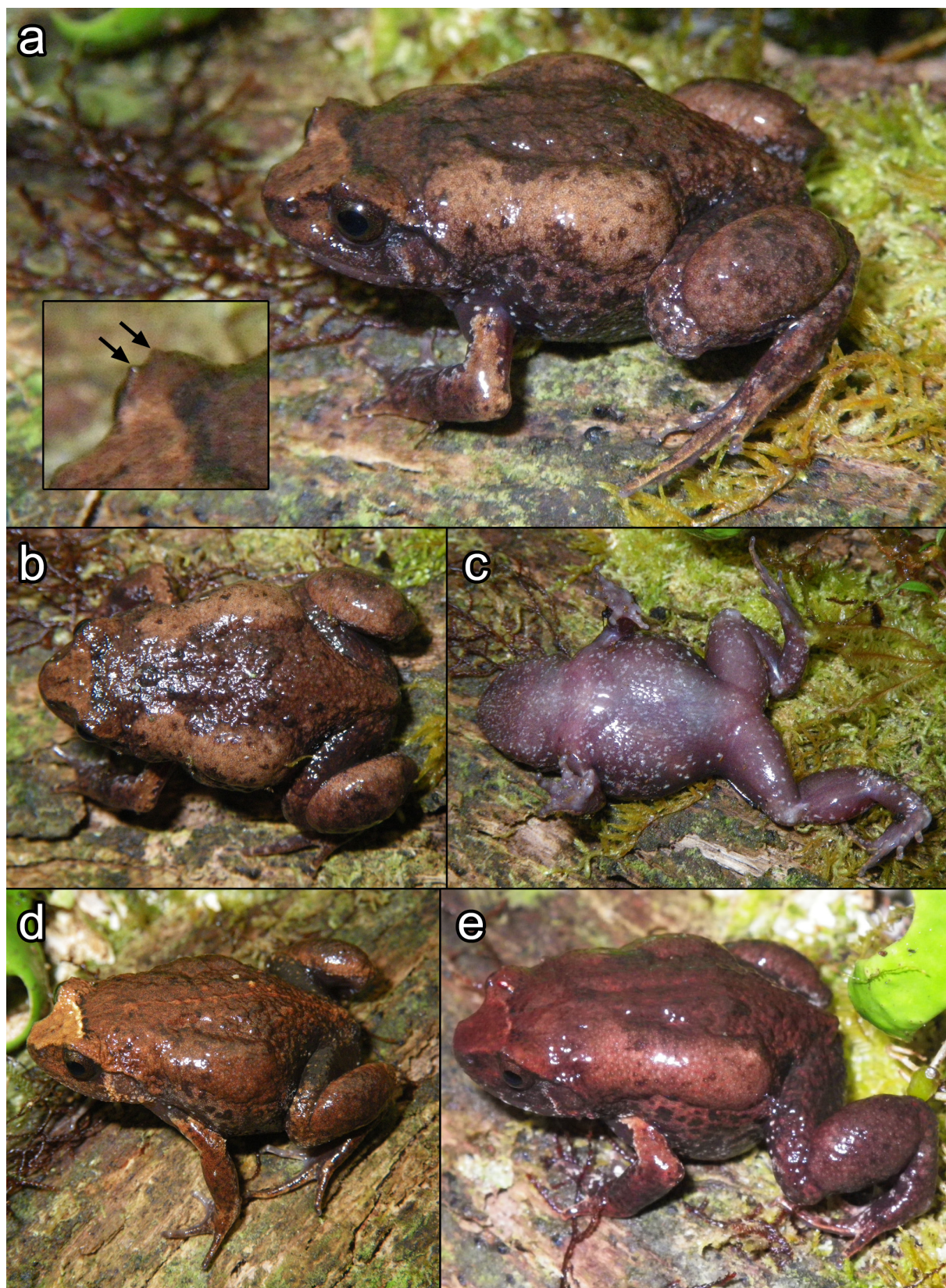


FIGURE 6. *Rhombophryne guentherpetersi* in life. (a–c) ZSM 607/2014 in (a) dorsolateral (with inset showing superciliary spines), (b) dorsal, and (c) ventral view; and (d, e) other specimens in dorsolateral view (assignment to field and collection numbers unknown).

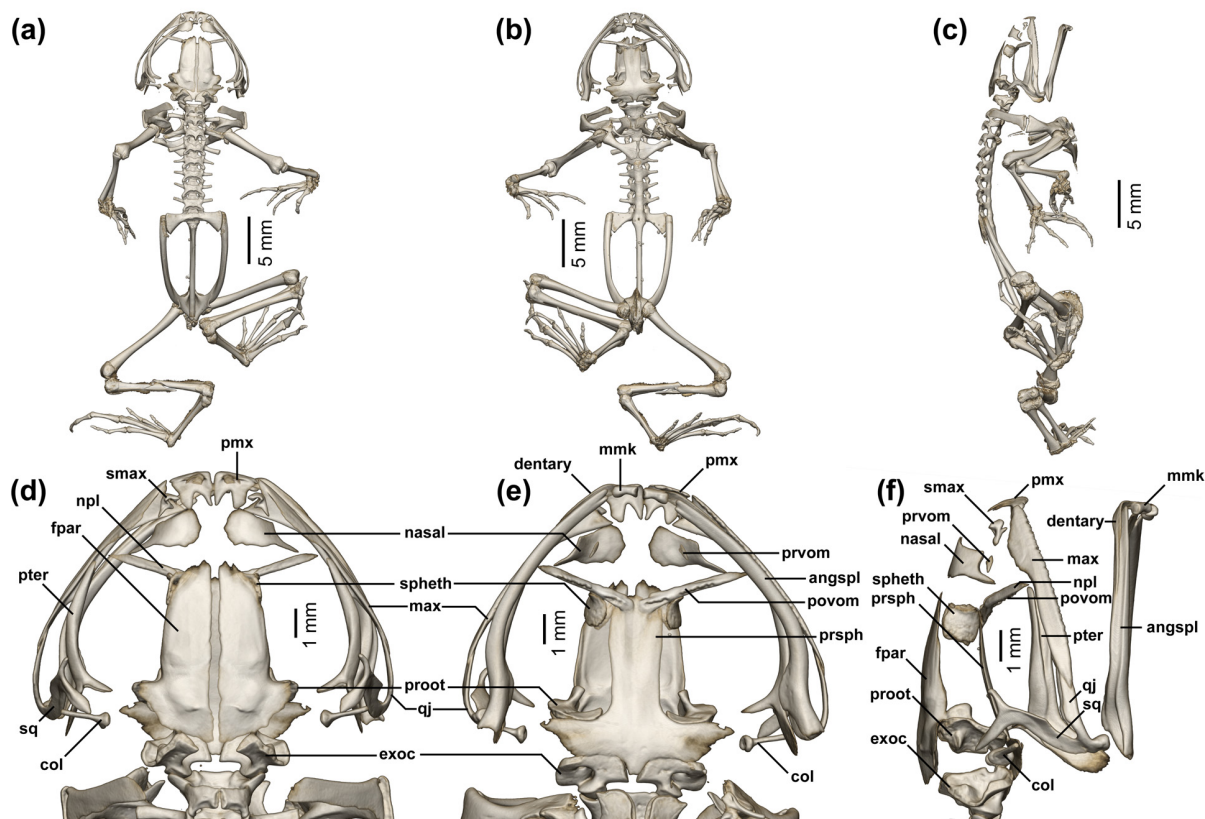


FIGURE 7. Osteology of *Rhombophryne guentherpetersi* (MNHN 1953.165). Full skeleton in (a) dorsal, (b) ventral, and (c) lateral view; skull in (d) dorsal, (e) ventral, and (f) lateral view. Abbreviations: angspl = angulosplenial, col = columella, exoc = exoccipital, fpar = frontoparietal, max = maxilla, mmk = mentomeckelian, npl = neopalatine, pmx = premaxilla, povom = postchoanal vomer, proot = prootic, prvom = prechoanal vomer, prsph = parasphenoid, pter = pterygoid, qj = quadratojugal, smax = septomaxilla, spheth = sphenethmoid, sq = squamosal.

Body robust. Head wider than long (HW/HL = 1.35). Pupils horizontally oval. Snout rounded in dorsal and lateral views. Canthus rostralis concave. Loreal region concave. Nostrils nearer to snout tip than to eye (END/NSD = 1.24), directed laterally, slightly protuberant. Tympanum distinct, TDH/ED = 0.47. Weak supratympanic fold, from middle rear of eye curving slightly over and behind tympanum toward the axilla. Two small superciliary spines above each eye. Vomerine teeth present, curved, not meeting at the midline.

Arms robust. Fingers without webbing; relative lengths 1<2<4<3, fourth finger distinctly longer than second; finger tips not expanded; fingers not reduced; nuptial pads absent; inner metacarpal tubercle present, outer metacarpal tubercle divided, faint; subarticular tubercles distinct, undivided. Hindlimbs short and thick; tibiotarsal articulation reaches the axilla; TIBL/SVL = 0.35. Strongly developed tibial glands cover almost the entirety of the dorsal tibia. Inner metatarsal tubercle present, enlarged, outer metatarsal tubercle absent. Toes unwebbed; relative lengths 1<2<5<3<4, fifth toe distinctly shorter than third. Toe tips not expanded.

Dorsal skin slightly granular except on the head, where it is slightly rougher, with a slightly raised ridge on the midline of the head. Dorsolateral folds absent. A porous glandular formation extends from the suprascapular region to the inguinal region on either side of the body. Ventral skin smooth.

Colouration of the holotype: (Figs 4, 5) Light reddish-brown above with irregular small dark speckling. Loreal and tympanic regions lighter than dorsal head, without speckling. Glandular formations on tibiae and dorsum darker brown, as are the anterior surfaces of head and above eyes. Flanks fading from dorsal colour to ventral colour. Venter uniformly tan to cream. Limbs coloured as the dorsum.

Variation. The type series is composed of two juveniles, one subadult, and one poorly preserved adult, in addition to the holotype. Our newly added material consists of three well-preserved adults, including the first male specimen. All specimens, including the juveniles, possess superciliary spines, but they are small and variable in

number, and in poorly preserved specimens cannot be well distinguished (but can be distinguished in life; see Fig. 6). ZSM 606/2014 has three supraciliary spines, whereas all other specimens have two. The paratype MNHN 1953.165B is darker than the rest of the type series and has much rougher skin (but is also particularly poorly preserved). All specimens, including the juveniles, have tibial glands, but these are less bulbous in the juveniles and subadult, becoming large only in the adults (confirming that all members of the type series are indeed conspecifics). The one male specimen is smaller than the adult females, but is in all other aspects highly similar in morphology (see Appendix 1). The tibiotarsal articulation reaches either the axilla or the tympanum. A prepollex is well developed in the one available male specimen, ZSM 607/2014. The species may have some degree of sexual size dimorphism, as the only male specimen is slightly smaller than all adult female specimens available (27.3 vs. 28.9–35.7 mm).

Colouration is relatively homogeneous, but shade and pattern differ somewhat (Fig. 6). The newly collected specimens are much darker brown in colour than the type series, but generally have commonalities to their colour patterns: a pair of blackish oblong markings above the suprascapular region (Fig. 6). These markings are present only in one member of the type series (MNHN 1973.592). The lateral body has several dark-brown flecks. These are present in all of the paratypes but not in the holotype. The venter is mottled dark and light brown in some specimens but is almost solid dark brown in others. A light brown interocular bar is sometimes present, anterior to which the snout is typically lighter brown than the dorsum. The dorsolateral glands can also be this light brown, or they can be continuous with the rest of the dorsum.

Remarks. The following inconsistencies exist between our re-description and the original description of this species by Guibé (1974): Supraciliary spines are present; these were apparently overlooked in his description. Tibiotarsal articulation was given as reaching the eye. This could not be verified in any member of the type series except the poorly preserved paratype MNHN 1973.592, the vertebral column of which is inverted (i.e. convex instead of concave), possibly misleading tibiotarsal articulation. The holotype is 10 mm longer than described (34.6 mm vs. 25 mm). Guibé (1974, 1978) stated that the prepollex was developed in males, but the type series does not contain any males. Nevertheless, we have confirmed this observation with a newly collected male specimen (see Variation above).

Natural history. At Andranomadio, specimens were found during the day in high-altitude rainforest with rather open canopy (2503 m a.s.l.), burrowed several centimetres deep in the ground. Another individual (ZSM 608/2014) was collected above the treeline (2732 m a.s.l.), in an area of grassland with some scattered heath, hidden under a stone during the day.

Distribution and conservation status. *Rhombophryne guentherpetersi* is currently listed in the IUCN Red List as Endangered under criterion B1ab(iii) (IUCN SSC Amphibian Specialist Group 2016a), meaning an extent of occurrence of $< 5000 \text{ km}^2$ (B1), a severely fragmented habitat or known from ≤ 5 locations (a), and an observed, estimated, inferred, or projected on-going decline in the area, extent and/or quality of habitat (b(iii)). At present, *R. guentherpetersi* is known only from the Tsaratanana Massif. The exact collecting locality of the type specimens is not clear (Guibé 1974), but three specimens were collected on a recent expedition to the Tsaratanana Massif (ZSM 606–607/2014 at 14.0801°S, 48.9854°E at 2503 m a.s.l; ZSM 608/2014 at 14.0665°S, 48.9832°E, 2732 m a.s.l.; Fig. 8). These two localities are well inside the protected area of Tsaratanana Strict Nature Reserve, to which only researchers and conservation workers are permitted access. Although it is possible that the species may occur in the forest corridor between Marojejy and Tsaratanana (COMATSA; see Rabearivony *et al.* 2015), which is pending official protected status, we consider this unlikely: we suspect that *R. guentherpetersi* is found only at high elevations, possibly near to and above the tree line, which in Tsaratanana is around 2550 m a.s.l. No part of the COMATSA corridor exceeds 2300 m a.s.l. The likely extent of occurrence of this species is therefore limited to an area of 36.4 km². Deforestation and habitat degradation pressure at such high altitude is minimal relative to the lower reaches of the forest, especially due to the strict conservation status of this forest. However, it is not free from threats: Climate change may be a significant factor for species living near the tops of mountains, as their niche space diminishes with rising temperatures. Fires in the high mountain grassland could swiftly eradicate the suitable open habitat and leave only forest habitat available. To balance (1) the small range of this species, (2) the highly protected status it enjoys, and (3) the threats that persist despite this protection, we propose to maintain a status of Endangered B1ab(iii) (IUCN 2012), but encourage further surveys within COMATSA and Tsaratanana Strict Nature Reserve in order to better understand the distribution and ecology of this species.

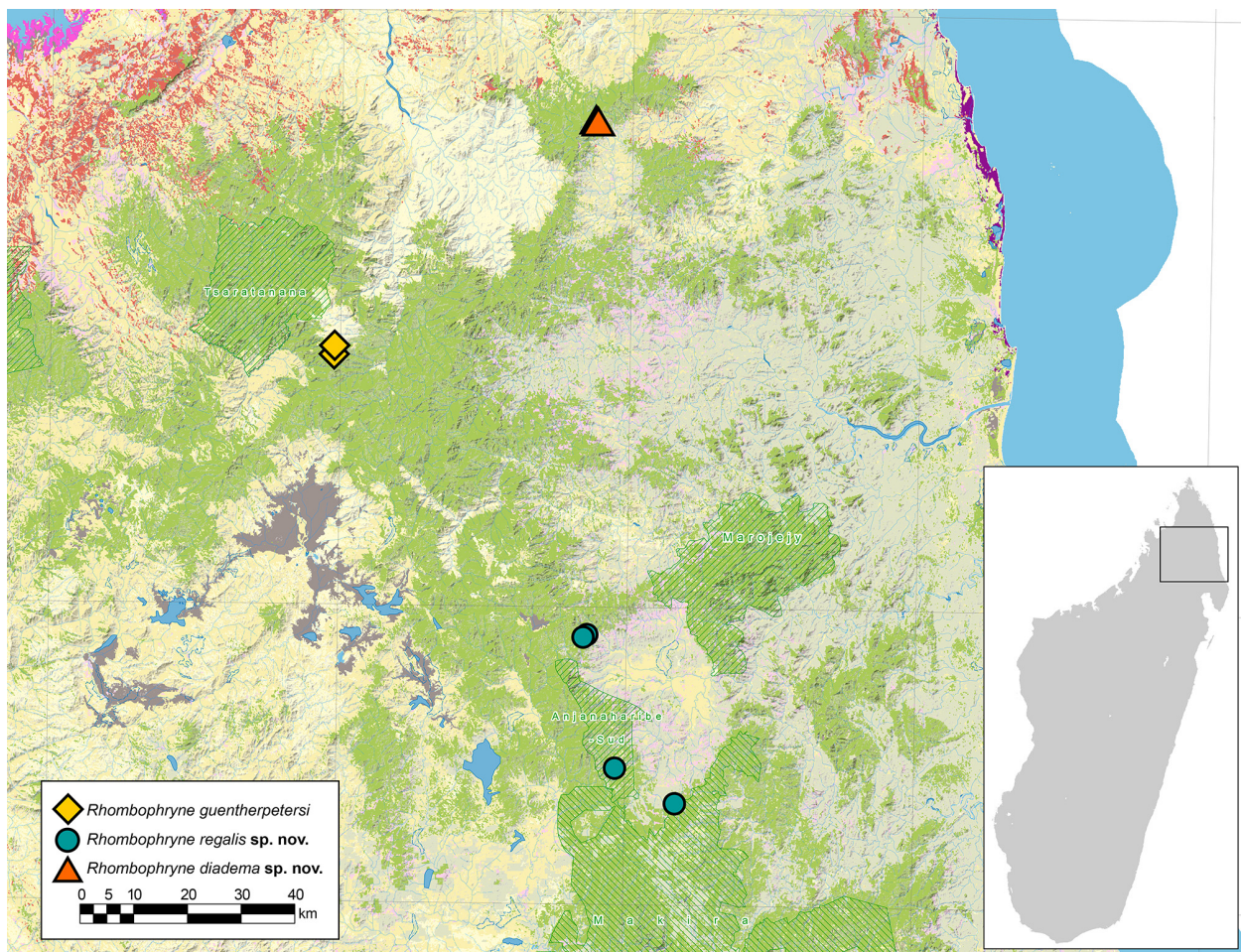


FIGURE 8. Map of the north of Madagascar showing the collection localities of specimens of the focal species of this paper, *Rhombophryne guentherpetersi*, *R. regalis* sp. nov., and *R. diadema* sp. nov. Basemap from www.vegmad.org. Hashing indicates protected areas; note that the full extent of Tsaratanana Strict Nature Reserve is not shown.

***Rhombophryne regalis* sp. nov.**

Suggested common name: Regal saw-browed diamond frog
(Figs 4, 5, 9, 10, S3–S7)

Naming remarks. This species has frequently been referred to as *Plethodontohyla* (after 2008, *Rhombophryne serratopalpebrosa* (Vences & Glaw 2003; Glaw & Vences 2007; Wollenberg *et al.* 2008; Vieites *et al.* 2009). It was figured as such on page 119 of Glaw & Vences (2007). We have referred to it as *R. sp. aff. serratopalpebrosa* (Scherz *et al.* 2015b), *R. sp. ‘Ambolokopatrika’* (Scherz *et al.* 2014, 2015a, 2016a, Lambert *et al.* 2017), and *R. sp. CaNEW Ambolokopatrika* (Scherz *et al.* 2016b). We consider it likely that some records from COMATSA (e.g. Rabearivony *et al.* 2015) refer to this species, but specimens and DNA samples are required to verify this.

Holotype. MRSN A4602 (FN 7292), adult male, captured 13 December 1997 by F. Andreone, J.E. Randrianirina, and G. Aprea at Camp 3 of Ambolokopatrika-Betaolana Forest, locally known as ‘Antsinjorano’ (14.5433°S, 49.4300°E), around 980 m a.s.l., in the Sava Region, northeastern Madagascar (Figs 4, 5, S3).

Paratypes. MRSN A4603 (FN 7146), adult female, same collection data as the holotype; MRSN A4619, subadult, and MRSN A4620, adult female, collected 6 December 1997 by F. Andreone, J.E. Randrianirina, and G. Aprea at Camp 2 of Ambolokopatrika-Betaolana Forest, locally known as ‘Andranomadio’ (14.5400°S, 49.4383°E), around 860 m a.s.l.; MRSN A4618, adult female, collected 26 June 1996 by F. Andreone and J.E. Randrianirina in Besariaka Forest, at the campsite locally known as ‘Ambozin’antsahamaloto’ (14.8283°S, 49.5958°E), around 800 m a.s.l.; MRSN A6058, adult female, collected January 1996 by F. Andreone, J.E.

Randrianirina, and H. Randriamahazo on the west slope of Anjanaharibe-Sud (Analabe) at 'Camp W1' (14.7783°S, 49.4634°E), around 1050 m a.s.l.

Diagnosis and comparisons. A species assigned to the genus *Rhombophryne* on the basis of molecular phylogenetic affinities (Fig. 3), and the possession of a clavicle combined with the absence of T- or Y-shaped terminal phalanges (vs. either absence of a clavicle or possession of a clavicle combined with T- or Y-shaped terminal phalanges in the morphologically similar *Plethodontohyla*). Within the genus *Rhombophryne*, it is assigned to the *R. serratopalpebrosa* species group on the basis of possessing supraciliary spines and molecular phylogenetic affinities (Fig. 3).

Rhombophryne regalis sp. nov. is distinguished from all congeners by the following unique suite of characters: SVL 20.2–26.5 mm; loreal region strongly concave, possessing an S-shaped fold behind the naris; tympanum distinct, TDH/ED = 0.47–0.67; weak supratympanic fold extending from rear corner of eye over tympanum toward axillary region; three supraciliary spines, the first of which is largest and pointed anteriorly, the second of which is smaller, and the third of which is diminutive; second finger slightly shorter than fourth, fifth toe distinctly shorter than third; tibiotarsal articulation reaching to or beyond the snout tip; TIBL/SVL = 0.47–0.56. Osteologically, it is characterised by an anteriorly broadening parasphenoid cultriform process, ventromedial contact of exoccipitals, straight postchoanal vomers, smoothly sigmoidal anterior edge of ventral ramus of squamosal, strong dorsal prominence on iliac shafts, and ossified pubis. Additionally, *R. regalis* is distinguished from all other *Rhombophryne* species for which molecular data are available by uncorrected pairwise distances of at least 6.1% in a segment of the 16S rRNA mitochondrial gene (Table 1).

Within the genus *Rhombophryne*, *R. regalis* sp. nov. can be distinguished from all species except members of the *R. serratopalpebrosa* group by the possession of supraciliary spines. Within the *R. serratopalpebrosa* group, *R. regalis* sp. nov. may be distinguished from *R. serratopalpebrosa*, which it most strongly resembles, by its smaller size (adult female SVL 20.2–26.5 mm vs. 28.5 mm; males unavailable from *R. serratopalpebrosa*), weak supratympanic fold (vs. strong supratympanic fold), possession of three supraciliary spines: 1st large, 2nd medium, 3rd diminutive (vs. four: 1st large, 2nd medium, 3rd small, 4th diminutive), smaller relative tympanum size (TDH/ED = 0.47–0.67 vs. 0.72), shorter relative forelimb length (FORL/SVL = 0.59–0.70 vs. 0.80), parasphenoid cultriform process broadening anteriorly (vs. not broadening), exoccipitals in ventromedial contact (vs. not in contact), broad (vs. narrow) quadratojugal–squamosal contact, anterior edge of squamosal ventral ramus smoothly sigmoidal (vs. stepped), and ossified (vs. unossified) pubis; from *R. vaventy* by its much smaller size (SVL 20.2–26.5 vs. 51.9 mm), weak supratympanic fold extending from posterior of eye over tympanum toward axillary region (vs. distinct supratympanic fold, curved over and behind the tympanum but not extending anterior to the tympanum), possession of three supraciliary spines: 1st large, 2nd medium, 3rd diminutive (vs. four, anterior two most distinct), shorter relative forelimb length (FORL/SVL = 0.59–0.70 vs. 0.76), and absence (vs. presence) of enlarged inner metatarsal tubercles; from *R. guentherpetersi* by its smaller size (SVL 20.2–26.5 vs. 27.3–35.7 mm), possession of three supraciliary spines: 1st large, 2nd medium, 3rd diminutive (vs. 2–3 small supraciliary spines), tibiotarsal articulation reaching at least the nostril (vs. reaching the insertion of the arms), longer relative tibia length (TIBL/SVL = 0.47–0.56 vs. 0.35–39), and absence of a dorsal tibial gland (vs. presence); from *R. ornata* by its smaller size (single known male SVL 22.4 vs. 33.0 mm), weak supratympanic fold extending from rear corner of eye over tympanum toward axillary region (vs. distinct supratympanic fold extending from rear corner of eye over and behind tympanum toward axilla; see Fig. 5), possession of three supraciliary spines: 1st large, 2nd medium, 3rd diminutive (vs. two of roughly equal size), thinner thighs (THIW/THIL = 0.26–0.34 vs. 0.36–0.40), slightly longer relative tibia length (TIBL/SVL = 0.47–0.56 vs. 0.38–0.46), tibiotarsal articulation reaching at least the nostril (vs. reaching between the tympanum and eye), and absence of reddish colour on the hidden portions of the legs (vs. presence); from *R. tany* by its weaker supratympanic fold (see Fig. 5), possession of three supraciliary spines: 1st large, 2nd medium, 3rd diminutive (vs. two of roughly equal size), considerably thinner thighs (THIW/THIL 0.26–0.34 vs. 0.41), longer relative tibia length (TIBL/SVL = 0.47–0.56 vs. 0.43), and tibiotarsal articulation reaching at least the nostril (vs. reaching between the tympanum and eye); and from *R. coronata* by possession of three supraciliary spines differing in size: 1st large, 2nd medium, 3rd diminutive (vs. three of roughly equal size), thinner thighs (THIW/THIL = 0.26–0.34 vs. 0.36–0.44), thinner shanks (TIBW/TIBL = 0.18–0.24 vs. 0.31–0.36), longer relative tibia length (TIBL/SVL = 0.47–0.56 vs. 0.35–0.39), and first toe unreduced (vs. sometimes reduced to a short nub; see Fig. 5).

Results

Description of the holotype. (Figs 4, 5, 9a, b) An adult male specimen in a moderately good state of preservation, though quite soft. Tissue samples taken from left thigh and tongue for sequencing. A small incision is present in the right side. The testes are well developed and mature, and can be easily identified.

Body robust. Head wider than long (HW/HL = 1.46). Pupils tiny and horizontally oblong (possibly deformed by preservation). Snout rounded in dorsal and lateral view. Canthus rostralis concave. Loreal region concave, with a subtle S-shaped fold that surmounts the nostril anteriorly (otherwise known only from *R. serratopalpebrosa*). Nostrils nearer to snout tip than to eye (END/NSD = 1.22), directed laterally, slightly protuberant. Tympanum distinct, TDH/ED = 0.47. Weak supratympanic fold, hardly noticeable anterior to tympanum but extending posterior to it toward the axillary region. Three supraciliary spines above each eye, the first large and anterior to the eye, the second smaller and above the eye, the third diminutive and over the posterior half of the eye (hardly perceptible without the aid of magnification). Vomerine teeth present in a straight row either side of the palate, approaching each other medially but separated by a small gap.

Arms slender. Fingers without webbing, relative lengths 1<2<4<3; fourth finger distinctly longer than second; finger tips not expanded; fingers not reduced (Fig. 5); nuptial pads absent; inner metacarpal tubercle present, outer metacarpal tubercle absent; subarticular tubercles weak, undivided. Hindlimbs fairly slender; tibiotarsal articulation reaches the snout tip; TIBL/SVL = 0.48. Inner metatarsal tubercle present, not enlarged, outer metatarsal tubercle absent, subarticular tubercles indistinct. Toes unwebbed; relative lengths 1<2<5<3<4, fifth toe distinctly shorter than third. Toe tips not expanded, third toe tip pointed.

Dorsal and ventral skin smooth in preservative, but quite bumpy in life (Fig. 9a). Dorsolateral folds absent.

Colouration of holotype: After 19 years in preservative, specimen dorsally brown, with two darker spots above the suprascapulae, anteriorly bordered by cream lines. A darker brown chevron extends from the inguinal regions on either side of the body to the mid-dorsum, bordered anteriorly and posteriorly by thin cream lines. Another cream line extends from the middle lateral side of the frog anteriorly over the axial pit, dorsally encircling the insertion of the arm. Over the suprascapular region, a clover-shaped dark brown marking is present, outlined with a thin cream border (much more distinct in life; see Fig. 9a). A dark brown interocular bar is also present, likewise bordered with cream. Laterally lighter brown, with a cream line extending from posterior of eye along anterior edge of tympanum to corner of mouth. Legs with one darker brown crossband each on the thigh, lower leg, tarsal, and metatarsal regions, that on the thigh with thin cream borders. Venter cream, with a darker chin. Colouration in life as in preservative, but more vibrant and clear, and somewhat more reddish (Fig. 9a).

Variation. All paratypes have been more strongly fixed than the holotype. Snout more or less truncate and squared. For variation in measurements, see Appendix 1. TDH larger in all paratypes than in the holotype (full range of TDH/ED = 0.47–0.67). Leg length varies, but the tibiotarsal articulation extends to or beyond the nostril. Supratympanic fold and supraciliary spines generally consistent, but influenced by quality of preservation. The tongues of the paratypes are broad, unlobed, and attached anteriorly (that of the holotype has been removed). No sexual size dimorphism is apparent. The paratypes are more uniformly brown dorsally than the holotype, mostly lacking dorsal patterns and cream colouration; ventrally similar, but can be more mottled with light brown. The dorsal skin of all paratypes is rougher than the holotype, both in preservative and in life (Fig. 9). Notes on osteological variability are given in the Osteology section, below.

Natural history. Several of the paratypes contain developing eggs, revealed by their slightly higher X-ray absorbance than the surrounding tissue in the micro-CT scans; MRSN A4620 had 11, and A6058 had 17. This suggests relatively small clutch sizes. Little is known about the species' life history. The individuals were usually found active on the ground during rainy weather at night. The type series was collected while installing basecamp and drift fences in primary, mid-altitude rainforest, confirming the species as at least partly fossorial.

Etymology. The species epithet is the Latin nominative singular two-ending adjective *regalis*, meaning 'kingly' or 'regal', and refers to the crown-like supraciliary spines that individuals of this species, and all other members of the *R. serratopalpebrosa* group, possess.

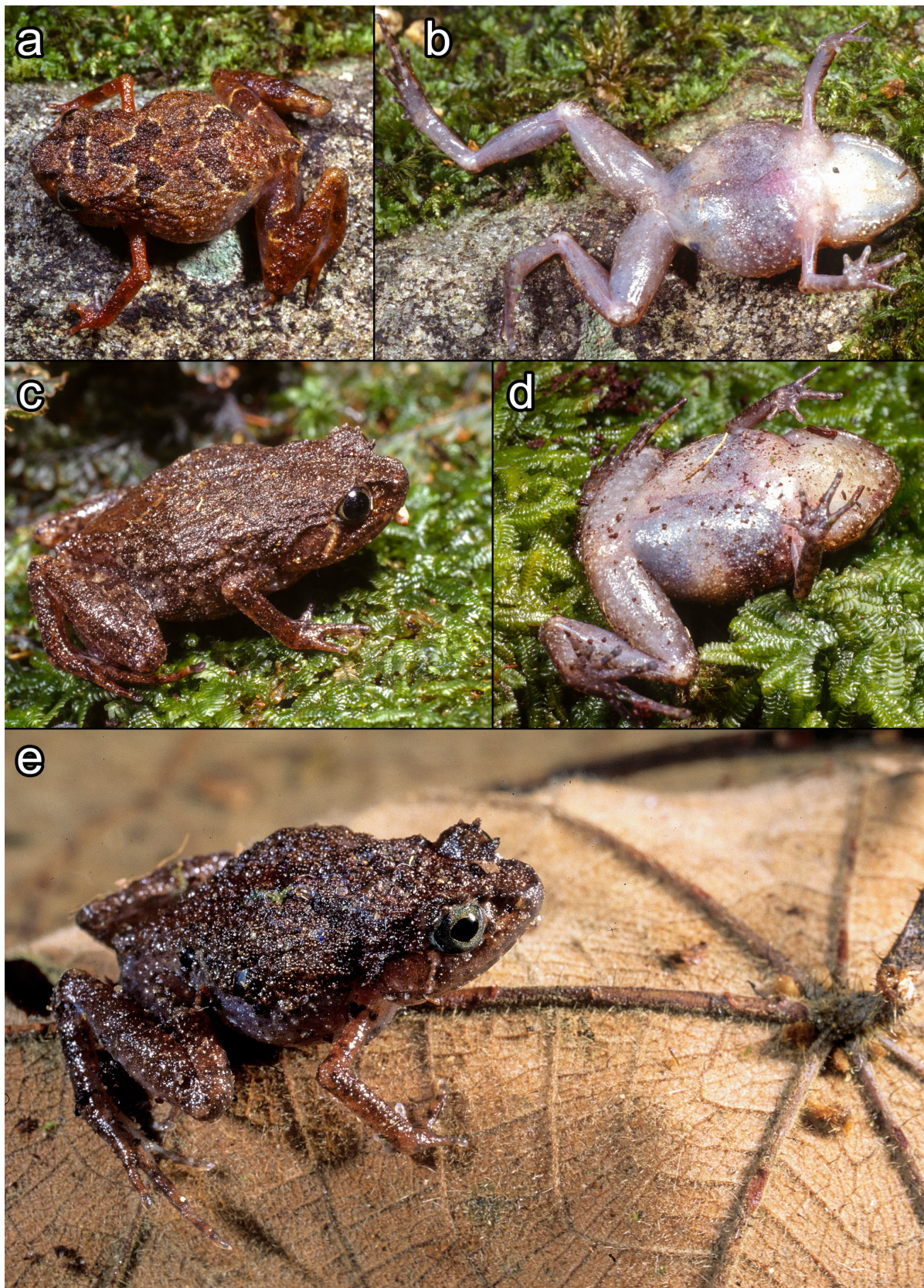


FIGURE 9. *Rhombophryne regalis* sp. nov. in life, showing the holotype (MRSN A4602) in (a) dorsal and (b) ventral view; paratype MRSN A4603 in (c) dorsolateral and (d) ventral view; and (e) an individual from Ambolokopatrika in dorsolateral view (assignment to field and collection numbers unknown).

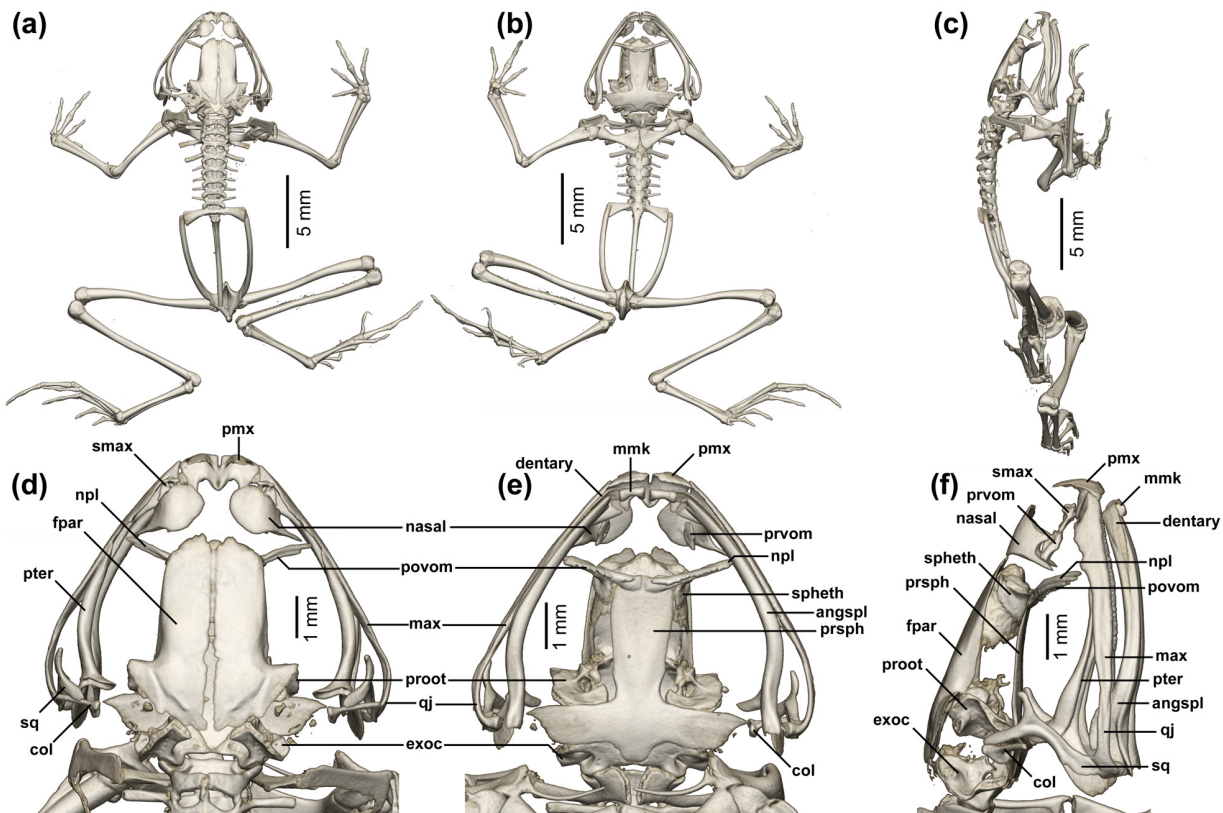


FIGURE 10. Osteology of *Rhombophryne regalis* sp. nov. (MRSN A4602). Full skeleton in (a) dorsal, (b) ventral, and (c) lateral view; skull in (d) dorsal, (e) ventral, and (f) lateral view. Abbreviations as in Fig. 7.

Distribution and conservation status. *Rhombophryne regalis* sp. nov. is reliably known from Anjanaharibe-Sud, Ambolokopatrika, and Besariaka, over an altitudinal range from 980 to 1050 m a.s.l. (Fig. 8). It may also be distributed south into Makira, northwest into COMATSA, southeast into Masoala, or northeast into Marojejy—a more detailed sampling including genetic material will be needed to assess its full distribution. Its currently known distribution encompasses an area of 213 km² over three threat-defined locations (TDLs). A TDL is defined by the IUCN (2012) as a ‘distinct area in which a single threatening event can rapidly affect all individuals of the taxon present’; here, we consider each of the three localities from which the new species is known to be separate TDLs, as deforestation, the greatest threat to these frogs, is generally localized, and disappearance of habitat in one of the locations will not affect the status of the others.

Records of ‘*R. serratopalpebrosa*’ from COMATSA by Rabearivony *et al.* (2015) probably refer to this species as well, but need to be verified with specimens. However, we hypothesise that it may in fact be distributed over an area of >7000 km² encompassing adjacent, mid-altitude rainforest in northern Madagascar. The habitat in all three of the confirmed locations where this species occurs is being degraded, despite partial protection—cattle grazing, slash-and-burn, and selective logging are widely practiced, leading to on-going decline in the extent and quality of available habitat. Due to its restricted known range but probable wider distribution, this species is a borderline case between Endangered and Vulnerable using the IUCN classification system. To avoid being inflationary, we conservatively propose a status of Vulnerable for this species according to the IUCN Red List criterion B1ab(iii) (as above, but extent of occurrence <20,000 km² and known from 10 or fewer locations) and recommend research to quantify its distribution in northern Madagascar’s rainforests.

***Rhombophryne diadema* sp. nov.**

Suggested common name: Diadem saw-browed diamond frog
(Figs 4, 5, 11, 12, S8)

Holotype. ZSM 1629/2012 (FGZC 3604), adult female, collected between the 26th and 30th of November by F. Glaw, O. Hawlitschek, T. Rajoafiarison, A. Rakotoarison, F.M. Ratsoavina, and A. Razafimanantsoa on the Sorata Massif at 13.6817°S, 49.4411°E, at 1339 m a.s.l., in the Sava Region, northeastern Madagascar (Figs 4, 5, S8).

Paratypes. ZSM 1628/2012 (FGZC 3731), adult male, and UADBA-A 60289 (FGZC 3611), adult female with large eggs, same data as holotype except collected at a creek above the campsite in Sorata (13.6780°S, 49.4404°E) at 1407 m a.s.l.

Diagnosis and comparisons. A species assigned to the genus *Rhombophryne* on the basis of molecular phylogenetic affinities (Fig. 3), and the possession of a clavicle combined with the absence of T- or Y-shaped terminal phalanges (vs. either absence of a clavicle or possession of a clavicle combined with T- or Y-shaped terminal phalanges in the morphologically similar *Plethodontohyla*). Within the genus *Rhombophryne*, it is assigned to the *R. serratopalpebrosa* group on the basis of possessing supraciliary spines and molecular phylogenetic data (Fig. 3).

Rhombophryne diadema sp. nov. is distinguished from all congeners by the following unique suite of characters: SVL 22.7–23.4 mm; tympanum indistinct, TDH/ED = 0.59–0.64; weak supratympanic fold extending from the rear corner of the eye over and behind tympanum toward the axilla; three supraciliary spines, the posterior-most considerably smaller than the anterior two; unreduced fingers, second finger distinctly shorter than fourth; tibiotarsal articulation reaching eye; TIBL/SVL = 0.44–0.46; and fifth toe distinctly shorter than third. Osteologically, it is characterised by an anteriorly broadening parasphenoid cultriform process, prechoanal portion of vomer non-radiate, postchoanal portion straight, broad quadratojugal-squamosal contact, stepped anterior edge of ventral ramus of squamosal, short humeral crista ventralis, weak dorsal prominence on iliac shafts, and partially ossified pubis. Additionally, *R. diadema* is separated from all other *Rhombophryne* species for which molecular data are available by uncorrected pairwise distances of at least 5.1% in a segment of the 16S rRNA mitochondrial gene (Table 1).

Within the genus *Rhombophryne*, *R. diadema* sp. nov. differs from all species except members of the *R. serratopalpebrosa* group by the possession of supraciliary spines. Within the *R. serratopalpebrosa* group, it differs from *R. serratopalpebrosa* by smaller size (SVL 22.7–23.4 vs. 28.5 mm), smaller relative tympanum size (TDH/ED = 0.59–0.64 vs. 0.78), a weak (vs. strong) supratympanic fold, three supraciliary spines (vs. four), shorter relative forelimb length (FORL/SVL 0.59 vs. 0.71), and shorter relative hindlimb length (HIL/SVL = 1.66 vs. 1.77); from *R. vaventy* by much smaller size (SVL 22.7–23.4 vs. 51.9 mm), larger relative tympanum size (TDH/ED = 0.59–0.64 vs. 0.46), narrower head (HW/HL = 1.46–1.59 vs. 1.70), a weak (vs. distinct) supratympanic fold (see Fig. 5), three (vs. four) supraciliary spines, tibiotarsal articulation reaching eye (vs. beyond snout tip), shorter relative forelimb length (FORL/SVL = 0.59 vs. 0.76), smaller relative tibia size (TIBL/SVL = 0.44–0.46 vs. 0.53), and smaller inner metacarpal tubercle size (IMCL/HAL 0.13–0.14 vs. 0.19); from *R. guentherpetersi* by smaller size (SVL 22.7–23.4 vs. 27.5–35.1 mm), three supraciliary spines, the anterior two of which are of medium size, the posterior-most of which is considerably smaller (vs. two to three small supraciliary spines), broader head (HW/HL = 1.46–1.59 vs. 1.34–1.41), tibiotarsal articulation reaching the eye (vs. reaching the insertion of the arms), longer relative tibia length (TIBL/SVL 0.44–0.46 vs. 0.32–0.36), partially ossified pubis (vs. unossified), and broader pectoral girdle (compare Fig. 7b with Fig. 12b); from *R. ornata* by smaller size (SVL 22.4–23.4 mm vs. 33.0 mm), a weak (vs. distinct) supratympanic fold, three supraciliary spines (vs. two), longer relative hindlimb length (HIL/SVL = 1.66 vs. 1.45–1.63), smaller relative inner metacarpal tubercle length (IMCL/HAL = 0.13–0.14 vs. 0.15–0.19), absence of reddish colour on the hidden portions of the legs (vs. presence), and ossified carpals and limb bone epiphyses (vs. unossified); from *R. tany*, which it most strongly resembles, by its weaker supratympanic fold (see Fig. 5 and compare Figs 1d and 11), three supraciliary spines (vs. two), slightly shorter forelimbs (FORL/SVL 0.59 vs. 0.63), slightly longer relative tibia length (TIBL/SVL 0.44–0.46 vs. 0.43), prootics in contact with parasphenoid alae (vs. not in contact), parasphenoid cultriform process broadening anteriorly (vs. having parallel edges), nasals not anterolaterally displaced (vs. displaced), quadratojugal-squamosal contact broad (vs. narrow), anterior edge of ventral ramus of squamosal distinctly stepped (vs. weakly stepped), dorsal prominence of iliac shafts weak (vs.

Results

strong), and partially ossified pubis (vs. unossified); from *R. regalis* by anterior-most superciliary spine sitting atop eye (vs. anterior to eye; see Fig. 5 and compare Figs 9 and 11), slightly shorter relative forelimb length (FORL/SVL = 0.59 vs. 0.59–0.70), shorter relative tibia length (TIBL/SVL 0.44–0.46 vs. 0.47–0.56), tibiotarsal articulation reaching the eye (vs. reaching the snout tip or beyond), exoccipitals ventromedially not in contact (vs. in contact), anterior edge of ventral ramus of squamosal stepped (vs. smoothly sigmoidal), dorsal prominence of iliac shafts weak (vs. strong), and partially ossified pubis (vs. ossified); and from *R. coronata*, which it also closely resembles, by much smaller size of the posterior-most superciliary spine (vs. three roughly equal-sized superciliary spines), larger relative tympanum size (TDH/ED 0.59–0.64 vs. 0.37–0.59), longer relative tibia length (TIBL/SVL 0.44–0.46 vs. 0.35–0.39), first toe unreduced (vs. sometimes reduced to a short nub; see Fig. 5), anterior edge of squamosal ventral ramus stepped (vs. straight), and sphenethmoids not exceeding postchoanal vomers (vs. exceeding postchoanal vomers).

Description of the holotype. (Figs 4, 5) An adult female specimen in a very good state of preservation. Tissue taken from the left thigh for genetic sequencing. A transverse incision present in the posterior abdomen.

Body robust. Head wider than long (HW/HL = 1.59). Pupils round. Snout rounded in dorsal and lateral views. Canthus rostralis concave. Loreal region slightly concave. Nostril nearer to snout tip of than to eye (END/NSD = 0.47), directed laterally, slightly protuberant. Internarial distance greater than distance from eye to nostril. Tympanum indistinct, TDH/ED = 0.64. Supratympanic fold weak, extending from the middle back of the eye over and behind the tympanum toward the axilla. A small granular bump is present posteroventral to both tympana. Three superciliary spines above each eye, the anterior two roughly equal in size, the posterior-most almost imperceptible without magnification. Vomerine teeth present, in straight rows either side of the palate, separated medially by a small gap. Tongue broad and unlobed, attached anteriorly.

Arms fairly slender. Fingers not reduced. Fingers without webbing; relative lengths 1<2<4<3; fourth finger distinctly longer than second. Finger tips not enlarged. Nuptial pads absent; inner metacarpal tubercle present, outer metacarpal tubercle absent, subarticular tubercles weak. Hindlimbs strongly built. Tibiotarsal articulation reaches the eye; TIBL/SVL = 0.46. Inner metatarsal tubercle present; outer metatarsal tubercle absent. Toes unwebbed; relative lengths 1<2<5<3<4; fifth toe distinctly shorter than third. Dorsal skin granular, rugose in life. Dorsolateral folds absent.

Colouration of the holotype: After two and a half years in preservative, dorsal body colour is dark brown flecked with black—in life, the body was a more reddish brown (Fig. 11a). The posterior half is lighter in colour than the anterior, particularly around the midline. Two light-brown lines run posteromedially from the eyes, approaching one another toward the midline but ending in the suprascapular region. These lines merge anterolaterally at the posterior of the eye with the lighter flank colouration, extending onto the lateral portions of the head. A whitish line runs from the posterior edge of the eye to the corner of the mouth. The arms are dorsally light brown flecked with black. The legs are dorsally light brown, with one dark crossband on the thigh, two on the shank—the proximal of which is less distinct than the distal—one on the tarsus, one on the metatarsals, and some black spots on the toes.

The ventral surface is cream, with a little brown speckling on the chin and below the insertions of the arms. The legs are ventrally flecked with light brown and cream. The iris is gold with black reticulations and a black periphery.

Variation. Morphologically, ZSM 1628/2012 agrees strongly with the holotype. Its tympanum is slightly smaller (TDH/ED = 0.59), and its tibia shorter (TIBL/SVL = 0.44). Its colouration is starkly different, however. Dorsally, it is uniformly an earthy brown. Crossbands on the shanks are faint but present, as is the light line running between the corner of the mouth and the posterior of the eye. Based on colour photographs (Fig. 11), UADBA-A 60289, which is female, also closely agrees in morphology with the rest of the type material. Its colouration is roughly intermediate between the other specimens, its dorsum being muddy brown flecked with white and black spots; a pair of small white spots being present between the anterior edges of the eyes, and again between the posterior edges, as well as over the suprascapular region. Its inguinal region is a yellowish cream. The crossbands on its legs are as in the holotype.

Etymology. The specific epithet *diadema* is the latinized Greek word for diadem, a small crown typically worn by female royalty. It refers to the superciliary spines borne by this species. It is a feminine nominative singular noun in apposition.

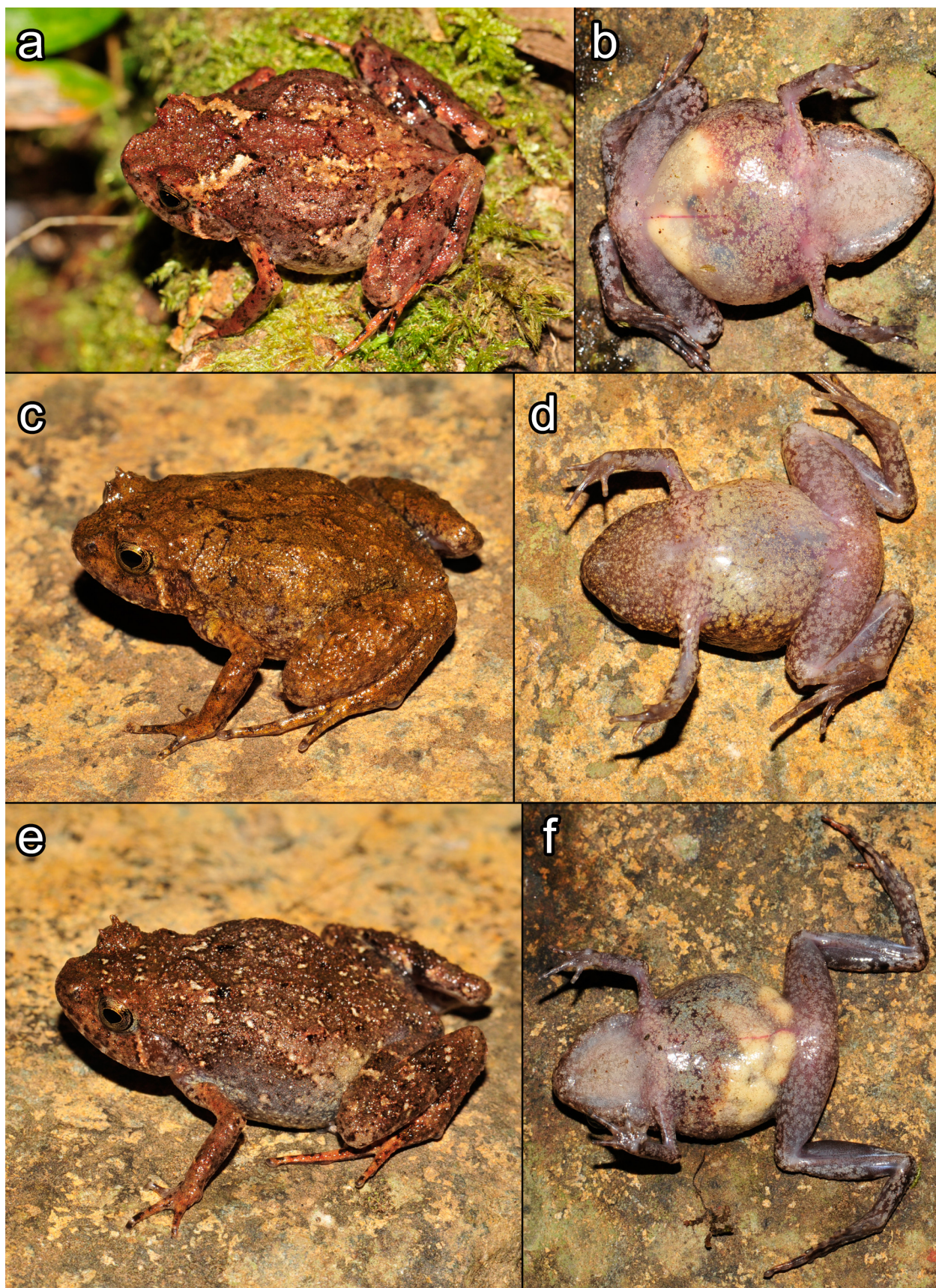


FIGURE 11. *Rhombophryne diadema* sp. nov. in life, showing the holotype ZSM 1629/2012 in (a) dorsal and (b) ventral view; paratype ZSM 1628/2012 in (c) lateral and (d) ventral view; and paratype UADBA-A 60289 in (e) lateral and (f) ventral view.

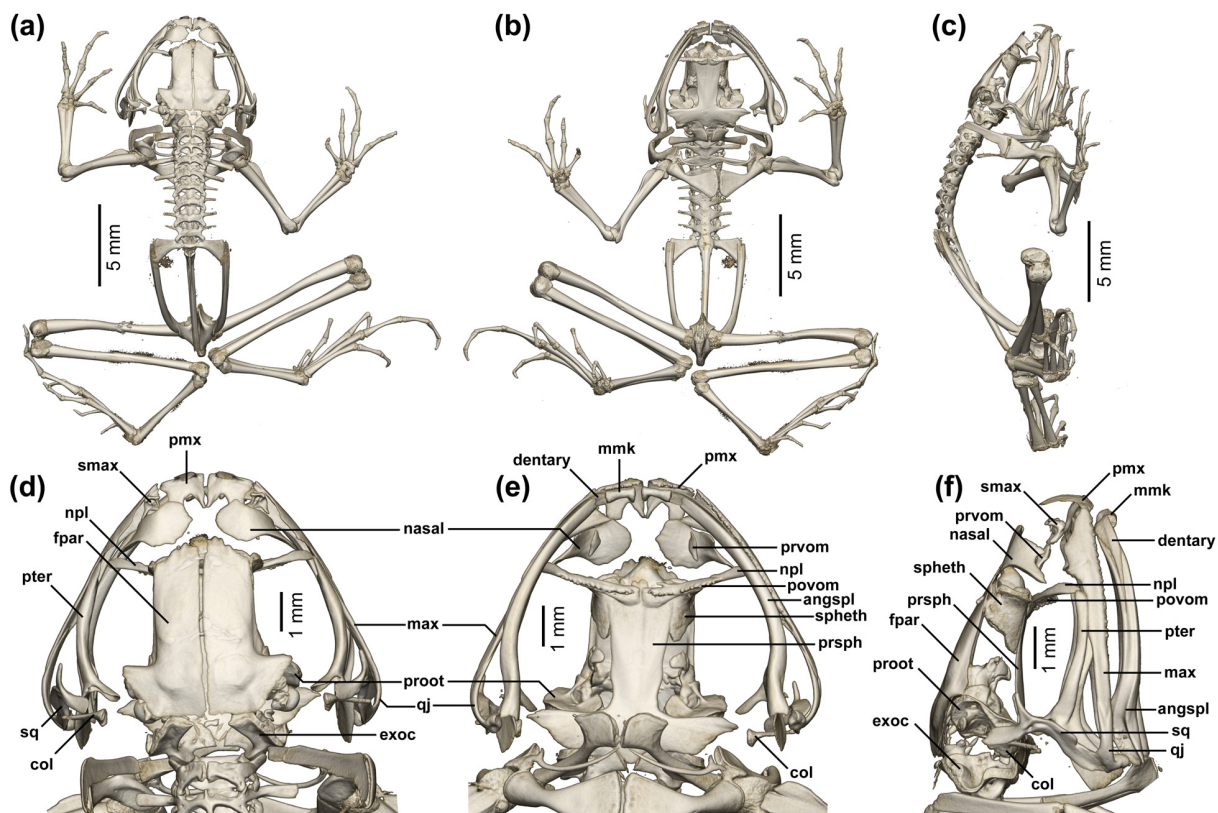


FIGURE 12. Osteology of *Rhombophryne diadema* sp. nov. (ZSM 1629/2012). Full skeleton in (a) dorsal, (b) ventral, and (c) lateral view; skull in (d) dorsal, (e) ventral, and (f) lateral view. Abbreviations as in Fig. 7.

Natural history. Individuals of this species were captured when active during the day jumping among the leaf-litter or near pitfall traps, suggesting a terrestrial, possibly partially fossorial lifestyle. The holotype contained at least 13 well-developed, yellow eggs (diameter 2.45 ± 0.25 mm), suggesting that the species was reproductively active at the end of November, around the start of the rainy season.

The montane rainforest of Sorata is under high human-disturbance pressure, especially due to the high number of zebu cattle, which are responsible for widespread forest disturbance in the area. The area where the specimens of this species were discovered was exceptionally intact, with dense leaf litter.

Distribution and conservation status. This species is known only from high altitudes (1339–1407 m a.s.l.) in the forest of the Sorata Massif in northern Madagascar (Fig. 8). This forest is unprotected and therefore threatened by deforestation and degradation without restriction. Additionally, species at high altitude may be threatened by climate change (Raxworthy 2008; Raxworthy *et al.* 2008), although this threat is most likely less imminent than that of deforestation. If this species is restricted to the Sorata Massif, then its extent of occurrence and optimistically estimated area of occupancy constitutes an area of only ~ 250 km² (calculated in Google Earth® Pro 6.1.0.500, Google Inc., Mountain View, CA). Due to its likely restriction to a small area of unprotected forest that is under threat from deforestation and possible long-term threat of climate change, *R. diadema* sp. nov. qualifies as Endangered under the IUCN Red List Criteria (2012) B1ab(iii) as defined for *R. guentherpetersi* above, similar to *R. longicrus*, which was described from the same area (Scherz *et al.* 2015b).

Osteology

In the following, we describe the generalized skeleton of members of the *R. serratopalpebrosa* group, noting where characters vary among and within species. This description incorporates all described species from the group. It should be noted that this osteological description is based on data from a renewed examination of all of the available material, and does not draw on descriptions previously published for *R. serratopalpebrosa*, *R. vaventy*, *R. ornata*, and *R. tany* (Scherz *et al.* 2014, 2015a). Descriptions of those species should be considered an update or

revision of previous conclusions and observations for reasons that are discussed at the end of this paper. These are the first published osteological descriptions for *R. coronata*, *R. guentherpetersi*, *R. diadema*, and *R. regalis*. Osteological figures (13–19) are drawn from the micro-CT scans of the holotype of *R. diadema* (ZSM 1629/2012). Videos of the skeletons of all of these species rendered as volumes are deposited at http://morphosource.org/Detail/ProjectDetail>Show/project_id/254. PDF-embedded 3D surface models of *R. coronata*, *R. vaventy*, *R. diadema*, *R. guentherpetersi*, *R. regalis*, and one specimen of *R. ornata* are provided as Supplemental Figs S1–S12; for a model of *R. serratopalpebrosa*, see Scherz *et al.* (2014); for models of *R. ornata* and *R. tany*, see Scherz *et al.* (2015a). Measurements following the scheme in Fig. 2 are provided in Table 2.

Ossification. The degree of skeletal ossification is highly variable in this group. The most extreme case is *R. ornata*, in which considerable portions of the postcranial skeleton are unossified, including the epiphyses of the femur, tibia, tarsals, carpals (but not including the phalanges and metacarpals), and the pubis. Articulations of these bones are therefore invisible in micro-CT scans. All other species are more strongly ossified. The degree of intraspecific variability in the extent of ossification is apparently moderate; in *R. ornata* (n = 3), all specimens lack ossification in the carpals, tarsals, and bone epiphyses. In *R. regalis* (n = 5), the extent of ossification varies in some skull bones (e.g. the prootic and squamosal), and is at least partially associated with developmental stage. A similar situation is visible in the skull of a young paratype of *R. ornata*, which is much less ossified than the adult holotype (Scherz *et al.* 2015a).

The lack of ossification in some specimens is not a result of specimen conservation modes: (1) specimens of *R. regalis* fixed and stored in ethanol have practically identical ossification patterns as those fixed in formalin and stored in ethanol, and (2) the most extremely unossified specimens, namely those of *R. ornata*, were fixed in ethanol. Thus despite the well-known demineralizing properties of formalin (e.g. Fonseca *et al.* 2008), the patterns we observe cannot be attributed to fixation chemicals. We tentatively interpret ossification states as true characters for the description of the skeleton here.

Cranium. (Figs 7, 10, 12, 13). *Shape and proportions.* The skull is widest at the quadratojugal slightly anterior to the columella (Fig. 2d), where it is 108–124% of the skull's length (Fig. 2c, Table 2). The rostrum is short; the distance from the anterior edge of the frontoparietals to the anterior face of the premaxilla (Fig. 2a) is 19–42% of the skull length (mean $33.6\% \pm 5.2\%$; 19% in *R. vaventy* is an outlier; Table 2). The braincase is broad; at the level of the mid-orbit (Fig. 2b) it is 22–33% of the maximum skull width (Table 2).

Neurocranium. The braincase is moderately well ossified; the sphenethmoid is not ossified medially; a mineral deposit is, however, present between the sphenethmoids in *R. ornata*, *R. coronata* (in one specimen extending posteriorly almost to contact with the prootics), *R. diadema*, *R. vaventy* (extending posteriorly to contact the prootics), *R. tany*, and some specimens of *R. regalis*; sphenethmoids are completely unossified in two juvenile/subadult specimens of *R. ornata*. The anteroventral margin of the sphenethmoid lies at the level of the postchoanal vomers (except in *R. coronata*, in which the bone has an anterior extension that reaches or surpasses the level of the posterior edge of the nasal), and its posterior margin does not exceed the midpoint of the orbit. The sphenethmoid is broadly separated from the prootic. It is generally in ventral contact with the parasphenoid, except in *R. guentherpetersi*. The exoccipitals approximate one another ventromedially (actually in contact in *R. regalis*), but not dorsomedially. The dorsal surface of the otic capsule is not ossified. The prootic is dorsally overlapped by the lateral flange of the frontoparietal; ventrally, the prootics are in contact with the parasphenoid alae (except in *R. tany*, *R. ornata*, *R. guentherpetersi*, *R. coronata*); they are broadly separated from each other.

The septomaxilla is roughly spiralled, the medial ramus extending posterodorsal to the posterior ramus; the anterior ramus is thick, possessing ventral and dorsal rami toward its lateral edge; the lateral ramus is oblique and can have a long acuminate posterolateral extension; the posterior ramus extends from the middle of the lateral ramus ventromedially and can bear a ventral ramus. Due to its small size and fine structure, scan quality has a strong impact on the resolution of this bone. Physical examination, or micro-CT scanning at higher resolution (e.g. based on only the heads or nasal capsules of animals) will be needed to establish structural variability in this bone.

The columella (or stapes) is well ossified, formed by the synostotic fusion of the long, thin pars media plectri (stylus) and the pars interna plectri (baseplate), which ranges from curved to somewhat bilobed (exceptionally stepped in *R. vaventy*).

Dorsal investing bones. The dorsal investing bones are well developed. The nasals are broad, isolated, and widely separated (except in *R. coronata*, in which they are narrowly separated; note the degree of variability in *R. regalis*, Figs S3–S7), situated directly dorsal or slightly anterodorsal to the prechoanal portion of vomer except in

Results

R. tany, in which they are anterolaterally displaced (but note intraspecific variability in *R. regalis* as well; Figs S3–S7), possessing an acuminate posterolateral maxillary process extending ventrolaterally toward the maxilla. An anterolateral knob can be present or absent, and is apparently intraspecifically variable (as assessed in *R. regalis*; see Figs S3–S7). The nasals curve ventrally toward their lateral edges, affording some protection of the nasal capsule; posteriorly broadly separated from the anterior end of the frontoparietals, except in *R. coronata*, in which they are almost in contact with the frontoparietals.

The frontoparietals are anteriorly roughly trapezoidal, their anterior margins oblique, their medial margins roughly parallel and narrowly separated, their lateral margins converging slightly anteriorly. Posteriorly they have flared lateral flanges with almost orthogonal anterior edges and oblique posterolateral edges, forming the dorsal anteromedial portion of the otic capsule and leaving the dorsal otic capsule unossified. They are clearly distinct from the exoccipitals, but not the prootics. Anteriorly, they can be in contact with the sphenethmoid, but this is variable within species. Posteriorly the frontoparietal bears a dorsal process in *R. vaventy* and *R. guentherpetersi*.

Ventral investing and palatal bones. The broad parasphenoid cultriform process (47–60% of braincase width at mid-orbit; Table 2) extends anteriorly from the anterior edge of the otic capsule to the level of the postchoanal vomers, which it overlaps and sometimes surpasses; it is 40–46% of the skull length (Table 2). The lateral edges curve slightly outward from its posterior end to encompass 20–30% of its length (Table 2), and then run subparallel (broadening anteriorly in *R. coronata*, *R. guentherpetersi*, *R. regalis*, and *R. diadema*). Its anterior end is truncate or rounded. The parasphenoid alae are long (each one generally longer than the cultriform process is wide at mid-orbit), perpendicular to the anteroposterior body axis, broadening slightly laterally, and distally acuminate, with oblique lateral edges. The posteromedial process lies slightly anterior to the level of the ventromedial exoccipitals and may therefore not participate in the foramen magnum (excluded by medial contact of exoccipitals in *R. regalis*).

The vomer is divided into pre- and postchoanal portions; the prechoanal portion is small, longer than broad, triradiate in *R. coronata*, *R. ornata*, *R. serratopalpebrosa*, and *R. vaventy*, with a thin lateral ramus extending from its lateral edge (a second posterolateral ramus is present in *R. vaventy*), or lacking distinct rami in *R. guentherpetersi* (in which it is strongly reduced), *R. diadema*, *R. regalis* (note variability in Figs S3–S7), and *R. tany*. The postchoanal portion overlaps the neopalatine for most of its length, and these bones are difficult to distinguish but apparently not fused. The vomerine teeth extend from a ventral ridge on the postchoanal vomer and may be arrayed in a straight (*R. diadema*, one specimen of *R. guentherpetersi*, two specimens of *R. ornata*, *R. regalis*, *R. serratopalpebrosa*, and *R. tany*), sigmoid (*R. coronata* and one specimen of *R. ornata*), or arcuate (*R. vaventy* and one specimen of *R. guentherpetersi*) pattern. In some species, the vomer bears a small disc-like (*R. serratopalpebrosa*, *R. ornata*), or large angular (*R. vaventy*) anterior projection from its anteromedial surface (absent or weak in *R. diadema*, *R. coronata*, *R. guentherpetersi*, *R. regalis*, and *R. tany*). Vomers medially separated by a small gap. The neopalatine approaches the maxilla distally but does not contact it. This complex is in dorsal contact with the parasphenoid medially.

Maxillary arcade. The maxillary arcade bears many small, often poorly resolved, teeth on the premaxilla and maxilla. The premaxillae are separated medially, and their anterodorsal alary processes rise in parallel or are weakly divergent from the midline. The pars palatina is broad, with two well-defined processes: the medial (palatine) process is thin and acuminate, and runs roughly parallel to or converges toward its contralateral; the lateral process is thicker and truncate. The premaxilla and maxilla are sometimes in lateral contact via a simple juxtaposition.

The maxilla is long, with a broad pars palatina along its lingual margin and a poorly developed pars facialis. The posterior end is acuminate and overlaps in a weak junction with the quadratojugal.

Suspensory apparatus. The triradiate pterygoid bears a curved anterior ramus with a sculpted ventrolateral face, oriented anterolaterally toward the maxilla, with which it articulates at the anteroventral corner of the orbit. This contact is obscured by mineralization in micro-CT scans but presumably is separated by the pterygoid cartilage on the medial margin of the maxilla. The posterior face of the medial ramus is strongly sculpted. The posterior ramus is broad and flat. The medial ramus is much shorter than the posterior ramus.

The quadratojugal is long, laterally curved, and slender, articulating anteriorly with the maxilla. It has a bulbous posteroventral process, and articulates dorsally with the ventral ramus of the squamosal (articulation narrow in *R. ornata*, *R. serratopalpebrosa*, *R. tany*, and *R. vaventy*, and broad in *R. coronata*, *R. guentherpetersi*, *R. regalis*, and *R. diadema*) through a small dorsal process.

TABLE 2. Skeletal measurements. All values are given in millimetres, and are not rounded due to the high resolution of the scans (14–40 μm per voxel). SVL is given for comparative purposes (see the text). Bone abbreviations follow Fig 7.

Species	Specimen No.	Sex	SVL	Skull width	Branimcase depth @ mid-orbit	Frontal @ mid-orbit (Fig. 2b)	Skull length (occipital condyle to pmx) (Fig. 2c)	Par-pmx distance (Fig. 2a)	Prsph length (Fig. 2e)	Prsph cultriform length (Fig. 2g)	Prsph cultriform length to waist (from otic capsule) (Fig. 2h)	Anterior edge of coracoid (Fig. 2m)	
<i>Rhomboophryne coronata</i>	ZSM 694/2001	M	20.4	9.32	1.58	2.63	1.44	7.97	2.71	5.04	3.53	1.03	2.47
<i>Rhomboophryne coronata</i>	ZSM 474/2005	M	19.4	8.29	1.45	2.61	1.30	6.98	2.08	4.36	3.03	0.91	2.12
<i>Rhomboophryne guentherpetersi</i>	ZSM 608/2014	F	28.9	11.25	1.60	3.43	2.02	10.24	3.99	6.38	4.67	0.96	2.73
<i>Rhomboophryne guentherpetersi</i>	MNHN 1953.165	F	34.6	12.03	2.01	3.61	1.75	10.25	3.65	6.03	4.38	1.13	2.82
<i>Rhomboophryne diadema</i>	ZSM 1629/2012	F	22.7	8.55	1.80	2.58	1.41	7.66	2.55	4.53	3.32	0.78	2.56
<i>Rhomboophryne ornata</i>	ZSM 1816/2010	M	33.0	14.60	1.95	3.39	1.81	11.76	4.88	6.71	5.17	1.28	4.00
<i>Rhomboophryne regalis</i>	MRSN A4602	M	22.4	8.22	1.37	2.64	1.43	7.49	2.51	4.49	3.02	0.60	2.63
<i>Rhomboophryne regalis</i>	MRSN A6058	F	20.2	8.69	1.49	2.87	1.55	8.04	2.66	4.79	3.42	0.73	2.63
<i>Rhomboophryne regalis</i>	MRSN A4620	F	22.9	8.63	1.37	2.73	1.65	7.86	2.48	4.52	3.21	0.93	2.56
<i>Rhomboophryne regalis</i>	MRSN A4618	F	26.5	10.11	1.39	2.91	1.67	8.53	2.92	4.92	3.38	0.99	3.14
<i>Rhomboophryne serratopalpebrosa</i>	MNHN 1975.24	F	28.5	12.02	1.88	3.38	1.73	10.40	3.49	6.10	4.33	1.20	3.41
<i>Rhomboophryne tany</i>	ZSM 1814/2010	M	24.6	9.87	1.83	3.15	1.49	8.50	3.36	4.82	3.41	0.90	2.67
<i>Rhomboophryne waventy</i>	ZSM 357/2005	M	51.9	21.89	2.91	4.70	2.73	16.61	3.19	8.98	7.55	1.70	6.01

....continued on the next page

Results

Species	Anterior edge of coracoid (Fig. 2J)	Coracoid width (Fig. 2i)	Coracoid width (Fig. 2k) (at ventral suture (Fig. 2i))	Coracoid width (Fig. 2k) (at internal end (Fig. 2k))	Anterior face of scapula (at longest point (Fig. 2n))	Coracoid width (Fig. 2j) (at thinnest point (Fig. 2j))	Postzyg. length (Fig. 2o)	Sacral diapophysis base width (Fig. 2q)	Sacral diapophysis distal width (Fig. 2p)	Postzyg. length (Fig. 2o)	Width of iliac shaft tips (Fig. 2s)	Length of femur (Fig. 2t)	Length of tibia (Fig. 2u)
<i>Rhombophryne coronata</i>	2.47	1.06	1.91	0.62	3.16	0.67	1.57	7.47	10.42	4.61	10.16	9.27	
<i>Rhombophryne coronata</i>	2.12	0.89	1.62	0.47	2.71	0.73	1.36	5.74	8.60	3.57	8.29	7.66	
<i>Rhombophryne guentherpersi</i>	2.73	1.21	2.11	0.72	4.11	1.03	1.84	9.48	13.28	5.21	10.76	10.48	
<i>Rhombophryne guentherpersi</i>	2.82	1.48	2.10	0.76	4.26	1.01	2.42	11.01	15.31	5.51	12.00	11.75	
<i>Rhombophryne diadema</i>	2.56	0.84	1.71	0.45	2.80	0.56	1.43	7.84	10.19	3.85	10.52	10.95	
<i>Rhombophryne ornata</i>	4.00	1.49	2.35	0.73	4.25	0.87	1.79	10.27	14.35	5.97	N/A	N/A	
<i>Rhombophryne regalis</i>	2.63	0.94	1.63	0.47	2.53	0.51	1.08	6.97	9.28	4.01	10.26	10.44	
<i>Rhombophryne regalis</i>	2.63	0.93	1.67	0.55	2.54	0.71	1.35	6.98	9.36	4.38	10.49	11.01	
<i>Rhombophryne regalis</i>	2.56	0.88	1.59	0.55	3.05	0.70	1.48	8.02	10.24	3.62	N/A	11.44	
<i>Rhombophryne regalis</i>	3.14	0.93	2.03	0.49	3.39	0.74	1.68	8.82	11.87	5.03	11.98	12.28	
<i>Rhombophryne serratopalpebrosa</i>	3.41	1.30	2.42	0.62	3.82	0.75	1.88	9.31	13.77	5.24	14.37	14.83	
<i>Rhombophryne tam</i>	2.67	1.07	2.05	0.50	3.27	0.71	1.38	7.56	10.71	4.67	10.59	10.81	
<i>Rhombophryne vaventy</i>	6.01	2.68	4.61	1.14	6.68	1.65	4.26	18.69	26.65	11.34	27.76	28.01	

TABLE 2. (Continued)

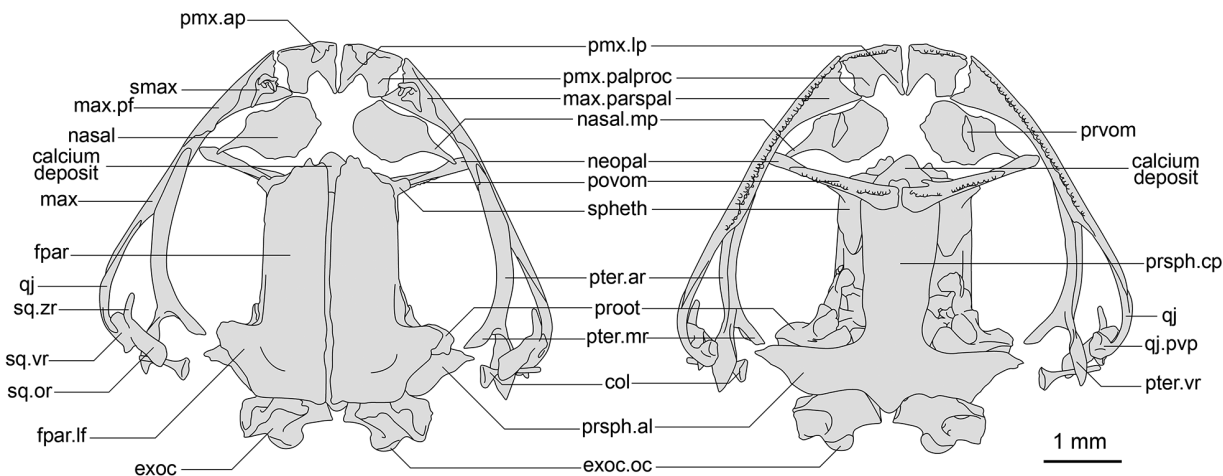


FIGURE 13. Terminology of skull osteology in dorsal view (left) and ventral view (right). Abbreviations: col = columella, exoc = exoccipital, exoc.oc = occipital condyle of exoccipital, fpar = frontoparietal, fpar.lf = frontoparietal lateral flange, max = maxilla, max(pf) = maxillary pars fascialis, max.parspal = maxillary pars palatina, nasal.mp = maxillary process of nasal, neopal = neopalatine, pmx.ap = premaxilla alary process, pmx.lp = premaxilla lateral process, pmx.palproc = premaxilla palatine process, povom = postchoanal vomer, proot = prootic, prvom = prechoanal vomer, prspb.cp = parasphenoid cultriform process, prspb.al = parasphenoid alae, pter.ar = pterygoid anterior ramus, pter.mr = pterygoid medial ramus, pter.vr = pterygoid ventral ramus, qj = quadratojugal, qj.pvp = quadratojugal posteroventral process, smax = septomaxilla, spheth = sphenethmoid, sq.or = squamosal otic ramus, sq.vr = squamosal ventral ramus, sq.zr = squamosal zygomatic ramus.

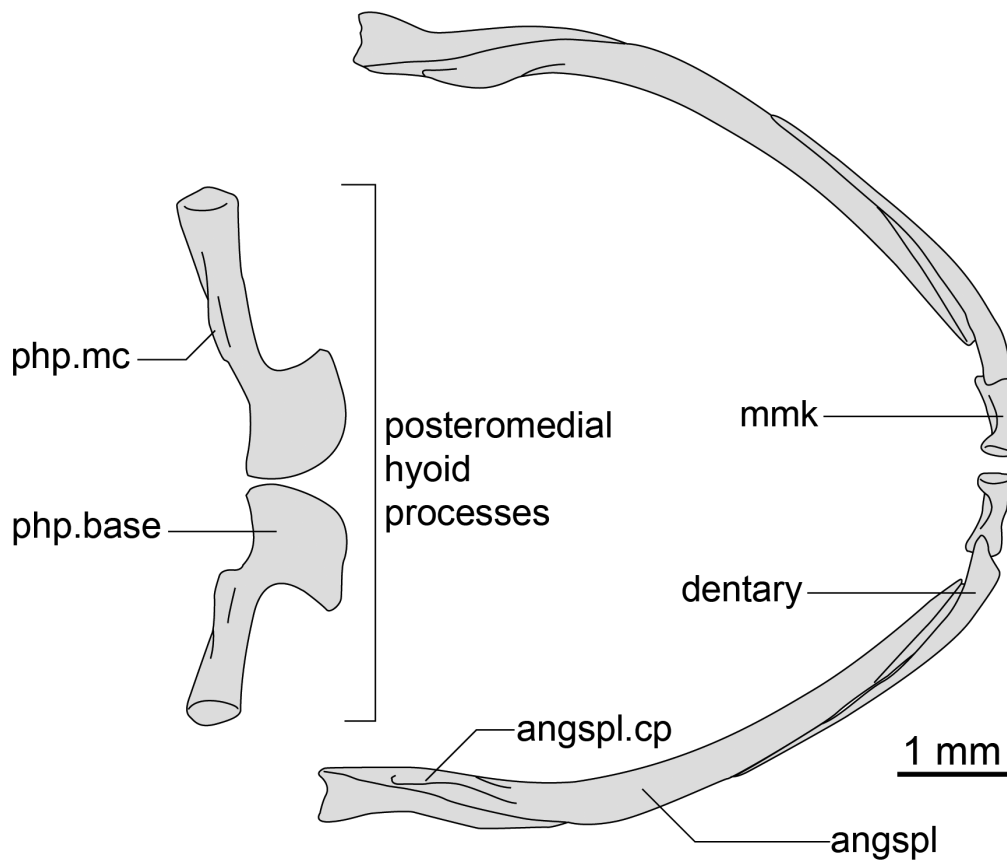


FIGURE 14. The posteromedial hyoid processes and mandible of the *R. serratopalpebrosa* species group shown in dorsal view. Abbreviations: mmk = mentomeckelian bone, angspl = angulosplenial, angspl.cp = angulosplenial coronoid process, php.base = base of posteromedial hyoid process, php.mc = medial crista of posteromedial hyoid process.

Results

The squamosal is dorsally bifurcated, broad and sculpted, extending anterodorsomedially from the quadratojugal to the level of the otic capsule, passing anterior to the columella; the anterior edge of its ventral ramus is stepped in *R. diadema*, *R. guentherpetersi*, *R. serratopalpebrosa*, intermediate between sigmoidal and stepped in *R. ornata* and *R. tany*, smoothly sigmoidal in *R. vaventy*, *R. tany*, and *R. regalis*, and straight in *R. coronata*. The otic ramus is laminar and is longer than the zygomatic ramus.

Mandible. (Fig. 14) The mandible is slim and edentate. The mentomeckelians are small and arcuate in ventral view, medially and laterally broadened, and separated medially by a narrow gap. The dentary is long and thin, posteriorly acuminate, and overlaps the angulosplenial for most of its length. It may be in contact with this bone posteriorly, but this is obscured in our scans. The angulosplenial is long and arcuate, laterally sculpted where it is in contact with Meckel's cartilage. The coronoid process is weak in *R. guentherpetersi*, but is a relatively long and strongly raised ridge in all other species.

Hyoid. (Fig. 14). The posteromedial processes of the hyoid are spade-shaped, with a distinct medial crista and a broad and flat base with a rounded anteromedial edge and sharp anterolateral and posteromedial corners; their angle is variable within species. No ossified parahyoid is present.

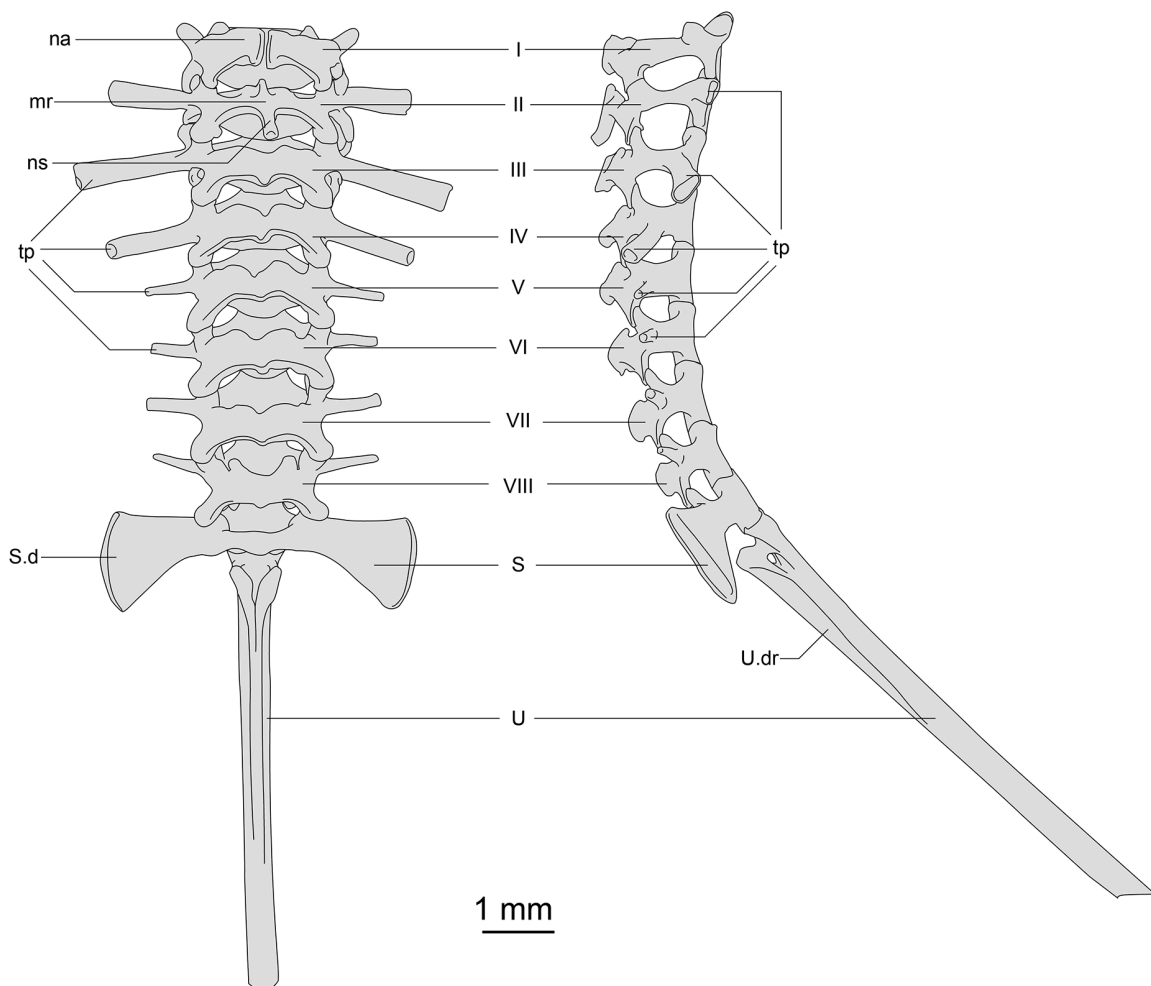


FIGURE 15. The vertebral column of the *R. serratopalpebrosa* species group shown in dorsal (left) and lateral (right) view. Abbreviations: I–VIII = presacral numbers, S = sacrum, S.d = sacral diapophysis, U = urostyle, U.dr = urostyle dorsal ridge, tp = transverse processes, mr = medial ridge, na = neural arch, ns = neural spine.

Postcranium. Vertebral column. (Fig. 15) Eight procoelous, unfused presacrals are present, each with round posterior articular processes. All vertebrae are non-imbricate. The neural arch of presacral I (atlas) can be complete or incomplete (variable within species); the neural arch of presacral II bears a raised medial ridge, which can extend outward from its anterior edge (variable) and posteriorly as a bulbous neural spine. Presacral III bears a

longer, more developed neural spine (weak in *R. vaventy*, *R. diadema*, and *R. ornata*; variable in *R. regalis* and *R. guentherpetersi*). The rest of the presacrals have raised posterior margins but lack strong neural spines (except possibly presacral IV, which often has a small medial knob that could be considered a neural spine).

The transverse processes of presacrals II–IV are thicker and broader than those of presacrals V–VIII, though their widths are variable due to the extent of ossification and thresholds in all species for which more than one specimen was available. The transverse processes of presacrals II and III are oriented ventrolaterally (II anteriorly, III posteriorly), whereas those of presacrals IV–VIII extend dorsolaterally (IV–VI strongly to weakly posteriorly, VII and VIII perpendicularly or anteriorly). The transverse processes of *R. guentherpetersi* are shortened relative to all other species (compare Fig. 7a to Figs 10a and 12a, and Figs S1–2 with S3–12).

The sacrum bears expanded diapophyses, the base 39–56% of the distal margin. The leading edge is straight and perpendicular to the longitudinal axis of the body in *R. coronata*, *R. diadema*, *R. regalis*, *R. tany*, some specimens of *R. guentherpetersi*, and *R. ornata*, but is anteriorly curved in *R. vaventy*, and slightly posteriorly curved in some specimens of *R. guentherpetersi* and *R. serratopalpebrosa*; the posterior edge is smoothly curved in all species. The urostyle is long (30–37% of SVL) and slender (thickened in one specimen of *R. coronata*, presumably a developmental defect), and bears a low dorsal ridge along a third (some specimens of *R. regalis*, *R. serratopalpebrosa*, and *R. tany*), half (*R. guentherpetersi*, some specimens of *R. regalis*), or over half (*R. diadema*, *R. ornata*, *R. coronata*, *R. tany*, and *R. vaventy*) of its length, beginning at its anterior end. Its articulation with the sacrum is bicondylar.

Pectoral girdle. (Fig. 16) Prezonal elements are not visible from micro-CT scans. The zonal portion has well-ossified coracoids, clavicles, scapulae, and cleithra. The girdle is laterally compressed in *R. guentherpetersi* through the shortening of the coracoids and clavicles (anterior edge of coracoid 8–9% of SVL vs. 11–13% in all other species; Table 2).

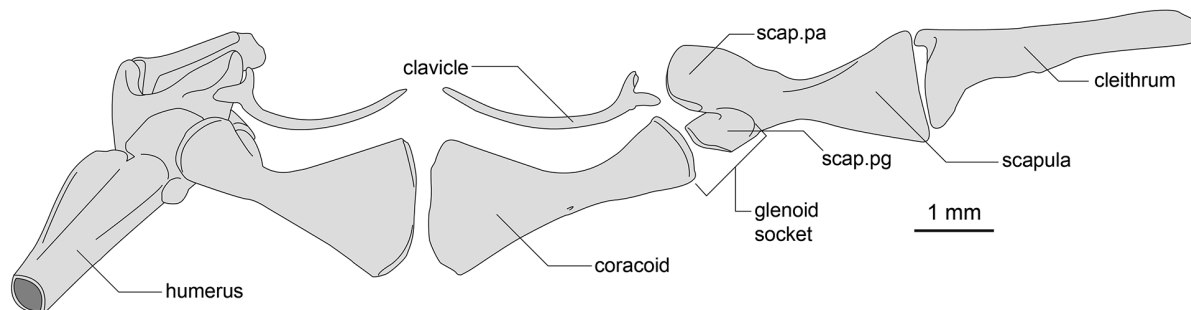


FIGURE 16. The pectoral girdle of the *R. serratopalpebrosa* species group in ventral view, articulated (left) and laid flat (right). Abbreviations: scap.pa = scapula pars acromialis, scap.pg = scapula pars glenoidalis.

The clavicles are long, slim, arcuate, and oriented anteromedially, with their medial tips distantly separated from one another (narrowly in *R. diadema*), more broadly separated than the coracoids, medially ending at about the same level as the middle of the lateral articulation with the scapula. The curve of the clavicle is almost always less strong than that of the anterior edge of the coracoid.

The coracoid is long (except in *R. guentherpetersi*) and strongly flared, with its sternal end much broader than its glenoid end (sternal end 142–218% of the glenoid end; Table 2). Its anterior edge is more strongly curved than the posterior edge. The midshaft width is 24–36% of the width of the expansion of the sternal end of the bone (Table 2).

The scapula is long (96–151% of coracoid length along its anterior edge; Table 2), with a broad pars acromialis that is clearly distinct from the pars glenoidalis, but approximately equal in length. The pars acromialis is weakly indented on its anterior surface.

The cleithrum is long (can be variable within species), anteriorly thicker, thinning posteriorly; broader at the scapular border, its posterior edge wavy with a distinct notch at the middle of its length (can be absent or asymmetrical). The suprascapula is unossified, but often has mineralization along its ventral and posterior edges.

The postzonal region (sternum) has no ossified elements but can show signs of weak anterior mineralization (e.g. in *R. vaventy*, Fig. S12).

Results

Forelimb and manus. (Fig. 17) The humerus bears ventral and lateral crista, and lacks a medial crista. The crista ventralis broadens proximally from the midpoint (closer to the proximal end in *R. diadema*, *R. coronata*, *R. regalis*), ending abruptly before reaching the unossified caput humeri in *R. ornata*, extending to the caput humeri in all other species (with an indentation of varying strength just before the caput humeri; see Fig. 17e). Sexual dimorphism in the length of the crista ventralis was not noted in *R. regalis*, one male and three females of which were scanned. The radio-ulna is broad. The sulcus intermedium is indicated by a distinct groove.

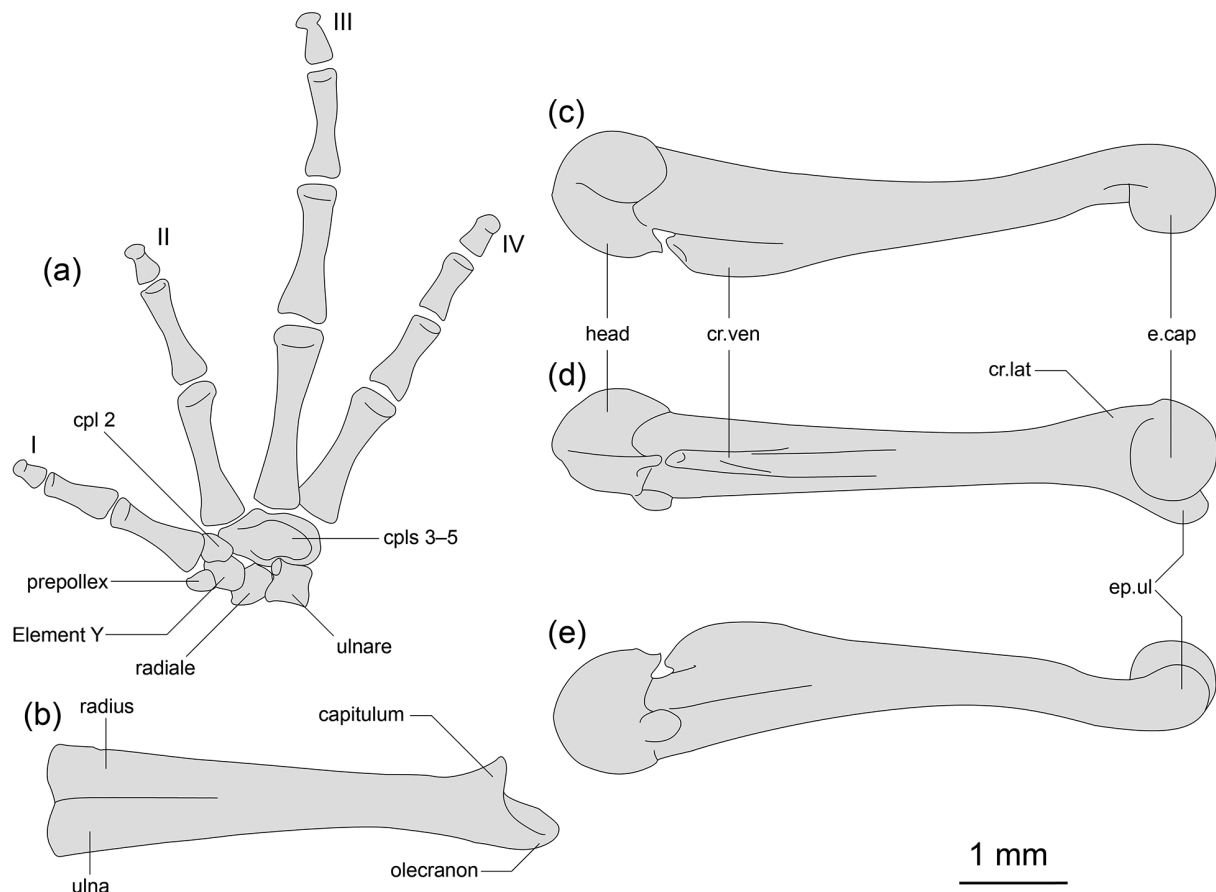


FIGURE 17. Forelimb anatomy of the *R. serratopalpebrosa* species group showing (a) left manus in ventral view, (b) left radio-ulna in dorsal view, and left humerus in (c) lateral, (d) ventral, and (e) medial view. Abbreviations: cpl(s) = carpal(s), cr.lat = crista lateralis, cr.ven = crista ventralis, e.cap = eminentia capitata, ep.ul = epicondylus ulnaris.

The carpals are totally unossified in *R. ornata* but are at least partially ossified in all other species. The carpus is composed of a radiale, ulnare, ossified prepollex element, Element Y, carpal 2, and a large post-axial element probably representing a fusion of carpals 3–5. The finger phalangeal formula is standard (2–2–3–3). Small distal knobs are present on the terminal phalanges of the fingers (not always well resolved in micro-CT scans and particularly sensitive to thresholds used). An ossified prepollex is not visible in adult specimens of *R. ornata* (1 adult male) and *R. tany* (1 adult male); is small in *R. coronata* (2 adult males; larger in one), *R. diadema* (1 adult female), *R. regalis* (1 adult male, 3 adult females; larger in the male), *R. guentherpetersi* (2 adult females), and *R. serratopalpebrosa* (1 adult female); and is large in *R. vaventy* (1 adult male).

Pelvic girdle. (Fig. 18) The pelvic girdle is 44–51% of the SVL in length, being considerably longer in *R. vaventy* than other species (erroneously described as ‘short’ by Scherz *et al.* 2014; see Table 2). The iliac shafts pass ventrolateral to, and extend beyond, the sacrum to a variable degree (note: this was previously considered a diagnostic feature in the distinction of *R. vaventy* and *R. serratopalpebrosa* [Scherz *et al.* 2014], but this joint is flexible and depends on the angle of fixation or mounting for micro-CT imagery, and this is therefore not a valuable character for taxonomic purposes). They are almost cylindrical, with a weak dorsal crest extending nearly their full length, except in one specimen of *R. coronata* (ZSM 474/2005, Fig. S10) in which they are teardrop-shaped in

cross-section and have a relatively strong dorsal crest. Each shaft bears a dorsal prominence (strong in *R. guentherpetersi*, *R. regalis*, *R. serratopalpebrosa*, and *R. tany*; weak in *R. diadema*, *R. vaventy*, and *R. coronata*; variable in *R. ornata*) and deep oblique groove. The ilia are posteriorly fused with the ischium (fusion not visible in *R. ornata* but presumably synchondrotic). The pubis is ossified in *R. regalis* and *R. coronata*, partially ossified in *R. diadema* and *R. vaventy*, and unossified in *R. ornata*, *R. tany*, *R. guentherpetersi*, *R. vaventy*, and *R. serratopalpebrosa* (note that the pubes of *R. serratopalpebrosa* and *R. vaventy* were mistakenly described as being ossified by Scherz *et al.* 2014; previous assessment of the ossification of the pubis was misled by the methodology used; this is discussed below). In a subadult *R. regalis*, the pubis is unossified, suggesting that ossification occurs only at or near maturity. Iliosacral articulation is type IIA sensu Emerson (1979). The overall length of the girdle is 229–283% of the distance between the anterior ends of the iliac shafts (Table 2).

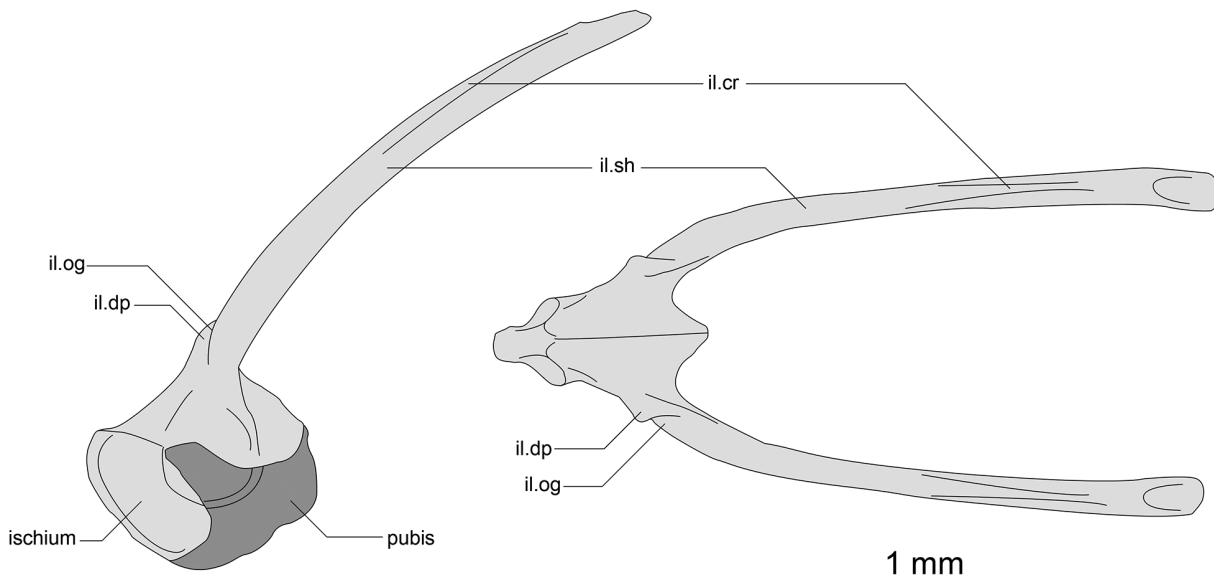


FIGURE 18. The pelvic girdle of the *R. serratopalpebrosa* species group in lateral and dorsal view. Darker colour indicates cartilage. Abbreviations: il.cr = iliac crest, il.sh = iliac shaft, il.dp = dorsal prominence of ilium, il.og = oblique groove of ilium.

Hindlimb and pes. (Fig. 19) The femur is weakly sigmoid. It is nearly equal in length to the tibiofibula (slightly longer in *R. coronata* and *R. guentherpetersi*, and slightly shorter in all other species; not assessable in *R. ornata* due to the lack of terminal ossification). The sulcus intermedius of the tibiofibula is weak. The tibiale and fibulare are much shorter than the tibiofibula. The bones are widely separated at their midpoint and fused at their proximal and distal heads. Two tarsals—T1 and T2+T3—are present, T1 being about half the size of T2+T3; a large centrale and ossified prehallux are also present. The toe phalangeal formula is standard (2–2–3–4–3), but development or ossification of the terminal phalanges is variable in *R. coronata* (one specimen 1–2–3–4–3 and one with a reduced terminal phalanx of the second digit). The terminal phalanges possess distal knobs, which can be weakly or strongly expanded but are never as broad as the base of the phalanx (again, not always well resolved; see comments on the manus, above).

Discussion

Systematics and evolution of the *R. serratopalpebrosa* species group. The addition of three species to the *R. serratopalpebrosa* species group (*R. guentherpetersi* and the new taxa *R. diadema* sp. nov. and *R. regalis* sp. nov.) brings it to a total of eight species. This clade therefore accounts for over half of the described diversity of *Rhombohryne*, and it is likely that it will remain the most diverse clade in the genus even once all other known candidates are described (Scherz *et al.* unpublished data). It is no surprise that the diversity of these frogs has gone unnoticed for so long, given their secretive nature, but it highlights the need for more thorough investigation of Madagascar's underappreciated microhylids.

Results

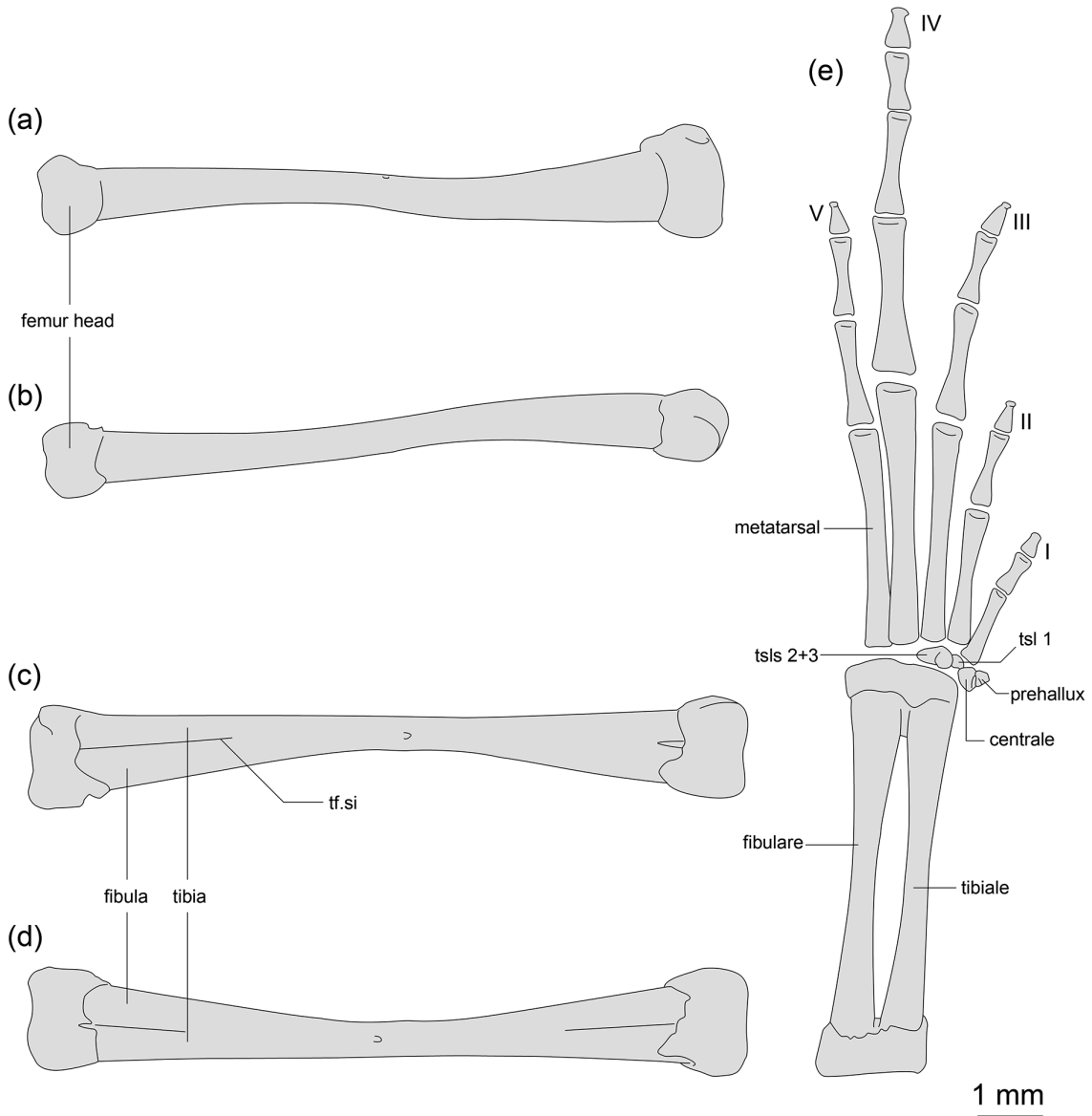


FIGURE 19. Hindlimb anatomy of the *R. serratopalpebrosa* species group showing the right femur in (a) medial and (b) lateral view, the right tibiofibula in (c) ventral and (d) dorsal view, and (e) the right pes and tibiale-fibulare in ventral view. Abbreviations: tf.si = sulcus intermedius of tibiofibula, tsl(s) = tarsal(s).

Rhombophryne guentherpetersi and *R. ornata* are differentiated by a small uncorrected pairwise difference of around 3% in the segment of the *16S* gene most widely used for amphibian barcoding in Madagascar (Vieites *et al.* 2009). This is below typical thresholds for flagging genetic lineages as potentially separate species (Vieites *et al.* 2009). However, evidence from a second segment of the *16S* gene, as well as the nuclear *sacs* gene, recover these species with much higher levels of differentiation, recapitulating their strong morphological distinction. This emphasises that, although the 3' portion of *16S* is generally a good marker for species recognition in frogs (e.g. Vences *et al.* 2005; Vieites *et al.* 2009), low p-distances do not always represent a lack of differentiation. In cases where non-genetic lines of evidence suggest the existence of differentiation that is not apparent from the barcode markers, additional genes should be sequenced to clarify the situation.

The morphological resemblance of *R. tany* and *R. diadema* sp. nov. is extreme, even for this complex, despite them not being especially closely related (5.4–5.5% uncorrected pairwise distance in a segment of the *16S* gene; not sister species). Indeed, they are almost indistinguishable in life (compare Fig. 1d with 11c). Only subtle

characters (especially the number of supraciliary spines, tibia length, strength of the supratympanic fold, and several osteological characters) were found to distinguish them. However, our dataset remains incomplete, and it is likely that, as for all members of this genus (e.g. Scherz *et al.* 2016a; Lambert *et al.* 2017), bioacoustic data will further assist in the differentiation of these species, if ever recordings can be made.

The affinities of *R. serratopalpebrosa* have remained uncertain throughout our revision of this complex. *Rhombophryne vaventy* occurs probably in close proximity (sympatrically or parapatrically) with it on the Marojejy Massif, but differs from it strongly in morphology (Scherz *et al.* 2014). *Rhombophryne regalis sp. nov.*, which is from areas near Marojejy but not yet known from the Massif itself, is morphologically more similar to *R. serratopalpebrosa* than any other *Rhombophryne* species currently known. It shares in particular the S-shaped fold before the naris, which is not known from any other member of this genus, and may be a synapomorphy of these two species, which we hypothesise to be sister to one another. Despite their similarity, the distinctiveness of *R. serratopalpebrosa* and *R. regalis sp. nov.* is sufficient that we think it unlikely that they will be revealed to be conspecific if ever genetic data become available from *R. serratopalpebrosa*. To test this hypothesis we emphasise the need to collect additional material of *R. serratopalpebrosa* from the type locality so that we can finally clarify its genetic relationships.

Biogeography and conservation of the *R. serratopalpebrosa* species group. Although sampling at present is sparse, the biogeographic patterns of the *R. serratopalpebrosa* group are worthy of remark (Fig. 20). The group has its centre of diversity in northern Madagascar, with three species probably co-occurring on the Tsaratanana Massif, two occurring in Sorata (the second being *R. vaventy*, based on a sequence of specimen AMNH A167315 from 13.6858°S, 49.4419°E from Frost *et al.* (2006) shown to be minimally divergent from *R. vaventy* by Scherz *et al.* 2016b and Lambert *et al.* 2017), two on Marojejy, and one in Anjanaharibe-Sud. *Rhombophryne coronata* is exceptional in being found in the central east of Madagascar, roughly 470 km south of the rest of the group. Additional surveys are needed in forests between Andasibe and Anjanaharibe-Sud to search for taxa that might tie *R. coronata* to the rest of the group, as no such records are currently known to exist. Given the sister relationship between *R. coronata* and the rest of the group, it is tempting to conclude that they may have originated in eastern Madagascar, and not in their centre of diversity in northern Madagascar. However, it must also be noted that the next closest group of *Rhombophryne* species, *R. minuta* and *R. longicrus*, are found in Marojejy and Sorata respectively, and therefore definitely have a northern distribution. It seems therefore more likely that they may have originated in northern Madagascar, with the lineage later giving rise to *R. coronata* subsequently moving southwards. This hypothesis will be worth testing explicitly once additional distribution data are available, taxonomy within the genus has been better resolved, and perhaps in light of a time-calibrated phylogeny.

TABLE 3. IUCN Red List status of members of the *R. serratopalpebrosa* group. Note that the statuses assigned to many species differ from recommendations given in their original descriptions (e.g. Scherz *et al.* 2014, 2015a). For explanation of criteria, see IUCN (2012) and the text above. AOO = Area of Occupancy, EOO = Extent of Occurrence.

Species	Status as of March 2017 ([†] indicates recommended status for new taxa)	No. of threat-defined locations as defined by the IUCN Red List	Estimated AOO (km ²)	Estimated EOO (km ²)
<i>R. serratopalpebrosa</i>	EN B1ab(iii)	1	Unknown	780
<i>R. coronata</i>	LC	~4*	>2600	37170*
<i>R. vaventy</i>	EN B1ab(iii)	2 [‡]	Unknown	~2000 [‡]
<i>R. ornata</i>	EN B1ab(iii)	1	Unknown	1236
<i>R. tany</i>	EN B1ab(iii)	1	Unknown	1236
<i>R. guentherpetersi</i>	EN B1ab(iii)	2	Unknown	<5000
<i>R. diadema</i> sp. nov.	EN B1ab(iii) [†]	1	250	250
<i>R. regalis</i> sp. nov.	VU B1ab(iii) [†]	3	Unknown	>7000

*The current EOO estimate of *R. coronata* includes records from Andringitra that require confirmation. These are not included in our map (Fig. 20) or the number of localities in this table.

[‡]A second locality for *R. vaventy* was published by Frost *et al.* (2006) as shown by Scherz *et al.* (2016b) and Lambert *et al.* (2017). This increases its EOO from 780 km² to around 2000 km², but does not change its IUCN status (EOO still below 5000 km²).

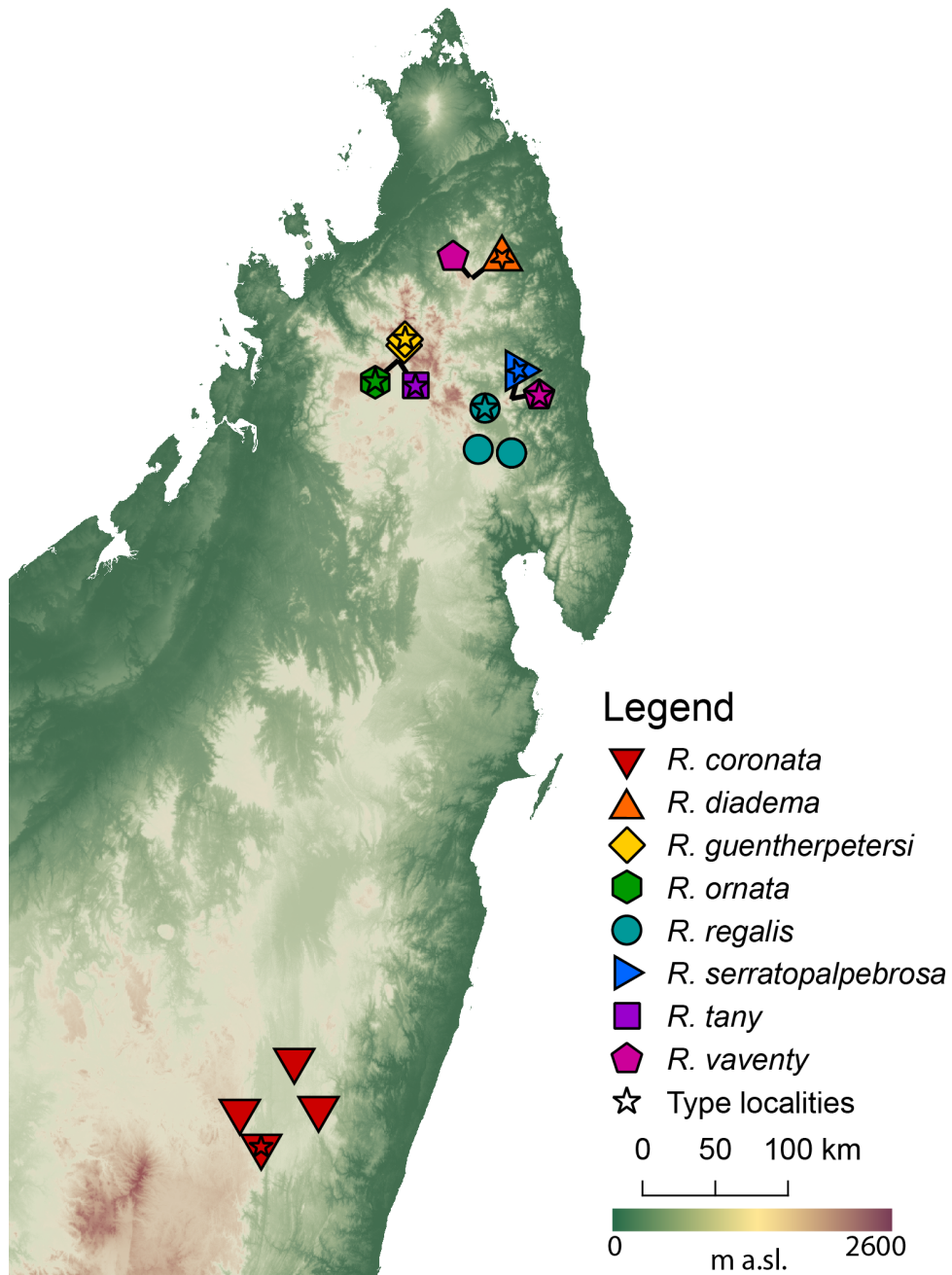


FIGURE 20. Map of northern Madagascar showing confirmed localities for all described members of the *Rhombophryne serratopalpebrosa* group. The type locality of *R. guentherpetersi* is inferred by us to be Maromokotro mountain. The second locality of *R. vaventy* in Sorata is from Frost *et al.* (2006) based on its relationships in Scherz *et al.* (2016b) and Lambert *et al.* (2017). Map produced in QGIS v2.8.2-Wien (QGIS Development Team, 2016) using SRTM 90 m raster data.

Considering their fairly small ranges and poor knowledge of their distribution, we currently consider almost all members of the *R. serratopalpebrosa* group as likely threatened (see Table 3). Only *R. coronata* is exempt, although it must be noted that its current assessment includes dubious records from Andringitra that are in need of taxonomic clarification (IUCN SSC Amphibian Specialist Group 2016b). We do not, however, consider any of these likely threatened species to be under immediate danger of extinction. Based on our current knowledge, the most threatened is undoubtedly *R. diadema*, which is known from a single location in forest that is currently unprotected and under heavy anthropogenic pressure. In all cases (including *R. coronata*), the future of the species

depends on the maintenance of the forests they inhabit. Madagascar is in the process of expanding its protected area network (Rabearivony *et al.* 2010, 2015). Depending on the effectiveness of the implementation of these new protected areas, this may result in the improvement of the conservation status of *R. diadema* and the rest of this species group. At present however, the fate of most, if not all members of this group, remains uncertain.

Digital osteology: surfaces vs. volumes. The osteology of the *Rhombophryne serratopalpebrosa* species group has been a major component in its taxonomic resolution over the last four years (Scherz *et al.* 2014, 2015a, present work). Our previous work on this genus has been done predominantly based on 3D surface models produced in Amira software (Scherz *et al.* 2014, 2015a,b, 2016a), whereas the osteological analysis presented here is based on examination of volumes rendered in VG Studio Max 2.2. As a result of this methodological change, we discovered at least one significant discrepancy between the osteology of this group as described here and as described by us previously: *R. vaventy* and *R. serratopalpebrosa* have unossified pubes, which were incorrectly described and depicted as ‘ossified’ by Scherz *et al.* (2014; see Fig. 21). Consequently, unossified pubes were misinterpreted as diagnostic of members of the genus from the Tsaratanana Massif in Scherz *et al.* 2015a (although the general pattern of low ossification of these species remains taxonomically valuable). Although this disparity does not have major consequences for our taxonomic interpretation, it raises issues on the analysis, representation, and interpretation of micro-CT data that must be discussed. This is particularly important as taxonomists increasingly add micro-CT to their toolbox of methods for incorporation in ‘integrative’ approaches.

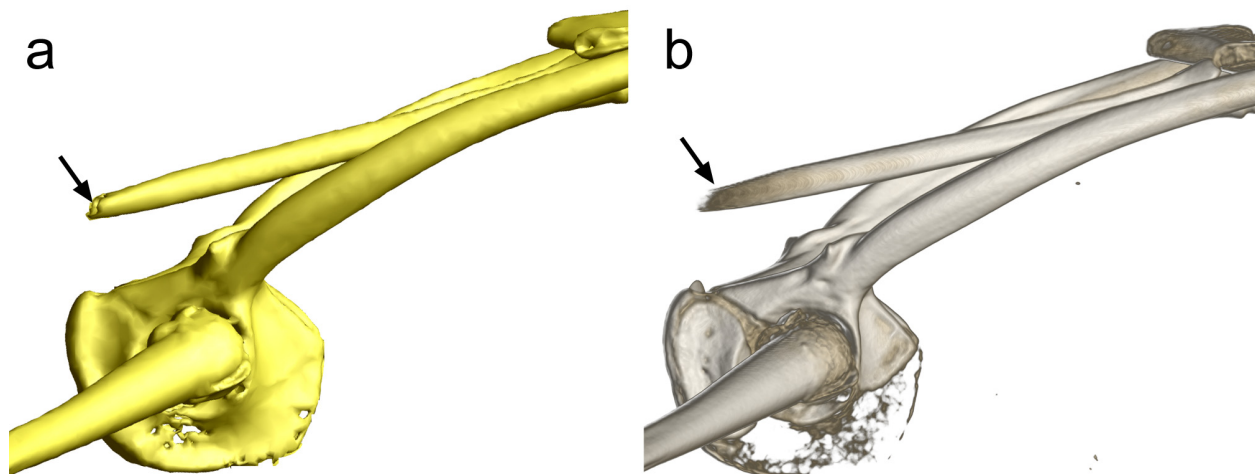


FIGURE 21. Comparison of (a) surface and (b) volume rendering of the same skeletal region of the same specimen; the acetabulum of *Rhombophryne serratopalpebrosa* (MNHN 1975.24). The surface rendering is that used in Scherz *et al.* (2014). The volume rendering was produced for this study. Note particularly the unossified state of the pubis in (b) compared to that reproduced in (a). The arrow indicates the end of the urostyle, which gradually thins towards its tip, but is shown to end abruptly in surface rendering due to the on/off characteristic of meshes.

Surface rendering depends on user-defined density thresholds and subsequent manual segmentation of structures that are either over- or under-rendered. The result is a three-dimensional surface of a single density, that can be converted to a PDF-embedded model that can easily be examined by an end-user (e.g. Figs S1–S12), making surface rendering appealing to the taxonomist and morphologist (Ruthensteiner & Heß 2008). However, display of all bone or bone-like structures as a single density provides a significant loss of information over that contained in raw images produced by micro-CT scanning—where grey values of voxels (3D pixels) are generally proportional to X-ray absorption—and can mislead interpretations. It was this property of surface models that led to the misinterpretation of the poorly ossified pubis of *R. serratopalpebrosa* as being bony in Scherz *et al.* (2014), whereas volume rendering shows that this is not the case; see Fig. 21). It is exceptionally difficult to set manual thresholds for surface rendering that accurately reflect boundaries between ossified and unossified structures, partially because these often form a continuum (consider the cleithrum and suprascapula for instance), and partially because the firm thresholds used in segmentation of one part of a micro-CT scan may not be adequate in another area due to scan artefacts and inconsistencies.

Surface models must also be simplified (i.e. reduction of the number of triangles in a mesh) and smoothed (i.e.

Results

planar alignment of neighbouring triangles) to remove the number of rendering artefacts that they contain, especially when they are either generated using a single general threshold, or when multiple manual thresholds have been applied. This can however introduce new artefacts that obscure or mislead interpretations. The neopalatine and postchoanal portion of the vomer appear as a single fused bone in the models and figures of Scherz *et al.* (2014), and indeed in our own Figs S1–12. This was cautiously interpreted as the postchoanal vomer “overlapping, fused with, or replacing the [neo]palatine” by Scherz *et al.* (2014). These bones are however easily distinguishable in volume renderings, though they overlap extensively. Their apparent fusion in surface rendering was presumably caused by simplification and subsequent smoothing, which removed any trace of the boundaries between them. This emphasises the caution needed to interpret character states based solely on surface rendered micro-CT scans.

Volume rendering depends on a user-defined density curve that modifies transparency based on voxel brightness, meaning that a variety of grey values are represented at transparencies and colours proportional to their x-ray absorption. Because portions of the volume can be segmented and given individual density curves, volume rendering can succumb to the same pitfalls as surface rendering, namely misrepresentation of low-absorption regions as high absorption (e.g. poorly ossified structures as bony). However, when a single density curve is applied to the whole dataset, as was done here, volume rendering presents a more data-rich and objective representation of the skeleton. Precisely how much more accurate this method is than surface rendering must be assessed using cleared and stained specimens in the future, but this is not possible in this genus with so few specimens available. The greatest drawback of volume rendering is that, so far as we know, volumes cannot yet be embedded into PDFs as manipulable 3D models in the way that surface models can. However, rotational videos of volumes can be produced that enable similar three-dimensionality for the end user without compromising the data (see supplemental videos at http://morphosource.org/Detail/ProjectDetail>Show/project_id/254).

We contend that vertebrate taxonomists using micro-CT should, when possible, base osteological descriptions on volume-based visualization (including figures), and provide surface models only as supplemental files to aid the reader in their understanding of the three-dimensional relationships and shapes of the described bones. Invertebrate taxonomists and morphologists working on structures other than bone should carefully consider the applications of the technique they are using, and, when basing figures on surface renderings, should make clear that relative density information is not represented.

Acknowledgements

We thank the Malagasy authorities for providing research permits to the authors over many years of collaboration with the Direction Générale des Forêts. We also thank B. Ruthensteiner, E.Z. Lattenkamp, A. Ohler, M. Kondermann, R.D. Randriaina, F.M. Ratsoavina, S. Rasamison, E. Rajeriarison, F. Randrianasolo, T. Rajoafiarison, and A. Razafimanantsoa for help in various aspects of this project. F. Andreone thanks J.E. Randrianirina, H. Randriamahazo, and G. Aprea for field companionship and assistance. Finally, we thank the Parc Botanique et Zoologique de Tsimbazaza for research authorisation and institutional collaboration. F. Kraus and J. Köhler provided excellent feedback and input on this manuscript, and we are grateful to them for taking the time to review it in such detail.

References

- AmphibiaWeb (2017) AmphibiaWeb: Information on amphibian biology and conservation. <http://amphibiaweb.org/> (accessed 6 March 2017)
- Andreone, F., Vences, M., Vieites, D.R., Glaw, F. & Meyer, A. (2005) Recurrent ecological adaptations revealed through a molecular analysis of the secretive cophyline frogs of Madagascar. *Molecular Phylogenetics and Evolution*, 34, 315–322. <https://doi.org/10.1016/j.ympev.2004.10.013>
- Blommers-Schlösser, R.M.A. & Blanc, C.P. (1991) Amphibiens (première partie). *Faune de Madagascar*, 75, 1–397.
- Boettger, O. (1880) Diagnoses reptilium et batrachiorum novorum a Carolo Ebenau in insula Nossi-Bé madagascariensi lectorum. *Zoologischer Anzeiger*, 3, 279–283.
- Boulenger, G.A. (1882) *Catalogue of the Batrachia Salientia s. Caudata in the collection of the British Museum. 2nd Edition.* Taylor and Francis, London, xvi + 503 pp.

- Bruford, M.W., Hanotte, O., Brookfield, J.F.Y. & Burke, T. (1992) Single-locus and multilocus DNA fingerprint. In: Hoelzel, A.R. (Ed.), *Molecular Genetic Analysis of Populations: A Practical Approach*. IRL Press, Oxford, pp. 225–270.
- Cope, E.D. (1889) The Batrachia of North America. *Bulletin of the United States National Museum*, 34, 1–525.
- Dayrat, B. (2005) Towards integrative taxonomy. *Biological Journal of the Linnean Society*, 85, 407–415.
<https://doi.org/10.1111/j.1095-8312.2005.00503.x>
- D'Cruze, N., Köhler, J., Vences, M. & Glaw, F. (2010) A new fat fossorial frog (Microhylidae: Cophylinae: *Rhombophryne*) from rainforest of the Forêt d'Ambre Special Reserve, northern Madagascar. *Herpetologica*, 66, 182–191.
<https://doi.org/10.1655/09-008R1.1>
- Edgar, R.C. (2004) MUSCLE: multiple sequence alignment with high accuracy and high throughput. *Nucleic Acids Research*, 32, 1792–1797.
<https://doi.org/10.1093/nar/gkh340>
- Emerson, S.B. (1979) The ilio-sacral articulation in frogs: form and function. *Biological Journal of the Linnean Society*, 11, 153–168.
<https://doi.org/10.1111/j.1095-8312.1979.tb00032.x>
- Fabrezi, M. & Alberch, P. (1996) The carpal elements of anurans. *Herpetologica*, 52, 188–204.
- Fonseca, A.A., Cherubini, K., Veeck, E.B., Ladeira, R.S. & Carapeto, L.P. (2008) Effect of 10% formalin on radiographic optical density of bone specimens. *Dentomaxillofacial Radiology*, 37, 137–141.
<https://doi.org/10.1259/dmfr/18109064>
- Frank, N. & Ramus, E. (1995) *Complete Guide to Scientific and Common Names of Amphibians and Reptiles of the World*. N. G. Publishing Inc., Pottsville, Pennsylvania, 377 pp.
- Frost, D.R., Grant, T., Faivovich, J., Bain, R.H., Haas, A., Haddad, C.F.B., de Sá, R.O., Channing, A., Wilkinson, M., Donnellan, S.C., Raxworthy, C.J., Campbell, J.A., Blotto, B.L., Moler, P., Drewes, R.C., Nussbaum, R.A., Lynch, J.D., Green, D.M. & Wheeler, W.C. (2006) The Amphibian Tree of Life. *Bulletin of the American Museum of Natural History*, 297, 1–370.
[https://doi.org/10.1206/0003-0090\(2006\)297\[0001:TATOL\]2.0.CO;2](https://doi.org/10.1206/0003-0090(2006)297[0001:TATOL]2.0.CO;2)
- Glaw, F., Köhler, J. & Vences, M. (2010) A new fossorial frog, genus *Rhombophryne*, from Nosy Mangabe Special Reserve, Madagascar. *Zoosystematics and Evolution*, 86, 235–243.
<https://doi.org/10.1002/zoos.201000006>
- Glaw, F. & Vences, M. (2007) *A Field Guide to the Amphibians and Reptiles of Madagascar*. Vences & Glaw Verlags GbR, Köln, 496 pp.
- Guibé, J. (1974) Batraciens nouveaux de Madagascar. *Bulletin du Muséum national d'Histoire Naturelle*, 3, 1170–1192.
- Guibé, J. (1975) Batraciens nouveaux de Madagascar. *Bulletin du Muséum National d'Histoire Naturelle, Paris, Serie 3, Zoologie*, 323, 1081–1089.
- Guibé, J. (1978) Les batraciens de Madagascar. *Bonner zoologische Monographien*, 11, 1–140.
- IUCN (2012) *IUCN Red List Categories and Criteria: Version 3.1*. IUCN, Gland & Cambridge. Available from: <http://www.iucnredlist.org/technical-documents/categories-and-criteria/2001-categories-criteria> (accessed 24 April 2017)
- IUCN SSC Amphibian Specialist Group (2016a) *Rhombophryne guentherpetersi*. The IUCN Red List of Threatened Species 2016: e.T57971A84181017. Available from: <http://www.iucnredlist.org/details/57971/0> (accessed 18 July 2016)
- IUCN SSC Amphibian Specialist Group (2016b) *Rhombophryne coronata*. The IUCN Red List of Threatened Species 2016: e.T57969A84180747. Available from: <http://www.iucnredlist.org/details/57969/0> (accessed 18 July 2016)
- Köhler, J., Vences, M., D'Cruze, N. & Glaw, F. (2010) Giant dwarfs: discovery of a radiation of large-bodied 'stump-toed frogs' from karstic cave environments of northern Madagascar. *Journal of Zoology*, 282, 21–38.
<https://doi.org/10.1111/j.1469-7998.2010.00708.x>
- Kumar, S., Stecher, G. & Tamura, K. (2016) MEGA7: Molecular Evolutionary Genetics Analysis Version 7.0 for Bigger Datasets. *Molecular Biology and Evolution*, 33, 1870–1874.
<https://doi.org/10.1093/molbev/msw054>
- Lambert, S.M., Hutter, C.R. & Scherz, M.D. (2017) Diamond in the rough: a new species of fossorial diamond frog (*Rhombophryne*) from Ranomafana National Park, southeastern Madagascar. *Zoosystematics and Evolution*, 93, 143–155.
<https://doi.org/10.3897/zse.93.10188>
- Lanfear, R., Calcott, B., Ho, S.Y.W. & Guindon, S. (2012) PartitionFinder: Combined selection of partitioning schemes and substitution models for phylogenetic analyses. *Molecular Biology and Evolution*, 29, 1695–1701.
<https://doi.org/10.1093/molbev/mss020>
- Meyer, C., Geller, J. & Paulay, G. (2005) Fine scale endemism on coral reefs: Archipelagic differentiation in turbinid gastropods. *Evolution*, 59, 113–125.
<https://doi.org/10.1554/04-194>
- Padial, J.M., Castroviejo-Fisher, S., Köhler, J., Vilà, C., Chaparro, J.C. & de la Riva, I. (2008) Deciphering the products of evolution at the species level: the need for an integrative taxonomy. *Zoologica Scripta*, 38, 431–447.
<https://doi.org/10.1111/j.1463-6409.2008.00381.x>
- Padial, J.M. & de la Riva, I. (2010) A response to recent proposals for integrative taxonomy. *Biological Journal of the Linnean Society*, 101, 747–756.
<https://doi.org/10.1111/j.1095-8312.2010.01528.x>

Results

- Padial, J.M., Miralles, A., De La Riva, I. & Vences, M. (2010) The integrative future of taxonomy. *Frontiers in Zoology*, 7, 16. <https://doi.org/10.1186/1742-9994-7-16>
- Palumbi, S.R., Martin, A., Romano, S., McMillan, W.O., Stice, L. & Grabowski, G. (1991) *The simple fool's guide to PCR, Version 2.0*. Privately published, University of Hawaii.
- Perl, R.G.B., Nagy, Z.T., Sonet, G., Glaw, F., Wollenberg, K.C. & Vences, M. (2014) DNA barcoding Madagascar's amphibian fauna. *Amphibia-Reptilia*, 35, 197–206. <https://doi.org/10.1163/15685381-00002942>
- Rabearivony, J., Rasamolina, M., Raveloson, J., Rakotomanana, H., Raselimanana, A.P., Raminosoa, N.R. & Zaonarivel, J.R. (2015) Roles of a forest corridor between Marojejy, Anjanaharibe-Sud and Tsaratanana protected areas, northern Madagascar, in maintaining endemic and threatened Malagasy taxa. *Madagascar Conservation & Development*, 10, 85–92. <https://doi.org/10.4314/mcd.v10i2.7>
- Rabearivony, J., Thorstrom, R., Rene de Roland, A., Rakotondratsima, M., Andriamalala, T.R.A., Sam, T.S., Razafimanjato, G., Rakotondravony, D., Raselimanana, A.P. & Rakotoson, M. (2010) Protected area surface extension in Madagascar: Do endemism and threatened species remain useful criteria for site selection? *Madagascar Conservation & Development*, 5, 35–47. <https://doi.org/10.4314/mcd.v5i1.57338>
- Rambaut, A. & Drummond, A.J. (2007) Tracer v1.5. Available from: <http://beast.bio.ed.ac.uk/Tracer> (Accessed 30 May 2017)
- Raxworthy, C.J. (2008) Global warming and extinction risks for amphibians in Madagascar: a preliminary assessment of upslope displacement. In: Andreone, F. (Ed.), *A Conservation Strategy for the Amphibians of Madagascar - Monografie*. Museo Regionale di Scienze Naturali, Torino, pp. 67–84.
- Raxworthy, C.J., Pearson, R.G., Rabibisoa, N., Rakotondrazafy, A.M., Ramanamanjato, J.-B., Raselimanana, A.P., Wu, S., Nussbaum, R.A. & Stone, D.A. (2008) Extinction vulnerability of tropical montane endemism from warming and upslope displacement: a preliminary appraisal for the highest massif in Madagascar. *Global Change Biology*, 14, 1703–1720. <https://doi.org/10.1111/j.1365-2486.2008.01596.x>
- Ronquist, F., Teslenko, M., van der Mark, P., Ayres, D.L., Darling, A., Höhna, S., Larget, B., Liu, L., Suchard, M.A. & Huelsenbeck, J.P. (2012) MRBAYES 3.2: Efficient Bayesian phylogenetic inference and model selection across a large model space. *Systematic Biology*, 61, 539–542. <https://doi.org/10.1093/sysbio/sys029>
- Ruthensteiner, B. & Heß, M. (2008) Embedding 3D models of biological specimens in PDF publications. *Microscopy Research and Technique*, 71, 778–786. <https://doi.org/10.1002/jemt.20618>
- Scherz, M.D., Glaw, F., Vences, M., Andreone, F. & Crottini, A. (2016a) Two new species of terrestrial microhylid frogs (Microhylidae: Cophylinae: *Rhombophryne*) from northeastern Madagascar. *Salamandra*, 52, 91–106.
- Scherz, M.D., Rakotoarison, A., Hawlitschek, O., Vences, M. & Glaw, F. (2015b) Leaping towards a saltatorial lifestyle? An unusually long-legged new species of *Rhombophryne* (Anura, Microhylidae) from the Sorata massif in northern Madagascar. *Zoosystematics and Evolution*, 91, 105–114. <https://doi.org/10.3897/zse.91.4979>
- Scherz, M.D., Ruthensteiner, B., Vences, M. & Glaw, F. (2014) A new microhylid frog, genus *Rhombophryne*, from northeastern Madagascar, and a re-description of *R. serratopalpebrosa* using micro-computed tomography. *Zootaxa*, 3860 (6), 547–560. <https://doi.org/10.11646/zootaxa.3860.6.3>
- Scherz, M.D., Ruthensteiner, B., Vieites, D.R., Vences, M. & Glaw, F. (2015a) Two new microhylid frogs of the genus *Rhombophryne* with supraciliary spines from the Tsaratanana Massif in northern Madagascar. *Herpetologica*, 71, 310–321. <https://doi.org/10.1655/HERPETOLOGICA-D-14-00048>
- Scherz, M.D., Vences, M., Rakotoarison, A., Andreone, F., Köhler, J., Glaw, F. & Crottini, A. (2016b) Reconciling molecular phylogeny, morphological divergence and classification of Madagascan narrow-mouthed frogs (Amphibia: Microhylidae). *Molecular Phylogenetics and Evolution*, 100, 372–381. <https://doi.org/10.1016/j.ympev.2016.04.019>
- Shen, X.X., Liang, D. & Zhang, P. (2012) The development of three long universal nuclear protein-coding locus markers and their application to osteichthyan phylogenetics with nested PCR. *PLoS ONE*, 7, e39256. <https://doi.org/10.1371/journal.pone.0039256>
- Stuart, S.N., Hoffmann, M., Chanson, J.S., Cox, N.A., Berridge, R.J., Ramani, P. & Young, B.E. (2008) *Threatened Amphibians of the World*. Lynx Edicions, Barcelona; IUCN, Gland & Conservation International, Arlington, Virginia, 758 pp.
- Trueb, L. (1968) Cranial osteology of the hylid frog, *Smilisca baudini*. *University of Kansas Publications, Museum of Natural History*, 18, 11–35.
- Trueb, L. (1973) Bones, frogs, and evolution. In: Vial, J.L. (Ed.), *Evolutionary biology of the anurans: Contemporary research on major problems*. University of Missouri Press, USA, pp. 65–132.
- Vences, M. & Glaw, F. (2003) New microhylid frog (*Plethodontohyla*) with a supraocular crest from Madagascar. *Copeia*, 2003, 789–793.

<https://doi.org/10.1643/ha02-285.1>

Vences, M., Glaw, F., Köhler, J. & Wollenberg, K.C. (2010) Molecular phylogeny, morphology and bioacoustics reveal five additional species of arboreal microhylid frogs of the genus *Anodonthyla* from Madagascar. *Contributions to Zoology*, 79, 1–32.

Vences, M., Kosuch, J., Glaw, F., Böhme, W. & Veith, M. (2003) Molecular phylogeny of hyperoliid treefrogs: biogeographic origin of Malagasy and Seychellelean taxa and re-analysis of familial paraphyly. *Journal of Zoological Systematics and Evolutionary Research*, 41, 205–215.

<https://doi.org/10.1046/j.1439-0469.2003.00205.x>

Vences, M., Thomas, M., Bonett, R.M. & Vieites, D.R. (2005) Deciphering amphibian diversity through DNA barcoding: chances and challenges. *Philosophical Transactions of the Royal Society B*, 360, 1859–1868.

<https://doi.org/10.1098/rstb.2005.1717>

Vieites, D.R., Wollenberg, K.C., Andreone, F., Köhler, J., Glaw, F. & Vences, M. (2009) Vast underestimation of Madagascar's biodiversity evidenced by an integrative amphibian inventory. *Proceedings of the National Academy of Sciences of the United States of America*, 106, 8267–8272.

<https://doi.org/10.1073/pnas.0810821106>

Watters, J.L., Cummings, S.T., Flanagan, R.L. & Siler, C.D. (2016) Review of morphometric measurements used in anuran species descriptions and recommendations for a standardized approach. *Zootaxa*, 4072 (4), 477–495.

<http://doi.org/10.11646/zootaxa.4072.4.6>

Wollenberg, K.C., Vieites, D.R., van der Meijden, A., Glaw, F., Cannatella, D.C. & Vences, M. (2008) Patterns of endemism and species richness in Malagasy cophyline frogs support a key role of mountainous areas for speciation. *Evolution*, 62, 1890–1907.

<https://doi.org/10.1111/j.1558-5646.2008.00420.x>

SUPPLEMENTARY FIGURE 1. Interactive PDF-3D model of the skeleton of *Rhombophryne guentherpetersi*, ZSM 608/2014 (DRV 6231). To activate the model, open the PDF in Adobe Acrobat IX or above, and click the image.

SUPPLEMENTARY FIGURE 2. Interactive PDF-3D model of the skeleton of *Rhombophryne guentherpetersi*, MNHN 1953.165 (holotype). To activate the model, open the PDF in Adobe Acrobat IX or above, and click the image.

SUPPLEMENTARY FIGURE 3. Interactive PDF-3D model of the skeleton of *Rhombophryne regalis*, MRSN-A4602 (FN 7292; holotype). To activate the model, open the PDF in Adobe Acrobat IX or above, and click the image.

SUPPLEMENTARY FIGURE 4. Interactive PDF-3D model of the skeleton of *Rhombophryne regalis*, MRSN-A6058 (paratype). To activate the model, open the PDF in Adobe Acrobat IX or above, and click the image.

SUPPLEMENTARY FIGURE 5. Interactive PDF-3D model of the skeleton of *Rhombophryne regalis*, MRSN-A4620 (paratype). To activate the model, open the PDF in Adobe Acrobat IX or above, and click the image.

SUPPLEMENTARY FIGURE 6. Interactive PDF-3D model of the skeleton of *Rhombophryne regalis*, MRSN-A4618 (paratype). To activate the model, open the PDF in Adobe Acrobat IX or above, and click the image.

SUPPLEMENTARY FIGURE 7. Interactive PDF-3D model of the skeleton of *Rhombophryne regalis*, MRSN-A4619 (paratype). To activate the model, open the PDF in Adobe Acrobat IX or above, and click the image.

SUPPLEMENTARY FIGURE 8. Interactive PDF-3D model of the skeleton of *Rhombophryne diadema*, ZSM 1629/2012 (FGZC 3604; holotype). To activate the model, open the PDF in Adobe Acrobat IX or above, and click the image.

SUPPLEMENTARY FIGURE 9. Interactive PDF-3D model of the skeleton of *Rhombophryne coronata*, ZSM 694/2001 (MV 2001-199; paratype). To activate the model, open the PDF in Adobe Acrobat IX or above, and click the image.

SUPPLEMENTARY FIGURE 10. Interactive PDF-3D model of the skeleton of *Rhombophryne coronata*, ZSM 474/2005 (ZCMV 2223). To activate the model, open the PDF in Adobe Acrobat IX or above, and click the image.

SUPPLEMENTARY FIGURE 11. Interactive PDF-3D model of the skeleton of *Rhombophryne ornata*, ZSM 2859/2010 (DRV 6156; paratype). To activate the model, open the PDF in Adobe Acrobat IX or above, and click the image.

SUPPLEMENTARY FIGURE 12. Interactive PDF-3D model of the skeleton of *Rhombophryne vaventy*, ZSM 357/2005 (FGZC 3876; holotype). To activate the model, open the PDF in Adobe Acrobat IX or above, and click the image.

APPENDIX 1. Raw measurements of the *Rhombophryne serratopalpebrosa* group. An explanation of the acronyms is given in the Materials and Methods. j = juvenile; sa = subadult; h = holotype; p = paratype; ND = not determined.

Collection Number	Field Number	Species	Type	Sex	SVL	HW	HL	ED	END	NSD	NND	TDH	TDV	HAL	UAL	LAL
MNHN 1975.24		<i>R. serratopalpebrosa</i>	h	F	28.5	12.3	8.2	3.1	1.9	3.2	2.2	2.0	9.2	5.6	8.0	
ZSM 0357/2005	FGZC 3876	<i>R. vaventy</i>	h	M	51.9	24.5	14.4	6.3	4.0	2.4	4.7	2.9	16.0	10.4	12.8	
ZSM 1816/2010	ZCMV 12384	<i>R. ornata</i>	h	M	33.0	14.6	9.7	3.9	2.3	1.6	3.4	2.4	8.7	6.4	8.3	
ZSM 2859/2010	DRV 06156	<i>R. ornata</i>	p	sa	21.7	9.0	6.5	2.9	1.8	1.1	2.1	1.4	5.1	3.8	4.7	
ZSM 1815/2010	ZCMV 12382	<i>R. ornata</i>	p	j	19.4	7.7	6.1	2.6	1.2	0.9	2.1	1.2	4.7	3.3	3.7	
UADBA-A 60834		<i>R. ornata</i>	p	sa	18.8	8.8	5.9	ND	ND	ND	3.0	ND	ND	4.9	2.9	3.4
UADBA-A 60835		<i>R. ornata</i>	p	sa	20.5	9.1	6.0	ND	ND	ND	2.7	ND	ND	4.6	3.5	4.4
UADBA-A 60734		<i>R. ornata</i>	p	sa	24.4	11.2	6.9	ND	ND	ND	2.5	ND	ND	6.0	3.1	4.5
MNHN 1953.165		<i>R. guentherpetersi</i>	h	F	34.6	11.7	8.7	3.4	2.0	1.6	3.2	1.6	2.2	8.1	5.4	7.4
MNHN 1953.165B		<i>R. guentherpetersi</i>	p	F	30.6	11.7	8.4	3.0	1.9	1.8	3.1	1.5	1.9	8.5	5.8	7.0
MNHN 1973.592		<i>R. guentherpetersi</i>	p	F	26.0	10.0	7.3	3.0	1.9	1.5	2.4	1.6	1.6	6.7	4.9	6.2
ZSM 608/2014	DRV 06231	<i>R. guentherpetersi</i>	--	F	28.9	11.5	8.3	3.1	1.8	1.6	3.0	1.6	1.9	7.5	4.3	5.7
ZSM 606/2014	DRV 06220	<i>R. guentherpetersi</i>	--	F	35.7	13.0	9.3	3.3	1.9	1.5	3.2	2.2	2.1	9.3	5.0	6.5
ZSM 607/2014	DRV 06223	<i>R. guentherpetersi</i>	--	M	27.3	10.6	7.5	3.1	1.8	1.6	2.7	1.4	1.3	7.5	4.2	5.3
MRSN A4602	FN 7292	<i>R. regalis</i>	h	M	22.4	9.1	6.3	2.4	1.5	1.2	2.2	1.1	1.3	4.5	3.6	5.0
MRSN A4603	FN 7146	<i>R. regalis</i>	p	F	24.1	9.7	7.4	2.8	1.8	1.4	2.5	1.9	1.7	5.1	3.9	5.1
MRSN A4618		<i>R. regalis</i>	p	F	26.5	10.0	7.6	2.8	1.9	1.4	3.0	1.6	1.6	6.0	4.3	6.0
MRSN A4619		<i>R. regalis</i>	p	sa	18.6	8.2	6.0	2.2	1.4	1.3	2.3	1.3	1.4	4.5	3.5	5.1
MRSN A4620		<i>R. regalis</i>	p	F	22.9	8.2	6.8	2.6	1.5	1.2	2.8	1.6	1.6	5.2	4.2	5.4
MRSN A6058		<i>R. regalis</i>	p	F	20.2	8.7	6.7	2.3	1.6	1.4	2.6	1.6	1.6	4.6	3.8	4.7
ZSM 1629/2012	FGZC 3604	<i>R. diadema</i>	h	F	22.7	9.8	6.2	2.7	1.6	1.1	2.9	1.8	1.8	5.6	2.9	4.9
ZSM 1628/2012	FGZC 3731	<i>R. diadema</i>	p	M	23.4	9.6	6.6	2.5	1.8	1.3	2.9	1.5	1.6	5.5	4.0	4.4
ZSM 694/2001	MV 2001-199	<i>R. coronata</i>	p	M	20.4	8.4	5.5	2.3	1.6	1.3	2.3	1.0	1.2	4.1	3.3	4.7
KU 340732	CRH 457	<i>R. coronata</i>	--	F	22.2	9.2	6.5	2.6	1.5	1.2	2.4	1.4	1.4	5.1	5.1	5.6
ZSM 474/2005	ZCMV 2223	<i>R. coronata</i>	--	A	19.4	8.4	5.4	2.4	1.4	0.9	2.1	0.9	0.9	4.1	2.4	3.8
ZSM 473/2005	ZCMV 2222	<i>R. coronata</i>	--	A	23.2	9.0	5.9	2.4	1.6	1.1	2.2	1.1	1.1	4.7	3.4	3.9
ZSM 1814/2010	ZCMV 12359	<i>R. tany</i>	h	M	24.6	10.6	6.9	2.5	1.5	1.2	2.6	1.5	1.4	5.8	4.7	5.0

.....continued on the next page

APPENDIX 1. (Continued)

Collection Number	Field Number	Species	FORL	THIL	THIW	TIBL	TIBW	TARL	FOL	FOTL	HIL	IMCL	IMTL
MNHN 1975.24		<i>R. serratopalpebrosa</i>	22.9	13.5	5.0	15.2	3.8	8.4	16.5	24.9	53.6	1.1	1.5
ZSM 0357/2005	FGZC 3876	<i>R. raveni</i>	39.2	26.9	9.2	27.5	6.7	14.8	28.6	43.4	97.8	3.0	4.0
ZSM 1816/2010	ZCMV 12384	<i>R. ornata</i>	23.4	15.3	5.5	15.1	3.8	8.4	15.3	23.6	54.0	1.6	1.3
ZSM 2859/2010	DRV 06156	<i>R. ornata</i>	13.6	8.9	3.3	8.2	2.3	5.3	9.2	14.4	31.6	1.0	1.0
ZSM 1815/2010	ZCMV 12382	<i>R. ornata</i>	11.7	8.7	3.4	8.3	2.1	4.7	9.1	13.9	30.8	0.9	1.1
UADBA-A 60834		<i>R. ornata</i>	11.2	8.3	ND	7.4	ND	4.5	7.4	11.9	27.6	0.8	ND
UADBA-A 60835		<i>R. ornata</i>	12.5	9.6	ND	8.9	ND	5.0	9.6	14.6	33.1	0.9	ND
UADBA-A 60734		<i>R. ornata</i>	13.6	10.9	ND	10.3	ND	6.1	10.8	16.8	38.0	0.9	ND
MNHN 1953.165		<i>R. guentherpetersi</i>	20.9	12.6	5.1	12.1	5.0	7.7	13.6	21.3	46.0	1.3	1.7
MNHN 1953.165B		<i>R. guentherpetersi</i>	21.2	12.5	5.0	11.7	4.8	5.9	13.8	19.7	43.8	1.4	1.4
MNHN 1973.592		<i>R. guentherpetersi</i>	17.9	9.8	3.6	10.1	3.5	5.4	10.9	16.3	36.1	1.1	1.2
ZSM 608/2014	DRV 06231	<i>R. guentherpetersi</i>	17.6	11.7	4.4	10.8	4.5	5.6	12.5	18.1	40.6	1.5	1.2
ZSM 606/2014	DRV 06220	<i>R. guentherpetersi</i>	20.9	13.2	5.6	13.2	5.6	6.8	15.0	21.8	48.3	1.8	1.8
ZSM 607/2014	DRV 06223	<i>R. guentherpetersi</i>	17.0	11.6	4.9	10.1	5.1	5.8	12.1	17.9	39.6	1.3	1.4
MRSN A4602	FN 7292	<i>R. regalis</i>	13.1	10.9	3.5	10.7	2.5	5.3	9.9	15.2	36.9	0.6	0.6
MRSN A4603	FN 7146	<i>R. regalis</i>	14.1	11.4	3.6	12.6	2.5	6.2	11.0	17.2	41.2	0.9	0.9
MRSN A4618		<i>R. regalis</i>	16.4	13.1	3.4	12.5	2.8	6.5	11.4	17.9	43.5	1.1	0.6
MRSN A4619		<i>R. regalis</i>	13.1	10.2	2.4	10.5	1.9	5.3	9.2	14.4	35.2	0.7	0.5
MRSN A4620		<i>R. regalis</i>	14.8	9.9	3.2	11.8	2.8	5.9	10.7	16.6	38.2	0.8	0.8
MRSN A6058		<i>R. regalis</i>	13.1	10.1	3.4	11.2	2.6	5.4	10.5	15.9	37.2	0.7	0.7
ZSM 1629/2012	FGZC 3604	<i>R. dialema</i>	13.5	9.8	3.2	10.4	2.2	6.2	11.2	17.4	37.6	0.8	0.5
ZSM 1628/2012	FGZC 3731	<i>R. dialema</i>	13.8	11.2	4.2	10.2	3.1	6.4	11.0	17.4	38.8	0.7	1.2
ZSM 694/2001	MV 2001-199	<i>R. coronata</i>	12.1	7.9	2.9	7.5	2.4	4.8	8.0	12.8	28.2	0.8	0.7
KU 340732	CRH 457	<i>R. coronata</i>	15.7	10.7	2.7	10.0	2.1	5.6	9.9	15.5	36.2	0.7	1.0
ZSM 474/2005	ZCMV 2223	<i>R. coronata</i>	10.3	8.1	3.5	7.6	2.7	4.0	8.1	12.1	27.8	0.0	1.1
ZSM 473/2005	ZCMV 2222	<i>R. coronata</i>	12.0	8.7	3.8	8.1	2.5	4.4	8.6	12.9	29.7	0.9	0.9
ZSM 1814/2010	ZCMV 12359	<i>R. tany</i>	15.6	10.8	4.4	10.5	2.8	6.3	10.9	17.2	38.4	0.8	0.8

Chapter 8. PAPER: Reconciling molecular phylogeny, morphological divergence and classification of Madagascan narrow-mouthed frogs (Amphibia: Microhylidae)

In this chapter I present a phylogenetic revision of the narrow-mouthed frog subfamily Cophylinae. The impetus for this study was a paper by Peloso et al. (2016), which proposed to revise the taxonomy of the group based on a phylogenomic analysis of the whole of Microhylidae. In this chapter, my colleagues and I reanalyse their data pertaining to the Cophylinae together with the extensive data available from our own work on these frogs. We find that many of their specimens were misidentified, which partly misled their conclusions. This showcases the importance of taxonomic verification of genetic samples used in proposing revisions to taxonomy, especially supraspecific taxonomy. We describe a new genus, *Anilany*, for the frog formerly called *Stumpffia helenae* due to its strong genetic and osteological differentiation. We also highlight the existence of miniaturised frogs with strong genetic divergence, which we suggest may constitute new genera; these are examined in greater detail in **chapter 9**. In the **supplementary material** of this manuscript (available online and on the appended CD), we provide a key to distinguish members of the genera *Plethodontohyla* and *Rhombophryne*. These genera are morphologically highly similar, but are not closely related, highlighting the convergence of external morphology over osteology during ecomorphological convergence in cophylinae frogs.

Scherz, M.D., Vences, M., Rakotoarison, A., Andreone, F., Köhler, J., Glaw, F. & Crottini, A. (2016) Reconciling molecular phylogeny, morphological divergence and classification of Madagascan narrow-mouthed frogs (Amphibia: Microhylidae). *Molecular Phylogenetics and Evolution*, 100(2016):372–381. DOI: 10.1016/j.ympev.2016.04.019

Digital Supplementary Materials on appended CD:

Supplementary Data 1 — Appendices A–C

Supplementary Figures C1–C5

Post-publication comments:

Peloso et al. (2017) reanalysed the dataset used in this paper with a larger outgroup sampling. They recovered near-identical topologies to ours, differing only in the relationships of unstable taxa that are highlighted as such in this chapter. Despite confirming our phylogenetic conclusions, they proposed to lump species again as originally proposed in their 2016 study. They implied that a lumped taxonomy would be preferable because it would reduce the risk that a species is mistakenly placed into the wrong genus—a conclusion that, although undeniably true, argues against supraspecific taxonomy of any kind. Curiously, they made this point in the discussion of two genera that are distinguished by obvious and clearly defining characters, *Stumpffia* and *Rhombophryne*, that can be identified with comparative ease (the former is generally much smaller, have narrower heads, and exhibit digital reduction not present in the latter). We responded (Scherz et al. 2017), showing that (1) Peloso et al. (2017) had mistakenly miscoded their reanalysis of the non-metric multidimensional scaling (NMDS) analysis on morphology performed in this study, obscuring the difference in morphology between *Stumpffia* and *Anilany*, and (2) their phylogeny supports that reported in this chapter except for the position of three unstable lineages. In that paper, we emphasise the role of supraspecific taxonomy in conveying information (a split taxonomy, where the taxa are morphologically distinct, is preferable to a lumped one that obscures such information), and promote a policy of economy of change to supraspecific taxa (Vences et al. 2013).



Reconciling molecular phylogeny, morphological divergence and classification of Madagascan narrow-mouthed frogs (Amphibia: Microhylidae)



Mark D. Scherz ^a, Miguel Vences ^b, Andolalao Rakotoarison ^b, Franco Andreone ^c, Jörn Köhler ^d, Frank Glaw ^a, Angelica Crottini ^{e,*}

^a Zoologische Staatssammlung München (ZSM-SNSB), Münchhausenstr. 21, 81247 München, Germany

^b Zoologisches Institut, Technische Universität Braunschweig, Mendelssohnstraße 4, 38106 Braunschweig, Germany

^c Museo Regionale di Scienze Naturali, Via G. Giolitti, 36, 10123 Torino, Italy

^d Hessisches Landesmuseum Darmstadt, Friedensplatz 1, 64283 Darmstadt, Germany

^e CIBIO, Research Centre in Biodiversity and Genetic Resources, InBIO, Universidade do Porto, Campus Agrário de Vairão, Rua Padre Armando Quintas, N° 7, 4485-661 Vairão, Portugal

ARTICLE INFO

Article history:

Received 19 November 2015

Revised 11 April 2016

Accepted 12 April 2016

Available online 13 April 2016

Keywords:

Cophylinae

Anilany gen. nov.

Cophyla

Platypelis

Rhomboophryne

Stumpffia

ABSTRACT

A recent study clarified several aspects of microhylid phylogeny by combining DNA sequences from Sanger sequencing and anchored phylogenomics, although numerous aspects of tree topology proved highly susceptible to data partition and chosen model. Although the phylogenetic results of the study were in conflict with previous publications, the authors made several changes to the taxonomy of Madagascar's cophyline microhylids. We re-analyzed part of their data together with our own molecular and morphological data. Based on a supermatrix of 11 loci, we propose a new phylogeny of the Cophylinae, and discuss it in the context of a newly generated osteological dataset. We found several sample misidentifications, partially explaining their deviant results, and propose to resurrect the genera *Platypelis* and *Stumpffia* from the synonymy of *Cophyla* and *Rhomboophryne*, respectively. We provide support for the previous genus-level taxonomy of this subfamily, and erect a new genus, *Anilany* gen. nov., in order to eliminate paraphyly of *Stumpffia* and to account for the osteological differences observed among these groups. Deep nodes in our phylogeny remain poorly supported, and future works will certainly refine our classification, but we are confident that these will not produce large-scale rearrangements.

© 2016 Elsevier Inc. All rights reserved.

1. Introduction

Narrow-mouthed frogs of the family Microhylidae are a species-rich and cosmopolitan group of anurans mainly distributed in the tropics. Many microhylids are characterized by their specialized hydrostatic tongue (Meyers et al., 2004), larval morphology (Wassersug, 1984, 1989; Wassersug and Pyburn, 1987; McDiarmid and Altig, 1999; Haas, 2003; Grosjean et al., 2007; Roelants et al., 2011), and osteology (e.g., Parker, 1934; Trueb et al., 2011). These specializations, especially the frequent reductions of skeletal elements, led to the description of a large number of supraspecific units

in this family. In consequence, narrow-mouthed frogs have had fewer species per genus and more monotypic genera than does any other species-rich anuran clade (Van der Meijden et al., 2007). Species contents of many genera have increased over the last decade, with intensive taxonomic revisions leading to the description of numerous new species of microhylids. Currently, 582 species are distinguished, allocated to 60 genera (AmphibiaWeb, 2016, accessed February 2016), compared to 400 species in 64 genera in 2007 (with currently 14 vs. formerly 22 monotypic genera).

Monophyly of the Microhylidae and its placement among neobatrachian frogs have been established in multiple studies (Frost et al., 2006; Roelants et al., 2007; Pyron and Wiens, 2011; Irisarri et al., 2012; Zhang et al., 2013). Various major clades within microhylids, typically each restricted to a single continent or biogeographical region, are well supported. Yet, despite dense taxon sampling for mitochondrial and nuclear DNA sequences (Frost et al., 2006; Van Boclaer et al., 2006; Van der Meijden et al., 2007; Matsui et al., 2011; Pyron and Wiens, 2011; Kurabayashi

* Corresponding author at: CIBIO/InBio, Centro de Investigação em Biodiversidade e Recursos Genéticos, Campus Agrário de Vairão, Rua Padre Armando Quintas, 4485-661 Vairão, Portugal.

E-mail addresses: mark.scherz@gmail.com (M.D. Scherz), m.vences@tu-braunschweig.de (M. Vences), andomailaka@gmail.com (A. Rakotoarison), Franco.Andreone@regione.piemonte.it (F. Andreone), joern.koehler@hlmd.de (J. Köhler), Frank.Glaw@zsm.mwn.de (F. Glaw), tiliquait@yahoo.it (A. Crottini).

et al., 2011; de Sá et al., 2012; Peloso et al., 2016), the relationships among deep intra-familial clades, including subfamilies and genera, have yet to be satisfactorily resolved.

One such subfamily that has, thus far, evaded full phylogenetic resolution is the Cophylinae, a Madagascar-endemic clade of currently 71 species subdivided in seven genera (AmphibiaWeb, 2016). Cophylines are characterized by nidiocolous (endotrophic) tadpoles, procoelous vertebral columns, and by stereotyped long series of tonal advertisement calls in most species, but otherwise are ecomorphologically highly diverse (Glaw and Vences, 2007). They range from some of the smallest terrestrial vertebrates (snout-vent length [SVL] approximately 10 mm) to the largest microhylids in the world (SVL over 105 mm), occur from just above sea level to montane habitats above 2500 m a.s.l., and have adapted to terrestrial (*Madecassophryne*, *Stumpffia*, some *Rhombophryne*, and some *Plethodontohyla*), fossorial (some *Rhombophryne* and some *Plethodontohyla*), arboreal (*Anodonthyla*, *Cophyla*, *Platypelis* and some *Plethodontohyla*) and rupicolous (*Anodonthyla montana*) habits (Andreone et al., 2005; Glaw and Vences, 2007).

In a recent study, Peloso et al. (2016) assembled a comprehensive dataset from classical Sanger sequencing and complemented it with an anchored phylogenomic dataset (Lemmon et al., 2012) for a subset of selected taxa aimed at revisiting the phylogeny of narrow-mouthed frogs. They provided a substantial advance in the understanding of microhylid relationships, but made some controversial changes in supraspecific classification. Especially controversial were changes to the genus-level classification of the Cophylinae, conflicting with all previous studies (e.g., Blommers-Schöller and Blanc, 1991; Andreone et al., 2005; Wollenberg et al., 2008). They suggested that *Platypelis* should be synonymized with *Cophyla*, and *Stumpffia* with *Rhombophryne*. These changes prompted us to revise their proposed classification of cophyline microhylids on the basis of improved Sanger sequence coverage and a newly obtained osteological dataset.

2. Materials and methods

We herein follow the traditional genus-level classification of cophylines (Glaw and Vences, 2007; AmphibiaWeb, 2016) rather than adopting the changes proposed by Peloso et al. (2016) [hereafter named PEL], anticipating our main conclusions. Our classification differs from that suggested by PEL in considering *Platypelis* a valid genus separate from *Cophyla*, and *Stumpffia* a valid genus separate from *Rhombophryne*.

Field numbers used in the main article text and supplemental materials refer to the zoological collections of Christopher Raxworthy (RAX), Frank Glaw (FGZC and FGMV), Miguel Vences (ZCMV, FGMV, and MVTIS), Franco Andreone (FAZC) Achille P. Raselimanana (APR) and Ylenia Chiari (YCHIA). For consistency with previous studies, we mention M. Kondermann DNA extraction numbers (MK). Institutional acronyms used in the main article text and in the supplemental material are as follows: American Museum of Natural History, – Amphibians (AMNH(-A)); Ambrose Monell Cryo Collection of the American Museum of Natural History (AMCC); Museum of Zoology of the University of Michigan (UMMZ); Senckenberg Museum of Natural History, Frankfurt (SMF); Museo Regionale di Scienze Naturali, Torino (MRSN); Université d'Antananarivo, Département de Biologie Animale (UADBA); Zoologisches Forschungsmuseum Alexander Koenig, Bonn (ZFMK); Zoological Museum Amsterdam (ZMA); Zoologische Staatssammlung München (ZSM).

2.1. Phylogenetic inference

We compiled a supermatrix of available DNA sequences for 11 loci and a total of 189 terminals (species and undescribed

candidate species). Data were largely retrieved from our own work published over the past 10 years (e.g., Andreone et al., 2005; Wollenberg et al., 2008; Crottini et al., 2012; Rakotoarison et al., 2012, 2015) and include data from all 38 taxa of Madagascan origin that were included in PEL. These comprised segments of mitochondrial genes: 12S rRNA (12S, 84 sequences), the 3' and the 5' ends of the mitochondrial 16S rRNA (16S_I, 183 sequences; 16S_II, 97 sequences), cytochrome *b* (cytb, 75 sequences), cytochrome oxidase subunit 1 (cox1, 127 sequences); and segments of six protein-coding nuclear genes: recombination-activating genes 1 and 2 (rag1, 57 sequences; rag2, 12 sequences), brain-derived neurotrophic factor (bdnf, 13 sequences), sascin (sacs, 14 sequences), titin (ttn, 15 sequences), and leucine-rich repeat and WD repeat-containing protein (kiaa1239, 18 sequences). A set of 52 sequences was newly obtained using published primers and wet-lab protocols (Van der Meijden et al., 2007; Vieites et al., 2009; Rakotoarison et al., 2012, 2015; Perl et al., 2014). Newly determined sequences were submitted to GenBank (KU937772–KU937817, KX033507–KX033512). The total matrix of gene segments used for analysis, their GenBank accession numbers, and the alignment, have been submitted to Dryad (doi:10.5061/dryad.1b2k5).

Terminals in our genetic analysis include (i) samples of all nominal species of cophylines and scaphiophrynines, including type species of most genera (exceptions: *Madecassophryne truebae*, the sole member of a monotypic genus for which no DNA sequence data are so far available; *Platypelis cowanni*, the type species of *Platypelis*; *Rhombophryne serratopalpebrata*; the recently described *Rhombophryne longicrus*—the sister species of *R. minuta*, see Scherz et al., 2015a; and *Stumpffia kibomena*, closely related to *S. grandis*, see Glaw et al., 2015), (ii) undescribed deep genetic lineages probably representing new species, named according to the standardized scheme proposed by Padial et al. (2010) with numbers of previously known candidate species following Vieites et al. (2009) and Perl et al. (2014), and (iii) cophylines and scaphiophrynines from the PEL dataset for two gene segments (cox1 and 16S) that overlapped the segments we sequenced. It is worth noting that, without considering PEL terminals, our matrix included a dense taxon sampling for all mitochondrial gene segments and for the nuclear rag1. For the other nuclear genes (rag2, bdnf, sacs, ttn, kiaa1239) at least one species per genus was used, with the exception of the bdnf gene fragment, where sequence of *Cophyla* is missing, and of the rag2 gene fragment, where sequences of *Cophyla* and *Anilany gen. nov.* (described herein) are missing.

As cryptic diversity is high in cophylines, we preferred taxonomically unambiguous samples for the construction of the tree shown in Fig. 1. Of the 66 described species used as ingroup terminals (cophylines) in Fig. 1, 25 (38%) were sampled from type specimens of the respective species, and other 20 (30%) from topotypical specimens. The remaining 21 described taxa (32%) of our terminals were diagnosed to species level based on morphology. Terminals from PEL in our study were included largely for comparative purpose, i.e., to assign them to species based on their clustering with sequences determined by ourselves.

Homologous sequences of *Kaloula pulchra* and of all representatives of the subfamily Dyscophinae were used for outgroup rooting. The outgroup and the representatives of the Scaphiophryninae (which are not the focus of this paper) were excluded from the tree in Fig. 1 for graphical purposes, but are shown in the complete tree in the Supplementary Information (Appendix C, Fig. C.1). Phylogenetic analyses were run for each separate gene segment to detect possible contaminants or wrongly labelled sequences.

Chromatograms of newly determined sequences were checked and sequences manually corrected, if necessary, in CodonCode Aligner 3.5.6 (CodonCode Corporation). We used MEGA 6 (Tamura et al., 2013) to align sequences using the MUSCLE algorithm under

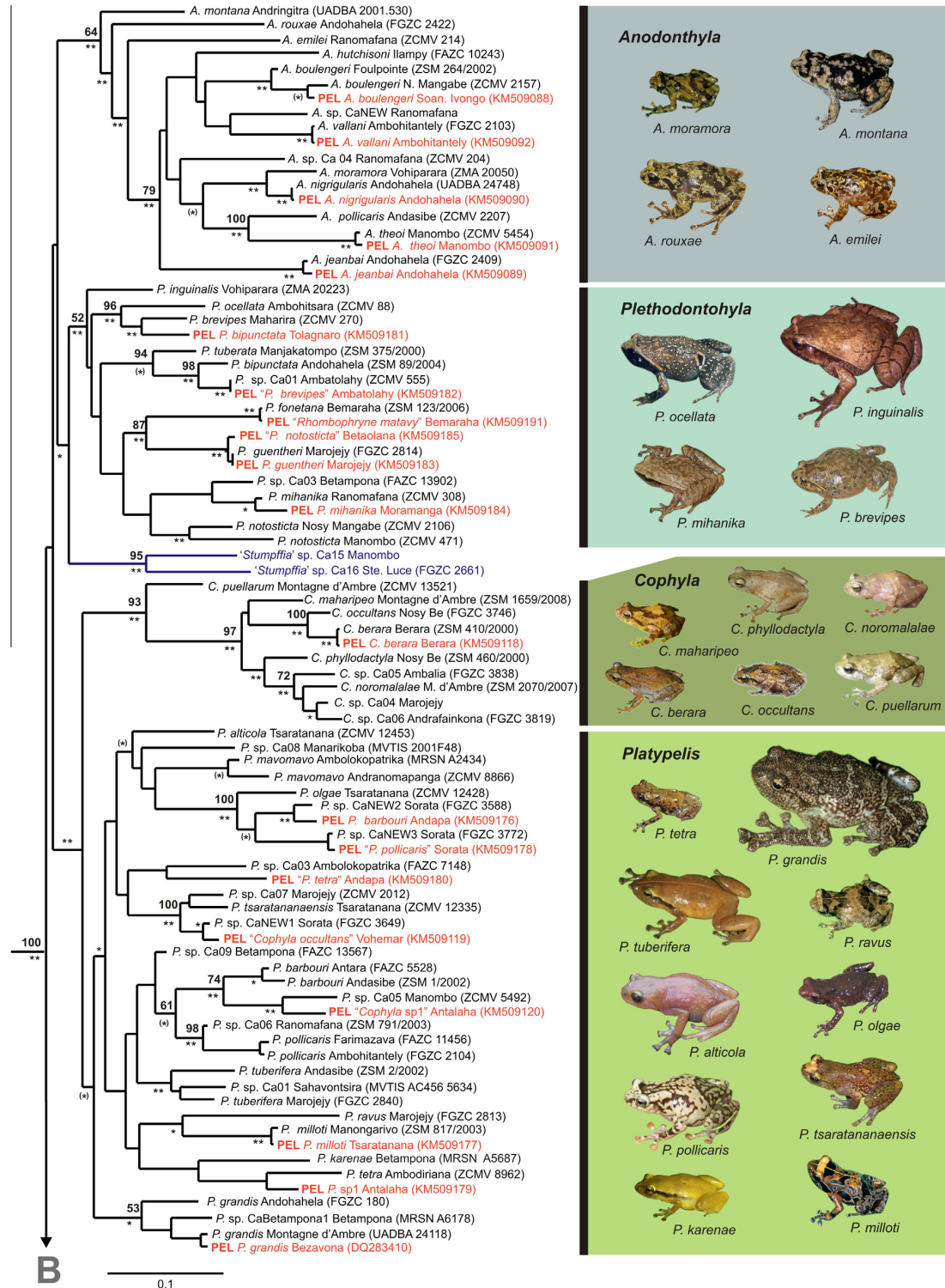


Fig. 1. Phylogram (50% majority rule consensus tree) from a Bayesian Inference analysis of the Cophylinae based on our supermatrix of data combined with the PEL Sanger sequences of the *16S*_J and *cox1* fragments. Terminals from the PEL study are indicated by the bold prefix PEL and are in red, with species names in quotation marks indicating misidentified samples. Asterisks mark posterior probabilities: (·) 0.85–0.94, · 0.95–0.98, ** 0.99–1. Numbers at nodes are MP bootstrap values (2000 replicates), shown only if >50%. In blue are the three deep clades that have been preliminarily assigned to *Stumpffia* sensu lato (two of which consist of undescribed species only, the third is herein described as genus *Anilany*). Name after the species refers to the sampling locality of the sample that was sequenced for the *16S*_J gene fragment. In brackets is the field number of the voucher specimens or the GenBank accession number of the *16S*_J gene fragment sequence. (For interpretation of the references to color in this figure legend, the reader is referred to the web version of this article.)

Results

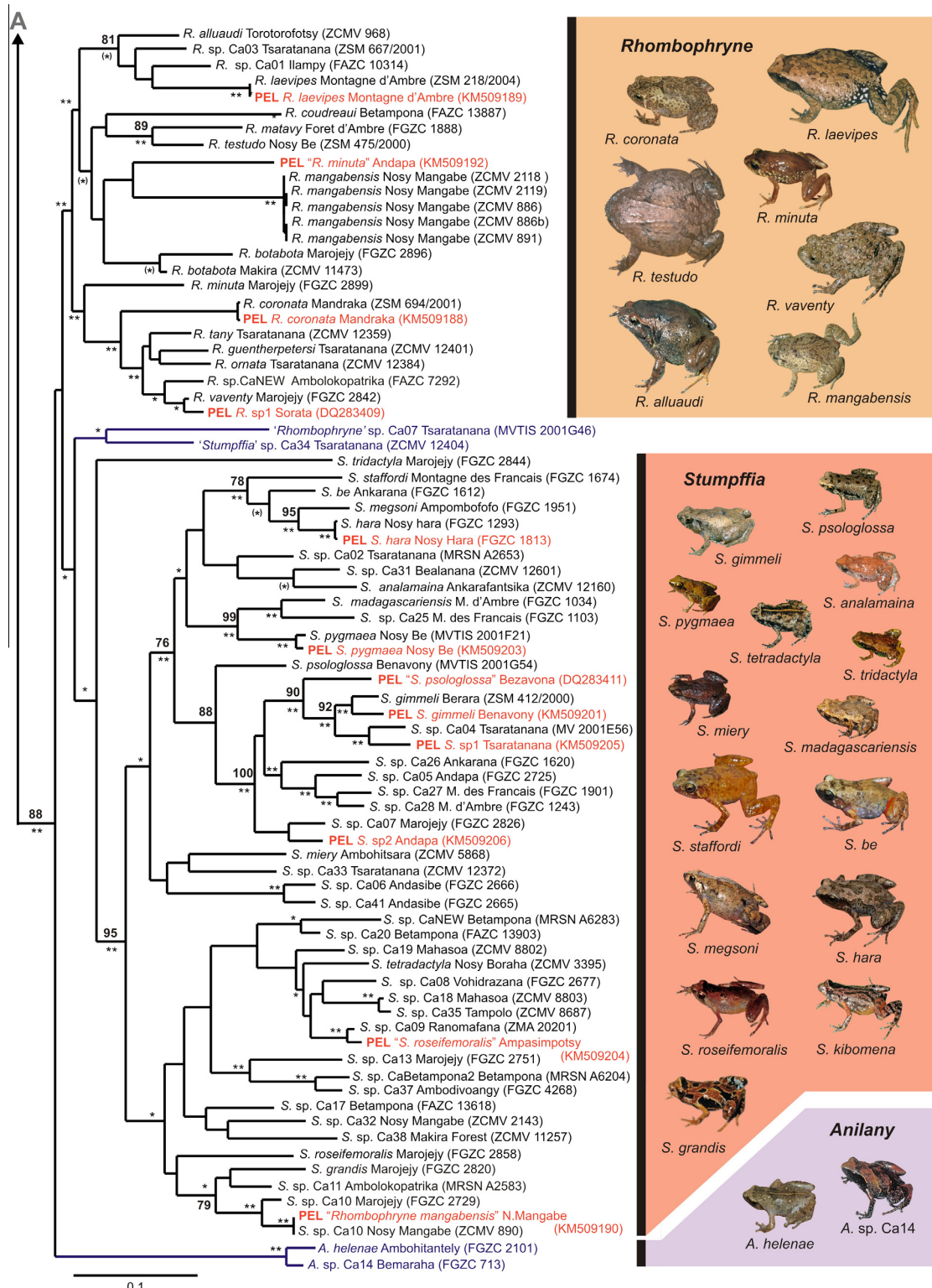


Fig. 1 (continued)

default settings. GBLOCKS 0.91b (Castresana, 2000) with default parameters was used to identify and to exclude nucleotide positions of unreliable alignment in the 12S and 16S gene fragments from the analyses. After exclusion of these positions, the alignment consisted of a total of 7646 bp.

PartitionFinder 1.1.1 software (Lanfear et al., 2012) was used to infer the best-fitting models of molecular evolution and partition scheme on the basis of the AICc criterion, using an input configuration file with 27 partitions, corresponding to individual codon positions for the eight protein-coding gene fragments and one partition each for every rRNA gene fragment. This represents the most finely partitioned scheme possible for our dataset. We used the 'greedy' algorithm (heuristic search) with branch lengths estimated as 'unlinked'. A total of 703 *a priori* schemes with varying degrees of complexity and the best-fit and the worst-fit schemes were statistically compared using AIC in PartitionFinder. The partition strategy including only two partitions (1st partition including 12S + 16S_I + 16S_II + 3rd codon position of *cox1* and *cytB*; 2nd partition including all remaining positions) yielded the lowest score and was therefore identified as the optimal partitioning scheme for our analyses. The GTR + I + G model was determined within PartitionFinder as the best-fitting model of substitution for the two suggested partitions. *Dyscophus insularis* was used *a priori* as outgroup in all MrBayes analyses. Partitioned Bayesian Inference analyses (BI) were performed in the MPI version of MrBayes 3.2 for Unix Clusters (Ronquist et al., 2012) and in the CIPRES portal (Miller et al., 2010) using MrBayes 3.2.6 running on XSEDE. We performed four runs of 100 million generations (starting with random trees) and four incrementally heated Markov chains (using default heating values), sampling the Markov chains at intervals of 1000 generations. Stabilization and convergence of likelihood values were assessed in Tracer 1.4 (Rambaut and Drummond, 2007) and occurred after about 35–40 million generations. Therefore, sixty million trees were retained post burn-in and used to generate the 50% majority-rule consensus tree.

Maximum Parsimony (MP) analysis was performed with TNT (Goloboff et al., 2008) after removal of unreliable alignment positions as identified by GBLOCKS. We used the multi command with 100 random sequence-addition replicates, followed by branch-swapping with tree-bisection and reconnection (command *break tbr*), with up to 1000 trees specified to be retained. We also executed 2000 MP bootstrap replicates in TNT (provided in the *Supplementary Information, Appendix C, Fig. C.2*).

2.2. Morphological examination and morphometrics

Specimen examination followed standard protocols for cophylid microhylids, taking note of characters that have been most informative for taxonomic work in this subfamily (for full details, see recent species descriptions, e.g. Köhler et al., 2010; Klages et al., 2013; Rakotoarison et al., 2012, 2015; Glaw et al., 2015; Scherz et al., 2015a,b). Overall, we have examined over 500 specimens collected by ourselves in the field.

Non-metric multidimensional scaling (NMDS) was performed in Past 3.07 (Hammer et al., 2001) using characters that showed potential diagnostic value in *Rhombophryne* and *Stumpffia*. 46 *Stumpffia* and 70 *Rhombophryne* specimens were examined to generate a morphological character matrix for this analysis. Measurements were taken using a digital calliper to 0.01 mm under a binocular dissecting microscope, rounded to 0.1 mm, and averaged across all specimens of each species. Measurements selected for inclusion in our analysis were: snout-vent length (SVL), head width (HW), head length (HL), eye-nostril distance (END), nostril-snout distance (NSD), forelimb length (given by the sum of hand length, lower arm length, and upper arm length), hindlimb length (given

by the sum of foot length, tarsus length, tibia length and thigh length).

For conclusions on the taxonomy of *Stumpffia*, *Rhombophryne*, *Plethodontohyla*, and *Stumpffia*-like genera, a total of 174 specimens belonging to these genera were examined. Specimens used by PEL (except those housed at the ZSM) were not examined. As outlined above, conclusions on these specimens are based on their genetic affinities.

2.3. Osteological analyses

High resolution micro-Computed Tomography (micro-CT) scans were produced on a phoenix nanotom m cone-beam micro-CT scanner (GE Measurement & Control, Wunstorf, Germany). Large specimens (>20 mm) were scanned using a standard target, with typical settings of 140 kV and 80 mA, using a timing of 500 ms for 2440 projections. Small specimens (<20 mm, especially *Stumpffia*) were scanned using a molybdenum element, at 70 kV and 160 mA, using a timing of 750 ms for 2440 projections. Models were prepared and examined in VG Studio Max 2.2 (Volume Graphics GMBH, Heidelberg, Germany). Selected specimens were processed into PDF-embedded 3D models using Amira 5.4.5 or 6.0 (FEI Visualization Sciences Group, Burlington MA, USA), and are provided in the *Supplementary Information (Appendix C, Figs. C.3–C.5)*. Osteological terminology follows Trueb (1968, 1973). Osteological examination was conducted based on both volume and surface renders. Because its X-ray absorption is low, cartilage is not rendered in normal micro-CT scans; cartilages are therefore omitted from our discussion here, and from figures.

3. Results and discussion

3.1. Misidentification of taxa in PEL

PEL produced a matrix of 66 homologous loci for 48 representative species generated with an anchored phylogenomic approach, plus Sanger sequencing of seven loci for 142 species. Five species of cophylines were included in the phylogenomic dataset (identified by the authors as: *Anodonthyla nigrigularis*, *Cophyla occultans*, *Platypelis pollicaris*, *Rhombophryne mangabensis*, and *Stumpffia roseifemoralis*). We applied a molecular taxonomic identification of these five taxa by comparing PEL 16S and *cox1* Sanger sequences against homologous sequences of all of Madagascar's cophylines as described above. We can confirm the identity of their *Anodonthyla nigrigularis* sequences. On the other hand, (i) their '*Platypelis pollicaris*' is an undescribed species of the genus *Platypelis* so far known only from the Sorata Mountains in northern Madagascar; (ii) their '*Cophyla occultans*' is another undescribed species of the genus *Platypelis* so far known only from the Sorata Mountains (see below for more details); (iii) their '*Stumpffia roseifemoralis*' is an undescribed species of the genus *Stumpffia* (*Stumpffia* sp. Ca9 Ranomafana); and (iv) their '*Rhombophryne mangabensis*' is an undescribed species of the genus *Stumpffia* similar to *Stumpffia grandis*. Thus, the phylogenomic dataset of PEL contains one *Anodonthyla*, two *Platypelis*, and two *Stumpffia*, and lacks genomic information for the genera *Madecassophryne*, *Plethodontohyla*, *Cophyla*, and *Rhombophryne* (*Anilany gen. nov.*, which we describe below, is also not included in their dataset).

Using the molecular taxonomic identification approach outlined above, we identified a number of sample misidentifications in PEL, and partly traced the origins of these (see *Supplementary Information, Appendix A* for details). Four of these errors affect phylogenetic and classificatory conclusions: (i) a sample from the holotype of *Plethodontohyla fonetana* was mistakenly supplied by our second author's institution (TU Braunschweig) as *Rhombophryne matavy*

and included in the PEL dataset as such, despite the respective 16S sequence being identical to a sequence of the same specimen, available in GenBank under the correct taxon name (EU341058) and despite the sampling locality being the type locality of *Plethodontohyla fonetana*, a site far away from the type locality of *R. matavy*; (ii) a sample of an undescribed species of *Stumpffia* was mistakenly supplied as *Rhombophryne mangabensis*, and included in the PEL dataset despite the respective 16S sequence being strongly divergent from a homologous sequence of the *R. mangabensis* holotype (KF611588); (iii) a sample named 'Cophyla sp.' in the PEL dataset (specimen RAN 42521 from Antalaha) does not agree or cluster with topotypical specimens of any of the nominal *Cophyla* species by its 16S or cox1 sequences, and instead probably belongs to an undescribed species of *Platypelis*; (iv) a sample named 'Cophyla occultans' in the PEL dataset (AMNH-A 167233/AMCC 103335) is very similar in 16S and cox1 (and forms a highly supported clade) to a sample of an undescribed species of *Platypelis* from the Sorata Mountains, both of which are within a well-supported clade also including *P. tsaratananaensis* and a further undescribed species of *Platypelis*, all of which superficially resemble *C. occultans*. Numerous additional inconsistencies, unjustified emendations and misspellings in PEL do not impact their phylogenetic conclusions; these are therefore corrected in *Supplementary Information, Appendix A* but not further discussed here.

3.2. Revised phylogeny of cophylinae

Bayesian Inference (BI) analysis of our supermatrix of 11 gene segments yielded a phylogenetic tree (Fig. 1) largely in agreement with those published by Andreone et al. (2005) and Wollenberg et al. (2008). The Cophylinae received maximum support as a monophyletic group, but deep nodes within the subfamily were basically unresolved. Of the six cophyline genera included and not considering the misidentifications of the PEL terminals, *Anodonthyla*, *Rhombophryne*, *Plethodontohyla* and *Cophyla* received high support (posterior probabilities ≥ 0.99), and the clade comprising *Platypelis* species received moderate support (PP = 0.91). A single named species assigned to the genus *Stumpffia* (*S. heleneae*), along with an undescribed candidate species, was the sister taxon to a clade comprising *Rhombophryne* and *Stumpffia*, thus rendering *Stumpffia* paraphyletic. We discuss this in more detail below, where we also erect a new genus for these *Stumpffia*-like frogs. Excluding these morphologically and genetically divergent frogs renders *Stumpffia* monophyletic with relatively high support (PP = 0.97), but as we explain, further divisions may be necessary in the future. *Cophyla* and *Platypelis* were sister clades, with high support for *Cophyla* (PP > 0.999).

Analyses of our matrix under MP yielded largely similar results. A total of 144 equally most parsimonious trees were obtained (tree length 17,840 steps). A strict consensus of these (*Supplementary Information, Appendix C, Fig. C.2*) closely matches the BI tree. Considering nominal species only, all traditional genera were recovered as monophyletic, although bootstrap support for these clades was usually low, and for some genera below 50% (Fig. 1). Differences to the BI tree were mostly apparent in the basal nodes of the *Stumpffia* clade: *S. tridactyla* was placed with a clade containing *S. heleneae* and two samples of undescribed miniaturized frogs from Tsaratanana and Tsingy de Bemaraha, and the two samples of undescribed miniaturized frogs from the Tsaratanana massif (clustering as the sister clade of *Stumpffia* sensu stricto in the BI analysis) were placed with the *S. heleneae* clade and within *Rhombophryne*, respectively.

Regarding the phylogenetic topology with sample identification amended, two major discordances between the MP tree of PEL and our BI phylogeny exist: (i) one unambiguous species of *Cophyla* (*C. berara*) is phylogenetically nested within *Platypelis* in the PEL tree, while this sequence is identical to our *C. berara* sample and clearly

within the *Cophyla* clade in our tree (also supported by our MP analysis); (ii) the four species of *Rhombophryne* included (*R. coronata*, *R. laevipes*, 'R. minuta', *R. sp.*) do not form a monophyletic group in the PEL tree, although all four terminals are included in the strongly supported *Rhombophryne* clade in our BI tree.

Based on our new phylogenetic analysis (Fig. 1), the re-identification of deviant PEL sequences, and newly obtained osteological data from CT scans, we discuss the evidence for separate generic classification of *Platypelis* vs. *Cophyla*, *Stumpffia* vs. *Rhombophryne*, and for recognizing new genus-level taxa within *Stumpffia* sensu lato. We formalize our suggestions on the basis of the taxon-naming criteria (TNCs) proposed by Vences et al. (2013). We focus on the nominal species in each clade because only fragmentary data are available for the many undescribed candidate species of cophylines included in our phylogenetic tree; where applicable, these fragmentary data do, however, support our conclusions.

3.3. *Cophyla* and *Platypelis*: morphologically similar sister genera

The *Cophyla/Platypelis* clade consists of unambiguously arboreal cophylines. The relationships within this clade have recently been discussed by Rakotoarison et al. (2015) and can be summarized as follows: (i) *Cophyla* and *Platypelis* are probably both monophyletic (as also supported by our tree; Fig. 1); (ii) *Cophyla* species are restricted to northern Madagascar, whereas *Platypelis* occurs across the entire humid biome of the island; (iii) no reliable external morphological characters exist to diagnose these two clades; (iv) all but one species of *Cophyla* lack a clavicle, while this element is present in all *Platypelis* species examined; (v) all species of *Cophyla* examined have medially fused vomers, whereas this element is either centrally divided or reduced in *Platypelis*.

The data available so far thus characterize *Cophyla* and *Platypelis* as monophyletic groups that can be diagnosed by a combination of osteological characters. Distinguishing the two genera is also informative from a biogeographic perspective. It is true, however, that the two clades together form a monophyletic group (satisfying the Stability of Monophly TNC; Vences et al., 2013) and might together become more easily diagnosable in external morphology (which would satisfy the Diagnosability TNC). Nevertheless, we here maintain both genera as valid taxa. This proposal is formalized in *Supplementary Information, Appendix A*. However, we emphasise that a comprehensive revision of osteological variation of *Platypelis* is pending, and that this should be combined with additional phylogenetic and phylogenomic data of both genera, *Cophyla* and *Platypelis*, for a definitive outcome.

3.4. *Stumpffia* and *Rhombophryne*: ecomorphologically distinct sister genera

Our BI phylogenetic tree recovered *Rhombophryne* as a monophyletic group within a paraphyletic *Stumpffia* sensu lato, with full support. The paraphyly of *Stumpffia* is caused by the highly divergent 'S.' *heleneae* clade, composed of 'S.' *heleneae* and 'S.' sp. Ca14. This clade is morphologically and osteologically distinct, in addition to its strong genetic differentiation from all other *Stumpffia*, and therefore warrants recognition as a new genus (erected below). This change renders *Stumpffia* sensu stricto a monophyletic genus and sister taxon to *Rhombophryne*, albeit with poor support ($P < 0.95$). Support increased ($P = 0.97$) for a clade of all species except for *S. tridactyla*. We emphasize that for several of the miniaturized species at the base of the tree, only a small number of genes have so far been sequenced, while for others a large number of sequences are available. This imbalance, along with very deep divergences, might add to the instability of basal nodes in the *Rhombophryne* + *Stumpffia* clade.

PEL did not recover *Stumpffia* and *Rhombophryne* as sister clades, and they are sister taxa in our analysis only after transferring part of *Stumpffia* to a separate genus. In such a situation, the Stability of Monophyly TNC (Vences et al., 2013) would suggest, other things being equal, a classification with both groups subsumed in a single genus with unequivocal support. However, the two clades are ecomorphologically highly distinct, and it is therefore worth exploring whether grouping them in a single genus (PEL) has advantages over a two-genera classification.

The differences between *Rhombophryne* and *Stumpffia* are exemplified by the two type species (neither of which was included in the PEL dataset), the miniaturized leaf-litter dweller *S. psoglossa* and the stout, fossorial *R. testudo* (3D models of the skeletons of the type specimens of these species are provided in **Supplementary Information, Appendix C, Figs. C.3–C.4**). These differences hold for most species in both clades, but some *Rhombophryne* are smaller and have more elongated bodies (e.g. *R. minuta*: max. SVL 22 mm; *R. longicrus*: max. SVL 28 mm), and some *Stumpffia* are relatively large (e.g. *S. staffordi*: max. 28 mm; Köhler et al., 2010). These exceptional species are deeply nested within their respective major clades (Fig. 1), suggesting extensive morphological homoplasy.

Defining morphological synapomorphies for *Rhombophryne* and *Stumpffia* is challenging because data are unavailable for many cophyline genera, and basal nodes in the subfamily are unresolved (Fig. 1). Still, it is possible to diagnose all or most species of the two genera by morphology; a NMDS analysis based on discrete coding of characters fully distinguished the two genera (Fig. 2). In more concrete terms, *Rhombophryne* are characterized (vs. *Stumpffia*) by the presence of vomerine teeth in all but one species (vs. absence), presence of maxillary teeth in all but one species (vs. absence), relatively wider heads in all species, larger body sizes in most species, a smaller braincase-width to head-width ratio, and (if present) clavicles curved along the antero-posterior axis (vs. straight) (see Fig. 3 and compare **Supplementary Information, Appendix C, Figs. C.4, C.5**). Given that both genera are monophyletic (after the transfer of 'S.' *heleneae* to a new genus, see below), all members of the two genera are morphologically

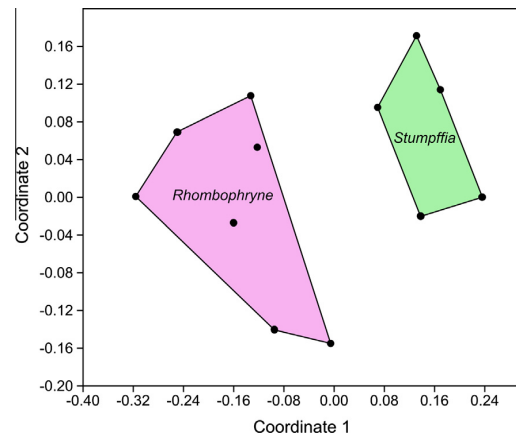


Fig. 2. Non-metric multidimensional scaling (NMDS) scatterplot of *Rhombophryne* and *Stumpffia* based on morphological characters (see **Supplementary Information, Appendix B, Tables B.1–B.2**). Convex hulls are drawn around each genus, showing clear distinction of genera based on our coding of their morphology.

diagnosable against each other, and with a few exceptions they occupy non-overlapping adaptive zones (leaf litter vs. soil): their synonymy is untenable. Thus, we strongly advocate continued recognition of *Stumpffia* as a valid genus distinct from *Rhombophryne*. This proposal is formalized in **Supplementary Information, Appendix A**, in which we provide a new and effective key to identify specimens to *Stumpffia*, *Stumpffia*-like genus-level clades (see below), *Rhombophryne*, and *Plethodontohyla*.

3.5. Convergent miniaturization: multiple *Stumpffia*-like genus-level clades

Non-monophyly of *Stumpffia* has been previously inferred (e.g., Wollenberg et al., 2008) but is complicated by the fact that many of the species involved are taxonomically undescribed. Three deep

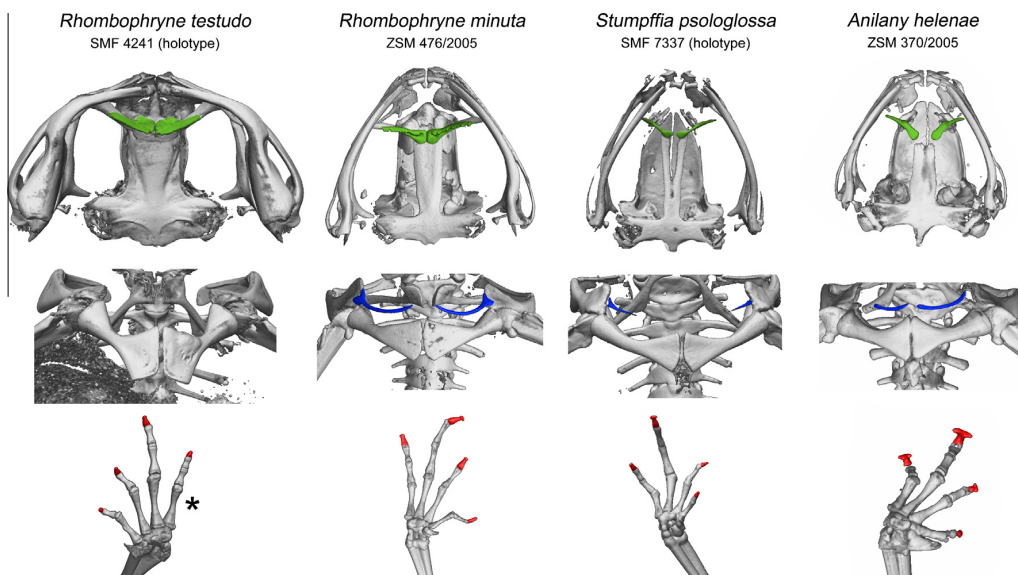


Fig. 3. Comparative micro-CT images of the heads, pectoral girdles, and hand bones of representative members of the genera *Rhombophryne*, *Stumpffia*, and *Anilany*. Postchoanal vomers/neopalatines are colored in green, clavicles in blue, and terminal phalanges in red. *The hands of SMF 4241 were poorly oriented in the micro-CT scan, so a hand of its sister species, *R. matavy* (ZSM 1628/2008), is shown in its stead. The hand morphology of these two species is highly similar. Not to scale. (For interpretation of the references to colour in this figure legend, the reader is referred to the web version of this article.)



Fig. 4. Representatives of *Stumpffia* and *Stumpffia*-like clades. (A) *S. tetracycla* (Nosy Boraha; holotype, ZFMK 52547); (B) *Anilany heleneae* (Ambohitantely; ZSM 370/2005); (C) 'Stumpffia' sp. Ca34 (Tsaratanana; ZSM 636/2014); (D) 'Stumpffia' sp. Ca15 (Manombo; ZMA 20172).

clades have been assigned to *Stumpffia*, mainly by their small body sizes (<16 mm), but probably do not belong to this genus: (i) 'S.' *heleneae* and an undescribed candidate species ('S.' sp. Ca14; discussed briefly above and in more detail in the next paragraph); (ii) two small-sized candidate species from south-eastern Madagascar ('S.' spp. Ca15 and Ca16; see Fig. 4) which, interestingly, have been recovered as more closely related to *Plethodontohyla* than to the *Stumpffia*-*Rhomboophryne* clade, supporting the hypothesis of Wollenberg et al. (2008) that they probably constitute a new genus (see Fig. 1); (iii) two divergent lineages from Tsaratanana ('R.' sp. Ca7 and 'S.' sp. Ca34), which fall within *Stumpffia* sensu stricto in the BI analysis (Fig. 1) but are within *Rhomboophryne* or the sister taxon to 'S.' *heleneae* under MP; these lineages are morphologically distinct, being miniaturized microhylids of different body shape than all other *Stumpffia* (Fig. 4), possessing both maxillary and vomerine teeth (absent in *Stumpffia* sensu stricto), and lacking clavicles (present in *Stumpffia* sensu stricto).

The second and third clades of these *Stumpffia*-like frogs contain only taxonomically undescribed lineages, and currently their

existence does not challenge the taxonomic definition of *Stumpffia*. We anticipate that these clades merit distinction as separate genera, which will be described together with the species in forthcoming revisions. The first clade, however, contains the nominal 'S.' *heleneae* (and its sister lineage, the undescribed 'S.' sp. Ca14, depicted in Fig. 4) and thus requires taxonomic discussion at this time. Wollenberg et al. (2008) revealed 'S.' *heleneae* to be the sister taxon to all other *Stumpffia*, although without statistical support; herein it is the sister taxon to the *Rhomboophryne* + *Stumpffia* clade. This species has long been known to be outstanding among *Stumpffia* in that it possesses dilated terminal disks of fingers and toes (Vallan, 2000). Micro-CT scans revealed that it also possesses T-shaped terminal phalanges of the fingers and toes (Fig. 3 and Supplementary Information, Appendix C, Fig. C.5). In *Stumpffia*, terminal phalanges are typically weakly distally expanded, knobbed, or unornamented, but a group of large-sized cave-adapted *Stumpffia* (*S. be*, *S. hara*, *S. megsoni*, *S. staffordi*) also possess expanded terminal phalanges and discs. 'Stumpffia' *heleneae* is the only nominal species to combine small size and expanded finger

and toe tips, but less ambiguously it also has a broad, flattened vomer that tapers slowly distally, rather than the vomer consisting of a thin rod of bone with a rounded proximal base as in *Stumpffia*, clavicles curved along the anteroposterior axis (straight in eight examined *Stumpffia* species), and the only male available for examination has a broad *crista ventralis* and *crista lateralis* of the humerus, as well as a strong prepollex, not known from any other *Stumpffia* (see *Supplementary Information, Appendix C, Fig. C.5*). Based on these morphological differences and the phylogenetic position apart from other *Stumpffia*, we transfer 'S.' *helenae* to a new genus:

Anilany gen. nov.

This published work and the nomenclatural acts it contains have been registered in ZooBank, the online registration system for the ICBN. The LSID (Life Science Identifier) for this publication is: urn:lsid:zoobank.org:act:DF982DCE-5CB9-4B01-9ED7-4D992170C603. The electronic edition of this work was published in a journal with an ISSN, and will be archived and made available from the following digital repository: <http://www.zenodo.org/>.

Type species: *Stumpffia helenae* [Vallan, 2000](#)

Diagnosis: Miniaturized terrestrial cophyline microhylids (14–16 mm adult SVL). Dilated terminal discs on fingers and toes. T-shaped terminal phalanges of fingers and toes, the distal tip broader than the base. Vomer broad, flattened, and not tapering strongly. Clavicles curved along the anteroposterior axis. Males with broad *crista ventralis* and *crista lateralis* of the humerus, and strongly developed, broad prepollex almost equal in length to the first metacarpal (not observed in females of *A.* sp. Ca14, possibly reflecting sexual dimorphism; males of this candidate species are unknown).

The new genus is morphologically distinguished from *Stumpffia* by the combination of small size (14–16 mm SVL) and dilated terminal discs of the fingers and toes, with T-shaped terminal phalanges of these digits with tips broader than their bases (found only in large-bodied *Stumpffia* species), curved clavicles (straight in all examined *Stumpffia* species), and broader vomer. Genetically, representatives of the new genus are strongly divergent from all nominal species of *Stumpffia*, and phylogenetically *Anilany* might be the sister genus of *Stumpffia* or of the *Rhombophryne* + *Stumpffia* clade.

A 3D model of the skeleton of a specimen of *A. helenae* is provided in *Supplementary Information, Appendix C, Fig. C.5*.

Included species: *Anilany helenae* ([Vallan, 2000](#)) and one undescribed candidate species (*Anilany* sp. Ca14).

Distribution: Central and western Madagascar. Known from rainforest in Ambohitantely Special Reserve (*Anilany helenae*) and dry forests in karstic limestone formations in Tsingy de Bemaraha National Park (*Anilany* sp. Ca14).

Etymology: *Anilany* is derived from the Malagasy contraction anilan'ny, meaning 'at the side of', as in the statement '*A. helenae* mianjera teo anilan'ny *Rhombophryne* + *Stumpffia*' (*S. helenae* falls at the side of *Rhombophryne* + *Stumpffia*), in reference to the phylogenetic position of this genus beside the *Rhombophryne* + *Stumpffia* clade. It is to be treated as an invariable feminine noun.

4. Conclusions

It is almost unavoidable that large-scale phylogenetic analyses with dense sampling will contain some errors in species identity of samples, especially because most organismal groups require alpha-taxonomic revision. This is particularly true for taxa from highly biodiverse developing countries where the lack of both well-maintained in-country natural history collections and a sufficiently high number of expert taxonomists precludes efficient cataloguing of biodiversity ([Paknia et al., 2015](#)). Sample misidenti-

fication is insidious; at higher taxonomic levels, the impact of individual misidentified samples is generally low, as their effect on deep tree topology is weak, especially when taxon sampling is dense. Investigating higher taxonomy using dense taxon sampling almost inevitably leads to conclusions being made also at lower taxonomic levels. Here, the impact of these misidentifications is much higher, and can mislead conclusions and cause taxonomic errors. Therefore, even when the main focus of a study is a higher taxonomic question, proofing procedures (e.g. performing blast searches of barcode sequences) should be implemented to ensure maximum possible confidence in sample identity.

Our re-analysis of the cophyline members of the PEL dataset revealed several misidentified taxa, partly caused by upstream sample confusion (for which the authors are not to blame, although precautionary procedures would have revealed these), and partly by incorrect taxonomic identification. While these misidentifications do not undermine the central conclusions of PEL—having likely had little impact on deep tree topology—we have here shown that they caused erroneous genus-level changes within the Cophylinea.

Based on our densely sampled phylogeny, together with morphological and osteological data, we have shown that (i) *Cophyla* and *Platypelis* are highly similar but monophyletic, diagnosable genera (although a thorough revision of their taxonomy will be necessary in future); (ii) *Rhombophryne* and *Stumpffia* sensu stricto are ecomorphologically distinct, monophyletic, diagnosable genera; (iii) two species formerly considered as *Stumpffia* fall outside the *Rhombophryne* + *Stumpffia* clade, and are transferred to the new genus *Anilany*, which is diagnosable in osteology; and (iv) two further clades of *Stumpffia*-like frogs may warrant recognition as new genera.

As discussed elsewhere ([Vences et al., 2013](#)), genus names are particularly relevant for the end users of taxonomies, such as conservation biologists and lawmakers. We therefore suggest that a general principle of economy of change in these names should apply. Making changes based on weakly supported clades can necessitate repeated revision before reaching a stable and unambiguous taxonomy (see *Supplementary Information, Appendix A.6* for a brief discussion of the new microhylid subfamily Chaperininae erected by PEL). Deep nodes in our phylogeny remain poorly resolved, and our revised classification is not free of ambiguities in diagnosing genera by morphology alone. Future revisions will doubtless refine this classification, as osteological datasets expand, candidate species are described, and genetic coverage improves. We are confident, though, that this will entail few large-scale rearrangements.

Acknowledgments

We thank B. Ruthensteiner for assistance related to micro-CT scanning, and Walter Cocca for his assistance in phylogenetic analyses. The osteological research was supported by a grant from the Wilhelm-Peters Fund of the Deutsche Gesellschaft für Herpetologie und Terrarienkunde (DGHT) to MDS and FG. The work of AC is supported by a Investigador FCT (IF) grant from the Portuguese "Fundação para a Ciencia e a Tecnologia" (IF/00209/2014), funded by Programa Operacional Potencial Humano (POPH) – Quadro de Referencia Estrategico Nacional (QREN) from the European Social Fund. Work of the authors over the past 25 years has been made possible by collaboration accords with the Université d'Antananarivo (Département de Biologie Animale). We are grateful to the Malagasy authorities for research and export permits. We thank also the editor, the two anonymous reviewers, and Pedro Peloso (corresponding author of the Cladistics publication here discussed) for their careful reading of our manuscript and their many insightful comments and suggestions.

Appendices A–C. Supplementary material

Appendix A. Comments and corrections on classificatory changes (A.1–A.6); Appendix B. Supplementary Tables (Table B.1–B.2); Appendix C. Supplementary Figures (Figure C.1–C.5). Supplementary data associated with this article can be found, in the online version, at <http://dx.doi.org/10.1016/j.ympev.2016.04.019>.

References

- AmphibiaWeb, 2016. <<http://amphibiaweb.org/>>. (accessed on 16 February 2016).
- Andreone, F., Vences, M., Vieites, D.R., Glaw, F., Meyer, A., 2005. Recurrent ecological adaptations revealed through a molecular analysis of the secretive cophyline frogs of Madagascar. *Mol. Phylogenet. Evol.* 34, 315–322.
- Blommers-Schöller, R.M.A., Blanc, C.P., 1991. Amphibiens (première partie). *Faune Madagascar* 75, 1–379.
- Castresana, J., 2000. Selection of conserved blocks from multiple alignments for their use in phylogenetic analysis. *Mol. Biol. Evol.* 17, 540–552.
- Crottini, A., Madsen, O., Pouc, C., Strauß, A., Vieites, D.R., Vences, M., 2012. Vertebrate time-tree elucidates the biogeographic pattern of a major biotic change around the K-T boundary in Madagascar. *Proc. Natl. Acad. Sci. USA* 109, 5358–5363.
- de Sá, R.O., Streicher, J.W., Sekonyela, R., Forlani, M.C., Loader, S.P., Greenbaum, E., Richards, S., Haddad, C.F.B., 2012. Molecular phylogeny of microhylid frogs (Anura: Microhylidae) with emphasis on relationships among New World genera. *BMC Evol. Biol.* 12, 1–21.
- Frost, D.R., Grant, T., Faivovich, J., Bain, R.H., Haas, A., Haddad, C.F.B., de Sá, R.O., Channing, A., Wilkinson, M., Donnellan, S.C., Raxworthy, C.J., Campbell, J.A., Blotto, B.L., Moler, P., Drewes, R.C., Nussbaum, R.A., Lynch, J.D., Green, D.M., Wheeler, W.C., 2006. The amphibian tree of life. *Bull. Amer. Mus. Nat. Hist.* 297, 1–291.
- Glaw, F., Vallan, D., Andreone, F., Edmunds, D., Dolch, R., Vences, M., 2015. Beautiful belly: a distinctive new microhylid frog (Amphibia: Stumpffia) from eastern Madagascar. *Zootaxa* 3925, 120–128.
- Glaw, F., Vences, M., 2007. A Field Guide to the Amphibians and Reptiles of Madagascar. Vences and Glaw Verlags GbR, Köln, Germany.
- Goloboff, P.A., Farris, J.S., Nixon, K.C., 2008. TNT, a free program for phylogenetic analysis. *Cladistics* 24, 774–786.
- Grosjean, S., Glos, J., Teschke, M., Glaw, F., Vences, M., 2007. Comparative larval morphology of Madagascan toadlets of the genus *Scaphiophryne*: phylogenetic and taxonomic inferences. *Zool. J. Linn. Soc. Lond.* 151, 555–576.
- Haas, A., 2003. Phylogeny of frogs as inferred from primarily larval characters (Amphibia: Anura). *Cladistics* 19, 23–89.
- Hammer, Ø., Harper, D.A.T., Ryan, P.D., 2001. PAST: Paleontological Statistics Software Package for Education. v3.07 available at: <<http://folk.uio.no/ohammer/past/>>.
- Irisarri, I., San Mauro, D., Abascal, F., Ohler, A., Vences, M., Zardoya, R., 2012. The origin of modern frogs (Neobatrachia) was accompanied by acceleration in mitochondrial and nuclear substitution rates. *BMC Genom.* 13, e626.
- Klages, J., Glaw, F., Köhler, J., Müller, J., Hipsley, C.A., Vences, M., 2013. Molecular, morphological and osteological differentiation of a new species of microhylid frog of the genus *Stumpffia* from northwestern Madagascar. *Zootaxa* 3717, 280–300.
- Köhler, J., Vences, M., D'Cruze, N., Glaw, F., 2010. Giant dwarfs: discovery of a radiation of large-bodied 'stump-toed frogs' from karstic cave environments of northern Madagascar. *J. Zool.* 282, 21–38.
- Kurabayashi, A., Matsui, M., Belabut, D.M., Yong, H., Ahmad, N., Sudin, A., Kuramoto, M., Hamidy, H., Sumida, M., 2011. From Antarctica or Asia? New colonization scenario for Australian-New Guinean narrow mouth toads suggested from the findings on a mysterious genus *Gastrophrynoidea*. *BMC Biol.* 11, 175.
- Landre, R., Calcott, B., Ho, S.Y.W., Guindon, S., 2012. PartitionFinder: combined selection of partitioning schemes and substitution models for phylogenetic analyses. *Mol. Biol. Evol.* 29, 1695–1701.
- Leempon, A.R., Emme, S., Lemmon, E.M., 2012. Anchored hybrid enrichment for massively high-throughput phylogenomics. *Syst. Biol.* 61, 727–744.
- McDiarmid, R.W., Altig, R., 1999. Tadpoles: The Biology of Anuran Larvae. Chicago University Press, Chicago, USA.
- Matsui, M., Hamidy, H., Belabut, D.M., Ahmad, N., Panha, S., Sudin, A., Khonsue, W., Oh, H., Yong, H., Jiang, J., Nishikawa, K., 2011. Systematic relationships of oriental tiny frogs of the family Microhylidae (Amphibia, Anura) as revealed by mtDNA genealogy. *Mol. Phylogenet. Evol.* 61, 167–176.
- Meyers, J.J., O'Reilly, J.C., Monroy, J.A., Nishikawa, K.C., 2004. Mechanism of tongue protraction in microhylid frogs. *J. Exp. Biol.* 207, 21–31.
- Miller, M.A., Pfeiffer, W., Schwartz, T., 2010. Creating the CIPRES Science Gateway for inference of large phylogenetic trees. In: Proceedings of the Gateway Computing Environments Workshop (GCE), 14 Nov. 2010, New Orleans, LA, pp. 1–8.
- Padial, J.M., Miralles, A., De La Riva, I., Vences, M., 2010. The integrative future of taxonomy. *Front. Zool.* 7, 16.
- Paknia, O., Rajaei, Sh.H., Koch, A., 2015. Lack of well-maintained natural history collections and taxonomists in megadiverse developing countries hampers global biodiversity exploration. *Org. Divers. Evol.* 15 (3), 1619–1629.
- Parker, B.A., 1934. A Monograph of the Frogs of the Family Microhylidae. The British Museum, London, UK.
- Peloso, P.L.V., Frost, D.R., Richards, S.J., Rodrigues, M.T., Donnellan, S., Matsui, M., Raxworthy, C.J., Biju, S.D., Lemmon, E.M., Lemmon, A.R., Wheeler, W.C., 2016. The impact of anchored phylogenomics and taxon sampling on phylogenetic inference in narrow-mouthed frogs (Anura, Microhylidae). *Cladistics* 32, 113–140.
- Perl, R.G.B., Nagy, Z.T., Sonet, G., Glaw, F., Wollenberg, K.C., Vences, M., 2014. DNA barcoding Madagascar's amphibian fauna. *Amphibia-Reptilia* 35, 197–206.
- Pyron, R.A., Wiens, J.J., 2011. A large-scale phylogeny of Amphibia including over 2800 species, and a revised classification of extant frogs, salamanders, and caecilians. *Mol. Phylogenet. Evol.* 61, 543–583.
- Rakotoarison, A., Crottini, A., Müller, J., Rodel, M.O., Glaw, F., Vences, M., 2015. Revision and phylogeny of narrow-mouthed treefrogs (*Cophyla*) from northern Madagascar: integration of molecular, osteological, and bioacoustic data reveals three new species. *Zootaxa* 3937, 61–89.
- Rakotoarison, A., Glaw, F., Vieites, D.R., Raminosoa, N.R., Vences, M., 2012. Taxonomy and natural history of arboreal microhylid frogs (*Platypelis*) from the Tsaratanana Massif in northern Madagascar, with description of a new species. *Zootaxa* 3563, 1–25.
- Rambaut, A., Drummond, A.J., 2007. Tracer v1.4 available at: <<http://beast.bio.ed.ac.uk/Tracer>>. Last accessed on 8 August 2015.
- Roelants, K., Gower, D.J., Wilkison, M., Loader, S.P., Biju, S.D., Guillaume, K., Moriau, L., Bossuyt, F., 2007. Global patterns of diversification in the history of modern amphibians. *Proc. Natl. Acad. Sci. USA* 104, 887–892.
- Roelants, K., Haas, A., Bossuyt, F., 2011. Anuran radiations and the evolution of tadpole morphospace. *Proc. Natl. Acad. Sci. USA* 108, 8731–8736.
- Ronquist, F., Teslenko, M., Van der Mark, P., Ayres, D.L., Darling, A., Höhna, S., Larget, B., Liu, L., Suchard, M.A., Huelsenbeck, J.P., 2012. MrBayes 3.2: efficient Bayesian phylogenetic inference and model choice across a large model space. *Syst. Biol.* 61, 539–542.
- Scherz, M.D., Rakotoarison, A., Hawlitschek, O., Vences, M., Glaw, F., 2015a. Leaping towards a saltatorial lifestyle? An unusually long-legged new species of *Rhomphophryne* (Anura, Microhylidae) from the Sorata massif in northern Madagascar. *Zoosyst. Evol.* 91, 105–114.
- Scherz, M.D., Ruthensteiner, B., Vieites, D.R., Vences, M., Glaw, F., 2015b. Two new microhylid frogs of the genus *Rhomphophryne* with superciliary spines from the Tsaratanana Massif in northern Madagascar. *Herpetologica* 71, 310–321.
- Tamura, K., Stecher, G., Peterson, D., Filipski, A., Kumar, S., 2013. MEGA6: molecular evolutionary genetics analysis. Version 6.0. *Mol. Biol. Evol.* 30, 2725–2729.
- Trueb, L., 1968. Cranial osteology of the hylid frog, *Smilisca baudini*. University of Kansas Publications, Museum of Natural History, vol. 18, pp. 11–35.
- Trueb, L., 1973. Bones, frogs, and evolution. In: Vial, J.L. (Ed.), *Evolutionary Biology of the Anurans: Contemporary Research on Major Problems*. University of Missouri Press, USA, pp. 65–132.
- Trueb, L., Diaz, R., Blackburn, D.C., 2011. Osteology and chondrocranial morphology of *Gastrophryne carolinensis* (Anura: Microhylidae), with a review of the osteological diversity of New World microhylids. *Phylomedusa* 10, 99–135.
- Vallan, D., 2000. A new species of the genus *Stumpffia* (Amphibia: Anura: Microhylidae) from a small forest remnant of the central high plateau of Madagascar. *Rev. Suisse Zool.* 107, 835–841.
- Van Boeckelaer, I., Roelants, K., Biju, S.D., Nagaraju, J., Bossuyt, F., 2006. Late Cretaceous vicariance in Gondwanan amphibians. *PLoS One* 1, e74.
- van der Meijden, A., Vences, M., Hoeegg, S., Boistel, R., Channing, A., Meyer, A., 2007. Nuclear gene phylogeny of narrow-mouthed toads (Family: Microhylidae) and a discussion of competing hypotheses concerning their biogeographical origins. *Mol. Phylogenet. Evol.* 44, 1017–1030.
- Vences, M., Guayasamin, J.M., Miralles, A., Riva, I.D.L., 2013. To name or not to name: criteria to promote economy of change in Linnaean classification schemes. *Zootaxa* 3363, 201–244.
- Vieites, D.R., Wollenberg, K.C., Andreone, F., Köhler, J., Glaw, F., Vences, M., 2009. Vast underestimation of Madagascar's biodiversity evidenced by an integrative amphibian inventory. *Proc. Natl. Acad. Sci. USA* 106, 8267–8272.
- Wassersug, R., 1984. The *Pseudohemisus* tadpole: a morphological link between microhylid (Orton type 2) and ranoid (Orton type 4) larvae. *Herpetologica* 40, 138–149.
- Wassersug, R., 1989. What, if anything is a microhylid (Orton type II) tadpole? *Fortsch. Zool.* 35, 534–538.
- Wassersug, R.J., Pyburn, W.F., 1987. The biology of the Peret toad, *Otophryne robusta* (Microhylidae), with special consideration of its fossorial larva and systematic relationships. *Zool. J. Linn. Soc. Lond.* 91, 137–169.
- Wollenberg, K.C., Vieites, D.R., van der Meijden, A., Glaw, F., Cannatella, D.C., Vences, M., 2008. Patterns of endemism and species richness in Malagasy cophyline frogs support a key role of mountainous areas for speciation. *Evolution* 62, 1890–1907.
- Zhang, P., Liang, D., Mao, R.L., Hillis, D.M., Wake, D.B., Cannatella, D.C., 2013. Efficient sequencing of anuran mtDNAs and a mitogenomic exploration of the phylogeny and evolution of frogs. *Mol. Biol. Evol.* 30, 1899–1915.

Chapter 9. MANUSCRIPT (accepted): Morphological and ecological convergence at the lower size limit for vertebrates highlighted by five new miniaturised microhylid frog species from three different Madagascan genera

In this chapter I present the description five new species of miniaturised cophyline frogs: three species within the new genus *Mini*, a miniaturised species of *Anodonthyla*, and a miniaturised species of *Rhombophryne*. These three lineages have independently evolved diminutive body size less than 12 mm, converging on being among the smallest terrestrial vertebrates on earth. As established in **chapters 6–8**, osteology is a rich source of taxonomic and evolutionary information. The miniaturised *Anodonthyla eximia*, shows many of the hallmarks of the genus *Anodonthyla*, especially in the blade-like shape of the prepollex, which is pronounced among males of that genus, and the arrangement of the bones of its palate, highlighting the phylogenetic contingency under which miniaturisation evolves in these frogs. Two species of the genus *Mini* retain teeth despite their small size, in contrast to the loss of teeth associated with miniaturisation in the diverse genus *Stumpffia* (Rakotoarison et al. 2017). Finally, *Rhombophryne proportionalis* presents an unusual case of so-called ‘proportional dwarfism’, that is, it has proportions resembling a larger frog species but at a smaller size, which is in strong contrast to the paedomorphism that typifies most miniaturised frogs. This paper highlights the ecological lability within the subfamily Cophylinae, particularly with respect to their body size evolution.

Scherz, M.D., Hutter, C.R., Rakotoarison, A., Riemann, J.C., Rödel, M.-O., Ndriantsoa, S.H., Glos, J., Hyde Roberts, S., Crottini, A., Vences, M. & Glaw, F. (accepted) Morphological and ecological convergence at the lower size limit for vertebrates highlighted by five new miniaturised microhylid frog species from three different Madagascan genera. PLoS One.

Digital Supplementary Materials on appended CD:

Supplementary Table S1 — GenBank accession numbers for 3' 16S rRNA sequences used in this study to calculate uncorrected pairwise distances.

Results

Morphological and ecological convergence at the lower size limit for vertebrates highlighted by five new miniaturised microhylid frog species from three different Madagascan genera

Mark D. Scherz^{1,2,3*}, Carl R. Hutter⁴, Andolalao Rakotoarison^{2,5}, Jana C. Riemann⁶, Mark-Oliver Rödel⁷, Serge H. Ndriantsoa⁵, Julian Glos⁶, Sam Hyde Roberts^{8,9}, Angelica Crottini¹⁰, Miguel Vences² & Frank Glaw¹

Short title: Five tiny new frogs from Madagascar

¹Sektion Herpetologie, Zoologische Staatssammlung München (ZSM-SNSB), München, Germany

²Division of Evolutionary Biology, Zoologisches Institut, Technische Universität Braunschweig, Braunschweig, Germany

³Systematische Zoologie, Department Biologie II, Biozentrum, Ludwig-Maximilians-Universität München, Planegg-Martinsried, Germany

⁴Biodiversity Institute and Department of Ecology and Evolutionary Biology, University of Kansas, Lawrence, KS, USA

⁵Mention Zoologie et Biodiversité Animale, Université d'Antananarivo, Antananarivo, Madagascar

⁶Institute of Zoology, Universität Hamburg, Hamburg, Germany

⁷Museum für Naturkunde – Leibniz Institute for Evolution and Biodiversity Science, Berlin, Germany

⁸SEED Madagascar, London, UK

⁹Oxford Brookes University, Oxford, UK

¹⁰CIBIO, Research Centre in Biodiversity and Genetic Resources, InBIO, Campus Agrário de Vairão, Universidade do Porto, Vairão, Portugal

*corresponding author: mark.scherz@gmail.com

Publication LSID: urn:lsid:zoobank.org:pub:91E597C8-7A80-46F9-B0E8-61F2524400F7

Abstract

Miniaturised frogs form a fascinating but poorly understood amphibian ecomorph and have been exceptionally prone to taxonomic underestimation. The subfamily Cophylinae (family Microhylidae), endemic to Madagascar, has a particularly large diversity of miniaturised species which have historically been attributed to the single genus *Stumpffia* largely based on their small size. Recent phylogenetic work has revealed that several independent lineages of cophyline microhylids evolved towards highly miniaturised body sizes, achieving adult snout–vent lengths under 16 mm. Here, we describe five new species belonging to three clades that independently miniaturised and that are all genetically highly divergent from their relatives: (i) a new genus (*Mini* gen. nov.) with three new species from southern Madagascar, (ii) one species of *Rhombophryne*, and (iii) one species of *Anodonthyla*. *Mini mum* sp. nov. from Manombo in eastern Madagascar is one of the smallest frogs in the world, reaching an adult body size of 9.7 mm in males and 11.3 mm in females. *Mini scule* sp. nov. from Sainte Luce in southeastern Madagascar is slightly larger and has maxillary teeth. *Mini ature* sp. nov. from Andohahela in southeast Madagascar is larger than its congeners but is similar in build. *Rhombophryne proportionalis* sp. nov. from Tsaratanana in northern Madagascar is unique among Madagascar's miniaturised frogs in being a proportional dwarf, exhibiting far less advanced signs of paedomorphism than other species of similar size. *Anodonthyla eximia* sp. nov. from Ranomafana in eastern Madagascar is distinctly smaller than any of its congeners and is secondarily terrestrial, providing evidence that miniaturisation and terrestriality may be evolutionarily linked. The evolution of body size in Madagascar's microhylids has been more dynamic than previously understood, and future studies will hopefully shed light on the interplay between ecology and evolution of these remarkably diverse frogs.

Keywords: Miniaturisation; Taxonomy; Systematics; Microhylidae; Amphibians; New Species; Madagascar; Frogs; Morphology; Osteology; Evolution; Convergent Evolution; Cophylinae, *Mini* gen. nov., *Mini mum* sp. nov., *Mini scule* sp. nov., *Mini ature* sp. nov., *Anodonthyla eximia* sp. nov., *Rhombophryne proportionalis* sp. nov.

Introduction

Miniaturisation is a common phenomenon in amphibians [1-4], and is especially widespread and extreme in frogs [4-6]. A large proportion of the world's smallest frogs belong to the highly diverse family Microhylidae [5-8]. Microhylid frogs exhibit high degrees of osteological variation, especially in the morphology of elements of the skull, hands, feet, and pectoral girdle [9]. The smallest species among the microhylids do not belong to a single clade however, but rather occur in various different subfamilies spread across the tropics, including New Guinea [5, 6, 8], Borneo [10, 11], South America [12, 13], and Madagascar [14, 15]. Even within single microhylid subfamilies, multiple independent instances of miniaturisation are evident from the interdigitation of miniaturised and non-miniaturised species in the respective phylogenetic trees [8, 15]. One of the best examples is the subfamily Cophylinae, endemic to Madagascar [15].

Cophylinae currently consists of 103 described species, divided across eight recognised genera. Two of the largest microhylids, *Platypelis grandis* and *Plethodontohyla inguinalis* are members of this subfamily, but it also contains frogs that are among the smallest in the world, such as *Stumpffia contumelia* (adult snout–vent length [SVL] 8.0–8.9 mm [14]). Historically all small to miniaturised terrestrial cophylines were placed in the genus *Stumpffia*, as they are superficially homogeneous in external morphology, bioacoustics, and ecology, but even early molecular phylogenetic results suggested that their diversity exceeded a single genus [16, 17]. Several lineages of cophylines have

Results

independently miniaturised, converging on a diminutive phenotype, and belonging to a number of different genus-level clades which, however, have not yet all been taxonomically named. The latest phylogenetic reconstructions [15, 18-21] have clarified this picture; Fig 1 illustrates a simplified view of the latest phylogeny of Tu et al. [20], with emphasis on previously undescribed, miniaturised lineages that do not belong to *Stumpffia*.

In 2016, we highlighted three deep clades of miniaturised frogs within the Cophylinae that we considered probably distinct from *Stumpffia* [15]. These were: (i) ‘*S.*’ *helenae*, which we transferred to a new genus *Anilany* in order to preserve the monophyly of *Stumpffia*—this decision was challenged by Peloso et al. [22], who preferred to subsume *Stumpffia*, *Anilany*, and the generally much larger and morphologically strongly distinct *Rhombophryne* into a single genus, but evidence from morphology and genetics argues against this lumping approach [23]; (ii) a clade of two undescribed lineages from south-eastern Madagascar (provisionally named ‘*S.*’ spp. Ca15 and Ca16), originally identified by Wollenberg et al. [17], which consistently fall sister to the large-bodied *Plethodontohyla*—a third member of this clade, ‘*S.*’ sp. Ca53 was sequenced and deposited in GenBank by Rakotoarison et al. [14] and included in the phylogeny of Tu et al. [20]; and (iii)

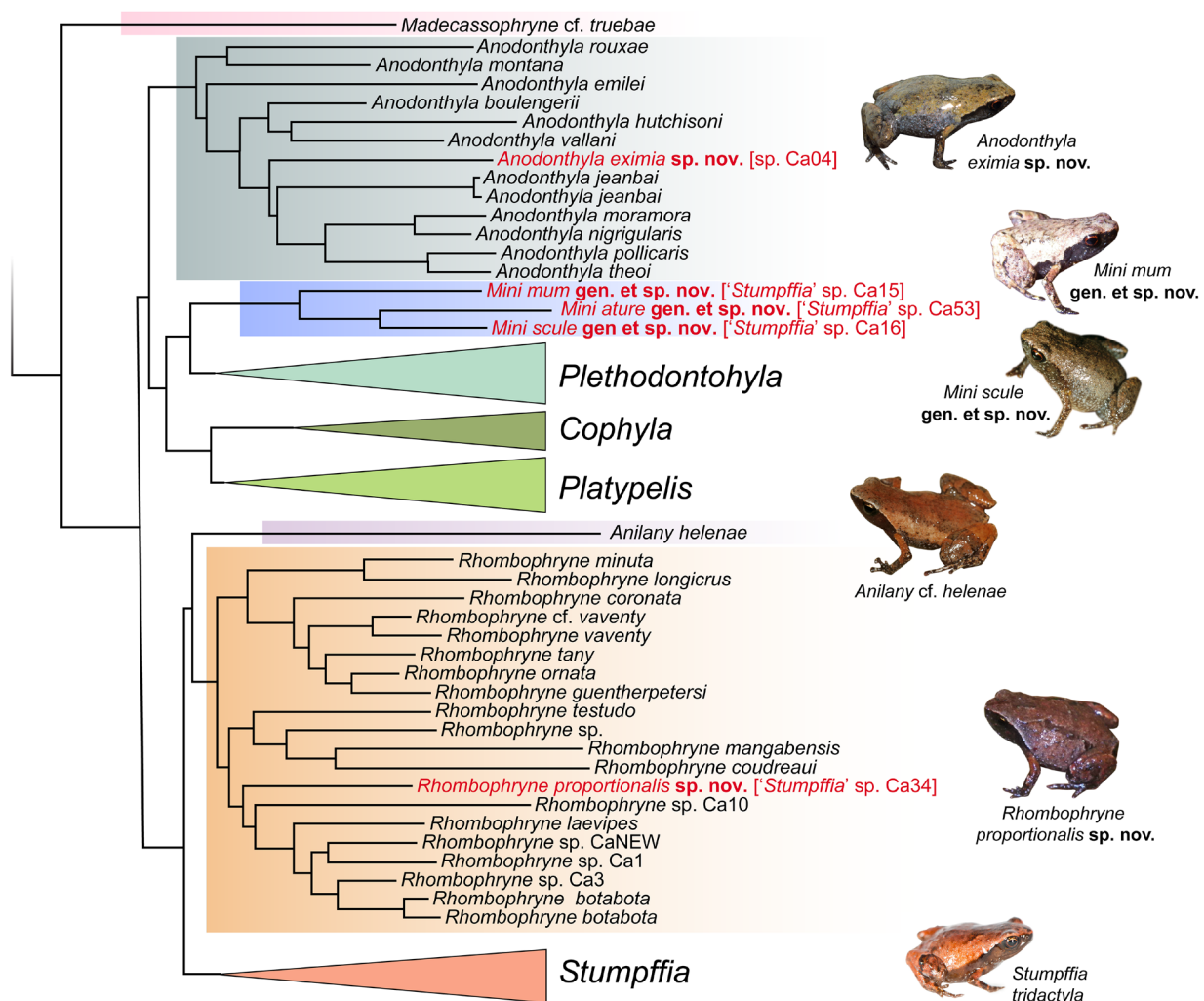


Fig 1. Stylised representation of the latest phylogeny of the microhylid subfamily Cophylinae.

Based on the phylogenetic tree of Tu et al. [20] (reconstructed from a concatenated multi-gene DNA sequence data set) with numerous nomenclatural updates. See that paper for support values and phylogenetic context. The sister species of *Rhombophryne proportionalis* sp. nov. is an undescribed candidate species (*R. sp. Ca7*) that is not included in this phylogeny; its taxonomy will be treated elsewhere. Taxa highlighted in red are those described herein. Inset photos show a selection of the new species described herein, and representatives of the other small-bodied genera, *Stumpffia* and *Anilany*. Inset photos are not to scale.

two frogs from Tsaratanana (*Rhombophryne* sp. Ca7 and 'S.' sp. Ca34), which were topologically unstable—these have since been found to fall within *Rhombophryne* ([20]; unpublished data), and only the latter is miniaturised, while the former is a frog of moderate-size (SVL 23.5–26.5 mm).

The phylogenetic position of *Stumpffia tridactyla* was also unstable [15, 22, 23] and the species was flagged as potentially divergent [23]. In light of our recent revision of the entirety of *Stumpffia* [14] and osteological data (unpublished observations), this species and its sister species, *S. contumelia*, form a clade sister to all other *Stumpffia* that we do not, at this time, consider to warrant genus-level recognition.

In previous work, we overlooked another miniaturised species that was included in our phylogeny [15, 20, 24] but not morphologically examined, namely *Anodonthyla* sp. Ca04 Ranomafana (ZCMV 204). The only available specimen of this species measures 11.3 mm SVL, and genetically and morphologically can be ascribed to *Anodonthyla*, representing an additional miniaturisation event within the Cophylinae.

In summary, there are three miniaturised species within an undescribed genus-level clade sister to *Plethodontohyla*, one miniaturised species of *Rhombophryne*, and one miniaturised species of *Anodonthyla*, all of which are awaiting taxonomic description. In the present paper, we provide formal descriptions of these taxa, with the aim of facilitating future research on the convoluted evolution of the frogs of the subfamily Cophylinae.

Materials and Methods

Ethics Statement

Approval for this study by an Institutional Animal Care and Use Committee (IACUC) was not required by Malagasy law, but all work complied with the guidelines for field research compiled by the American Society of Ichthyologists and Herpetologists (ASIH), the Herpetologists' League (HL), and the Society for the Study of Amphibians and Reptiles (SSAR). All field research, collecting of specimens, including in situ euthanasia of specimens, were approved by the Madagascan Ministère de l'Environnement des Eaux et des Forêts (Direction des Eaux et Forêts, DEF) under the following permits:

64/10/MEF/SG/DGF/DCB.SAP/SLRSE, 238-MINENV.EF/SG/DGEF/DPB/SCBLF/RECH, 045/12/MEF/SG/DGF/DCB.SAP/SCB, 238-MINENVEF/SG/DGEF/DPB/SCBLF, 218-MEEF/DEF/SPN/FSE/AUT, 198/16/MEEF/SG/DGF/DSAP/SCB.Re. Export of specimens was approved by the DEF under permits: 135N-EA07/MG10, 103C-EA03/ MG05, 044N-EA04/MG12, 094C-EA03/MG04, 094C-EA03/MG04, export 356N-EA12/MG16. Specimens were anaesthetised and subsequently euthanized following approved methods (MS222 solution; approved by the American Veterinary Medical Association) that do not require approval by an ethics committee, after consultation of the Animal Welfare Officer of TU Braunschweig.

Voucher specimens

Our study areas were as follows: Sainte Luce (ca. 24.75–24.76°S, 47.17–47.18°E); Tsaratanana (ca. 14.08–14.12°S, 48.97–48.99°E); Manombo (ca. 23.02–23.03°S, 47.72–47.73°E); Nahampoana (ca. 24.98°S, 46.98°E); Andohahela (ca. 24.75°S, 46.85°E). Field numbers used in this study refer to the zoological collections of Frank Glaw (FGZC), Miguel Vences (ZCMV), David R. Vieites (DRV), Serge H. Ndriantsoa (NSH), Angelica Crottini (ACZCV), and Sam Hyde Roberts (SHR). The following institutional acronyms are used: Zoologische Staatssammlung München, Munich (ZSM), amphibian collections of the Mention Zoologie et Biodiversité Animale of the Université d'Antananarivo (UADBA-A), Museum für Naturkunde, Berlin (ZMB), Muséum National d'Histoire Naturelle, Paris (MNHN), Zoologische Forschungsmuseum Alexander Koenig,

Results

Bonn (ZFMK), Zoological Museum of Amsterdam (ZMA)—today part of the Naturalis Biodiversity Centre, Leiden. Collected voucher specimens were fixed in the field in 90% ethanol and some subsequently transferred to 70% ethanol for long-term storage. Tissue samples (muscle or a limb) were preserved in 99% ethanol in the field, before specimen fixation.

Morphological measurements

Morphological examination was done under a binocular dissecting microscope. Measurements were taken with a digital calliper to the nearest 0.01 mm by MDS and rounded to the nearest 0.1 mm, with ratios calculated prior to rounding to avoid compound rounding errors. Measurement scheme followed our previous work [25-28]. The scheme is repeated here for convenience verbatim from Scherz et al. [25]: ‘SVL (snout–vent length), HW (maximum head width), HL (head length, from the maxillary commissure to the snout tip. Note: this is measured along the jaw, and not parallel to the longitudinal axis of the animal), ED (horizontal eye diameter), END (eye–nose distance, from the anterior eye to the posterior of the naris), NSD (nostril–snout tip distance, from the centre of the naris), NND (internarial distance, from the centre of each naris), TDH (horizontal tympanum diameter), TDV (vertical tympanum diameter), HAL (hand length, from the carpal–radioulna articulation to the tip of the longest finger), LAL (lower arm length, from the carpal–radioulna articulation to the radioulna–humeral articulation), UAL (upper arm length, from the radioulna–humeral articulation to the trunk, measured along the posterior aspect of the arm), FORL (forelimb length, given by the sum of HAL, LAL, and UAL), FOL (foot length, from the tarsal–metatarsal articulation to the tip of the longest toe), TARL (tarsal length, from the tarsal–metatarsal articulation to the tarsal–tibiofibular articulation), FOTL (foot length including tarsus, given by the sum of FOL and TARL), TIBL (tibiofibula length, from the femoral–tibiofibular articulation to the tarsal–tibiofibular articulation), TIBW (maximum tibiofibula [=shank] width), THIL (thigh length, from the vent to the femoral–tibiofibular articulation), THIW (thigh width at thickest point, measured in supine position), HIL (hindlimb length, given by the sum FOL, TARL, TIBL, and THIL), IMCL (maximum length of inner metacarpal tubercle), IMTL (maximum length of the inner metatarsal tubercle).’ Comparison to *Stumpffia* species based on external morphology is done in relation to the data presented by Rakotoarison et al. [14]. Morphological terminology referring to digits of the hands and feet is based on Rakotoarison et al. [14].

Micro-Computed Tomography

Micro-Computed Tomography (micro-CT) scans were produced in a nanotom m cone-beam scanner (phoenix|x, GE Measurement & Control, Wunstorf, Germany). Specimens were placed in small vessels such as Eppendorf tubes or film canisters and fixed in place using polystyrene and thin wooden struts. A small volume of ethanol was added to the container to prevent desiccation, and a lid was firmly shut to prevent excessive evaporation. Scan times were maximally 30 minutes. Standard scanning parameters were 750 ms exposures at 140 kV and 80 μ A for 2440 projections under fastscan parameters, with a 0.1 mm copper filter and a tungsten target, but small deviations were necessary in some cases. Scans were initially reconstructed in datos|x reconstruct software (GE Measurement & Control) and were then visualised in 8-bit under phong volume rendering settings in VG Studio Max 2.2 (Volume Graphics GMBH, Heidelberg, Germany) using a custom preset (available upon request). Osteological description was based on volume-renderings of the micro-CT data, following recommendations of Scherz et al. [25]. Osteological terminology follows Trueb [29-31] and Fabrezi and Alberch [32]. Rotational videos of micro-CT data were produced in VG Studio Max 2.2 following the methods outlined in Scherz et al. [25], and these together with DICOM image stacks of the scans produced in this study are available from http://morphosource.org/Detail/ProjectDetail>Show/project_id/464.

Bioacoustics

Recordings were made in the field using digital recorders (Tascam DR07 or DR05, Tascam DR-40, Roland EDIROL R-09) with internal or external (Sennheiser ME66/K6) microphone, or with an analogue Sony WM-D6C tape recorder with a Vivanco EM 238 external microphone in the case of the new *Anodonthyla* and early recordings from Nahampoana. Call analysis was conducted in Audacity 2.2.0 (<https://github.com/audacity/audacity>). Recordings with background wind were run through a decaying hi-pass filter in Audacity set at ca. 3 kHz to clean the audio prior to analysis. Frequency information was obtained through Fast Fourier Transformation (FFT; width 1024 points). The spectrogram was obtained using the Hanning window function with 256 bands resolution. Bioacoustic parameters are given as mean \pm standard deviation, with range in brackets. We measured dominant frequency, call duration, inter-call silent interval, and, where relevant, notes per call. Terminology follows the note-centred approach of Köhler et al. [33].

Molecular phylogenetics

We here present only minimal genetic data, because relevant genetic conclusions have been reported elsewhere [15, 17-21]; see Fig 1. Sequences of a 3' segment of the *16S rRNA* mtDNA gene were downloaded from GenBank (see S1 Table for full list of GenBank accession numbers used) and complemented by sequences of 11 additional specimens to verify their identity (GenBank accession numbers of new sequences: MK459307–MK459317). Separate alignments were constructed for the three genera concerned here: (1) *Mini* gen. nov. and *Plethodontohyla*, (2) *Rhombophryne*, and (3) *Anodonthyla*. Sequences were aligned using MUSCLE [34], and manually checked and trimmed in MEGA7 [35]. We herein also report uncorrected pair-wise distances (p-distances) between species in the *16S rRNA* gene, calculated in MEGA7 [35].

Taxonomic approach

Species described herein were identified initially based on molecular differentiation from other species, and morphological characters were then interrogated for diagnostic features, taking into account their phylogenetic position based on molecular data. Description schemes loosely follow Rakotoarison et al. [14], especially in the respect of comparing new material with a minimum possible set of other species in order to promote brevity. We follow the recommendations of Vences et al. [36] with regard to the economy of change in our consideration of the taxonomy of higher taxa.

Nomenclatural acts

The electronic edition of this article conforms to the requirements of the amended International Code of Zoological Nomenclature (ICZN), and hence the new names contained herein are available under that Code from the electronic edition of this article. This published work and the nomenclatural acts it contains have been registered in ZooBank, the online registration system for the ICZN. The ZooBank LSIDs (Life Science Identifiers) can be resolved and the associated information viewed through any standard web browser by appending the LSID to the prefix '<http://zoobank.org/>'. The LSID for this publication is: urn:lsid:zoobank.org:pub:91E597C8-7A80-46F9-B0E8-61F2524400F7. The journal's eISSN is 1932-6203. The article has been archived and is available from the following repositories: PubMed Central and LOCKSS.

Miniaturisation terminology

Clarke [4] discussed the definition of miniaturisation in the different clades of amphibians. He considered 25–30 mm SVL to represent the ‘critical division in anurans,’ with specimens of small-

Results

Table 1. Morphological measurements (in mm) of new species of miniaturised cophyline microhylids. Measurement abbreviations are listed in the Materials and Methods. A = Adult, M = Male, F = Female (lowercase indicates probable subadult), p = paratype, h = holotype (holotypes are also bolded), na = not available.

Collection Number	Field Number	Species	Status	SVL	HW	HL	ED	END	NSD	NND	TDH	TDV	HAL	UAL	LAL	FORL	FARL	THIL	THIW	TIBW	TARL	FOL	FOTL	HIL	IMCL	IMTL			
ZSM	ZCMV	<i>Rhombophryne proportionalis</i> sp. nov.	h	M	12.3	4.1	2.4	1.2	0.6	0.7	1.5	0.7	2.4	2.1	1.9	6.4	4.3	4.2	2.7	4.2	1.8	2.3	4.4	6.7	15.0	0.4	0.5		
1826/2010	12404	<i>Rhombophryne proportionalis</i> sp. nov.	p	M	11.0	4.1	2.6	1.0	0.5	0.7	1.2	0.8	0.7	1.6	1.6	2.1	5.4	3.8	4.3	2.1	3.9	1.4	2.4	3.9	6.3	14.6	0.3	0.3	
ZSM	DRV 6224	<i>Rhombophryne proportionalis</i> sp. nov.	p	M	11.5	3.8	2.4	1.1	0.6	0.6	1.1	na	na	2.0	1.3	1.8	5.1	3.8	4.4	2.2	3.9	1.3	1.8	3.8	5.6	13.9	0.3	0.5	
ZSM	636/2014	<i>Rhombophryne proportionalis</i> sp. nov.	p	M	11.5	3.8	2.4	1.1	0.6	0.6	1.1	na	na	2.0	1.3	1.8	5.1	3.8	4.4	2.2	3.9	1.3	1.8	3.8	5.6	13.9	0.3	0.5	
ZSM	ZCMV	<i>Rhombophryne proportionalis</i> sp. nov.	p	M?	8.2	3.0	2.1	1.2	0.5	0.6	1.6	0.6	1.5	1.4	1.6	4.5	3.1	3.5	1.9	4.1	1.4	2.3	3.1	5.4	13.0	0.0	0.3		
ZSM	ZCMV	<i>Minimium</i> gen. et sp. nov. h	M?	M?	8.8	3.0	2.2	1.2	0.6	0.7	1.2	0.4	1.1	1.8	1.6	4.5	2.7	4.6	1.7	4.1	1.3	2.7	3.8	6.4	15.1	0.0	0.4		
ZSM	ZCMV	<i>Minimium</i> gen. et sp. nov. p	M?	M?	8.8	3.0	2.2	1.2	0.6	0.7	1.2	0.4	1.1	1.8	1.6	4.5	2.7	4.6	1.7	4.1	1.3	2.7	3.8	6.4	15.1	0.0	0.4		
ZSM	1840/2010	<i>Rhombophryne proportionalis</i> sp. nov.	p	M?	9.2	3.3	2.3	1.2	0.5	0.7	1.2	0.3	0.4	1.5	1.6	1.9	5.0	3.4	3.6	1.7	4.3	1.4	2.8	3.8	6.6	14.5	0.2	0.4	
ZSM	ZCMV	<i>Minimium</i> gen. et sp. nov. p	F	11.3	3.5	2.7	1.3	0.6	0.6	1.2	0.6	0.7	1.7	1.8	2.0	5.5	3.7	5.3	1.7	4.6	1.4	2.8	4.1	6.9	16.7	0.0	0.0		
ZMA	20172	<i>Minimium</i> gen. et sp. nov. p	M	9.7	3.2	2.8	1.1	0.7	0.7	1.2	0.5	0.5	1.3	1.5	1.7	4.6	3.0	4.5	1.6	3.8	1.1	2.5	3.5	5.9	14.2	0.0	0.0		
ZMB	557	<i>Minimium</i> gen. et sp. nov. p	M?	10.5	3.3	2.8	1.1	0.7	0.7	1.2	0.6	0.6	1.8	1.8	1.9	5.5	3.6	4.0	1.6	4.6	1.4	2.6	3.6	6.3	14.8	0.0	0.2		
ZMB	NSH 2583	<i>Minimium</i> gen. et sp. nov. p	M?	9.9	3.3	2.5	1.2	0.6	0.6	1.1	0.6	0.6	1.6	na	na	na	4.2	1.9	4.3	1.2	na	na	na	na	na	na	na	na	
ZMB	NSH 2584	<i>Minimium</i> gen. et sp. nov. p	M	9.7	3.2	2.8	1.1	0.7	0.7	1.2	0.5	0.5	1.3	1.5	1.7	4.6	3.0	4.5	1.6	3.8	1.1	2.5	3.5	5.9	14.2	0.0	0.0		
ZSM	FGZC	<i>Miniscale</i> gen. et sp. nov. h	M?	M?	10.5	3.3	2.8	1.1	0.7	0.7	1.2	0.6	0.6	1.8	1.8	1.9	5.5	3.6	4.0	1.6	4.6	1.4	2.6	3.6	6.3	14.8	0.0	0.2	
ZSM	2662	<i>Miniscale</i> gen. et sp. nov. p	M?	M?	9.9	3.3	2.5	1.2	0.6	0.6	1.1	0.6	0.6	1.6	na	na	na	4.2	1.9	4.3	1.2	na	na	na	na	na	na	na	na
ZSM	FGZC	<i>Miniscale</i> gen. et sp. nov. p	M?	M?	10.8	3.6	2.8	1.4	0.6	0.7	1.4	0.5	0.4	1.7	1.9	2.3	5.9	4.0	4.5	2.0	4.3	1.6	2.6	4.0	6.6	15.4	0.3	0.3	
ZSM	2661	<i>Miniscale</i> gen. et sp. nov. p	A	A	10.2	3.4	2.7	1.2	0.6	0.7	1.3	0.7	1.8	2.1	2.2	6.0	4.0	4.8	1.9	4.7	1.7	3.1	4.1	7.2	16.6	0.2	0.5		
ZSM	577/2016	<i>Miniscale</i> gen. et sp. nov. p	A	A	10.7	3.5	2.8	1.4	0.6	0.8	1.4	0.7	0.7	1.7	2.0	2.4	6.1	4.1	5.1	1.8	4.6	1.4	3.2	4.1	7.4	17.1	0.2	0.3	
UADBA-A	0383	<i>Miniscale</i> gen. et sp. nov. p	M	M	10.2	3.4	2.7	1.2	0.6	0.7	1.3	0.7	1.8	2.1	2.2	6.0	4.0	4.8	1.9	4.7	1.7	3.1	4.1	7.2	16.6	0.2	0.5		
Uncat-	0384	<i>Miniscale</i> gen. et sp. nov. p	M	M	10.2	3.4	2.7	1.2	0.6	0.7	1.3	0.7	1.8	2.1	2.2	6.0	4.0	4.8	1.9	4.7	1.7	3.1	4.1	7.2	16.6	0.2	0.5		
ZSM	ACZCV	<i>Miniscale</i> gen. et sp. nov. p	A	A	10.7	3.5	2.8	1.4	0.6	0.8	1.4	0.7	0.7	1.7	2.0	2.4	6.1	4.1	5.1	1.8	4.6	1.4	3.2	4.1	7.4	17.1	0.2	0.3	
UADBA-A	0385	<i>Miniscale</i> gen. et sp. nov. p	A	A	9.2	3.2	2.4	1.2	0.7	0.6	1.1	0.5	0.5	1.4	1.5	1.9	4.8	3.3	4.0	1.8	4.2	1.4	2.5	3.4	5.9	14.2	0.3	0.4	
Uncat-	0386	<i>Miniscale</i> gen. et sp. nov. p	M	M	9.4	3.1	2.2	1.1	0.6	0.6	1.2	0.6	1.3	1.4	1.6	4.4	2.9	4.1	1.7	4.0	1.4	2.4	3.7	6.0	14.1	0.3	0.5		
UADBA-A	0387	<i>Miniscale</i> gen. et sp. nov. p	f	f	8.4	3.1	2.2	1.1	0.6	0.6	1.2	0.6	1.3	1.4	1.6	4.4	2.9	4.1	1.7	4.0	1.4	2.4	3.7	6.0	14.1	0.3	0.5		
ZFMK	—	<i>Miniscale</i> Naham-	—	A	10.5	4.0	2.8	1.4	0.6	0.8	1.4	0.6	0.6	1.8	1.8	2.3	5.9	4.1	4.9	2.0	4.1	1.7	2.7	4.0	6.7	15.7	0.3	0.6	
53775	—	<i>Miniscale</i> Naham-	—	A	14.9	5.6	3.8	1.5	0.8	0.8	1.8	0.7	0.8	2.3	1.6	2.5	6.4	4.8	4.6	2.7	5.1	2.0	2.9	5.0	7.9	17.6	0.3	0.3	
ZSM	FGZC	<i>Minature</i> gen. et sp. nov. h	A	A	11.3	3.5	2.6	1.2	0.7	0.8	1.4	0.6	0.7	1.6	1.3	1.7	4.6	3.3	4.1	1.7	4.4	1.6	2.8	3.8	6.6	15.1	0.3	0.4	
86/2004	0151	<i>Anodonthyla extima</i> sp.	h	M	11.3	3.5	2.6	1.2	0.7	0.8	1.4	0.6	0.7	1.6	1.3	1.7	4.6	3.3	4.1	1.7	4.4	1.6	2.8	3.8	6.6	15.1	0.3	0.4	
20246	204	—	—	—	—	—	—	—	—	—	—	—	—	—	—	—	—	—	—	—	—	—	—	—	—	—	—		

er sizes ‘exhibiting physiological and ecological modifications’ associated with miniaturisation. Thus, he considered 20–25 mm specimens ‘small’, and specimens below 20 mm ‘miniaturised’, with no further refinement for smaller taxa. Trueb and Alberch [37] considered any frog smaller than 25 mm to be ‘small’, with the further categorisation of ‘dwarf’ for frogs under 14 mm. Clarke [4] considered this scheme to be ‘too restrictive in the case of the extreme-small-size category’. We here opt for a compromise between these two schemes and consider species below 12 mm to be ‘extremely miniaturised’, below 16 mm to be ‘highly miniaturised’, below 20 mm to be ‘miniaturised’, and below 24 mm to be ‘small’.

Results

The miniaturised members of the subfamily Cophylinae, considering the described diversity and the undescribed lineages outlined in the Introduction, are morphologically, ecologically, and bioacoustically highly similar: they are terrestrial, leaf-litter dwelling frogs that predominantly emit their advertisement calls during the day. Their calls (with few exceptions, including the undescribed miniaturised *Rhombophryne*) consist of single, high-pitched, tonal notes emitted at regular intervals. Most if not all use ‘slow-motion’ walking [38, 39] as their primary mode of locomotion when undisturbed. All exhibit outward signs of reduction in length and/or number of digits, and almost all lack strongly expanded terminal discs (present only in larger species of *Stumpffia*, and in *Anilany heleneae*). Eye size is rather small, but nevertheless relatively larger compared to head length (ED up to 57% of HL; Table 1) than in non-miniaturised cophylines (e.g. maximum 45% in the *Rhombophryne serratopalpebrosa* species group; [25]). Finally, they are all inconspicuous in colour dorsally, with only a few larger species of *Stumpffia* possessing red on the hidden surfaces of their legs and on their venters [14].

Despite these strong similarities, detailed morphological (including osteological) assessment of the specimens representing the deep lineages outlined above (in the Introduction) yielded characters that differ significantly between them and all other cophylines. Of particular note are characters of the skull and hands, which show strong signs of miniaturisation and corresponding convergence, but also retain hallmarks of their evolutionary history shared with their non-miniaturised closest relatives.

Specimens belonging to the miniaturised clade sister to *Plethodontohyla* differ from all *Stumpffia* species by their curved clavicles, broad contact between the neopalatine and the straight-edged cultriform process of the parasphenoid (vs narrow contact and obliquely-edged), and a fused or lost carpal 2 (present in *Stumpffia*). The three deep lineages within this clade (Fig 1) differ from one another strongly in the state of the palate and dentition: the lineage from Manombo (‘*Stumpffia*’ sp. Ca15 in Scherz et al. [15]) lacks teeth altogether, while that from Sainte Luce (‘*Stumpffia*’ sp. Ca16 in Scherz et al. [15]) has both maxillary and premaxillary teeth. The lineage from Andohahela (‘*Stumpffia*’ sp. Ca53 in Tu et al. [20]) differs from both of these lineages in having a much larger body size, from the lineage from Manombo by possessing teeth, and from the lineage from Sainte Luce by a number of skull characters, including proportionally smaller braincase, broader contact between quadratojugal and maxilla, and proportionally smaller nasals.

Specimens belonging to the miniaturised *Rhombophryne* species (‘*Stumpffia*’ sp. Ca34 in Scherz et al. [15]) are morphologically (and genetically) homogeneous. This species differs from all other miniaturised species of the subfamily Cophylinae by the presence of vomerine teeth. It also differs from most *Stumpffia* by the total absence of clavicles, the presence of a strong lateral head colour border (thus far known only in *Anilany* and two much larger *Stumpffia* species, *S. be* and *S. hara* among small-sized cophylines), and very different hand and skull morphology, which is similar to larger *Rhombophryne* in its possession of a distinct first finger and toe (strongly reduced or absent in most *Stumpffia* species, especially those of similar size). Numerous characters separate this

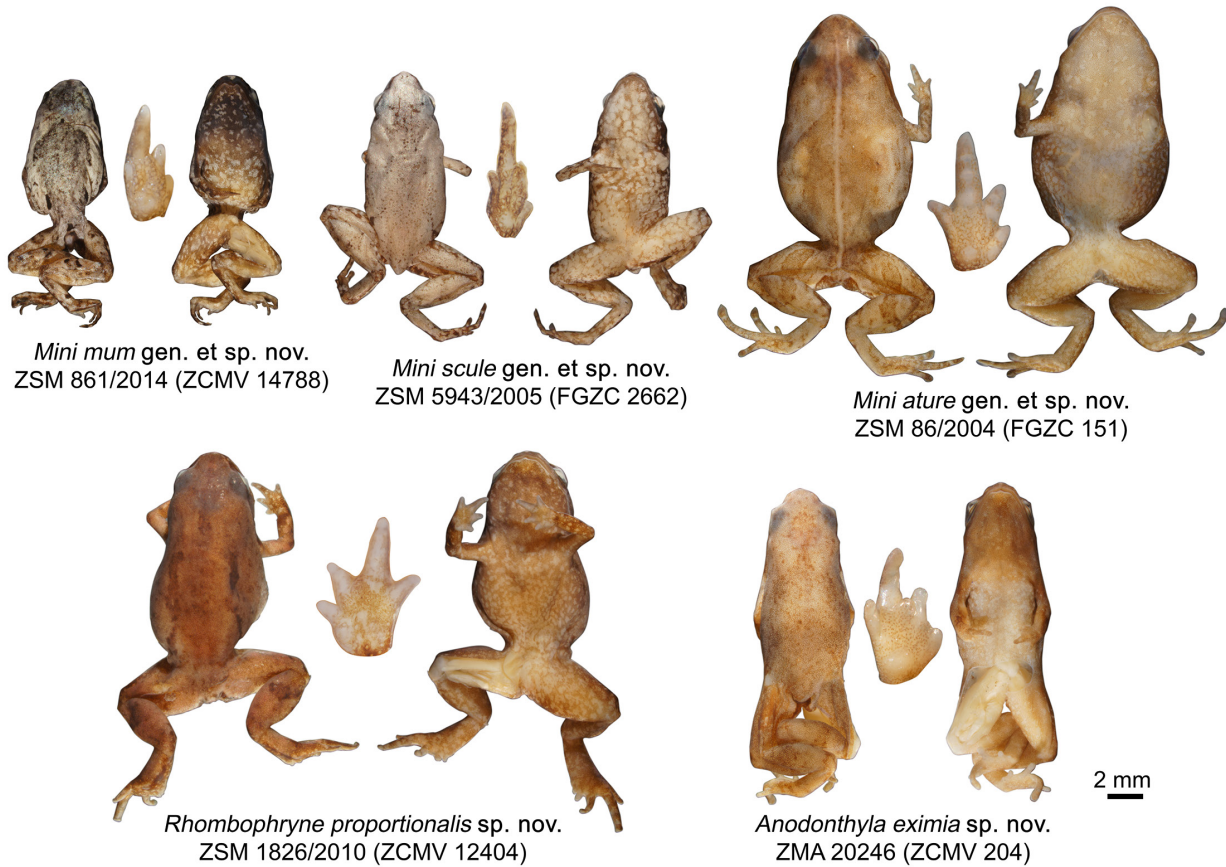


Fig 2. Holotypes of the new species described in this paper and their hands.

Whole specimens in dorsal (left) and ventral (right) view. Hand images not to scale.

species from all other *Rhombophryne* species, the most distinct of which being its considerably smaller body size. It also has a highly distinct call.

The sole available specimen of the miniaturised lineage within the genus *Anodonthyla*, ZMA 20246 (ZCMV 204), is an adult male, collected while presumably calling. It retains the synapomorphies of that genus, some of which are also related to sexual dimorphism in other members of the genus: a long and cultriform prepollex exceeding the length of the first metacarpal (present only in males of *Anodonthyla*), curved clavicles with distal knobs, and T-shaped terminal phalanges of toes 2–5 and the third finger. It differs from all *Anodonthyla* species by the absence of ossification in the sphenethmoid, and by the absence of strongly expressed humeral spurs or crests found in males of many species [24].

In summary, each of the five undescribed, species-level lineages of miniaturised frogs within the Cophylinae possess diagnostic characters. The three species forming a genus-level clade share synapomorphies that distinguish them from their sister genus, *Plethodontohyla*, and indeed all other miniature frogs from Madagascar. We therefore describe a new genus containing three new species, and one new species each of *Rhombophryne* and *Anodonthyla*.

Mini gen. nov.

urn:lsid:zoobank.org:act:67171236-00A2-428B-8194-584BF52E84E6

(Figs 2–9, Table 1)

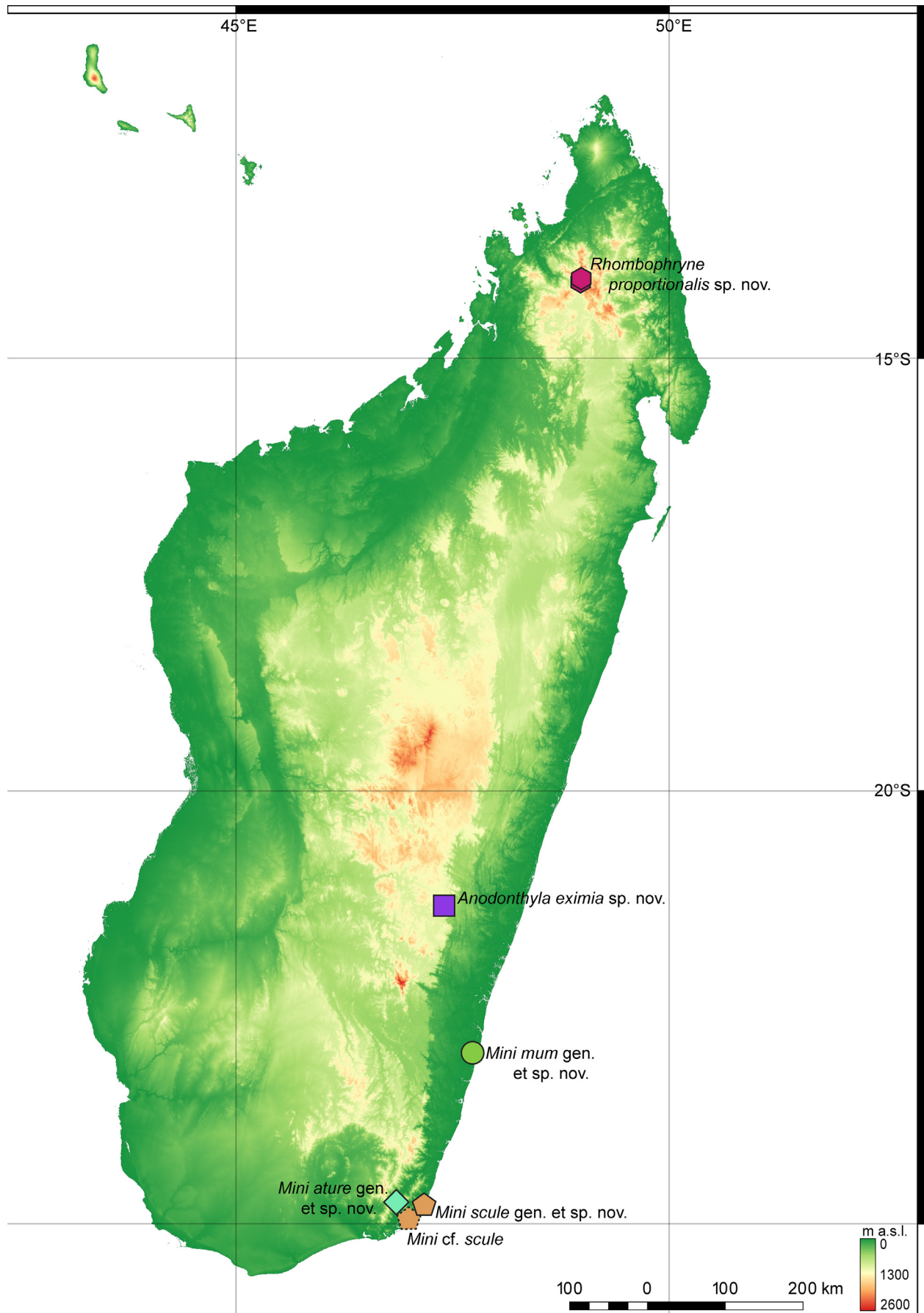


Fig 3. Currently known localities of the new taxa described in this paper.

The base map is USGS SRTM 1-Arc second digital elevation model.

Results

Type species. *Mini mum* sp. nov.

Contents. *Mini mum* sp. nov., *M. scule* sp. nov., and *M. ature* sp. nov.

Etymology. The genus name is derived from English prefix ‘mini-’, denoting a small version of an object. We treat this name as an arbitrary combination of letters in the sense of the International Code of Zoological Nomenclature Articles 30.1.4.1 and 30.2.2, and we assign it the feminine gender. We have searched all available taxonomic databases and could not find any evidence that this name has ever been used to refer to a genus of animals, and we therefore conclude that it is available.

Diagnosis. Diminutive terrestrial frogs (adult SVL 8.2–14.9 mm), assigned to the Madagascar-endemic subfamily Cophylinae on the basis of divided vomers, procoelous vertebral column, divided sphenethmoids, and genetic affinities. Skin smooth to slightly granular, occasionally iridescent. A lateral colour border is present but varies in intensity among species. Highly reduced fingers and toes, fusion or loss of carpal 2, and paedomorphic skull morphology: laterally displaced narrow nasals, teeth absent from vomer, in some species present on the maxilla and premaxilla, otic capsule sometimes dorsally ossified, brain case comprising most of the skull’s length and width.

All members of the genus *Mini* gen. nov. resemble miniaturised to extremely miniaturised members of the genus *Stumpffia*. However, all species can be distinguished from *Stumpffia* on the basis of their curving clavicles and a fused or lost carpal 2. In the species accounts below, we provide detailed distinctions from *Stumpffia* relevant to each species.

Justification. The erection of the genus *Mini* is justified by significant genetic differentiation from all other major cophyline lineages (see Fig 1), by the fact that it does not form a monophyletic group with the genus *Stumpffia*, and furthermore by the strong morphological differences (including but not restricted to the much smaller size) to all species of its sister clade, *Plethodontohyla*. The following characters distinguish the genus from all *Plethodontohyla* species, including juveniles: digital reduction of the fingers and toes (vs no reduction), laterally displaced and reduced nasals (vs large nasals situated anterior to frontal), parasphenoid cultriform process shorter than frontoparietals (vs roughly equal in length to the frontoparietals) and considerably narrower than alary processes (vs as wide or wider), vomerine teeth absent (vs present), carpal 2 absent (vs present). Uncorrected p-distances between *Mini* and *Plethodontohyla* range from 8.3–13.3% in the 3' fragment of 16S rRNA analysed here, and they have been found to be sister to *Plethodontohyla* in all phylogenetic analysis since their first inclusion in genetic datasets [15, 17, 20, 22] (except the DNA barcoding study of Vieites et al. [40], where they were placed at the base of *Rhombohypyne*+*Stumpffia*+*Anilany*, but that study lacks any resolution at deep nodes, and was not intended to provide phylogenetic hypotheses at deep levels).

Distribution. The genus *Mini* is apparently endemic to low-elevation habitats (0–350 m a. s. l.) of southeastern Madagascar (Fig 3).

Mini mum sp. nov.

urn:lsid:zoobank.org:act:237AA825-4612-4591-9CC8-764DAD646B48

(Figs 1–6, Tables 1, 2)

Remark. This species was previously listed as *Stumpffia* sp. 10 [17]; *Stumpffia* sp. 15/Ca15 [15, 40]; *Stumpffia* sp. aff. *tetradactyla* “Southeast” [41]; and *Stumpffia* sp. 10 KCW-2008 (EU341082) [20].

Holotype (Figs 2, 4, 6). ZSM 861/2014 (ZCMV 14788), an adult presumed male specimen collected in Manombo Special Reserve (23.0294°S, 47.7312°E, 7 m a.s.l.), Atsimo-Atsinanana



Fig 4. *Mini mum* gen. et sp. nov. in life and its habitat in Manombo Special Reserve.

(a-c) ZSM 861/2014, holotype, in (a) anterolateral view on a thumbnail, (b) dorsolateral view on a leaf, (c) ventral view. (d, e) ZSM 862/2014, paratype, in (d) ventral view, and (e) lateral view on a thumbnail. (f, g) ZMB 83194, paratype, in (f) dorsolateral view, and (g) ventral view. (h) ZMB 81993, paratype, in dorsolateral view. (i) ZMA 20172 in posterodorsolateral view. (j) Habitat of the new species in Manombo Special Reserve.

Results

Region, former Fianarantsoa province, southeastern Madagascar on 30 November 2014 by A. Rakotoarison and E. Rajeriarison.

Paratypes (Fig 4). ZSM 862/2014 (ZCMV 14789), an adult presumed male specimen with the same collection data as the holotype; ZMA 20172 (ZCMV 557), an adult presumed male specimen, and ZMA 20191 (ZCMV 558, GenBank accession number EU341082 for *12S rRNA* gene, *tRNA-Val*, and *16S rRNA* gene), an unsexed specimen collected in Manombo Special Reserve (23.0284°S, 47.7316°E, 44 m a.s.l.) on 2 February 2004 by D.R. Vieites and C. Woodhead; ZMB 81993 (NSH 2584) and ZMB 83194 (NSH 2583), adult male and female specimens (respectively) collected in Manombo Special Reserve (23.0249°S, 47.7311°E, ca. 20 m a.s.l.) on 28 March 2012 by J.C. Riemann, S.H. Ndriantsoa, A. Rakotoarison, J. Glos and M.-O. Rödel.

Diagnosis. An extremely miniaturised frog assigned to *Mini* gen. nov. on the basis of its small size, curved clavicles, laterally displaced and reduced nasals, and fusion or loss of carpal 2. This assignment is supported by its genetic affinities (Fig 1; [15, 17, 20]). It is separated by uncorrected p-distances of 10.0–11.2% in the analysed 3' fragment of the *16S rRNA* gene from other members of the genus *Mini* gen. nov., and 8.3–12.4% from all members of the genus *Plethodontohyla*.

Mini mum sp. nov. is characterised by the unique combination of the following characters (n = 4 male specimens, 1 female specimen): (1) male SVL 8.2–9.7 mm, female SVL 11.3 mm; (2) ED/HL 0.38–0.56; (3) HW/SVL 0.28–0.37; (4) FARL/SVL 0.30–0.38; (5) TIBL/SVL 0.39–0.50; (6) HIL/SVL 1.47–1.72; (7) fingers 1, 2, and 4 strongly reduced; (8) toe 1 absent, toes 2 and 5 quite reduced; (9) maxillary and premaxillary teeth absent; (10) vomerine teeth absent; (11) strong lateral colour border present; (12) black inguinal spots absent; (13) postchoanal vomer present, spatulate, medially fused to parasphenoid; (14) nasal cultriform and laterally displaced; (15) quadratojugal-maxilla contact weak; (16) zygomatic ramus of squamosal short, narrow, and horizontal; (17) clavicles present, curving with simple lateral articulations, medially not bulbous; (18) prepollex small or absent; (19) carpal 2 absent or fused to post-axial carpal 3–5 element; (20) finger phalangeal formula 1-2-3-2; (21) toe phalangeal formula 1-2-3-4-3; (22) single-note, unpulsed calls, not emitted in series; (23) frequency modulated calls; (24) call dominant frequency 8089 ± 140 Hz (n = 35); (25) call duration 74.8 ± 7.0 ms (n = 35); (26) inter-call interval 4299.8 ± 1604.9 ms (n = 34).

Within the genus *Mini* gen. nov., the new species is unique in lacking teeth, and possessing a strong lateral colour border. See other species described below for respective diagnoses.

This species is particularly similar to some extremely miniaturised *Stumpffia* species, but it can be distinguished from all *Stumpffia* based on the condition of the carpals, and all *Stumpffia* except *S. tridactyla*, *S. contumelia*, and *S. obscoena* by the extent of reduction of its fingers and toes. It differs from all of these in possessing curved clavicles (vs absent in *S. contumelia* and *S. obscoena* and straight or absent in *S. tridactyla*; unpublished data), and presence of neopalatine and divided vomer (vs absence of neopalatine and non-divided vomer in *S. obscoena*, *S. tridactyla*, and *S. contumelia*; unpublished data).

Calls resemble those of *S. miery*, *S. tridactyla*, *S. contumelia*, and *S. obscoena*, but are shorter in duration and lower in frequency than *S. obscoena* (duration 74.8 ± 7.0 ms vs 144 ± 8 ms; frequency 8089 ± 140 Hz vs 8361 ± 69 Hz); longer in duration and higher in frequency than *S. contumelia* (duration 74.8 ± 7.0 ms vs 42 ± 4 ms; frequency 8089 ± 140 Hz vs 7493 ± 50 Hz); shorter in duration and higher in frequency than *S. tridactyla* (duration 74.8 ± 7.0 ms vs 132 ± 23 ms; frequency 8089 ± 140 Hz vs 7244 ± 200 Hz); and slightly longer inter-call interval than *S. miery* (4299.8 ± 1604.9 ms vs 3102 ± 456 ms).

Holotype description. Specimen in a good state of preservation, a piece of the left thigh re-

moved as a tissue sample. Body oblong; head wider than long, narrower than body width; snout rounded in dorsal view, pointed in lateral view; nostrils directed laterally, not protuberant, slightly further from tip of snout than from eye; canthus rostralis indistinct, straight; loreal region flat, vertical; tympanum indistinct, round, about 49% of eye diameter; round pupil; supratympanic fold absent; tongue long, broadening slightly posteriorly, attached anteriorly, not notched; maxillary teeth absent; vomerine teeth absent; choanae small and round. Forelimbs slender; subarticular tubercles single, indistinct except on third finger; outer metacarpal tubercle rounded; inner metacarpal tubercle indistinguishable from reduced first finger; hand without webbing; first, second, and fourth fingers strongly reduced, third finger basally broadened; relative length of fingers $1 < 4 < 2 < 3$, fourth finger slightly more reduced than second; finger tips not expanded into discs. Hindlimbs slender; TIBL 50% of SVL; lateral metatarsalia strongly connected; inner metatarsal tubercle indistinguishable from completely reduced first toe; outer metatarsal tubercle absent; no webbing between toes; first toe absent, second and fifth toes extremely reduced; relative length of toes $2 < 5 < 3 < 4$; fifth toe distinctly shorter than third. Skin on dorsum smooth, without distinct dorsolateral folds. Ventral skin smooth.

After four years in 70% ethanol, the dorsum is metallic silver centrally on the trunk, bluish silver on the head, and laterally light silver, with dark oblong markings in the inguinal region (Fig

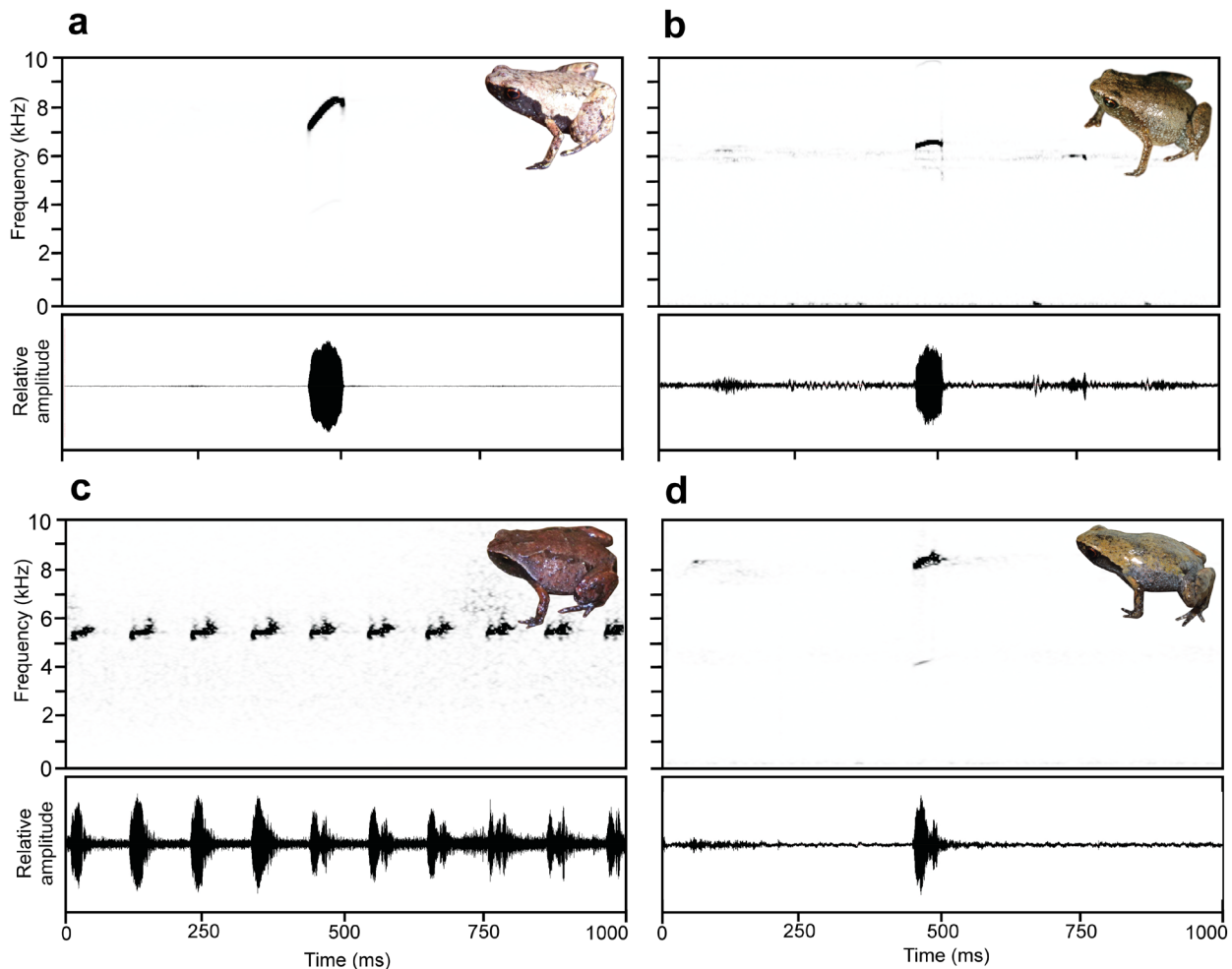


Fig 5. One-second spectrograms and oscillograms of the calls of the new species described here.

Insets represent the respective species but not the calling specimens. (a) *Mini mum* gen. et sp. nov., paratype ZMB 81993 from Manombo, (b) *Mini scule* gen. et sp. nov., ZSM 265/2018 from Sainte Luce, (c) *Rhombophryne proportionalis* sp. nov., part of a call (note series) of a specimen from Bepia campsite, Tsaratanana (not collected), (d) *Anodonthyla eximia* sp. nov., specimen not collected, from Maharira (Ranomafana).

Results

2). There is a strong dorsolateral colour border to the ebony lateral colouration, extending from the side of the head to the legs. The lateral colouration fades to the more burnt umber ventral colouration, especially dark anteriorly, flecked with beige, fading posteriorly through larger fleck sizes to beige at the posterior abdomen. Dorsally, the legs are mottled cream and grey brown with a dark cloacal region. Ventrally the legs are brown flecked with beige. The arms are silvery dorsally and ebony laterally and ventrally. Colour in life (Fig 4a-c) as in preservative but browner in every aspect and less obviously iridescent, with a red iris.

Variation. For variation in measurements among specimens, see Table 1. Non-ovigerous specimens with darkened throats are presumed to be males, in keeping with the one call voucher, ZMB 81993. In general, all examined specimens agree with the holotype in morphology, but female ZMB 83194 is more rotund in body shape in preservative, but had a longer, depressed body profile in life (Fig 4f-g). ZMB 83194 and 83193 varied in life from smooth to slightly granular skin, with a very faintly bulging vertebral line. The colouration in life varied rather strongly (Fig 4). Lateral and ventral colouration was more or less consistently dark brown with light flecks, but ZMB 81993 had bright bluish-white flecks laterally. The strength of the flank colour border varied from stark in ZSM 862/2014 to weak in ZMB 83194. Dorsal colouration varied from solid tan in ZSM 862/2014 to mottled beige and dark brown in ZMB 83194. Iris colouration was consistently red to reddish copper. In preservative, paratypes are less iridescent than the holotype, and ZMB 81993 and 83914 are faded to light brown.

Bioacoustics. Calls recorded from specimen ZMB 81993 (Fig 5a, Table 2) during the day on 28 March 2012 (see paratype section for locality data). Air temperature was 21.7°C. The specimen was calling under dense leaf litter. Estimated call parameters were as follows (n = 35 in all cases except inter-call and call intervals, where n = 34): Calls consisting of a single note were emitted at regular intervals without defined call series. Calls had linear upward frequency modulation with a downward hooked tail, with an initial dominant frequency around 7000 Hz, rising gradually to ca. 8250 Hz, and with a tail-end dropping down to ca. 7500 Hz again. For detailed parameters, see

Table 2. Bioacoustic parameters of new species of miniaturised cophyline microhylids.

Data on *S. miery* from Rakotoarison et al. [14], provided for comparison with the sympatric *A. eximia*. Values are presented as mean ± standard deviation, with range in brackets. na = not applicable. *In all species except *R. proportionalis* calls consist of a single note according to the definition herein, and in these species call duration is therefore synonymous with note duration.

	Dominant frequency (Hz)	Call duration (ms)*	Inter-call interval (ms)	Note duration (ms)*	Inter-note interval (ms)	Notes per series	Notes analysed*
<i>Minimium</i> gen. et sp. nov.	8089 ± 140 (7676–8306)	74.8 ± 7.0 (57–87)	4299.8 ± 1604.9 (3136–10139)		na	na	n = 35
<i>Miniscule</i> gen. et sp. nov.	6675 ± 64 (6549–6768)	121.9 ± 8.7 (108–140)	1905.1 ± 398.3 (1589–4122)		na	na	n = 51
ZSM 265/2018							
<i>Rhombophryne proportionalis</i> sp. nov. (Camp Bepia)	5460 ± 117 (5166–5732)	1328.0 ± 284.1 (905–1765, n = 6)	62753 ± 20613 (38952–74744, n = 3)	45.4 ± 8.2 (27–60)	63.0 ± 9.0 (45–88)	13 ± 3 (9–17, n = 6)	n = 79
<i>Anodonthyla eximia</i> sp. nov.	8406 ± 78 (8349–8540)	59.6 ± 6.5 (53–68)	3749.0 ± 1149.9 (2654–5172)		na	na	n = 5
<i>Stumpffia miery</i>	8057 ± 137 (7751–8225)	73 ± 12 (51–88)	3102 ± 456 (2679–4247)		na	na	n = 10

Table 2.

Osteology (Fig 6). Based on ZSM 861/2014 (figured), and ZSM 862/2014, ZMA 20172, ZMB 81993 and ZMB 83194 (not figured). Note that the skulls of ZSM 861–862/2014 are somewhat distorted in fixation, especially with respect to the maxillary arcade and mandible. The skull and pectoral girdle of ZMB 81993 are quite badly damaged, and both of its hindlimbs are fractured, as are the coracoids and left ilium of ZMB 83194.

Cranium (Fig 6d-g). Shape and proportions. Skull short and rounded, longer than wide, widest at the bowing of the quadratojugal roughly in line with the anterior face of the prootic. Braincase proportionally broad, with an extremely short rostrum.

Neurocranium. Ossification generally high, lower in ZSM 862/2014 than other specimens. Anterior cone of sphenethmoid ossified and in contact with the frontoparietals in ZSM 861/2014 and ZMB 83194 and 81993, but no sphenethmoid ossification in the other specimens. Prootic in dorsal contact with lateral flange of frontoparietal, ventral contact with parasphenoid alae, not approaching contralateral ventrally. Septomaxilla minuscule, very tightly curled, not further discussed due to low ossification and insufficient resolution. Columella (stapes) well ossified, pars media plectra (stylus) long and nearly straight, broadening distally, posteriorly and dorsally oriented toward the dorsally elongated pars interna plectra (baseplate). Nasal narrow and cultriform, laterally displaced (in line with anterior end of frontoparietal), curved downward laterally, the acuminate maxillary process not distinct and not closely approaching maxillary pars facialis, broadly separated from contralateral. Frontoparietal with rounded anterior edge, laterally rather straight-edged, with short lateral flange covering prootic, posteriorly strongly connected to exoccipital, anteroventrally contacting sphenethmoid in ZSM 861/2014, lacking any dorsal process, separated from contralateral by a narrow gap with a small rhomboid facet at the level of the prootics, possibly constituting the pineal foramen.

Parasphenoid with narrow, rather straight-edged cultriform process and slightly broader perpendicular alae, considerably shorter than frontoparietals, in contact with exoccipitals postero-dorsally, prootics dorsally along the edges of the alae, anteroventrally in contact with postchoanal vomer and not in contact with neopalatine; posteromedial process not participating in foramen magnum. Vomer divided into pre- and postchoanal portions; prechoanal portion narrow, simple, sickle-shaped, without a lateral ramus; postchoanal portion spatulate and edentate, narrowly separated from its contralateral on the midline, in dorsal contact with the parasphenoid proximally and the neopalatine distally, lacking an anterior projection. Neopalatine simple, straight, almost indistinguishable from lateral postchoanal portion of vomer, laterally broadly separated from the maxilla, not exceeding the lateral-most point of the postchoanal vomer.

Maxillary arcade gracile, maxilla and premaxilla edentate, anterior extension of maxilla not exceeding lateral extent of premaxilla. Premaxilla with a narrow acuminate dorsal alary process rising laterally, pars palatina shallowly divided into a narrow palatine process and broad, squared lateral process. Maxilla with a low triangular pars facialis and a narrow pars palatina, its posterior tip acuminate and barely contacting the quadratojugal, the lingual surface of the pars palatina followed by but not contacting the anterior ramus of the pterygoid, presumably separated by the pterygoid cartilage. Pterygoid with an exceptionally short medial ramus, long anterior ramus, and broad posterior ramus, posteriorly weakly calcified to the quadratojugal complex. Quadratojugal bowed laterally, broadly connected to the ventral ramus of the squamosal, bearing a small posteroventral knob, weakly anteriorly connected to the maxilla; the articulation of the mandible is apparently somewhat fortified by the mineralisation of the posterior ramus of the pterygoid+squamosal+quadratojugal posteroventral knob. Squamosal with a slender, rather straight ventral ramus, broadened, nearly vertical otic ramus, and short, thin, horizontal zygomatic ramus.

Results

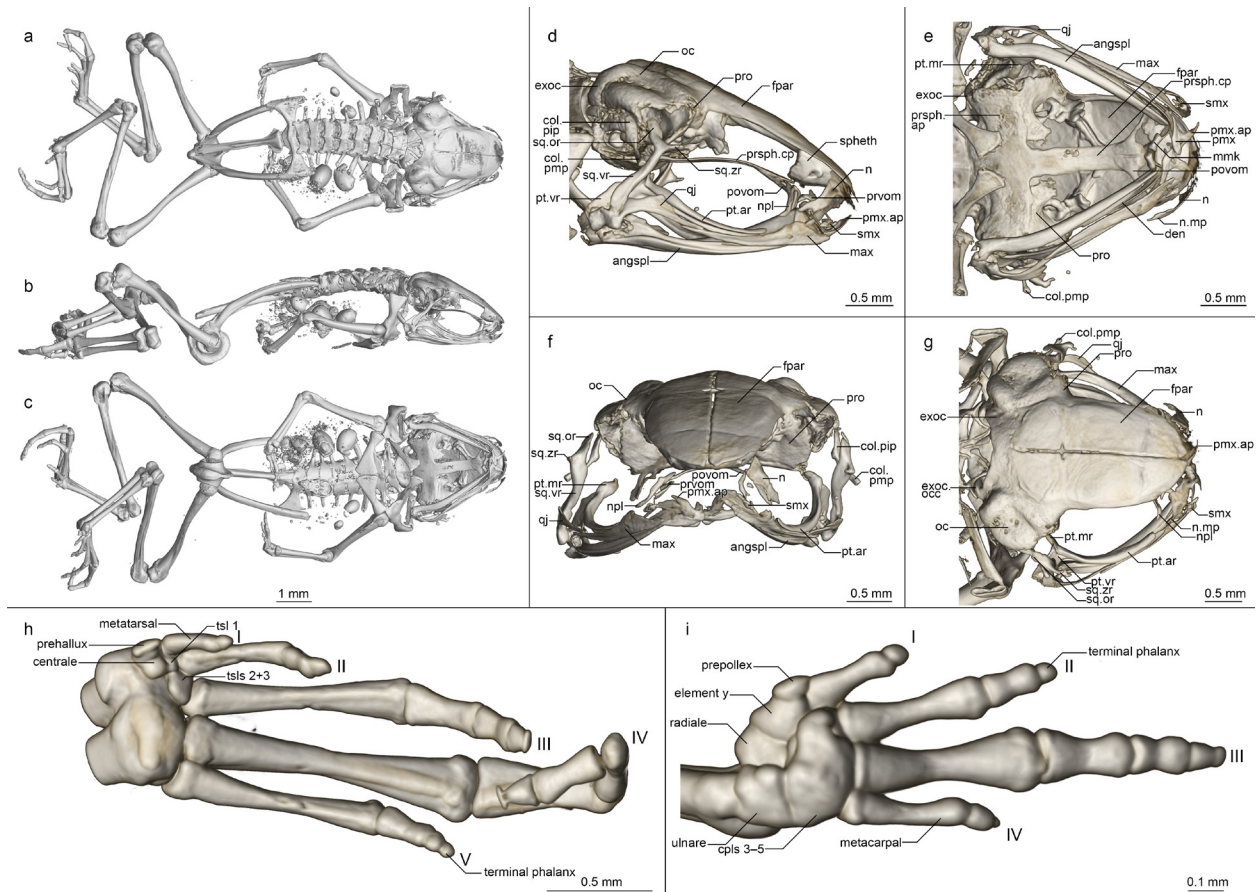


Fig 6. Osteology of *Mini mum* gen. et sp. nov. holotype (ZSM 861/2014).

(a-c) Whole skeleton in (a) dorsal, (b) lateral, and (c) ventral view. (d-g) Skull in (d) lateral, (e) ventral, (f) anterior, and (g) dorsal view. (h) Foot in ventral view. (i) Hand in ventral view. Abbreviations for all osteological figures: angspl, angulosplenial; col.pip, pars interna plectra of columella; col.pmp, pars media plectra of columella; cpl(s), carpal(s); den, dentary; exoc, exoccipital; exoc.occ, occipital condyle of exoccipital; fpar, frontoparietal; max, maxilla; max.fp, facial process of maxilla; mmk, mentomeckelian; n, nasal; n.mp, maxillary process of nasal; npl, neopalatine; oc, otic capsule; prsph.ap, parasphenoid alary process; prsph.cp, parasphenoid cultriform process; prsph.pmp, parasphenoid posteromedial process; pmx, premaxilla; pmx.ap, premaxilla ascending process; pmx.lp, premaxilla lateral process; pmx.pp, premaxilla palatine process; povom, postchoanal portion of vomer; pro, prootic; prvom, prechoanal portion of vomer; pt.ar, pterygoid anterior ramus; pt.mr, pterygoid medial ramus; pt.vr, pterygoid ventral ramus; qj, quadratojugal; smx, septomaxilla; spheth, sphenethmoid; sq.or, squamosal otic ramus; sq.vr, squamosal ventral ramus; sq.zr, squamosal zygomatic ramus; ts1, tarsals; ts2-3, tarsals; vt, vomerine teeth.

Mandible slim and edentate, largely unremarkable, with a weakly raised coronoid process on the angulosplenial. Mentomeckelians separated from the dentary, with small hooked ventrolateral projections.

Posteromedial processes of hyoid proximally rounded with a broad medial crista.

Postcranial Skeleton (Fig 6a-c, h, i). Eight procoelous presacrals, all much broader than long, lacking neural spines, with round posterior articular processes, presacral I with a complete neural arch, presacrals II–IV with thicker and longer transverse processes than V–VIII. Sacrum with expanded diapophyses, the leading and trailing edges roughly equally angled, the articulation type IIB *sensu* Emerson [42]. Urostyle bicondylar, long, broadening posteriorly, with a somewhat flared head and a low dorsal ridge.

Pectoral girdle without ossified prezonal or postzonal elements, with ossified clavicles. Clavicle thin and weakly curved, with a simple lateral junction, slightly shorter than the coracoid. Coracoid fairly narrow, weakly flared laterally, strongly flared medially with a straight medial articular

surface with the contralateral. Scapula slender, with a thin pars acromialis, the cleitheral border straight. Cleithrum ossified for half the width of the scapular border, thickened anteriorly. Suprascapula unossified.

Humerus with a well-developed crista ventralis and no medial or lateral cristae. Radioulna slender with a distinct sulcus intermedius. Carpals apparently reduced, composed of radiale, ulnare, element Y, prepollex, and a large post-axial element formed by carpals 3–5. Carpal 2 has either been lost or fused to the latter element. Finger phalangeal formula is reduced (1-2-3-2), and the terminal phalanges of the first, second and fourth fingers are small, round elements.

Pubis ossified; iliac shafts passing ventral to and beyond sacrum, oblong in cross-section, with a weak dorsal crest, without a dorsal prominence and with a shallow oblique groove. Femur weakly sigmoid, lacking a posterior crest. Tibiofibula slightly longer than femur in length, with a sulcus intermedius. Tibiale and fibulare fused proximally and distally. T1 and T2+3 tarsals present, T1 considerably smaller than T2+3. Centrale present, slightly smaller than T2+3. Prehallux small. Phalangeal formula reduced (1-2-3-4-3). Terminal phalanges of toes 3 and 4 with knobs, those of other toes small, round elements.

Distribution, natural history, and conservation status. This species is known only from Manombo Special Reserve, southeast Madagascar (Fig 3). The habitat consists of low, comparatively open forest with small trees, many lianas and a very thick layer of dead leaves (Fig 4j). Calls were emitted by males during the day, hiding within the leaf litter or between roots, separated from other calling males by several metres. The female paratype ZMB 83194 contains four eggs (visualised by micro-CT scan, not extracted for physical examination). Manombo Special Reserve covers an area of 52.66 km². We estimate that this species occurs from 0–100 m a.s.l. within lowland forests in and around this reserve. Although lowland species from areas with low topographical complexity tend not to be extreme micro-endemics [43], extremely miniaturized frogs in Madagascar almost always are [14, 17], so the full extent of this species' range is not likely to be large. Littoral forest in the area where the species occurs is extremely reduced, so other sites outside the Special Reserve are likely to be small and under high pressure. We therefore recommend this species be listed as Critically Endangered according to the IUCN Red List Criterion CR B1ab(iii) [44], in line with other endemics from Manombo Special Reserve (e.g. *Guibemantis diphonous* [45]).

The gut of ZSM 861/2014 contains four or five arthropods visible from micro-CT scans, tentatively identified as oribatid mites.

Etymology. We use the specific epithet 'mum' as an arbitrary combination of letters, in order to form a pun on 'minimum' from the name in apposition, in reference to the fact that this is among the smallest known frogs from Madagascar and the world. It is to be regarded as an invariable noun.

Miniscule sp. nov.

urn:lsid:zoobank.org:act:AC570728-78AE-4FDB-B9BE-87DB553C5ABE

(Figs 1-3, 7, 8, Tables 1, 2)

Remarks. This species was previously listed as *Stumpffia* sp. 9 [17]; *Stumpffia* sp. 16/Ca16 [15, 40, 46]; *Stumpffia* sp. aff. *tetradactyla* "Southeast" [41]; and *Stumpffia* sp. 16 MV-2009 (KC351485) [20].

ZFMK 53775 (Fig 7d, e), a specimen from Nahampoana in southeastern Madagascar (ca. 24.975°S, 46.980°E, ca. 60 m a.s.l.), collected by F. Glaw and J. Müller on 4 January 1992, is sim-

Results



Fig 7. *Mini scule* gen. et sp. nov. in life and its habitat in Sainte Luce Reserve.

(a, b) ZSM 5943/2005, holotype, in (a) dorsolateral and (b) ventral view. Black lines in the two pictures are scanning artefacts from damaged analogue slides. (c) Probably ZSM 5942/2005, paratype, in dorsolateral view. (d-f) ZSM 265/2018 (SHR 09112018) in (d) dorsal, (e) dorsolateral, and (f) ventral view. Note the numerous pink cf. *Endotrombicula* mites on the abdomen and legs. (g) Habitat in Sainte Luce Special Reserve. (h, i) *Mini* cf. *scule* from Nahampoana, ZFMK 53775 in (h) lateral and (i) ventral view.

ilar to *M. scule* sp. nov. and we consider it possible that it is a member of this species. However, in the absence of genetic data from this specimen and population, we here do not consider it within the definition of *M. scule* sp. nov. and refer to it as *M. cf. scule*.

Holotype (Figs 2, 7, 8). ZSM 5943/2005 (FGZC 2662, GenBank accession number KC351485 for *16S rRNA* gene), an adult presumed male specimen collected in Sainte Luce Reserve forest at the QMM climate station (24.7798°S, 47.1713°E, 23 m a.s.l.), Anosy Region, former Toliara province, southeastern Madagascar on 4 February 2005 by F. Glaw and P. Bora.

Paratype (Fig 7). ZSM 5942/2005 (FGZC 2661, GenBank accession number EU341081 for *12S rRNA* gene, *tRNA-Val*, and *16S rRNAe* genes), an adult presumed male specimen with the same collection data as the holotype. The hands and feet of this specimen were all removed as tissue samples. ZSM 265/2018 (SHR 09112018), an adult male specimen collected while calling in Sainte Luce Reserve parcel S9 (24.7606°S, 47.1732°E, 28 m a.s.l.) on 8 November 2018 by S. Hyde Roberts. Additionally, the following five specimens collected by S. Hyde Roberts between 8 and 20 October 2016 in Sainte Luce Reserve: UADBA-A Uncatalogued (ACZCV 0386, GenBank accession number MK459315 for *16S rRNA* gene) an unsexed adult specimen, and UADBA-A Uncatalogued (ACZCV 0387, GenBank accession number MK459316 for *16S rRNA* gene), a juvenile female specimen (sexed by incision, small dark brown egg follicles present), both collected at 24.754–24.755°S, 47.173°E, ca. 20 m a.s.l.; ZSM 577/2016 (ACZCV 0383, GenBank accession number MK459312 for *16S rRNA* gene), an adult unsexed specimen collected at 24.7600°S, 47.1746°E, ca. 20 m a.s.l.; UADBA-A Uncatalogued (ACZCV 0384, GenBank accession number MK459313 for *16S rRNA* gene), an adult male specimen collected at 24.7604°S, 47.1737°E, ca. 20 m a.s.l.; ZSM 578/2016 (ACZCV 0385, GenBank accession number MK459314 for *16S rRNA* gene), an adult unsexed specimen collected at 24.7550°S, 47.1735°E, ca. 20 m a.s.l.

Diagnosis. An extremely miniaturised frog assigned to *Mini* gen. nov. on the basis of its small size, curved clavicles, laterally displaced and reduced nasals, and fusion or loss of carpal 2. This assignment is supported by its genetic affinities (Fig 1; [15, 17, 20]). It is separated by uncorrected p-distances of 10.4–11.2% in the analysed 3' fragment of the *16S rRNA* gene from other members of the genus *Mini* gen. nov., and 9.7–13.3% from all members of the genus *Plethodontohyla*.

Mini scule sp. nov. is characterised by the unique combination of the following characters (n = 3 probable male and 3 adult unsexed specimens): (1) male SVL 9.9–10.5 mm (adult SVL up to 10.8 mm); (2) ED/HL 0.40–0.51; (3) HW/SVL 0.31–0.38; (4) FARL/SVL 0.34–0.39; (5) TIBL/SVL 0.39–0.47; (6) HIL/SVL 1.41–1.68; (7) fingers 1, 2, and 4 strongly reduced; (8) toe 1 absent, toes 2 and 5 quite reduced; (9) maxillary and premaxillary teeth present; (10) vomerine teeth absent; (11) lateral colour border occasionally present; (12) black inguinal spots generally absent; (13) postchoanal vomer present, spatulate, medially fused to parasphenoid; (14) nasal cultriform and laterally displaced; (15) quadratojugal-maxilla contact weak; (16) zygomatic ramus of squamosal short, thick, and horizontal; (17) clavicles present, curving with simple lateral articulations, medially not bulbous; (18) prepollex small or absent; (19) carpal 2 absent or fused to post-axial carpal 3–5 element; (20) finger phalangeal formula 0-2-3-2; (21) toe phalangeal formula 1-2-3-4-3; (22) single-note, unpulsed calls, not emitted in series; (23) non-frequency modulated calls; (24) call dominant frequency 6675 ± 64 Hz (n = 51); (25) call duration 121.9 ± 8.7 ms (n = 51); (26) inter-call interval 1905.1 ± 398.3 ms (n = 50).

Within the genus *Mini* gen. nov., the new species can be distinguished from *M. mum* sp. nov. by the presence of maxillary and premaxillary teeth (vs absence), and less distinct lateral colour border. For diagnosis against *M. ature* sp. nov., see the diagnosis of that species, below.

Results

This species is particularly similar to some extremely miniaturised *Stumpffia* species, but it can be distinguished from all *Stumpffia* based on the condition of the carpals, from almost all *Stumpffia* by the possession of maxillary and premaxillary teeth (present only in *S. spandei*, *S. miovaova*, *S. makira*, *S. diutissima*; unpublished data), and from all *Stumpffia* except *S. tridactyla*, *S. contumelia*, and *S. obscoena* by the extremely reduced fingers and toes. It differs from these latter three species in lacking a strong lateral colour border (vs present), curved clavicles (vs absent in *S. contumelia* and *S. obscoena* and straight or absent in *S. tridactyla*; unpublished data), and presence of neopalatine and divided vomer (vs absence of neopalatine and non-divided vomer in *S. obscoena*, *S. tridactyla*, and *S. contumelia*; unpublished data).

Calls differ significantly from *M. mum* sp. nov. in frequency, duration, and inter-call intervals (see Table 2), but resemble those of numerous *Stumpffia* species. For distinction, compare the values given in Table 5 of Rakotoarison et al. [14]. In call duration, the calls are most similar to *S. gimmeli*, *S. larinki*, and *S. tridactyla*, but they are higher in dominant frequency than *S. gimmeli* and *S. larinki* (6675 ± 64 Hz vs 4823 ± 302 Hz in *S. gimmeli* and 2914 ± 124 Hz in *S. larinki*), and lower in dominant frequency with a longer inter-call interval than *S. tridactyla* (dominant frequency 6675 ± 64 Hz vs 7244 ± 200 Hz; inter-call interval 1905.1 ± 398.3 ms vs 1012 ± 39 ms).

Holotype description. Specimen in a moderately good state of preservation, the left arm removed as a tissue sample. Body oblong; head wider than long, narrower than body width; snout rounded in dorsal view, squared in lateral view; nostrils directed laterally, not protuberant, equidistant between tip of snout and eye; canthus rostralis indistinct, straight; loreal region flat, vertical; tympanum indistinct, round, about 55% of eye diameter; supratympanic fold absent; tongue long and thin, attached anteriorly, not notched; maxillary teeth present; vomerine teeth absent; choanae small and round, located very far forward. Forelimbs slender; subarticular tubercles single, indistinct; outer/palmar metacarpal tubercle rounded; inner metacarpal tubercle small and indistinct; hand without webbing; first, second, and fourth fingers strongly reduced, third finger basally broadened; relative length of fingers $1 < 4 < 2 < 3$, fourth finger slightly more reduced than second; finger tips not expanded into discs. Hind limbs slender; TIBL 43% of SVL; lateral metatarsalia strongly connected; inner metatarsal tubercle indistinguishable from completely reduced first toe; outer metatarsal tubercle absent; no webbing between toes; first toe absent, second and fifth toes extremely reduced; relative length of toes $2 < 5 < 3 < 4$; fifth toe distinctly shorter than third. Skin on dorsum smooth, without distinct dorsolateral folds. Ventral skin smooth.

After 12 years in 70% ethanol, the dorsum is metallic silver over the whole body, excepting brown colour in the inguinal region and the posterior surface of the thigh (Fig 2). There is a moderately distinct colour border between the dorsal and ventral colouration that runs the length of the flank. The side of the head is dark brown, but this becomes increasingly flecked with cream posteriorly. The ventral and lower lateral colouration is cream flecked with brown, most densely on the anterior abdomen, and most loosely at the posterior abdomen. This flecking becomes akin to ocelli on the ventral surfaces of the legs. Colour pattern in life was the same as in preservative, but dorsal colouration was bronze instead of silver (compare Fig 7a, b with Fig 2). Iris was rust red.

Variation. For measurements, see Table 1. The paratypes strongly resemble the holotype in morphology. Colouration among paratypes is highly variable. ZSM 5942/2005 resembles the holotype but is steelier in colour (Fig 7c). Dark markings in the inguinal region are present in ZSM 5942/2005 and ZSM 265/2018, and both specimens have a more distinctly black flank than the holotype (Fig 7c-f). ZSM 265/2018 additionally has broad burnt umber crossband on its thighs and shanks.

Bioacoustics. Calls recorded from ZSM 265/2018 by S. Hyde Roberts (Fig 4b, Table 2) on 8 November 2018 at 10h16, at an air temperature of 30.4°C. The individual was found in forest habitat (parcel S9 at 24.7606°S, 47.1732°E, 28 m a.s.l.), ca. 3 m from a lentic stream, with an estimated canopy height of 11 m and canopy cover of ~70% after a night of heavy rain. Call details (n = 51 in all cases except inter-call intervals, where n = 30): Calls consisted of a single note and were emitted at regular intervals without defined call series. Calls were not or only very slightly frequency modulated. For detailed call parameters, see Table 2.

Osteology (Fig 8). Based on ZSM 5942/2005 (not figured) and ZSM 5943/2005 (figured).

Cranium (Fig 8c-f). Shape and proportions. Skull narrow, longer than wide, widest at the level of the dorsal end of the squamosal and the anterior edge of the otic capsule. Braincase proportionally broad, with a short rostrum.

Neurocranium. Ossification varies: highly ossified in ZSM 5942/2005 with ossified otic capsules, less ossified in ZSM 5943/2005, without otic capsule ossification. Only the anterior cone of the sphenethmoid is ossified and contacts the frontoparietal dorsally but is not in contact with any other bones. Prootic in dorsal contact with lateral flange of frontoparietal, ventral contact with parasphenoid alae, not approaching contralateral ventrally. Septomaxilla minuscule, very tightly curled, with a long and thin posterior ramus. Columella (stapes) well ossified, pars media plectra (stylus) long and nearly straight, posteriorly and dorsally oriented toward the elongated pars interna plectra (baseplate). Nasal narrow and cultriform, laterally displaced, curved downward laterally, the acuminate maxillary process not closely approaching maxillary pars facialis, broadly separated from contralateral. Frontoparietal with rounded anterior edge, laterally rather straight-

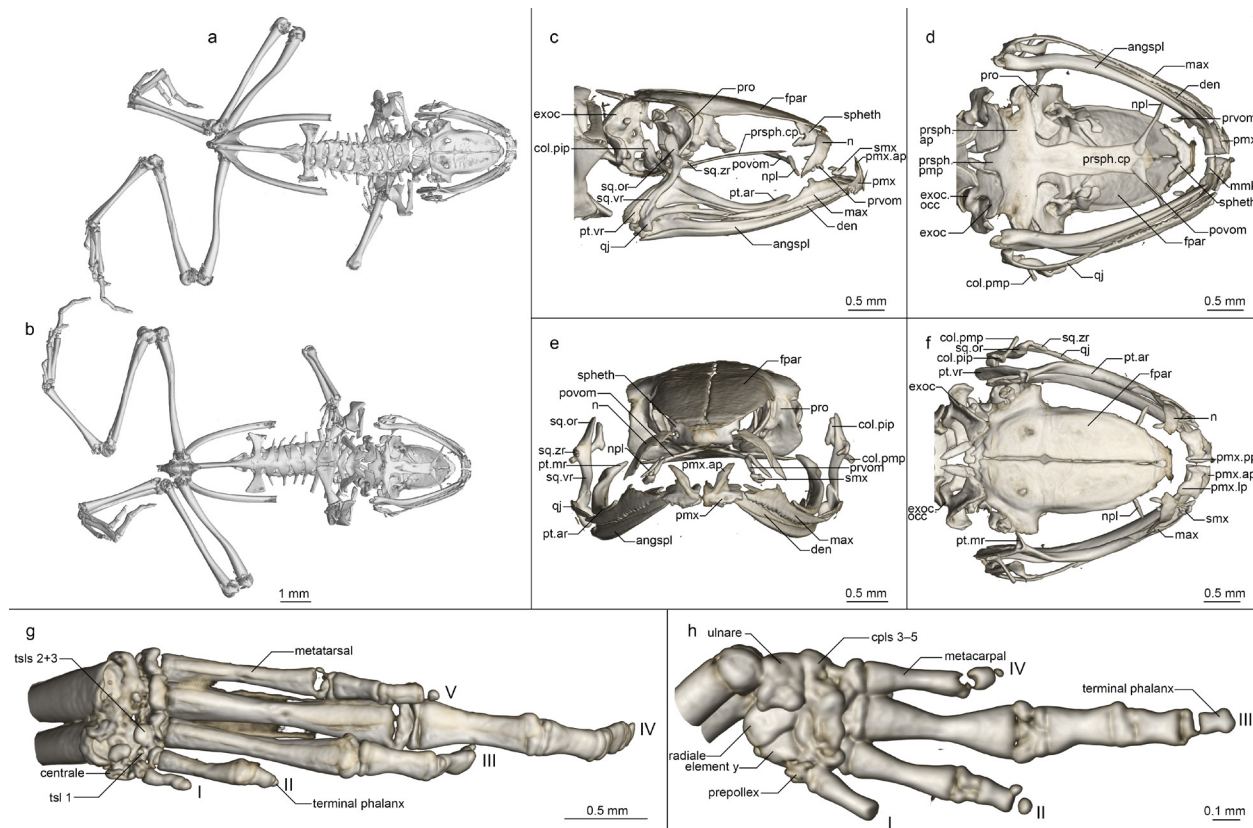


Fig 8. Osteology of *Mini scule* gen. et sp. nov. holotype (ZSM 5943/2005).

(a, b) Whole skeleton in (a) dorsal and (b) ventral view. (c-f) Skull in (c) lateral, (d) ventral, (e) anterior, and (f) dorsal view. (g) Foot in ventral view. (h) Hand in ventral view. For abbreviations, see Fig 6.

Results

edged, with short lateral flange covering prootic, posteriorly strongly (ZSM 5942/2005) or weakly (ZSM 5943/2005) connected to exoccipital, anteroventrally contacting sphenethmoid, lacking any dorsal process, separated from contralateral by a narrow gap, with a clear, rhomboid facet at the level of the prootics, which may represent a pineal foramen.

Parasphenoid with narrow, rather straight-edged cultriform process and slightly broader posterior-curved alae, considerably shorter than frontoparietals, in contact with exoccipitals postero-dorsally, prootics dorsally along the edges of the alae, anteroventrally in contact with postchoanal vomer and not in contact with neopalatine; posteromedial process not participating in foramen magnum. Vomer divided into pre- and postchoanal portions; prechoanal portion narrow, simple, curved, with a suggestion of a lateral ramus; postchoanal portion spatulate and edentate, narrowly separated from its contralateral on the midline, in dorsal contact with the parasphenoid proximally and the neopalatine distally, lacking an anterior projection. Neopalatine simple, straight, weakly distinguishable from lateral postchoanal portion of vomer, laterally broadly separated from the maxilla, not exceeding the lateral-most point of the postchoanal vomer.

Maxillary arcade gracile, maxilla and premaxilla bearing numerous small teeth, anterior extension of maxilla exceeding lateral extent of premaxilla but not in contact with it. Premaxilla with a narrow acuminate dorsal alary process rising laterally, pars palatina shallowly divided into a narrow palatine process and broad lateral process. Maxilla with a low triangular pars facialis and a narrow pars palatina, its posterior tip acuminate and barely contacting the quadratojugal, the lingual surface of the pars palatina in contact with the anterior ramus of the pterygoid. Pterygoid with an exceptionally short medial ramus, long anterior ramus, and broad posterior ramus, posteriorly calcified to the quadratojugal complex. Quadratojugal weakly bowed laterally, broadly connected to the ventral ramus of the squamosal, bearing a small posteroventral knob, weakly anteriorly connected to the maxilla; the articulation of the mandible is apparently fortified by the mineralisation of the posterior ramus of the pterygoid+squamosal+quadratojugal posteroventral knob. Squamosal with a slender, sigmoid ventral ramus, broadened otic ramus, and short, thick zygomatic ramus, the otic ramus oriented dorsally and posteriorly, the zygomatic ramus horizontal.

Mandible slim and edentate, largely unremarkable, with a moderately raised coronoid process on the angulosplenial. Mentomeckelians separated from the dentary, with slightly bulbous, almost hooked ventrolateral projections sometimes present (present in ZSM 5942/2005, absent in ZSM 5943/2005).

Posteromedial processes of hyoid proximally rounded with a broad medial crista.

Postcranial skeleton (Fig 8a, b, g, h). Eight procoelous presacrals, with some differentiation errors in ZSM 5942/2005 leading to a transverse process forming on the head of the urostyle; all presacrals much broader than long, lacking neural spines, with round posterior articular processes, presacral I with a more or less complete neural arch, presacrals II–IV with thicker and longer transverse processes than V–VIII. Sacrum with expanded diapophyses, the leading and trailing edges roughly equally angled, the articulation type IIB *sensu* Emerson [42]. Urostyle bicondylar, long, not broadening posteriorly, with a somewhat flared head in ZSM 5943/2005 and with a low dorsal ridge.

Pectoral girdle without ossified prezonal or postzonal elements, with ossified clavicles, badly fractured in ZSM 5942/2005. Clavicle thin and weakly curved, with a simple lateral junction, shorter than the coracoid. Coracoid fairly narrow, not flared laterally, strongly flared medially with a curved medial articular surface with the contralateral. Scapula slender, with a thin pars acromialis, the cleithral border straight. Cleithrum ossified for two thirds the width of the scapular border, thickened anteriorly. Suprascapula unossified.

Arms and legs described only from ZSM 5943/2005, as the limbs of ZSM 5942/2005 were removed for DNA sequencing. Humerus with a well-developed crista ventralis and no medial or

lateral cristae. Radioulna slender with a distinct sulcus intermedius. Carpals poorly ossified, composed of radiale, ulnare, element Y, and large post-axial element formed by carpals 3–5. Carpal 2 has either been lost or fused to the latter element. Finger phalangeal formula is reduced (0-2-3-2), and the terminal phalanges of the second and fourth fingers are small, round elements. Prepollex absent.

Pubis unossified in ZSM 5943/2005 and fully ossified in ZSM 5942/2005; iliac shafts passing ventral to and beyond sacrum, oblong in cross-section, with a weak dorsal crest and without a dorsal prominence and with a shallow oblique groove. Femur weakly sigmoid, lacking a posterior crest. Tibiofibula equal to femur in length, with a sulcus intermedius. Tibiale and fibulare fused proximally and distally. T1 and T2+3 tarsals present, T1 considerably smaller than T2+3. Centrale present, slightly smaller than T2+3. Prehallux diminutive. Phalangeal formula reduced (1-2-3-4-3). Terminal phalanges of toes 3 and 4 with knobs, those of other toes small, round elements.

Distribution, natural history, and conservation status. This species is known only from Sainte Luce, southeast Madagascar (Fig 6). Records of ‘*Stumpffia tridactyla*’ from Mandena [47], and Vohimena mountains and the southern Anosy mountain chain [48], and of ‘*Stumpffia* sp. aff. *tetradactyla* “Southeast”’ from Tsitongambarika [49] may refer to this species but require verification. A specimen from Nahampoana (ZFMK 53775) resembles this species, but due to the lack of genetic data, we cannot confirm its identity. Calls of *Stumpffia*-like frogs from Nahampoana were described in Glaw and Vences [50], but these were lower in dominant frequency (ca. 5 kHz), and longer in call duration (ca. 250 ms) than those recorded in Sainte Luce that are here assigned to *M. scule* sp. nov. Two separate ‘*Stumpffia*’ calls from Nahampoana were included in Vences et al. [51], one as Track 51, ‘*Stumpffia* sp. (Nahampoana)’, and a second as Cut 2 of Track 37, ‘*Stumpffia tetradactyla*’.

This species appears restricted to areas of deep leaf litter concomitant with semi-permanent water bodies such as shallow and slow-moving forest streams. Individuals call from concealed positions on adjacent stream banks during the day. Sainte Luce consists of 17 forest fragments (numbered S1–S17), covering approximately 1600 Ha of littoral forest. At present we assume that this species is microendemic to these forest fragments, and we have directly observed it in fragments S7, S8, and S9, but it appears to be absent from S1 and S2. It may also occur in other parcels of lowland forest nearby. Based on its current estimated Extent of Occurrence (=Area of Occupancy) of < 10 km² in forest that is threatened and declining in quality despite protection status, we recommend this species be listed as Critically Endangered according to the IUCN Red List Criterion CR B1ab(iii) [44]. So far, no other described amphibian species are known to be restricted to Sainte Luce.

Etymology. We use the specific epithet ‘scule’ as an arbitrary combination of letters, in order to form a pun on ‘minuscule’ from the name in apposition, in reference to the fact that it is among the smallest known frogs from Madagascar and in the world. It is to be regarded as an invariable noun.

Miniature sp. nov.

urn:lsid:zoobank.org:act:0C1C4CE2-419A-4030-86D1-B1B89793697D

(Figs 1-3, 9, Table 1)

Remark. This species was previously listed as *Stumpffia* sp. Ca53 MV2017(MF867231) by Tu et al. [20], though with incorrect accession number (correct number is MF768231).

Results

Holotype (Figs 2, 9). ZSM 86/2004 (FGZC 0151, GenBank accession numbers MF768231 and MK459307 for 5' and 3' fragments of the *16S rRNA* gene, respectively, and MF768147 for *cox1* gene), a presumed adult specimen collected in Andohahela National Park between Isaka and Eminiminy above 'Camp 1' (ca. 24.75°S, 46.85°E, ca. 350 m) between 29 and 31 January 2004 by F. Glaw, M. Puente, M. Teschke (née Thomas), and R.D. Randriaina.

Diagnosis. A highly miniaturised frog assigned to *Mini* gen. nov. on the basis of its small size, curved clavicles, laterally displaced and reduced nasals, and fusion or loss of carpal 2. This assignment is supported by its genetic affinities (Fig 1; [20]). It is separated by uncorrected p-distances of 10.0–10.6% in the analysed 3' fragment of the *16S rRNA* gene from other members of the genus *Mini* gen. nov., and 10.8–13.7% from all members of the genus *Plethodontohyla*.

Mini ature sp. nov. is characterised by the unique combination of the following characters (n = 1 specimen): (1) SVL 14.9 mm; (2) ED/HL 0.38; (3) HW/SVL 37.2; (4) FARL/SVL 0.32; (5) TIBL/SVL 0.34; (6) HIL/SVL 1.18; (7) finger 1 strongly reduced, 2 and 4 reduced; (8) toe 1 absent, toes 2 and 5 quite reduced; (9) maxillary and premaxillary teeth present; (10) vomerine teeth absent; (11) lateral colour border absent; (12) black inguinal spots present; (13) postchoanal vomer present, spatulate, medially fused to parasphenoid; (14) nasal cultriform and laterally displaced; (15) quadratojugal-maxilla contact strong and broad; (16) zygomatic ramus of squamosal long, thin, curved, and horizontal; (17) clavicles present, curving with simple lateral articulations, medially not bulbous; (18) prepollex thin and cultriform; (19) carpal 2 absent or fused to post-axial carpal 3–5 element; (20) finger phalangeal formula 1-2-3-3; (21) toe phalangeal formula 1-2-3-4-3; (22–26) calls unknown.

Within the genus *Mini* gen. nov., the new species can be distinguished by its distinctly larger body size (14.9 mm vs 8.2–11.3 mm), shorter relative hindlimb length (HIL/SVL 1.18 vs 1.41–1.72) and phalangeal formula of fingers (1-2-3-3 vs 1-2-3-2 in *M. mum* sp. nov. and 0-2-3-2 in *M. scule* sp. nov.). Additionally, it can be distinguished from *M. mum* sp. nov. by the presence of maxillary and premaxillary teeth (vs absence), and less distinct lateral colour border, and *M. scule* sp. nov. by proportionally smaller nasals and braincase, broader quadratojugal-maxillary contact, and vertical dorsal process of premaxilla (vs anterior).

This species is particularly similar to some highly miniaturised *Stumpffia* species, but it can be distinguished from all *Stumpffia* based on the condition of the carpals and the presence of curved clavicles, and most *Stumpffia* by the presence of maxillary and premaxillary teeth.

Holotype description. Specimen in a moderately good state of preservation, the left arm removed as a tissue sample, the whole body somewhat dorsoventrally flattened in preservative. Body oblong; head wider than long, narrower than body width; snout slightly pointed in dorsal view, pointed in lateral view; nostrils directed laterally, not protuberant, equidistant between tip of snout and eye; canthus rostralis rounded, indistinct, slightly concave; loreal region flat, vertical; tympanum indistinct, round, ~48% of eye diameter; supratympanic fold absent; tongue long, broadening posteriorly, attached anteriorly, not notched; maxillary teeth present; vomerine teeth present; choanae small and round. Forelimb slender; subarticular tubercles single, elongated; outer/palmar metacarpal tubercle small and round; inner metacarpal tubercle slightly smaller than outer/palmar; hand without webbing; first finger strongly reduced, second and fourth fingers reduced, third finger basally broadened; relative lengths of fingers 1<2=4<3, fourth and second finger equal in length; finger tips not expanded into discs. Hindlimbs stocky; TIBL 34% of SVL; lateral metatarsalia strongly connected; inner metatarsal tubercle indistinguishable from first toe; outer metatarsal tubercle absent; no webbing between toes, second and fifth toes reduced; relative lengths of toes 2<5<3<4, fifth toe distinctly shorter than third; toe tips slightly pointed distally.

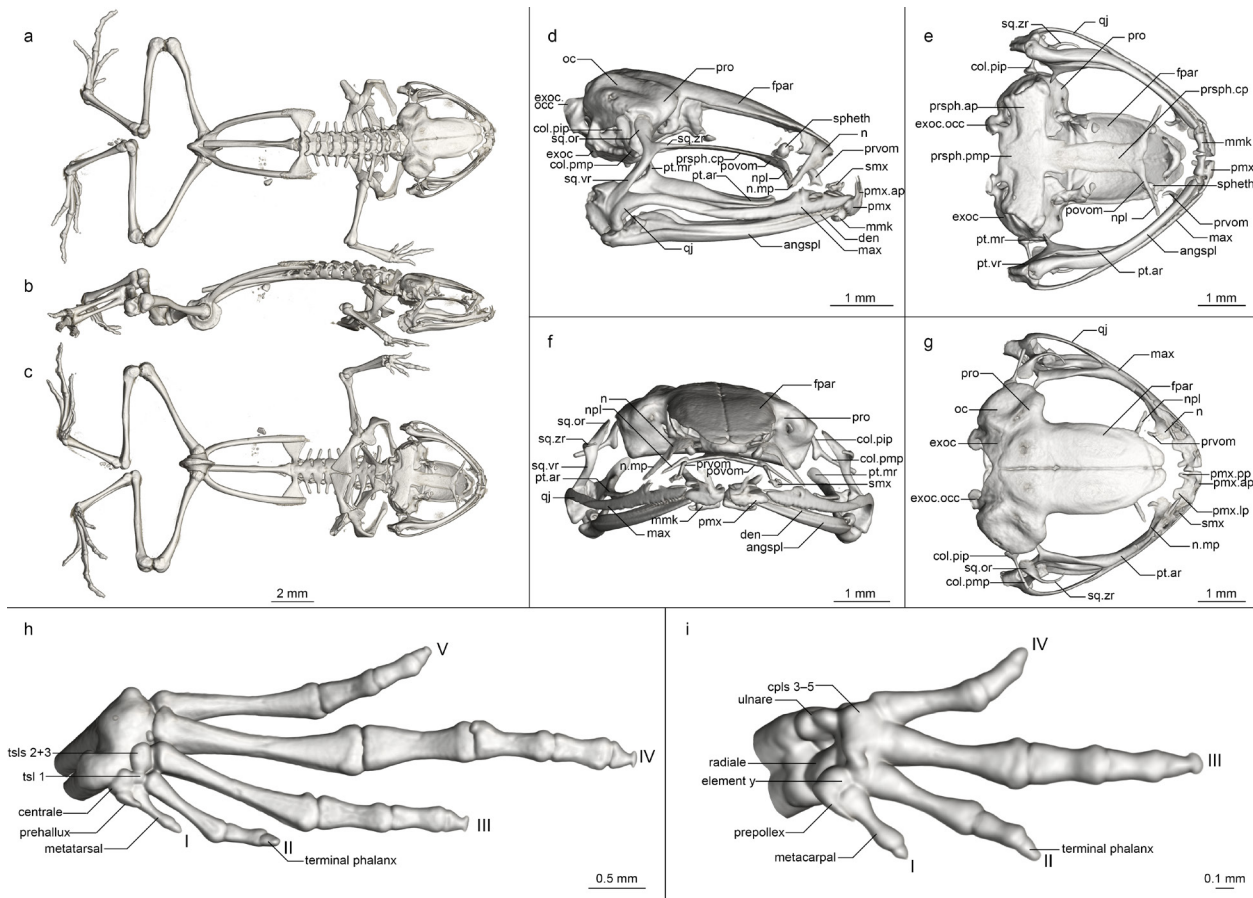


Fig 9. Osteology of *Miniature* gen. et sp. nov. holotype (ZSM 86/2004).

(a-c) Whole skeleton in (a) dorsal, (b) lateral, and (c) ventral view. (d-g) Skull in (d) lateral, (e) ventral, (f) anterior, and (g) dorsal view. (h) Foot in ventral view. (i) Hand in ventral view. For abbreviations, see Fig 6.

Skin on dorsum smooth without a distinct dorsolateral fold, but with a distinct colour border, see below. Ventral skin smooth.

After 14 years in 70% ethanol, the dorsum is light brown, paler—almost beige—laterally, and slightly translucent, with a thin beige vertebral stripe and a darkened area on the posterior head. The skin above the eyes is translucent and dark in colour through the presence of the eyes beneath. The dorsal forelimb is beige flecked with brown, the hand is lighter medially, and the fingers have faint cream annuli. The dorsal hindlimb is beige in base colour with several brown crossbands on the thigh and shank that line up when the leg is folded together. A trapezoid of brown is present around the vent. The foot is dorsally as the forelimb with a light annulus before each distal phalanx. A distinct colour border that is not straight is present laterally, running along the canthus rostralis from the nostril through the eye, through the supratympanic region along the torso to the inguinal region. Small oblong dark brown spots are present in the inguinal region. The side of the head is dark brown. Ventral to this colour border the frog is mocha speckled with beige, lightening ventrally to beige with loose cream speckles. The ventral skin is translucent, and some of the organs can be seen through it. The chin is not differently coloured than the rest of the ventral body. This pattern continues onto the ventral limbs. No data on life colouration are available.

Variation. This species is currently known from a single specimen only.

Results

Osteology (Fig 9). Based on ZSM 86/2004 (figured).

Cranium (Fig 9d-g). Shape and proportions. Skull almost equilateral, roughly as wide as long, widest at quadratojugal-squamosal junction, lateral to the otic region. Braincase moderately broad, rostrum not shortened.

Neurocranium. Well ossified, including the otic capsules. The anterior cone of the sphenethmoid is ossified and contacts the frontoparietal dorsally but is not in contact with any other bones; small isolated lateral mineralisations of this bone are also present anterodorsal to the anterior tip of the cultriform process of the parasphenoid. Prootic in dorsal contact with lateral flange of frontoparietal, ventral contact with parasphenoid alae, not approaching contralateral ventrally. Septomaxilla minuscule, relatively poorly mineralised, and therefore not further discussed here. Columella (stapes) well ossified, pars media plectra (stylus) long and nearly straight, weakly posteriorly and dorsally oriented toward the reniform, dorsally elongated pars interna plectra (baseplate). Nasal narrow and cultriform, laterally displaced, curved downward laterally, acuminate maxillary process not closely approaching maxillary pars facialis, broadly separated from contralateral. Frontoparietal with rounded anterior edge, laterally bulging, with short lateral flange covering prootic, posteriorly strongly connected to exoccipital, anteroventrally contacting sphenethmoid, lacking any dorsal process.

Parasphenoid with narrow, rather straight-edged cultriform process and broad perpendicular alae, considerably shorter than frontoparietals, in contact with exoccipitals posterodorsally, prootics dorsally along the edges of the alae, anteroventrally in contact with postchoanal vomer and not in contact with neopalatine; posteromedial process excluded from participating in foramen magnum by exoccipitals. Vomer divided into pre- and postchoanal portions; prechoanal portion narrow, arcuate, triradiate, with a short lateral and anterior ramus and long, curving posterior ramus; postchoanal portion spatulate and edentate, contacting its contralateral on the midline, in dorsal contact with the parasphenoid proximally and the neopalatine distally, lacking an anterior projection. Neopalatine simple, straight, almost indistinguishable from lateral postchoanal portion of vomer, laterally broadly separated from the maxilla, not exceeding the lateral-most point of the postchoanal vomer.

Maxillary arcade fairly slight, maxilla and premaxilla bearing numerous diminutive teeth, anterior extension of maxilla exceeding lateral extent of premaxilla but not in contact with it. Premaxilla with a broad acuminate dorsal alary process rising laterally, pars palatina shallowly divided into a narrow palatine process and broad lateral process. Maxilla with a low triangular pars facialis and a narrow pars palatina, its posterior tip acuminate and broadly overlapping the quadratojugal, the lingual surface of the pars palatina running parallel to but not touching the anterior ramus of the pterygoid.

Pterygoid with a short medial ramus, long anterior ramus, and broad posterior ramus and posterolaterally calcified to the quadratojugal complex. Quadratojugal weakly bowed laterally, broadly connected to the ventral ramus of the squamosal, bearing a small posteroventral knob; the articulation of the mandible is apparently fortified by the mineralisation of the posterior ramus of the pterygoid+squamosal+quadratojugal posteroventral knob. Squamosal with a slender ventral ramus, broadened otic ramus, and long, thin zygomatic ramus, the otic ramus oriented slightly dorsally and posteriorly, the zygomatic ramus horizontal and strongly curved.

Mandible slim and edentate, largely unremarkable, with a low coronoid process on the angulosplenial. Mentomeckelians separated from the dentary, with slightly bulbous, almost hooked ventrolateral projections.

Posteromedial processes of hyoid proximally rounded with a broad medial crista.

Postcranial skeleton (Fig 9a-c, h, i). Eight procoelous unfused presacrals, much broader than long, lacking neural spines, with round posterior articular processes, presacral I with a complete

neural arch, presacrals II–IV with thicker and longer transverse processes than V–VIII. Sacrum with expanded diapophyses, the leading and trailing edges roughly equally angled, the articulation type IIB *sensu* Emerson [42]. Urostyle bicondylar, long, not broadening posteriorly, without lateral processes and with a low dorsal ridge.

Pectoral girdle without ossified prezonal or postzonal elements, with ossified clavicles. Clavicle thin and curved, with a simple lateral junction, shorter than the coracoid. Coracoid fairly narrow, not flared laterally, strongly flared medially with a large medial articular surface with the contralateral. Scapula slender, with a thin pars acromialis, the cleithral border concave. Cleithrum ossified for two thirds the width of the scapular border, thickened anteriorly. Suprascapula unossified.

Humerus with a well-developed crista ventralis and no medial or lateral cristae. Radioulna slender with a distinct sulcus intermedius. Carpals poorly ossified, composed of radiale, ulnare, prepollical element, element Y, and large post-axial element formed by carpals 3–5. Carpal 2 has either been lost or fused to the latter element. Finger phalangeal formula is reduced (1-2-3-3), and the terminal phalanx of the first finger is a small, round element. Small distal knobs on terminal phalanx of finger 3. Prepollex thin and cultriform and extending only to the base of the first metacarpal.

Pubis calcified, iliac shafts passing ventral to and beyond sacrum, nearly cylindrical, without a dorsal crest and with a weak dorsal prominence and shallow oblique groove. Femur weakly sigmoid, almost lacking a posterior crest. Tibiofibula shorter than femur, with a sulcus intermedius. Tibiale and fibulare fused proximally and distally. T1 and T2+3 tarsals present, T1 considerably smaller than T2+3, plus a small additional ossification (possibly a sesamoid) between the bases of metatarsals 2 and 3. Centrale present, roughly the size of T2+3. Prehallux subtriangular. Phalangeal formula reduced (1-2-3-4-3). Terminal phalanges of toes 2–4 with almost T-shaped knobs.

Distribution, natural history, and conservation status. This species is known only from a single specimen from Andohahela National Park in southeast Madagascar (Fig 6). The species is larger than the other members of the genus *Mini*, and its ecology may differ accordingly. Advertisement calls were not recorded. At present it is not possible to estimate its distribution or population status, and we prefer to suggest this species be considered Data Deficient until more information is available.

Etymology. We use the specific epithet ‘ature’ as an arbitrary combination of letters, in order to form a pun on ‘miniature’ from the name in apposition, in reference to the small size of this species. It is to be regarded as an invariable noun.

Rhombophryne proportionalis sp. nov.

urn:lsid:zoobank.org:act:1A79607B-E9D4-4214-BF47-9BC0B4320E5F

(Figs 1, 2, 3, 5, 10, 11, Tables 1, 2)

Remark. This species was previously referred to as *Stumpffia* sp. Ca34 [15, 46] and as *Stumpffia* sp. 39 MV-2012 (KC351481) [20].

Holotype. ZSM 1826/2010 (ZCMV 12404, GenBank accession number KC351380 and KU937808 for 5' and 3' fragments of the *16S rRNA* gene, respectively, and KF611640 for the *coxI* gene), an adult male specimen (seen calling, not recorded) collected at Bepia Campsite on



Fig 10. *Rhombophryne proportionalis* sp. nov., holotype ZSM 1826/2010, in life.

(a) dorsolateral, (b) dorsal, and (c) ventral view.

the Tsaratanana massif (Camp 3; 14.1182°S, 48.9782°E, 2294 m a.s.l.), Diana Region, former Antsiranana province, northern Madagascar on 16 June 2010 by M. Vences, D.R. Vieites, R.D. Randrianiaina, S. Rasamison, and E. Rajeriarison.

Paratypes. ZSM 1840/2010 (ZCMV 12405, GenBank accession number KC351481 and MK459317 for 5' and 3' fragments of the *16S rRNA* gene, respectively), adult male specimen with the same collection data as the holotype; and ZSM 636/2014 (DRV 6224), an adult presumed male specimen collected at Andranomadio Campsite in Tsaratanana (Camp 4; 14.0801°S, 48.9854°E, 2503 m a.s.l.) on 16 June 2010 by the same collectors.

Diagnosis. A diminutive frog assigned to the genus *Rhombophryne* on the basis of absence of clavicles, presence of vomerine, maxillary, and premaxillary teeth, short and broad skull, and ge-

netic affinities. It is separated by uncorrected p-distances of 7.0–12.9% in the analysed 3' fragment of the *16S rRNA* gene from other members of the genus *Rhombophryne*.

Rhombophryne proportionalis sp. nov. is characterised by the unique combination of the following characters (n = 3 male specimens): (1) male SVL 11.0–12.3 mm; (2) ED/HL 0.40–0.48; (3) HW/SVL 0.33–0.37; (4) FARL/SVL 0.33–0.35; (5) TIBL/SVL 0.34–0.36; (6) HIL/SVL 0.21–1.32; (7) finger 1 reduced, 2 and 4 short; (8) toe 1 highly reduced, 2 somewhat reduced; (9) maxillary and premaxillary teeth present; (10) vomerine teeth present; (11) lateral colour border absent; (12) black inguinal spots sometimes present; (13) postchoanal vomer present, spatulate, medially fused to parasphenoid; (14) nasal broad and not laterally displaced; (15) quadratojugal-maxilla contact strong and broad; (16) zygomatic ramus of squamosal long, thick, curved, and horizontal; (17) clavicles absent; (18) prepollex short and triangular; (19) carpal 2 present; (20) finger phalangeal formula 2-2-3-3; (21) toe phalangeal formula 2-2-3-4-3; (22) unpulsed calls emitted in series of 9–17 calls at irregular intervals; (23) non-frequency modulated calls; (24) call dominant frequency 5460 ± 117 Hz (n = 79); (25) call duration 45.4 ± 8.2 ms (n = 79); (26) inter-call interval 63.0 ± 9.0 ms (n = 73).

Among extremely miniaturized cophyline, this species is unique in possessing vomerine teeth. It can be distinguished from almost all other miniaturised species in lacking clavicles (also absent in *S. contumelia*, *S. obscoena*, *S. davidattenboroughi*, *S. makira*, *S. achillei*, and *S. analanjirofo*, and some specimens of *S. tridactyla*, unpublished data). It is also characterised by a dark colouration of the lateral surface of the head with a distinct colour border, and less reduced fingers and toes. Confusion with juvenile *Rhombophryne* species is still possible, but these have much larger teeth proportional to their skull size, and most lack the distinct lateral head colouration and possess clavicles. The call is unique among the frogs of Madagascar and is instantly distinctive in being emitted as a rapid, high-pitched series of tonal notes.

Holotype description. Specimen in a good state of preservation, part of the right thigh removed as a tissue sample. Body somewhat rhomboid; head wider than long, narrower than body; snout rounded in dorsal view, squared in lateral view; nostrils directed laterally, not protuberant, closer to eye than to tip of snout; canthus rostralis rounded, concave; loreal region flat, vertical; tympanum indistinct, round, about 57% of eye diameter; supratympanic fold distinct, weakly raised, curving slightly from posterior corner of eye over tympanum toward axilla; tongue very broad, disc-like, posteriorly free, unlobed; maxillary teeth present; vomerine teeth present in two tiny patches either side of the midline; choanae rounded. Forelimbs slender; subarticular tubercles faint, single; outer metacarpal tubercle faint, paired; inner metacarpal tubercle distinct, elongated; hand without webbing; first finger reduced, second and fourth short; relative length of fingers $1 < 2 = 4 < 3$; finger tips not expanded. Hind limbs robust; TIBL 34% of SVL; lateral metatarsalia strongly connected; inner metatarsal tubercle thin and indistinct; outer metatarsal tubercle small and indistinct; no webbing between toes; first toe highly reduced, second toe short; relative length of toes $1 < 2 < 5 < 3 < 4$; fifth toe distinctly shorter than third. Skin on dorsum smooth in preservative, without distinct dorsolateral folds. In life, the dorsal skin was smooth was scattered tubercles, and distinct ridges above the scapular region (Fig 10). Ventral skin smooth in preservative, granular in life.

After eight years in 70% ethanol, the dorsum is chocolate brown in colour, darker over the head, with a faint dark brown line running from the inguinal region anteriorly toward the eye. The dorsal leg has a dark brown crossband on the shank. The lateral head has a distinct colour border to the dorsum, being a much darker brown, its border defined by the supratympanic fold. The flank has an indistinct colour border to the venter. The venter is brown with cream flecks, slightly darker and less flecked on the chin. The ventral legs and arms are as the ventral abdomen in colour. The bottom of the foot is dark brown along the medial half. Colour in life as in preservative but more vibrant.

Variation. For measurements, see Table 1. The paratypes are in general very similar to the holotype in morphology. ZSM 636/2014 is slightly smaller than the other specimens, and has a slightly shorter, more rounded head. Its supratympanic fold is also less curved than those of the other specimens, being rather more straight from the eye to above the arm. ZSM 1840/2010 has a more massive body than the others. The colouration of the specimens is relatively consistent, with the whole venter of ZSM 1840/2010 being darker than those of the other two specimens. The dorsolateral lines of the holotype are present in ZSM 1840/2010, but not in ZSM 636/2014, instead being broken in that specimen into spots above the suprascapular region and lines in the inguinal region. The crossbands of the shanks are less distinct in ZSM 1840/2010 than the other two specimens.

Bioacoustics. Specimens called only during the day, from open, shrubby landscape between dense vegetation, on the ground. In some areas, numerous specimens could be heard calling in a chorus. Calls were recorded from an uncollected specimen by M. Vences (Fig 5c, Table 2) at around 11h40 on 15 June 2010 in Camp Bepia (14.11822°S, 048.97822°E, 2294 m a.s.l.), and further calls were heard but not recorded at Camp Andranomadio (14.0801°S, 048.9854°E, 2503 m a.s.l.). A precise description of the call structure is difficult; the vocalization is a series of short tonal units that cannot readily be assigned to units. In past studies, we have described roughly comparable structures differently: in *Stumpffia psologlossa*, where the units have a very short duration, as a single call composed of pulses [14], in *Rhombophryne mangabensis* as a series of notes [52], and in *R. minuta* two closely spaced units were seen as components of a single note [52]. To allow comparison within *Rhombophryne* we here define the tonal units in the vocalizations of the new species as notes, and the entire series as a call, but emphasize that it also would be possible to define each unit as call and the entire series as call series, or to consider each unit as a pulse as their duration falls within the 5–50 ms range for which the pulse category was recommended by Köhler et al. [33].

Calls are rapid series of high-pitched slightly frequency modulated notes. Each call consists of a series of 9–17 notes, and calls are repeated at long and irregular intervals. For detailed call parameters, see Table 2.

Osteology (Fig 11). Based on ZSM 1826/2010 (figured) and ZSM 636/2014 (not figured).

Cranium (Fig 11c–f). Shape and proportions. Skull short and stout, relatively wide, widest at quadratojugal anterior to the otic region. Short rostrum. Braincase broad.

Neurocranium. Well ossified except the weakly calcified otic capsules. Sphenethmoid well ossified, in contact with the frontoparietal in ZSM 1826/2010 but not in ZSM 636/2014, with a calcified anterior medial cone; broadly separated from prootic. Prootic in dorsal contact with lateral flange of frontoparietal, ventral contact with parasphenoid alae, not approaching contralateral. Septomaxilla minuscule, roughly spiralled, similar in shape to those of other *Rhombophryne* (see [25]). Columella (stapes) well ossified, pars media plectra (stylus) steeply sloping upwards proximally to its broad, bilobed, flattened pars interna plectra (baseplate). Nasal broad, curved over the nasal capsule, triangular, acuminate maxillary process not closely approaching maxillary pars facialis, broadly separated from contralateral, situated anterior to frontoparietal. Frontoparietal with slanted anterior edge, laterally bulging, with short lateral flange covering prootic, posteriorly weakly connected to exoccipital, anteroventrally contacting sphenethmoid, lacking any dorsal process (suggestions of such processes in ZSM 1826/2010).

Parasphenoid with broad, squared cultriform process and broad perpendicular alae, shorter than frontoparietals, posteromedial process not participating in foramen magnum, anteroventrally in

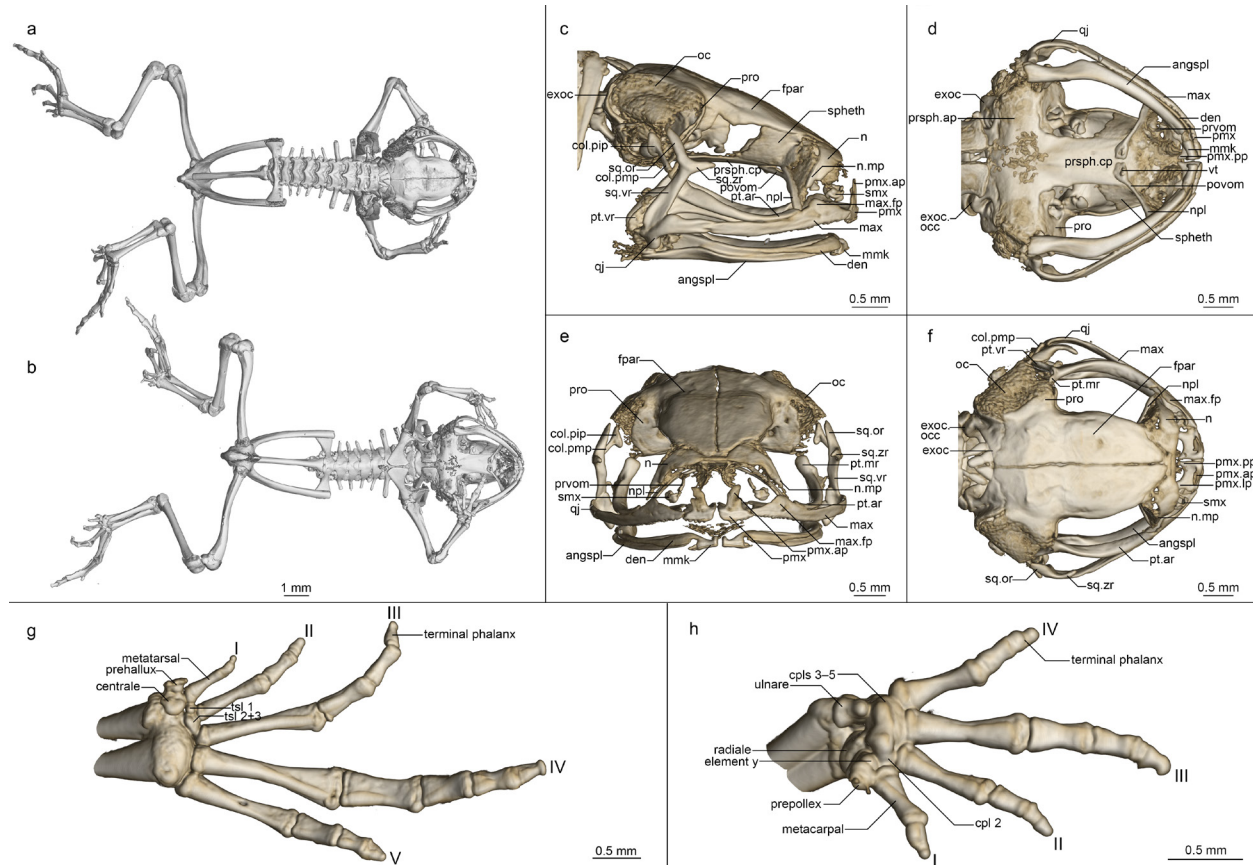


Fig 11. Osteology of *Rhombophryne proportionalis* sp. nov. holotype (ZSM 1826/2010).

(a, b) Whole skeleton in (a) dorsal and (b) ventral view. (c-f) Skull in (c) lateral, (d) ventral, (e) anterior, and (f) dorsal view. (g) Foot in ventral view. (h) Hand in ventral view. For abbreviations, see Fig 6.

contact with postchoanal vomer and not in contact with neopalatine. Vomer divided into pre- and postchoanal portions; prechoanal portion narrow, arcuate, triradiate, with a short lateral and anterior ramus and long posterior ramus; postchoanal portion spatulate bearing a single vomerine tooth or a pair thereof, separated from contralateral by a narrow space, in dorsal contact with the parasphenoid proximally and the neopalatine distally, lacking an anterior projection. Neopalatine laminar, broader than lateral postchoanal portion of vomer, laterally approaching but not contacting the maxilla, exceeding the lateral-most point of the postchoanal vomer to approach the anterior tip of the parasphenoid but not in contact with it, such that the vomer contacts the neopalatine near its midpoint and not at its terminus.

Maxillary arcade quite robust, maxilla and premaxilla bearing numerous diminutive teeth, premaxilla and maxilla in narrow contact anteriorly. Premaxilla with a broad acuminate dorsal alary process rising vertically, pars palatina shallowly divided into a narrow palatine process and broad lateral process. Maxilla with a low triangular pars facialis and a narrow pars palatina, its posterior tip acuminate and broadly overlapping the quadratojugal, the lingual surface of the pars palatina in broad contact with the anterior ramus of the pterygoid.

Pterygoid with a short medial ramus, long anterior ramus with broad contact with the maxilla, leaving a channel for the pterygoid cartilage, posterior ramus broad and posterolaterally calcified to the quadratojugal complex. Quadratojugal bowed laterally, broadly connected to the ventral ramus of the squamosal, and with a broad articular surface with the maxilla, bearing a large posteroventral knob. Squamosal with a broadened ventral ramus and narrow otic and zygomatic rami, the otic ramus long and thin and oriented dorsally, the zygomatic ramus short and thin, oriented anteriorly.

Mandible slim and edentate, largely unremarkable, with a low coronoid process on the angu-

Results

losplenial. Mentomeckelians strongly connected to the dentary, with unusual, flat ventrolateral projections.

Posteromedial processes of hyoid proximally pointed with a broad medial crista.

Postcranial skeleton (Fig 11a, b, g, h). Eight procoelous unfused presacrals, much broader than long, lacking neural spines, with round posterior articular processes, presacral I with a mostly complete neural arch, presacrals II–IV with thicker and longer transverse processes than V–VIII. Sacrum with expanded diapophyses, the leading and trailing edges roughly equally angled, the articulation type IIB *sensu* Emerson [42]. Urostyle bicondylar, long, broadening posteriorly, without lateral processes and with a low dorsal ridge.

Pectoral girdle without ossified prezonal or postzonal elements, lacking ossified clavicles. Coracoid broad, strongly flared with a large medial articular surface with the contralateral. Scapula also robust, with a broad pars acromialis distinct from the pars glenoidalis. Cleithrum ossified for half the width of the scapular border, acuminate, thickened anteriorly. Suprascapula unossified.

Humerus with a well-developed crista ventralis and no medial or lateral cristae. Radioulna broad with a distinct sulcus intermedius. Carpals well ossified in ZSM 1826/2010 and poorly ossified in ZSM 636/2014, composed of radiale, ulnare, prepollical element, element Y, carpal 2, and large post-axial element formed by carpals 3–5. Finger phalangeal formula is standard (2-2-3-3). Small distal knobs on terminal phalanges of the fingers. A very small prepollex is present in ZSM 1826/2010 but is not visible in ZSM 636/2014.

Pubis partly calcified, iliac shafts passing ventral to and beyond sacrum, nearly cylindrical, without a dorsal crest and with a weak dorsal prominence and shallow oblique groove. Femur weakly sigmoid with a low posterior crest. Tibiofibula shorter than femur, with a sulcus intermedius. Tibiale and fibulare weakly fused proximally and distally. T1 and T2+3 tarsals present, T1 considerably smaller than T2+3. Centrale present but not large. Prehallux unossified. Phalangeal formula standard (2-2-3-4-3).

Distribution, natural history, and conservation status. *Rhombophryne proportionalis* sp. nov. is known from two localities (Bepia and Andranomadio) on the Tsaratanana massif in northern Madagascar. Both of these sites fall within the Tsaratanana National Park (formerly a Strict Nature Reserve). It is a terrestrial species that lives among the leaf litter. Two other cophyline frogs, *Platypelis alticola* and *P. tsaratananaensis*, are also known from these locations, and both are currently listed as Endangered, due to their small distribution < 2000 km², presence in a single threat-defined location, and potentially on-going decline in habitat quality. We therefore suggest *R. proportionalis* sp. nov. also to be Endangered, following the same rationale.

Etymology. The species epithet is the Latin adjective *proportionalis* meaning ‘proportional’, in reference to the comparatively proportional dwarfism that this species has apparently undergone (see discussion). It is a feminine adjective in the nominative singular.

Anodonthyla eximia sp. nov.

urn:lsid:zoobank.org:act:2C419E74-C13D-447D-BDCF-312324515EAE

(Figs 1, 2, 3, 5, 12, 13, Tables 1, 2)

Remark. This species was previously listed as *A.* sp. Ranomafana (Maharira) [24], *A.* sp. Ca04 Ranomafana (ZCMV204) [15] and *Anodonthyla* sp. 4 Ranomafana [20].



Fig 12. *Anodonthyla eximia* sp. nov. holotype (ZMA 20246) in life.

(a) dorsolateral, (b) ventral, and (c) posterodorsal view.

Holotype. ZMA 20246 (ZCMV 204, GenBank accession number GU177052 and FJ559111 for the 5' and 3' fragments of the *16S rRNA* gene, respectively, and GU177063 for the *cox1* gene), an adult male specimen (vocal sac inflated when collected) collected from a campsite at the base of Maharira mountain (21.3258°S, 47.4025°E, approx. 1248 m a.s.l.) in Ranomafana National Park, Vatovavy-Fitovinany Region, former Fianarantsoa province, southeastern Madagascar on 25 January 2004 by M. Vences, I. de la Riva, and E. Rajeriarison.

Diagnosis. An extremely miniaturised frog assigned to the genus *Anodonthyla* on the basis of the possession of a large, cultriform prepollex, T-shaped terminal phalanges, absence of postchoanal vomer, and by its genetic affinities. It is separated by uncorrected p-distances of 9.3–17.0% in the analysed 3' fragment of the *16S rRNA* gene from all other members of the genus *Anodonthyla*.

Anodonthyla eximia sp. nov. is characterised by the unique combination of the following characters (n = 1 male specimen): (1) male SVL 11.3 mm; (2) ED/HL 0.45; (3) HW/SVL 0.31; (4) FARL/SVL 0.30; (5) TIBL/SVL 0.39; (6) HIL/SVL 1.34; (7) finger 1 highly reduced, other fingers small; (8) toe 1 absent, toes 2 and 5 quite reduced; (9) maxillary and premaxillary teeth absent;

Results

(10) vomerine teeth absent; (11) lateral colour border absent; (12) black inguinal spots absent; (13) postchoanal vomer absent; (14) nasal subrectangular with an acuminate maxillary process, not displaced; (15) quadratojugal-maxilla contact absent; (16) zygomatic ramus of squamosal short, thin, and anterodorsally oriented; (17) clavicles present, curving with simple lateral articulations, medially bulbous; (18) prepollex cultriform, longer than first metatarsal; (19) carpal 2 present; (20) finger phalangeal formula 1-2-3-3; (21) toe phalangeal formula 2-2-3-4-3; (22) single-note, unpulsed calls, not emitted in series; (23) weakly frequency modulated calls; (24) call dominant frequency 8406 ± 78 Hz (n = 5); (25) call duration 59.6 ± 6.5 ms (n = 5); (26) inter-call interval 3749.0 ± 1149.9 ms (n = 4).

This species is considerably smaller than all other *Anodonthyla* species (11.3 mm vs 15–34 mm), and as such is only possible to confuse with juveniles of its congeners. In addition to its small size, it can be distinguished from all other *Anodonthyla* species by the absence of flared crests on the humerus in adult males. Among similarly sized adult frogs in Madagascar, it can be distinguished by the possession of a large inner metacarpal tubercle with a large, cultriform prepollex (present only in male *Anodonthyla*, much smaller in all other species except *Anilany*, where it is broad and triangular instead of cultriform), and a laterally displaced neopalatine not in contact with the sphenethmoid or vomer (neopalatine either in contact with sphenethmoid or in contact with vomer in all other species; in some species of *Stumpffia*, the neopalatine is lost, unpublished data).

Holotype description. Specimen in a good state of preservation, a piece of the right thigh removed as a tissue sample. Body oblong; head wider than long, narrower than the body width; snout rounded in dorsal and lateral view; nostrils directed laterally, not protuberant, closer to eye than to tip of snout; canthus rostralis rounded, straight; loreal region concave, vertical; tympanum indistinct, round, about 46% of eye diameter; supratympanic fold weak, not raised, straight from posterior corner of eye to axilla; tongue long, thin, attached anteriorly, not notched; maxillary teeth absent, vomerine teeth absent; choanae oblong, very small. Forelimbs relatively broad; subarticular tubercles indistinct, single; outer metacarpal tubercle small, indistinct, single; inner metacarpal tubercle large and distinct, bulging outward strongly, underlain by cultriform prepollex; hand without webbing; all fingers short, first highly reduced and only marginally longer than the prepollex; relative length of fingers 1<2=4<3, fourth finger equal in length to second; tip of third finger marginally expanded, other fingers not expanded into discs. Hind limbs robust; TIBL 39% of SVL; lateral metatarsalia strongly connected; inner metatarsal tubercle rounded, indistinguishable from first toe; outer metatarsal tubercle absent; no webbing between toes; first toe practically absent, second and fifth toes shortened; relative length of toes 2<5<3<4; fifth toe distinctly shorter than third. Skin on dorsum smooth, without distinct dorsolateral folds. Ventral skin smooth.

After 13 years in 70% ethanol, the dorsum is pale brown with a faint darker brown chevron over the scapular region (Fig 2). The dorsal legs have faint dark brown crossbands, especially on the shanks. The dorsal colouration fades over the shanks to cream, which is continuous on the venter. The lateral head is dark brown, with a distinct border to the dorsum and flank formed by the supratympanic fold. The chin is a lighter brown than the dorsum but distinctly not the cream of the abdomen. The ventral legs are translucent cream. Colour in life as in preservative but more vibrant; the venter was slate grey with blue-cream flecks.

Bioacoustics. Calls recorded from an unknown specimen by M. Vences at 08h45, on 26 January 2004 at Maharira in Ranomafana National Park (21.3258°S, 047.4025°E, 1248 m a.s.l.) in the leaf litter of primary rainforest, referred to this species (Fig 4d, Table 2). The holotype and single known specimen of this species was collected during careful searches of the leaf litter from the

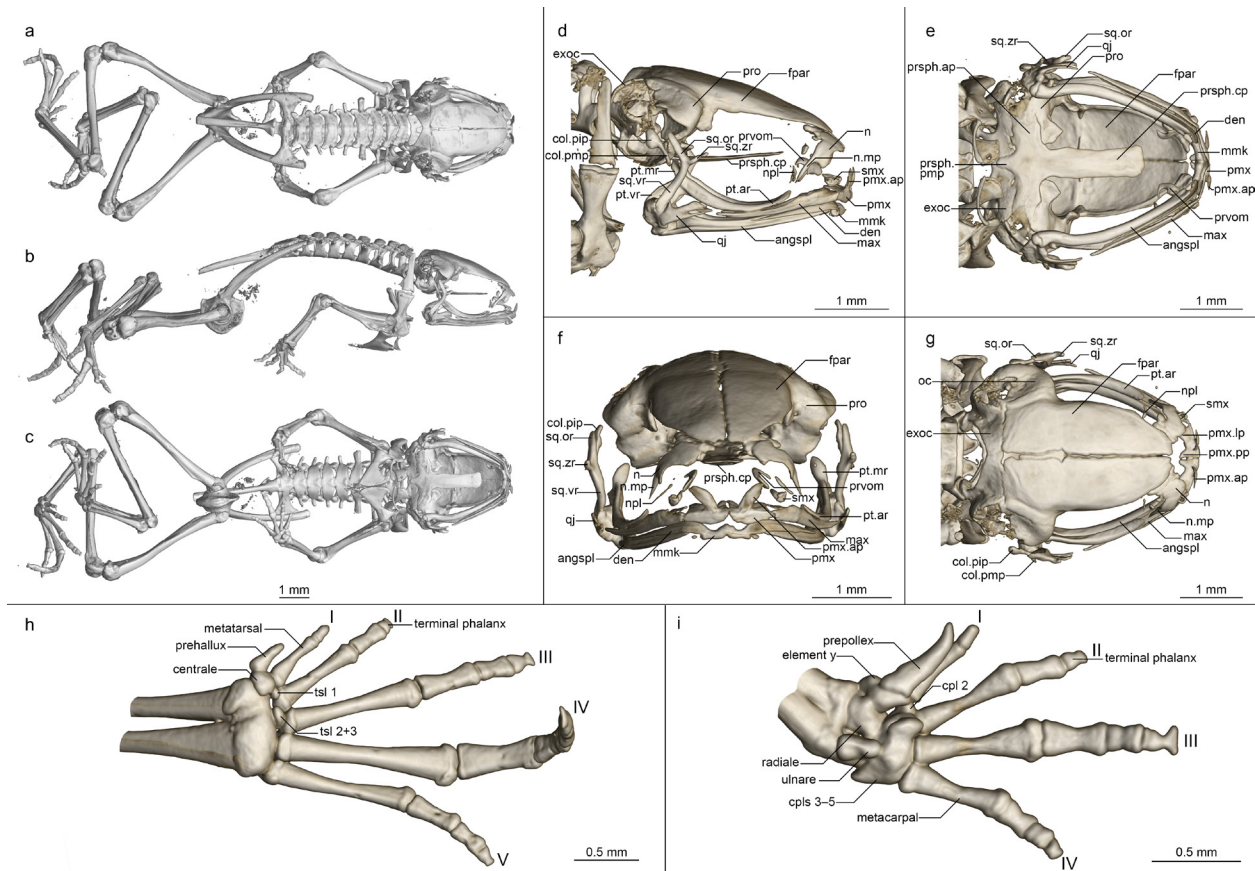


Fig 13. Osteology of *Anodonthyla eximia* sp. nov. holotype (ZMA 20246).

(a-c) Whole skeleton in (a) dorsal, (b) lateral, and (c) ventral view. (d-g) Skull in (d) lateral, (e) ventral, (f) anterior, and (g) dorsal view. (h) Foot in ventral view. (i) Hand in ventral view. For abbreviations, see Fig 6.

exact spot where similar calls were heard, and upon capture, had an apparent partially inflated vocal sac. No other calls assignable to a miniature frog were heard in the area at this time in the morning. Assignment of the calls to this species therefore is the most likely hypothesis but remains tentative. The call bears remarkable resemblance to that of *Stumpffia miery* (Table 2), which is also known from lower elevations in Ranomafana National Park, and detailed future field study will be required to confirm its assignment to *Anodonthyla eximia* sp. nov.

Calls were emitted as part of a large chorus in the early hours of the morning following cyclonic rainfall after the retreat of major flooding of the area. Calls consisted of a single note and were emitted at regular intervals without defined call series. Calls were weakly frequency modulated with an increase in pitch, but recording quality is too poor for detailed analysis. For approximate call parameters, see Table 2.

Osteology (Fig 13). Based on ZMA 20246 (figured).

Cranium (Fig 13d-g). Shape and proportions. Skull short and rounded, longer than wide, widest at the bowing of the quadratojugal roughly in line with the anterior face of the prootic. Braincase proportionally broad, with an extremely short rostrum.

Neurocranium. Moderately ossified, otic capsules partly ossified. Sphenethmoid unossified. Prootic in dorsal contact with lateral flange of frontoparietal, ventral contact with parasphenoid alae, not approaching contralateral. Septomaxilla minuscule, very tightly curled, not further discussed due to low ossification and insufficient resolution. Columella (stapes) well ossified, pars media plectra (stylus) long and slightly curved, posteriorly and dorsally oriented toward the broad-

Results

ened, somewhat posteriorly oriented pars interna plectra (baseplate). Nasal narrow, retaining the shape of larger cophyline: subrectangular with an elongated, acuminate maxillary process that does not closely approach the maxillary pars facialis; displaced laterally, broadly separated from contralateral. Frontoparietal with rounded anterior edge, laterally rather straight-edged, with short lateral flange covering prootic, posteriorly strongly connected to exoccipital, lacking any dorsal process, separated from contralateral by a narrow gap with a small rhomboid facet at the level of the prootics, which may represent a pineal foramen.

Parasphenoid with narrow, rather straight-edged cultriform process and roughly equally broad perpendicular alae, considerably shorter than frontoparietals, in contact with exoccipitals postero-dorsally, prootics dorsally along the edges of the alae, anteroventrally free; posteromedial process long but not participating in foramen magnum. Vomer lacking postchoanal portion (typical of *Antodonthyla*); prechoanal portion strongly curved, bearing a small lateral ramus. Neopalatine simple and very thin, laterally displaced, not contacting any other ossified elements.

Maxillary arcade gracile, maxilla and premaxilla edentate, anterior extension of maxilla not exceeding lateral extent of premaxilla. Premaxilla with a narrow dorsal alary process rising laterally, pars palatina shallowly divided into a narrow palatine process and broad lateral process. Maxilla practically lacking a pars facialis and bearing a narrow pars palatina, its posterior tip acuminate and not contacting the quadratojugal, the lingual surface of the pars palatina contacting the anterior ramus of the pterygoid, which has taken over the articulation. Pterygoid with a short medial ramus, long and strongly curved anterior ramus, and broad posterior ramus, posteriorly calcified to the quadratojugal complex. Quadratojugal bowed laterally, rather short, broadly connected to the ventral ramus of the squamosal, bearing a small posteroventral knob, anteriorly dividing and with decreasing ossification, not connected to the maxilla; the articulation of the mandible is apparently somewhat fortified by the mineralisation of the posterior ramus of the pterygoid+squamosal+quadratojugal posteroventral knob. Squamosal with a slender, rather straight ventral ramus, thin, posterodorsally oriented otic ramus, and short, thin, anterodorsally oriented zygomatic ramus.

Mandible slim and edentate, largely unremarkable, with a weakly raised coronoid process on the angulosplenial. Mentomeckelians separated from the dentary, with small, poorly ossified hooked ventrolateral projections.

Posteromedial processes of hyoid proximally rounded without an obvious medial crista.

Postcranial skeleton (Fig 13a-c, h, i). Eight procoelous presacrals, all much broader than long, lacking neural spines, with round posterior articular processes, presacral I with a complete neural arch, presacrals II–IV with thicker and longer transverse processes than V–VIII. Sacrum with flared diapophyses, the leading and trailing edges roughly equally curved, the articulation type IIB *sensu* Emerson [42]. Urostyle bicondylar, long, broadening gently posteriorly, with a somewhat flared head and a low dorsal ridge.

Pectoral girdle without ossified prezonal or postzonal elements, with ossified clavicles. Clavicle thin and curved, with a simple lateral junction, equal in length to the coracoid, medially bulbous. Coracoid broad, flared laterally and strongly flared medially with a curving medial articular surface with the contralateral. Scapula robust, with a broad pars acromialis, the cleithral border straight. Cleithrum ossified for three-quarters the width of the scapular border, thickened anteriorly. Suprascapula unossified.

Humerus with a well-developed crista ventralis and no medial or lateral cristae. Radioulna slender with a distinct sulcus intermedius. Carpals composed of radiale, ulnare, element Y, prepollex, carpal 2, and a large post-axial element formed by carpals 3–5. Prepollex extremely long and acuminate, longer than first metacarpal. Finger phalangeal formula is reduced (1-2-3-3), and the terminal phalanx of the first finger small and columnar, others bearing T-shaped knobs.

Pubis ossified; iliac shafts passing ventral to and beyond sacrum, oblong in cross-section, with

a weak dorsal crest, a distinct dorsal prominence, and a shallow oblique groove. Femur weakly sigmoid, bearing a distinct posterior crest. Tibiofibula slightly shorter than femur in length, with a sulcus intermedius. Tibiale and fibulare fused proximally and distally. T1 and T2+3 tarsals present, T1 considerably smaller than T2+3. Centrale present, larger than other tarsals. Prehallux elongated, half the length of first metatarsal. Phalangeal formula standard (2-2-3-4-3). Terminal phalanx of toe 1 a small round element, those of toes 2–5 with T-shaped knobs.

Etymology. The species epithet *eximia* is the feminine form of the Latin adjective *eximus* meaning ‘remarkable’ or ‘special’, in reference to the surprisingly small body size and terrestrial habits of this *Anodonthyla* species.

Distribution, natural history, and conservation status. *Anodonthyla eximia* sp. nov. is known only from Maharira in Ranomafana National Park (Fig 6). It is a terrestrial species. Nothing else is known of its natural history. It is likely that this species should be classified as Vulnerable like other species from Maharira (e.g. *Gephyromantis runewsweeki*), but as we know almost nothing of its range and ecology, we instead recommend that it be considered Data Deficient until more data are available.

Discussion

Genus-level taxonomy of the Cophylinae

Mini adds a ninth genus to the Cophylinae for a unique clade of miniaturised frogs that falls sister to the large-bodied *Plethodontohyla* (Fig 1). Although body size is the most obvious character that differentiates these two sister genera, they are also distinguished by a number of osteological features, and can be identified without skeletal analysis by their digital reduction (present in *Mini*, absent in *Plethodontohyla*) and vomerine teeth (absent in *Mini*, present in *Plethodontohyla*). Despite these differences and consistent recovery of the two genera as being reciprocally monophyletic in genetic analyses, the uncorrected p-distances between these genera in the 3' fragment of the 16S rRNA mitochondrial gene analysed here are at first glance surprisingly small at 8.3–13.3% (these distances would be distinctly higher if insertions and deletions would be considered in their calculation). Nevertheless, we consider the differences between these clades sufficiently great and robust that we regard them as constituting separate genera. Aside from their morphological and osteological differentiation, a further argument for their classification in distinct genera comes from the strength of support for their sister-group relationship; while the two clades here seen as genera *Plethodontohyla* and *Mini* have been placed sister to each other in most molecular analyses so far, support values for this grouping often were low, and typically lower than the respective support for each of the two clades. The clade stability criterion [36] is therefore better served considering both clades as separate genera.

The relationship of *Mini* to *Plethodontohyla* is analogous to the relationship of *Stumpffia* to *Rhombophryne*: a genus-level sister clade of miniaturised frogs (although *Stumpffia* also contains several non-miniaturised species), recovered in robust genetic phylogenies as reciprocally monophyletic, and distinguished by several diagnostic characters [14, 15, 23]. Peloso et al. [19] argued for the lumping of *Stumpffia*, *Rhombophryne*, and later also *Anilany* [22] into a single genus, *Rhombophryne*. In response, we showed that the initial argument for lumping was based on misidentified specimens [15], and subsequently incorrectly coded morphology, ignoring various unique diagnostic features of *Anilany*, and the relationships of particularly unstable taxa (most notably *Stumpffia tridactyla*) [23]. We revised the taxonomy of the genus *Stumpffia*, describing 26 new species, and providing a more robust phylogeny that resolved the phylogenetic position of *Stumpffia tridactyla* [14]. Despite this progress, the Amphibian Species of the World database

Results

(ASW) currently continues to use the lumped taxonomy, in contrast to AmphibiaWeb and other researchers that have adopted our proposed taxonomy (e.g. [20, 53]). The newly described *Rhombophryne proportionalis*, which is the only miniaturised *Rhombophryne* so far known, is highly distinct from *Stumpffia*, lacking, for example, the externally obvious digital reduction that is present in all miniaturised species of *Stumpffia*, and differing in body shape and proportions [14]. This demonstrates that even miniaturised *Rhombophryne* species can be distinguished by external morphology from *Stumpffia* species, providing still further support for the recognition of *Rhombophryne*, *Stumpffia*, and *Anilany* as separate genera.

More than one way to shrink a frog

Paedomorphosis constitutes the retention of characteristics typical of earlier developmental stages of an ancestor in later stages of development [54–56]. The vast majority of amphibians achieve reduced body size via paedomorphosis, retaining in particular paedomorphic head morphology (relatively larger eyes, larger relative brain-case size) [5–8, 13, 14, 57–62]. The species we have described here of the genera *Mini* and *Anodonthyla* fit this pattern, but *Rhombophryne proportionalis* demonstrates that this is not the only way that anurans can achieve reduced body size.

Rhombophryne proportionalis would probably have been considered by Alberch et al. [55] and Gould [54] to represent a case of ‘proportional dwarfism’, that is, a reduction in body size without alteration of body proportions, relative to the ancestral shape. Klingenberg [56] considered cases of proportional dwarfism sufficiently rare that he more or less dismissed them and considered it impossible for body size to reduce without resulting in related changes in shape. Yet, while the proportions of *R. proportionalis* do not perfectly match those of larger *Rhombophryne* species, it certainly is nearer to their proportions than any other cophyline frog of comparable size (compare [14], and note its short and rounded snout in Fig 2) and its skull morphology in particular is almost unmodified compared to other *Rhombophryne* species (e.g. compare Fig 11 with *R. serratopapilosa* species group [25]), except in the anterior shift of the jaw joint, which is common in miniaturised frogs [62]. Its proportions differ from those of juvenile *Rhombophryne*, for example in having a proportionally shorter head (HL/SVL 0.20–0.24 vs 0.31 and 0.33 in juvenile *R. ornata* and *R. regalis*, respectively; unpublished data). It is also the smallest of the cophylines to retain vomerine teeth, and these again are not like those of juvenile *Rhombophryne* (which are disproportionately large) but rather more like those of adult, large-bodied species. Thus, *R. proportionalis* is a remarkable case of miniaturisation through proportional dwarfism.

Loss of digits, while a corollary of miniaturisation, is not a form of paedomorphosis [63], but rather a commonly arising morphological homoplasy resulting from miniaturisation through functional constraint of the limb primordium [2, 63, 64]. In our recent revision of the genus *Stumpffia*, we commented on the pattern of digit loss across that genus [14], and noted that it apparently departed from known patterns of digit reduction in reduced frogs [62, 63]. *Mini* has reduced its digits in a manner comparable with *Stumpffia*, and its reduction is further accentuated by the apparent loss of carpal 2. Curiously, although *M. mum* is smaller than almost all *Stumpffia* species, its toes are less reduced than the smallest *Stumpffia*, suggesting that absolute adult body size is not the only factor determining the degree of digital reduction; data on the embryos of extremely miniaturised cophylines are needed to understand if limb bud size may be responsible for this change.

The digits of *Anodonthyla eximia* retain the hallmarks of *Anodonthyla*, most obviously in the long cultriform prepollex that characterises males of that genus, but also in the possession of a T-shaped phalanx on the third finger. Its digital formula is also only weakly reduced. In this context, it is, once again, remarkable that *R. proportionalis* has undergone only minimal digital loss, having reduced the first phalanx of the first toe, and has not undergone any loss of the fingers, which sets it apart from comparatively miniaturised cophylines. More notably still, its relative

finger lengths (see Fig 11) are highly similar to those of larger *Rhombophryne* (e.g. [25]). Both of these cases suggest that miniaturisation is occurring in a contingent, rather than a deterministic fashion in these frogs.

Underestimated diversity of miniaturised frogs

Globally, miniaturised frogs are thought to comprise a unique ecomorph, specialised to hide in small places and occupy a lower position in the trophic ladder than larger species [5]. Part of the reason this ecomorph has only recently been acknowledged [6] is taxonomic underestimation; it was not possible to understand how many lineages have evolved independently to occupy the miniaturised frog niche while so much of the diversity was undescribed. The diversity was also further obscured by morphology-based supraspecific taxonomy influenced by homoplastic characters [2] that suggested fewer instances of miniaturisation than revealed by DNA-based phylogenetics. In light of the recent taxonomic descriptions (e.g. [5, 6, 10, 14, 57, 60, 65-69]) and strongly supported phylogenetic studies of miniaturised frogs however (e.g. [8, 14, 58, 65, 70-74]), it is becoming clear that the diversity of these frogs is astonishingly high, at both the species and supraspecific levels. The emerging picture of the diversity of miniaturised lineages of cophyline microhylids is a perfect example: newly discovered small microhylids from Madagascar were generally assigned ad hoc to *Stumpffia* based on their size, although keys for described species did exist [75, 76]. Genetic differentiation of different undescribed lineages initially assigned to *Stumpffia* flagged them as belonging to separate deep clades, prompting closer inspection that has yielded the new species described here. This transition of understanding drives home the importance of genetics in shedding light on groups with potentially extensive ecology-linked homoplasy, like fossorial squamates (e.g. [77, 78]).

Based on current understanding of the phylogeny of the Cophylineae [15, 20], the five new species of miniaturised frogs described here represent three additional separate cases of extreme miniaturisation of body size. The total evolutionary lability of cophyline body size is thus only just emerging: *Stumpffia* and *Anilany* have also miniaturised, but due to instability of their relationships in available phylogenetic hypotheses with respect to *Rhombophryne*, we cannot currently establish if they reduced in size independently or if they stem from a small or miniaturised common ancestor. *Platypelis karenae* (SVL 16.1–18.3 mm) and *P. tetra* (17.5–19.4 mm among the type series) are also miniaturised species [79], but uncertainty surrounding their taxonomic position means that body size evolution in *Platypelis* is unclear. Finally, and perhaps most remarkably, two of the largest species of microhylids in the world, *Plethodontohyla inguinalis* and *Platypelis grandis*, are also members of this subfamily. To understand the apparently volatile evolution of body size within cophylines, and indeed other aspects of their evolutionary history such as ecology (see below) and digits (see above), detailed analysis will need to be conducted on a robust and densely sampled phylogeny—a project on which we are currently working. Further future expansions should look at patterns across the whole of the Microhylidae, as the Cophylineae are just one of the several subfamilies that exhibit remarkably extensive, interdigitated miniaturisation [8, 11, 13, 65].

Drivers of miniaturisation in frogs

Lehr and Coloma [7] suggested that miniaturisation may enable frogs to exploit new food resources that are not available to larger frogs. Kraus [5] expanded on this hypothesis, suggesting that miniaturisation may evolve as a means to exploit leaf-litter or mossy habitats; doing so may simultaneously open access to prey that is inaccessible to larger species that cannot penetrate these complex habitats, while also providing enhanced shelter from predators. But exploiting this opportunity comes at the cost of a higher surface-area–volume ratio, leading to more rapid desiccation [80], which Kraus [5] considered as an explanation for the distribution of the smallest frogs

exclusively in wet, tropical forests.

Our current data, especially with regard to the new species described here, appears to corroborate these hypotheses. Almost all of Madagascar's miniaturised microhylids are leaf-litter dwellers, except some few *Stumpffia* species from high elevations (e.g. *S. tridactyla*) that are also associated with moss. *Anodonthyla eximia* in particular seems to support the hypothesis of Kraus [5] that miniaturisation is an evolutionary means of exploiting leaf-litter and mossy habitats: In general, *Anodonthyla* are arboreal or scansorial frogs [24, 41]. *Anodonthyla eximia* is not only considerably smaller than any other member of the genus (11.3 mm SVL; the next smallest species is *A. pollicaris* at 16.3–18.3 mm SVL) but is also the only apparently terrestrial, leaf-litter-dwelling member of the genus. The transition to miniaturisation in this species thus seems to have come hand-in-hand with a transition to terrestriality. Complementing the very rudimentary natural history information available for this enigmatic species should be a high priority for future field studies in Ranomafana National Park.

Curiously, the miniaturised and arboreal species *Platypelis karenae* (mentioned above) seems to contradict this prediction. Perhaps leaf-axil phytotelmic habits of this species have allowed it to miniaturise without ecological transition by exploiting smaller leaf axils than are available to larger frogs—a hypothesis compatible with our own observations, and, for example, *Microhyla bornensis*, an extremely miniaturised microhylid that breeds in pitcher plants [10, 11]. As a further deviation, the pyxicephalid *Microbatrachella capensis* (15–18 mm SVL) occurs in the South African fynbos shrubland vegetation, with acidic water and a dense humus layer, and breeds in swamps where its regular exotrophic tadpoles develop, while other miniaturized species of *Cacosternum*, such as *C. boettgeri*, (18–19 mm SVL) even occur in drier grassland areas, without apparent dependence on large quantities of leaf litter [81]. These cases indicate potential for uncoupling of typical trends of ecological change that accompany miniaturisation, similar to the pattern observed in African puddle frogs, Phrynobatrachidae, wherein terrestrialisation from predominantly aquatic habits was found to be uncoupled from miniaturisation [70]. Studying these exceptional cases in greater detail may reveal additional factors involved in miniaturisation, and drivers of miniaturisation without terrestrialisation.

Acknowledgements

We are indebted to numerous individuals in the Direction Général des Forêts and Madagascar National Parks for providing us with permits to conduct the research associated with this study of the last 30 years, and export collected material. This study was carried out under collaboration accords with the Mention Zoologie et Biodiversité Animale (former Département de Biologie Animale), Université de Madagascar, and the Ministry for Environment and Forests of the Republic of Madagascar. Micro-CT scanning was facilitated by A. Cerwenka and B. Ruthensteiner. We wish to thank P. Bora, J. Müller, M. Puente, E. Rajeriarison, T. Rajoafiarison, F. Randrianasolo, R.D. Randrianaina, F.M. Ratsoavina, I. de la Riva, M. Teschke (née Thomas), D.R. Vieites, and C. Woodhead for their assistance in the field.

References

1. Rieppel O. Miniaturization in tetrapods: consequences for skull morphology. *Symposia of the Zoological Society of London*. 1996;69:47–61.
2. Hanken J, Wake DB. Miniaturization of body size: organismal consequences and evolutionary significance. *Annual Review of Ecology and Systematics*. 1993;24:501–19.
3. Hanken J. Morphological novelty in the limb skeleton accompanies miniaturization in salamanders. *Science*. 1985;229:871–4.

4. Clarke BT. Small size in amphibians—its ecological and evolutionary implications. *Symposia of the Zoological Society of London*. 1996;69:201–24.
5. Kraus F. At the lower size limit for tetrapods, two new species of the miniaturized frog genus *Paedophryne* (Anura, Microhylidae). *ZooKeys*. 2011;154:71–88. doi: 10.3897/zook-
eys.154.1963.
6. Rittmeyer EN, Allison A, Gründler MC, Thompson DK, Austin CC. Ecological guild evolution and the discovery of the world’s smallest vertebrate. *PLoS One*. 2012;7(1):e29797. doi: 10.1371/journal.pone.0029797.
7. Lehr E, Coloma LA. A minute new Ecuadorian Andean frog (Anura: Strabomantidae, *Pristimantis*). *Herpetologica*. 2008;64(3):354–67.
8. Oliver PM, Iannella A, Richards SJ, Lee MSY. Mountain colonisation, miniaturisation and ecological evolution in a radiation of direct-developing New Guinea frogs (*Choerophryne*, Microhylidae). *PeerJ*. 2017;5:e3077. doi: 10.7717/peerj.3077.
9. Parker HW. Monograph of the frogs of the family Microhylidae. London, UK: Trustees of the British Museum; 1934.
10. Das I, Haas A. New species of *Microhyla* from Sarawak: Old World’s smallest frogs crawl out of miniature pitcher plants on Borneo (Amphibia: Anura: Microhylidae). *Zootaxa*. 2010;2571:37–52.
11. Matsui M. Taxonomic revision of one of the Old World’s smallest frogs, with description of a new Bornean *Microhyla* (Amphibia, Microhylidae). *Zootaxa*. 2011;2814(1):33–49. doi: 10.11646/zootaxa.2814.1.3.
12. Peloso PLV, Sturaro MJ, Forlani MC, Motta AP, Wheeler WC. Phylogeny, taxonomic revision, and character evolution of the genera *Chiasmocleis* and *Syncope* (Anura, Microhylidae) in Amazonia, with descriptions of three new species. *Bulletin of the American Museum of Natural History*. 2014;386:1–112.
13. de Sá RO, Tonini JFR, van Huss H, Long A, Cuddy T, Florlani MC, et al. Multiple connections between Amazonia and Atlantic Forest shaped the phylogenetic and morphological diversity of *Chiasmocleis* Mehely, 1904 (Anura: Microhylidae: Gastrophryninae). *Molecular Phylogenetics and Evolution*. 2019;130:198–210. doi: 10.1016/j.ympev.2018.10.021.
14. Rakotoarison A, Scherz MD, Glaw F, Köhler J, Andreone F, Franzen M, et al. Describing the smaller majority: Integrative taxonomy reveals twenty-six new species of tiny microhylid frogs (genus *Stumpffia*) from Madagascar. *Vertebrate Zoology*. 2017;67(3):271–398.
15. Scherz MD, Vences M, Rakotoarison A, Andreone F, Köhler J, Glaw F, et al. Reconciling molecular phylogeny, morphological divergence and classification of Madagascan narrow-mouthed frogs (Amphibia: Microhylidae). *Molecular Phylogenetics and Evolution*. 2016;100:372–81. doi: 10.1016/j.ympev.2016.04.019.
16. Andreone F, Vences M, Vieites DR, Glaw F, Meyer A. Recurrent ecological adaptations revealed through a molecular analysis of the secretive cophyline frogs of Madagascar. *Molecular Phylogenetics and Evolution*. 2005;34(2):315–22. doi: 10.1016/j.ympev.2004.10.013.
17. Wollenberg KC, Vieites DR, van der Meijden A, Glaw F, Cannatella DC, Vences M. Patterns of endemism and species richness in Malagasy cophyline frogs support a key role of mountainous areas for speciation. *Evolution*. 2008;62(8):1890–907. doi: 10.1111/j.1558-5646.2008.00420.x.
18. de Sá RO, Steicher JW, Sekonyela R, Forlani MC, Loader SP, Greenbaum E, et al. Molecular phylogeny of microhylid frogs (Anura: Microhylidae) with emphasis on relationships among New World genera. *BMC Evolutionary Biology*. 2012;12:241. doi: 10.1186/1471-2148-12-241.

Results

19. Peloso PLV, Frost DR, Richards SJ, Rodrigues MT, Donnellan S, Matsui M, et al. The impact of anchored phylogenomics and taxon sampling on phylogenetic inference in narrow-mouthed frogs (Anura, Microhylidae). *Cladistics*. 2016;32(2):113–40. doi: 10.1111/cla.12118.
20. Tu N, Yang M, Liang D, Zhang P. A large-scale phylogeny of Microhylidae inferred from a combined dataset of 121 genes and 427 taxa. *Molecular Phylogenetics and Evolution*. 2018;126:85–91.
21. van der Meijden A, Vences M, Hoegg S, Boistel R, Channing A, Meyer A. Nuclear gene phylogeny of narrow-mouthed toads (Family: Microhylidae) and a discussion of competing hypotheses concerning their biogeographical origins. *Molecular Phylogenetics and Evolution*. 2007;44:1017–30. doi: 10.1016/j.ympev.2007.02.008.
22. Peloso PLV, Raxworthy CJ, Wheeler WC, Frost DR. Nomenclatural stability does not justify recognition of paraphyletic taxa: A response to Scherz et al. (2016). *Molecular Phylogenetics and Evolution*. 2017;111(2017):56–64. doi: 10.1016/j.ympev.2017.03.016.
23. Scherz MD, Vences M, Rakotoarison A, Andreone F, Köhler J, Glaw F, et al. Lumping or splitting in the Cophylinae (Anura: Microhylidae) and the need for a parsimony of taxonomic changes: a response to Peloso et al. (2017). *Salamandra*. 2017;53(3):479–83.
24. Vences M, Glaw F, Köhler J, Wollenberg KC. Molecular phylogeny, morphology and bioacoustics reveal five additional species of arboreal microhylid frogs of the genus *Anodonthyla* from Madagascar. *Contributions to Zoology*. 2010;79(1):1–32.
25. Scherz MD, Hawlitschek O, Andreone F, Rakotoarison A, Vences M, Glaw F. A review of the taxonomy and osteology of the *Rhombophryne serratopalpebrosa* species group (Anura: Microhylidae) from Madagascar, with comments on the value of volume rendering of micro-CT data to taxonomists. *Zootaxa*. 2017;4273(3):301–40. doi: 10.11646/zootaxa.4273.3.1.
26. Scherz MD, Glaw F, Vences M, Andreone F, Crottini A. Two new species of terrestrial microhylid frogs (Microhylidae: Cophylinae: *Rhombophryne*) from northeastern Madagascar. *Salamandra*. 2016;52(2):91–106.
27. Scherz MD, Ruthensteiner B, Vieites DR, Vences M, Glaw F. Two new microhylid frogs of the genus *Rhombophryne* with supraciliary spines from the Tsaratanana Massif in northern Madagascar. *Herpetologica*. 2015;71(4):310–21. doi: 10.1655/HERPETOLOGICA-D-14-00048.
28. Scherz MD, Rakotoarison A, Hawlitschek O, Vences M, Glaw F. Leaping towards a saltatorial lifestyle? An unusually long-legged new species of *Rhombophryne* (Anura, Microhylidae) from the Sorata massif in northern Madagascar. *Zoosystematics and Evolution*. 2015;91(2):105–14. doi: 10.3897/zse.91.4979.
29. Trueb L. Cranial osteology of the hylid frog, *Smilisca baudini*. University of Kansas Publications, Museum of Natural History. 1968;18(2):11–35.
30. Trueb L. Patterns of diversity in the lissamphibian skull. In: Hanken J, Hall BK, editors. The Skull, Volume 2: Patterns of Structural and Systematic Diversity. 2. Chicago IL, USA: University of Chicago Press; 1993. p. 255–343.
31. Trueb L. Bones, frogs, and evolution. In: Vial JL, editor. Evolutionary Biology of the Anurans: Contemporary Research on Major Problems. USA: University of Missouri Press; 1973. p. 65–132.
32. Fabrezi M, Alberch P. The carpal elements of anurans. *Herpetologica*. 1996;52(2):188–204.
33. Köhler J, Jansen M, Rodríguez A, Kok PJR, Toledo LF, Emmrich M, et al. The use of bioacoustics in anuran taxonomy: theory, terminology, methods and recommendations for best practice. *Zootaxa*. 2017;4251(1):1–124. doi: 10.11646/zootaxa.4251.1.1.
34. Edgar RC. MUSCLE: multiple sequence alignment with high accuracy and high throughput. *Nucleic Acids Research*. 2004;32(5):1792–7.

35. Kumar S, Stecher G, Tamura K. MEGA7: Molecular Evolutionary Genetics Analysis version 7.0 for bigger datasets. *Molecular Biology and Evolution*. 2016;33(7):1870–4. doi: 10.1093/molbev/msw054.
36. Vences M, Guayasamin JM, Miralles A, de la Riva I. To name or not to name: Criteria to promote economy of change in Linnaean classification schemes. *Zootaxa*. 2013;3636(2):201–44. doi: 10.11646/zootaxa.3636.2.1.
37. Trueb L, Alberch P. Miniaturisation and the anuran skull: a case study of heterochrony. In: Duncker HR, Fleischer G, editors. *Functional Morphology of Vertebrates*. Stuttgart, Germany: Gustav Fisher Verlag; 1985. p. 113–21.
38. Vallan D. A new species of the genus *Stumpffia* (Amphibia: Anura: Microhylidae) from a small forest remnant of the central high plateau of Madagascar. *Revue suisse de Zoologie*. 2000;107:835–41.
39. Vences M, Glaw F. Revision der Gattung *Stumpffia* Boettger 1881 aus Madagaskar mit Beschreibung von zwei neuen Arten (Amphibia, Anura, Microhylidae). *Acta Biologica Benrodis*. 1991;3:203–19.
40. Vieites DR, Wollenberg KC, Andreone F, Köhler J, Glaw F, Vences M. Vast underestimation of Madagascar's biodiversity evidenced by an integrative amphibian inventory. *Proceedings of the National Academy of Sciences of the USA*. 2009;106(20):8267–72. doi: 10.1073/pnas.0810821106.
41. Glaw F, Vences M. *A Field Guide to the Amphibians and Reptiles of Madagascar*. 3rd Edition. Cologne, Germany: Vences & Glaw Verlags GbR; 2007. 496 p.
42. Emerson SB. The ilio-sacral articulation in frogs: form and function. *Biological Journal of the Linnean Society*. 1979;11:153–68. doi: 10.1111/j.1095-8312.1979.tb00032.x.
43. Rodríguez A, Börner M, Pabijan M, Gehara M, Haddad CFB, Vences M. Genetic divergence in tropical anurans: deeper phylogeographic structure in forest specialists and in topographically complex regions. *Evolutionary Ecology*. 2015;29:765–85.
44. IUCN. *IUCN Red List Categories and Criteria: Version 3.1*. 2nd Edition ed. Gland, Switzerland and Cambridge, UK: IUCN; 2012.
45. IUCN SSC Amphibian Specialist Group. *Guibemantis diphonus*. The IUCN Red List of Threatened Species. 2016;2016:e.T88219153A312479. doi: 10.2305/IUCN.UK.2016-1.RLTS.T88219153A88312479.en. Downloaded on 29 October 2018.
46. Perl RGB, Nagy ZT, Sonet G, Glaw F, Wollenberg KC, Vences M. DNA barcoding Madagascar's amphibian fauna. *Amphibia-Reptilia*. 2014;35:197–206. doi: 10.1163/15685381-00002942.
47. Ramanamanjato J-B. Reptile and amphibian communities along the humidity gradient and fragmentation effects in the littoral forests of southeastern Madagascar. In: Ganzhorn JU, Goodman SM, Vinczelette M, editors. *Biodiversity, Ecology and Conservation of Littoral Ecosystems in Southeastern Madagascar, Tolagnaro (Fort Dauphin)*. SI/MAB Series. Washington DC, USA: Smithsonian Institution; 2007. p. 167–79.
48. Lewis Environmental Consultants. *Madagascar Mineral Project. Environmental impact assessment study. Part I: Natural environment. Appendix IV: Faunal Study: QIT Madagascar Minerals S. A.*; 1992.
49. Ramanamanjato J-B, Soanary CH. The herpetofauna of Tsitongambarika Forest. In: International B, editor. *Tsitongambarika Forest, Madagascar—Biological and socio-economic surveys, with conservation recommendations*. Cambridge, UK: BirdLife International; 2011. p. 34–41.
50. Glaw F, Vences M. *A Fieldguide to the Amphibians and Reptiles of Madagascar*. Second Edi-

Results

- tion. Cologne, Germany: Vences & Glaw Verlags GbR; 1994. 478 p.
51. Vences M, Glaw F, Marquez R, editors. The Calls of the Frogs of Madagascar. 3 Audio CD's and booklet. Madrid, Spain: Fonoteca Zoológica; 2006.
 52. Glaw F, Köhler J, Vences M. A new fossorial frog, genus *Rhombophryne*, from Nosy Mangabe Special Reserve, Madagascar. *Zoosystematics and Evolution*. 2010;86(2):235–43. doi: 10.1002/zoot.201000006.
 53. Feng Y-J, Blackburn DC, Liang D, Hillis DM, Wake DB, Cannatella DC, et al. Phylogenomics reveals rapid, simultaneous diversification of three major clades of Gondwanan frogs at the Cretaceous–Paleogene boundary. *Proceedings of the National Academy of Sciences of the USA*. 2017;114(29):E5864–E70. doi: 10.1073/pnas.1704632114.
 54. Gould SJ. *Ontogeny and Phylogeny*. Cambridge, MA USA: Harvard University Press; 1977. 501 p.
 55. Alberch P, Gould SJ, Oster GF, Wake DB. Size and shape in ontogeny and phylogeny. *Paleobiology*. 1979;5:296–317.
 56. Klingenberg CP. Heterochrony and allometry: the analysis of evolutionary change in ontogeny. *Biological Reviews*. 1998;73:79–123.
 57. Kraus F. New genus of diminutive microhylid frogs from Papua New Guinea. *ZooKeys*. 2010;48:39–59. doi: 10.3897/zookeys.48.446.
 58. Clemente-Carvalho RBG, Klaczko J, Perez SI, Alves ACR, Haddad CFB, dos Reis SF. Molecular phylogenetic relationships and phenotypic diversity in miniaturized toadlets, genus *Brachycephalus* (Amphibia: Anura: Brachycephalidae). *Molecular Phylogenetics and Evolution*. 2011;61(1):79–89. doi: 10.1016/j.ympev.2011.05.017.
 59. Padial JM, Grant T, Frost DR. Molecular systematics of terraranas (Anura: Brachycephaloidea) with an assessment of the effects of alignment and optimality criteria. *Zootaxa*. 2014;3825(1):1–132. doi: 10.11646/zootaxa.3825.1.1.
 60. Ribeiro LF, Bornschein MR, Belmonte-Lopes R, Firkowski CR, Morato SAA, Pie MR. Seven new microendemic species of *Brachycephalus* (Anura: Brachycephalidae) from southern Brazil. *PeerJ*. 2015;3:e1011. doi: 10.7717/peerj.1011.
 61. Klages J, Glaw F, Köhler J, Müller J, Hipsley CA, Vences M. Molecular, morphological and osteological differentiation of a new species of microhylid frog of the genus *Stumpffia* from northwestern Madagascar. *Zootaxa*. 2013;3717(2):280–300. doi: 10.11646/zootaxa.3717.2.8.
 62. Yeh J. The effect of miniaturized body size on skeletal morphology in frogs. *Evolution*. 2002;56(3):638–41.
 63. Alberch P, Gale EA. A developmental analysis of an evolutionary trend: digital reduction in amphibians. *Evolution*. 1985;39(1):8–23.
 64. Alberch P, Gale EA. Size dependence during the development of the amphibian foot: colchicine-induced digital loss and reduction. *Journal of Embryology and Experimental Morphology*. 1983;76:177–97.
 65. Poyarkov NA, Suwannapoom C, Pawangkhanant P, Aksornneam A, Van Duong T, Korost DV, et al. A new genus and three new species of miniaturized microhylid frogs from Indochina (Amphibia: Anura: Microhylidae: Asterophryinae). *Zoological Research*. 2018;39(3):130.
 66. Blackburn DC. Description and phylogenetic relationships of two new species of miniature *Arthroleptis* (Anura: Arthroleptidae) from the Eastern Arc Mountains of Tanzania. *Breviora*. 2009;517:1–17.
 67. Garg S, Suyesh R, Sukesan S, Biju SD. Seven new species of Night Frogs (Anura, Nyctibatrachidae) from the Western Ghats Biodiversity Hotspot of India, with remarkably high diversity

- of diminutive forms. *PeerJ*. 2017;5:e3007. doi: 10.7717/peerj.3007.
- 68. Monteiro JPdC, Condez TH, Garcia PCdA, Comitti EJ, Amaral IB, Haddad CFB. A new species of *Brachycephalus* (Anura, Brachycephalidae) from the coast of Santa Catarina State, southern Atlantic Forest, Brazil. *Zootaxa*. 2018;4407(4). doi: 10.11646/zootaxa.4407.4.2.
 - 69. Günther R, Richards S. Three new species of the microhylid frog genus *Choerophryne* (Amphibia, Anura, Microhylidae) from Papua New Guinea. *Zoosystematics and Evolution*. 2017;93(2):265–79. doi: 10.3897/zse.93.11576.
 - 70. Zimkus BM, Lawson L, Loader SP, Hanken J. Terrestrialization, miniaturization and rates of diversification in African puddle frogs (Anura: Phrynobatrachidae). *PLoS One*. 2012;7(4):e35118. doi: 10.1371/journal.pone.0035118.
 - 71. Blackburn DC. Biogeography and evolution of body size and life history of African frogs: Phylogeny of squeakers (*Arthroleptis*) and long-fingered frogs (*Cardioglossa*) estimated from mitochondrial data. *Molecular Phylogenetics and Evolution*. 2008;49:806–26. doi: 10.1016/j.ympev.2008.08.015.
 - 72. Lourenco-De-Moraes R, Dias IR, Mira-Mendes CV, de Oliveira RM, Barth A, Ruas DS, et al. Diversity of miniaturized frogs of the genus *Adelophryne* (Anura: Eleutherodactylidae): A new species from the Atlantic Forest of northeast Brazil. *PLoS One*. 2018;13:e0201781. doi: 10.1371/journal.pone.0201781.
 - 73. Rodríguez A, Poth D, Schulz S, Gehara M, Vences M. Genetic diversity, phylogeny and evolution of alkaloid sequestering in Cuban miniaturized frogs of the *Eleutherodactylus limbatus* group. *Molecular Phylogenetics and Evolution* 2013;68:541–54.
 - 74. Köhler F, Günther R. The radiation of microhylid frogs (Amphibia: Anura) on New Guinea: A mitochondrial phylogeny reveals parallel evolution of morphological and life history traits and disproves the current morphology-based classification. *Molecular Phylogenetics and Evolution*. 2008;47:353–65. doi: 10.1016/j.ympev.2007.11.032.
 - 75. Guibé J. Les batraciens de Madagascar. *Bonner zoologische Monographien*. 1978;11:1–140.
 - 76. Blommers-Schlösser RMA, Blanc CP. Amphibiens (première partie). *Faune de Madagascar*. 1991;75(1):1–397.
 - 77. Mott T, Vieites DR. Molecular phylogenetics reveals extreme morphological homoplasy in Brazilian worm lizards challenging current taxonomy. *Molecular Phylogenetics and Evolution*. 2009;51(2):190–200. doi: 10.1016/j.ympev.2009.01.014.
 - 78. Heideman NJL, Mulcahy DG, Sites JW, Hendricks MGJ, Daniels SR. Cryptic diversity and morphological convergence in threatened species of fossorial skinks in the genus *Scelotes* (Squamata: Scincidae) from the Western Cape Coast of South Africa: Implications for species boundaries, digit reduction and conservation. *Molecular Phylogenetics and Evolution*. 2011;61(3):823–33. doi: 10.1016/j.ympev.2011.08.021.
 - 79. Rosa GM, Crottini A, Noël J, Rabibisoa N, Raxworthy CJ, Andreone F. A new phytotelmic species of *Platypelis* (Microhylidae: Cophylinae) from the Betampona Reserve, eastern Madagascar. *Salamandra*. 2014;50(4):201–14.
 - 80. Tracy CR, Christian KA, Tracy CR. Not just small, wet, and cold: effects of body size and skin resistance on thermoregulation and arboreality of frogs. *Ecology*. 2010;91(5):1477–84. doi: 10.1890/09-0839.1.
 - 81. Du Preez LH, Carruthers VC. A complete guide to the frogs of Southern Africa. Cape Town, South Africa: Random House Struik; 2017. 400 p.

Chapter 10. MANUSCRIPT (in prep.): Ecomorphological evolution of Madagascar's narrow-mouthed frogs (Anura, Microhylidae)

In this chapter I present an unpublished manuscript that features the latest work on the subfamily Cophylinae. In this manuscript, my colleagues and I present a new reconstruction of the subfamily Cophylinae based on a phylotranscriptomic tree, a phylogenomic tree produced using target capture methods, and a supermatrix tree of the entire subfamily using a rigid skeleton based on genomic trees. We discuss the taxonomic implications of our robust phylogenetic relationships. We show that the ancestrally terrestrial frogs originated in northeastern Madagascar, and subsequently diversified across the expanding biomes during the Paleogene, transitioning repeatedly toward arboreality following the humidification of the island. We find that fossoriality and arboreality have strongly influenced morphometric evolution, and that miniaturisation has been accompanied by a homogenisation of morphology.

Scherz, M.D., Hutter, C.R., Rödel, M.-O., Rancilhac, L., Künzel, S., Rakotoarison, A., Drehlich, C., Philippe, H., Glaw, F., Vences, M. Ecomorphological evolution of Madagascar's narrow-mouthed frogs (Anura, Microhylidae). Unpublished manuscript

Digital Supplementary Materials on appended CD:

Supplementary Figure 1 — Six-category ancestral state reconstruction of ecology in the Cophylinae.

Supplementary Figure 2 — \log_{10} maximum body size by ecology in the Cophylinae.

Supplementary Table 1 — The 50 smallest frogs in the world.

Supplementary Table 2 — Supermatrix table of single gene sequences of Cophylinae at individual level.

Supplementary Table 3 — Supermatrix table of single gene sequences of Cophylinae at species level.

Supplementary Table 4 — Cophylinae frog measurement database.

Supplementary Table 5 — Newly assigned species numbers based on 3' 16S rRNA mitochondrial genes.

Supplementary Table 6 — Ancestral sizes of clades and their 95% Confidence Intervals (CI).

Supplementary Trees

Ecomorphological evolution of Madagascar's narrow-mouthed frogs (Anura, Microhylidae)

Mark D. Scherz^{1,2,3,*}, Carl R. Hutter⁴, Mark-Oliver Rödel⁵, Loïs Rancilhac², Sven Künzel⁶, Andola-lao Rakotoarison⁷, Carmen Drehlich², Hervé Philippe⁸, Frank Glaw¹, Miguel Vences²

Short title: Narrow-mouthed frog evolution

¹Sektion Herpetologie, Zoologische Staatssammlung München (ZSM-SNSB), München, Germany

²Division of Evolutionary Biology, Zoologisches Institut, Technische Universität Braunschweig, Braunschweig, Germany

³Systematische Zoologie, Department Biologie II, Biozentrum, Ludwig-Maximilians-Universität München, Planegg-Martinsried, Germany

⁴Biodiversity Institute and Department of Ecology and Evolutionary Biology, University of Kansas, Lawrence, KS, USA

⁵Museum für Naturkunde – Leibniz Institute for Evolution and Biodiversity Science, Berlin, Germany

⁶Max-Planck Institute for Evolutionary Biology, Plön, Germany

⁷Mention Zoologie et Biodiversité Animale, Université d'Antananarivo, Antananarivo, Madagascar

⁸Centre for Biodiversity Theory and Modelling, Station d'Ecologie Théorique et Expérimentale du CNRS, Moulis, France

*corresponding author: mark.scherz@gmail.com

Introduction

The emerging picture of convergent evolution shows that apparent determinism in phenotypic outcome of adaptation into a similar niche or due to similar selective pressures often shows signs of contingency upon close inspection (e.g. Bergmann and Morinaga in press). Ecomorphs (sometimes called ‘ecological guilds’ or ‘ecotypes) represent astonishingly repetitive convergent evolution. The best-examined examples stem from the anoles of Central America and the islands of the Caribbean. Island radiations may harbour the same anole ecomorphs, yet they are generally convergently derived from single colonists (reviewed in Losos 2011). Such examples of serial convergence are excellent systems in which to study the principles of phenotypic evolution.

Frogs exhibit a remarkably conserved set of ecomorphs, only few of which are unique to single clades. Globally, communities consist of a limited number of oft repeated ecomorphs, from the stereotypical treefrog with its broad toe pads, to the pond frogs with highly webbed feet and long powerful legs, to digging frogs with broad heads and short limbs. In several cases, these ecomorphs have evolved within single radiations (e.g. Bossuyt and Milinkovitch 2000), making them anuran parallels of the anole convergence story. Narrow-mouthed frogs (family Microhylidae) are a curious case among frogs. They are a diverse (657 species; AmphibiaWeb 2019) comparatively old family (Feng et al. 2017) distributed throughout the tropics, and globally exhibit a wide range of ecomorphs, including tree frogs, litter frogs, aquatic or semi-aquatic frogs, scansorial bouldering or karst-living frogs, and especially burrowers and miniaturised frogs.

Of particular note is the propensity of microhylid frogs to become miniaturised. Indeed, among the top 50 smallest frogs in the world, 35 are microhylids (Supplementary Table 1). Miniaturisation in microhylids is almost always accompanied by terrestriality and constitutes a unique ecomorph (Clarke 1996; Rittmeyer et al. 2012; **chapter 9**). Smaller body size opens up novel ecological niches (Clarke 1996; Miller 1996; Lehr and Coloma 2008; Lee et al. 2014), allows exploitation of new nutrition sources (Clarke 1996; Lehr and Coloma 2008), and can be strongly favoured by selection (Clarke 1996). Miniaturised frogs are an important ecomorph in the tropics (Kraus 2011). Yet, aside from miniaturisation, little about ecomorphological evolution in microhylids has been studied (but see Blackburn et al. 2013; Rivera et al. 2017).

In this study, we look at morphological evolution across the Madagascar-endemic microhylid subfamily Cophylinae. The nine cophyline genera (**chapter 9**) currently consist of 108 species (AmphibiaWeb 2019). Molecular phylogenetic work revealed that these frogs have been ecologically highly labile in their evolutionary past, with ecomorphology in several cases belying evolutionary relationships (Andreone et al. 2005; Wollenberg et al. 2008). In recent work, we have shown that miniaturised frogs in this subfamily are not only extremely speciose (Rakotoarison et al. 2017a), but also phylogenetically diverse, belonging to four separate genera (see **chapter 9** for an overview). A similar diversity and non-monophyly is seen among burrowing and arboreal/scansorial lineages. At the same time as they have diversified ecologically, these frogs have spread across Madagascar, and their biogeography is nearly as complex as their ecomorphological evolution.

In this chapter, we examine the biogeography, and the evolution of body size and morphology within the microhylid subfamily Cophylinae, based on a new phylogeny with a backbone constrained on topologies recovered from two genomic datasets (transcriptome and target enrichment).

Methods

Sequencing and molecular phylogenetics

Sanger sequences. We compiled all of the sequences of cophyline frogs present on GenBank, and sorted them into a supermatrix, giving a row to each specimen and a column to each marker. This method was designed to get explicit information on the specimen-sequence matchup of every

sequence, so that even chimeric sequences in our supermatrix could be traced to specimens for morphological verification. This is intended as a quality control step to reduce the risk of misidentification and prevent mixed-species chimeras in our supermatrix. We expanded this dataset with numerous additional new sequences produced using primers and protocols from previous studies (Table 1). This resulted in a supermatrix of 1300 specimens (Supplementary Table 2). In a second step, we reduced this supermatrix to include a single tip per species, with each component of the chimera identified (Supplementary Table 3). Specimens were chosen for maximum coverage, so

Table 1. Primers used for Sanger sequencing in this study.

Gene	Primer- Name	Sequence (5'-3')	Source
Cytb	Cytb-a	CCATGAGGACAAATATCATTYGRGG	1
	Cytb-c	CTACTGGTTGTCCTCCGATTATGT	1
12S	12SA-L	AAACTGGGATTAGATACCCCACTAT	2
	12SB-H	GAGGGTGACGGCGGTGTGT	2
16S 3'	16SA-L	CGCCTGTTATCAAAACAT	2
	16SBH-NEW	CCTGGATTACTCCGGTCTGA	2
16S 5'	16SL3	AGCAAAGAHYWWACCTCGTACCTTTGCAT	3
	16SAH	ATGTTTTGATAAACAGGCG	3
ND1	L3914	GCCCCATTGACCTCACAGAAGG	4
	H4419	GGTATGGGCCAAAGCT	4
ND2/	L4437	AAGCTTCGGGCCATACC	5
COI	H6564	GGGTCTCCTCCTCCAGCTGGTC	6
COI	dgLCO1490	GGTCAACAAATCATAAAGAYATYGG	7
	dgHCO2198	TAAAACTTCAGGGTGACCAAAR AAY CA	7
SACS	SACSF2	AAYATHACNAAYGCNTGYTAYAA	8
	SACSR2	GCRAARTGNCCRTTNACRTGRAA	8
	SACSNF2	TGYTAYAAYGAYTGYCCNTGGAT	8
	SACSNR2	CKGTGRGGYTTYTTARTTRTG	8
KIAA1239	KIAA1239F1	CARCCTGGGTNTTYCARTGYAA	8
	KIAA1239R1	ACMACAAAYGGTCRTTRTGNGT	8
	KIAA1239NF1	GAGCCNGAYATHTTYTTYGTNAA	8
	KIAA1239NR1	TTCACRAANCCMCCNGAAAAYTC	8
TTN	TTNF1	TATGCTGARAAYATNGCNGGNAT	8
	TTNR1	CCMCCRTCAAAYARNGGYTT	8
	TTNNF1	GATGGNMGKTGGYTNAARTGYAA	8
	TTNNR1	AGRTCRTANACNGGYTTYTTRTT	8
BDNF	BDNF-F2	CCATCCTTTCCTKACTATGGT	9
	BDNF-R2	TATCTTCCCCTTTAATGGTCA	new
RAG1	MartFL1	AGCTGGAGYCARTAYCAYAARATG	10
	MartR6	GTGTAGAGCCARTGRTGYTT	10
	Amp F2	ACNGGNMGICARATCTTYCARCC	10
	RAG1_UC_R	TTGGACTGCCTGGCATTCAT	11
H3	H3F	ATGGCTCGTACCAAGCAGACVGC	12
	H3R	ATATCCTTRGGCATRATRGTGAC	12

¹Bossuyt and Milinkovitch (2000), ²Palumbi et al. (1991), ³Vences et al. (2003), ⁴Macey et al. (1998b), ⁵Macey et al. (1997), ⁶Macey et al. (1998a), ⁷Meyer (2003), ⁸Shen et al. (2012), ⁹Lee et al. (2005), ¹⁰Chiari et al. (2004), ¹¹Rakotoarison et al. (2015), ¹²Colgan et al. (1998)

Results

that a chimera consisted of a minimum number of specimens positively identified as conspecifics. Chimeras were only produced from specimens confirmed to be conspecific by close matches in at least one gene fragment.

Probe design. The sequence capture probe set used for this study is the FrogCap Ranoidea v1 probe set (<https://github.com/chutter/FrogCap-Sequence-Capture>; Hutter et al. in prep). Probe design is summarized here and will be published in detail by Hutter et al. (in prep.). Probes were synthesized as biotinylated RNA oligos in a myBaits kit (Arbor Biosciences, formerly MYcroarray Ann Arbor, MI) by matching 25 publicly available transcriptomes to the *Nanorana parkeri* and *Xenopus tropicalis* genomes using the program BLAT (Kent 2002). Matching sequences were clustered by their genomic coordinates to detect presence/absence across species and to achieve full locus coverage. To narrow the locus selection to coding regions, each cluster was matched to available coding region annotations from the *Nanorana* genome using the program EXONERATE (Slater and Birney 2005). Loci from all matching species were then aligned using MAFFT (Katoh and Standley 2013) and subsequently separated into 120 bp-long bait sequences with 2x tiling (50% overlap among baits) using the myBaits-2 kit (40,040 baits) with 120mer sized baits. These loci have an additional bait at each end extending into the intronic region to increase the coverage and capture success of these areas. Baits were then filtered, retaining those: without sequence repeats; with a GC content of 30–50%; and baits that did not match to their reverse complement or multiple places in the genome. Additionally, 700 ultra-conserved elements (UCEs) and 40 commonly used Sanger-based legacy loci from phylogenetic analyses of frogs (i.e. RAG1, POMC, TYR) were included to enable direct comparisons and inclusion of publicly available data from past phylogenetic studies.

Library preparation and sequencing. Genomic DNA was extracted from 25 tissue samples using a PROMEGA Maxwell bead extraction robot. The resultant DNA was quantified using a Quantus DNA Broad-range assay (PROMEGA). Approximately 500 ng total DNA was acquired and set to a volume of 50 μ l through dilution (with H_2O) or concentration (using a vacuum centrifuge) of the extraction when necessary.

The genomic libraries for the samples were prepared by Arbor Biosciences library preparation service. Prior to library preparation, the genomic DNA samples were quantified with fluorescence and up to 4 μ g was then taken to sonication with a QSonica Q800R instrument. After sonication and SPRI bead-based size-selection to modal lengths of roughly 300 nt, up to 500 ng of each sheared DNA sample were taken to Illumina Truseq-style sticky-end library preparation. Following adapter ligation and fill-in, each library was amplified for 6 cycles using unique combinations of i7 and i5 indexing primers, and then quantified with fluorescence. For each capture reaction, 125 ng of 8 libraries were pooled, and subsequently enriched for targets using the MYbaits v 3.1 protocol. Following enrichment, library pools were amplified for 10 cycles using universal primers and subsequently pooled in equimolar amounts for sequencing. Samples were sequenced on an Illumina HiSeq 3000 with 150 bp paired-end reads.

Data processing pipeline. A bioinformatics pipeline for filtering adapter contamination, assembling loci, and exporting alignments is coded in R and available at (<https://github.com/chutter/FrogCap-Sequence-Capture>). The pipeline is scripted in R statistical software (R Core Team 2014) using the BIOCONDUCTOR suit of packages (Ramos et al. 2018) in addition to open source software publicly available and commonly used in bioinformatics. First, the raw reads were cleaned of adapter contamination, low complexity sequences, and other sequencing artefacts using the program FASTP (default settings; Chen et al. 2017). Adapter-cleaned reads were then matched to

a database of bacterial and other genomes to ensure that no contamination was in the final dataset (Hutter et al. in prep will contain a reference genome list). We decontaminated the adapter-cleaned reads with the program BWA (Li and Durbin 2009), where we matched the cleaned reads to each contamination genome at >95 percent similarity. Each reference was indexed (function: *bwa index*) and reads were mapped to each reference (function: *bwa mem*), using SAMTOOLS (Li et al. 2009) to convert between file-types (functions: *view* and *fastq*). Next, we merged paired-end reads using BBMERGE (Bushnell et al. 2017) from BBTOOLS (<https://jgi.doe.gov/data-and-tools/bbtools/>). BBMERGE also fills in missing gaps between non-overlapping paired-end reads by assembling the missing data from the other paired-end reads. Exact duplicates were also removed when both read pairs were duplicated using ‘dedupe’ from BBTOOLS. Additionally, duplicates from the set of merged paired-end contigs were removed if they were exact duplicates or were contained within another merged contig.

The merged singletons and paired-end reads were next *de novo* assembled using the program SPADES v.3.12 (Bankevich et al. 2012), which runs BAYESHAMMER (Nikolenko et al. 2013) error correction on the reads internally. Data were assembled using several different k-mer values (21, 33, 55, 77, 99, 127), where orthologous contigs resulting from the different k-mer assemblies were merged. We used the DIPSPADES (Sofanova et al. 2015) function from this program to better assemble exons that were polymorphic by generating a consensus sequence from both haplotypes from orthologous regions.

The consensus haplotype contigs were then matched against reference loci sequences from the *N. parkeri* genome used to design the probes with BLAST (*dc-megablast*), keeping only those contigs that matched uniquely to the reference probe sequences. Contigs were discarded if they did not match to at least 30 percent of the reference locus. Finally, we merged all discrete contigs that matched to the same reference locus, joining them together with Ns based on their match position within the locus. The final set of matching contigs were named with the name of the locus followed by the sample name in a single file to be parsed out separately for multiple sequence alignment.

Finally, we assembled mitochondrial genomes for each sample, separating, and annotating genes from Illumina sequence data. We used an assembly pipeline using a ‘bait fishing’ approach that uses SPADES. We used the *Nanorana parkeri* mitochondrial genome as a reference and extracted the cleaned raw reads that matched to this genome. We next assembled the separated reads and using the resulting contigs and we matched the cleaned reads again to these contigs and assembled them. We continued this process iteratively until no new portions of the mitochondrial genome could be assembled. Next, we used BLAST to match the assembled contigs to the separated mitochondrial markers and trimmed them to reference markers. This resulted in a collection of assembled mitochondrial markers that were aligned and trimmed as described in the next section.

Alignment and trimming. The final set of matching loci was next aligned on a locus-by-locus basis using MAFFT local pair alignment (max iterations = 1000; ep = 0.123; op = 3). We screened each alignment for samples that were greater than 40 percent divergent from the consensus sequence, which are almost always incorrectly assigned contigs. Alignments were kept if they had greater than 3 taxa, had more than 100 base pairs, and a mean breadth of coverage of greater than 50 percent across the alignment. Alignments were next saved into usable datasets for phylogenetic analyses and data type comparisons: 1) all-markers, includes all the unique alignments that matched to target loci, unfiltered for exons and introns; 2) exons, each alignment was adjusted to be in an open-reading frame and trimmed to the largest reading frame that accommodated >90% of the sequences and alignments with no clear reading frame were discarded; 3) introns, the exon previously delimited was trimmed out of the original contig and the two remaining intronic regions were concatenated; 4) proteins, exon nucleotide sequences were translated into their corresponding amino acid protein sequences; 5) genes, exons from the same gene were concatenated and treated as a single locus; and 6) mitochondrial, markers that were assembled separately from

Results

the raw reads (described above). We applied internal trimming only to the all-markers dataset and alignments that were non-coding (i.e. rRNA, UCEs, introns) using TRIMAL (automatic1 function; Capella-Gutiérrez et al. 2009). All alignments were externally trimmed to ensure that at least 50 percent of the samples had sequence data present.

Transcriptomics. We used transcriptomics as a secondary source of deep phylogenomic node resolution (Irisarri et al. 2017; Rodríguez et al. 2017) to ratify the phylogenetic relationships reconstructed from the target capture method outlined above. Samples of ten ingroups and two outgroups (*Scaphiophryne calcarata* and *Dyscophus guineti*) were taken from freshly euthanised specimens and deposited in RNAlater. RNA was extracted using a trizol-extraction protocol from pooled tissue samples (skin, muscle, liver) from single individuals. Libraries were prepared following the Illumina TruSeq mRNA protocol and sequenced on an Illumina NextSeq machine. Reads were pre-processed, and transcriptomes assembled de novo in Trinity v. 2.1.0 (Grabherr et al. 2011). Orthologs were translated into amino acid sequences and added to the multi-gene alignment of vertebrates of Irisarri et al. (2017) in FORTY-Two (<https://bitbucket.org/dbaurain/42/>). Contaminations (non-vertebrates, cross-contaminations), misalignments, and possible paralogues were removed following Irisarri et al. (2017). The specific pipeline used is detailed in **chapter 11**, but briefly consists of (1) invertebrate sequence fishing using BLAST, (2) redundancy and implausible divergence exclusion, (3) patristic-distance outlier exclusion, (4) removal of highly divergent paralogs (possible orthologs). Nucleotide sequences were then recovered from retained AA alignments from the original assemblies using LEEL (written by D. Baurain) and assembled using SCAFos (Roure et al. 2007).

Phylogeny estimation

Concatenated tree datasets. We first estimated concatenated phylogenetic trees by creating separate datasets with variable amounts of missing sequence data for the FrogCap and transcriptome datasets. For the transcriptome dataset, several samples with a relatively small amount of data sequenced were excluded in case the missing data gave no clear support. We separated alignment matrices into three different amounts of completeness (70, 80, and 90 percent), where individual markers were only retained if the number of samples in each alignment met that completeness threshold. We used maximum likelihood (ML) and Bayesian inference (BI) approaches to generate phylogenetic hypotheses from each of the three resulting datasets. First, we used the maximum-likelihood method IQ-TREE v.1.6.7 (Nguyen et al. 2015) to estimate phylogenetic trees from concatenated data. For these analyses, we employed models of molecular evolution identified via MODELFINDER (Kalyaanamoorthy et al. 2017) built into IQ-Tree, which identified an optimal partitioning scheme and models of molecular evolution for each partition. We assessed support for the resulting topology using 1000 ultrafast bootstrap replicates (Minh et al. 2013). Additionally, we also used EXABAYES (Aberer et al. 2014) for BI analyses, which can analyse genome-scale data while being computationally tractable. With EXABAYES, we analysed a fully partitioned dataset by marker, where we used the GTR+GAMMA model (the only model available) for the nucleotide sequences. Two coupled chains were run twice independently for 200,000 generations to verify independent convergence. We checked for convergence by ensuring that ESS values were greater than 100 for all parameters.

Concatenated gene jackknifing. We scripted a gene-jackknifing workflow to estimate concatenated trees utilizing full model selection and partitioning across data matrices, which were often not computationally tractable on full datasets. In addition, this approach allowed us to verify that the topology was consistent across the jackknife replicates. The jackknifing approach used ML

with IQ-TREE and followed the procedure: 1) Genes for the data matrix were randomly selected without replacement, where genes were selected up until a threshold of 200,000 bp had been reached so that each matrix was nearly the same size; 2) We partitioned by codon position for exons and by marker for non-coding regions; 3) We used MODELFINDER to select the best model for each partition; 4) we ran the analysis 1000 times to generate 1000 jackknife tree replicates; and 5) the 1000 replicate trees were summarized by generating a maximum clade credibility tree, which collapsed nodes into polytomies that were not supported by at least 50% of the jackknife replicates. The script was coded in R and is available on GitHub (<https://github.com/chutter/Frog-Cap-Sequence-Capture>).

Gene trees and species trees. Recent studies have suggested that concatenation analyses can be statistically inconsistent in the presence of incomplete lineage sorting or anomaly zones that result in species trees that are different from their gene trees (Degnan and Rosenberg 2009; Roch and Steel 2015). To address this possibility, we used the software ASTRAL-III (Zhang et al. 2018), which conducts a summary-coalescent species tree analysis that is statistically consistent under the multi-species coalescent model. As input for ASTRAL-III, individual trees for each gene and marker were needed, so we performed maximum likelihood (ML) concatenation analyses on each alignment using IQ-TREE. We ran the analyses separately on the exon, intron, protein, and gene datasets; and we also combined the exon and intron datasets together in a final analysis. To improve accuracy, we collapsed branches that were below 10% bootstrap support (Zhang et al. 2018). Finally, we used local branch support to assess topological support for the coalescent trees generated by ASTRAL-III because this method out-performs multi-locus bootstrapping (Sayyari and Mirarab 2016).

Time-calibrated phylogeny estimation. We generated time calibrated phylogenetic trees from the topologies generated via ASTRAL III using the MCMCTree program in the PAML package (Yang 1997, 2007). For these analyses, we follow this program's requirement by setting all branch lengths in the input phylogeny to the same length. We then used PAML's BASEML function to generate branch lengths for the input topology via Maximum Likelihood as a single partition with the GTR + Gamma model (dividing the alignment into multiple partitions would be computationally intractable). For the calibration ages, we calibrated the phylogeny using divergence dates estimated from Feng et al. (2017) for shared nodes, which estimated a time-calibrated phylogeny across all anurans using 8 fossil calibration points and 95 loci. We selected three calibration points using the highest posterior density 95% confidence intervals (HPD 95% CI), which were: 1) The crown age of Cophylinae (all genera except basal *Madecassophryne* which was not included in Feng et al. 2017) of 27.6–44.1 Myr; 2) the crown age of Scaphiophryninae of 41.4–58.2 Myr; and 3) the age of Scaphiophryninae + Cophylinae at 50.2–66.1 Myr.

For MCMCTree analyses of the input phylogeny with branch lengths generated via BASEML, we set priors as follows: (a) overall substitution rate: rgene gamma = (1, 16.7, 1), (b) rate drift parameter: sigma2 gamma = (1, 4.5, 1); (c) alpha for gamma rates at sites = 0.5. We next applied a T probability distribution between the age ranges above with soft bounds and 2.5 percent tail probabilities. We set rate priors for internal nodes using the independent rates model. We ran MCMCTree for 100,000 generations, sampling every 100 generations, with a burn-in of 25 percent and ran each analysis twice to assess convergence.

Morphological and ecological data collection

Morphometrics. External morphometric measurements were taken from specimens by the first author using a digital calliper to the nearest 0.01 mm, rounded to 0.1 mm. The following measure-

Results

ments were taken: SVL, snout–vent length; HW, head width at widest point; HL, head length, from the commissure of the law to the anterior-most point of the jaw diagonally; ED, eye diameter at widest point; END, eye–nostril distance, from the anterior edge of the eye to the centre of the nares; NND, nostril–nostril distance, from their centres; TDH, horizontal tympanum diameter; TDV, vertical tympanum diameter; HaL, hand length, from the base of the manus to the tip of the longest (third) finger; LAL, lower-arm length, from the base of the manus to the humero-radioulnar articulation; UAL, upper arm length, posteriorly along the brachium from its insertion to the humero-radioulnar articulation; FARL, forearm length, given by the sum of HaL and LAL; FORL, forelimb length, given by the sum of HaL, LAL, and UAL; THIL, thigh length, from the cloaca to the knee; THIW, thigh width, at the widest point lateral to the abdomen; TIBL, tibia length, from the knee to the tibiotarsal articulation; TIBW, tibia width at widest point; TARL, tarsus length, from tibiotarsal articulation to the tarsal-metatarsal articulation; FOL, foot length, from the tarsal-metatarsal articulation to the end of the longest (fourth) toe; HIL, hindlimb length, given by the sum of THIL, TIBL, TARL, and FOL; IMCL, inner metacarpal tubercle length; IMTL, inner metatarsal tubercle length. A complete database of measured specimens is provided as Supplementary Table 4. Size dimorphism was calculated by the largest known male body size divided by the largest known female body size of each species, where available.

We followed the terminological scheme of **chapter 9** to refer to miniaturised lineages, expanded also to include larger body size ranges: ‘extremely miniaturised’ ≤ 12 mm < ‘highly miniaturised’ ≤ 16 mm < ‘miniaturised’ ≤ 20 mm < ‘small’ ≤ 24 mm < ‘medium’ ≤ 36 mm < ‘large’. These cut-offs were used in reconstructing the number of miniaturisation events within the subfamily (see below).

Ecology. Ecological data on species was coded based on our own observations and data available in the literature, primarily Glaw and Vences (2007) and subsequent publications. Species were coded as being terrestrial, arboreal, scansorial, fossorial, or rupicolous.

Comparative evolutionary analysis.

Comparative evolutionary analysis was conducted in R 3.5.2 (R Core Team 2014), mostly in the RStudio 1.1.423 environment (RStudio Team 2016).

Biogeographic reconstruction. Biogeography was reconstructed using BioGeoBEARS (Bio-Geography with Bayesian (and Likelihood) Evolutionary Analysis in R Scripts; Matzke 2014). Our approach followed that recently employed for Madagascan frogs of the genus *Boophis* (Hutter et al. 2018). Distribution of tips was coded based on published and unpublished data into the ten ecoregions Boumans et al. (2007), which are based on Wilmé et al. (2006): Sambirano, North, North East, North Central-East, South Central-East, South East, South, West, Central, and North West. We tested the LaGrange DEC (Dispersal-Extinction-Cladogenesis), DIVALIKE (Dispersal-Vicariance Analysis), and BayArea-like models. Founder events (models +J) were not run, due to concerns that these violate the time-dependent nature of biogeographic reconstructions (Ree and Sanmartín 2018), and because Madagascar, as a continent-like setting, is *a priori* considered unlikely to have founder-event speciation. Maximum ancestral range was set as five areas (the maximum in our extant taxon set). Models were compared based on Akaike Information Criterion (AIC) weights.

Phylogenetic Principal Component Analysis. Phylogenetic Principal Component Analysis (pPCA) was conducted on morphometric data using the PHYL.PCA() function in the PHYTOOLS 0.6-60 package in R (Revell 2012). We performed phylogenetic regression of data against body size

(Revell 2009) using the `PHYL.RESID()` function in `PHYTOOLS`, and performed pPCA on the covariance matrix of SVL and measurement residuals, under Pagel's λ model. By doing so, pPCA axes are rendered both evolutionarily orthogonal and phylogenetically uncorrelated (Revell 2009), and capture shape variation, so downstream analyses were conducted on principal components (PCs).

Ancestral state reconstruction. Ancestral state reconstruction was conducted using `PHYTOOLS`. Continuous characters were mapped using the `CONTMAP()` function, which uses ML estimation of states at nodes with the `FASTANC()` function by re-rotting the tree at all internal nodes and computing the contrasts state of the root under each configuration (Revell 2012), and interpolates states along edges following Felsenstein (1985). Ecological evolution was mapped using the ML-based `ACE()` function in the package `APE` (Paradis et al. 2004), which uses a joint estimation procedure from tip and branch data descending from each node to estimate the state at the node. We implemented a model with equal rates.

Testing ecological correlation of traits. We tested for differences in continuous variables and PCs between species ecologies using phylogenetic ANOVA with the function `PHYLANOVA()` in `PHYTOOLS` (Revell 2012). Ecological niches were supplied as the grouping factors. P-values were based on 1000 simulations (Garland et al. 1993). Post-hoc tests were conducted with Holm-adjusted P-values (Holm 1979). We also performed these tests for miniaturised versus non-miniaturised species, using a threshold of 20 mm as the boundary between these classes.

Phylogenetic signal. We tested the phylogenetic signal of ecological and morphological evolution of characters using the function `PHYLOSIG()` in `PHYTOOLS`. This function evaluates the strength of phylogenetic signal according to Pagel's λ (Pagel 1999) and Blomberg's K (Blomberg et al. 2003). Phylogenetic signal analysis was not conducted on PCs, as pPCA results in phylogenetically uncorrelated axes.

Results

Molecular phylogeny of the Cophylinae

Transcriptomes were produced from ten ingroup taxa (all nominal genera except *Anilany*) and two outgroups (*Dyscophus guineti* and *Scaphiophryne calcarata*). The sequence-capture (SC) dataset consisted of 31 ingroup taxa and five species of the subfamilies Scaphiophryinae and Dyscophinae as hierarchical outgroups. Due to the minimal overlap in the alignments between the transcriptomic and SC datasets, we consider them to constitute pseudo-independent tests of phylogenetic relationships. These two genomic approaches produced a congruent backbone for the phylogeny of genera within Cophylinae (Fig. 1; full trees are provided as Supplementary Trees): A basal split between all taxa and *Madecassophryne*, followed by a major divide between the *Rhombophryne*-clade (*Rhombophryne*, *Stumpffia*, and *Anilany*) and the *Cophyla*-clade (*Cophyla*, *Platypelis*, *Plethodontohyla*, *Mini*, and *Anodonthyla*) were found in all phylogenies and configurations. Within the *Cophyla*-clade, *Anodonthyla* was always the most basally diverging genus, and *Plethodontohyla*+*Mini* were always recovered as sister to the *Cophyla*+*Platypelis* clade.

The transcriptome dataset lacked *Anilany* and was therefore inadequate for testing the hypothesis of reciprocal monophyly of *Stumpffia* and *Rhombophryne*. SC datasets recovered reciprocally monophyletic *Rhombophryne* and *Stumpffia*, with *Anilany* always placed sister to *Stumpffia*. *Rhombophryne proportionalis* fell sister to other *Rhombophryne* in the SC dataset, but sampling of that genus was not adequate to test whether or not the species falls within it or sister to it. This

Results

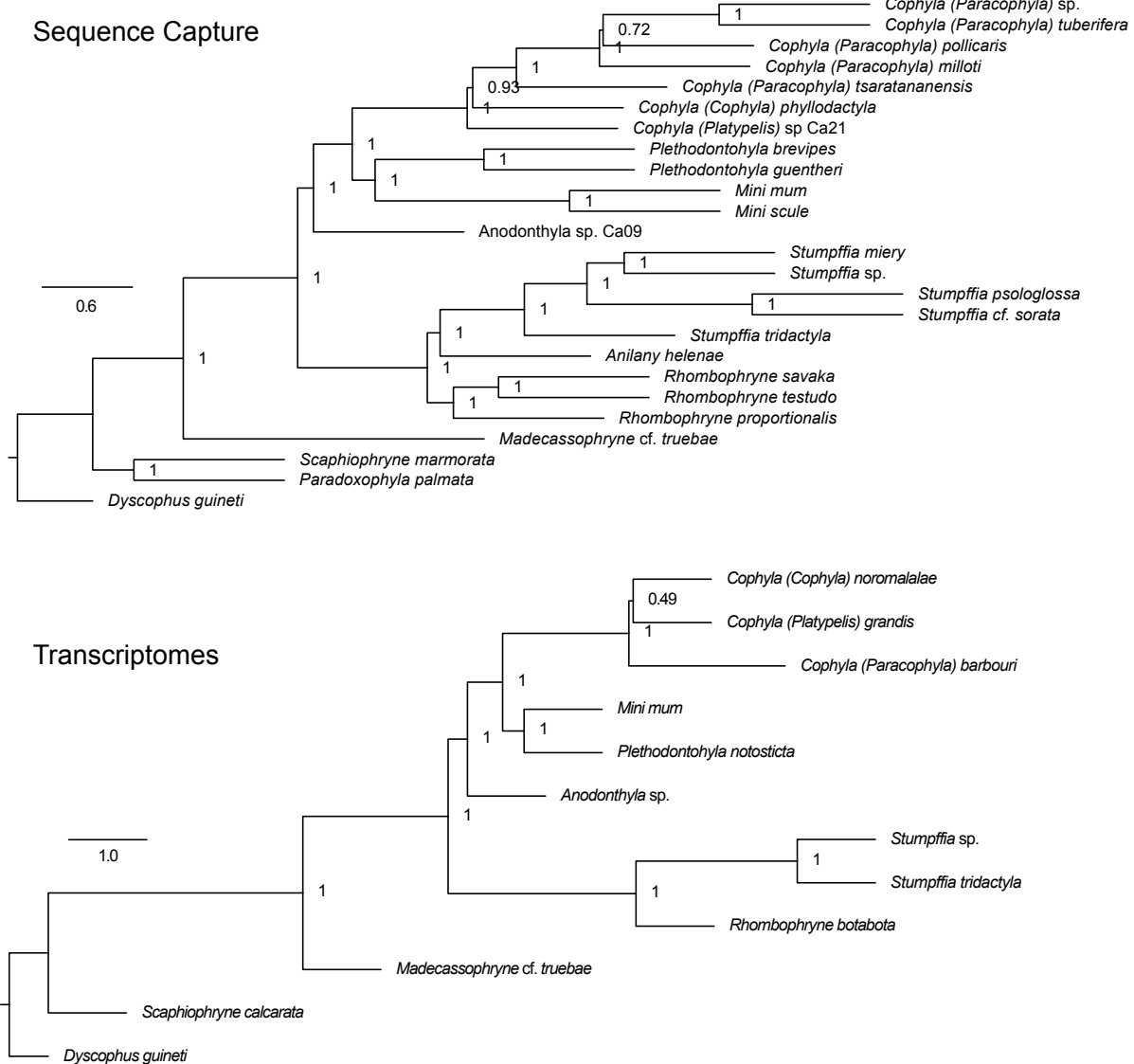


Fig. 1. Multiple Species Coalescent Model phylogenomic trees reconstructed from codons within Sequence Capture and Transcriptome datasets in ASTRAL-III.

Numbers at nodes represent quartet support (a metric of the degree of gene tree conflict around the branch; Sayyari and Mirarab 2016).

genomic support for the monophyly and distinctness of these genera provides unequivocal support for the continued recognition of all three genera as taxonomically valid, supported also on morphological grounds (see below).

In transcriptomic trees, *Platypelis* was found to be paraphyletic, with *P. barbouri* sister to a clade consisting of *P. grandis* and *Cophyla* (Fig. 1). In SC trees, *Platypelis grandis* was recovered as paraphyletic in trees constructed under the Multiple Species Coalescent Model (reconstructed in ASTRAL-III), with one lineage basally diverging from the whole clade and another sister to *Cophyla* (Fig. 1). Most phylogenies lacked this second *P. grandis*, and placed *P. grandis* sister to *Cophyla+Platypelis* (Supplementary Trees). Below, we discuss the ramifications of these findings and propose taxonomic changes to accommodate them.

Our species-level phylogeny contains 204 tips. Our dated phylogeny (conducted with MCMC-Tree) suggests that Cophylinae and Scaphiophryinae diverged in the late Palaeocene, 54.71–75.53 Ma b.p. (Fig. 2). *Madecassophryne* diverged in the early Eocene, 50.21–66.18 Ma b.p.

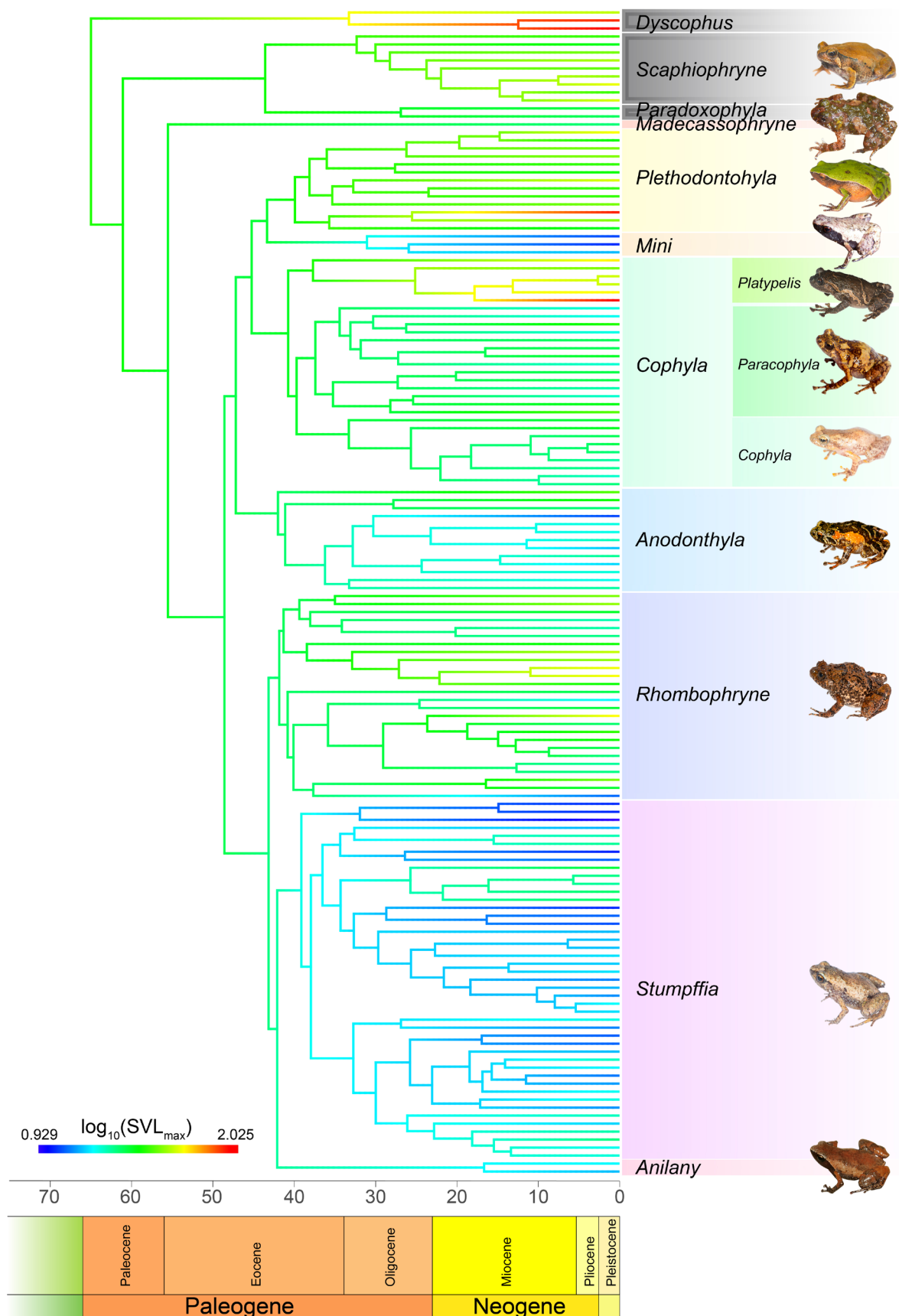
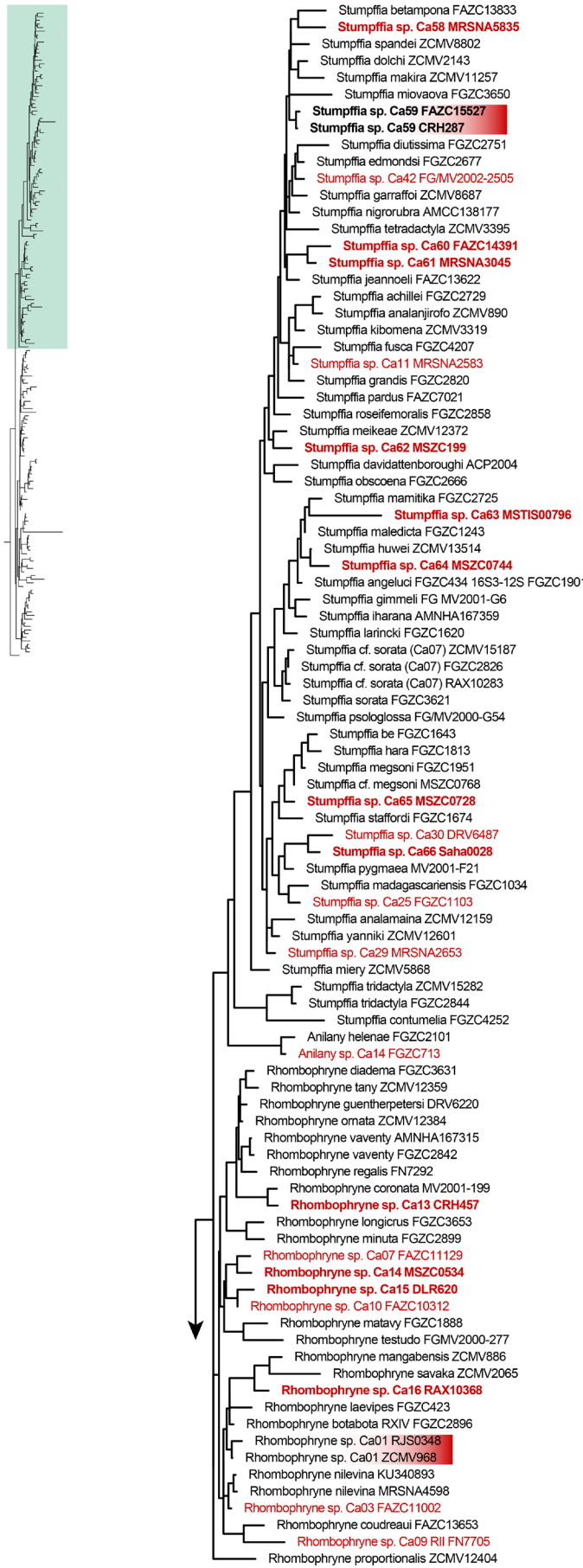


Fig. 2. Dated phylogeny and ancestral size reconstruction of $\log_{10}(\text{SVL}_{\text{max}})$ of the Cophylinae.
Inset frog photos are scaled to be equal in size.

Results



with the major clades mentioned above diverging in the Eocene 45.07–54.19 Ma b.p. By ca. 40 Ma b.p., all currently recognised genera had diverged.

We reconstructed a taxon-dense 3' 16S rRNA tree in order to identify undescribed species-level lineages within the Cophylinae that do not yet bear candidate numbers, in order to update our estimate of the taxonomic gap present in this subfamily (Fig. 3). It contained 176 ingroup tips, constituting 141 lineages differing by at least 3% uncorrected p-distance from all other tips. Five pairs of nominal taxa were found to differ by less than 3% in this fragment, but all differed by at least 2% except *Anodonthyla nigrigularis* and *A. moramora* (1.5%), which however differ by 3.7% in the 5' fragment of the 16S rRNA gene. Of the recognised lineages, 32 are newly identified in this study or have been found in previous studies but not assigned candidate species status. Following thresholds established previously (Vieites et al. 2009), we consider these to constitute new candidate species and assign them new candidate numbers in Supplementary Table 5. In several cases, species complexes exist where the nominal species cannot be distinguished among the possible lineages, namely *Platypelis grandis* (four potential lineages), *Plethodontohyla ocellata* (two), *P. notosticta* (two), *P. tetra* (five), and *Anodonthyla boulengeri* (five). In these instances, we have tentatively assigned the name to

← Fig. 3. Maximum likelihood reconstruction of the 3' 16S rRNA mitochondrial gene fragment for the Cophylinae.

Red tips are candidate species, red shaded lineages together represent a singly candidate species. Bolded names are those established for the first time in this study. Continued below. Outgroups (Scaphiophryiniae and Dyscophiniae) omitted for graphical purposes.

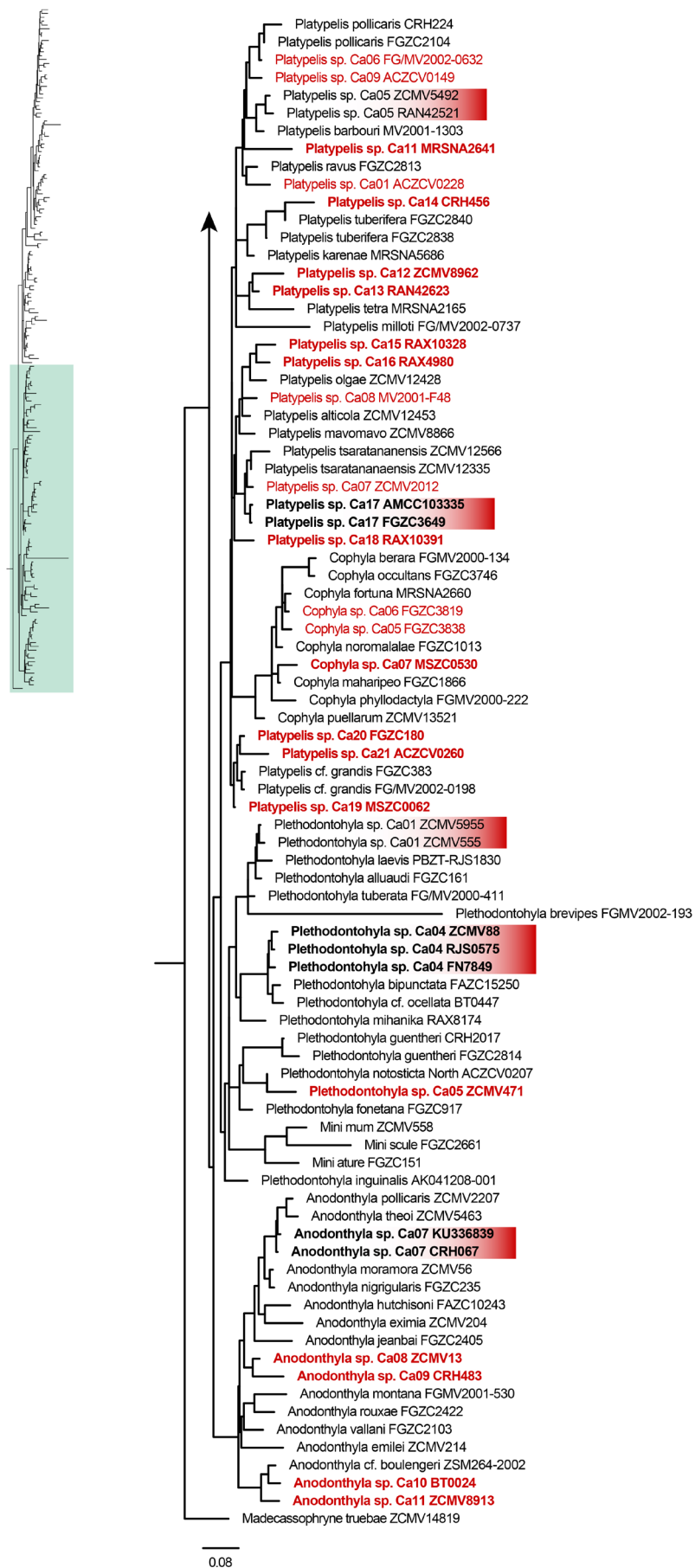


Fig. 3. continued

either (a) the lineage known to occur closest to the type locality, or (b) the most widespread lineage. These cases will need to be studied in more detail to establish the correct assignment of names.

Taxonomic reconciliation of *Platypelis* and *Cophyla*

The paraphyly of *Platypelis* must be taxonomically reconciled. There are two alternative solutions: (1) synonymising the clade within the genus *Cophyla* as proposed by Peloso et al. (2016, 2017), or (2) dividing the clade into three separate genera. There are advantages to either option: with the former, the diagnosability of the clade becomes indisputable, and its long-term stability is assured. With the latter, more subtle distinctions are possible among genera, and the divergent morphology of *P. grandis* no longer need be reconciled within the diversity of *Platypelis*, enhancing diagnosability of both genera. We opt for a compromise: we herewith formally sink these taxa into *Cophyla*, but we erect three subgenera: *Cophyla* Boettger, 1880 (contents unchanged), *Platypelis* Boulenger, 1882 (restricted to *P. grandis* and *P. cowanii* [type species], which are morphologically undoubtedly closely related), and we resurrect *Paracophyla* Millot & Guibé, 1951 (type species *P. tuberculata*, a synonym of *P. barbouri*) for the third subgenus, containing all other *Platypelis* species. For distinction among these subgenera, see the discussion.

Results

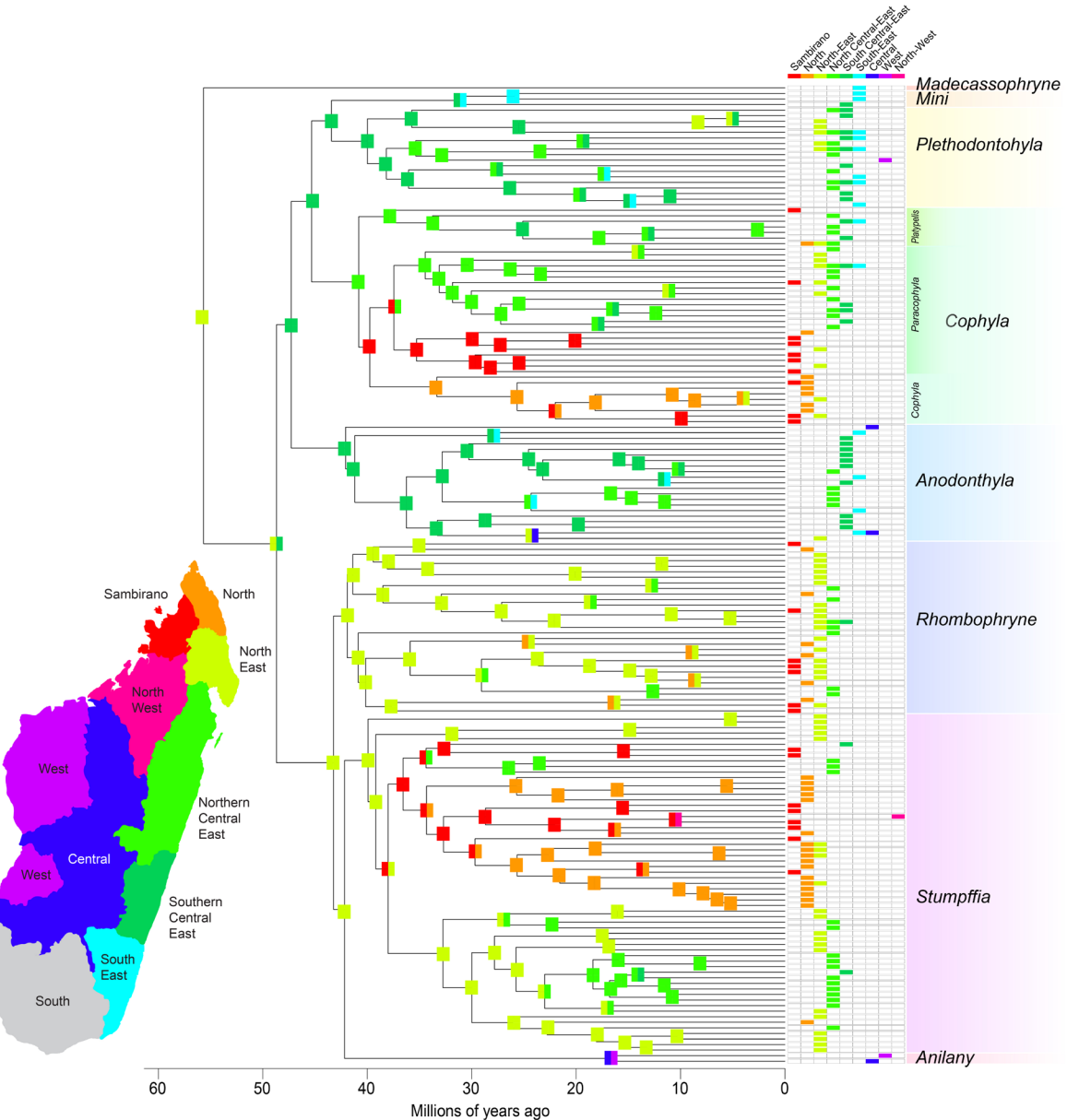


Fig. 4. Biogeographic reconstruction of the subfamily Cophylinae under the DIVALIKE model of BioGeoBEARS.

Squares at nodes indicate most likely distributions, and colours correspond regions on the map. Outgroups (Scaphiophryinae and Dyscophinae) omitted for graphical purposes.

Biogeography

BioGeoBEARS recovered DIVALIKE as the optimal model (Table 2, Fig. 4). This model places the origin of the subfamily in the North East of Madagascar, and the major division between the *Cophyla*- and *Rhombophryne*-clades being one between the South Central East and North East, respectively. The largely terrestrial genera of the latter clade apparently originated in the north of

Table 2. BioGeoBEARS model values.

Model	Log likelihood	Parameters	Dispersal	Extinction	AIC
DIVALIKE	-749.89382	2	0.01	0.01	1503.8
DEC	-772.47225	2	0.01	0.01	1548.9
BAYAREALIKE	-865.98532	2	0.01	0.01	1736.0

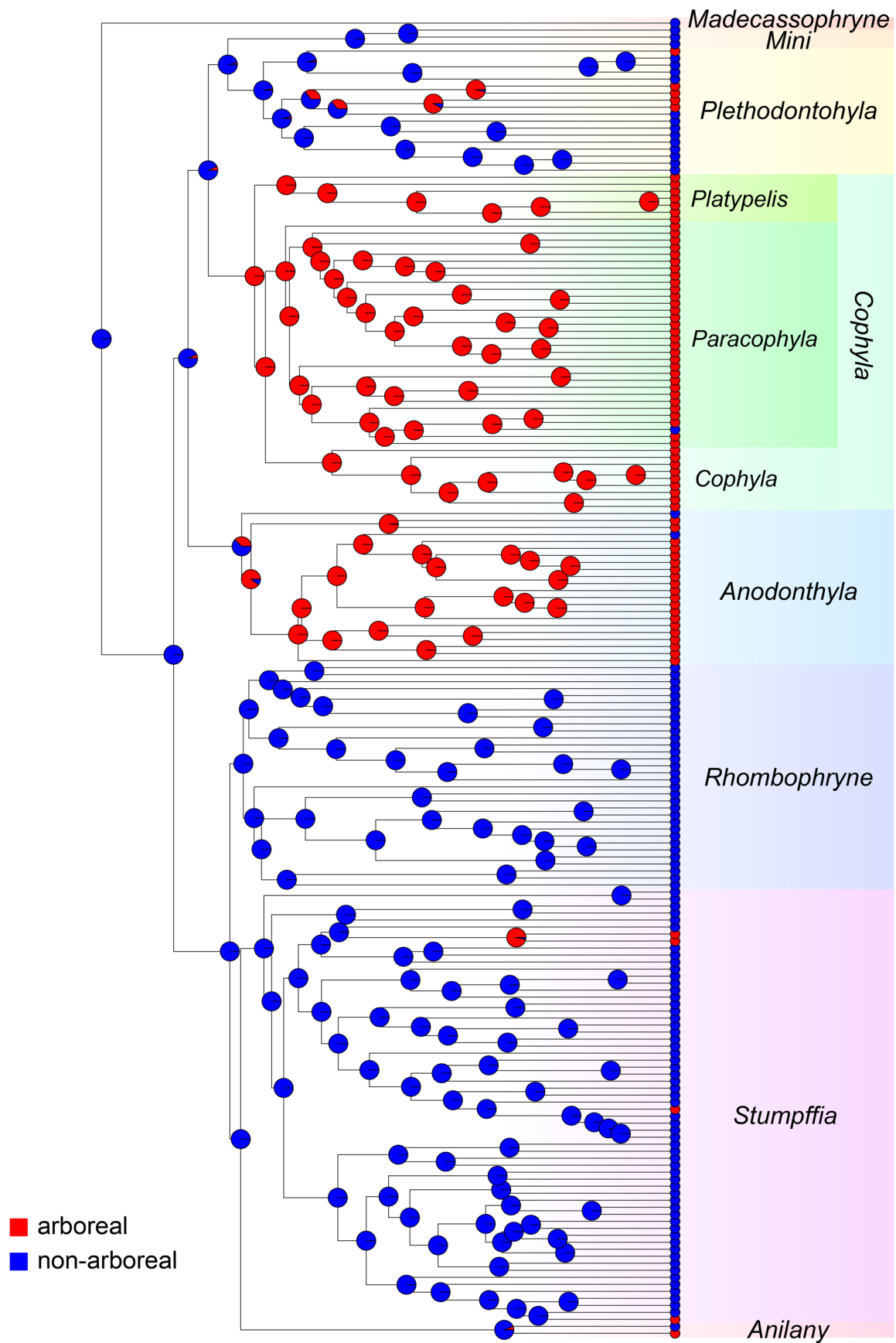


Fig. 5. Ancestral reconstruction of arboreality within Cophylinae.

Pie slices indicate relative likelihood of either state at each node. Outgroups (Scaphiophryninae and Dyboschinae) omitted for graphical purposes.

Results

the island, whereas the largely arboreal species originated in the Central East. Both clades subsequently exchanged lineages, starting with a move northward in *Cophyla* around 40 Ma, and several clades of *Rhombophryne* and *Stumpffia* moving southwards around 30 Ma.

Body size evolution

Body size evolution within Cophylinae was found to have strong phylogenetic signal (Pagel's λ 1.039541, $P = 3.808702 \times 10^{-34}$; Blomberg's $K = 2.082735$, $P = 0.001$). Ancestral size reconstruction estimated the ancestral body size of all cophylines at 29.4 mm (95% CI: 22.0–39.1 mm; Fig. 2, Supplementary Table 6). The first major divide within the subfamily, that between the *Cophyla*-clade and the *Rhombophryne*-clade, came with a slight decrease in body size of the latter (23.7 mm, 95% CI: 20.0–28.1 mm) compared to the former (27.0 mm, 95% CI: 22.4–32.5 mm). Three genera, namely *Stumpffia*, *Anilany*, and *Mini* have an estimated ancestral body size under 20 mm (*Stumpffia* 18.4 mm [95% CI: 15.4–22.1 mm], *Anilany* 17.4 mm [13.1–23.2 mm], *Mini* 18.3 mm [13.6–24.4 mm]). Body size over 30 mm was reconstructed at the base of *Platypelis* s. s. (33.6 mm, 95% CI: 26.5–42.7 mm) and *Plethodontohyla* (33.2 mm, 95% CI: 27.0–40.8 mm).

Nine species-level lineages consist of species under 12 mm, but only two pairs (*Stumpffia tridactyla* and *S. contumelia*, and *Mini scule* and *M. mum*) stem from an ancestor reconstructed as probably being also extremely miniaturised—all other lineages have apparently achieved these sizes independently, meaning seven lineages have independently converged on extremely miniaturised body sizes. Additionally, *Rhombophryne proportionalis*, though not an extremely miniaturised species, has apparently reached a highly miniaturised state from a medium to large ancestor, making it remarkable within the subfamily.

Stumpffia appears to have originated from a highly miniaturised ancestor, and within *Stumpffia* two moderately diverse lineages (*S. be* species group and *S. grandis* species group) have apparently transitioned back to larger body sizes from miniaturised states, and *S. meikeae* and *S. nigrorubra* also apparently have returned to larger body sizes from clades with highly miniaturised ancestors.

Ecomorphological evolution

Ancestral state reconstruction of arboreality vs. non-arboreal habits found the ancestral state of cophylines to be non-arboreal, with a likelihood of 0.999 (Fig. 5). Transition rate between arboreal and terrestrial and back under an equal rates model was 0.2475 (SE = 0.0538). The divergence of the two major clades (*Rhombophryne*-clade and *Cophyla*-clade) was not initially linked with an ecological transition, but rather the major transitions to arboreality are reconstructed as having occurred twice in the *Cophyla*-clade, i.e. once within *Anodonthyla* subsequent to the divergence of *A. montana*, and once at the base of *Cophyla* s. l. The scansorial species of *Plethodontohyla* do not form a monophyletic group and are reconstructed instead as three independent transitions to arboreality. Within *Cophyla* s. l. and *Anodonthyla*, one lineage each has transitioned to terrestriality. In the former, this is a montane species, *C. (P.) olgae*, which has apparently become rupicolous or terrestrial, whereas in *Anodonthyla*, the hyper-miniaturised *A. eximia* has transitioned to becoming terrestrial. For a more extensive ecomorphological reconstruction using finer ecological classes, see Supplementary Figure 1.

Body sizes do not differ between arboreal and non-arboreal species (phyloANOVA, $F = 4.792862$, $P = 0.435$), but finger and toe widths do (third finger tip width, phyloANOVA, $F = 31.047117$, $P = 0.001$; fourth toe tip width, phyloANOVA, $F = 56.367296$, $P = 0.001$).

In a pPCA of the morphometric data on cophylines (Fig. 6; corrected for body size, see methods above), the first principal component (PC1) is strongly weighted by hindlimb length (thigh, tibia, and foot length, all negative), PC2 is strongly negatively weighted by head and thigh width and positively weighted by upper and lower arm length, PC3 is strongly weighted by foot length (neg-

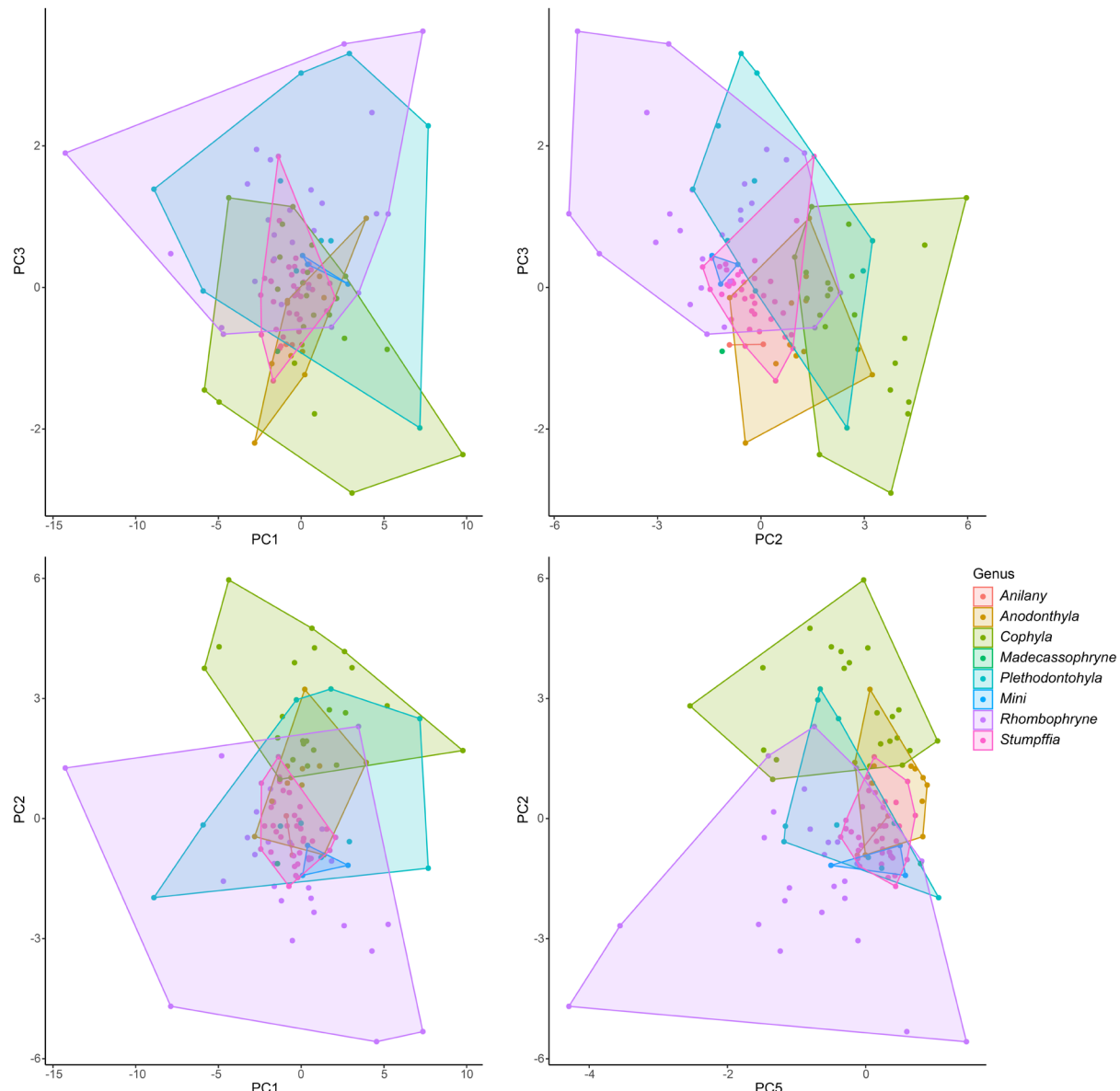


Fig. 6. Phylogenetic Principal Component Analysis plots of cophyline morphometric data.

ative) and its inverse relationship with thigh length and head width (positive), and PC4 is strongly negatively weighted by hand length and head width. Together, these four PCs account for 82% of the variation in the data, and ten components are required to account for 95%.

In phylogenetic ANOVA on the first ten PCs, only three were found to differ significantly among arboreal and non-arboreal species: PC2 ($F = 75.333178$, $P = 0.002$), PC8 (weighted strongly only by foot length; $F = 23.440843$, $P = 0.031$), and PC9 (weighted strongly positively by tarsus length and negatively by upper arm length and thigh width; $F = 26.604865$, $P = 0.019$). In pairwise tests based on more refined ecological classifications, significant differences were found in PC1 between fossorial and terrestrial species ($t = 3.753434$, $P = 0.04$), suggesting that fossoriality invokes major morphological changes related to head and thigh width (typified by the *Rhombophryne testudo* species group, which have exceptionally short limbs and broad heads). PC2 was significantly different among finer ecology classifications ($F = 27.696988$, $P = 0.001$). Of the non-arboreal species, only rupicolous species do not differ from arboreal species in PC2 (rupicolous vs arboreal, $t = 3.032399$, $P = 0.352$; rupicolous vs scansorial, $t = 2.067363$, $P = 0.477$), indicating that rupicolous species strongly resemble arboreal species in head and thigh widths, and in forelimb lengths, consistent with their clambering behaviour, lending credence to our combining these factors in our ancestral state reconstruction, above. Finger and toe tip measurements had only weak weights in

Results

all of these first ten components.

Of the first ten PCs, only PC5 was found to be significantly associated with miniaturisation (phyloANOVA, $F = 14.650061$, $P = 0.039$), and miniature and non-miniaturised species differed strongly in variance (F-test, $F_{45,61} = 0.1115$, $P = 4.447 \times 10^{-12}$). PC5 was loaded most strongly positively by thigh length and width, and negatively by tibia length.

Discussion

We have here provided the most robust phylogenetic analysis of the subfamily Cophylinae to date. Our genomic analyses, composed of both sequence capture (SC) and transcriptomic data, have resolved most of the phylogenetic relationships within the subfamily, including confidently showing that (1) *Madecassophryne* is the basal-most member of the subfamily, and is highly isolated from all other taxa, (2) *Anilany* is consistently recovered as sister to *Stumpffia* (present in SC datasets only), and these are sister to *Rhombophryne*, forming one of the two major clades within the subfamily, (3) a second major clade is composed of *Anodonthyla*, *Plethodontohyla* and *Mini*, and *Cophyla* s. l., in which *Anodonthyla* diverged first, followed by the divergence between *Cophyla* s. l. and *Plethodontohyla* and *Mini*, and (4) *Platypelis* as formerly defined is taxonomically unstable and occasionally recovered as paraphyletic. The overall topology corroborates that recovered in the most recent study on microhylids as a whole (Tu et al. 2018).

Although the resolution is dramatically improved in comparison to previous work, containing several orders of magnitude more sequence data, some nodes within the subfamily remain unresolved. In particular the nodes within the redefined genus *Cophyla* are unstable. It is not clear to which subgenus *Platypelis* is most closely related; it was reconstructed as basally divergent, and sister to subgenus *Cophyla* in various different analyses. A broader taxon sampling within these clades will be needed to establish whether this is an artefact of our sampling, or whether other patterns such as incomplete lineage sorting may be responsible for the lack of resolution.

In order to reconcile the non-monophyly of *Platypelis* as previously defined, we have subsumed it as a subgenus within *Cophyla*, restricted it to *Platypelis grandis* and *P. cowanii*, and resurrected the former genus-level name *Paracophyla* for the other taxa formerly assigned to *Platypelis*. This action is in accordance with the proposed criteria for economy of changes to Linnaean classification schemes (Vences et al. 2013), specifically:

(1) the Monophyly Criterion: the newly defined genus is unquestionably monophyletic, whereas *Platypelis* as previously defined was found to be paraphyletic. The proposed subgenera are also monophyletic according to our current knowledge.

(2) the Clade Stability Criterion: under our revised taxonomy, the genus *Cophyla* is unquestionably stable and monophyletic. We have opted to erect subgenera instead of recognising the individual clades as genera in order to ensure that that Clade Stability of the genus is upheld. Our analyses showed that the relationships among *Platypelis* s. s. and the other subgenera are not wholly stable, and therefore treating these as separate genera would be a less stable solution than subsuming them within a single genus, while also erecting subgenera for the three diagnosable clades within the genus.

(3) the Phenotypic Diagnosability Criterion: the genus *Cophyla* as redefined here is much easier to diagnose than previously; it contains most of the arboreal members of the Cophylinae, and can be distinguished from *Anodonthyla* (mostly arboreal) by the presence of teeth in most individuals and absence of flared humeral crests and cuneate prepollex in males (the prepollex can be long, but when it is, it is also very broad and not pointed, as in *Anodonthyla*), and from arboreal *Plethodontohyla* by the different body shape and the absence of a distinct colour border between the dorsum and the venter. The individual subgenera are also more easily diagnosable than the previous two-genus taxonomy, because *Platypelis* and *Paracophyla* are now restricted, and differences

between them can be highlighted. The circumscription of the three subgenera is straightforward: *Platypelis* s. s. are comparatively large-bodied frogs (SVL 30–106 mm) with broad heads (HW/HL 1.35–1.89), generally rough skin, strongly expanded terminal discs, clavicles present, and paired post-choanal vomers; *Paracophyla* are small to moderate-sized frogs (SVL 16.1–39.3 mm) with moderately broad heads (HW/HL 0.96–1.54), smooth to rough skin, moderately to strongly expanded terminal discs, clavicles present, and paired or reduced post-choanal vomers; and *Cophyla* s. s. are moderate-sized frogs (SVL 17.5–33.6 mm) with moderately broad heads (HW/HL 1.03–1.42), generally smooth skin, moderately expanded terminal discs, lacking clavicles except in one species, and all possessing a single, medial post-choanal vomer.

Peloso et al. (2016) previously proposed also that *Platypelis* and *Cophyla* be subsumed into a single genus. Scherz et al. (2016) argued that this decision was premature for three reasons: (1) most of their samples concerning *Platypelis* and *Cophyla* were misidentified (two of their three ‘*Cophyla*’ samples were *Platypelis* [now *Paracophyla*] species); (2) previous studies looking specifically at these two genera had recovered them as reciprocally monophyletic and osteologically diagnosable (Rakotoarison et al. 2012, 2015); and (3) in our re-analysis with correctly identified specimens and considerably more data pertaining to this clade, we too recovered the genera to be reciprocally monophyletic, albeit with modest support (Scherz et al. 2016). In that study, we recommended that the taxonomic changes proposed by Peloso et al. (2016) be rejected pending more information. Here we have provided that additional information and found that the clade does indeed merit recognition as a single genus.

Revising the number of candidate species in Cophylinae

The formal numbering of candidate species of Vieites et al. (2009) recognised 57 candidate species within the Cophylinae. 38 of those original candidates have since been taxonomically addressed, with five being assigned to existing names (Rakotoarison et al. 2017a, in press; Bellati et al. 2018), and the rest becoming new species. New candidate numbers within this scheme have also been assigned (Klages et al. 2013; Perl et al. 2014; Rakotoarison et al. 2015, 2017a; Scherz et al. 2016). However, in several cases candidate numbers within *Stumpffia* have been given to two separate clades. Several publications following Klages et al. (2013) made use of candidate numbers submitted to GenBank by those authors that were not published in the text—published were numbers up to and including *Stumpffia* sp. 31, but numbers spp. 32–43 were submitted to GenBank. More confusingly still, this has not been done in a consistent manner. For example, the candidate numbers *S.* spp. Ca35, Ca37, and Ca41 used in Scherz et al. (2016) refer to those numbers from the GenBank series of Klages et al. (2013), but Ca32 in Scherz et al. (2016) refers to the Ca32 of Perl et al. (2014), not that of Klages et al. (2013). Similarly, Ca53 was deposited in GenBank by Rakotoarison et al. (2017a) but never mentioned in the text, and was published for the first time in a phylogeny by Tu et al. (2018) (it is not a *Stumpffia* but a species of *Mini*, see **chapter 9**). In addition to these numbered candidate species, several have been identified without assigning new numbers (Scherz et al. 2016; Penny et al. 2017; Bellati et al. 2018), and a number of taxa in Peloso et al. (2016) were identified as distinct candidate species by Scherz et al. (2016).

The production of our specimen-level supermatrix allowed us to reconcile the various informal names applied to significant lineages within the Cophylinae. In Fig. 3 and Supplementary Table 5, we have provided new candidate numbers for all hitherto unnumbered candidate lineages following the justifications and thresholds of Vieites et al. (2009). This results in a total of 52 candidate species. The genus breakdown of these candidates is as follows: *Anodonthyla* (5), *Mini* (0), *Made-cassophryne* (0), *Rhombophryne* (9), *Plethodontohyla* (3), *Cophyla* (*Paracophyla*: 14, *Cophyla*: 3, *Platypelis*: 3), *Stumpffia* (14), and *Anilany* (1). In summary, despite ten years of taxonomic progress, including the description or resurrection of 54 species, the number of candidate species has decreased by just five. Species discovery is almost keeping pace with our rate of description.

Results

We note also that additional candidate numbers will eventually need to be given for lineages that are present in other genes in our supermatrix but not the analysed segment of the 16S rRNA gene.

Biogeography

It has long been clear that the Cophylinae have their centre of diversity and endemism in northern Madagascar (Wollenberg et al. 2008; Brown et al. 2014, 2016). Our analysis also found the North East of the island also to be the centre of origin of the subfamily. This is surprising for two reasons: (1) one of the major clades originated in the South East or South Central East, and (2) the most basally divergent lineage, *Madecassophryne*, is restricted to the South East of the island (Rakotoarison et al. 2017b). This suggests that *Madecassophryne* and the *Cophyla*-clade may have independently expanded from the North East southwards, along with several additional southward expansions of individual taxa or small clades.

The divergence between the *Rhombophryne*-clade (*Rhombophryne*, *Stumpffia*, and *Anilany*) and the *Cophyla*-clade (*Cophyla*, *Platypelis*, *Plethodontohyla*, *Mini*, and *Anodonthyla*) was associated with a major geographic shift in the early Eocene, with the former clade originating in the North East, while the latter clade originated in the South Central-East. Within the *Rhombophryne*-clade, most species remained in the north, with transitions between the North East, North, and Sambirano regions, with a few taxa moving south into the North Central-East repeatedly. The origin of *Anilany* is associated with a movement into Central and West Madagascar, away from *Stumpffia* and *Rhombophryne*. Within the *Cophyla*-clade, *Anodonthyla* originated in the South Central East and spread southwards. *Cophyla* and *Platypelis* moved northwards, with radiations occurring in the North Central-East, and the origin of *Cophyla* in particular associated with a diversification in the North. *Plethodontohyla* radiated northwards from the South Central-East, while their sister clade moved south to the South East.

In the mid-to-late Eocene, between 35 and 40 Ma, two clades, namely *Paracophyla* + *Cophyla* s.s. and a major clade within *Stumpffia* moved into the Sambirano region and thence into the North. In the former clade, this transition was preceded by a spread north through the North Central East. The timing of these movements coincide with warming and increasing moisture across the whole of the island, and in the Sambirano region in particular (see Ali and Huber 2010).

Andreone et al. (2005) suggested that if microhylids were present in Madagascar during the Mesozoic, they would likely have been adapted to seasonal, drier climes initially, and later colonised forests as they spread across Madagascar. Our reconstruction places the diversification of these frogs post-Mesozoic, but is still consistent with their diversification being associated with the humidification of the island during the Eocene. The initial spread of the frogs may have been tied with the expansion of rainforests along the east of the island, but this remains speculative.

Ecomorphological evolution

The evolution of ecomorphology within the Cophylinae has been dynamic, involving repeated transitions between states. This fact was highlighted already in the first genetic study to look at the subfamily in detail (Andreone et al. 2005). In that study, it was stated that it was ‘difficult to make statements about their ancestral life style, i.e., whether they were terrestrial or arboreal.’ This we have now clarified: Cophylinae were ancestrally terrestrial and evolved to become arboreal or scansorial around nine times independently. Andreone et al. (2005) suggested that *Anodonthyla montana* represented a transition to terrestrial from an arboreal ancestor. Interestingly, our ancestral state reconstruction suggests rather than the genus was ancestrally terrestrial and became arboreal only after the divergence of *A. montana*, with one transition to terrestrial occurring in the highly miniaturised *A. eximia*. However, it should be noted that the ancestral state of *Anodonthyla* is recovered with a partial likelihood of being arboreal, and *A. montana*, as a high-ele-

vation species, is consistent with the overall pattern of high-elevation endemics becoming more terrestrial. The only other transition from arboreality to terrestriality present in our reconstruction, namely *Cophyla (Paracophyla) olgae*, is also consistent with this pattern. We thus think it likely that the ecology of *A. montana* is secondarily terrestrial, and that elevation has indeed played a role in evolution of terrestriality in these frogs.

In our pPCA of morphometric relationships, the two axes explaining most variation (PCs 1 and 2) were related to fossoriality and arboreality. Morphologically, rupicolous cophyline species are highly similar to arboreal species, suggesting similar adaptive pressures between these two ecologies. This is consistent also with Australian microhylids living in boulder fields, with similarly enlarged fingers and scuttling locomotion (e.g. Hoskin 2013). Despite a significant association between arboreal habits and relatively broader finger and toe discs, these were not weighted strongly in PCs; the dominant axes of variation were related to proportions of the limbs and head.

Miniaturisation is perhaps the most remarkable evolutionary feature of the Cophylinae, as our phylogeny shows that they have repeatedly independently converged on body sizes under 12 mm, among the smallest frog species in the world (Supplementary Table 1). By correcting for body size in our pPCA, we were able to establish syndromes of miniaturisation beyond isometric scaling factors. PC5 was significantly correlated with miniaturisation; no other significant component correlations were found. This indicates that miniaturised species typically have relatively broader, longer thighs and relatively shorter tibias than non-miniaturised species. Variance in PC5 decreased dramatically with decreasing body size, suggesting that there may be constraints on this suite of characters in smaller frogs that do not act on larger species. Reduced body size is also associated with terrestrialisation (Supplementary Figure 2).

Osteology of the Cophylinae will be an important avenue for future exploration of ecomorphological evolution in these frogs. All nine instances of the evolution of arboreality reconstructed here are tied with the expansion of terminal phalanges into T- or Y-shaped elements. In **chapter 9** we showed that miniaturisation is associated with contingent, and not deterministic, osteological changes. In future, it will be interesting to establish the connection between ecology and osteology to features more likely to be driven by homoplasy through convergence than phylogeny.

Within the Microhylidae, only the subfamily Asterophryinae has more species than Cophylinae, and the two have approximately the same level of ecological diversity (Zweifel 1972; Burton 1986; AmphibiaWeb 2019). Numerous parallels exist between these two subfamilies. Both, for example, have high levels of variation in the state of the pectoral girdle, the shape and proportions of the skull, especially with respect to the palate, and terminal phalanges of the digits (Burton 1986). Comparison of the innumerable niche transitions within these two radiations will shed light on the way in which microhylids evolve morphological syndromes.

Acknowledgements

We wish to thank Joan Garcia-Porta and F. Andreone for their various contributions to this study. This project has been made possible by our long-term collaborations with the Mention Zoologie et Biodiversité Animale of the Université d’Antananarivo. We thank the Direction Général des Forêts and Madagascar national Parks for providing us with permits for fieldwork and export over the last three decades.

References

- Aberer AJ, Kober K, Stamatakis A (2014) ExaBayes: massively parallel Bayesian tree inference for the whole-genome era. *Molecular Biology and Evolution* 31(10): 2553–2556.
- Ali JR, Huber M (2010) Mammalian biodiversity on Madagascar controlled by ocean currents.

Results

- Nature 463: 653–656. doi:10.1038/nature08706
- AmphibiaWeb. (2019) AmphibiaWeb: Information on amphibian biology and conservation. Available at: <http://amphibiaweb.org>. Accessed 15 February 2019
- Andreone F, Vences M, Vieites DR, Glaw F, Meyer A (2005) Recurrent ecological adaptations revealed through a molecular analysis of the secretive cophyline frogs of Madagascar. Molecular Phylogenetics and Evolution 34(2): 315–322. doi:10.1016/j.ympev.2004.10.013
- Bankovich A, Nurk S, Antipov D, Gurevich AA, Dvorkin M, Kulikov AS, Lesin VM, Nikolenko SI, Pham S, Prjibelski AD, Pyshkin AV (2012) SPAdes: a new genome assembly algorithm and its applications to single-cell sequencing. Journal of Computational Biology 19(5): 455–477.
- Bellati A, Scherz MD, Megson S, Hyde Roberts S, Andreone F, Rosa GM, Noël J, Randrianirina JE, Fasola M, Glaw F, Crottini A (2018) Resurrection and re-description of *Plethodontohyla laevis* (Boettger, 1913) and transfer of *Rhombophryne alluaudi* (Mocquard, 1901) to the genus *Plethodontohyla* (Microhylidae: Cophylinae). Zoosystematics and Evolution 94(1): 109–135. doi:10.3897/zse.94.14698
- Bergmann PJ, Morinaga G (in press) The convergent evolution of snake-like forms by divergent evolutionary pathways in squamate reptiles. Evolution doi:10.1111/evo.13651
- Blackburn DC, Siler CD, Diesmos AC, McGuire JA, Cannatella DC, Brown RM (2013) An adaptive radiation of frogs in a Southeast Asian island archipelago. Evolution 67(9): 2631–2646. doi:10.1111/evo.12145
- Blomberg SP, Garland TJ, Ives AR (2003) Testing for phylogenetic signal in comparative data: Behavioral traits are more labile. Evolution 57: 717–745.
- Bossuyt F, Milinkovitch MC (2000) Convergent adaptive radiations in Madagascan and Asian ranid frogs reveal covariation between larval and adult traits. Proceedings of the national Academy of Sciences of the USA 97: 6585–6590.
- Boumans L, Vieites DR, Glaw F, Vences M (2007) Geographical patterns of deep mitochondrial differentiation in widespread Malagasy reptiles. Molecular Phylogenetics and Evolution 45(3): 822–839. doi:10.1016/j.ympev.2007.05.028
- Brown JL, Cameron A, Yoder AD, Vences M (2014) A necessarily complex model to explain the biogeography of the amphibians and reptiles of Madagascar. Nature Communications 5: 5046. doi:10.1038/ncomms6046
- Brown JL, Sillero N, Glaw F, Bora P, Vieites DR, Vences M (2016) Spatial biodiversity patterns of Madagascar’s amphibians and reptiles. PLoS One 11(1): e0144076. doi:10.1371/journal.pone.0144076
- Burton TC (1986) A reassessment of the Papuan subfamily Asterophryinae (Anura: Microhylidae). Records of the South Australian Museum 19: 405–450.
- Bushnell B, Rood J, Singer E (2017) BBMerge – Accurate paired shotgun read merging via overlap. PLoS ONE 12(10): e0185056. doi:10.1371/journal.pone.0185056
- Capella-Gutiérrez S, Silla-Martínez JM, Gabaldón T (2009) trimAl: a tool for automated alignment trimming in large-scale phylogenetic analyses. Bioinformatics 25(15): 1972–1973.
- Chen S, Huang T, Zhou Y, Han Y, Xu M, Gu J (2017) AfterQC: automatic filtering, trimming, error removing and quality control for fastq data. BMC Bioinformatics 18(13): 80.
- Chiari Y, Vences M, Vieites DR, Rabemananjara F, Bora P, Ramilijaona Ravoahangimalala O, Meyer A (2004) New evidence for parallel evolution of colour patterns in Malagasy poison frogs (Mantella). Mol Ecol 13(12): 3763–3774. doi:10.1111/j.1365-294X.2004.02367.x
- Clarke BT (1996) Small size in amphibians—its ecological and evolutionary implications. Sym-

- posia of the Zoological Society of London 69: 201–224.
- Colgan DJ, McLauchlan A, Wilson GDF, Livingston SP, Edgecombe GD, Macaranas J, Cassis G, Gray MR (1998) Histone H3 and U2 snRNA DNA sequences and arthropod molecular evolution. *Australian Journal of Zoology* 46: 419–437. doi:10.1071/ZO98048
- Degnan JH, Rosenberg NA (2009) Gene tree discordance, phylogenetic inference and the multi-species coalescent. *Trends in Ecology and Evolution* 24(6): 332–340.
- Felsenstein J (1985) Phylogenies and the comparative method. *American Naturalist* 125: 1–15.
- Feng Y-J, Blackburn DC, Liang D, Hillis DM, Wake DB, Cannatella DC, Zhang P (2017) Phylogenomics reveals rapid, simultaneous diversification of three major clades of Gondwanan frogs at the Cretaceous–Paleogene boundary. *Proceedings of the National Academy of Sciences of the USA* 114(29): E5864–E5870. doi:10.1073/pnas.1704632114
- Garland TJ, Dickerman AW, Janis CM, Jones JA (1993) Phylogenetic analysis of covariance by computer simulation. *Systematic Biology* 42: 265–292.
- Glaw F, Vences M (2007) A field guide to the amphibians and reptiles of Madagascar. Vences & Glaw Verlags GbR, Cologne, Germany, 496 pp.
- Grabherr MG, Haas BJ, Yassour M, Levin JZ, Thompson DA, Amit I, Adiconis X, Fan L, Raychowdhury R, Zeng Q, Chen Z, Mauceli E, Hacohen N, Gnirke A, Rhind N, Palma FD, Birren BW, Nusbaum C, Lindblad-Toh K, Friedman N, Regev A (2011) Trinity: reconstructing a full-length transcriptome without a genome from RNA-Seq data. *Nature Biotechnology* 29: 644–652.
- Holm S (1979) A simple sequentially rejective multiple test procedure. *Scandinavian Journal of Statistics* 6: 65–70.
- Hoskin CJ (2013) A new frog species (Microhylidae: *Cophixalus*) from boulder-pile habitat of Cape Melville, north-east Australia. *Zootaxa* 3722(1): 61–72. doi:10.11646/zootaxa.3722.1.5
- Hutter CR, Lambert SM, Andriampenomanana ZF, Glaw F, Vences M (2018) Molecular systematics and diversification of Malagasy bright-eyed tree frogs (Mantellidae: *Boophis*). *Molecular Phylogenetics and Evolution* 127: 568–578. doi:10.1016/j.ympev.2018.05.027
- Irisarri I, Baurain D, Brinkmann H, Delsuc F, Sire J-Y, Kupfer A, Petersen J, Jarek M, Meyer A, Vences M, Philippe H (2017) Phylogenomic consolidation of the jawed vertebrate timetree. *Nature Ecology and Evolution* 1(9): 1370–1378. doi:10.1038/s41559-017-0240-5
- Kalyaanamoorthy S, Minh BQ, Wong TK, von Haeseler A, Jermiin LS (2017) ModelFinder: fast model selection for accurate phylogenetic estimates. *Nature Methods* 14(6): 587.
- Katoh K, Standley DM (2013) MAFFT multiple sequence alignment software version 7: improvements in performance and usability. *Molecular Biology and Evolution* 30(4): 772–780. doi:10.1093/molbev/mst010
- Kent W (2002) BLAT—the BLAST-like alignment tool. *Genome Research* 12: 656–664.
- Klages J, Glaw F, Köhler J, Müller J, Hipsley CA, Vences M (2013) Molecular, morphological and osteological differentiation of a new species of microhylid frog of the genus *Stumpffia* from northwestern Madagascar. *Zootaxa* 3717(2): 280–300. doi:10.11646/zootaxa.3717.2.8
- Kraus F (2011) At the lower size limit for tetrapods, two new species of the miniaturized frog genus *Paedophryne* (Anura, Microhylidae). *ZooKeys* 154: 71–88. doi:10.3897/zook- eys.154.1963
- Lee JH, Choi T-J, Nam SW, Kim YT (2005) Isolation and characterization of Brain-Derived Neurotrophic Factor gene from Flounder (*Paralichthys olivaceus*). *Journal of Microbiology and Biotechnology* 15(4): 838–843.

Results

- Lee MSY, Cau A, Nash D, Dyke GJ (2014) Sustained miniaturization and anatomical innovation in the dinosaurian ancestors of birds. *Science* 345(6196): 562–566. doi:10.1126/science.1252243
- Lehr E, Coloma LA (2008) A minute new Ecuadorian Andean frog (Anura: Strabomantidae, *Pristimantis*). *Herpetologica* 64(3): 354–367.
- Li H, Durbin R (2009) Fast and accurate short read alignment with Burrows-Wheeler Transform. *Bioinformatics* 25: 1754–1760.
- Li H, Handsaker B, Wysoker A, Fennell T, Ruan J, Homer N, Marth G, Abecasis G, Durbin R, 1000 Genome Project Data Processing Subgroup (2009) The sequence alignment/map (SAM) format and SAMtools. *Bioinformatics* 25: 2078–2079.
- Losos JB (2011) Lizards in an Evolutionary Tree. University Of California Press, Berkeley CA, USA, 507 pp.
- Macey JR, Larson A, Ananjeva NB, Fang Z, Papenfuss TJ (1997) Two novel gene orders and the role of light-strand replication in rearrangement of the vertebrate mitochondrial genome. *Molecular Biology and Evolution* 14: 91–104.
- Macey JR, Schulte JAI, Ananjeva NB, Larson A, Rastegar-Pouyani N, Shammakov SM, Papenfuss TJ (1998a) Phylogenetic relationships among agamid lizards of the *Laudakia caucasia* species group: Testing hypotheses of biogeographic fragmentation and an area cladogram for the Iranian Plateau. *Molecular Phylogenetics and Evolution* 10: 118–131.
- Macey JR, Schulte JAI, Larson A, Fang Z, Wang Y, Tuniyev BS, Papenfuss TJ (1998b) Phylogenetic relationships of toads in the *Bufo bufo* species group from the eastern escarpment of the Tibetan Plateau: A case of vicariance and dispersal. *Molecular Phylogenetics and Evolution* 9: 80–97.
- Matzke NJ (2014) Model selection in historical biogeography reveals that founder-event speciation is a crucial process in island clades. *Systematic Biology* 63: 951–970.
- Meyer CP (2003) Molecular systematics of cowries (Gastropoda: Cypraeidae) and diversification patterns in the tropics. *Biological Journal of the Linnaean Society* 79: 401–459. doi:10.1046/j.1095-8312.2003.00197.x
- Miller PJ (1996) The functional ecology of small fish: some opportunities and consequences. *Symposia of the Zoological Society of London* 69: 175–199.
- Minh BQ, Nguyen MAT, von Haeseler A (2013) Ultrafast approximation for phylogenetic bootstrap. *Molecular Biology and Evolution* 30(5): 1188–1195.
- Nguyen L-T, Schmidt HA, von Haeseler A, Minh BQ (2015) IQ-TREE: a fast and effective stochastic algorithm for estimating maximum-likelihood phylogenies. *Molecular Biology and Evolution* 32(1): 268–274. doi:10.1093/molbev/msu300
- Nikolenko SI, Korobeynikov AI, Alekseyev MA (2013) BayesHammer: Bayesian clustering for error correction in single-cell sequencing. *BMC Genomics* 14(Suppl. 1): S7.
- Pagel M (1999) Inferring the historical patterns of biological evolution. *Nature* 401: 877–884.
- Palumbi SR, Martin A, Romano S, McMillan WO, Stice L, Grabowski G (1991) The Simple Fool's Guide to PCR, Version 2.0. Privately published, University of Hawaii, 45 pp.
- Paradis E, Claude J, Strimmer K (2004) APE: Analyses of Phylogenetics and Evolution in R language. *Bioinformatics* 20(2): 289–290. doi:10.1093/bioinformatics/btg412
- Peloso PLV, Frost DR, Richards SJ, Rodrigues MT, Donnellan S, Matsui M, Raxworthy CJ, Biju SD, Lemmon EM, Lemmon AR, Wheeler WC (2016) The impact of anchored phylogenomics and taxon sampling on phylogenetic inference in narrow-mouthed frogs (Anura, Microhylidae). *Cladistics* 32(2): 113–140. doi:10.1111/cla.12118

- Peloso PLV, Raxworthy CJ, Wheeler WC, Frost DR (2017) Nomenclatural stability does not justify recognition of paraphyletic taxa: A response to Scherz et al. (2016). *Molecular Phylogenetics and Evolution* 111(2017): 56–64. doi:10.1016/j.ympev.2017.03.016
- Penny SG, Crottini A, Andreone F, Bellati A, Rakotozafy LMS, Holderied MW, Schwitzer C, Rosa GM (2017) Combining old and new evidence to increase the known biodiversity value of the Sahamalaza Peninsula, Northwest Madagascar. *Contributions to Zoology* 86(4): 273–296.
- Perl RGB, Nagy ZT, Sonet G, Glaw F, Wollenberg KC, Vences M (2014) DNA barcoding Madagascar's amphibian fauna. *Amphibia-Reptilia* 35: 197–206. doi:10.1163/15685381-00002942
- R Core Team (2014) R: A language and environment for statistical computing. R Foundation for Statistical Computing, Vienna, Austria. <http://www.R-project.org/>.
- Rakotoarison A, Crottini A, Müller J, Rödel M-O, Glaw F, Vences M (2015) Revision and phylogeny of narrow-mouthed treefrogs (*Cophyla*) from northern Madagascar: integration of molecular, osteological, and bioacoustic data reveals three new species. *Zootaxa* 3937(1): 61–89. doi:10.11646/zootaxa.3937.1.3
- Rakotoarison A, Glaw F, Vieites DR, Raminosoa NR, Vences M (2012) Taxonomy and natural history of arboreal microhylid frogs (*Platypelis*) from the Tsaratanana Massif in northern Madagascar, with description of a new species. *Zootaxa* 3563: 1–25.
- Rakotoarison A, Scherz MD, Bletz MC, Razafindraibe JH, Glaw F, Vences M (in press) Diversity, elevational variation, and phylogenetic origin of stump-toed frogs (Microhylidae, Cophylinae, *Stumpffia*) on the Marojejy massif, northern Madagascar. *Salamandra*
- Rakotoarison A, Scherz MD, Glaw F, Köhler J, Andreone F, Franzen M, Glos J, Hawlitschek O, Jono T, Mori A, Ndriantsoa SH, Raminosoa Rasoamampionona N, Riemann JC, Rödel M-O, Rosa GM, Vieites DR, Crottini A, Vences M (2017a) Describing the smaller majority: Integrative taxonomy reveals twenty-six new species of tiny microhylid frogs (genus *Stumpffia*) from Madagascar. *Vertebrate Zoology* 67(3): 271–398.
- Rakotoarison A, Scherz MD, Glaw F, Vences M (2017b) Rediscovery of frogs belonging to the enigmatic microhylid genus *Madecassophryne* in the Anosy Massif, south-eastern Madagascar. *Salamandra* 53(4): 507–518.
- Ramos M, Schiffer L, Re A, Azhar R, Basunia A, Rodriguez C, Chan T, Chapman P, Davis SR, Gomez-Cabrero D, Culhane AC (2018) Software for the integration of multiomics experiments in Bioconductor. *Cancer Research* 77(21): e39–e42.
- Ree RH, Sanmartín I (2018) Conceptual and statistical problems with the DEC+J model of founder-event speciation and its comparison with DEC via model selection. *Journal of Biogeography* 45(4): 741–749. doi:10.1111/jbi.13173
- Revell LJ (2009) Size-correction and principal components for interspecific comparative studies. *Evolution* 63: 3258–3268. doi:10.1111/j.1558-5646.2009.00804.x
- Revell LJ (2012) phytools: An R package for phylogenetic comparative biology (and other things). *Methods in Ecology and Evolution* 3: 217–223.
- Rittmeyer EN, Allison A, Gründler MC, Thompson DK, Austin CC (2012) Ecological guild evolution and the discovery of the world's smallest vertebrate. *PLoS One* 7(1): e29797. doi:10.1371/journal.pone.0029797
- Rivera JA, Kraus F, Allison A, Butler MA (2017) Molecular phylogenetics and dating of the problematic New Guinea microhylid frogs (Amphibia: Anura) reveals elevated speciation rates and need for taxonomic reclassification. *Molecular Phylogenetics and Evolution* 112: 1–11. doi:10.1016/j.ympev.2017.04.008
- Roch S, Steel M (2015) Likelihood-based tree reconstruction on a concatenation of aligned se-

Results

- quence data sets can be statistically inconsistent. *Theoretical Population Biology* 100: 56–62.
- Rodríguez A, Burgon JD, Lyra M, Irisarri I, Baurain D, Blaustein L, Göçmen S, Künzel S, Mable BK, Nolte AW, Veith M, Steinfartz S, Elmer KR, Philippe H, Vences M (2017) Inferring the shallow phylogeny of true salamanders (*Salamandra*) by multiple phylogenomic approaches. *Molecular Phylogenetics and Evolution* 115: 16–26.
- Roure B, Rodriguez-Ezpeleta N, Philippe H (2007) SCaFoS: a tool for selection, concatenation and fusion of sequences for phylogenomics. *BMC Evolutionary Biology* 7: S2.
- RStudio Team (2016) RStudio: Integrated Development for R. RStudio, Inc., Boston, MA. <http://www.rstudio.com/>.
- Sayyari E, Mirarab S (2016) Fast coalescent-based computation of local branch support from quartet frequencies. *Molecular Biology and Evolution* 33(7): 1654–1668.
- Scherz MD, Vences M, Rakotoarison A, Andreone F, Köhler J, Glaw F, Crottini A (2016) Reconciling molecular phylogeny, morphological divergence and classification of Madagascan narrow-mouthed frogs (Amphibia: Microhylidae). *Molecular Phylogenetics and Evolution* 100: 372–381. doi:10.1016/j.ympev.2016.04.019
- Shen X-X, Liang D, Zhang P (2012) The development of three long universal nuclear protein-coding locus markers and their application to osteichthyan phylogenetics with nested PCR. *PLoS ONE* 7(6): e39256. doi:10.1371/journal.pone.0039256
- Slater GSC, Birney E (2005) Automated generation of heuristics for biological sequence comparison. *BMC Bioinformatics* 6(1): 31.
- Sofanova Y, Bankevich A, Pevzner PA (2015) dipSPAdes: assembler for highly polymorphic diploid genomes. *Journal of Computational Biology* 22(6): 528–545.
- Tu N, Yang M, Liang D, Zhang P (2018) A large-scale phylogeny of Microhylidae inferred from a combined dataset of 121 genes and 427 taxa. *Molecular Phylogenetics and Evolution* 126: 85–91.
- Vences M, Guayasamin JM, Miralles A, de la Riva I (2013) To name or not to name: Criteria to promote economy of change in Linnaean classification schemes. *Zootaxa* 3636(2): 201–244. doi:10.11646/zootaxa.3636.2.1
- Vences M, Kosuch J, Glaw F, Böhme W, Veith M (2003) Molecular phylogeny of hyperoliid treefrogs: biogeographic origin of Malagasy and Seychellean taxa and re-analysis of familial paraphyly. *Journal of Zoological Systematics and Evolutionary Research* 41: 205–215. doi:10.1046/j.1439-0469.2003.00205.x
- Vieites DR, Wollenberg KC, Andreone F, Köhler J, Glaw F, Vences M (2009) Vast underestimation of Madagascar's biodiversity evidenced by an integrative amphibian inventory. *Proceedings of the National Academy of Sciences of the USA* 106(20): 8267–8272. doi:10.1073/pnas.0810821106
- Wilmé L, Goodman SM, Ganzhorn JU (2006) Biogeographic evolution of Madagascar's microendemic biota. *Science* 312(5776): 1063–1065. doi:10.1126/science.1122806
- Wollenberg KC, Vieites DR, van der Meijden A, Glaw F, Cannatella DC, Vences M (2008) Patterns of endemism and species richness in Malagasy cophyline frogs support a key role of mountainous areas for speciation. *Evolution* 62(8): 1890–1907. doi:10.1111/j.1558-5646.2008.00420.x
- Yang Z (1997) PAML: a program package for phylogenetic analysis by maximum likelihood. *Bioinformatics* 13(5): 555–556.
- Yang Z (2007) PAML 4: Phylogenetic Analysis by Maximum Likelihood. *Molecular Biology and*

Evolution 24: 1586–1591.

Zhang C, Rabiee M, Sayyari E, Mirarab S (2018) ASTRAL-III: polynomial time species tree reconstruction from partially resolved gene trees. *BMC Bioinformatics* 19(6): 153.

Zweifel RG (1972) A revision of the frogs of the subfamily Asterophryinae, family Microhylidae. *Bulletin of the American Museum of Natural History* 148(413–546)

Supplementary Figure 1. Six-category ancestral state reconstruction of ecology in the Cophylinae.

Supplementary Figure 2. \log_{10} maximum body size by ecology in the Cophylinae. Points are jittered on the x-axis.

Supplementary Table 1. The 50 smallest frogs in the world, updated from the tables of on the table by Lehr and Coloma (2008) and Kraus (2011), plus Rittmeyer et al. (2012). All measurements in mm.

Supplementary Table 2. Supermatrix table of single gene sequences of Cophylinae at individual level.

Supplementary Table 3. Supermatrix table of single gene sequences of Cophylinae at species level.

Supplementary Table 4. Cophylinae frog measurement database. All values in mm.

Supplementary Table 5. Newly assigned species numbers based on 3' 16S rRNA mitochondrial genes.

Supplementary Table 6. Ancestral sizes of clades and their 95% Confidence Intervals (CI). All values in mm.

Supplementary Trees

Section 4: Consolidating taxonomic datasets for macroevolutionary studies

In this section, I present a single chapter pertaining to the evolution of chameleons. This study is based on harvesting data from taxonomic descriptions and field guides and using these data to shed light on the evolution of ornamentation in chameleons.

Chapter 11. MANUSCRIPT (in prep.): Genital and external ornaments are evolutionarily uncoupled in chameleons

In this chapter, I present an analysis of the evolution of sexual ornamentation of chameleons. Chameleons are among the most physically ornamented of all vertebrates, and thus an excellent group of organisms for the study of sexual communication. For this chapter, we constructed a morphological dataset by harvesting information largely from existing taxonomic literature and photographs in field guides. We analysed these data on a dated species-level phylogeny with a phylogenetic backbone using phylogenetic comparative methods. We compared the importance of body size, ecology, and sexual selection on ornamentation evolution. The results show that genital and external ornamentation are evolutionarily uncoupled yet are both under sexual selection. This study demonstrates the extent of macroevolutionary questions that can be answered using a taxonomy-based data collection strategy.

Scherz, M.D., Rancilhac, L., Garcia-Porta, J., Bruy, T., Irisarri, I., Künzel, S., Stützer, D., Glaw, F., Prötz, D., Tolley, K.A., Meyer, A., Böhme, W., Philippe, H. & Vences, M. Genital and external ornaments are evolutionarily uncoupled in chameleons. Unpublished manuscript.

Digital Supplementary Materials on appended CD:

Supplementary Data 1 — Legacy gene sequence data

Supplementary Data 2 — Morphological data

Supplementary Methods

Supplementary Results

Genital and external ornaments are evolutionarily uncoupled in chameleons

Mark D. Scherz^{1,2,*}, Loïs Rancilhac², Joan Garcia-Porta³, Teddy Bruy², Iker Irisarri⁴, Sven Künzel⁵, Dominik Stützer², Frank Glaw¹, David Prötzl¹, Krystal Tolley^{6,7}, Axel Meyer⁸, Wolfgang Böhme⁹, Hervé Philippe¹⁰, Miguel Vences²

¹Zoologische Staatssammlung München (ZSM-SNSB), Münchhausenstr. 21, 81247 München, Germany.

²Zoologisches Institut, Technische Universität Braunschweig, Mendelssohnstr. 4, 38106 Braunschweig, Germany

³Department of Biology, Washington University in Saint Louis, St. Louis, MO 63130, USA

⁴Department of Biodiversity and Evolutionary Biology, Museo Nacional de Ciencias Naturales, José Gutiérrez Abascal 2, 28006 Madrid, Spain

⁵Max-Planck Institute for Evolutionary Biology, August-Thienemann-Str. 2

24306 Plön, Germany

⁶South African National Biodiversity Institute, Kirstenbosch Research Centre, Private Bag X7, Claremont 7735, South Africa

⁷Centre for Ecological Genomics and Wildlife Conservation, University of Johannesburg, Auckland Park 2000, South Africa

⁸Fakultät Biologie, Universität Konstanz, 78457 Konstanz, Germany

⁹Abteilung Wirbeltiere, Zoologische Forschungsmuseum Alexander Koenig, Adenauerallee 160, 53113 Bonn, Germany

¹⁰Centre for Biodiversity Theory and Modelling, Station d'Ecologie Théorique et Expérimentale du CNRS, 09200 Moulis, France

*corresponding author, e-mail: mark.scherz@gmail.com

Background

Sexual selection is a strong driver of morphological evolution. It can drive and reinforce speciation itself (reviewed by [1]), and often gives rise to ornaments or weapons [2-4]—physical manifestations of sexual communication. Such structures, from the shimmering plumage of the peacock’s tail to the weighty antlers of an elk, have fascinated and enthralled naturalists for centuries, inspiring generations of biologists, including the likes of Darwin [5], to ponder their origins and function. Sexual communication is possibly the most ubiquitous purpose of communication in the animal kingdom. More often than not, signals are multimodal and complex, raising questions on how the evolution of signal complexity is driven [6-8]. Understanding of this process is emerging, but is still fraught with uncertainties and, occasionally, contradictions, which may be traced to lack of understanding of mechanisms for signal production, the way in which sexual and natural selection are acting on them, and how different modules and aspects of complex signals are related to one another [6].

Four major non-exclusive hypotheses have been put forward to explain the evolution of signal complexity in communication [8]: (1) sociality, e.g. species with greater sexual selection evolve larger repertoires of signals to outcompete rivals; (2) ecology, e.g. amount and monotony of background noise causes species to elaborate signals to stand out; (3) allometry, e.g. larger species have a greater surface area over which to elaborate ornaments or colour patterns, and (4) neutrality, e.g. drift in vocal repertoire complexity of wide-ranging species (for more information, see [8] and references therein). Applying this conceptual framework to sexual ornamentation, we can derive the proximal causes of the evolution of such extreme and often costly structures—a critical part of the endeavour to understand the evolutionary origins of some of the most striking and baffling features in the animal kingdom.

Ornamentation of male genitalia can be just as bizarrely complex and exaggerated as any head-dress. The intriguing diversity and complexity of such structures is particularly well known in insects and reptiles, where it can be extravagant and of high taxonomic value [9-12]. It is also driven by sexual selection, especially male-male competition, male-female conflict, and male-female co-evolution (reviewed in [13]). These forms of selection may also influence external ornamentation, e.g. the evolution of weaponry in males that physically battle for mates, and we might therefore expect a positive correlation between external and genital ornaments. On the other hand, if the selective forces drive pre-copulatory barriers, they may also manifest as negative correlation between genital and external ornaments [14]—we refer to the latter as the ‘ornament trade-off hypothesis’.

Chameleons, highly visual animals with often pronounced external and genital ornamentation are chameleons (reviewed in [15]), are a great model to disentangle the potential selective forces that drive signal complexity. The 212 currently described species of this lizard group [16], divided into the two subfamilies Brookesiinae (leaf chameleons from Madagascar) and Chamaeleoninae (‘true’ chameleons from Madagascar, Africa, and Eurasia), range in external ornamentation from hardly any ornaments to some of the most ornamented tetrapods ever. They can be adorned with a broad array of physical ornaments, including spines, horns, sails, crests, and skin flaps, which are used in ritualised displays or physical battles (reviewed by [17]). Structural (as opposed to chromatic) ornamentation in chameleons often exhibits sexual ornamentation dimorphism (SOD). Across the family, taxa exhibit varying degrees and directions of sexual size dimorphism (SSD). Furthermore, the hemipenes of chameleons are elaborately ornamented (surveyed in [18]), more so than in many other squamates, and are taxonomically informative [18-20], though often more-so at supraspecific levels than between closely related taxa [21, 22]. Their gross morphological evolution has been suggested to be strongly affected by body size and ecology [20, 23], but sexual selection in chameleons is thought to be strong. Finally, they have radiated into multiple environments, from closed rainforests to desert, allowing the exploration of environmental effects on the complexity and development of visual structures. Although little is known of the ecology of most

species, on the whole most chameleons are coercive maters [24], but have female or mutual mate choice [25, 26], and the direction of the action of sexual selection on head morphology is apparently affected by ecology, specifically the openness of habitats [27, 28]. There is thus pretence for suspecting that sociality, allometry, and ecology are affecting the evolution of their external and genital ornamentation complexity. These amazing lizards are therefore an ideal model group to test the relative strength and interplay of these mechanisms.

Based on a new, nearly fully taxon-sampled tree of the family Chamaeleonidae to elucidate the factors driving the degree and complexity of chameleon physical external ornamentation as well as genital ornamentation, using the step-by-step hypothesis-testing approach based on that of Ord and Garcia-Porta [8].

Methods

Phylogenomic backbone tree

To resolve deep nodes in the chameleon phylogeny, we took a phylogenomic approach [29, 30]. We sequenced mixed-tissue transcriptomes from 12 species (*Bradyopodium pumilum*, *Brookesia* sp., *Calumma ambreense*, *Calumma* cf. *nasutum*, *Calumma gastrotaenia*, *Chamaeleo chamaeleon* (chimera of *C. c. chamaeleon* with *C. c. recticristata*), *Furcifer pardalis*, *Kinyongia boehmei*, *Palleon lolontany*, *Rhampholeon acuminatus*, *Rieppeleon brevicaudatus* (chimera of two specimens), and *Trioceros hoehneli*), representing 10 of the 12 described chameleon genera on the Illumina NextSeq platform. *De novo* assembly was conducted in TRINITY v. 2.1.0 [31] and open reading frames extracted with Transdecoder. Using the high-quality vertebrate alignments of Irisarri et al. [29] as a reference, homologous sequences from the new transcriptomes were added with FORTY-Two (<https://bitbucket.org/dbaurain/42/>), and alignments were filtered for possible contaminations and paralogs following Irisarri et al. [29] (see Supplementary Methods for details). The original amino acid alignments were back-translated into nucleotide alignments using LEEL (written by D. Baurain) for further phylogenomic analyses. Relevant taxa were extracted from the taxonomically broader alignments and we retained only genes with a maximum of one species missing in both African and Madagascan large-bodied chameleons. The final dataset was assembled with SCAFFOS [32], creating two chimeric OTUs for *Chamaeleo chamaeleon* (*C. c. chamaeleon* + *C. c. recticristata*) and *Rieppeleon brevicaudatus* (two different individuals). Preliminary phylogenetic analyses were performed using RAxML [33] (detailed in Supplementary Methods) in order to determine the best merging strategy to adopt to assemble the final alignment. We finally created chimeras for the two taxa for which we had several transcriptomes (*C. chamaeleo* and *R. brevicaudatus*). The final alignment consisted of 4,230 genes, 12 taxa, and 9,903,111 nucleotide positions of which 374,450 are parsimony-informative. The matrix was partitioned by gene, and the best-fitting substitution model was selected for each partition using MODELFINDER [34], as implemented in IQ-TREE [35], followed by tree reconstruction. Node support was assessed using ultrafast bootstrapping [36] with 1000 replicates.

Extended all-taxon multigene data set

We extended an available six-marker, 174-taxon phylogenetic dataset [37] by adding (1) partial sequences of an additional seven nuclear genes for representatives of all chameleon genera, used previously [37]; (2) new published sequences for additional species, many new species described since 2013; (3) newly obtained sequences for the first six gene fragments for newly described species, mostly from Madagascar, and to fill a few gaps in the previous supermatrix; (4) newly obtained sequences for selected species of *Calumma* and *Furcifer* of five additional nuclear markers (BDNF, KIAA123, SACS, and a second fragment of the RAG1 gene; see Supplementary Meth-

Results

ods for primers and protocols). Our final taxon set included 212 chameleon taxa for the following genes: RAG1 (3' and 5'), PRLR, C-mos, BDNF, KIAA1239, SACS, R35, AKAP9, BACH1, BACH2, MSH6, NKTR, REV3L, ND2, ND4, 16S. The alignment is included as Supplementary Data 1.

We used three alternative backbone topologies produced from phylotranscriptomic analyses (mostly differing in the position of the long-branch taxon, *Rieppeleon*) as topological constraints and analysed the supermatrix under ML with a by-gene partitioned RAxML analysis (GTR+Γ4 models); each analysis was replicated five times, and the tree with highest likelihood was chosen. Branch support was assessed with 100 bootstrap replicates.

Timetree inference

We produced time-calibrated ultrametric trees of our three backbone topologies. Squamate outgroups representing relevant clades whose divergences could be time-constrained with fossil evidence were added to the phylotranscriptomic dataset (Supplementary Methods, Table S6). This resulted in a total of 39 taxa (12 chameleons and 27 outgroup taxa) and a total of 8,055,531 bp. Prior calibrations were applied to 11 nodes in the outgroup set (Supplementary Methods) using four alternative prior calibration distributions, following dos Reis et al. [38] (see Supplementary Methods for details). Divergence times of the 4,230 genes in the dataset was estimated with MCMCTREE [39] within the PAML package [40] using approximate likelihood calculation [41]. For each of the four calibration settings, two MCMC chains were run for a total of 502 million generations, sampling every 1,000 and the first 2 million excluded as burn-in. For each calibration setting, three independent runs were performed to control for convergence issues, which was assessed in TRACER v 1.7.1 [42].

Estimated ages for four within chameleons and agamids were used as secondary calibrations for a second molecular clock analyses on the taxon-rich tree (detailed in Supplementary Methods) using MCMCTREE with similar parameters as above. Convergence was reached at 6 million generations, discarding the first million as burn-in. Posterior ages of crucial nodes for all analyses are tabulated in Table SM7. Because estimated node ages were overall similar across all analyses and to previously inferred ages [37], we averaged node ages across three replicates of 95% HPD calibration with the SUMTREES package from DENDROPy v 3.12.1 [43]. The three resulting ultrametric trees (one for each of the three alternative topologies) were used for downstream analyses. Results are reported based on values from our preferred tree topology (due to similarity to Tolley et al. [37], see Supplementary Results, Fig. SR1) except where they differed between topologies.

Morphological data collection

Body size was taken per sex for each species (SVL_m and SVL_f for males and females, respectively) from the literature, retaining the largest records available. Body size was log-transformed in analyses. The midpoint of body size measures was calculated as well (indicated by SVL_{mid}). Sexual size dimorphism (SSD) is given by $\text{SVL}_m/\text{SVL}_f$ (not log-transformed). Morphological data were obtained from photographs and text descriptions in the literature and supplemented with examination of voucher specimens. Hemipenis morphology was coded based on illustrations, photographs, micro-CT scans, and examination of voucher specimens. We coded eleven external morphological ornament characters (five binary, six ordinal), and 17 hemipenis ornament characters (seven binary, ten ordinal). Ordinal coded characters were subjectively ordered from least (0) to most ornamented (max); for coding scheme see Supplementary Methods. For data, see Supplementary Data.

In the text we refer to the *degree* of ornamentation. This is a summary variable, given as the sum of states of ornamentation, such that a species with little or unelaborate ornamentation has low values, and a species with elaborate or complex ornamentation has high values. Dimorphism

in external ornamentation (SOD) is given as the number of characters in which males differ from females to avoid inflation as a result of ordered characters. SOD and SSD are our two proxies of sexual selection.

We took habitat as a proxy for species ecology. We recoded species largely following the scheme of Tolley et al. [37] as occurring in scrub, savannah, grassland, rainforest edge, rainforest interior, or dry forest. We also simplified these habitat classes into a binary canopy-openness factor, with the first three being considered as open canopy, the latter three as closed canopy habitats.

The full morphological dataset is provided as Supplementary Data.

Statistical analysis

Data analysis was conducted in R 3.5.1 [44] in RStudio 1.1.423 [45]. Phylogenetic analyses used the packages APE 5.2 [46], PHYTOOLS 0.6-60 [47], GEIGER 2.0.6 [48]. Analyses were conducted on three alternate topologies independently (see supplementary information). Results are reported only from our preferred topology (which agrees most closely with previous topologies [37]) except where topologies differed in statistical significance. Plotting was partially done in GGPlot2 3.1.0 [49]. Phylogenetic linear regression models (PLRMs) were calculated using the package PHYLOLM 2.6 [50] with Pagel's λ [51] model. To test the ornament trade-off hypothesis, we fitted a PLRM between size-corrected residuals of external and genital ornamentation. Phylogenetic ANOVAs were calculated with phylANOVA() function in PHYTOOLS, with 10,000 simulations to produce more robust P-values. Residuals were calculated using the correlation structure computed by means of Pagel's λ [51].

Phylogenetic signal was tested using the phylosig() function in PHYTOOLS, which tests the presence of phylogenetic signal with two metrics, Pagel's λ [51] and Blomberg's K [52], using size-corrected residuals for all variables except body size.

To test the hypothesis that environment openness results in different selective regimes on external and genital ornamentations, we compared two Brownian and four Ornstein-Uhlenbeck (OU) models for goodness of fit using OUWE [53]. These models are constructed as follows: BM1, single rate Brownian model; BMS, Brownian model with a separate rate parameter for each state; OUM, OU model with different state means (μ) and a single constraint value (α) and rate (σ^2) for each selective regime; OUMV, OUM model with different σ^2 per regime; OUMA, OUM model with different α for each regime; and OUMVA, OUM model with different α and σ^2 per regime. Models were tested over a set of 300 simulated character maps produced in with the make.simmap() function in PHYTOOLS, and outputs were summarised; the optimal model was concluded to be the most frequently supported across all character simulations (support for that model is given as a percentage of the full reconstructions). Models were compared based on their AICc weights.

Phylogenetic path analysis was conducted in PHYLOPATH [54, 55]. Paths were constructed to contain six variables: midpoint of body size, degree of external ornamentation, degree of ornamentation dimorphism, sexual size dimorphism ($= \text{SVL}_m / \text{SVL}_f$), degree of genital ornamentation, and habitat openness (open vs. closed, as a proxy for ecology). Based on the results presented here, and hypothetically likely scenarios, we constructed 26 alternative path models to explain ornamentation of genitals and external morphology (Fig. SR3). The models within 2 CICc were averaged to produce an optimal model.

Results

RNAseq-based phylogenies differed in topology from previous reconstructions [37], particularly in the relationships between the Malagasy genera *Calumma* and *Furcifer*, and the position of *Rieppeleon*. For the latter, three alternative topolgoies were recovered among differently filtered

Results

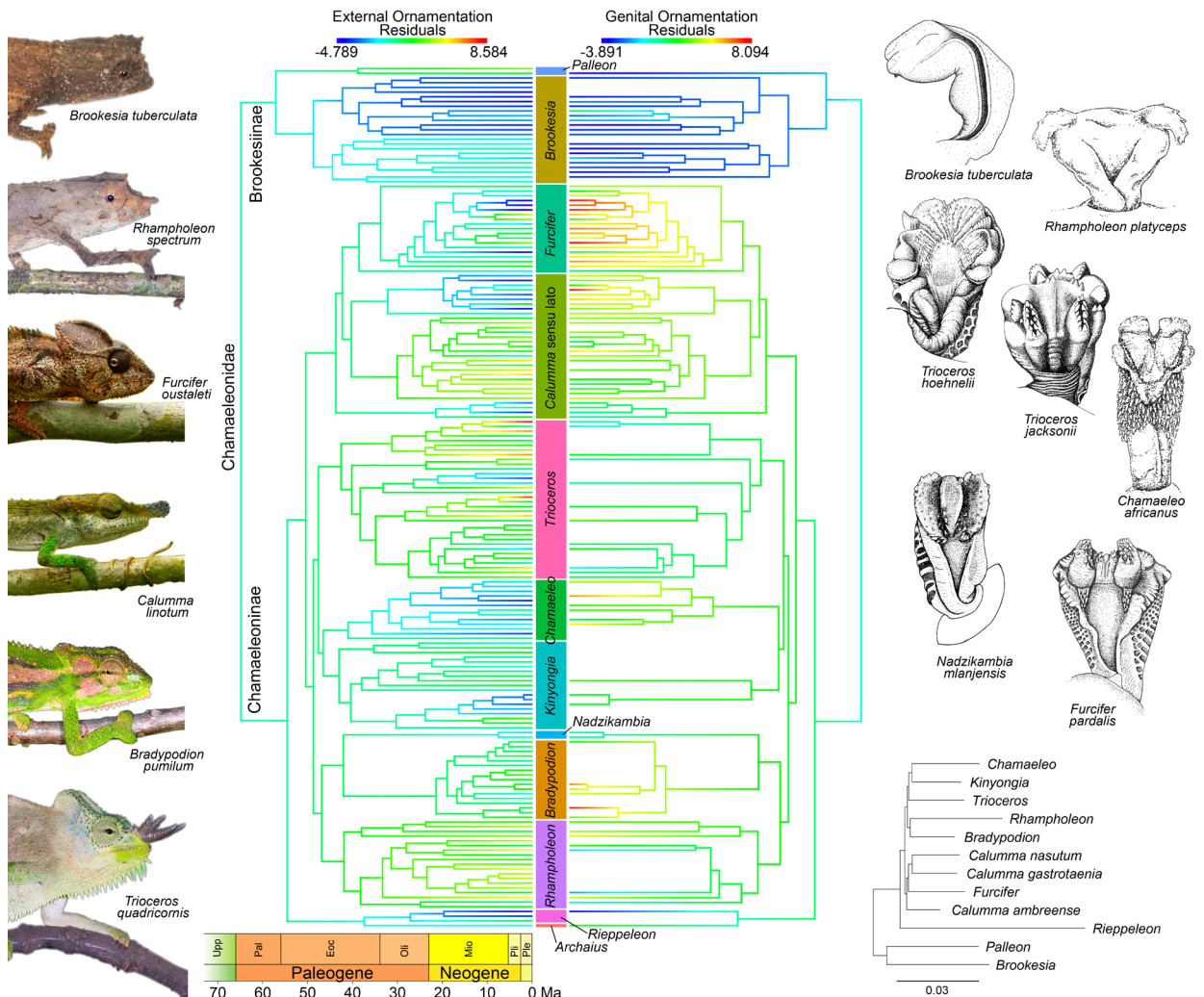


Fig. 1. Evolution of ornamentation of external ornaments and genitals in chameleons.

Trees show only taxa for which respective data are available; for the full genetic trees with support values, see Fig SR2 in the Supplementary Results. Inset chameleon heads and hemipenes showcase part of the variability in ornamentation. Inset tree is the phylotranscriptomic phylogeny with the same backbone topology as that used for the species tree. Support at all nodes is 100%. Missing genera were placed based on non-transcriptomic phylogenies: *Nadzikambia* was placed sister to *Bradypodion* and *Archaius* sister to *Rieppeleon*.

phylotranscriptomic data sets (Fig. SR1, Table SM4), with no topology being clearly favoured over the others. These differed mostly in the position of *Rieppeleon* and the relative position of the Malagasy genera *Calumma* and *Furcifer* (Fig. SR1). We consider the topology most closely resembling previous work [37] (Fig. 1) *a priori* to be the most likely, but to overcome the topological intractability we used all three alternative topologies as backbone constraints for taxon-rich phylogenies, and tested hypotheses on all three. Except where results differed among topologies, results are here reported only for the preferred one. Our dated phylogenies placed the divergence of the two subfamilies in the Upper Cretaceous, with most modern genera originating in the Eocene.

Hemipenis data were available from 109 species of the 200 coded for external morphology. Ancestral state reconstruction of genital and external ornamentation size residuals (Fig. 1) shows that Brookesiinae (*Brookesia* and *Palleon*) are distinguished by low levels of ornamentation in both external and genital morphology, in a pattern clearly distinct from Chamaeleoninae (all other chameleon genera). For both sets of ornamentation, low and high levels of ornamentation have

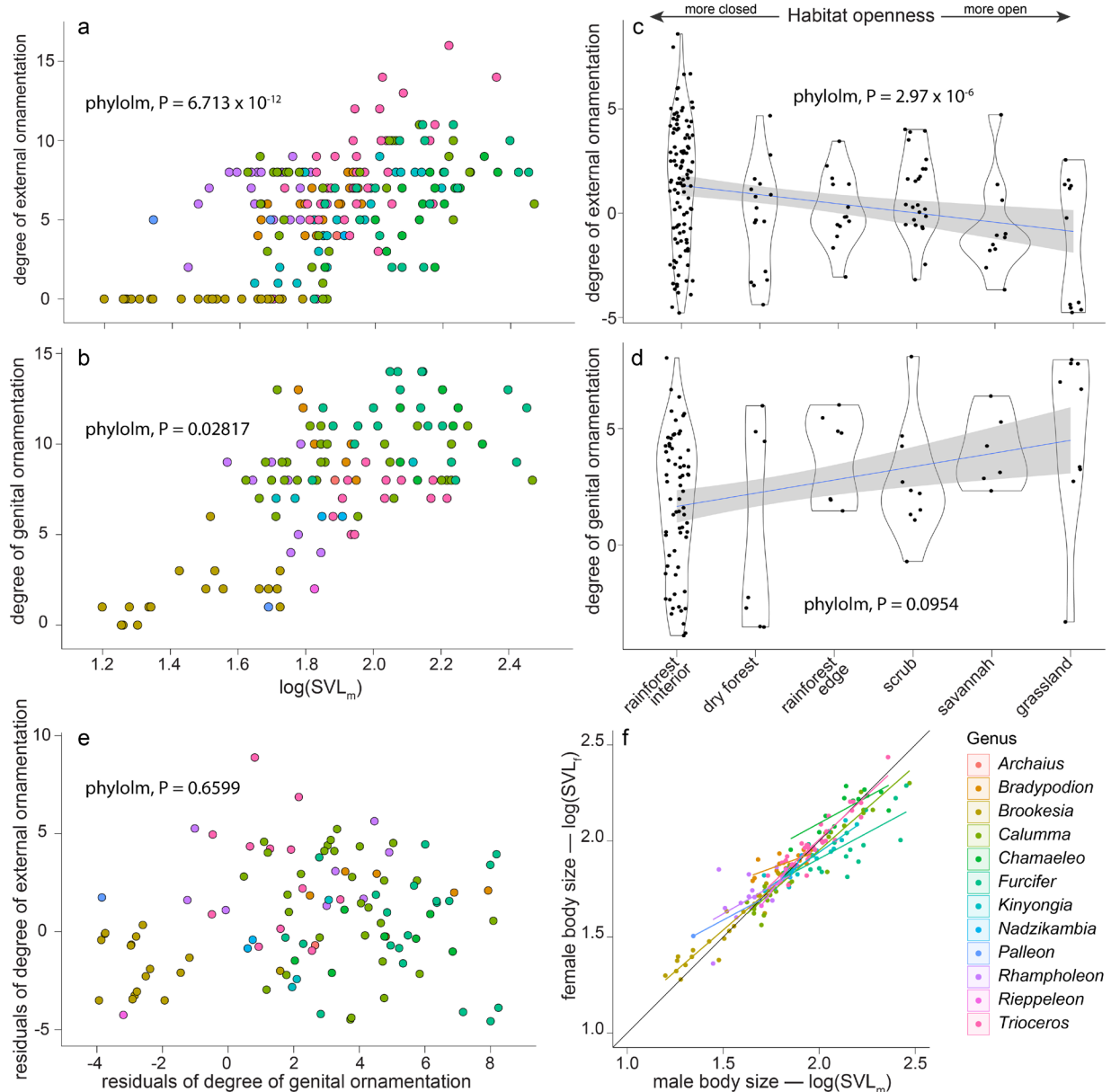


Fig. 2. Ornamentation evolution within chameleons.

(a-b) Scatterplots of the degree of (a) external and (b) genital ornamentation against male body size. (c-d) Violin plots of degree of (c) external and (d) genital ornamentation against ranked openness scores. Trend line indicated in blue with standard error in grey. Points are jittered. (e) Scatterplot of size-corrected phylogenetic residuals of genital and external ornamentation against one another. (f) Scatterplot of male and female body size per species. Coloured trend lines indicate linear trends per genus. Species below the line have male-biased sexual size dimorphism, and vice versa.

emerged repeatedly across Chamaeleoninae, and correspondence between genital and external ornamentation is not obvious to the eye.

Neutrality. Evolution of the degree of external ornamentation in chameleons (Fig. 1) has only weak phylogenetic signal (Blomberg's $K = 0.8052556$, $P = 0.001$, Pagel's $\lambda = 0.7983883$ $P = 8.215671 \times 10^{-21}$), whereas the degree of genital ornamentation (Fig. 1) had elevated phylogenetic signal ($K = 2.103076$, $P = 0.001$; $\lambda = 0.8209686$, $P = 3.84641 \times 10^{-24}$), as is body size (SVL_{mid} , $K = 2.051809$, $P = 0.001$; $\lambda = 0.9963342$, $P = 1.893447 \times 10^{-46}$). Phylogenetic size-corrected residuals

Results

(PSRs) of SOD and SSD have very little phylogenetic signal (SOD, $K = 0.5585963$, $\lambda = 0.751535$; SSD, $K = 0.4880256$, $\lambda = 0.4643452$).

Allometry. Chameleon ornamentation is strongly related to body size. External and genital ornamentation are both significantly positively correlated with SVL (PLRM of external ornamentation $P = 6.713 \times 10^{-12}$; genital ornamentation $P = 0.02817$; Fig. 2a–b). In both cases, the degree of ornamentation is less in Brookesiinae than Chamaeleoninae. There is also a strong correlation between SSD and body size SVL_{mid} ($P = 9.275 \times 10^{-5}$). In all genera except *Rieppeleon* and *Nadzikambia*, smaller species have relatively larger females than larger species (Fig. 2f). There is an inversion point around a male SVL of 60–80 mm—below this size, females tend to be larger than males, and above this size, males tend to be larger than females, except in *Chamaeleo*, which has larger females above this size, and *Trioceros*, which generally shows little sexual size dimorphism. The pattern across the family is consistent with Rensch's rule [56, 57].

Sexual selection. Our two proxies of sexual selection, SSD and SOD, are not equivalent: PSRs of SSD in chameleons are not correlated with PSRs of the degree of SOD ($P = 0.3506$). External and genital ornamentation have inverse relationships with these two proxies of sexual selection: the degree of genital ornamentation is not correlated with SOD ($P = 0.9359$) but is positively correlated with SSD ($P = 0.01667$), whereas the degree of external ornamentation is strongly positively correlated with the SOD ($P = 1.338 \times 10^{-11}$) but is not correlated with SSD ($P = 0.1005$).

This brings us to the ornament trade-off hypothesis, stated above: is there a relationship between genital and external ornaments? The prediction of a trade-off between selection on genital and external ornaments would lead to a negative correlation between these ornaments. There is considerable variation within most genera in the degree of external and genital ornamentation (Fig. 2e), but overall there is no correlation between these features (PLRM of PSRs: $P = 0.6599$), rejecting this hypothesis.

Ecology. Male body size and SOD differ significantly between open and closed habitats (phyLA-NOVA: SVL_m $F = 16.748593$, $P = 0.0479$; SOD $F = 22.024396$, $P = 0.0257$). Yet the degree of external and genital ornamentation, and SSD do not differ significantly ($P > 0.09$). Brookesiinae skew these results however, as they are not found in open habitats; in Chamaeleoninae alone, degree of external ornamentation $F = 14.78189$, $P = 0.0499$) and SOD ($F = 25.182925$, $P = 0.0083$) differ significantly between habitats, but SSD, genital ornamentation, and male body size do not ($P > 0.2$).

In a crude PLRM analysis, in which we ranked habitat types from least to most open, (0 rainforest interior, 1 dry forest, 2 forest edge, 3 scrub, 4 savannah, and 5 grassland), and ran a PLRM against ornamentation and dimorphism residuals, we found a significant negative correlation between habitat openness and PSRs of the degree of external ornamentation ($P = 2.97 \times 10^{-6}$; Fig. 2c), and an insignificant positive correlation between habitat openness and PSRs of the degree of genital ornamentation ($P = 0.0954$; Fig. 2d). A significant negative relationship was also found between habitat openness and PSRs of SOD ($P = 1.89 \times 10^{-5}$), but not SSD ($P = 0.09547$) or body size itself ($P = 0.7013$). These results were the same when only Chamaeleoninae were used and are robust to topology. As Brookesiinae are found only in rainforest interior and dry forest, we did not analyse them separately here.

Our OUWIE analyses are consistent with the existence of different selective regimes in open and closed habitats. These regimes differ in rate, strength of stabilising selection, and trait optima (OUMVA model). By contrast, genital ornamentation regimes are consistent with Brownian motion with separate rates for open and closed habitats (BMS model). SOD is consistent with the

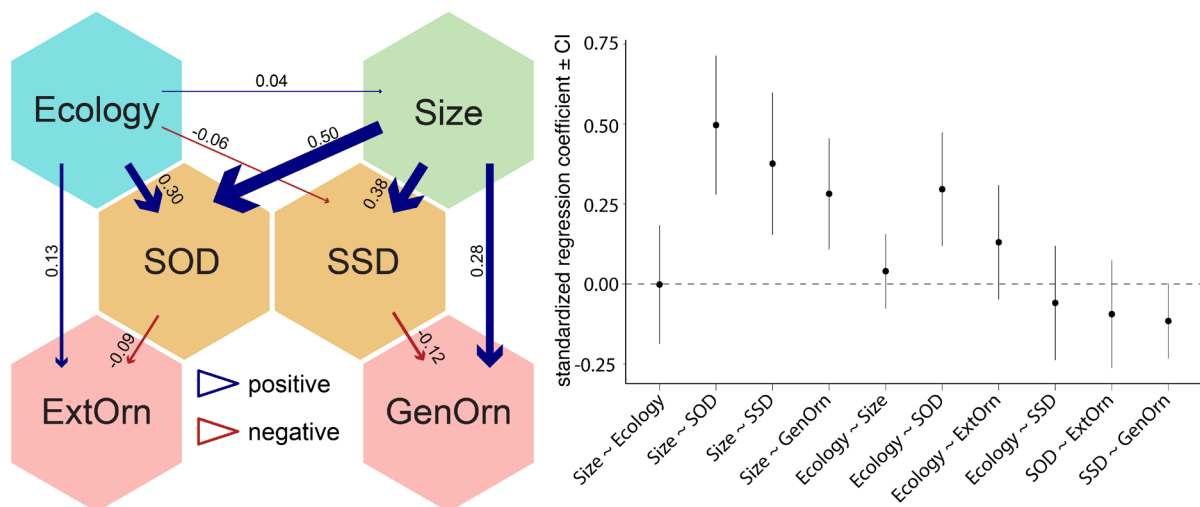


Fig. 3. Average of two best-scoring phylogenetic path analysis models and the standardised regression coefficients of its components.

SSD = sexual size dimorphism, SOD = sexual external ornamentation dimorphism, ExtOrn = external ornamentation, GenOrn = genital ornamentation.

OUMVA model, or a marginally simpler OUMV model, which does not include alternative values of stabilising selection strength.

Multifactorial comparison and phylogenetic path analysis. We built PLRMs of the multifactorial effects that potentially influence genital and external ornamentation: degree of genital ornamentation $\sim \log(\text{SVL}_{\text{mid}})$ + degree of external ornamentation + habitat openness + SOD + SSD, and the same model with external and genital ornamentation swapped. In the former model, body size ($P = 0.009103$) and SSD ($P = 0.032903$) had a significant effect on genital ornamentation of all chameleons, and all other elements were insignificant ($P > 0.1$). In the external ornamentation model, SOD had the strongest effect ($P = 4.975 \times 10^{-9}$), SSD ($P = 0.000284$) and habitat openness ($P = 0.006486$) also had highly significant effects, and body size had a marginally insignificant effect ($P = 0.050873$). For Chamaeleoninae alone, no factors were significant in the genital model, but SSD was closest ($P = 0.08592$), while in the external ornamentation model, the significant factors did not differ (SOD $P = 7.63 \times 10^{-8}$, SSD $P = 0.0008649$, habitat openness $P = 0.0092553$), and size had a less significant effect ($P = 0.1405476$). These models indicate that size and SSD have a strong effect on genital ornamentation, whereas SOD and habitat have the strongest effects on external ornamentation.

To investigate the relative importance of the different components in determining ornamentation, we conducted a phylogenetic path analysis. The two best models had identical weights and probabilities, and differed only in the direction of the influence of ecology and size on one another, both of which were insignificant, so we averaged them (Fig. 3). In this model, ecology drives ornamentation dimorphism, external ornamentation, and weakly also influences size dimorphism and size itself; size drives ornamentation and size dimorphism, as well as genital ornamentation; and ornamentation dimorphism influences external ornamentation and size dimorphism influences genital ornamentation. These two models had a cumulative weight of 0.756. These results are consistent with those found in our multifactorial PLRM analysis.

Discussion

In this study we have used the complete radiation of chameleons to untangle different potential drivers of signal complexity. The trade-off (negative correlation) predicted between the degree of external and genital ornamentation predicted by the ornament trade-off hypothesis [14] is not found, but neither is the positive correlation we might expect if sexual selection was having holistic effects on the degree of ornamentation. The evolution of complexity in external and genital ornamentation appears to be uncoupled in chameleons, driven by different forms of sexual selection; a finding robust to topological uncertainty of deep nodes within the chameleon tree that persists despite our phylotranscriptomic approach.

We used two separate proxies for sexual selection: sexual external ornamentation dimorphism (SOD) and sexual size dimorphism (SSD). We find SOD to be strongly related to habitat openness and body size. The role of body size may simply be related to the surface area over which to host ornaments [8], whereas that of habitat openness is consistent with field observations [28, 58, 59] that have suggested that signal complexity in closed-canopy environments helps chameleons stand out, whereas open-canopy environments have reduced visibility distance, resulting in greater emphasis on performance over signalling [28]. This is consistent with SOD being driven most strongly by female mate choice [60]. Given the role of SOD and habitat openness recovered in our path model, we conclude that complexity of external ornamentation in chameleons is driven by two factors: (1) the strength of female choice, which is strongly related to ecology because habitat openness has a strong effect on the ability to perceive signals, and thus the need to invest in them, and (2) natural selection, possibly because habitat openness influences the costliness of ornamentation, counter-balancing sexual selection, e.g. if ornament elaboration results in increased predation risk or decreased resource acquisition.

SSD is found to be strongly related to body size, with some effect of habitat openness. Chameleon SSD is generally consistent with Rensch's rule [56, 57]; in most species with larger females, we find decreasing SSD with greater body size, and in most species with larger males we find greater SSD with greater body size. SSD and body size directly were recovered as promoting genital ornamentation complexity in chameleons. This leads us to conclude that allometry has a strong effect on genital ornamentation, probably again due to physical limitations on hemipenial ornamentation, as evidenced by the simple (though still taxonomically valuable [19, 20, 61]) hemipenes of most *Brookesia* species. The role of SSD is probably related to its relationship with mating system, which is potentially a key factor determining genital ornamentation. Although chameleons in general are polygamous, the degree of mate guarding by males does seem to be related to body size, with greater fidelity (and thus perhaps less frequent polygyny) in species with females substantially larger than males [17]. However, SSD can have multiple drivers: male-biased SSD is driven largely by male-male competition or female choice, whereas female-biased SSD is generally driven by fecundity selection (reviewed in [62]). What is clear is that the mode of selection is different from that driving external ornamentation.

In the terms of Ord and Garcia-Porta [8], our results show that ornament complexity evolution is related to social factors (different kinds of sexual selection) in chameleons, but the strength and direction of influence that these factors have are dependent upon ecology and allometry. For hemipenes, allometry also plays an important role, probably due to physiological limitations, whereas for external ornamentation, ecology itself has an important role, possibly due to natural selection. Complex external ornamentation, while acting as a pre-copulatory selective substrate, does not seem to influence the strength of selection on the intromittent organs. Genital and external ornaments therefore do not act in a redundant manner in response to an overarching selective pressure, as is the case of the complex 'courtship phenotype' of birds of paradise [7], but rather, they are separate modules of the sexual selective substrate, without co-dependency.

This surprising result has important implications for broader patterns that have been noted pre-

viously. Iguanid lizards, which have marked SSD and SOD, have simple hemipenes, while varanid lizards, which may have SSD but lack SOD, have elaborate and highly diagnostic hemipenes [63]. Our results suggest that these patterns may be more strongly related to the ecology and mating systems of these lizards, than to any trade-off. The potential for different selective pressures to act separately and differently on different modules of the sexual selective substrate may have important implications for our understanding of why the same components can be negatively correlated in one taxon, and positively correlated in another, e.g. plumage vibrancy and song complexity in different groups of birds [7, 64, 65].

The comparative phylogenetic framework we have used has helped us to elucidate the overall patterns and their potential drivers. This must now be supplemented by more extensive work on chameleon behaviour and ecology to better understand the factors driving their ornamentation. Perhaps most importantly, we need to understand how ornaments are perceived [6]. A critical step will be investigating the function of genital ornamentation; cryptic female choice may be playing an important role if genital ornaments are used in assessing male quality, but male-male competition or sexual conflict could be at play if the chameleons use hemipenial spines to scar the female reproductive tract or remove sperm from previous mating events. Currently, our lack of functional understanding of these organs precludes the ability to fully deduce their evolutionary drivers. Nevertheless, with this study, we have taken the first step toward understanding sexual ornamentation in one of the most elaborately ornamented tetrapod groups ever to exist.

Acknowledgements

We are very grateful to the following colleagues for their various contributions to the realisation of this project: C. Liedtke, E. Sherratt, G. T. Lloyd, D. Hone, E. Z. Lattenkamp, and T. Ziegler. Photos of chameleons in life were kindly provided by W. Conradie, the late B. Branch, E. van Heygen, and C. Anderson. M. Kondermann, G. Keunecke, E. Öztel, S. Szefs, and T. Townsend helped with laboratory work. We thank S. Álvarez-Carretero and M. Dos Reis for help in setting up MCMCTree analyses.

References

1. Ritchie M.G. 2007 Sexual Selection and Speciation. *Annual Review of Ecology, Evolution, and Systematics* **38**, 79–102. (doi:10.1146/annurev.ecolsys.38.091206.095733).
2. Rico-Guevara A., Hurme K.J. in press Intrasexually selected weapons. *Biological Reviews*. (doi:10.1111/brv.12436).
3. McCullough E.L., Miller C.W., Emlen D.J. 2010 Why sexually selected weapons are not ornaments. *Trends in Ecology and Evolution* **31**(10), 742–751. (doi:10.1016/j.tree.2016.07.004).
4. Hone D.W.E., Naish D. 2013 The ‘species recognition hypothesis’ does not explain the presence and evolution of exaggerated structures in non-avian dinosaurs. *Journal of Zoology* **290**, 172–180. (doi:10.1111/jzo.12035).
5. Darwin C. 1871 *The descent of man, and selection in relation to sex*. London, United Kingdom, John Murray.
6. Eliason C.M. 2018 How do complex animal signals evolve? *PLoS Biology* **16**(12), e3000093. (doi:10.1371/journal.pbio.3000093).
7. Ligon R.A., Diaz C.D., Morano J.L., Troscianko J., Stevens M., Moskaland A., Laman T.G., Scholes E., III. 2018 Evolution of correlated complexity in the radically different courtship signals of birds-of-paradise. *PLoS Biology* **16**(11), e2006962 (2006924 pp.). (doi:10.1371/journal.pbio.2006962).

Results

8. Ord T.J., Garcia-Porta J. 2012 Is sociality required for the evolution of communicative complexity? Evidence weighed against alternative hypotheses in diverse taxonomic groups. *Philosophical Transactions of the Royal Society B: Biological Sciences* **367**, 1811–1828. (doi:10.1098/rstb.2011.0215).
9. Edwards R. 1993 Entomological and mammalogical perspectives on genital differentiation. *Trends in Ecology and Evolution* **8**, 406–409.
10. Böhme W. 1988 Zur Genitalmorphologie der Sauria: funktionelle und stammesgeschichtliche Aspekte. *Bonner zoologische Monographien* **27**, 1–176.
11. Cope E.D. 1896 On the hemipenes of the Sauria. *Proceedings of the Academy of Natural Sciences of Philadelphia* **48**, 461–467.
12. Cope E.D. 1895 The classification of the Ophidia. *Transactions of the American Philosophical Society* **18**, 186–219.
13. Hosken D.J., Stockley P. 2004 Sexual selection and genital evolution. *Trends in Ecology and Evolution* **19**(2), 87–93. (doi:10.1016/j.tree.2003.11.012).
14. Böhme W., Ziegler T. 2008 A review of iguanian and anguimorph lizard genitalia (Squamata: Chamaeleonidae; Varanoidea, Shinisauridae, Xenosauridae, Anguidae) and their phylogenetic significance: comparisons with molecular data sets. *Journal of Zoological Systematics and Evolutionary Research* **47**(2), 189–202. (doi:10.1111/j.1439-0469.2008.00495.x).
15. Anderson C.V., Higham T.E. 2013 Chameleon Anatomy. In *Biology of the Chameleons* (eds. Tolley K.A., Herrel A.), pp. 7–56. Berkeley and Los Angeles, California, USA and London, England, University of California Press.
16. Uetz P., Hošek J. 2016 The Reptile Database, <http://www.reptile-database.org>, accessed: 14 March 2019. (
17. Stuart-Fox D.M. 2013 Chameleon Behavior and Color Change. In *Biology of the Chameleons* (eds. Tolley K.A., Herrel A.), pp. 115–130. Berkeley and Los Angeles, California, USA and London, England, University of California Press.
18. Klaver C., Böhme W. 1986 Phylogeny and classification of the Chamaeleonidae (Sauria) with special reference to hemipenis morphology. *Bonner zoologische Monographien* **22**, 1–64.
19. Scherz M.D., Köhler J., Rakotoarison A., Glaw F., Vences M. 2019 A new dwarf chameleon, genus *Brookesia*, from the Marojejy massif in northern Madagascar. *Zoosystematics and Evolution* **95**(1), 95–106. (doi:10.3897/zse.95.32818).
20. Glaw F., Köhler J., Townsend T.M., Vences M. 2012 Rivaling the world's smallest reptiles: discovery of miniaturized and microendemic new species of leaf chameleons (*Brookesia*) from northern Madagascar. *PLoS One* **7**(2), e31314 (31324 pp.). (doi:10.1371/journal.pone.0031314).
21. Prötz D., Scherz M.D., Ratsoavina F.M., Vences M., Glaw F. submitted Untangling the trees: Revision of the *Calumma nasutum* complex (Squamata: Chamaeleonidae). *Vertebrate Zoology*.
22. Prötz D., Vences M., Scherz M.D., Vieites D.R., Glaw F. 2017 Splitting and lumping: An integrative taxonomic assessment of Malagasy chameleons in the *Calumma guibei* complex results in the new species *C. gehringi* sp. nov. *Vertebrate Zoology* **67**(2), 231–249.
23. Townsend T.M., Vieites D.R., Glaw F., Vences M. 2009 Testing species-level diversification hypotheses in Madagascar: the case of microendemic *Brookesia* leaf chameleons. *Systematic Biology* **58**(6), 641–656. (doi:10.1093/sysbio/syp073).
24. Stuart-Fox D.M., Whiting M.J. 2005 Male dwarf chameleons assess risk of courting large, aggressive females. *Biology Letters* **1**, 231–234. (doi:10.1098/rsbl.2005.0299).

25. Cuadrado M. 2001 Mate guarding and social mating system in male common chameleons (*Chamaeleo chamaeleon*). *Journal of Zoology* **255**, 425–435.
26. Karsten K.B., Andriamandimbiarisoa L.N., Fox S.F., Raxworthy C.J. 2009 Social behavior of two species of chameleons in Madagascar: insights into sexual selection. *Herpetologica* **65**(1), 54–69.
27. Stuart-Fox D.M., Moussalli A. 2008 Selection for social signalling drives the evolution of chameleon colour change. *PLoS Biology* **6**(1), e25.
28. Measey G.J., Hopkins K., Tolley K.A. 2009 Morphology, ornaments and performance in two chameleon ecomorphs: is the casque bigger than the bite? *Zoology* **112**, 217–226. (doi:10.1016/j.zool.2008.09.005).
29. Irisarri I., Baurain D., Brinkmann H., Delsuc F., Sire J.-Y., Kupfer A., Petersen J., Jarek M., Meyer A., Vences M., et al. 2017 Phylogenomic consolidation of the jawed vertebrate timetree. *Nature Ecology and Evolution* **1**(9), 1370–1378. (doi:10.1038/s41559-017-0240-5).
30. Rodríguez A., Burgos J.D., Lyra M., Irisarri I., Baurain D., Blaustein L., Göçmen S., Künzel S., Mable B.K., Nolte A.W., et al. 2017 Inferring the shallow phylogeny of true salamanders (*Salamandra*) by multiple phylogenomic approaches. *Molecular Phylogenetics and Evolution* **115**, 16–26.
31. Grabherr M.G., Haas B.J., Yassour M., Levin J.Z., Thompson D.A., Amit I., Adiconis X., Fan L., Raychowdhury R., Zeng Q., et al. 2011 Trinity: reconstructing a full-length transcriptome without a genome from RNA-Seq data. *Nature Biotechnology* **29**, 644–652.
32. Roure B., Rodriguez-Ezpeleta N., Philippe H. 2007 SCaFoS: a tool for selection, concatenation and fusion of sequences for phylogenomics. *BMC Evolutionary Biology* **7**, S2.
33. Stamatakis A. 2014 RAxML Version 8: A tool for phylogenetic analysis and post-analysis of large phylogenies. *Bioinformatics* **30**(9), 1312–1313. (doi:10.1093/bioinformatics/btu033).
34. Kalyaanamoorthy S., Minh B.Q., Wong T.K., von Haeseler A., Jermiin L.S. 2017 ModelFinder: fast model selection for accurate phylogenetic estimates. *Nature Methods* **14**(6), 587.
35. Nguyen L.-T., Schmidt H.A., von Haeseler A., Minh B.Q. 2015 IQ-TREE: a fast and effective stochastic algorithm for estimating maximum-likelihood phylogenies. *Molecular Biology and Evolution* **32**(1), 268–274. (doi:10.1093/molbev/msu300).
36. Hoang D.T., Chernomor O., von Haeseler A., Minh B.Q., Vinh L.S. 2018 UFBoot2: Improving the ultrafast bootstrap approximation. *Molecular Biology and Evolution* **35**, 518–522. (doi:10.1093/molbev/msx281).
37. Tolley K.A., Townsend T.M., Vences M. 2013 Large-scale phylogeny of chameleons suggests African origins and Eocene diversification. *Proceedings of the Royal Society of London B* **280**(1759), 20130184 (20130188 pp.). (doi:10.1098/rspb.2013.0184).
38. dos Reis M., Thawornwattana Y., Angelis K., Telford M.J., Donoghue P.C.J., Yang Z. 2015 Uncertainty in the timing of origin of animals and the limits of precision in molecular timescales. *Current Biology* **25**, 2939–2950.
39. dos Reis M., Donoghue P.C.J., Yang Z. 2016 Bayesian molecular clock dating of species divergences in the genomics era. *Nature Reviews Genetics* **17**(2), 71–80.
40. Yang Z. 2007 PAML 4: Phylogenetic Analysis by Maximum Likelihood. *Molecular Biology and Evolution* **24**, 1586–1591.
41. dos Reis M., Yang Z. 2011 Approximate likelihood calculation on a phylogeny for Bayesian estimation of divergence times. *Molecular Biology and Evolution* **28**, 2161–2172.
42. Rambaut A., Drummond A.J., Xie D., Baele G., Suchard M.A. 2018 Posterior summarisation in Bayesian phylogenetics using Tracer 1.7. *Systematic Biology* **67**(5), 901–904. (doi:10.1093/

Results

- sysbio/syy032).
43. Sukumaran J., Holder M.T. 2010 DendroPy: A Python library for phylogenetic computing. *Bioinformatics* **26**, 1569–1571.
 44. R Core Team. 2014 R: A language and environment for statistical computing. R Foundation for Statistical Computing, Vienna, Austria. <http://www.R-project.org/>.
 45. RStudio Team. 2016 RStudio: Integrated Development for R. RStudio, Inc., Boston, MA. <http://www.rstudio.com/>.
 46. Paradis E., Schliep K. in press ape 5.0: an environment for modern phylogenetics and evolutionary analyses in R. *Bioinformatics*, bty633. (doi:10.1093/bioinformatics/bty633).
 47. Revell L.J. 2012 phytools: An R package for phylogenetic comparative biology (and other things). *Methods in Ecology and Evolution* **3**, 217–223.
 48. Harmon L.J., Weir J.T., Brock C.D., Glor R.E., Challenger W. 2008 GEIGER: investigating evolutionary radiations. *Bioinformatics* **24**, 129–131.
 49. Wickham H. 2016 *ggplot2: Elegant Graphics for Data Analysis*. New York NY, USA, Springer-Verlag.
 50. Ho L.S.T., Ane C. 2014 A linear-time algorithm for Gaussian and non-Gaussian trait evolution models. *Systematic Biology* **63**(3), 397–408.
 51. Pagel M. 1999 Inferring the historical patterns of biological evolution. *Nature* **401**, 877–884.
 52. Blomberg S.P., Garland T.J., Ives A.R. 2003 Testing for phylogenetic signal in comparative data: Behavioral traits are more labile. *Evolution* **57**, 717–745.
 53. Beaulieu J.M., O'Meara B. 2016 OUwie: Analysis of Evolutionary Rates in an OU Framework. R package version 1.50. <https://CRAN.R-project.org/package=OUwie>.
 54. von Hardenberg A., Gonzalez-Voyer A. 2013 Disentangling evolutionary cause-effect relationships with phylogenetic confirmatory path analysis. *Evolution* **67**(2), 378–387. (doi:10.1111/j.1558-5646.2012.01790.x).
 55. van der Bijl W. 2018 phylopath: Easy phylogenetic path analysis in R. *PeerJ* **6**, e4718. (doi:10.7717/peerj.4718).
 56. Rensch B. 1948 Histological Changes Correlated with Evolutionary Changes of Body Size. *Evolution* **2**(3), 218–230. (doi:10.2307/2F2405381).
 57. Rensch B. 1950 Die Abhängigkeit der relativen Sexualdifferenz von der Körpergrösse. *Bonner Zoologische Beiträge* **1**, 58–69.
 58. da Silva J.M., Herrel A., Measey G.J., Tolley K.A. 2014 Sexual dimorphism in bite performance drives morphological variation in chameleons. *PLoS One* **9**(1), e86846. (doi:10.1371/journal.pone.0086846).
 59. da Silva J.M., Tolley K.A. 2013 Ecomorphological variation and sexual dimorphism in a recent radiation of dwarf chameleons (*Bradypodion*). *Biological Journal of the Linnean Society* **109**, 113–130.
 60. Andersson M. 1994 *Sexual Selection*. Princeton NJ, USA, Princeton University Press.
 61. Glaw F., Vences M., Ziegler T., Böhme W., Köhler J. 1999 Specific distinctness and biogeography of the dwarf chameleons *Brookesia minima*, *B. peyrierasi* and *B. tuberculata* (Reptilia: Chamaeleonidae): evidence from hemipenial and external morphology. *Journal of Zoology* **247**, 225–238.
 62. Blanckenhorn W.U. 2005 Behavioral causes and consequences of sexual size dimorphism. *Ethology* **111**(11), 977–1016. (doi:10.1111/j.1439-0310.2005.01147.x).
 63. Ziegler T., Böhme W. 1997 Genitalstrukturen und Paarungsbiologie bei squamaten Reptilien,

- speziell den Platynota, mit Bemerkungen zur Systematik. *Mertensiella* **8**, 1–207.
64. Badyaev A.V., Hill G.E., Weckworth B.V. 2002 Species divergence in sexually selected traits: increase in song elaboration is related to decrease in plumage ornamentation in finches. *Evolution* **56**, 412–419.
65. Gonzalez-Voyer A., den Tex R.-J., Castelló A., Leonard J.A. 2013 Evolution of acoustic and visual signals in Asian barbets. *Journal of Evolutionary Biology* **26**, 647–659.

Discussion

'There is considerable doubt in the minds of some taxonomists and even more in the minds of most nontaxonomists as to what the real functions of the systematist are.'

— Ernst Mayr, 1942, *Systematics and the Origin of Species from the Viewpoint of a Zoologist*, p. 8

The work that I have presented here has resulted in the description of sixteen new frog species, two new frog genera, and robust new phylogenetic hypotheses regarding the evolution of chameleons and a subfamilial radiation of frogs, with implications for the conservation, biogeography, and evolution of all of these taxa. Here, I first discuss the overall implications of my research on each topic (conservation, biogeography, ecomorphology, and macroevolution), and then go on to discuss our growing knowledge of the biodiversity of Madagascar, and the implications of that growth on our ability to use the island as a model system.

Conservation implications

The tropics are bearing the brunt of the impacts of human population growth and resource demands. Deforestation rates in tropical forests are extremely high, as are other forms of anthropogenic pressure that are altering and deteriorating tropical ecosystems (reviewed by Barlow et al. 2018). Amphibians and reptiles, as a consequence of their environmental sensitivity (outlined in the **Introduction**) are at the front line of threat (reviewed by Böhm et al. 2013 and Catenazzi 2015), made still worse by global spread of diseases, to which humans also contribute substantially (Olson et al. 2013; Lorch et al. 2016; Spitzen-van der Sluijs et al. 2016; O'Hanlon et al. 2018).

Given these global trends, conservation assessment and action are more important today than ever. As many others have argued in the past (see summaries in Dubois 2003 and Vogel Ely et al. 2017), conservation is strongly dependent on taxonomy, because species are the units that are managed. Often, it seems that this, when acknowledged, is taken to refer only to taxonomists' capacity to describe new species, but the duties of taxonomists lie not only in producing new names, but also careful revision of existing names and resolution of complexes (Dubois 2003). As experts on any given taxon, taxonomists are uniquely well suited to be involved in conservation assessment action. Indeed, species descriptions are now often accompanied by recommendations for conservation assessments, like those given here in **chapters 1–3, 5–7 and 9**.

In addition to individuals who actively work on conservation of specific taxa, many Red List assessors are taxonomists. Assessors are arranged into Specialist Groups for major taxa (e.g. the Amphibian Specialist Group, of which I am a member). These specialist groups coordinate the conservation assessments across higher taxa (<https://www.iucn.org/commissions/ssc-groups>). This inclusion reflects the acknowledgement by the IUCN of the unique suitability of taxonomists to assess the conservation needs of their focal taxa. One benefit of involving taxonomists directly in the conservation assessment process is that new species can be incorporated more quickly. Ideally this would also mean that the assessments of species for which taxonomic data are inadequate, such as species complexes, would reflect that status and list the species as Data Deficient (DD).

Although assessments of species complexes often include notes stating that their taxonomy is uncertain, their statuses do not reflect that uncertainty. As explained in **chapter 1**, the assessment of species complexes falls under IUCN guidelines that recommend they be treated as single species and assessed according to the distribution and knowledge of the whole of that 'species', or be omitted altogether. When a species complex stretches over a large area, the result is often a status

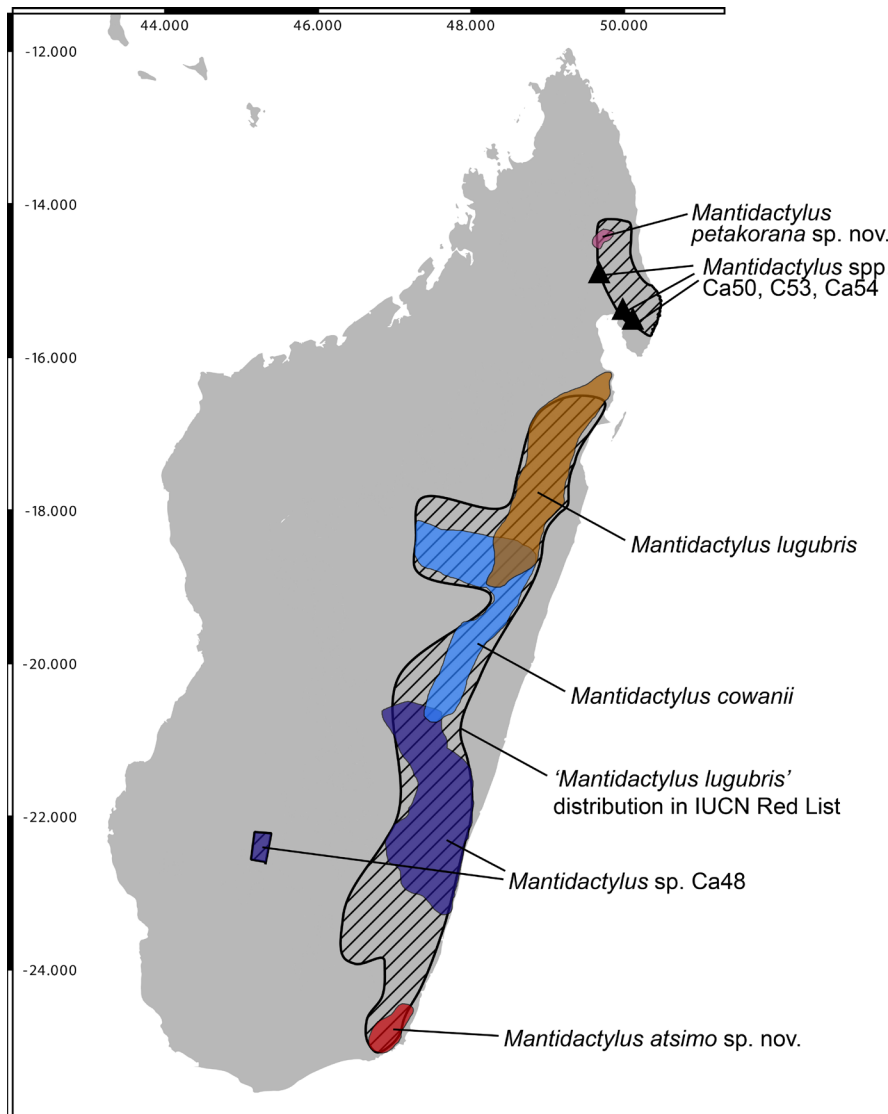


Fig. 2. Map of Madagascar showing the current IUCN Red List distribution of '*Mantidactylus lugubris*' (hatched areas), which refers to the entirety of the complex, versus the distributions of the species and candidate species in the complex.

The large distribution of the complex meant that the taxon was assessed as Least Concern. Yet, at the time of assessment (17 May 2016), it was already clear that certain lineages, such as those in the north, could be excluded from the circumscription of *M. lugubris*. My colleagues and I argue in **chapter 1** that such cases should be listed in the Red List under the most restrictive definition available, or assessed as a whole complex as Data Deficient.

of Least Concern for the whole of the complex, when any one species-level lineage within it might be on the verge of extinction (McLeod 2010; Gehara et al. 2014; see Fig. 2). Such assessments, I argue in **chapter 1**, hinder more than they help, because they fail to capture the threat status of any constituent species in the complex, and these could quietly go extinct without any change to the status of the complex as a whole.

A more reasonable practice for such complexes would be to treat them as DD. This is possible, but only if practically no information is available for the species, because of another IUCN recommendation: ‘taxa that are poorly known can often be assigned a threat category on the basis of background information concerning the deterioration of their habitat and/or other causal factors; therefore the liberal use of “Data Deficient” is discouraged.’ (IUCN 2012, p. 7). In practice, this suggestion means that species that are known from single individuals are often given threat statuses based on extreme extrapolation from a single data point; for example, we suggested *Rhombohphryne savaka* be assessed as Endangered in **chapter 6**, although only two specimens of the species were known at the time.

For species complexes, the combination of these two recommendations means that they are generally assessed as single species and assigned a non-DD category. The case of *Mantidactylus lugubris*, the species complex discussed in **chapter 1**, is typical in this regard. Currently, it is assessed as Least Concern because its circumscription refers to a number of candidate species that are widespread along the eastern escarpment of Madagascar and an isolated pocket in the west. As

Discussion

is evident in Fig. 2, the current assessment is not appropriate for any of the constituent lineages within the complex, and inflates their conservation status. While it is now possible to refine the Red List status for the described lineages as a result of our taxonomic treatment of the complex (**chapter 1**), a status of DD would have been more appropriate, and indeed more informative, to apply to the whole of the complex before our taxonomic revision.

The motivation for the IUCN's avoidance of the use of the DD category is understandable. As it does not constitute a threatened status, DD species are omitted from conservation prioritisation lists. As a result, these species may be nearing extinction without us being aware of how threatened they are (Butchart and Bird 2010; Howard and Bickford 2014). I would argue, however, that extrapolating from poor data is equally undesirable. I would also contend that a threat status may reflect the need for conservation of a species, but a status of DD better reflects the need for fundamental research on that species.

Taking up this point, there have recently been a couple of papers that have attempted to extrapolate from what little data are available on DD species in the Red List to propose research prioritisation. Nori and Loyola (2015) mapped DD species against a database of the world's protected areas and assessed the fraction of overlap, and Nori et al. (2018) used the distribution of DD species to identify focal areas where research is needed. Unfortunately, I would argue that these studies are, in part, based on a misunderstanding of the meaning of the DD criterion. DD species are generally those for which information on range are completely inadequate, for example species described from broad type localities like 'Madagascar' that have then not been found again, or, in some groups, species known from single individuals (note: criteria are applied inconsistently among major taxa, and even within taxa across different regions of the world). Mapping species that are more or less definitionally unreliable to map is unlikely to produce especially trustworthy results. Nevertheless, Nori and colleagues' emphasis on the need for research into DD species demonstrates the value of the criterion in promoting that research.

My colleagues and I argue in **chapter 1** that Data Deficient is an appropriate and valuable criterion for species complexes where taxonomy is wholly or largely uncertain. Sometimes, taxonomic complexes are understood to contain nominal lineages and unnamed lineages that simply have not yet been described. In these latter cases, we argue that assessment should be based on a restrictive definition of the taxon (as restricted as possible, if deemed possible by the assessors and taxonomists), with other lineages excluded until they are taxonomically addressed. In doing so, their assessments would better reflect the status of the species for which they are intended, and need not be updated every time a new species is described from the complex. Under the current policy, dozens of taxa included in the Red List as Least Concern at present refer to several species, each of which is presumably threatened in its own right. Such complexes are well known and widespread both geographically and taxonomically (e.g. Fritz et al. 2010; McLeod 2010; Gehara et al. 2014; He and Jiang 2015). Changing that policy as we recommend would better reflect the importance of taxonomy in anchoring the Red List, and potentially improve the future outlook for this overlooked and underappreciated cryptic diversity.

Biogeography of herpetofauna in northern Madagascar

Madagascar as a whole is exceptional in terms of biodiversity and microendemism, but the north of the island is particularly rich (Brown et al. 2014, 2016). The varied topography and strongly separated drainage basins (Wilmé et al. 2006) make this area especially valuable for biogeographical study, highlighted by numerous studies (Wilmé et al. 2006; Boumans et al. 2007; Maminirina et al. 2008; Raxworthy et al. 2008; Wollenberg et al. 2008, 2011; Andreone et al. 2009; Pearson and Raxworthy 2009; Gehring et al. 2013; Brown et al. 2014, 2016; Blair et al. 2015; Rabearivony et al. 2015). Although the complex topography and poor roads in the area make access to large

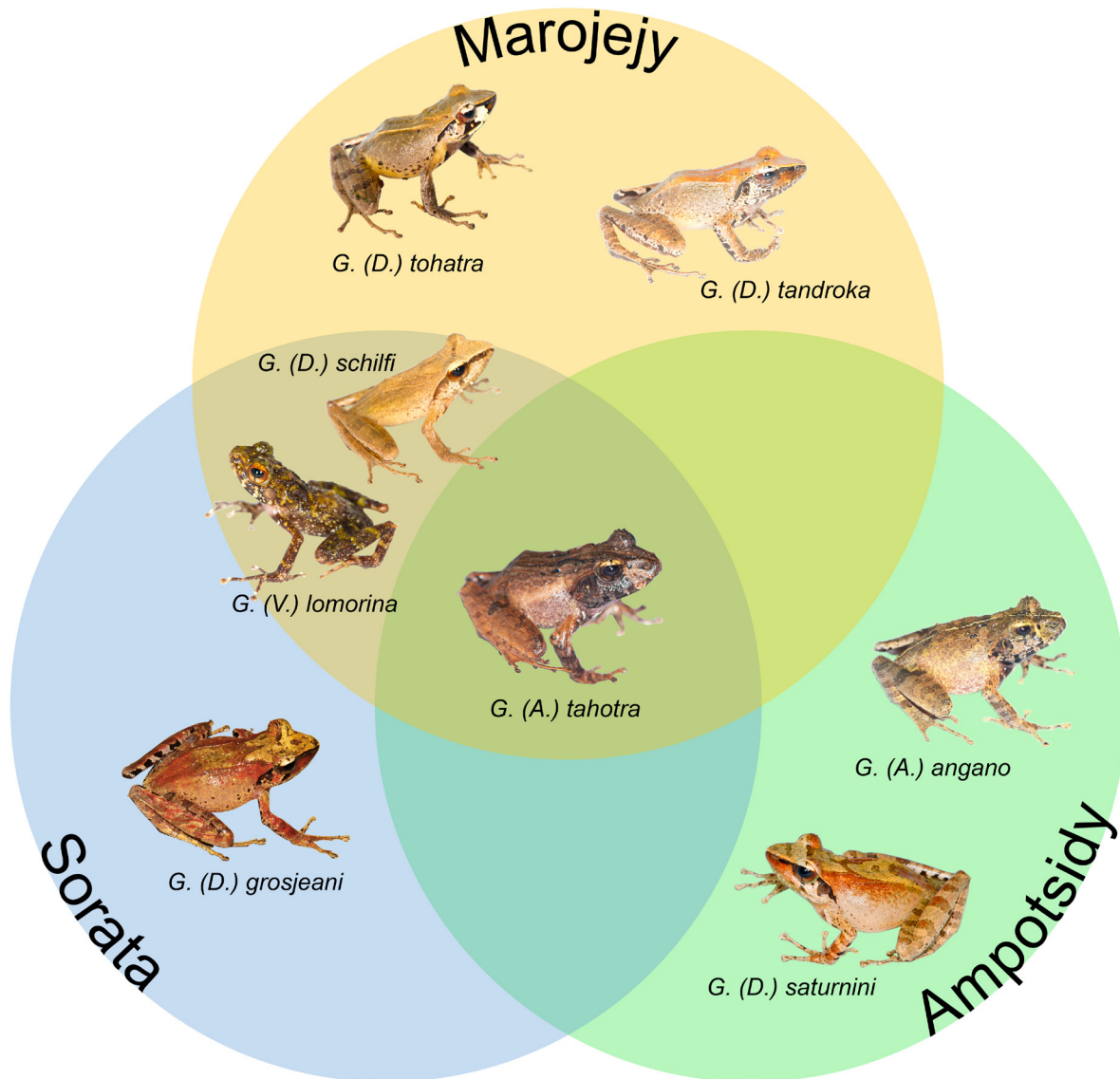


Fig. 3. A Venn-diagram of *Gephyromantis* species occurring across the mountainous massifs of northern Madagascar.

G. (L.) horridus-ranjomavo is not included here because of insufficient clarity in the relationships of the *Laurentomantis* in this region. For a map indicating the location of these three massifs, see Fig. 1 in the **Introduction**. Subgenus abbreviations: *A.* = *Asperomantis*, *D.* = *Duboimantis*, *V.* = *Vatomantis*

swathes of the northern forests challenging, there have recently been a number of well-vouchered herpetological surveys at various sites across the north of Madagascar. These have yielded sufficient samples that we can start to identify trends in the distribution and phylogenetic relationships of species across the region. Such trends are interesting, because they can shed light on processes involved in the generation and maintenance of species diversity in a hotspot of biodiversity where the community turnover is especially stark.

Gephyromantis are among the several amphibian clades with their centres of diversity and endemism in north Madagascar (Kaffenberger et al. 2012; Brown et al. 2016), making them a potentially insightful study system for the understanding of biogeography in this area. Ecological differentiation among the six subgenera of *Gephyromantis* is such that members of many different subgenera often occur syntopically, or at least in close sympatry; for example, the following species co-occur at ca. 1350 m a.s.l. on the Marojejy massif: *G. (Vatomantis) lomorina*, *G. (Laurentomantis) ranjomavo*, *G. (Duboimantis) schilfi*, *G. (Asperomantis) tahotra*, *G. (D.) tandroka*,

Discussion

and *G. klemmeri* (subgenus assignment of *G. klemmeri* is discussed in **chapter 3**). We might thus expect that biogeographic patterns among the different subgenera differ according to their ecologies. Nevertheless, my work points toward the existence of overarching patterns that hold for the genus as a whole.

Although the deepest nodes within the genus are still quite poorly resolved (Kaffenberger et al. 2012; discussed pertaining to *Laurentomantis* and *Vatomantis* in **chapter 3**), *Gephyromantis* is currently thought to have its origins in the north or northeast (Kaffenberger et al. 2012). However, at least one of the six subgenera appears to have expanded back into the north from further south (Kaffenberger et al. 2012). The papers I present in **chapters 2–5** deal with the subgenera *Asperomantis*, *Duboimantis*, and *Vatomantis*. Briefly, according to Kaffenberger et al. (2012), *Asperomantis*, leaf-litter dwelling frogs with exotrophic tadpoles, apparently originated in northern Madagascar, and spread south to reach Ranomafana in the south central east (see also Vences et al. 2017)—*G. (Asperomantis) angano* described in **chapter 2**, being possibly a relatively deep lineage from this subgenus, lends still greater weight to this interpretation; *Vatomantis*, mossy-looking frogs often found near moderately fast-flowing streams, are restricted entirely to north eastern Madagascar, with no members of the subgenus hitherto found outside of that region—*G. (Vatomantis) lomorina* described in **chapter 3** extends the range of that subgenus further into the north of Madagascar; and *Duboimantis*, leaf-litter dwelling frogs similar to *Asperomantis* but mostly of larger body size and with endotrophic (non-feeding) tadpoles, is divided between a basally diverged clade with its origins in the central east and a northern clade spread across most of the north of Madagascar—*G. (Duboimantis) tohatra* described in **chapter 4** and *G. (D.) saturnini* and *G. (D.) grosjeani* described in **chapter 5** all belong to a small part of the northern clade, adding still more evidence of local diversification of this subgenus in the north.

My work in **section 2** focussed largely on three massifs, Marojejy, Sorata (and the nearby Andravory massif), and Ampotsidy in the Bealanana District, which together form three corners of an almost equilateral triangle (see Fig. 1 in the **Introduction** for geographic context). The simplicity (or reducibility) of this system lends itself to biogeographic study. These areas are connected by a single continuous mountain range (see **figure 6 in chapter 2** and **figure 11 in chapter 5**) that reaches its maximum height at Maromakotro, Madagascar's highest peak, which lies almost directly between Ampotsidy and Sorata. Given that elevation-bands of frogs in Madagascar are usually (though not always) quite restricted, we can predict that direct connectivity between these two massifs might be limited. Of the species discussed in **section 2**, five are exclusive to one massif, and two are shared across two massifs, and one occurs on all three (see Fig. 3). The latter, *G. (A.) tahotra*, has also been recorded from Matsabory Maiky, a locality on the southwest side of the Tsaratanana massif, lying between Ampotsidy and Sorata (see **figure 7 in chapter 2**).

Based on these limited data, we may already distinguish that there is a greater degree of connectivity between Marojejy and Sorata, than between either of those massifs and Ampotsidy. Data from Cophylinae seem to conform to this pattern as well: *Rhombophryne longicrus* from Sorata is sister to *R. minuta* from Marojejy (Scherz et al. 2015a). In **chapter 8**, a *Rhombophryne* species from Sorata was found to be sister to or conspecific with *R. vaventy*, which is found around 1350 m a.s.l. on Marojejy (discussed also in Lambert et al. 2017 and **chapter 10**), and in **chapter 7**, *R. diadema* from Sorata is found to belong to a clade of frogs from Tsaratanana, which may be sister to lineages from Marojejy, but no *Rhombophryne* species are known from Ampotsidy. The same is true of *Stumpffia* species, of which my colleagues and I have described several from Sorata (Rakotoarison et al. 2017), but only few are known from the Bealanana District (data on these have not yet been analysed). Curiously, the *Stumpffia* species of Marojejy generally have closer affinities with species from further south along the east coast of Madagascar, except one species, *S. sorata*, which belongs to a clade from the north of the island and seems to have spread to Marojejy from the north (Rakotoarison et al. in press).

Among reptiles, the best studied group in this area of Madagascar are chameleons of the *Calumma nasutum* species group. These small chameleons, characterised by a narrow body profile and a dermal rostral appendage, are widespread across the East and North of the island and have been the subject of a recent revision by my colleagues and me (Prötzl et al. 2015, 2017, 2018b, 2018c, submitted). *Calumma uetzi* is found in both Sorata and Marojejy (Prötzl et al. 2018c), but curiously its sister species, *C. roaloko*, is found hundreds of kilometres further south in Andasibe (Prötzl et al. 2018b). These are closely related to *C. boettgeri* and *C. linotum*, the former of which is from Nosy Be, the latter from Montagne d'Ambre and a second locality west of Tsaratanana, thus forming a clade across the northern side of the Tsaratanana massif, extending also west and north. A trio of morphologically similar species, *C. gehringi*, *C. guibei*, and *C. lefona*, form a clade restricted to the area south and southwest of Tsaratanana, but in **chapter 11**, these species were found to not be closely related to other members of the complex (albeit with relatively poor support), and their biogeographic and morphological relationships are particularly puzzling. In *C. clade G (radamanus*; clade name from Gehring et al. 2012, taxon name from Prötzl et al. submitted), a very widespread species, populations from Sorata are most closely related to individuals from the lowland site Fanambana, and these clades are sister to a clade from Marojejy (Prötzl et al. submitted). *Calumma* sp. 'ratnasariae' (clade I) meanwhile is only found in the Bealanana District (Prötzl et al. submitted). Finally, *C. nasutum* (clade K) is found in Sorata and also the Andasibe region (Prötzl et al. submitted), showing a remarkably similar phylogeographic relationship to that seen between *C. uetzi* and *C. roaloko*. Except in the long-distance relationships, the arrangement of members of this complex appear to reflect the same configurations as I have illustrated for the frogs above; a greater similarity between Marojejy and Sorata than either has to the Bealanana District.

Small mammal distributions studied by Maminirina et al. (2008) show less clear patterns, with greater community assembly resemblance of large distances along the east coast of Madagascar. Their dendograms of Euclidean similarity among sites in northern and eastern Madagascar do not show clear patterns for tenrecs or nesomyid rodents, and some community relationships reconstructed are surprising, such as the strong similarity between Bemanevika 1600 m a.s.l. (this is a site near to Ampotsidy), and Andohahela at 1500 m a.s.l. (this is in the far south east of Madagascar). The differences in patterns may be related to taxonomic philosophy (samples are not genetically verified, so genetic patterns among massifs are not clear), or possibly the differences in age of the clades (unlikely, as both tenrecs and *Gephyromantis* frogs originated around 30 Ma; Wollenberg et al. 2011; Everson et al. 2016), their respective centres of origin, and most likely, differences in vagility and thermal tolerance between mammals and amphibians.

A remarkable fact that is becoming evident from the increasing data from different amphibian taxa examined, is that taxa shared (or forming sister pairs) among these massifs are usually found at 1300 m a.s.l. and above. Indeed, in Rakotoarison et al. (in press), my colleagues and I have shown that connectivity between populations of the one species of *Stumpffia* that occurs in both Sorata and Marojejy (*S. sorata*) is greatest at around this elevation, despite the species occurring over an elevational range of 1000 m. This is remarkable because there is currently no geographical connection at such high elevations; the highest single-elevation connection between Sorata and Marojejy today is at ca. 1120 m a.s.l.

Why are community assemblies so similar at 200 m above the minimum connection point? In several cases, including many *Gephyromantis*, an elevation range encompassing more than 200 m of elevation would be sufficient to explain connectivity. The apparent lack of such connectivity in Sorata and Ampotsidy is misleading, because those areas are without forest at 1100 m a.s.l. and their assemblies cannot, therefore, be compared. However, the potential role of paleoclimatic shifts is probably also significant; ranges that were formally more connected during warmer periods may now be isolated, and will continue to become more so if the climate continues to warm. The presence of sister pairs of a wide variety of ages between massifs suggests that connectivity may also

Discussion

be transient, with the separate massifs behaving like species pumps during climatic oscillations.

Understanding the diversity of clades must be informed by their biogeographical context, especially in topographically and climatically heterogeneous regions (Esquerré et al. 2019). The separate subgenera of *Gephyromantis* are semi-independent replicated radiations of frogs across northern Madagascar. This gives them the potential to be used as a model group in which to study biogeographic patterns of diversification and distribution, and the influence of ecology on these patterns (Wollenberg Valero 2015). For example, we might expect that riparian species such as members of the subgenus *Vatomantis* exhibit patterns more confined by watersheds than those of the more terrestrial *Duboinantis*. The diversification of *Gephyromantis* has occurred within the last 30 Ma (Wollenberg et al. 2011), and their biogeography can be expected to reflect well this span of time. The taxonomic groundwork for such investigation is approaching completion, but current sampling across the massifs remains insufficient to investigate such patterns in detail. More thorough exploration is needed in the corridor between Tsaratanana and Marojejy (Rabearivony et al. 2015). With data from these areas, it would be possible to construct ecological resistance maps (e.g. in MaxEnt Phillips et al. 2006). Alignment of such maps across taxa may identify common points of phylogeographic discontinuity, which would shed light on biogeographic barriers. Eventually, the comparison of patterns between different taxa, e.g. those between *Gephyromantis* and cophylines, which are also highly diverse and have complex biogeographic history in this area (**chapter 10**) may yield congruent timing and shifts that will shed light on the origin of diversity in this hyper-diverse area.

Ecomorphological evolution in cophylines

In the last 10 years, 56 new species of cophyline microhylid frogs have been described (including two that were resurrected), with 29 having been described in 2017 alone (Lambert et al. 2017; Rakotoarison et al. 2017; **chapter 7**), more than doubling the known diversity of the subfamily. This has resulted in a dramatic increase in our knowledge about the ecomorphological evolution of these frogs, which was already highlighted as fascinating in the 1920s by Noble and Parker (1926), and became only more interesting once genetic data became available from them (Andreone et al. 2005). Subsequent discoveries and taxonomic descriptions have further complicated the picture (Glaw et al. 2007; Wollenberg et al. 2008; Köhler et al. 2010; **chapter 9**), making the group still more interesting.

Osteological characters have long been used in phylogenetic reconstruction. Indeed, for palaeontological analysis, there are currently few alternatives. Osteological data has long been considered of great importance in the taxonomy of microhylid frogs, and cophylines are no exception (Noble and Parker 1926; Parker 1934; Guibé 1978; Blommers-Schlösser and Blanc 1991; Wu 1994). The recent advances of genetic methods have shown numerous osteology-based phylogenies to have been misled by homoplasies (e.g. the emergence of the Toxicofera clade from genetics that had no osteological precedent; Fry et al. 2005). Cophylinae was similarly affected. Early morphology-based phylogenetic hypotheses for this subfamily suggested that it either evolved from an ancestrally arboreal form with one transition to terrestriality (Noble and Parker 1926) or a terrestrial form with two transitions to arboreality (Blommers-Schlösser and Blanc 1993). In his unpublished doctoral thesis, Wu (1994) reconstructed osteology-based phylogenies of the microhylids that indicated a terrestrial origin with at least one transition to arboreality, and either two reversals or a second transition to arboreality. These morphological phylogenies were robustly shown by genetic phylogenies to be incorrect (Andreone et al. 2005; van der Meijden et al. 2007; Wollenberg et al. 2008)—instead, these phylogenies, and later, more robust reconstructions (Peloso et al. 2016, 2017; Tu et al. 2018; **chapters 8 and 10**), revealed a pattern of ecomorphological reticulation and extensive homoplasy across this subfamily.

Early attempts to reconstruct cophyline phylogeny based on osteology were misled by homoplasies arising from convergent evolution. Yet, in **chapters 6–9** (and previously also in Scherz et al. 2014, 2015a, 2015b) I have shown that modern methods of osteological study centred around micro-CT have reaffirmed the value and importance of osteology for cophyline taxonomy. This method is faster and easier to work with and communicate about than traditional osteological study and can be performed on type material without damaging it—an important distinction that ensures that osteology's relevance in the midst of constantly emerging new methods remains undiminished. Like any new technology, micro-CT is not without its own set of caveats of course, such as the often subjective nature of data visualisation (discussed in **chapter 7**), but awareness of these is growing, and micro-CT is being increasingly widely implemented (reviewed by Faulwetter et al. 2013 and Broeckhoven and du Plessis 2018). With the dramatic increase in feasibility of producing robust, DNA-based phylogenies, focus on extant taxa has recently shifted from using osteology and other morphological data as the basis of phylogenetic reconstruction, to examining that morphological data in phylogenetically explicit frameworks.

This shift in focus is a fundamental one: a move from phylogeny as the end-goal, to phylogeny as a tool by which to contextualise phenotypic evolution. This allows us to overcome the problem of extensive homoplasy in phenotypes, and turn it into research questions: how and why have species converged in morphology? Did that convergence yield similar evolutionary trajectories? To what extent are the morphological consequences of ecological convergence deterministic in nature? Cophylines are a promising group in which to address these kinds of questions. I have demonstrated this applicability already in **chapter 10** for morphometrics, but osteological data will also be valuable, especially in investigating the ecomorphological evolution, and particularly the miniaturisation, of these frogs.

Ecomorphs are a fascinating property of convergent evolution, suggesting of an 'optimal' phenotype for exploitation of a certain niche. The best examples of ecomorph evolution stem from anoles (see Losos 2011), but at a global scale, frogs display an equally astonishing degree of ecomorphological convergence (Bossuyt and Milinkovitch 2000; Moen et al. 2013; Vidal-García and Keogh 2015, 2017; Moen and Wiens 2017). Burrowing and arboreal frogs tend to be the most distinctly characteristic ecomorphs, the former having short, stout limbs and broad heads, the latter having generally longer limbs, and the characteristic broadened finger tips (as discussed in **chapter 10**). Across the tropics, miniaturised frogs form their own, only recently recognised ecomorph (Rittmeyer et al. 2012). Recent taxonomic advances on miniaturised frogs of Asia (e.g. Garg et al. 2017; Oliver et al. 2017; Poyarkov et al. 2018), Madagascar (e.g. Rakotoarison et al. 2017; **chapter 9**), Africa (e.g. Zimkus et al. 2012), and South America (e.g. Ribeiro et al. 2015; Lourenco-De-Moraes et al. 2018) have shown that the diversity of this guild has been underappreciated, and is extremely great. The smallest of these frogs do not reach 10 mm adult body size, making them the smallest tetrapods in terms of snout–vent length and amongst the smallest vertebrates of all.

In **chapters 8–10**, I discussed the miniaturised members of Cophylinae. Until genetic evidence became available, small species of microhylids from Madagascar were generally considered undescribed members of the genus *Stumpffia*, but Wollenberg et al. (2008) already revealed that species from southern Madagascar constituted a separate major clade. In **chapter 8**, my colleagues and I showed that there are in fact multiple lineages of miniaturised frogs, and in **chapter 9** we went on to describe three of these (one new genus and two new species from existing genera). This taxonomic investigation revealed indeed that an additional miniaturised lineage, *Anodonthyla eximia*, had gone unnoticed in previous discussions. In **chapter 10**, the phylogenetic resolution achieved by our new phylotranscriptomic and genomic trees yielded further clarity regarding the evolution of small body size in this subfamily, showing that body size has strong phylogenetic signal, and is not strongly linked to any particular shifts in overall morphometric relationships, yet extremely

miniaturised forms have evolved in several independent lineages.

The repeated evolution of body sizes near the minimum limit across the whole anuran order, and moreover repeatedly within single subfamilies, is suggestive of an evolutionary motif among frogs. Yet, although there has been some limited theoretical work on the topic (Alberch and Gale 1985; Trueb and Alberch 1985; Hanken and Wake 1993; Fabrezi and Alberch 1996), there is no empirical understanding of the drivers or selective advantage of miniaturisation among frogs. Integration of comparative phylogenetic methods like those employed in **chapters 10 and 11** and experimental evo-devo approaches may be a promising route to elucidate the mechanisms at work, and their evolutionary context. Of particular interest from an evolutionary perspective will be the clarification of the role of contingency and determinism in generating the miniaturised phenotype, and the role of ontogeny versus novelty in this process.

Macroevolution and taxonomy

In **sections 1–3** and the relevant sections of the discussion above, I have illustrated ways in which taxonomic papers themselves can be opportunities to develop and explore hypotheses regarding species and higher taxa, their biology, conservation, and evolution. Often these questions expand beyond the scope of what can reasonably be included in a taxonomic paper, and these then manifest as separate studies (e.g. **chapter 10**). In **section 4**, I have demonstrated the way that adequately detailed and illustrated descriptions themselves can also serve as data sources that can be harvested in order to construct datasets on morphology or ecology. This means that taxonomic papers can serve not only as science in their own right, but also as baseline data for larger-scale evolutionary exploration.

In **chapter 11**, I have demonstrated this function in chameleons. Morphological and ecological data were harvested from taxonomic literature and taxonomy-oriented field guides (Glaw and Vences 2007; Tilbury 2018). By means of this approach, we assembled data on external ornament morphology and body sizes for 200 species of chameleons, and on male genital morphology for 109 species. Using this dataset in a comparative phylogenetic framework based on a newly produced time-calibrated species-level phylogeny, I implemented a step-by-step hypothesis-testing approach to deduce the drivers of complexity in genital and external ornamentation. The results of this study are consistent with genital and external ornaments being under different forms of sexual selection and being evolutionarily uncoupled. Genital ornamentation is associated with allometry and size dimorphism, suggesting a role of intrasexual competition and mating system in determining ornament elaboration. On the other hand, external ornaments were associated with ecology and ornamentation dimorphism, suggesting a role of mate choice and extrinsic factors (e.g. background noise and predation pressure) in determining ornamentation complexity. This is the first study to address the macroevolution of ornamentation in chameleons in anything other than a descriptive manner. While a rather large body of literature exists that addresses the evolution and drivers of external ornamentation (e.g. Omland 1996; Badyaev et al. 2002; Kraaijeveld et al. 2007; Ligon et al. 2018) and genital ornamentation (e.g. Eberhard 1985; Böhme 1988; Böhme and Sieling 1993; Ziegler and Böhme 1997; Arnqvist 1998; Hosken and Stockley 2004; Andonov et al. 2017) independently, little discussion exists on their interaction (but see Böhme 1988; Böhme and Sieling 1993; Ziegler and Böhme 1997; Böhme and Ziegler 2008). Our comparative framework allowed us to address this question and showed that the differing forms of sexual selection acting on either results in their evolutionary independence.

Chapter 11 reveals factors involved in macroevolutionary patterns governing ornamentation in chameleons, but it also highlights basic research on chameleons that is wholly lacking. Firstly, mating systems across the family are only characterised in a handful of species, so understanding the direction of mate choice and degree of choosiness cannot be correlated against ornamentation

patterns. Secondly, we do not understand the functional morphology of genital ornamentation in chameleons, in large part because the female genital anatomy of chameleons has not been described in detail from any member of the family. Studying female genital morphology would be a realm of taxonomic interest, because females of several species cannot be distinguished from one another based on external morphology (Glaw and Vences 2007; Tilbury 2018). Thirdly, the study also omits two important aspects of chameleon courtship, namely colouration and behaviour, which are undoubtedly of importance, and need to be studied in greater detail. Finally, this study focussed on morphological aspects related to sexual selection, but the evolution of other aspects of morphology has also not yet been studied in these lizards. Different chameleon clades have evolved strikingly convergent morphologies in a manner similar to anoles but without the drive of island colonisation. Studying this may help us understand how adaptive phenotypic radiations with convergence occur in continental systems.

With the description of approximately 20,000 species and subspecies per year (<http://www.organismnames.com/>), taxonomic and systematic literature provides an enormous and rapidly expanding source of data. Phylogenetic comparative methods provide a framework into which this data can be integrated and analysed. It will be important to bear in mind the limitations of such an approach, such as the potential for misidentification of specimens to mislead conclusions if source data produced by others are not critically assessed (a problem discussed in **chapter 8**), and the potential problems that can arise from inaccurate phylogenetic reconstruction. With proper precautions, however, these problems can be mitigated, and the realm of questions that can be addressed is vast.

Madagascar as an island model system for continental evolution

Taxonomic inventory: an end in sight?

In the search for evolutionary systems that can be used as insular models for continental dynamics, no landmass ticks more boxes than Madagascar. To realise the potential of that system, a foundation must first be laid, and that foundation is in characterising the biodiversity of the island, its distribution and interrelations, and its origins. It is unrealistic in as short a space as a single doctoral thesis to hope to make revolutionary strides toward the goal of completing the taxonomic inventory of the herpetofauna of the island, which has already been underway since the end of the 18th century and which we know to include at least 200 species awaiting description (Vieites et al. 2009; Nagy et al. 2012; **chapter 10**). Yet, by using new methods in an integrative manner, comparatively large strides in the direction of completion can be made. Within the chapters presented in this thesis (specifically **chapters 1–9**), I have described 16 new frog species and two new frog genera. Including other work in which I have collaborated during my doctoral studies that number rises to 45 frog species and 13 reptile species (a full publication list is presented in my **Curriculum Vitae**, below), representing some 9% of all amphibian species and 2% of all reptile species described globally within this period (Uetz and Hošek 2016; AmphibiaWeb 2019). The foundation of the system is rapidly expanding and improving.

At a rate of ~50 species per three years, or ~17 species per year, we might hope for a completion of Madagascar's taxonomic inventory in the next decade or two. I am hesitant to predict such a windfall however, for two reasons: Firstly, species discovery is almost keeping pace with taxonomic description. Of the 16 species described here, five were not identified as candidate species before the start of my doctoral research (species described in **chapters 3–5 and 9**), and numerous new candidate species are identified in **chapter 10**. Secondly, the 'ease' of description of any given undescribed species-level lineage is contingent on two factors: (1) distinctiveness (ease of characterisation), and (2) taxonomic complexity (ease of resolution). As taxonomic resolution of a fauna progresses, I would argue that these factors become increasingly critical in determining the rate of

Discussion

resolution; they result in decreases in the yield of new species per unit effort, discussed by Costello et al. (2013). Highly distinctive species are readily described because they are easy to characterise, and because their taxonomic complexity is generally low. *Tsingymantis antitra* (Glaw et al. 2006) and *Plethodontohyla fonzana* (Glaw et al. 2007) were among the most distinctive recently discovered frogs in Madagascar, making their description straightforward. *Gephyromantis lomorina* described in **chapter 3** was similarly distinct, and its description was complicated only by its implications for the higher taxa *Vatomantis* and *Laurentomantis* and the species *G. klemmeri*.

On the other hand, species where the distinctiveness is lower and taxonomic complexity is greater, especially cryptic species and members of unresolved species complexes where names cannot be unambiguously allocated to species-level units, are more challenging to describe. Their descriptions take longer because more effort must go into clarifying existing names or identifying diagnostic features. **Chapter 7** is a good illustration of this point. In that paper, my colleagues and I revised the *Rhombohryne serratopalpebrosa* species group, involving the allocation of an existing species to the group and clarification of its identity (*R. guentherpetersi*) and description of two species, one of which (*R. regalis*) had been confused with *R. serratopalpebrosa* itself since 2007, and the other of which (*R. diadema*) is morphologically highly similar to another species (*R. tany*). This paper was predicated on two previous papers on the species group, wherein the identity of *R. serratopalpebrosa* had been addressed (Scherz et al. 2014, 2015b), and on detailed osteological study based on micro-CT scans. This taxonomic description was thus more complicated and took proportionally longer than a similar description of more distinctive and/or less complex taxa would have been.

As we proceed with the taxonomic resolution of Madagascar's herpetofauna, the distinctiveness of the remaining units is likely to decrease on average because we preferentially describe species that are readily described, and their taxonomic complexity is likely to increase on average simply because complexes are more time-consuming to resolve taxonomically. This will result in more complicated and thus slower progress. In part this limitation will be alleviated by emerging methods, such as target capture for sequencing old and damaged museum material (e.g. Ruane and Austin 2017) and micro-CT for accessing internal anatomy of old types (e.g. Scherz et al. 2014), increasing the available data and possibly revealing diagnostic characters. Further strides in increasing the rate of taxonomic resolution could be made by (1) focussing on diagnosis, rather than detailed descriptions containing both taxonomically informative and non-informative features of new species, as advocated by Renner (2016), (2) inclusion of DNA sequence data in diagnoses, as advocated by Tautz et al. (2003) and Renner (2016), (3) reducing the superfluous information in taxonomic description to a minimum (reduction of introduction, methods, and discussion to minimal information), and (4) perhaps most importantly, training of more taxonomists.

I would argue that an increase in rate at the cost of the valuable insights that we can gain on other aspects of the biology of the taxa (as demonstrated in the above discussion and throughout the rest of my thesis), is not, however, a worthwhile trade. The benefits of describing species, e.g. conservation feasibility and biodiversity quantification, are contingent upon our understanding of their biology, distribution, and evolution. A middle ground must be found that maximises utility and speed without compromising valuable information. The recent monograph on *Stumpffia* frogs from Madagascar by my colleagues and me is a good example of such a reconciliation (Rakotoarison et al. 2017); in this work, we described 26 new species of *Stumpffia* and provided accounts of all 15 previously described species in just 127 pages (average of ca. 3 pages per species). This included detailed accounts of the morphology, colouration, bioacoustics, and diagnostic features of each species, as well as photographs of the animals in life, natural history data (where available), preliminary conservation assessment, and molecular phylogenetic reconstructions of their relationships. This shows that integrative taxonomy can be utilised in an efficient way for monographic works describing dozens of taxa. The integrative approach also lines up with the accu-

mulation of criteria that support the distinction of lineages at species level under the USC, giving taxonomic hypotheses proposed in an integrative framework greater support. In more challenging groups, such as the frogs of the subgenus *Brygoomantis* (genus *Mantidactylus*) which have numerous ambiguous names, cryptic morphology, and complex and variable calls, such monographs will be more complicated, but would provide a valuable basis for future work. Incorporation of, for example, brief accounts of diagnostic apomorphic DNA sequence data would be easy to integrate and lend still more utility to the format.

A model system in development

As we approach the completion of the taxonomic inventory of Madagascar's herpetofauna, new opportunities are opening to gain insights into the origins and biogeography of the island's fauna. From the work I have presented here, new patterns in the biogeography of northern Madagascar have been identified, and supporting evidence is accumulating from a variety of different taxa. A great deal remains to be done in this regard, and studies on different taxa will be particularly insightful in understanding the generality and timing of these patterns, while understanding their causes will require more detailed sampling and modelling approaches. Large-scale modelling approaches, like those of Brown et al. (2014; 2016) have already shed some light on broad patterns of diversification and endemism of herpetofauna across the island, but finer-scale analyses would be desirable for more specific analysis and predictions. Those finer-scale analyses will become more feasible as our taxonomic inventory approaches completion and we gain more data on the distribution of poorly known taxa.

At the same time, we are beginning to understand the factors driving evolution of Madagascar's herpetofauna, from their ecomorphology (e.g. Rodríguez et al. 2015; Wollenberg Valero et al. 2017; Hutter et al. 2018b; **chapter 10**) to their sexual ornamentation (**chapter 11**). These taxon-specific approaches are promising insular models for continent-scale dynamics, but it will be important to also place them in an ecological context. For that, work is needed on broad-scale ecosystem evolution across Madagascar, and also on evolutionary community assembly. Particularly interesting insights may be afforded by investigation of (1) amphibians of different levels of distinction and the role of niche differentiation in permitting co-occurrence or driving ecological divergence or extinction/dominance dynamics, (2) the interplay between amphibian and snake diversity, as many of Madagascar's snakes are anurophagous (e.g. Hutter et al. 2018a), and (3) the interplay of lizard and bird diversity, as many of Madagascar's birds will opportunistically feed on lizards, but may also compete with them for insect prey (Hasegawa et al. 2009). Elucidating such ecological interactions will make the system's applicability to continent-scale patterns much stronger.

It is always desirable to consider biogeographic model systems in isolation, but the origins of their taxa are important. They determine, for example, whether challenges and opportunities of the system are totally novel to the colonist or might already have adaptive precedence. So, if Madagascar is to be our model system, understanding the origins of its fauna is important. At present, much remains uncertain regarding the island's herpetofauna, and indeed most other taxa (Crottini et al. 2012a). Recent work on mantellid frogs suggests an Out-of-Asia origin (Yuan et al. 2018), and similar affiliations are likely for the two separate microhylid clades (Dyscophinae and Scaphiophryninae+Cophylinae) (Tu et al. 2018), but this remains uncertain. Still less clarity is present in reptiles; in chameleons, for example, the new phylogenetic hypotheses presented in **chapter 11** cast doubt on the question of whether the family originated in Madagascar or Africa (Tolley et al. 2013). This is another area where systematic research is needed at higher taxonomic levels, in order to clarify relationships and identify how many times the island was colonised, when, and what the consequences might have been to the already extant fauna. As I stated in the **Introduction**, the lack of a recent fossil record means that we must infer these patterns from the extant fauna. With resolution of origins and timing of colonisations, we can start to build a picture of the origins of

one of the planet's most diverse and endemic faunas.

Conclusions

The processes leading to the formation and perpetuation of species, and how species assemblages are formed and evolve together, are questions of central interest in biological science, but are still not fully understood. In the 160 years since Darwin's revelations were published, we have begun to approach answers to these questions, with studies in laboratory and natural settings, with experimental approaches and observational studies, and with holistic analyses. In assembling the puzzle of how biodiversity is formed and maintained, a thorough understanding of the individual pieces, which are most commonly species, is critical to slotting them into their proper place. In this thesis, my goal was to thoroughly characterise pieces of the puzzle, examine their relationships, identify patterns among them, and place them into context, shedding light on the processes involved in their evolution.

As I have illustrated above, in our efforts to piece together the puzzle of evolution, systematics generates a wealth of data beyond giving names to the pieces: Conservation insights help us to understand which pieces are on the verge of being lost. Information on distribution and phylo-geographic relationships helps us to place pieces in spatial and evolutionary context. Phenotypic data further our understanding of evolutionary relationships among taxa and shed light on the connections and patterns in the evolutionary puzzle. Finally, stepping back and viewing pieces in a macroevolutionary context helps us understand evolutionary drivers and determinants, and the big picture begins to emerge.

Studying these aspects in an evolutionary Petri dish like Madagascar illuminates how process and context work together in the generation of biodiversity at a continental scale, yet in an insular system. With this thesis, I have contributed to the advancement of our understanding of the evolutionary processes generating and shaping the unique biodiversity of this remarkable island. Connecting these parts of the puzzle will be instrumental in deepening our understanding of the processes that have resulted in the unparalleled diversity of reptiles and amphibians in Madagascar, building the foundation for later extrapolation to general evolutionary principles.



References

- Adams D (1980) The Restaurant at the End of the Universe. Pan Books, London, UK, 208 pp.
- Adams JW, Olah A, McCurry MR, Potze S (2015) Surface model and tomographic archive of fossil primate and other mammal holotype and paratype specimens of the Ditsong National Museum of Natural History, Pretoria, South Africa. PLoS One 10(10): e0139800 (0139814 pp.). doi:10.1371/journal.pone.0139800
- Agnarsson I, Kuntner M (2007) Taxonomy in a changing world: seeking solutions for a science in crisis. Systematic Biology 56(3): 531–539. doi:10.1080/10635150701424546
- Alberch P, Gale EA (1985) A developmental analysis of an evolutionary trend: digital reduction in amphibians. Evolution 39(1): 8–23.
- Ali JR, Huber M (2010) Mammalian biodiversity on Madagascar controlled by ocean currents. Nature 463: 653–656. doi:10.1038/nature08706
- Ali JR, Meiri S (in press) Biodiversity growth on the volcanic ocean islands and the roles of in situ cladogenesis and immigration: case with the reptiles. Ecography doi:10.1111/ecog.04024
- Allentoft M, Rasmussen A, Kristensen H (2018) Centuries-old DNA from an extinct population of Aesculapian Snake (*Zamenis longissimus*) offers new phylogeographic insight. Diversity 10(1): 14. doi:10.3390/d10010014
- AmphibiaWeb. (2019) AmphibiaWeb: Information on amphibian biology and conservation. Available at: <http://amphibiaweb.org>. Accessed 15 February 2019
- Andonov K, Natchev N, Kornilev YV, Tsankov N (2017) Does sexual selection influence ornamentation of hemipenes in Old World snakes? The Anatomical Record 300: 1680–1694.
- Andreone F (2004) Crossroads of herpetological diversity: Survey work for an integrated conservation of amphibians and reptiles in northern Madagascar. Italian Journal of Zoology 71(sup2): 229–235. doi:10.1080/11250000409356640
- Andreone F (2008) A Conservation Strategy for the Amphibians of Madagascar. Monograph XLV. Museo Regionale di Scienze Naturali, Torino, 452 pp.
- Andreone F, Glaw F, Mattioli F, Jesu R, Schimmenti G, Randrianirina JE, Vences M (2009) The peculiar herpetofauna of some Tsaratanana rainforests and its affinities with Manongarivo and other massifs and forests of northern Madagascar. Italian Journal of Zoology 76(1): 92–110. doi:10.1080/11250000802088603
- Andreone F, Rosa GM, Noel J, Crottini A, Vences M, Raxworthy CJ (2010) Living within fallen palm leaves: the discovery of an unknown *Blommersia* (Mantellidae: Anura) reveals a new reproductive strategy in the amphibians of Madagascar. Naturwissenschaften 97(6): 525–543. doi:10.1007/s00114-010-0667-x
- Andreone F, Vences M, Vieites DR, Glaw F, Meyer A (2005) Recurrent ecological adaptations revealed through a molecular analysis of the secretive cophyline frogs of Madagascar. Molecular Phylogenetics and Evolution 34(2): 315–322. doi:10.1016/j.ympev.2004.10.013
- Arnqvist G (1998) Comparative evidence for the evolution of genitalia by sexual selection. Nature 383: 784–786.
- Badyaev AV, Hill GE, Weckworth BV (2002) Species divergence in sexually selected traits: increase in song elaboration is related to decrease in plumage ornamentation in finches. Evolution 56: 412–419.
- Barlow J, França F, Gardner TA, Hicks CC, Lennox GD, Berenguer E, Castello L, Economo EP, Ferreira J, Guénard B, Gontijo Leal C, Isaac V, Lees AC, Parr CL, Wilson SK, Young PJ, Graham NAJ (2018) The future of hyperdiverse tropical ecosystems. Nature 559(7715):

References

- 517–526. doi:10.1038/s41586-018-0301-1
- Blackburn DC (2008) Biogeography and evolution of body size and life history of African frogs: Phylogeny of squeakers (*Arthroleptis*) and long-fingered frogs (*Cardioglossa*) estimated from mitochondrial data. *Molecular Phylogenetics and Evolution* 49: 806–826. doi:10.1016/j.ympev.2008.08.015
- Blair C, Noonan BP, Brown JL, Raselimanana AP, Vences M, Yoder AD (2015) Multilocus phylogenetic and geospatial analyses illuminate diversification patterns and the biogeographic history of Malagasy endemic plated lizards (Gerrhosauridae: Zonosaurinae). *Journal of Evolutionary Biology* 8(2): 481–492. doi:10.1111/jeb.12586
- Blaxter M, Mann J, Chapman T, Thomas F, Whitton C, Floyd R, Abebe E (2005) Defining operational taxonomic units using DNA barcode data. *Philosophical Transactions of the Royal Society B* 360: 1935–1943. doi:10.1098/rstb.2005.1725
- Bletz MC, Scherz MD, Rakotoarison A, Lehtinen R, Glaw F, Vences M (2018) Stumbling upon a new frog species of *Guibemantis* (Anura: Mantellidae) on top of the Marojejy Massif in northern Madagascar. *Copeia* 106(2): 255–263. doi:10.1643/CH-17-655
- Blommers-Schöller RMA, Blanc CP (1991) Amphibiens (première partie). *Faune de Madagascar* 75(1): 1–397.
- Blommers-Schöller RMA, Blanc CP (1993) Amphibiens (deuxième partie). *Faune de Madagascar* 75(2): 385–530.
- Böhm M, Collen B, Baillie JEM, Bowles P, et al. (2013) The conservation status of the world's reptiles. *Biological Conservation* 157: 372–385. doi:10.1016/j.biocon.2012.07.015
- Böhme W (1988) Zur Genitalmorphologie der Sauria: funktionelle und stammesgeschichtliche Aspekte. *Bonner zoologische Monographien* 27: 1–176.
- Böhme W, Sieling U (1993) Zum Zusammenhang zwischen Genitalstruktur, Paarungsverhalten und Fortpflanzungserfolg bei squamaten Reptilien: erste Ergebnisse. *Herpetofauna* 15: 15–23.
- Böhme W, Ziegler T (2008) A review of iguanian and anguimorph lizard genitalia (Squamata: Chamaeleonidae; Varanoidea, Shinisauridae, Xenosauridae, Anguidae) and their phylogenetic significance: comparisons with molecular data sets. *Journal of Zoological Systematics and Evolutionary Research* 47(2): 189–202. doi:10.1111/j.1439-0469.2008.00495.x
- Bossuyt F, Milinkovitch MC (2000) Convergent adaptive radiations in Madagascan and Asian ranid frogs reveal covariation between larval and adult traits. *Proceedings of the National Academy of Sciences of the USA* 97: 6585–6590.
- Boumans L, Vieites DR, Glaw F, Vences M (2007) Geographical patterns of deep mitochondrial differentiation in widespread Malagasy reptiles. *Molecular Phylogenetics and Evolution* 45(3): 822–839. doi:10.1016/j.ympev.2007.05.028
- Box GEP (1976) Science and statistics. *Journal of the American Statistical Association* 71: 791–799.
- Branch WR, Bayliss J, Tolley KA (2014) Pygmy chameleons of the *Rhampholeon platyceps* complex (Squamata: Chamaeleonidae): Description of four new species from isolated ‘sky islands’ of northern Mozambique. *Zootaxa* 3814(1): 1–36. doi:10.11646/zootaxa.3814.1.1
- Briggs JC (2003) The biogeographic and tectonic history of India. *Journal of Biogeography* 30(3): 381–388. doi:10.1046/j.1365-2699.2003.00809.x
- Broekhoven C, du Plessis A (2018) X-ray microtomography in herpetological research: a review. *Amphibia-Reptilia* 39(4): 377–401. doi:10.1163/15685381-20181102
- Brown JL, Cameron A, Yoder AD, Vences M (2014) A necessarily complex model to explain the

- biogeography of the amphibians and reptiles of Madagascar. *Nature Communications* 5: 5046 (5010 pp.). doi:10.1038/ncomms6046
- Brown JL, Sillero N, Glaw F, Bora P, Vieites DR, Vences M (2016) Spatial biodiversity patterns of Madagascar's amphibians and reptiles. *PLoS One* 11(1): e0144076 (0144026 pp.). doi:10.1371/journal.pone.0144076
- Burbrink FT, Gehara M (2018) The biogeography of deep time phylogenetic reticulation. *Systematic Biology* 67(5): 743–755. doi:10.1093/sysbio/syy019
- Burrell AS, Disotell TR, Bergey CM (2015) The use of museum specimens with high-throughput DNA sequencers. *Journal of Human Evolution* 79: 35–44. doi:10.1016/j.jhevol.2014.10.015
- Butchart SHM, Bird JP (2010) Data Deficient birds on the IUCN Red List: What don't we know and why does it matter? *Biological Conservation* 143(1): 239–247. doi:10.1016/j.biocon.2009.10.008
- Catenazzi A (2015) State of the world's amphibians. *Annual Review of Environment and Resources* 40(1): 91–119. doi:10.1146/annurev-environ-102014-021358
- Chapman AD (2009) Numbers of living species in Australia and the world. Australian Government, Department of the Environment, Water, Heritage and the Arts, Canberra ACT, Australia.
- Chatterjee S, Goswami A, Scotese CR (2013) The longest voyage: Tectonic, magmatic, and paleoclimatic evolution of the Indian plate during its northward flight from Gondwana to Asia. *Gondwana Research* 23(1): 238–267. doi:10.1016/j.gr.2012.07.001
- Clayton A. (2011) A review of policies to combat deforestation in Madagascar. In: Africa Portal. Vol. 12. CIGI, Ontario, Canada
- Consiglio T, Schatz GE, McPherson G, Lowry PP, 2nd, Rabenantoandro J, Rogers ZS, Rabevohitra R, Rabehivitra D (2006) Deforestation and plant diversity of Madagascar's littoral forests. *Conservation Biology* 20(6): 1799–1803. doi:10.1111/j.1523-1739.2006.00562.x
- Costello MJ, Wilson S, Houlding B (2013) More taxonomists describing significantly fewer species per unit effort may indicate that most species have been discovered. *Systematic Biology* 62(4): 616–624. doi:10.1093/sysbio/syt024
- Coyne JA, Orr HA (2004) *Speciation*. Oxford University Press, Oxford, UK, 545 pp.
- Crottini A, Madsen O, Pouc C, Strauß A, Vieites DR, Vences M (2012a) Vertebrate time-tree elucidates the biogeographic pattern of a major biotic change around the K–T boundary in Madagascar. *Proceedings of the National Academy of Sciences of the USA* 109(14): 5358–5363. doi:10.1073/pnas.1118605109
- Crottini A, Miralles A, Glaw F, Harris DJ, Lima A, Vences M (2012b) Description of a new pygmy chameleon (Chamaeleonidae: *Brookesia*) from central Madagascar. *Zootaxa* 3490: 63–74.
- Darwin C (1845) *Journal of Researches into the Natural History and Geology of the countries visited during the voyage of H.M.S. Beagle round the world*. John Murray, London, UK.
- Darwin C (1859) *On the Origin of Species by Means of Natural Selection or the Preservation of Favoured Races in the Struggle for Life*. John Murray, London, UK.
- Dayrat B (2005) Towards integrative taxonomy. *Biological Journal of the Linnean Society* 85: 407–415. doi:10.1111/j.1095-8312.2005.00503.x
- de Carvalho MR, Bockmann FA, Amorim DS, Brandão CRF, de Vivo M, de Figueiredo JL, Britski HA, de Pinna MCC, Menezes NA, Marques FPL, Papavero N, Cancello EM, Crisci JV, McEachran JD, Schelly RC, Lundberg JG, Gill AC, Britz R, Wheeler QD, Stiassny MLJ, Parenti LR, Page LM, Wheeler WC, Faivovich J, Vari RP, Grande L, Humphries CJ, DeSalle R, Ebach MC, Nelson GJ (2007) Taxonomic impediment or impediment to

References

- taxonomy? A commentary on systematics and the cybertaxonomic-automation paradigm. *Evolutionary Biology* 34(3): 140–143. doi:10.1007/s11692-007-9011-6
- de Queiroz K (1998) The General Lineage Concept of species, species criteria, and the process of speciation. In Howard DJ & Berlocher SH (eds). *Endless Forms: Species and Speciation*. Oxford University Press, Oxford, UK: pp. 57–75.
- de Queiroz K (2005a) Ernst Mayr and the modern concept of species. *Proceedings of the National Academy of Sciences of the USA* 102: 6600–6607. doi:10.1073/pnas.0502030102
- de Queiroz K (2005b) A unified concept of species and its consequences for the future of taxonomy. *Proceedings of the California Academy of Sciences, series 4* 56(18): 196–215.
- de Queiroz K (2007) Species concepts and species delimitation. *Systematic Biology* 56(6): 879–886. doi:10.1080/10635150701701083
- de Wit MJ (2003) Madagascar: heads it's a continent, tails it's an island. *Annual Review of Earth and Planetary Sciences* 31(1): 213–248. doi:10.1146/annurev.earth.31.100901.141337
- Derryberry EP, Claramunt S, Derryberry G, Chesser RT, Cracraft J, Aleixo A, Pérez-Emán J, Remsen J, J. V., Brumfield RT (2011) Lineage diversification and morphological evolution in a large-scale continental radiation: the Neotropical Ovenbirds and Woodcreepers (Aves: Furnariidae). *Evolution* 65(10): 2973–2986. doi:10.1111/j.1558-5646.2011.01374.x
- Du Puy DJ, Moat J (2003) Using Geological Substrate to Identify and Map Primary Vegetation Types in Madagascar and the Implications for Planning Biodiversity Conservation. In Goodman SM & Benstead JP (eds). *The Natural History of Madagascar*. The University of Chicago Press, Chicago, IL: pp. 51–67.
- Dubois A (2003) The relationships between taxonomy and conservation biology in the century of extinctions. *Comptes Rendus Biologies* 326: 9–21. doi:10.1016/S1631-0691(03)00022-2
- Eberhard WG (1985) Sexual selection and animal genitalia. Harvard University Press, Harvard, Massachusetts, USA.
- Esquerre D, Brennan IG, Catullo RA, Torres-Pérez F, Keogh JS (2019) How mountains shape biodiversity: the role of the Andes in biogeography, diversification and reproductive biology in South America's most species rich lizard radiation (Squamata: Liolaemidae). *Evolution* 73(2): 214–230. doi:10.1111/evo.13657
- Evans SE, Jones MEH, Krause DW (2008) A giant frog with South American affinities from the Late Cretaceous of Madagascar. *Proceedings of the National Academy of Sciences of the USA* 105(8): 2951–2956. doi:10.1073/pnas.0707599105
- Everson KM, Soarimalala V, Goodman SM, Olson LE (2016) Multiple loci and complete taxonomic sampling resolve the phylogeny and biogeographic history of tenrecs (Mammalia: Tenrecidae) and reveal higher speciation rates in Madagascar's humid forests. *Systematic Biology* 65(5): 890–909. doi:10.1093/sysbio/syw034
- Fabrezi M, Alberch P (1996) The carpal elements of anurans. *Herpetologica* 52(2): 188–204.
- Faulwetter S, Vasileiadou A, Kouratoras M, Dailianis T, Arvanitidis C (2013) Micro-computed tomography: Introducing new dimensions to taxonomy. *Zookeys* 263: 1–45.
- Flynn JJ, Wyss AR (2003) Mesozoic terrestrial vertebrate faunas: the early history of Madagascar's vertebrate diversity. In Goodman SM & Benstead JP (eds). *The Natural History of Madagascar*. Chicago University Press, Chicago IL, USA: pp. 34–40.
- Fouquet A, Gilles A, Vences M, Marty C, Blanc M, Gemmell NJ (2007) Underestimation of species richness in neotropical frogs revealed by mtDNA analyses. *PLoS One* 2(10): e1109 (1110 pp.). doi:10.1371/journal.pone.0001109
- Fritz U, Gong S, Auer M, Kuchling G, Schneeweiss N, Hundsdörfer AK (2010) The world's eco-

- nominally most important chelonians represent a diverse species complex (Testudines: Trionychidae: *Pelodiscus*). *Organisms Diversity & Evolution* 10(3): 227–242. doi:10.1007/s13127-010-0007-1
- Fry BG, Vidal N, Norman JA, Vonk FJ, Scheib H, Ramjan SF, Kuruppu S, Fung K, Hedges SB, Richardson MK, Hodgson WC, Ignjatovic V, Summerhayes R, Kochva E (2005) Early evolution of the venom system in lizards and snakes. *Nature* 439(7076): 584–588. doi:10.1038/nature04328
- Ganzhorn JU, Lowry PP, Schatz GE, Sommer S (2009) The biodiversity of Madagascar: one of the world's hottest hotspots on its way out. *Oryx* 35(4): 346–348. doi:10.1046/j.1365-3008.2001.00201.x
- Gardner TA, Barlow J, Peres CA (2007) Paradox, presumption and pitfalls in conservation biology: The importance of habitat change for amphibians and reptiles. *Biological Conservation* 138(1-2): 166–179. doi:10.1016/j.biocon.2007.04.017
- Garg S, Suyesh R, Sukesan S, Biju SD (2017) Seven new species of Night Frogs (Anura, Nyctibatrachidae) from the Western Ghats Biodiversity Hotspot of India, with remarkably high diversity of diminutive forms. *PeerJ* 5: e3007 (3050 pp.). doi:10.7717/peerj.3007
- Gehara M, Crawford AJ, Orrico VGD, Rodríguez A, Lötters S, Fouquet A, Barrientos LS, Brusquetti F, De la Riva I, Ernst R, Urrutia GG, Glaw F, Guayasamin JM, Hölting M, Jansen M, Kok PJR, Kwet A, Lingnau R, Lyra M, Moravec J, Pombal JP, Jr., Rojas-Runjaic FJM, Schulze A, Señaris JC, Solé M, Rodrigues MT, Twomey E, Haddad CFB, Vences M, Köhler J (2014) High levels of diversity uncovered in a widespread nominal taxon: continental phylogeography of the Neotropical tree frog *Dendropsophus minutus*. *PLoS One* 9(9): e103958 (103912 pp.). doi:10.1371/journal.pone.0103958
- Gehring P-S, Glaw F, Gehara M, Ratsoavina FM, Vences M (2013) Northern origin and diversification in the central lowlands? – Complex phylogeography and taxonomy of widespread day geckos (*Phelsuma*) from Madagascar. *Organisms Diversity & Evolution* 13(4): 605–620. doi:10.1007/s13127-013-0143-5
- Gehring P-S, Pabijan M, Ratsoavina FM, Köhler J, Vences M, Glaw F (2010) A Tarzan yell for conservation - a new chameleon, *Calumma tarzan* sp. n., proposed as a flagship species for the creation of new nature reserves in Madagascar. *Salamandra* 46(3): 167–179.
- Gehring P-S, Ratsoavina FM, Vences M, Glaw F (2011) *Calumma vohibola*, a new chameleon species (Squamata: Chamaeleonidae) from the littoral forests of eastern Madagascar. *African Journal of Herpetology* 60(2): 130–154. doi:10.1080/21564574.2011.628412
- Gehring P-S, Tolley KA, Eckhardt FS, Townsend TM, Ziegler T, Ratsoavina FM, Glaw F, Vences M (2012) Hiding deep in the trees: discovery of divergent mitochondrial lineages in Malagasy chameleons of the *Calumma nasutum* group. *Ecology and Evolution* 2(7): 1468–1479. doi:10.1002/ece3.269
- Gignac PM, Kley NJ, Clarke JA, Colbert MW, Morhardt AC, Cerio D, Cost IN, Cox PG, Daza JD, Early CM, Echols MS, Henkelman RM, Herdina AN, Holliday CM, Li Z, Mahlow K, Merchant S, Müller J, Orsbon CP, Paluh DJ, Thies ML, Tsai HP, Witmer LM (2016) Diffusible iodine-based contrast-enhanced computed tomography (diceCT): an emerging tool for rapid, high-resolution, 3-D imaging of metazoan soft tissues. *Journal of Anatomy* 228(6): 889–909. doi:10.1111/joa.12449
- Gillespie RG, Baldwin BG (2010) Island biogeography of remote archipelagos: Interplay between ecological and evolutionary processes. In Losos JB & Ricklefs RE (eds). *The theory of island biogeography revisited*. Princeton University Press, Princeton NJ, USA: pp. 358–387.
- Glaw F, Hoegg S, Vences M (2006) Discovery of a new basal relict lineage of Madagascan frogs

References

- and its implications for mantellid evolution. *Zootaxa* 1334: 27–43.
- Glaw F, Köhler J, Bora P, Rabibisoa NHC, Ramlilaona O, Vences M (2007) Discovery of the genus *Plethodontohyla* (Anura: Microhylidae) in dry western Madagascar: description of a new species and biogeographic implications. *Zootaxa* 1577: 61–68.
- Glaw F, Köhler J, Townsend TM, Vences M (2012) Rivaling the world's smallest reptiles: discovery of miniaturized and microendemic new species of leaf chameleons (*Brookesia*) from northern Madagascar. *PLoS One* 7(2): e31314 (31324 pp.). doi:10.1371/journal.pone.0031314
- Glaw F, Köhler J, Vences M (2009) A distinctive new species of chameleon of the genus *Furcifer* from the Montagne d'Ambre rainforest of northern Madagascar. *Zootaxa* 2269: 32–42.
- Glaw F, Köhler J, Vences M (2011) New species of *Gephyromantis* from Marojejy National Park, northeast Madagascar. *Journal of Herpetology* 45(2): 155–160. doi:10.1670/10-058.1
- Glaw F, Scherz MD, Prötzl D, Vences M (2018) Eye and webbing colouration as predictors of specific distinctness: a genetically isolated new treefrog species of the *Boophis albilabris* group from the Masoala peninsula, northeastern Madagascar. *Salamandra* 54(3): 163–177.
- Glaw F, Vences M (2006) Phylogeny and genus-level classification of mantellid frogs (Amphibia, Anura). *Organisms Diversity & Evolution* 6(3): 236–253. doi:10.1016/j.ode.2005.12.001
- Glaw F, Vences M (2007) A field guide to the amphibians and reptiles of Madagascar. Vences & Glaw Verlags GbR, Cologne, Germany, 496 pp.
- Goodman SM, Benstead JP (2005) Updated estimates of biotic diversity and endemism for Madagascar. *Oryx* 39(1): 73–77. doi:10.1017/S0030605305000128
- Goodman SM, Raherilalao MJ, Wohlhauser S (2019) Les aires protégées terrestres de Madagascar : Leur histoire, description et biote / The terrestrial protected areas of Madagascar: Their history, description, and biota. 1. Association Vahatra, Antananarivo, Madagascar, 424 pp.
- Grant RB, Grant PR (2003) What Darwin's Finches can teach us about the evolutionary origin and regulation of biodiversity. *BioScience* 53(10): 965–975. doi:10.1641/0006-3568(2003)053[0965:WDFCTU]2.0.CO;2
- Green GM, Sussman RW (1990) Deforestation history of the eastern rain forests of Madagascar from satellite images. *Science* 248(4952): 212–215.
- Guibé J (1978) Les batraciens de Madagascar. *Bonner zoologische Monographien* 11: 1–140.
- Hanken J, Wake DB (1993) Miniaturization of body size: organismal consequences and evolutionary significance. *Annual Review of Ecology and Systematics* 24: 501–519.
- Harper GJ, Steininger MK, Tucker CJ, Juhn D, Hawkins F (2007) Fifty years of deforestation and forest fragmentation in Madagascar. *Environmental Conservation* 34(4): 1–9. doi:10.1017/s0376892907004262
- Hasegawa M, Mori A, Nakamura M, Mizuta T, Asai S, Ikeuchi I, Rakotomanana H, Okamiya T, Yamagishi S (2009) Consequence of inter class competition and predation on the adaptive radiation of lizards and birds in the dry forest of western Madagascar. *Ornithological Science* 8: 55–66.
- Hausdorf B (2011) Progress toward a general species concept. *Evolution* 65(4): 923–931. doi:10.1111/j.1558-5646.2011.01231.x
- Hawlitschek O, Scherz MD, Ruthensteiner B, Crottini A, Glaw F (2018) Computational molecular species delimitation and taxonomic revision of the gecko genus *Ebenavia* Boettger, 1878. *The Science of Nature* 105: 49. doi:10.1007/s00114-018-1574-9
- Hawlitschek O, Toussaint EFA, Gehring P-S, Ratsoavina FM, Cole N, Crottini A, Noppper J, Lam AW, Vences M, Glaw F (2016) Gecko phylogeography in the Western Indian Ocean region:

- the oldest clade of *Ebenavia inunguis* lives on the youngest island. *Journal of Biogeography* 44: 409–420. doi:10.1111/jbi.12912
- He K, Jiang X-L (2015) Mitochondrial phylogeny reveals cryptic genetic diversity in the genus *Niviventer* (Rodentia, Muroidea). *Mitochondrial DNA* 26(1): 48–55. doi:10.3109/19401736.2013.823167
- Heaney LR (2007) Is a new paradigm emerging for oceanic island biogeography? *Journal of Biogeography* 34(5): 753–757. doi:10.1111/j.1365-2699.2007.01692.x
- Hebert PDN, Cywinski A, Ball SL, DeWaard JR (2003) Biological identifications through DNA barcodes. *Proceedings of the Royal Society of London B* 270(1512): 313–321. doi:10.1098/rspb.2002.2218
- Hewitt G (2000) The genetic legacy of the Quaternary ice ages. *Nature* 405: 907. doi:10.1038/35016000
- Hillis DM (2019) Species delimitation in herpetology. *Journal of Herpetology* 53(1): 3–12. doi:10.1670/18-123
- Horning NR (2008) Madagascar's biodiversity conservation challenge: from local- to national-level dynamics. *Environmental Sciences* 5(2): 109–128. doi:10.1080/15693430801912246
- Hortal J, de Bello F, Diniz-Filho JAF, Lewinsohn TM, Lobo JM, Ladle RJ (2015) Seven shortfalls that beset large-scale knowledge of biodiversity. *Annual Review of Ecology, Evolution, and Systematics* 46: 523–549. doi:10.1146/annurev-ecolsys-112414-054400
- Hosken DJ, Stockley P (2004) Sexual selection and genital evolution. *Trends in Ecology and Evolution* 19(2): 87–93. doi:10.1016/j.tree.2003.11.012
- Howard SD, Bickford DP (2014) Amphibians over the edge: silent extinction risk of Data Deficient species. *Diversity and Distributions* 20(7): 837–846. doi:10.1111/ddi.12218
- Hughes DF, Kusamba C, Behangana M, Greenbaum E (2017) Integrative taxonomy of the Central African forest chameleon, *Kinyongia Adolfifridericci* (Sauria: Chamaeleonidae), reveals underestimated species diversity in the Albertine Rift. *Zoological Journal of the Linnean Society* zlx005 doi:10.1093/zoolinnean/zlx005
- Hutter CR, Andriampenomanana ZF, Razafindraibe J, Rakotoarison A, Scherz MD (2018a) New dietary data from *Compsophis* and *Alluaudina* species (Squamata: Lamprophiidae: Pseudoxyrhophiinae), and implications for their dietary complexity and evolution. *Journal of Natural History* 52(39–40): 2497–2510. doi:10.1080/00222933.2018.1543732
- Hutter CR, Lambert SM, Andriampenomanana ZF, Glaw F, Vences M (2018b) Molecular systematics and diversification of Malagasy bright-eyed tree frogs (Mantellidae: *Boophis*). *Molecular Phylogenetics and Evolution* 127: 568–578. doi:10.1016/j.ympev.2018.05.027
- IUCN (2012) IUCN Red List Categories and Criteria: Version 3.1. IUCN, Gland, Switzerland and Cambridge, UK.
- IUCN. (2019) IUCN Red List of Threatened Species. Version 2018.2. Available at <http://www.iucnredlist.org>. Accessed: 15 February 2019
- Jagoutz O, Royden L, Holt AF, Becker TW (2015) Anomalously fast convergence of India and Eurasia caused by double subduction. *Nature Geoscience* 8: 475. doi:10.1038/ngeo2418
- Jenkins RKB, Tognelli MF, Bowles P, Cox N, Brown JL, Chan L, Andreone F, Andriamazava A, Andriantsimanarilafy RR, Anjerieina M, Bora P, Brady LD, Hantalalaina EF, Glaw F, Griffiths RA, Hilton-Taylor C, Hoffmann M, Katariya V, Rabibisoa NH, Rafanomezantsoa J, Rakotomalala D, Rakotondravony H, Rakotondrazafy NA, Ralambonirainy J, Ramamanjato J-B, Randriamahazo H, Randrianantoandro JC, Randrianasolo HH, Randrianirina JE, Randrianizahana H, Raselimanana AP, Rasolohery A, Ratsoavina FM, Raxworthy CJ,

References

- Robson Manitrandrasana E, Rollande F, van Dijk PP, Yoder AD, Vences M (2014) Extinction risks and the conservation of Madagascar's reptiles. *PLoS One* 9(8): e100173 (100114 pp.). doi:10.1371/journal.pone.0100173
- Joppa LN, Roberts DL, Pimm SL (2011) The population ecology and social behaviour of taxonomists. *Trends in Ecology and Evolution* 26(11): 551–553. doi:10.1016/j.tree.2011.07.010
- Jury MR (2003) The Climate of Madagascar. In Goodman SM & Benstead JP (eds). *The Natural History of Madagascar*. The University of Chicago Press, Chicago IL: pp. 75–87.
- Kaffenberger N, Wollenberg KC, Köhler J, Glaw F, Vieites DR, Vences M (2012) Molecular phylogeny and biogeography of Malagasy frogs of the genus *Gephyromantis*. *Molecular Phylogenetics and Evolution* 62(1): 555–560. doi:10.1016/j.ympev.2011.09.023
- Köhler J, Vences M, D'Cruze N, Glaw F (2010) Giant dwarfs: discovery of a radiation of large-bodied 'stump-toed frogs' from karstic cave environments of northern Madagascar. *Journal of Zoology* 282(1): 21–38. doi:10.1111/j.1469-7998.2010.00708.x
- Kotov AA, Gololobova MA (2016) Traditional taxonomy: Quo vadis? *Integrative Zoology* 11: 500–505. doi:10.1111/1749-4877.12215
- Kraaijeveld K, Kraaijeveld-Smit FJL, Komdeur J (2007) The evolution of mutual ornamentation. *Animal Behaviour* 74(4): 657–677. doi:10.1016/j.anbehav.2006.12.027
- Krause DW (2003) Late Cretaceous vertebrates of Madagascar: a window into Gondwanan biogeography at the end of the Age of Dinosaurs. In Goodman SM & Benstead JP (eds). *The Natural History of Madagascar*. Chicago University Press, Chicago IL, USA: pp. 40–47.
- Krause DW, Evans SE, Gao K-Q (2003) First definitive record of Mesozoic lizards from Madagascar. *Journal of Vertebrate Paleontology* 23(4): 842–856.
- Kremen C, Cameron A, Moilanen A, Phillips SJ, Thomas CD, Beentje H, Dransfield J, Fisher BL, Glaw F, Good TC, Harper GJ, Hijmans RJ, Lees DC, Louis Jr. EE, Nussbaum RA, Raxworthy CJ, Razafimpanahana A, Schatz GE, Vences M, Vieites DR, Wright PC, Zjhra ML (2008) Aligning conservation priorities across taxa in Madagascar with high-resolution planning tools. *Science* 320(5873): 222–226. doi:10.1126/science.1155193
- Kuchta SR, Wake DB (2016) Wherfore and whither the ring species? *Copeia* 104(1): 189–201. doi: 10.1643/OT-14-176
- Kusky TM, Toraman E, Raharimahefa T, Rasoazanamparany C (2010) Active tectonics of the Alaotra–Ankay Graben System, Madagascar: Possible extension of Somalian–African diffusive plate boundary? *Gondwana Research* 18(2): 274–294. doi:10.1016/j.gr.2010.02.003
- Laduke T, Krause DW, Scanlon JD, Kley NJ (2010) A late cretaceous (Maastrichtian) snake assemblage from the Maevarano formation, Mahajanga basin, Madagascar. *Journal of Vertebrate Paleontology* 30(1): 109–138.
- Lambert SM, Hutter CR, Scherz MD (2017) Diamond in the rough: a new species of fossorial diamond frog (*Rhombophryne*) from Ranomafana National Park, southeastern Madagascar. *Zoosystematics and Evolution* 93(1): 143–155. doi:10.3897/zse.93.10188
- Ligon RA, Diaz CD, Morano JL, Troscianko J, Stevens M, Moskaland A, Laman TG, Scholes E, III (2018) Evolution of correlated complexity in the radically different courtship signals of birds-of-paradise. *PLoS Biology* 16(11): e2006962 (2006924 pp.). doi:10.1371/journal.pbio.2006962
- Lorch JM, Knowles S, Lankton JS, Michell K, Edwards JL, Kapfer JM, Staffen RA, Wild ER, Schmidt KZ, Ballmann AE, Blodgett D, Farrell TM, Glorioso BM, Last LA, Price SJ, Schuler KL, Smith CE, Wellehan JFX, Blehert DS (2016) Snake fungal disease: an emerging threat to wild snakes. *Philosophical Transactions of the Royal Society B* 371(1709): 20150457 (20150458 pp.). doi:10.1098/rstb.2015.0457

- Losos JB (2011) Lizards in an Evolutionary Tree. University Of California Press, Berkeley CA, USA, 507 pp.
- Losos JB, Ricklefs RE (2009) Adaptation and diversification on islands. *Nature* 457: 830–836. doi:10.1038/nature07893
- Lourenco-De-Moraes R, Dias IR, Mira-Mendes CV, de Oliveira RM, Barth A, Ruas DS, Vences M, Solé M, Bastos RP (2018) Diversity of miniaturized frogs of the genus *Adelophryne* (Anura: Eleutherodactylidae): A new species from the Atlantic Forest of northeast Brazil. *PLoS One* 13: e0201781 (0201717 pp.). doi:10.1371/journal.pone.0201781
- Lowry II PP, Phillipson PB, Andrimahefarivo L, Schatz GE, Rajaonary F, Andriambololonera S (2019) Flora. In Goodman SM, Raherilalao MJ & Wohlhauser S (eds). *Les aires protégées terrestres de Madagascar : Leur histoire, description et biote / The terrestrial protected areas of Madagascar: Their history, description, and biota*. Association Vahatra, Antananarivo, Madagascar: pp. 243–255.
- MacArthur RH, Wilson EO (1963) An equilibrium theory of insular zoogeography. *Evolution* 17: 373–387.
- Madagascar Catalogue (2019) Catalogue of the Vascular Plants of Madagascar. Missouri Botanical Garden, St. Louis, U.S.A. & Antananarivo, Madagascar [<http://www.tropicos.org/Project/Madagascar>. Accessed: February, 2019].
- Maestri R, Monteiro LR, Fornel R, Upham NS, Patterson BD, de Freitas TRO (2017) The ecology of a continental evolutionary radiation: Is the radiation of sigmodontine rodents adaptive? *Evolution* 71(3): 610–632. doi:10.1111/evo.13155
- Maminirina CP, Goodman SM, Raxworthy CJ (2008) Les micro-mammifères (Mammalia, Rodentia, Afrosoricida et Soricomorpha) du massif du Tsaratanana et biogéographie des forêts de montagne de Madagascar. *Zoosystema* 30: 695–721.
- Martin EA, Ratsimiseta L, Laloë F, Carrière SM (2009) Conservation value for birds of traditionally managed isolated trees in an agricultural landscape of Madagascar. *Biodiversity and Conservation* 18(10): 2719–2742. doi:10.1007/s10531-009-9671-x
- Mayden RL (1997) A hierarchy of species concepts: the denouement in the saga of the species problem. In Claridge MF, Dawah HA & Wilson MR (eds). *Species: The Units of Biodiversity*. Chapman & Hall, London, UK: pp. 381–424.
- Mayr E (1942) Systematics and the origin of species from the viewpoint of a zoologist Columbia University Press, New York NY, USA, 334 pp.
- Mayr E (1957) Species concepts and definitions. In Mayr E (ed). *The Species Problem*. Washington, DC, USA, American Association for Advancement of Science: pp. 1–22.
- McCormack JE, Tsai WLE, Faircloth BC (2016) Sequence capture of ultraconserved elements from bird museum specimens. *Molecular Ecology Resources* 16(5): 1189–1203. doi:10.1111/1755-0998.12466
- McLeod DS (2010) Of Least Concern? Systematics of a cryptic species complex: *Limnonectes kuhlii* (Amphibia: Dicroidiidae). *Molecular Phylogenetics and Evolution* 56: 991–1000. doi:10.1016/j.ympev.2010.04.004
- Meiri S (2018) Traits of lizards of the world: variation around a successful evolutionary design. *Global Ecology and Biogeography* 27: 1168–1172. doi:10.1111/geb.12773
- Moen DS, Irschick DJ, Wiens JJ (2013) Evolutionary conservatism and convergence both lead to striking similarity in ecology, morphology and performance across continents in frogs. *Proceedings of the Royal Society of London B* 280(1773): 20132156 (20132159 pp.). doi:10.1098/rspb.2013.2156

References

- Moen DS, Wiens JJ (2017) Microhabitat and climatic niche change explain patterns of diversification among frog families. *The American Naturalist* 190(1): 29–44. doi:10.1086/692065
- Myers N, Mittermeier RA, Mittermeier CG, da Fonseca GAB, Kent J (2000) Biodiversity hotspots for conservation priorities. *Nature* 403: 853–858.
- Nagy ZT, Sonet G, Glaw F, Vences M (2012) First large-scale DNA barcoding assessment of reptiles in the biodiversity hotspot of Madagascar, based on newly designed COI primers. *PLoS One* 7(3): e34506 (34511 pp.). doi:10.1371/journal.pone.0034506
- Nguyen CV, Lovell DR, Adcock M, La Salle J (2014) Capturing natural-colour 3D models of insects for species discovery and diagnostics. *PLoS One* 9(4): e94346 (94311 pp.). doi:10.1371/journal.pone.0094346
- Noble GK, Parker HW (1926) A synopsis of the brevicipitid toads of Madagascar. *American Museum Novitates* 232: 1–21.
- Nori J, Loyola R (2015) On the worrying fate of data deficient amphibians. *PLoS One* 10(5): e0125055 (0125058 pp.). doi:10.1371/journal.pone.0125055
- Nori J, Villalobos F, Loyola R (2018) Global priority areas for amphibian research. *Journal of Biogeography* 41(11): 2588–2594. doi:10.1111/jbi.13435
- O'Hanlon SJ, Rieux A, Farrer RA, Rosa GM, et al. (2018) Recent Asian origin of chytrid fungi causing global amphibian declines. *Science* 360(6389): 621–627. doi:10.1126/science.aar1965
- Oliver PM, Iannella A, Richards SJ, Lee MSY (2017) Mountain colonisation, miniaturisation and ecological evolution in a radiation of direct-developing New Guinea frogs (*Choerophryne*, *Microhylidae*). *PeerJ* 5: e3077 (3023 pp.). doi:10.7717/peerj.3077
- Olson DH, Aanensen DM, Ronnenberg KL, Powell CI, Walker SF, Bielby J, Garner TW, Weaver G, Bd Mapping G, Fisher MC (2013) Mapping the global emergence of *Batrachochytrium dendrobatidis*, the amphibian chytrid fungus. *PLoS One* 8(2): e56802 (56813 pp.). doi:10.1371/journal.pone.0056802
- Omland KE (1996) Female mallard mating preferences for multiple male ornaments: I. Natural variation. *Behavioral Ecology and Sociobiology* 39(6): 353–360.
- Pabijan M, Wollenberg KC, Vences M (2012) Small body size increases the regional differentiation of populations of tropical mantellid frogs (Anura: Mantellidae). *Journal of Evolutionary Biology* 25(11): 2310–2324. doi:10.1111/j.1420-9101.2012.02613.x
- Padial JM, de la Riva I (2010) A response to recent proposals for integrative taxonomy. *Biological Journal of the Linnean Society* 101: 747–756. doi:10.1111/j.1095-8312.2010.01528.x
- Padial JM, Miralles A, De La Riva I, Vences M (2010) The integrative future of taxonomy. *Frontiers in Zoology* 7: 16. doi:10.1186/1742-9994-7-16
- Paknia O, Rajaei Sh. H, Koch A (2015) Lack of well-maintained natural history collections and taxonomists in megadiverse developing countries hampers global biodiversity exploration. *Organisms Diversity & Evolution* 15: 619–629. doi:10.1007/s13127-015-0202-1
- Parker HW (1934) Monograph of the frogs of the family Microhylidae. Trustees of the British Museum, London, UK.
- Pavón-Vázquez CJ, García-Vázquez UO, Bryson RW, Feria-Ortiz M, Manríquez-Morán NL, de Oca AN-M (2018) Integrative species delimitation in practice: Revealing cryptic lineages within the short-nosed skink *Plestiodon brevirostris* (Squamata: Scincidae). *Molecular Phylogenetics and Evolution* 129: 242–257. doi:10.1016/j.ympev.2018.08.020
- Pearson RG, Raxworthy CJ (2009) The evolution of local endemism in madagascar: watershed versus climatic gradient hypotheses evaluated by null biogeographic models. *Evolution*

- 63(4): 959–967. doi:10.1111/j.1558-5646.2008.00596.x
- Peloso PLV, Frost DR, Richards SJ, Rodrigues MT, Donnellan S, Matsui M, Raxworthy CJ, Biju SD, Lemmon EM, Lemmon AR, Wheeler WC (2016) The impact of anchored phylogenomics and taxon sampling on phylogenetic inference in narrow-mouthed frogs (Anura, Microhylidae). *Cladistics* 32(2): 113–140. doi:10.1111/cla.12118
- Peloso PLV, Raxworthy CJ, Wheeler WC, Frost DR (2017) Nomenclatural stability does not justify recognition of paraphyletic taxa: A response to Scherz et al. (2016). *Molecular Phylogenetics and Evolution* 111(2017): 56–64. doi:10.1016/j.ympev.2017.03.016
- Perl RGB, Nagy ZT, Sonet G, Glaw F, Wollenberg KC, Vences M (2014) DNA barcoding Madagascar's amphibian fauna. *Amphibia-Reptilia* 35: 197–206. doi:10.1163/15685381-00002942
- Phillips SJ, Anderson RP, Schapire RE (2006) Maximum entropy modeling of species geographic distributions. *Ecological Modelling* 190(3): 231–259. doi:10.1016/j.ecolmodel.2005.03.026
- Poe S, Anderson CG (2019) The existence and evolution of morphotypes in *Anolis* lizards: coexistence patterns, not adaptive radiations, distinguish mainland and island faunas. *PeerJ* 6: e6040 (6019 pp.). doi:10.7717/peerj.6040
- Poe S, Nieto-montes de oca A, Torres-carvajal O, De Queiroz K, Velasco JA, Truett B, Gray LN, Ryan MJ, Köhler G, Ayala-varela F, Latella I (2017) A phylogenetic, biogeographic, and taxonomic study of all extant species of *Anolis* (Squamata; Iguanidae). *Systematic Biology* 66(5): 663–697. doi:10.1093/sysbio/syx029
- Poux C, Madsen O, Marquard E, Vieites DR, de Jong WW, Vences M (2005) Asynchronous colonization of Madagascar by the four endemic clades of primates, tenrecs, carnivores, and rodents as inferred from nuclear genes. *Systematic Biology* 54(5): 719–730. doi:10.1080/10635150500234534
- Poyarkov NA, Suwannapoom C, Pawangkhanant P, Aksornneam A, Van Duong T, Korost DV, Che J (2018) A new genus and three new species of miniaturized microhylid frogs from Indochina (Amphibia: Anura: Microhylidae: Asterophryinae). *Zoological Research* 39(3): 130.
- Prötz D, Heß M, Scherz MD, Schwager M, van't Padje A, Glaw F (2018a) Widespread bone-based fluorescence in chameleons. *Scientific Reports* 8: 698 (699 pp.). doi:10.1038/s41598-017-19070-7
- Prötz D, Lambert SM, Andrianasolo GT, Hutter CR, Cobb KA, Scherz MD, Glaw F (2018b) The smallest 'true chameleon' from Madagascar: a new, distinctly colored species of the *Calumma boettgeri* complex (Squamata, Chamaeleonidae). *Zoosystematics and Evolution* 94(2): 409–423. doi:10.3897/zse.94.27305
- Prötz D, Ruthensteiner B, Scherz MD, Glaw F (2015) Systematic revision of the Malagasy chameleons *Calumma boettgeri* and *C. linotum* (Squamata: Chamaeleonidae). *Zootaxa* 4048(2): 211–231. doi:10.11646/zootaxa.4048.2.4
- Prötz D, Scherz MD, Ratsoavina FM, Vences M, Glaw F (submitted) Untangling the trees: Revision of the *Calumma nasutum* complex (Squamata: Chamaeleonidae). *Vertebrate Zoology*
- Prötz D, Vences M, Hawlitschek O, Scherz MD, Ratsoavina FM, Glaw F (2018c) Endangered beauties: micro-CT cranial osteology, molecular genetics and external morphology reveal three new species of chameleons in the *Calumma boettgeri* complex (Squamata: Chamaeleonidae). *Zoological Journal of the Linnean Society* 184(2): 471–498. doi:10.1093/zoolinnean/zlx112
- Prötz D, Vences M, Scherz MD, Vieites DR, Glaw F (2017) Splitting and lumping: An integrative taxonomic assessment of Malagasy chameleons in the *Calumma guibei* complex results in the new species *C. gehringi* sp. nov. *Vertebrate Zoology* 67(2): 231–249.

References

- Rabearivony J, Rasamolina M, Raveloson J, Rakotomanana H, Raselimanana AP, Raminosoa NR, Zaonarivelo JR (2015) Roles of a forest corridor between Marojejy, Anjanaharibe-Sud and Tsaratanana protected areas, northern Madagascar, in maintaining endemic and threatened Malagasy taxa. *Madagascar Conservation & Development* 10(2): 85–92. doi:10.4314/mcd.v10i2.7
- Rakotoarison A, Scherz MD, Bletz MC, Razafindraibe JH, Glaw F, Vences M (in press) Diversity, elevational variation, and phylogenetic origin of stump-toed frogs (Microhylidae, *Cophylinae*, *Stumpffia*) on the Marojejy massif, northern Madagascar. *Salamandra*
- Rakotoarison A, Scherz MD, Glaw F, Köhler J, Andreone F, Franzen M, Glos J, Hawlitschek O, Jono T, Mori A, Ndriantsoa SH, Raminosoa Rasoamampionona N, Riemann JC, Rödel M-O, Rosa GM, Vieites DR, Crottini A, Vences M (2017) Describing the smaller majority: Integrative taxonomy reveals twenty-six new species of tiny microhylid frogs (genus *Stumpffia*) from Madagascar. *Vertebrate Zoology* 67(3): 271–398.
- Ramanamanjato J-B (2008) Reptile and amphibian communities along the humidity gradient and fragmentation effects in the littoral forests of southeastern Madagascar. In Ganzhorn JU, Goodman SM & Vinczelette M (eds). *Biodiversity, Ecology and Conservation of Littoral Ecosystems in Southeastern Madagascar*, Tolagnaro (Fort Dauphin). Smithsonian Institution, Washington DC, USA: pp.
- Ramos EKS, de Magalhães RF, Marques NCS, Baêta D, Garcia PCA, Santos FR (2019) Cryptic diversity in Brazilian endemic monkey frogs (Hylidae, Phylomedusinae, *Pithecopus*) revealed by multispecies coalescent and integrative approaches. *Molecular Phylogenetics and Evolution* 132: 105–116. doi:10.1016/j.ympev.2018.11.022
- Ratnasingham S, Hebert PDN (2007) BOLD: The Barcode of Life Data System (<http://www.barcodinglife.org>). *Molecular Ecology Resources* 7(3): 355–364. doi:10.1111/j.1471-8286.2007.01678.x
- Raxworthy CJ (1988) Reptiles, rainforest and conservation in Madagascar. *Biological Conservation* 43: 181–211.
- Raxworthy CJ, Nussbaum RA (1996) Montane amphibian and reptile communities in Madagascar. *Conservation Biology* 10(3): 750–756.
- Raxworthy CJ, Pearson RG, Zimkus BM, Reddy S, Deo AJ, Nussbaum RA, Ingram CM (2008) Continental speciation in the tropics: contrasting biogeographic patterns of divergence in the *Uroplatus* leaf-tailed gecko radiation of Madagascar. *Journal of Zoology* 275(4): 423–440. doi:10.1111/j.1469-7998.2008.00460.x
- Renner SS (2016) A return to Linnaeus's focus on diagnosis, not description: the use of DNA characters in the formal naming of species. *Systematic Biology* 65(6): 1085–1095. doi:10.1093/sysbio/syw032
- Ribeiro LF, Bornschein MR, Belmonte-Lopes R, Firkowski CR, Morato SAA, Pie MR (2015) Seven new microendemic species of *Brachycephalus* (Anura: Brachycephalidae) from southern Brazil. *PeerJ* 3: e1011 (1035 pp.). doi:10.7717/peerj.1011
- Riedel A, Sagata K, Suhardjono YR, Tänzler R, Balke M (2013) Integrative taxonomy on the fast track - towards more sustainability in biodiversity research. *Frontiers in Zoology* 10: 15. doi:10.1186/1742-9994-10-15
- Riedel A, Tänzler R, Balke M, Rahmadi C, Suhardjono YR (2014) Ninety-eight new species of *Trigonopterus* weevils from Sundaland and the Lesser Sunda Islands. *Zookeys* 467: 1–162. doi:10.3897/zookeys.467.8206
- Rittmeyer EN, Allison A, Gründler MC, Thompson DK, Austin CC (2012) Ecological guild evolution and the discovery of the world's smallest vertebrate. *PLoS One* 7(1): e29797 (29711

- pp.). doi:10.1371/journal.pone.0029797
- Rodríguez A, Börner M, Pabijan M, Gehara M, Haddad CFB, Vences M (2015) Genetic divergence in tropical anurans: deeper phylogeographic structure in forest specialists and in topographically complex regions. *Evolutionary Ecology* 29: 765–785.
- Roux C, Fraïsse C, Romiguier J, Anciaux Y, Galtier N, Bierne N (2016) Shedding light on the grey zone of speciation along a continuum of genomic divergence. *PLoS Biology* 14(12): e2000234 (2000222 pp.). doi:10.1371/journal.pbio.2000234
- Ruane S, Austin CC (2017) Phylogenomics using formalin-fixed and 100+ year-old intractable natural history specimens. *Molecular Ecology Resources* 17(5): 1003–1008. doi:10.1111/1755-0998.12655
- Samonds KE, Godfrey LR, Ali JR, Goodman SM, Vences M, Sutherland MR, Irwin MT, Krause DW (2012) Spatial and temporal arrival patterns of Madagascar's vertebrate fauna explained by distance, ocean currents, and ancestor type. *Proceedings of the National Academy of Sciences of the USA* 109: 5352–5357. doi:10.1073/pnas.1113993109
- Samonds KE, Godfrey LR, Ali JR, Goodman SM, Vences M, Sutherland MR, Irwin MT, Krause DW (2013) Imperfect isolation: factors and filters shaping Madagascar's extant vertebrate fauna. *PLoS One* 8(4): e62086 (62015 pp.). doi:10.1371/journal.pone.0062086
- Schatz GE (2000) Endemism in the Malagasy tree flora. In Lourenço WR & Goodman SM (eds). *Diversity and endemism in Madagascar*. Société de Biogéographie, MNHN ORSTOM, Paris, France: pp. 1–9.
- Scheffers BR, Joppa LN, Pimm SL, Laurance WF (2012) What we know and don't know about Earth's missing biodiversity. *Trends in Ecology and Evolution* 27(9): 501–510. doi:10.1016/j.tree.2012.05.008
- Scherz MD, Köhler J, Rakotoarison A, Glaw F, Vences M (2019) A new dwarf chameleon, genus *Brookesia*, from the Marojejy massif in northern Madagascar. *Zoosystematics and Evolution* 95(1): 95–106. doi:10.3897/zse.95.32818
- Scherz MD, Rakotoarison A, Hawlitschek O, Vences M, Glaw F (2015a) Leaping towards a saltatorial lifestyle? An unusually long-legged new species of *Rhombophryne* (Anura, Microhylidae) from the Sorata massif in northern Madagascar. *Zoosystematics and Evolution* 91(2): 105–114. doi:10.3897/zse.91.4979
- Scherz MD, Ruthensteiner B, Vences M, Glaw F (2014) A new microhylid frog, genus *Rhombophryne*, from northeastern Madagascar, and a re-description of *R. serratopalpebrosa* using micro-computed tomography. *Zootaxa* 3860(6): 547–560. doi:10.11646/zootaxa.3860.6.3
- Scherz MD, Ruthensteiner B, Vieites DR, Vences M, Glaw F (2015b) Two new microhylid frogs of the genus *Rhombophryne* with supraciliary spines from the Tsaratanana Massif in northern Madagascar. *Herpetologica* 71(4): 310–321. doi:10.1655/HERPETOLOGICA-D-14-00048
- Scherz MD, Vences M, Rakotoarison A, Andreone F, Köhler J, Glaw F, Crottini A (2017) Lumping or splitting in the Cophylinae (Anura: Microhylidae) and the need for a parsimony of taxonomic changes: a response to Peloso et al. (2017). *Salamandra* 53(3): 479–483.
- Schlick-Steiner BC, Steiner FM, Seifert B, Stauffer C, Christian E, Crozier RH (2010) Integrative taxonomy: a multisource approach to exploring biodiversity. *Annual Review of Entomology* 55(1): 421–438. doi:10.1146/annurev-ento-112408-085432
- Schliewen UK, Klee B (2004) Reticulate sympatric speciation in Cameroonian crater lake cichlids. *Frontiers in Zoology* 1(1): 5. doi:10.1186/1742-9994-1-5
- Scott DM, Brown D, Mahood S, Denton B, Silburn A, Rakotondraparany F (2006) The impacts of forest clearance on lizard, small mammal and bird communities in the arid spiny

References

- forest, southern Madagascar. *Biological Conservation* 127: 72–87. doi:10.1016/j.biocon.2005.07.014
- Seehausen O, Takimoto G, Roy D, Jokela J (2008) Speciation reversal and biodiversity dynamics with hybridization in changing environments. *Molecular Ecology* 17(1): 30–44. doi:10.1111/j.1365-294X.2007.03529.x
- Shaw KL, Gillespie RG (2016) Comparative phylogeography of oceanic archipelagos: Hotspots for inferences of evolutionary process. *Proceedings of the National Academy of Sciences of the USA* 113(29): 7986–7993. doi:10.1073/pnas.1601078113
- Simpson GG (1961) *Principles of Animal Taxonomy*. Columbia University Press, New York NY, USA, xii + 247 pp.
- Skukumaran J, Knowles LL (2017) Multispecies coalescent delimits structure, not species. *Proceedings of the National Academy of Sciences of the USA* 114(7): 1607–1612. doi:10.1073/pnas.1607921114
- Smith MA, Fisher BL, Hebert PDN (2005) DNA barcoding for effective biodiversity assessment of a hyperdiverse arthropod group: the ants of Madagascar. *Philosophical Transactions of the Royal Society B* 360(1462): 1825–1834. doi:10.1098/rstb.2005.1714
- Solís-Lemus C, Knowles LL, Ané C (2015) Bayesian species delimitation combining multiple genes and traits in a unified framework. *Evolution* 69: 492–507. doi:10.1111/evo.12582
- Spitzen-van der Sluijs A, Martel A, Asselberghs J, Bales EK, Beukema W, Bletz MC, Dalbeck L, Goverse E, Kerres A, Kinet T, Kirst K, Laudelout A, Marin da Fonte LF, Nöllert A, Ohlhoff D, Sabino-Pinto J, Schmidt BR, Speybroeck J, Spikmans F, Steinfartz S, Veith M, Vences M, Wagner N, Pasmans F, Lötters S (2016) Expanding distribution of lethal amphibian fungus *Batrachochytrium salamandrivorans* in Europe. *Emerging Infectious Diseases* 22(7): 1286–1288. doi:10.3201/eid2207.160109
- Stipala J, Lutzmann N, Malonza PK, Wilkinson P, Godley B, Nyamache J, Evans MR (2012) A new species of chameleon (Squamata: Chamaeleonidae) from the Aberdare Mountains in the central highlands of Kenya. *Zootaxa* 3391: 1–22.
- Sung Y-H, Karraker NE, Hau BCH (2012) Terrestrial herpetofaunal assemblages in secondary forests and exotic *Lophostemon confertus* plantations in South China. *Forest Ecology and Management* 270: 71–77. doi:10.1016/j.foreco.2012.01.011
- Tautz D, Arctander P, Minelli A, Thomas RH, Vogler AP (2003) A plea for DNA taxonomy. *Trends in Ecology and Evolution* 18(2): 70–74. doi:10.1016/S0169-5347(02)00041-1
- Tilbury CR (2018) Chameleons of Africa: An Atlas, Including the Chameleons of Europe, the Middle East and Asia. Chimaira Buchhandelsgesellschaft mbH, Frankfurt am Main, Germany, 643 pp.
- Tilbury CR, Tolley KA (2009) A new species of dwarf chameleon (Sauria; Chamaeleonidae, *Bradypodion* Fitzinger) from KwaZulu Natal South Africa with notes on recent climatic shifts and their influence on speciation in the genus. *Zootaxa* 2226: 43–57.
- Tilbury CR, Tolley KA (2015) Contributions to the herpetofauna of the Albertine Rift: Two new species of chameleon (Sauria: Chamaeleonidae) from an isolated montane forest, south eastern Democratic Republic of Congo. *Zootaxa* 3905(3): 345–364. doi:10.11646/zootaxa.3905.3.2
- Tolley KA, Townsend TM, Vences M (2013) Large-scale phylogeny of chameleons suggests African origins and Eocene diversification. *Proceedings of the Royal Society of London B* 280(1759): 20130184 (20130188 pp.). doi:10.1098/rspb.2013.0184
- Trueb L, Alberch P (1985) Miniaturisation and the anuran skull: a case study of heterochromy. In Duncker HR & Fleischer G (eds). *Functional morphology of vertebrates*. Gustav Fisher

- Verlag, Stuttgart, Germany: pp. 113–121.
- Tu N, Yang M, Liang D, Zhang P (2018) A large-scale phylogeny of Microhylidae inferred from a combined dataset of 121 genes and 427 taxa. *Molecular Phylogenetics and Evolution* 126: 85–91.
- Uetz P, Hošek J. (2016) The Reptile Database, <http://www.reptile-database.org>, accessed: 14 March 2019
- van der Meijden A, Vences M, Hoegg S, Boistel R, Channing A, Meyer A (2007) Nuclear gene phylogeny of narrow-mouthed toads (Family: Microhylidae) and a discussion of competing hypotheses concerning their biogeographical origins. *Molecular Phylogenetics and Evolution* 44: 1017–1030. doi:10.1016/j.ympev.2007.02.008
- Vences M, Guayasamin JM, Miralles A, de la Riva I (2013) To name or not to name: Criteria to promote economy of change in Linnaean classification schemes. *Zootaxa* 3636(2): 201–244. doi:10.11646/zootaxa.3636.2.1
- Vences M, Köhler J, Pabijan M, Bletz M, Gehring P-S, Hawlitschek O, Rakotoarison A, Ratsoavina FM, Andreone F, Crottini A, Glaw F (2017) Taxonomy and geographic distribution of Malagasy frogs of the *Gephyromantis asper* clade, with description of a new subgenus and revalidation of *Gephyromantis ceratophrys*. *Salamandra* 53(1): 77–98.
- Vences M, Thomas M, Bonett RM, Vieites DR (2005a) Deciphering amphibian diversity through DNA barcoding: chances and challenges. *Philosophical Transactions of the Royal Society B* 360: 1859–1868. doi:10.1098/rstb.2005.1717
- Vences M, Thomas M, van der Meijden A, Chiari Y, Vieites DR (2005b) Comparative performance of the 16S rRNA gene in DNA barcoding of amphibians. *Frontiers in Zoology* 2: 5. doi:10.1186/1742-9994-2-5
- Vences M, Wollenberg KC, Vieites DR, Lees DC (2009) Madagascar as a model region of species diversification. *Trends in Ecology and Evolution* 24(8): 456–465. doi:10.1016/j.tree.2009.03.011
- Vidal-García M, Keogh JS (2015) Convergent evolution across the Australian continent: ecotype diversification drives morphological convergence in two distantly related clades of Australian frogs. *Journal of Evolutionary Biology* 28: 2136–2151. doi:10.1111/jeb.12746
- Vidal-García M, Keogh JS (2017) Phylogenetic conservatism in skulls and evolutionary lability in limbs – morphological evolution across an ancient frog radiation is shaped by diet, locomotion and burrowing. *BMC Evolutionary Biology* 17(1): 165. doi:10.1186/s12862-017-0993-0
- Vieites DR, Wollenberg KC, Andreone F, Köhler J, Glaw F, Vences M (2009) Vast underestimation of Madagascar's biodiversity evidenced by an integrative amphibian inventory. *Proceedings of the National Academy of Sciences of the USA* 106(20): 8267–8272. doi:10.1073/pnas.0810821106
- Vogel Ely C, de Loreto Bordignon SA, Trevisan R, Boldrini II (2017) Implications of poor taxonomy in conservation. *Journal for Nature Conservation* 36: 10–13. doi:10.1016/j.jnc.2017.01.003
- Warren BH, Simberloff D, Ricklefs RE, Aguilée R, Condamine FL, Gravel D, Morlon H, Mouquet N, Rosindell J, Casquet J, Conti E, Cornuault J, Fernández-Palacios JM, Hengl T, Norder SJ, Rijssdijk KF, Sanmartín I, Strasberg D, Triantis KA, Valente LM, Whittaker RJ, Gillespie RG, Emerson BC, Thébaud C (2015) Islands as model systems in ecology and evolution: prospects fifty years after MacArthur-Wilson. *Ecology Letters* 18(2): 200–217. doi:10.1111/ele.12398
- Warren BH, Strasberg D, Bruggemann JH, Prys-Jones RP, Thébaud C (2010) Why does the biota

References

- of the Madagascar region have such a strong Asiatic flavour? *Cladistics* 26(5): 526–538. doi:10.1111/j.1096-0031.2009.00300.x
- Wells NA (2003) Some hypotheses on the Mesozoic and Cenozoic paleoenvironmental history of Madagascar. In Goodman SM & Benstead JP (eds). *The Natural History of Madagascar*. The University of Chicago Press, Chicago, IL: pp. 16–34.
- Wheeler QD, Bourgoin T, Coddington J, Gostony T, Hamilton A, Larimer R, Plaszek A, Schauff M, Solis MA (2012) Nomenclatural benchmarking: the roles of digital typification and telemicroscopy. *ZooKeys* 209: 193–202. doi:10.3897/zookeys.209.3486
- Whittaker RJ, Fernández-Palacios JM (2007) *Island Biogeography Ecology, Evolution, and Conservation*. Oxford University Press, Oxford, UK.
- Wiens JJ, Pyron RA, Moen DS (2011) Phylogenetic origins of local-scale diversity patterns and the causes of Amazonian megadiversity. *Ecology Letters* 14: 643–652.
- Will KW, Mishler BD, Wheeler QD (2005) The perils of DNA barcoding and the need for integrative taxonomy. *Systematic Biology* 54(5): 844–851. doi:10.1080/10635150500354878
- Wilmé L, Goodman SM, Ganzhorn JU (2006) Biogeographic evolution of Madagascar's microendemic biota. *Science* 312(5776): 1063–1065. doi:10.1126/science.1122806
- Wollenberg KC, Vieites DR, Glaw F, Vences M (2011) Speciation in little: the role of range and body size in the diversification of Malagasy mantellid frogs. *BMC Evolutionary Biology* 11: 217. doi:10.1186/1471-2148-11-217
- Wollenberg KC, Vieites DR, van der Meijden A, Glaw F, Cannatella DC, Vences M (2008) Patterns of endemism and species richness in Malagasy cophyline frogs support a key role of mountainous areas for speciation. *Evolution* 62(8): 1890–1907. doi:10.1111/j.1558-5646.2008.00420.x
- Wollenberg Valero KC (2015) Evidence for an intrinsic factor promoting landscape genetic divergence in Madagascan leaf-litter frogs. *Frontiers in Genetics* 6(155): 1–7. doi:10.3389/fgene.2015.00155
- Wollenberg Valero KC, Garcia-Porta J, Rodríguez A, Arias M, Shah A, Randrianaaina RD, Brown JL, Glaw F, Amat F, Künzel S, Metzler D, Isokpehi RD, Vences M (2017) Transcriptomic and macroevolutionary evidence for phenotypic uncoupling between frog life history phases. *Nature Communications* 8: 15213 (15219 pp.). doi:10.1038/ncomms15213
- Wu S-H. (1994) Phylogenetic relationships, higher classification, and historical biogeography of the microhyloid frogs (Lissamphibia: Anura: Brevicipitidae and Microhylidae), p. 284. Vol. Doctor of Philosophy (Biology). University of Michigan
- Yang Z, Rannala B (2010) Bayesian species delimitation using multilocus sequence data. *Proceedings of the National Academy of Sciences of the USA* 107(20): 9264–9269. doi:10.1073/pnas.0913022107
- Yoder AD, Nowak MD (2006) Has vicariance or dispersal been the predominant biogeographic force in Madagascar? Only time will tell. *Annual Review of Ecology, Evolution, and Systematics* 37(1): 405–431. doi:10.1146/annurev.ecolsys.37.091305.110239
- Yuan Z-Y, Zhang B-L, Raxworthy CJ, Weisrock DW, Hime PM, Jin J-Q, Lemmon EM, Lemmon AR, Holland SD, Kortyna ML, Zhou W-W, Peng M-S, Che J, Prendini E (2018) Natatanuran frogs used the Indian Plate to step-stone disperse and radiate across the Indian Ocean. *National Science Review* 0: 1–5. doi:10.1093/nsr/nwy092
- Ziegler T, Böhme W (1997) Genitalstrukturen und Paarungsbiologie bei squamaten Reptilien, speziell den Platynota, mit Bemerkungen zur Systematik. *Mertensiella* 8: 1–207.
- Zimkus BM, Lawson L, Loader SP, Hanken J (2012) Terrestrialization, miniaturization and rates

of diversification in African puddle frogs (Anura: Phrynobatrachidae). PLoS One 7(4): e35118 (35111 pp.). doi:10.1371/journal.pone.0035118

Zimkus BM, Lawson LP, Barej MF, Barratt CD, Channing A, Dash KM, Dehling JM, Du Preez L, Gehring P-S, Greenbaum E, Gvoždík V, Harvey J, Kielgast J, Kusamba C, Nagy ZT, Pabijan M, Penner J, Rödel M-O, Vences M, Lötters S (2017) Leapfrogging into new territory: How Mascarene ridged frogs diversified across Africa and Madagascar to maintain their ecological niche. Molecular Phylogenetics and Evolution 106: 254–269. doi:10.1016/j.ympev.2016.09.018

Curriculum Vitae



Mark D. Scherz, MSc



Website: <http://www.markscherz.com> • Twitter: @MarkScherz
ORCID: 0000-0002-4613-7761

Higher Education

PhD candidate in Evolutionary Biology & Systematics

Ludwig-Maximilians Universität München &
Technische Universität Braunschweig

Since Oct 2015

'Taxonomy as a window to evolution: insights from
the reptiles and amphibians of Madagascar'

Supervised by Prof. Miguel Vences, Dr Frank Glaw, and Prof. Gerhard Haszprunar



MSc Evolution, Ecology & Systematics, 1.48 (Very Good)

Ludwig-Maximilians Universität München

Oct 2013 – Sept 2015

'Disentangling cryptic genera of Madagascan narrow-mouthed frogs
(Anura: Microhylidae: Cophylinae) with an integrative dataset'

Supervised by Dr Frank Glaw and Prof. Gerhard Haszprunar

BSc Biological Sciences with Honours (Zoology), First Class

University of Edinburgh

Aug 2009 – July 2013

'The Paraphyly of Ratites Just Doesn't Fly'

Supervised by Prof. Andrew Rambaut

Research Experience

Research Assistant

Zoologische Staatssammlung München

Since Oct 2013
Munich, Germany

- Taxonomic and systematic research on the amphibians and reptiles of Madagascar
- Micro-computed tomography (micro-CT) scanning of museum specimens
- Herpetological specimen preparation, cataloguing, and curation assistance
- Supervision of MSc and BSc students (see Supervision section below)

Fieldwork Experience

Team Leader, Research Coordinator

PhD research expedition

Nov 2017 – Jan 2018
Montagne d'Ambre, Madagascar

Herpetological Researcher

Expedition to Marojejy

Nov – Dec 2016
Marojejy, Madagascar

International Science Officer, Taxonomist

Expedition Angano

Dec 2015 – Jan 2016
Bealanana, Madagascar

Herpetological Research Intern

DEAL Mayotte

Nov – Dec 2014
Mayotte, France

Herpetological Research Leader, Deputy Team Leader

Operation Wallacea

June – Aug 2012
Mahavelo, Madagascar

Team Leader, Research Coordinator, Herpetological Researcher

Madagascar 2011: Project Kobokara

July – Sept 2011
Kobokara, Madagascar

Grants and Competitive Funding

2011 & 2015 – 2016 Successfully raised funds for expeditions from numerous prestigious and competitive grants, from organisations including the Royal Geographical Society, Mohamed bin Zayed Species Conservation Fund, Scientific Exploration Society, and Zoological Society of London

2015 DGH Wilhelm-Peters-Fonds 2015 — Deutsche Gesellschaft für Herpetologie und Terrarienkunde

2015 SSAR Travel and Registration Grant — Gans Collections and Charitable Fund

Academic Honours and Awards

- 2013 The Zoological Society of London's Charles Darwin Award and Marsh Prize for outstanding work in zoology (awarded in 2014)
- 2013 Ashworth Prize: Top Student in the Zoology Honours class of 2013, University of Edinburgh

Mark D. Scherz

mark.scherz@gmail.com

www.markscherz.com

Research-related Activities & Editorial Support

Editorial Work

Since 2018 Associate Editor, *Herpetological Conservation and Biology*
 2017 English Language editor for a paper in *Nature Communications*

Peer Review

(see: publons.com/a/812520/)

Amphibia-Reptilia, *Biodiversity Data Journal*, *Biology Letters*, *Journal of Herpetology*, *Herpetological Conservation and Biology*, *Herpetology Notes*, *PeerJ*, *Zoological Research*, *Zookeys*, *Zoosystematics and Evolution*, *Zootaxa*.

Workshops Attended

June 2018 Getting Funded: Writing an individual fellowship application, IMPRS/BioScript

Academic Society & Organisation Memberships

Since 2018 Deutsche Zoologische Gesellschaft
 Since 2018 European Society for Evolutionary Biology
 Since 2015 Deutsche Gesellschaft für Herpetologie und Terrarienkunde,
 Since 2013 IUCN/SSC Amphibian Specialist Group for Madagascar

Supervision

Since 2018 1 MSc student, ongoing
 2017 3 MSc students & 1 BSc student, 3–6 months each
 2016 1 BSc student, 3 months

Supervision included training in micro-CT scanning and reconstruction, external and osteological morphological analysis and description of reptiles and amphibians, statistical analysis, introduction to R or Past3, handling and analysing Sanger sequence data, and scientific writing.

Additional supervision experience in Madagascar, involving several BSc and MSc students during and after fieldwork. This entailed training in a wide array of skills, from fieldwork techniques to basic statistics.

Teaching

Since 2016 Instructor and trainer in micro-CT scanner use and model reconstruction
 2017 – 2018 Teaching assistant, BD08 Morphologie der Wirbeltiere (morphology of vertebrates) course, TU Braunschweig
 2011 – 2013 Voluntary speaker on topics related to herpetology, evolution, and field research, Edinburgh University Zoological Society
 2009 – 2013 Teacher of beginner, advanced, wildlife, travel and macro photography, Edinburgh University Photography Society

Competences & Skills

Software

General — Microsoft Office, EndNote
 Statistical — R, Past3, ImageJ
 Phylogenetics — BEAST, Geneious, RAxML, MrBayes, PAUP*4, Mesquite, MEGA7, etc.
 Acoustic analysis — Audacity, Adobe Audition
 Graphical — Adobe Creative Suite, Inkscape
 Micro-CT — Amira, VGStudio, Drishti
 Various others — e.g. QGIS

Technology and Equipment

nanotom m micro-CT scanner, Marantz PMD661 mkII, Sennheiser condenser microphones, DSLR cameras, GPS, Microsoft Windows and Apple Macintosh

Languages

English (mother tongue)	•	German (fluent)
French (working knowledge)	•	Malagasy (basic)

Public Outreach

- Science blogging at <http://www.markscherz.com>; occasionally invited entries elsewhere, e.g. Oxford University Press blog
- Twitter outreach and scientific networking, @markscherz
- Scientific Podcast: 'SquaMates, a totally serious herpetological podcast' co-hosted with E. Kocak and G. N. Ugueto <http://www.squamatespod.com>, @squamatespod
- Wikipedia editor, <http://en.wikipedia.org/wiki/Special:Contributions/Mark.scherz>
- Occasional popular science articles in print in *Elaphe*
- Assistant during open days at the Zoologische Staatssammlung München since 2013

Curriculum Vitae

Mark D. Scherz

mark.scherz@gmail.com

www.markscherz.com

Conferences and Seminars

*T = Talk, *A = Attendee

Graduiertenforum Fachgruppe Morphologie, Deutsche Zoologische Gesellschaft
Deutsche Zoologische Gesellschaft (DZG)
Evolution 2018
Societas Europaea Herpetologica (SEH)
Society for the Study of Amphibians and Reptiles (SSAR)
A Conservation Strategy for the Amphibians of Madagascar 2 (ACSAM2)

11 – 13 October 2018 *T
11 – 14 September 2018 *T
18 – 23 August 2018 *A
19 – 22 September 2017 *T
30 July – 2 August 2015 *T
19 – 22 August 2014 *T

Peer-Reviewed Publications

(for updates and PDFs see www.markscherz.com/publications)

43. Köhler, J., Vences, M., **Scherz, M.D.** & Glaw, F. (in press) A new species of nocturnal gecko, genus *Paroedura*, from the karstic Tsingy de Bemaraha formation in western Madagascar. *Salamandra*.
42. Rakotoarison, A.*, **Scherz, M.D.***, Bletz, M.C., Razafindraibe, J.H., Glaw, F. & Vences, M. (in press) Diversity, elevational variation, and phylogenetic origin of stump-toed frogs (Microhylidae, Cophylinae, *Stumpffia*) on the Marojejy massif, northern Madagascar. *Salamandra*.
41. **Scherz, M.D.**, Köhler, J., Rakotoarison, A., Glaw, F. & Vences, M. (2019) A new dwarf chameleon, genus *Brookesia*, from the Marojejy massif in northern Madagascar. *Zoosystematics and Evolution*, 95:95–106. DOI: 10.3897/zse.95.32818
40. Chretien, J., Wang-Claypool, C.Y., Glaw, F. & **Scherz, M.D.** (2019) The bizarre skull of *Xenophylops* sheds light on synapomorphies of Typhlopoidae. *Journal of Anatomy*, Early View. DOI: 10.1111/joa.12952
39. Ratsoavina, F.M., Raselimanana, A.P., **Scherz, M.D.**, Rakotoarison, A., Glaw, F. & Vences, M. (2019) Finaritra! A new leaf-tailed gecko (*Uroplatus*) species from Marojejy National Park in north-eastern Madagascar. *Zootaxa*, 4545:563–577. DOI: 10.11646/zootaxa.4545.4.7
38. Hutter, C.R., Andriampenomanana, Z.F., Razafindraibe, J., Rakotoarison, A. & **Scherz, M.D.** (2018) New dietary data from *Compsophis* and *Alluaudina* species (Squamata: Lamprophiidae: *Pseudoxyrhophiinae*), and implications for their dietary complexity and evolution. *Journal of Natural History*, 52:2497–2510. DOI: 10.1080/00222933.2018.1543732
37. **Scherz, M.D.**, Glaw, F., Rakotoarison, A., Wagler, M. & Vences, M. (2018) Polymorphism and synonymy of *Brookesia antakarana* and *B. ambreensis*, leaf chameleons from Montagne d'Ambre in north Madagascar. *Salamandra*, 54:259–268. (with cover image)
36. Prötzl, D., Lambert, S.M., Andrianasolo, G.T., Hutter, C.R., Cobb, K.A., **Scherz, M.D.** & Glaw, F. (2018) The smallest 'true chameleon' from Madagascar: a new, distinctly colored species of the *Calumma boettgeri* complex (Squamata, Chamaeleonidae). *Zoosystematics and Evolution*, 94:409–423. DOI: 10.3897/zse.94.27305
35. Sentíš, M.*, Chang, Y.*., **Scherz, M.D.**, Prötzl, D. & Glaw, F. (2018) Rising from the ashes: resurrection of the Malagasy chameleons *Furcifer monoceras* and *Furcifer voeltzkowi* (Squamata: Chamaeleonidae), based on micro-CT analyses and external morphology. *Zootaxa*, 4483(3):549–566. DOI: 10.11646/zootaxa.4483.3.7
34. Rasolonjatovo, S.M., **Scherz, M.D.**, Raselimanana, A.P. & Vences, M. (2018) Tadpole predation by *Mantidactylus bellyi* Mocquard, 1895 with brief description of the site and morphological measurements of the specimen. *Herpetology Notes*, 11:747–750.
33. Glaw, F., **Scherz, M.D.**, Prötzl, D. & Vences, M. (2018) Eye and webbing colouration as predictors of specific distinctness: a genetically isolated new treefrog species of the *Boophis albilabris* group from the Masoala peninsula, northeastern Madagascar. *Salamandra*, 54:163–177.
32. Hawlitschek, O., **Scherz, M.D.**, Ruthensteiner, B., Crottini, A. & Glaw, F. (2018) Computational molecular species delimitation and taxonomic revision of the gecko genus *Ebenavia* Boettger, 1878. *The Science of Nature*, 105:49. DOI: 10.1007/s00114-018-1574-9
31. Lehtinen, R.M., Glaw, F., Vences, M., Rakotoarison, A. & **Scherz, M.D.** (2018) Two new *Pandanus* frogs (*Guibemantis*: Mantellidae: Anura) from northern Madagascar. *European Journal of Taxonomy*, 451:1–20. DOI: 10.5852/ejt.2018.451
30. **Scherz, M.D.**, Rakotoarison, A., Ratsoavina, F.M., Hawlitschek, O., Vences, M. & Glaw, F. (2018) Two new Madagascan frog species of the *Gephyromantis* (*Duboisimantis*) *tandroka* complex from northern Madagascar. *Alytes*, 36:130–158.
29. Gehring, P.-S., Siarabi, S., **Scherz, M.D.**, Ratsoavina, F.M., Rakotoarison, A., Glaw, F. & Vences, M. (2018) Genetic differentiation and species status of the large-bodied leaf-tailed geckos *Uroplatus fimbriatus* and *U. giganteus*. *Salamandra*, 54:132–146. (with cover image)
28. Bletz, M.C., **Scherz, M.D.**, Rakotoarison, A., Lehtinen, R., Glaw, F. & Vences, M. (2018) Stumbling upon a new frog species of *Guibemantis* (Anura: Mantellidae) on top of the Marojejy Massif in northern Madagascar. *Copeia*, 106(2):255–263. DOI: 10.1643/CH-17-655 (with cover image)

Mark D. Scherz

mark.scherz@gmail.com

www.markscherz.com

27. Prötzl, D., Vences, M., Hawlitschek, O., **Scherz, M.D.**, Ratsoavina, F.M. & Glaw, F. (2018) Endangered beauties: three new species of chameleons in the *Calumma boettgeri* complex (Squamata: Chamaeleonidae). *Zoological Journal of the Linnean Society*, 184(2):471–498. DOI: 10.1093/zoolinnean/zlx112
26. **Scherz, M.D.**, Hawlitschek, O., Razafindraibe, J.H., Megson, S., Ratsoavina, F.M., Rakotoarison, A., Bletz, M.C., Glaw, F. & Vences, M. (2018) A distinctive new frog species (Anura, Mantellidae) supports the biogeographic linkage of the montane rainforest massifs of northern Madagascar. *Zoosystematics and Evolution*, 94(2):247–261. DOI: 10.3897/zse.94.21037
25. Augros, S., **Scherz, M.D.**, Wang-Claypool, C.Y., Montfort, L., Glaw, F. & Hawlitschek, O. (2018) Comparative perch heights and habitat plant usage of day geckos (*Phelsuma*) in the Comoros Archipelago (Squamata: Gekkonidae). *Salamandra*, 54(1):71–74.
24. Bellati, A.*, **Scherz, M.D.***, Megson, S., Hyde Roberts, S., Andreone, F., Rosa, G.M., Noël, J., Randrianirina, J.E., Fasola, M., Glaw, F. & Crottini, A. (2018) Resurrection and re-description of *Plethodontohyla laevis* (Boettger, 1913) and transfer of *Rhombophryne alluaudi* (Mocquard, 1901) to the genus *Plethodontohyla* (Microhylidae: Cophylinae). *Zoosystematics and Evolution*, 94(1):109–135. DOI: 10.3897/zse.94.14698
23. Prötzl, D., Heß, M., **Scherz, M.D.**, Schwager, M., van't Padje, A. & Glaw, F. (2018) Widespread bone-based fluorescence in chameleons. *Scientific Reports*, 8:698. DOI: 10.1038/s41598-017-19070-7
22. **Scherz, M.D.**, Vences, M., Borrell, J., Ball, L., Nomenjanahary, D.H., Parker, D., Rakotondratsima, M., Razafimandimbry, E., Starnes, T., Rabearivony, J. & Glaw, F. (2017) A new frog species of the subgenus *Asperomantis* (Anura, Mantellidae, Gephyromantis) from the Bealanana District of northern Madagascar. *Zoosystematics and Evolution*, 93(2):451–466. DOI: 10.3897/zse.93.14906 (with cover image)
21. **Scherz, M.D.**, Razafindraibe, J.H., Rakotoarison, A., Dixit, N.M., Bletz, M.C., Glaw, F. & Vences, M. (2017) Yet another small brown frog from high altitude on the Marojejy Massif, northeastern Madagascar (Anura: Mantellidae). *Zootaxa*, 4347(3):572–582. DOI: 10.11646/zootaxa.4347.3.9
20. Ratsoavina, F.M., Gehring, P.-S., **Scherz, M.D.**, Vieites, D.R., Glaw, F. & Vences, M. (2017) Two new species of leaf-tailed geckos (*Uroplatus*) from the Tsaratanana mountain massif in northern Madagascar. *Zootaxa*, 4347(3):446–464. DOI: 10.11646/zootaxa.4347.3.2
19. Rakotoarison, A., **Scherz, M.D.**, Glaw, F., Köhler, J., Andreone, F., Franzen, M., Glos, J., Hawlitschek, O., Jono, T., Mori, A., Ndriantsoa, S.H., Raminosoa Rasoamampionona, N., Riemann, J.C., Rödel, M.-O., Rosa, G.M., Vieites, D.R., Crottini, A. & Vences, M. (2017) Describing the smaller majority: Integrative taxonomy reveals twenty-six new species of tiny microhylid frogs (genus *Stumpffia*) from Madagascar. *Vertebrate Zoology*, 67(3):271–398. (with cover image)
18. Rakotoarison, A., **Scherz, M.D.**, Glaw, F. & Vences, M. (2017) Rediscovery of frogs belonging to the enigmatic microhylid genus *Madecassophryne* in the Anosy Massif, south-eastern Madagascar. *Salamandra*, 53:507–518.
17. Prötzl, D., Vences, M., **Scherz, M.D.**, Vieites, D.R. & Glaw, F. (2017) Splitting and lumping: An integrative taxonomic assessment of Malagasy chameleons in the *Calumma guibei* complex results in the new species *C. gehringi* sp. nov. *Vertebrate Zoology*, 67:231–249.
16. **Scherz, M.D.**, Vences, M., Rakotoarison, A., Andreone, F., Köhler, J., Glaw, F. & Crottini, A. (2017) Lumping or splitting in the Cophylinae (Anura: Microhylidae) and the need for a parsimony of taxonomic changes: a response to Peloso et al. (2017). *Salamandra*, 53:479–483.
15. **Scherz, M.D.**, Hawlitschek, O., Andreone, F., Rakotoarison, A., Vences, M. & Glaw, F. (2017) A review of the taxonomy and osteology of the *Rhombophryne serratopalpebrosa* species group (Anura: Microhylidae) from Madagascar, with comments on the value of volume rendering of micro-CT data to taxonomists. *Zootaxa*, 4273(3):301–340. DOI: 10.11646/zootaxa.4273.3.1
14. Lambert, S.M., Hutter, C.R. & **Scherz, M.D.** (2017) Diamond in the rough: a new species of fossorial diamond frog (*Rhombophryne*) from Ranomafana National Park, southeastern Madagascar. *Zoosystematics and Evolution*, 93:143–155. DOI: 10.3897/zse.93.10188
13. **Scherz, M.D.**, Daza, J.D., Köhler, J., Vences, M. & Glaw, F. (2017) Off the scale: a new species of fish-scale gecko (Squamata: Gekkonidae: *Geckolepis*) with exceptionally large scales. *PeerJ*, 5:e2955. DOI: 10.7717/peerj.2955
12. Hawlitschek, O., Wang-Claypool, C.Y., **Scherz, M.D.**, Montfort, L., Soumille, O. & Glaw, F. (2016) New size record of the snake genus *Liophidium* by the island endemic *L. mayottensis*. *Spixiana*, 39(2):287–288.
11. Lattenkamp, E.Z., Mandák, M. & **Scherz, M.D.** (2016) The advertisement call of *Stumpffia* be Köhler, Vences, D'Cruze & Glaw, 2010 (Anura: Microhylidae: Cophylinae). *Zootaxa*, 4205(5):483–485. DOI: 10.11646/zootaxa.4205.5.7
10. Ceriaco L.M.P., Gutierrez, E.E., Dubois, A., +493 signatories (2016). Photography-based taxonomy is inadequate, unnecessary, and potentially harmful for biological sciences. *Zootaxa*, 4196(3):435–445. DOI: 10.11646/zootaxa.4196.3.9
9. **Scherz, M.D.**, Glaw, F., Vences, M., Andreone, F. & Crottini, A. (2016) Two new species of terrestrial microhylid frogs (Microhylidae: Cophylinae: Rhombophryne) from northeastern Madagascar. *Salamandra*, 52(2):91–106.

Curriculum Vitae

Mark D. Scherz

mark.scherz@gmail.com

www.markscherz.com

8. **Scherz, M.D.**, Vences, M., Rakotoarison, A., Andreone, F., Köhler, J., Glaw, F. & Crottini, A. (2016) Reconciling molecular phylogeny, morphological divergence and classification of Madagascan narrow-mouthed frogs (Amphibia: Microhylidae). *Molecular Phylogenetics and Evolution*, 100(2016):372-381. DOI: 10.1016/j.ympev.2016.04.019
7. Hawlitschek, O., **Scherz, M.D.**, Straube, N. & Glaw, F. (2016) Resurrection of the Comoran fish scale gecko *Geckolepis humbloti* Vaillant, 1887 reveals a disjunct distribution caused by natural overseas dispersal. *Organisms, Diversity & Evolution*, 16:289–298. DOI: 10.1007/s13127-015-0255-1
6. Prötzl, D., Ruthensteiner, B., **Scherz, M.D.** & Glaw, F. (2015) Systematic revision of the Malagasy chameleons *Calumma boettgeri* and *C. linotum* (Squamata: Chamaeleonidae). *Zootaxa*, 4048:211–231. DOI: 10.11646/zootaxa.4048.2.4
5. **Scherz, M.D.**, Ruthensteiner, B., Vieites, D.R., Vences, M. & Glaw, F. (2015) Two new microhylid frogs of the genus *Rhombophryne* with superciliary spines from the Tsaratanana Massif in northern Madagascar. *Herpetologica*, 71(4):310–321. DOI: 10.1655/HERPETOLOGICA-D-14-00048 (with cover image)
4. Eudeline, R., Wang, C. & **Scherz, M.D.** (2015). Predation attempt of *Rhombophryne laevipes* by *Compsophis albiventris*. *Herpetology Notes*, 8:393–394.
3. **Scherz, M.D.**, Rakotoarison, A., Hawlitschek, O., Vences, M., Glaw, F. (2015) Leaping towards a saltatorial lifestyle? An unusually long-legged new species of *Rhombophryne* (Anura, Microhylidae) from the Sorata massif in northern Madagascar. *Zoosystematics and Evolution*, 91(2):105–114. DOI: 10.3897/zse.91.4979
2. Martins, A.C., **Scherz, M.D.** & Renner, S.S. (2014) Several origins of floral oil in the Angelonieae, a Southern Hemisphere disjunct clade of Plantaginaceae. *American Journal of Botany*, 101:2113–2120. DOI: 10.3732/ajb.1400470
1. **Scherz, M.D.**, Ruthensteiner, B., Vences, M. & Glaw, F. (2014) A new microhylid frog, genus *Rhombophryne*, from northeastern Madagascar, and a re-description of *R. serratopalpebrosa* using micro-computed tomography. *Zootaxa*, 3860:547–560. DOI: 10.11646/zootaxa.3860.6.3

Asterisks (*) indicate shared first authorships

Books

2. Andreone, F., Crottini, A., Rosa, G.M., Rakotoarison, A., **Scherz, M.D.** & Raselimanana, A.P. (2018) *Les Amphibiens du Nord de Madagascar*. Association Vahatra, Antananarivo, Madagascar, 355 pp.
1. **Scherz, M.D.**, May, M., Taylor, J., Smith, N.J., Tsiafa, H.A., Danvi, M.T., Rakotomalala, M. & Rabemazaka, J. (2013) *Project Kobokara 2011: Final Report*. Amazon, Charleston SC, USA, 97 pp. ISBN 978-1482028751

All supplementary files are provided on the appended CD



Gephyromantis (Vatomantis) lomorina